

AD-A159 082

PROCEEDINGS OF THE SHIP CONTROL SYSTEMS SYMPOSIUM (5TH)

1/4

HELD AT U S NAVAL... (U) DAVID W TAYLOR NAVAL SHIP

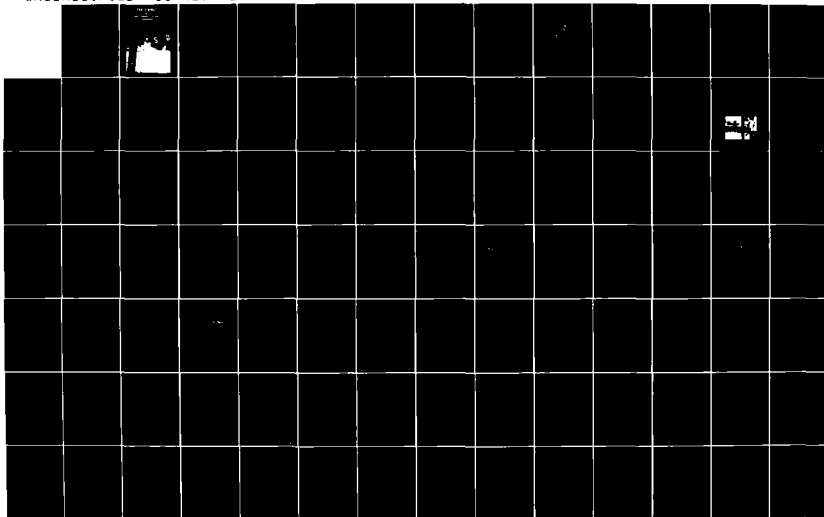
RESEARCH AND DEVELOPMENT CENTER ANN... P MARTIN ET AL.

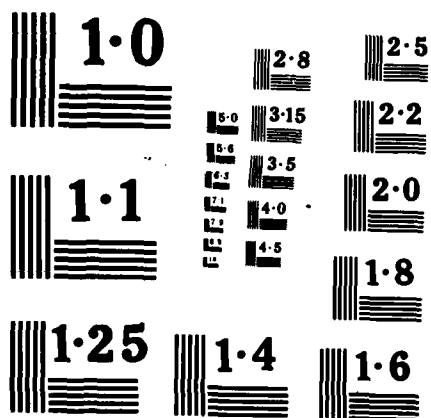
UNCLASSIFIED

03 NOV 78

F/G 13/10

NL





# PROCEEDINGS

①

## **FIFTH SHIP CONTROL SYSTEMS SYMPOSIUM**

OCTOBER 30 – NOVEMBER 3, 1978

VOLUME 2

This document has been approved  
for public release and sale; its  
distribution is unlimited.

AD-A159 082

DTIC FILE COPY

DTIC  
ELECTE  
SEP 9 1985  
D



-: PUBLICATION INFORMATION :-

These papers were printed just as received from the authors in order to assure their availability for the Symposium.

Statements and opinions contained therein are those of the authors and are not to be construed as official or reflecting the views of the Navy Department or of the naval service at large.

Any paper involved with copyrighting is prominently marked with the copyright symbol and was released for publication in these Proceedings.

Requests for information regarding the Proceedings, the Symposium, or the sponsor - David W. Taylor Naval Ship Research and Development Center - should be addressed to the Commander, David W. Taylor Naval Ship Research and Development Center, Bethesda, Maryland 20084 (Attn: Code 273).

Accession No.	
NTIS Class	X
DTIC TAB	
Unannounced	
Justification	
By	
For	
Availability	
A-1	





## VOLUME 2

### CONTENTS

#### Page

#### SESSION D:

Chairman: LCDR W. Verhage  
The Royal Netherlands Naval  
College (Neth)

LMT Ship Handling Simulator ; . . . . . D 1-1  
P. Martin (France)

Ship Control Centre Training Facilities for the  
Royal Navy; . . . . . D 2-1  
CDR N. J. Locke and LCDR M. A. Phelps (UK)

On the Ship Maneuverability Transducer Controlled  
by Mini-Computer for Training Ship Onboard  
Ship Handling Simulator ; . . . . . D 3-1  
K. Karasuno, S. Matsuki and  
M. Okumura (Japan)

#### SESSION E1:

Chairman: Mr. R. Stankey  
Technical Manager  
Ship Control Systems  
NAVSEC (USA)

Modern Control Theory for Dynamic Positioning of  
Vessels ; . . . . . E1 1-1  
O. Ropstad, Kongsberg (Norway)

The Design and Simulation of Navigation and Ship  
Control Algorithms for a Minesweeper; . . . . . E1 2-1  
J. R. Moon and J. R. E. Thomas (UK)

Automatic and Manual Control of the "Tripartite"  
Minehunter in the Hover and Track Keeping  
Modes - Preliminary Design Study. . . . . E1 3-1  
A. W. Brink and A. Stuurman (Neth)

Over )

SESSION E2:

Chairman: CAPT E. J. Healey  
Director, Marine and Electrical  
Engineering  
National Defence Headquarters  
(Canada)

Reversing Dynamics of a Gas Turbine Ship with  
Controllable-Pitch Propeller; . . . . . E2 1-1  
C. J. Rubis and T. R. Harper (USA)

Transient Behavior of Gasturbo-electric Propulsion  
Plant with Single Shaft Gas-turbine and Fixed  
Pitch Propeller; . . . . . E2 2-1  
E. Rohkamm (W. Ger)

Gas-Turbine Simulation Technique for Ship Propul-  
sion Dynamics and Control Studies . . . . . E2 3-1  
T. L. Bowen (USA)

SESSION F1:

Chairman: Mr. A. C. Pijcke  
The Netherlands Maritime  
Institute

New Ship Technical Control Systems for the Royal  
Norwegian Navy; . . . . . F1 1-1  
CAPT O. Ronning and E. Engebretsen (Norway)

The Development of a Machinery Control and Surveil-  
lance System for a Mine Counter Measures Vessel; . . . . . F1 2-1  
R. R. Cummings and T. Turner (UK)

Marine Gas Turbine Health/Performance Monitoring. . . . . F1 3-1  
R. Harris and G. Keating (UK)

Developments in Marine Gas Turbine Condition  
Monitoring Systems; . . . . . F1 4-1  
F. L. Foltz (USA)

SESSION F2:

Chairman: Mr. W. Ellsworth  
Head, Systems Development  
Department  
DTNSRDC (USA)

Elements of an Integrated Control System for Large  
Surface Effect Ships (SES). . . . . See Vol. 6  
W. Malone (USA)

Manual Steering of a Simulated Surface-Effect Ship. . . . . See Vol. 6  
W. F. Clement and R. W. Allen (USA)

→ Optimal Control of Hydrofoil Ship Lateral Dynamics. . . . . F2 3-1  
P. H. Whyte, D.R.E.A. (Canada)

System Analysis Techniques for Designing Ride Control  
Systems for SES Craft in Waves. . . . . See Vol. 6  
P. Kaplan and Sydney Davis (USA)

SESSION G:

Chairman: CAPT T. L. Albee  
Head, Ship System Engineering and  
Design Department  
NAVSEC (USA)

→ Future Propulsion Control Systems Functional  
Requirements; ~~and~~. . . . . G 1-1  
C. French and A. M. Dorrian (UK)

An Analogue Present, A Digital Future for Marine  
Propulsion Control. . . . . G 2-1  
N. D. Probert (UK)

Current and Future Developments in Marine Gas Turbine  
Control Systems . . . . . G 3-1  
M. J. Joby and R. J. Eves (UK)

A High Power Superconducting Ship Propulsion  
System - Its Control Functions and Possible  
Control Schemes . . . . . G 4-1  
T. C. Bartram and R. T. S. Locock (UK)

List of Authors, Session Chairmen, and Guest  
Speakers. . . . . AI-1

## LMT SHIP HANDLING SIMULATOR

By Patrick Martin  
LMT

### ABSTRACT

As in the field of aviation, the development of simulators in recent years enables bridge officers to complete their practical training. The purpose of this paper is to introduce the ship simulator developed by LMT in France.

This simulator consists of a bridge containing the controls, instruments and equipment used on the simulated ship. The bridge is located at the center of a visual system displaying a seascape containing the usual features such as coastline, buoys, landmarks and other ships. The behavior of the ship, the instrument readings and the external scene all respond realistically to commands from the bridge. From an instructor's station, exercises can be supervised and disturbing factors can be introduced into the exercise to train the crew in specific maneuvers.

### INTRODUCTION

The growth in shipping traffic density and the ever increasing size of modern ships have made ship owners, Navies and organizations such as the IMCO, aware of the importance of bridge officer training.

Conscious of these facts and on the advice of the French Navy, shipowners and the IMCO, LMT Simulators and Electronic Systems Division decided to design a ship's bridge simulator. The project received financial support from the French Government and, in January 1978, had progressed to the point where a feasibility prototype was put into operation.

### PURPOSE OF THE SIMULATOR

As in civil aviation, where pilots are now being trained almost exclusively on flight simulators, the ship simulator must be capable of providing all or part of the practical training previously taking place on board ship.

The simulator must therefore faithfully reproduce the environment and the reactions of the ship being steered.

The ship's bridge simulator provides, in particular, supplementary practical training to that given in Merchant Navy schools and in Defense Training Centers.

The practical training which both Merchant and military navies alike believe desirable, should meet two main requirements; it should accustom the bridge officers to the reactions and the instrumentation of the ship being handled and it should accustom them to take correct

decisions and action in response to external events.

Training of this kind applied to large ships is difficult to provide using a small training ship.

#### ADVANTAGES OF THE SIMULATOR

The simulator has many advantages over the conventional training ship:

- it is continuously available for training, independently of weather or tidal conditions. Modern simulation techniques, well proven in many existing installations in all countries, provide an equipment with extremely high reliability. At LMT we can cite the example of the AIRBUS flight simulator installed at Toulouse, France which is used 20 hours per day for pilot training. Moreover the complete independence of the system from weather constraints enables users to adhere to a planned training schedule throughout the year.
- being shore based, it can accept a rapid turn round of trainees. Ideally a simulator of this type would be located close to the Naval School's classrooms so that simulator sessions can be readily interleaved with sessions of theoretical training.
- its operating costs are relatively low. Only one or two persons are employed a few hours daily for operation and maintenance of the simulator. Also, since the electronic equipment used is not only highly modular but common to all types of simulator, repair costs are greatly minimized.
- it has high educational value. The great asset of a simulator is that it can be used to set up situations which are usually difficult to reproduce in reality and which are potential risk situations at sea. The instructor has complete freedom of choice of the training area, tidal conditions, wind force, visibility and the maneuvers of other ships in the training area. The instructor also has a number of particularly effective means of noting and measuring the trainees' progress.

#### DESCRIPTION (figure 1)

The bridge simulator consists of five main assemblies:

- a seascape image generation system,
- a seascape visual display system,
- the bridge,
- a digital computer,
- an instructor's station.

#### Image Generator (figure 2)

The seascape viewed by the occupants of the bridge must have all the characteristics indispensable for good training. In particular, the scene changes as it would, if observed from a ship under way, and it is possible to take bearings and alignments on objects which are

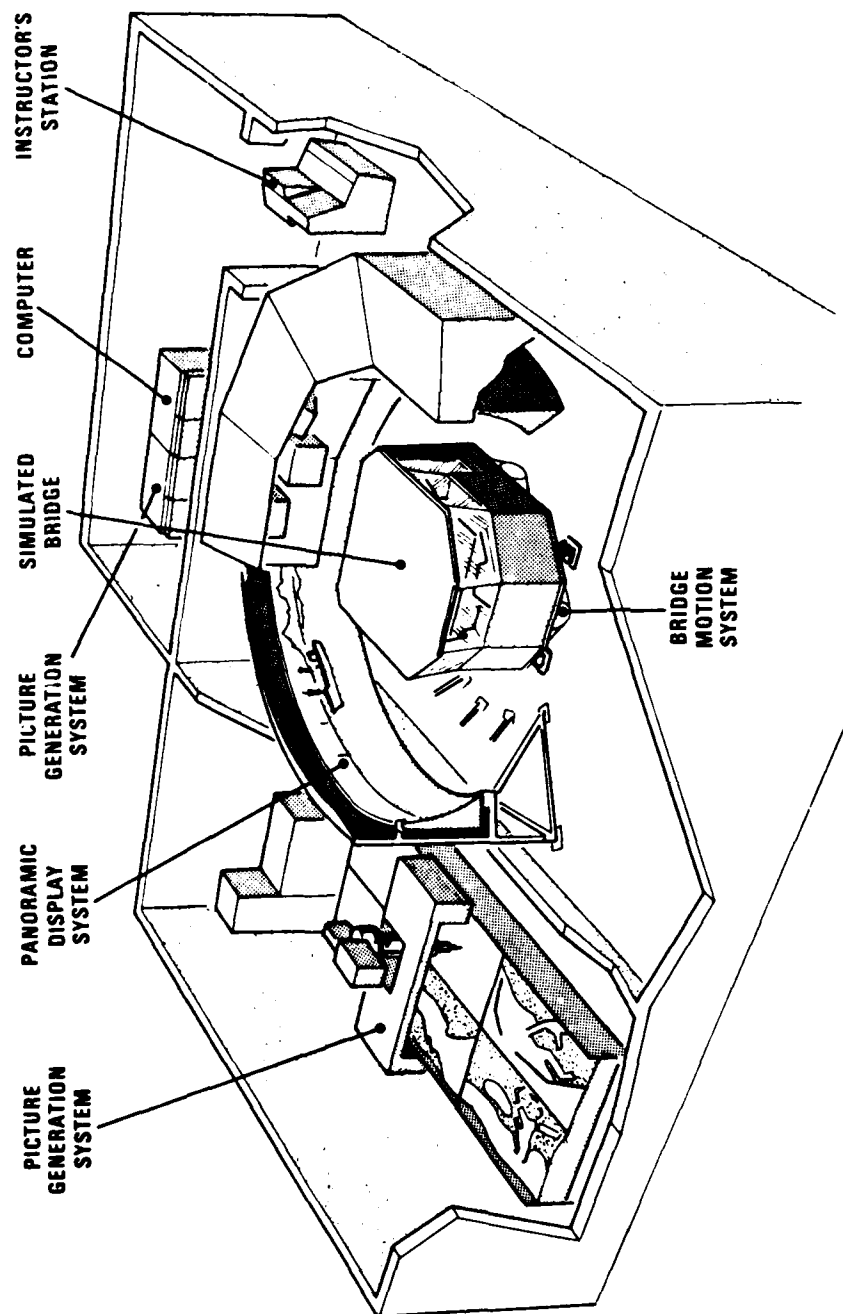


Figure 1 - LMT Ship Handling Simulator  
D 1-3

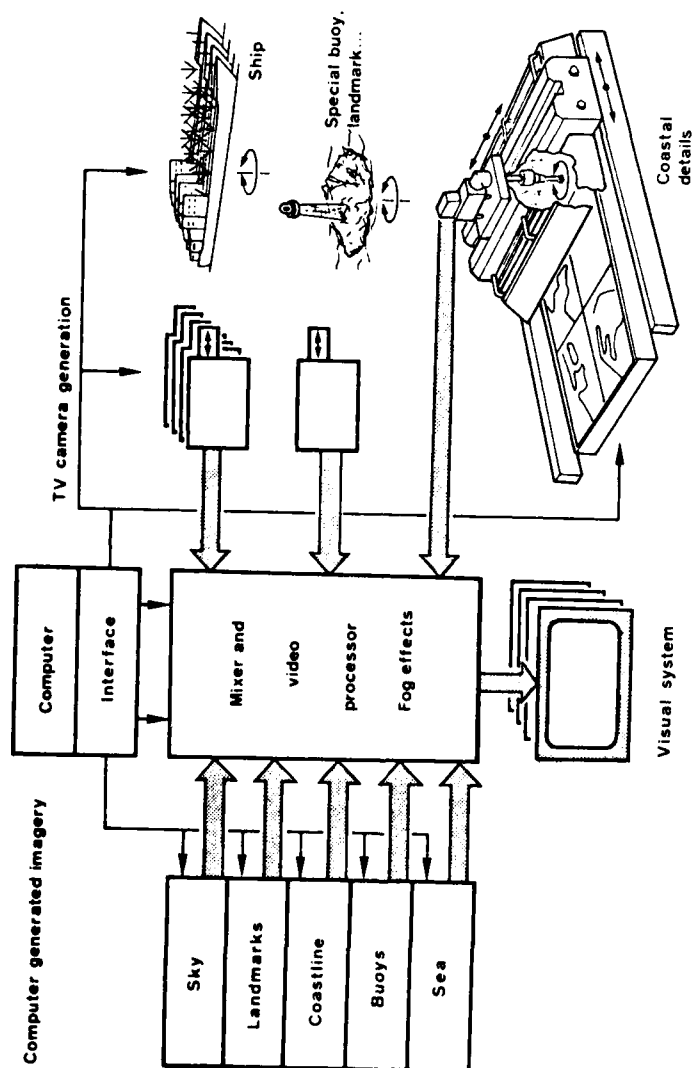


Figure 2 - Image Generation System

located correctly in distance and perspective.

To meet these requirements, the system employed provides a television image. This technique is, in fact, the only one allowing total freedom of movement for the image, as opposed to techniques relying on films or transparencies. Moreover, by conventional inlaying techniques, the television image allows objects to mask one another depending on their respective distances from the observer.

The image contains all the usual features of a seascape: sky, sea, coast, landmarks, buoys, other shipping, etc. There are two broad divisions of features: static features, which include buoys and landmarks and mobile features, such as the sea and other ships.

The static features enable the ship's position to be obtained from bearings and alignments. This training is indispensable to accustom bridge officers to steer the ship through difficult channels where the slightest deviation from course could have serious consequences.

The use of mobile features is mainly for training in busy shipping lanes. The simulation of other ships, in unlimited number, makes it possible to create situations in which the bridge officer's decision or action is vital.

The television image is composed of as many images as there are basic elements in the scene. Each basic image can be generated either by a scale model and T.V. camera or by purely digital computing techniques.

Computer generated image technology has not yet progressed to the stage where highly detailed images can be obtained at a reasonable cost. This technique is therefore used only for objects of simple shape with few details. Where the scene requires a great amount of detail, the camera/model board solution provides the best cost-effective compromise and is employed.

Instructor selected visibility conditions affect the image realistically depending on the distance of each object.

The image generator can reproduce full daylight, dusk and night conditions. At night, surrounding ships' lights and shore lights are reproduced in correct color and flashing sequence.

This system of image generation by processing each basic image, provides great flexibility in the composition of the final image and many possibilities for extension or modification.

#### Visual Display System

Technically this part is the most difficult to realize for, in order to immerse the trainee in surroundings which are as realistic as possible, the image displayed must be as faithful as possible and cover a wide field of view.

To give this impression of realism, the image is in color and is seen at infinity. The infinity image is obtained by using an annular mirror from which are reflected the images displayed on a number of television monitor screens.

The visual display system is modular which means that the field of



view can cover up to 360°. The use of television monitors in a precision optical system gives an image resolution comparable to that of the human eye. The scene viewed thus contains sufficient detail for visual navigation.

#### Bridge

The bridge, located at the center of the visual display system contains all the equipment of a modern ship's bridge. The controls and indicators respond realistically to crew action or to external agencies. The main instruments fitted to modern ships can be simulated: gyro compass, autopilot, Decca, Omega, Loran, echo sounder, Satellite navigation systems, etc. The bridge is also equipped with a radar display giving an image which is coherent with the visual environment.

The bridge layout is usually standardized so that the same equipment may be used for training crews in handling different types of ship. The system is, of course, capable of simulating any type of ship from super tankers to coastal patrol boats, at the choice of the instructor.

#### Computer System (figure 3)

The simulator is controlled by a digital computer. In the computer memory are stored all the characteristics of the ships simulated as well as relevant curves of external parameters. This set of information is known as a mathematical model. The mathematical model chosen is capable of interpreting orders received from the bridge and of determining the reaction of the ship in a given environment. It computes acceleration, speed and position and the indications displayed on bridge instruments and at the instructor's station. The mathematical model also takes into account various external parameters such as atmospheric conditions, current, depth of water, movement of other ships, etc.

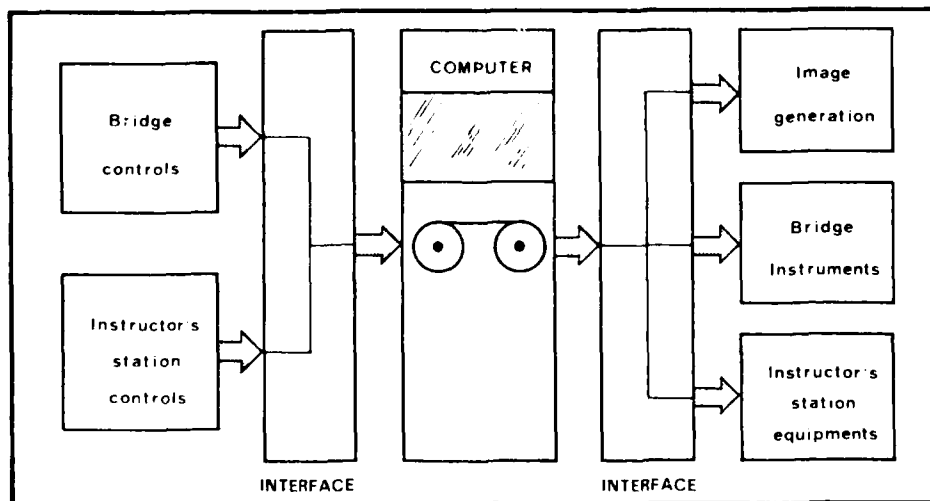


Figure 3 - Computer System

The computer processes all the data from the various controls several times a second and instantaneously transmits the corresponding effects to the visual system and to the bridge instruments.

This dialogue takes place via an interface which is an electronic

unit linking the computer to the bridge equipment. The interface converts digital signals, understood by the computer, into analog signals which actuate the instruments. It likewise converts signals from the bridge controls into digital form.

#### Instructor's Station

The instructor's station is used for:

- exercise management and supervision
- introducing effects into the simulation.

Exercise Management and Supervision. The means provided for exercise management and supervision include the following:

- a system which continuously displays on a cathode ray tube the navigation parameters selected by the instructor.
- a track recorder displaying on the corresponding marine chart the track of own ship and other ships.
- system initial setting controls used to select a particular configuration at the start of an exercise. The configuration can either be pre-programmed and selected by push button or be set up entirely by the instructor. The main factors involved in this setting up are the positions and initial speeds of the various ships.
- a "freeze" control is provided so that the simulation can be suspended allowing the instructor to point out a specific situation to the crew.
- an exercise sequence recorder continuously records the latest half hour of the exercise in progress. This allows the instructor to replay this sequence to point out any possible errors to the crew. The recording can also be stored and used for demonstration in future exercises.
- an interphone for communication between the bridge and the instructor's station.

Introduction of Effects. At any time during an exercise the instructor can introduce various effects into the simulation. Some of these effects are :

- various malfunctions which could affect the ship's engines, controls or other equipment. These malfunctions can render the equipment totally unserviceable or partly unserviceable, in which events the crew will be expected to make a diagnosis and to use the appropriate standby measures.
- sea state conditions, in particular the current force and direction at the simulated ship's position.
- wind force and direction.
- visibility conditions. Visibility can depend on the time of day which can be progressively changed from noon to full night. At night, the lights in the scene appear in color and with the appro-

Table 1. Particulars of Training Ship "FUKAF-MARU"

A	1. 10
2. 10	2. 10
3. 10	3. 10
4. 10	4. 10
5. 10	5. 10
6. 10	6. 10
7. 10	7. 10
8. 10	8. 10
9. 10	9. 10
10. 10	10. 10
11. 10	11. 10
12. 10	12. 10
13. 10	13. 10
14. 10	14. 10
15. 10	15. 10
16. 10	16. 10
17. 10	17. 10
18. 10	18. 10
19. 10	19. 10
20. 10	20. 10
21. 10	21. 10
22. 10	22. 10
23. 10	23. 10
24. 10	24. 10
25. 10	25. 10
26. 10	26. 10
27. 10	27. 10
28. 10	28. 10
29. 10	29. 10
30. 10	30. 10
31. 10	31. 10
32. 10	32. 10
33. 10	33. 10
34. 10	34. 10
35. 10	35. 10
36. 10	36. 10
37. 10	37. 10
38. 10	38. 10
39. 10	39. 10
40. 10	40. 10
41. 10	41. 10
42. 10	42. 10
43. 10	43. 10
44. 10	44. 10
45. 10	45. 10
46. 10	46. 10
47. 10	47. 10
48. 10	48. 10
49. 10	49. 10
50. 10	50. 10
51. 10	51. 10
52. 10	52. 10
53. 10	53. 10
54. 10	54. 10
55. 10	55. 10
56. 10	56. 10
57. 10	57. 10
58. 10	58. 10
59. 10	59. 10
60. 10	60. 10
61. 10	61. 10
62. 10	62. 10
63. 10	63. 10
64. 10	64. 10
65. 10	65. 10
66. 10	66. 10
67. 10	67. 10
68. 10	68. 10
69. 10	69. 10
70. 10	70. 10
71. 10	71. 10
72. 10	72. 10
73. 10	73. 10
74. 10	74. 10
75. 10	75. 10
76. 10	76. 10
77. 10	77. 10
78. 10	78. 10
79. 10	79. 10
80. 10	80. 10
81. 10	81. 10
82. 10	82. 10
83. 10	83. 10
84. 10	84. 10
85. 10	85. 10
86. 10	86. 10
87. 10	87. 10
88. 10	88. 10
89. 10	89. 10
90. 10	90. 10
91. 10	91. 10
92. 10	92. 10
93. 10	93. 10
94. 10	94. 10
95. 10	95. 10
96. 10	96. 10
97. 10	97. 10
98. 10	98. 10
99. 10	99. 10
100. 10	100. 10

The performance of the three transduce systems were studied in full-scale trial to find advantage or disadvantage. In case of yaw motion by large helm operation, it is easy to reproduce a mock yaw motion, but there is some problems on the performance in yaw motion by small helm operation. It is necessary for the device to be able to reproduce the course keeping/alter course maneuvering motions under the actual disturbance by wind and wave in view of a basic ship handling operation. Therefore criteria of the performance in mock yaw motion are examined with the analysed results of 5° zig-zag maneuvering experiments. On the other hand in case of mock ahead motion, criteria of the performance in the motion are examined with the response analysis to step movement of CPP control lever in ordinary operation.

#### BASIC DESIGN CONCEPTION OF TRANSDUCE SYSTEM FOR CHANGING SHIP MANEUVERABILITY

The ship maneuverability transducer is boarded on training ship and used in actual environment. These facts are most different from ship handling simulators on land. The most important point in designing this device is safety of the ship from avoiding collision. For this purpose change-over switch is placed on navigation console in order to change ship control mode from CPU to normal at once. For safety of ship, reliability of every calculations and easy operation of the device are essential. For these requirments a general purpose digital mini-computer is used in the device. The digital computer takes some advantages as follows; 1)conducting accurate real time calculation for slow movement as ship motion, 2)storing computer program in simple floppy disk sheet, 3)selecting any desired program in floppy disk sheet on occasion, 4)no need of checking after programs are completed.

#### DEVICE OF SHIP MANEUVERABILITY TRANSDUCER

The device receives input signals from the steering wheel/CPP control lever and provides output signals calculated from input signals for steering gear/CPP driving unit. Accordingly, signals of driving part are not the same as signals of operation part. As the results

the movement of the steering wheel (CPP control lever). The third system is called MODIFIED CLOSED SYSTEM which joints CLOSED SYSTEM to OPEN SYSTEM for compensating the steering (CPP) response.

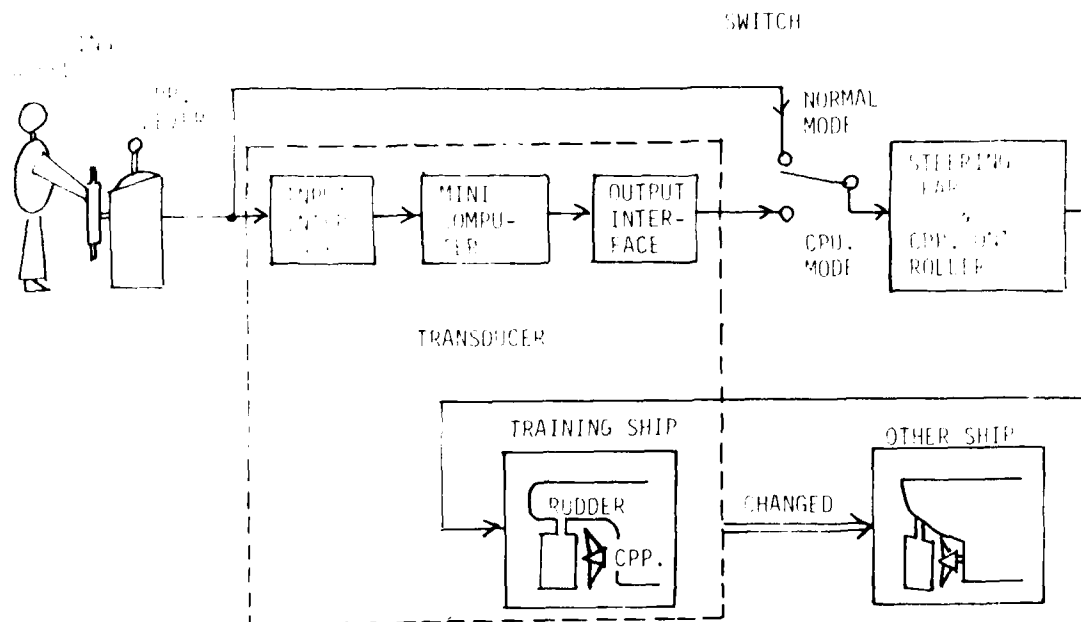


Figure 1. Block Diagram of Ship Maneuverability Transducer

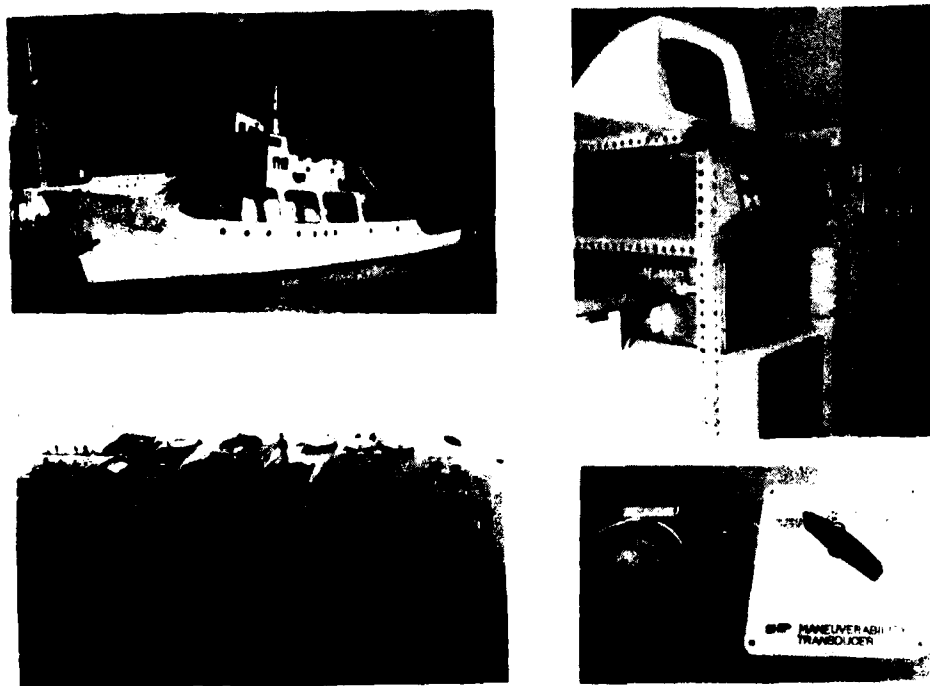


Figure 2. General View of Training Ship and Maneuverability Transducer

ON THE SHIP MANEUVERABILITY TRANSDUCER CONTROLLED BY MINI-  
COMPUTER FOR TRAINING SHIP -- ONBOARD SHIP HANDLING SIMULATOR

by Satoru Matsuki, Keiichi Karasuno  
and Muneyuki Okumura  
Kobe University of Mercantile Marine

ABSTRACT

Training ship FUKAE-MARU 360 GT equipped on board a ship maneuverability transducer, which is a device changing her own maneuverability to other ship's one apparently. In order to change her own maneuverability of yaw(ahead) motions, a mini-computer is linked between the steering wheel(CPP control lever) and the steering gear(CPP driver). The computer controls rudder deflection (CPP blades angle) to realize an optional maneuvering motion characterized by a different maneuverability from the original one. Accordingly a ship operator on board is possessed with the illusion that he handles another ship. As the transducer on board can immitate other ship's maneuvering motion, the training ship may be called a onboard ship handling simulator. The mock ship ranges from the original training ship to any large ship; using Nomoto's steering quality indices K-T, turning ability index K is 0.05—0.2 (1/sec) and course stability index T is 10—150 (sec), where the original indices of the training ship are  $K=0.2$  (1/sec) and  $T=13$  (sec) at ship speed 9 knots.

This device must be useful for

- 1)ship handling training for students
- 2)studies of man-machine system on ship handling
- 3)studies of correlation in man-machine system between full-scale ship and ship handling simulator

INTRODUCTION

The procedures of ship handling are generally different in ship's scale and maneuverability. A good ship handling requires enough experience and perception especially in VLCC. Referring to its education and training, we have one small training ship of 37m length. It is necessary for our students to experience to handle every size of ships. Therefore changing her ship maneuverability from original one to others temporarily by any means, gives the student useful experience with only one ship. This device, which can change a ship's own maneuverability to others, may be called a SHIP MANEUVERABILITY TRANSDUCER. The device is designed and prepared mainly for training our students as mentioned and studies of ship handling. A mini-computer in the device links the steering wheel(CPP control lever) to steering gear(CPP driver) and controls rudder deflection(CPP blades angle) in order to realize an aimed ship motion<sup>(1,2,3,4)</sup> (see Figs.1,2 and Table 1).

In this paper changing the characteristics of yaw and ahead motion is dealt respectively and the employed methods of the change are three transduce systems as follows. The first system is called OPEN SYSTEM which controls rudder deflection(CPP blades angle) by only one computer input from movement of the steering wheel(CPP control lever). The second system is called CLOSED SYSTEM which controls ship yaw angle(ship speed) following target computed by the computer input from

In a typical exercise the SCC instructor will set a machinery condition by keying the VDU and selecting the simulation programme. The trainees will carry out watchkeeping duties in response to orders from the "Bridge", the instructor in the observation room. The Engineer Officer of the Watch (EOOW) may require an item of machinery to be checked, so a watchkeeper will be sent to the machinery compartment. He will see on the VDU screen there a plan of the machinery with a code against each item and he will select the location of the machine by keying the code number. The VDU will name the machine selected and a view of it will appear on the back projection screen. It may be the wrong one. The observation room instructor will be able to monitor this. The watchkeeper may check a machine by interrogating the VDU for data such as lub oil level, discharge pressure and so on. A fault may have been programmed in; he will report back to the SCC. The exercise may continue thus or the instructors may inject problems by selecting an exercise which sets off warnings and alarms. The SCC team then carry out a breakdown drill to render the machinery safe and maintain manoeuvrability. The programming of the exercises will be done in the preparation of the course, initially by the manufacturer and later by SULTAN staff after appropriate training.

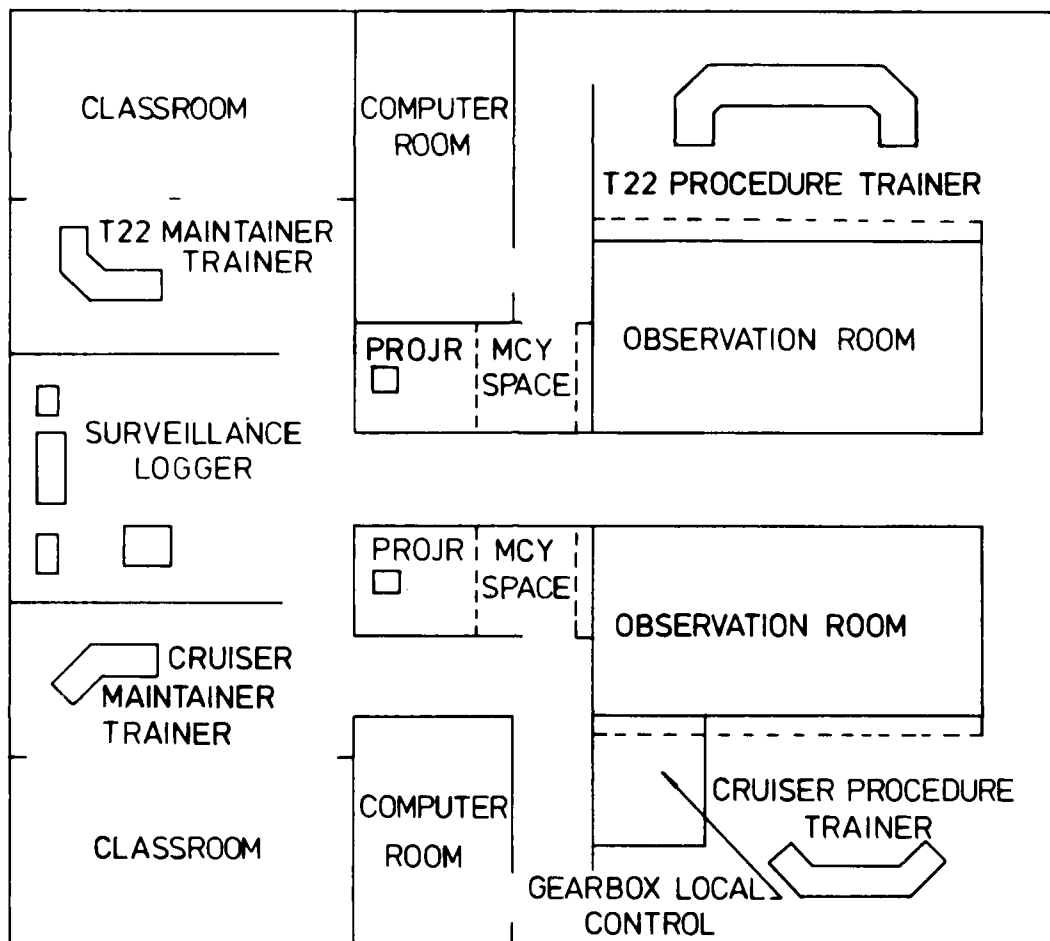
#### MAINTAINER TRAINERS

These will be sited adjacent to classrooms so that instruction on the equipment can be followed in drawings and handbooks by members of the class seated at desks. The equipment will comprise a part of a working shaft set of panels, chassis, modules and wiring. An instructors' console will enable faults to be introduced for diagnosis. Solid state logic and slave actuators will simulate the functions of the controls. Built in test equipment will be available for testing. A set of Data Logger equipment will be provided to demonstrate its functioning.

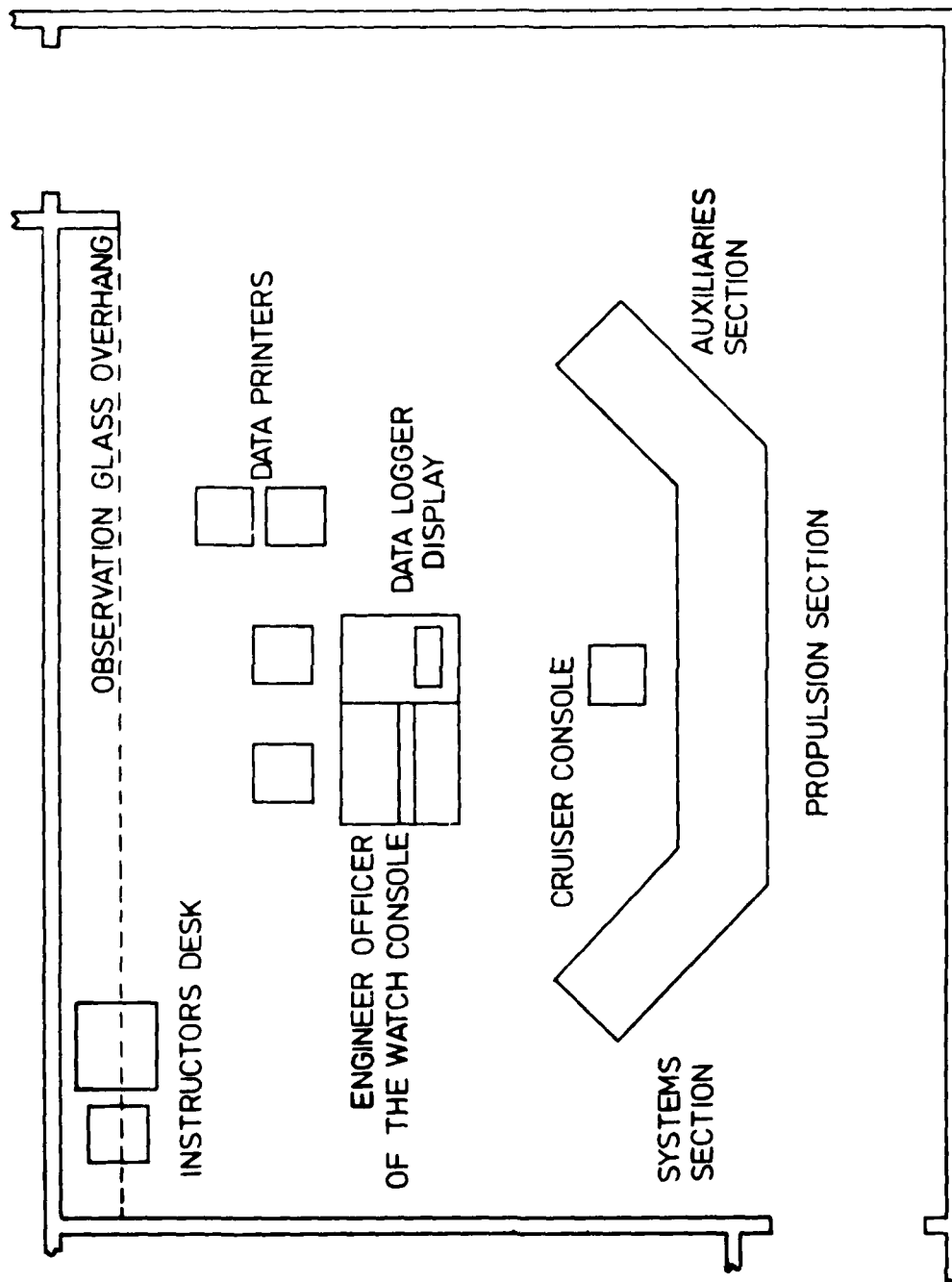
The Maintainer Trainers will teach fault-diagnosis of the control system by observation of the operation of the console and by use of the test equipment. The Procedure Trainers will not show faults in the control system but will be used to teach how to deal with faults in the plant by reverting to alternative modes. Thus the two sets of training equipment have different but complementary roles. A single general purpose set of equipment would have been more expensive and could not have met the requirements for course scheduling for operator and maintainer training.

#### CONCLUSION

This paper has shown how the use of training simulators for machinery has developed in the Royal Navy. The review has, of necessity, been limited to five classes of surface ship. The value of carrying out an appraisal of early simulators and courses and of justifying the acquisition of new simulators has been demonstrated. The need to consider training equipment design at the same time as a new machinery system is designed cannot be over-emphasised. In the current work the lengthy research has delayed the placing of contracts for training facilities but tendering companies have appreciated the completeness of specifications and firm price contracts have been possible. The new facilities will make use of latest digital computer techniques but the course content and structure will need to be fully prepared for procedure programming.

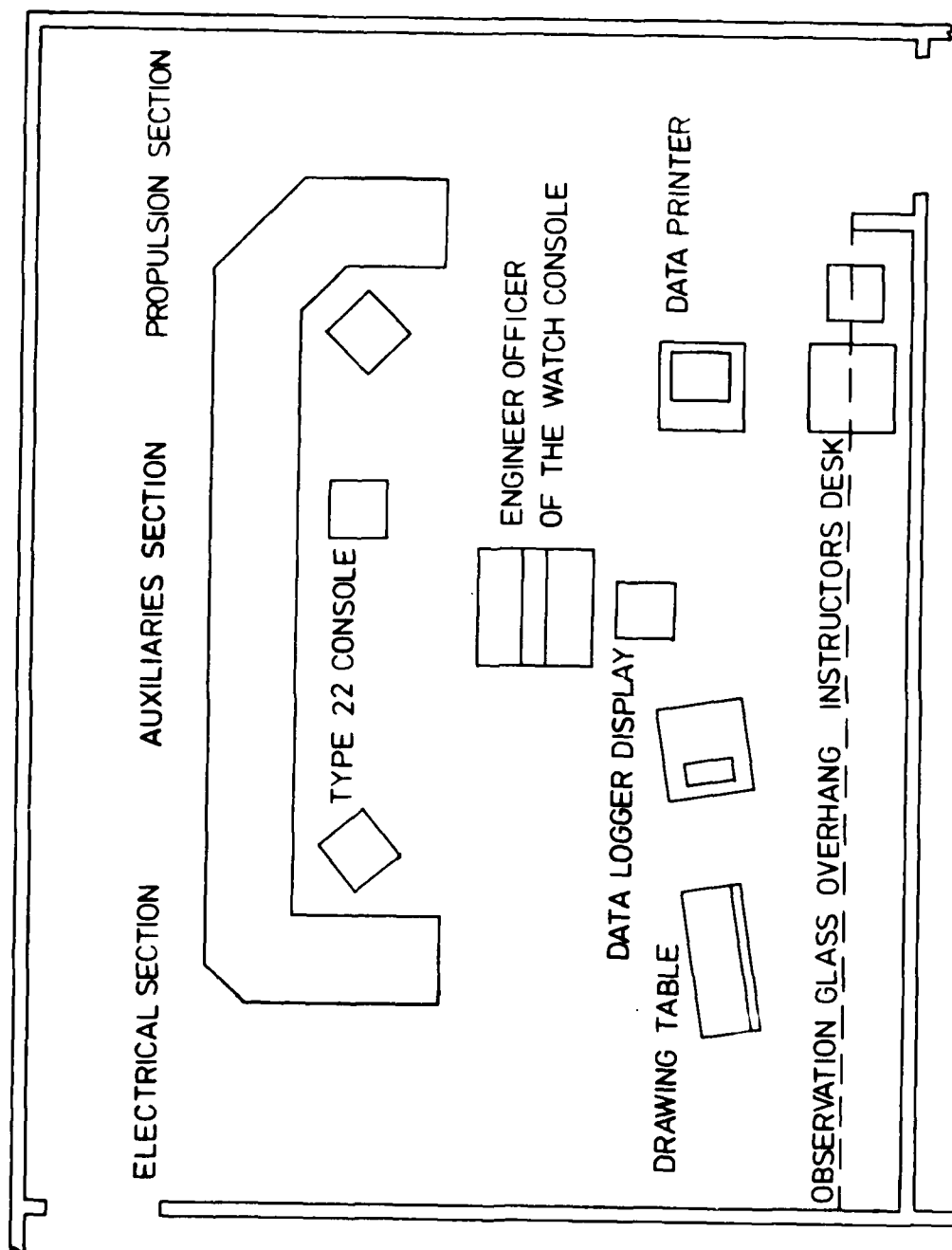


HMS SULTAN-TYPE 22/ CRUISER SHIP CONTROL CENTRE  
 FIG 4. NOT TO SCALE TRAINING FACILITIES



CRUISER SHIP CONTROL CENTRE PROCEDURE TRAINER.  
FIG 3.  
NOT TO SCALE.





TYPE 22 FRIGATE SHIP CONTROL CENTRE PROCEDURE TRAINER  
FIG. 2.  
NOT TO SCALE

Branch will be structured to include both disciplines. During the initial part of the course it is envisaged that systems will be taught with the aid of printed notes, overhead projectors and wall-drops. Subsequently the operation of a system will be explained by the use of an animated diagram where it is an important, complex system. The diagrams, by means of illuminated panels and flow lines driven by solid state devices, will demonstrate the working of the system in a pictorial form. It will also show how the relevant section of the control console relates to the system and the way in which system conditions are indicated on the control console. The trainee will be able to see that changes of state in one part of the system have implications for another part of a system and by this understanding he will be able to take the most appropriate action at any time under normal or breakdown conditions.

#### PROCEDURE TRAINERS

Full scale mock-ups of the ship control centres (SCC), consoles and local control positions are being provided. At an early stage of equipment definition it was accepted that the accuracy of simulation necessary for procedure training did not justify the high cost of total simulation.

A digital simulation system is being developed to cover a wide range of machinery and systems in such a way as to avoid the need for accurate and extensive mathematical modelling. This is saving cost on both software and hardware.

The control of a particular exercise or group of routines will be by "scenario", which will contain scripted directions to the procedure trainer and will also monitor the required actions of the student. Where applicable, the scenario will call for an input from the mathematical model but where a non-modelled system is concerned, its simulation will be under the direct control of the scenario.

There will be the ability to run through exercises and routines initially in slow time and then at real time. The instructor will have the facility to freeze an exercise at any point or allow it to continue in an unexpected direction by calling up further scenarios.

Exercises will be tied to the practice of normal and emergency procedures. Tasks external to the SCC will be accomplished in a realistic machinery compartment where the trainee will key a visual display unit to select the appropriate action. Compartment realism will be achieved by the use of back projection screens showing selected views of machinery. Communications will be as provided in the ship. The Type 22 Procedure Trainer SCC layout is shown in Figure 2 and that of the Cruiser Procedure Trainer in Figure 3.

There will be two instructors' consoles with visual display units, one in the SCC and one in the observation room. The latter will incorporate bridge control simulation. The observation room will enable extra members of a class or visitors to the facility to watch procedures without intruding upon the realism. The complete plan of the training facilities showing the various compartments is shown in Figure 4.

## PROPOSED TRAINING FACILITIES

The initial recommendation was for a systems-orientated PJT course with simple consoles for familiarisation and a properly structured onboard training course. In discussions with authorities concerned the possibilities were shown to be limited by operational considerations and by the likelihood of variation in standards between ships. Therefore it was decided that the Consultant should develop the specifications for the most suitable shore training facilities.

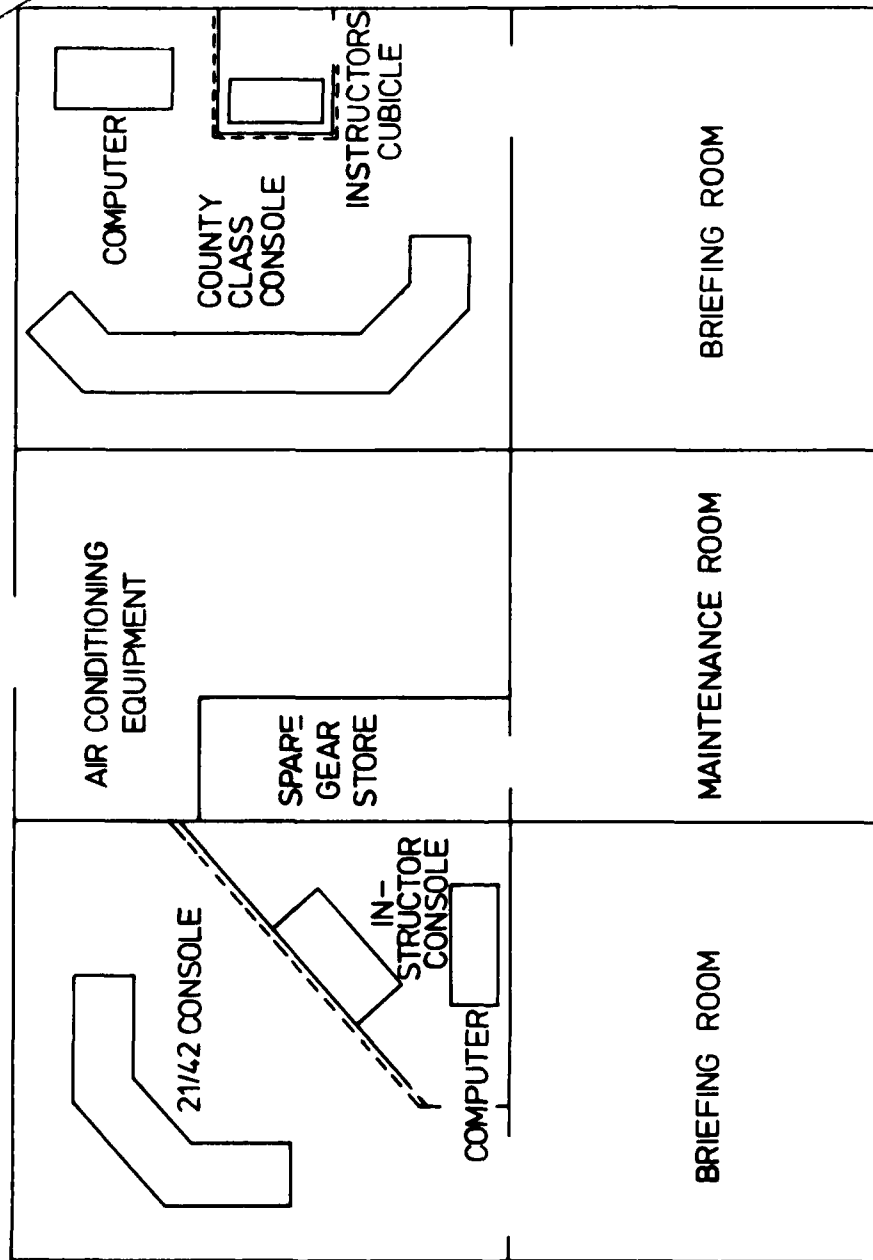
It should be borne in mind that Naval machinery operation is complex in comparison with Merchant Ship practice due to the requirements for (a) a wide variation in power to manoeuvre the warship in action and (b) a number of alternative systems available to maintain power in the event of action damage or breakdown.

The general recommendations for training were as follows:-

- (a) The operators must be trained to appreciate the machinery state from the surveillance systems provided and to take the appropriate actions in the normal and breakdown modes. To instil confidence in the plant as a whole the facility should include a representative machinery space environment for local control and communications.
- (b) For breakdown drills requiring diagnostic ability operators be given an understanding of systems such as transmission, fuel, controls and the like. To achieve this a series of training aids in the earlier stages of the course will be necessary.
- (c) Simulators which accurately represent the performance of ships equipment are not necessary to train individual operators in their tasks, however, for training watchkeeping teams, low cost, low fidelity simulators are justified.
- (d) For control system maintenance training, working equipment must be used, suitably arranged to teach fault-finding. The equipment and course must demonstrate upkeep policy and should include a thorough grounding in the use of test facilities.
- (e) The indirect costs and the instructor/trainee costs over a thirty year period were shown to be five times the life-cycle costs of the training equipment. Therefore to reduce costs significantly the length of course and the number of instructors should be kept to the minimum.
- (f) To ensure that the PJT course is kept to a minimum the balance between the career course and the PJT should be regularly reviewed.

## TRAINING AIDS

For personnel joining the Type 22 frigate or the Command Cruiser the intention is to provide an integrated electro-mechanical systems based course which will be common for both mechanically trained and electrically trained personnel. In time the Marine Engineering



TYPE 21/42 AND COUNTY CLASS MACHINERY CONTROL ROOM SIMULATORS  
FIG 1.  
NOT TO SCALE.

In a very short time it became apparent that this simulator was the most effective training aid employed in the instruction of personnel about to join this class of ship. Within a year, HMS SULTAN, the Naval Marine Engineering School where the simulator was installed, was providing the Fleet with an operator who was both competent and confident. He required much less on-job training and was more readily integrated into the ship's company. The simulator was also used for refresher training for the complete watchkeeping crews from particular ships.

#### THE TYPE 21/42 SIMULATOR

When HMS SULTAN was tasked to provide training for the new gas turbine and electronic control systems of the SHEFFIELD Class it became clear that the operator training task could best be met by the provision of a second simulator like that for the COUNTY Class. A proposal was also raised to obtain working sections of a console to provide maintenance training for the electronic controls. This was considered necessary due to the difficulty of giving the control system maintainers "on-job" training. The proposals were accepted and the contract for the simulator was placed in 1970 with the same manufacturer as before. It was later amended to include the provision of console sections for the AMAZON Class. For the first time with a new class of ship the watchkeepers were able to take advantage of simulator training before Contractor's Sea Trials. Known as HMS AYLESBURY, this simulator was a copy of the Type 42 console with additional panels to represent the Type 21 layout. An instructors' console and bridge console were provided behind a glass partition. An annex was added to represent machinery spaces as for the COUNTY Class facility. (Figure 1).

The maintainer training console was purchased from the controls system manufacturer and was delivered to HMS COLLINGWOOD, the Naval Weapon Electrical School in 1971. It has been used for PJT courses for teaching first-level fault-finding and for training Electrical Artificers in fault diagnosis and rectification, to enable them to work within the marine engineering departments in ships. A departure from previous practice has been adopted in the Type 21/42 PJT courses in that the mechanical and electrical technicians do almost a common course.

At the technician level, the duration of the course is nine weeks. The various items of machinery and systems particular to the ships are covered in the classroom in some detail, from the point of view of construction and operation. This is done with the aid of overhead projectors, wall-drops and where possible, static items of machinery. Practical maintenance training on the control system is given by means of the maintenance trainer, on which it is possible to inject numerous faults, see the effect of each fault on the front panels of the console and locate the source of the fault by the use of the test gear as supplied to the ship. The final week is spent with the simulator and it forms the focal point of the course. It is during this week that the trainees can consolidate and build on the knowledge gained in the classroom over the previous eight weeks. There is opportunity for each trainee to become familiar with the duties of the other members of the watch. The instructors can give a series of exercises of varying difficulty to extend the watchkeepers capabilities. At the end of such a course and more especially during team training sessions, the trainees can be assessed on their ability

classroom aids and some real items of equipment to be found on the ships. This training catered for early ships of the LEANDER, TRIBAL and COUNTY Classes, with reasonable success. Nevertheless, a number of incidents occurred with the COUNTY Class propulsion plant, involving operation of boilers, gearboxes and auxiliaries, which suggested that a fresh look be taken at the training provided, especially that concerned with operating procedures.

#### THE TRAINING TASK

In these ships the operator was faced, for the first time, with unmanned machinery spaces and a machinery control room from which the main propulsion plant and the major units of auxiliary machinery and systems could be operated in automatic or remote control. Primary surveillance was carried out by the operator from the control room using the extensive instrumentation displayed. In removing the watchkeeper from the machinery space environment in which he had been trained, to the air-conditioned control room, the senses of hearing, smell, feel and to a certain extent, sight, on which he had depended were of little value to him. To interpret the information presented to him in the remote position he required a different appreciation of the machinery and systems. To meet this situation the decision was taken in 1966 to obtain a machinery control room simulator to achieve the following purposes:-

- (a) To facilitate the exercising of emergency drills in safety and allow them to be taken further than would be possible in any "live" drill aboard ship, thus giving greater coverage of the emergency aspects of operation than could be achieved aboard ships.
- (b) To allow greater pressure to be placed on trainees so that they acquire much improved confidence in their ability to cope with any situation.
- (c) To increase the competence of operators with a wider range of tasks which could be carried out and thus reduce the amount of on-job training required.

#### THE COUNTY CLASS SIMULATOR

The first simulator was ordered in 1966 and it is still in service. Known as HMS BUCKINGHAMSHIRE, it consists of a steam plant control console on which many of the gauges respond to the push-buttons and levers through an analogue computer. There is an instructors' console by means of which faults can be introduced and operators can be guided by the instructor on correct drills and procedures. It is very realistic for the watchkeepers in charge of the boilers and steam turbines but it has limitations for the chief of the watch. The effects of cross-connecting units are not simulated and links with the imaginary machinery spaces and gas turbine control room have to be provided by the instructor from his cubicle. An annex with suitable communications has been added to represent compartments from which trainees can respond to broadcast instructions. Control system maintenance training is given during pneumatic controls courses for which an equipment demonstration area is provided.

## SHIP CONTROL CENTRE TRAINING FACILITIES FOR THE ROYAL NAVY

By Commander N J Locke  
C.Eng., F.I.Mar.E., M.I.Mech.E., RN  
and Lieutenant Commander M A Phelps, B.Sc., RN

### ABSTRACT

The development of warship propulsion machinery over the last ten years has resulted in the use of centralised controls and fewer watchkeepers. Present day machinery operators have to be well trained to manage the whole plant from a remote position. Computer simulation techniques have enabled shore-based facilities to be developed for pre-joining training and for continuation training. To obtain the most cost-effective facilities, detailed studies were undertaken, past methods were reviewed and objectives were clarified.

### INTRODUCTION

Until the 1960's the Royal Navy traditionally carried out its Marine Engineering operating training at sea. This was by the long established method of "double-banking" personnel with qualified operators until suitable, by observation or by examination, to take over the duty. Shore training was limited to career training in the basic principles of machinery operation and, more especially, machinery maintenance. This method of on-job training was cost-effective and satisfactory because the large number of technical personnel manning those ships could easily include a number of trainees without affecting operating efficiency.

From the early 1950's developments in machinery design were influenced by the need to provide remote operation of machinery for transit of nuclear fall-out. This resulted in the provision of a machinery control room; a small compartment above the main machinery spaces in which the individual control systems of the propulsion plant were combined for the convenience of manoeuvring. The control room was provided with little in the way of surveillance instrumentation but was equipped with the means of stopping the engines in an emergency. Any additional or standby machinery required was prepared and started by the watchkeepers in the machinery spaces. The trend towards the remote control of machinery was accompanied by the need to reduce the number of watchkeepers, in order to make savings on the manpower costs of ships. Both of these developments made the traditional on-job training methods less effective. The problem was compounded in the early 1960's by the increased complexity of modern high-performance machinery in the new design of ships, for which the shore-based career training courses were inadequate.

Pre-joining training courses (PJT courses) were introduced to give the officers and senior ratings concerned a broad understanding of the special features of the ship to which they were going. These courses tended to concentrate on the machinery and systems and were developed into longer, more detailed courses utilising comprehensive

priate flash. Additionally the instructor can introduce the effect of various densities of fog so that objects are more or less masked depending on their distance.

- modification of the type and position of the various buoys so that the exercise can be adapted to suit the training requirements.
- modification of course and speed of other ships so that the bridge crew meet realistically changing situations which train them to take the correct decisions and to maneuver accordingly.

#### SHIP SIMULATOR PROTOTYPE

As a first stage in the design of this simulator LMT has constructed a prototype to test the validity of the technical solutions adopted and specifically to test the visual projection system which is the original feature of this bridge simulator.

The prototype is installed, in LMT's TRAPPES factory, near PARIS, and simulates the handling of a 220 000 tonne tanker in an area containing other ships.



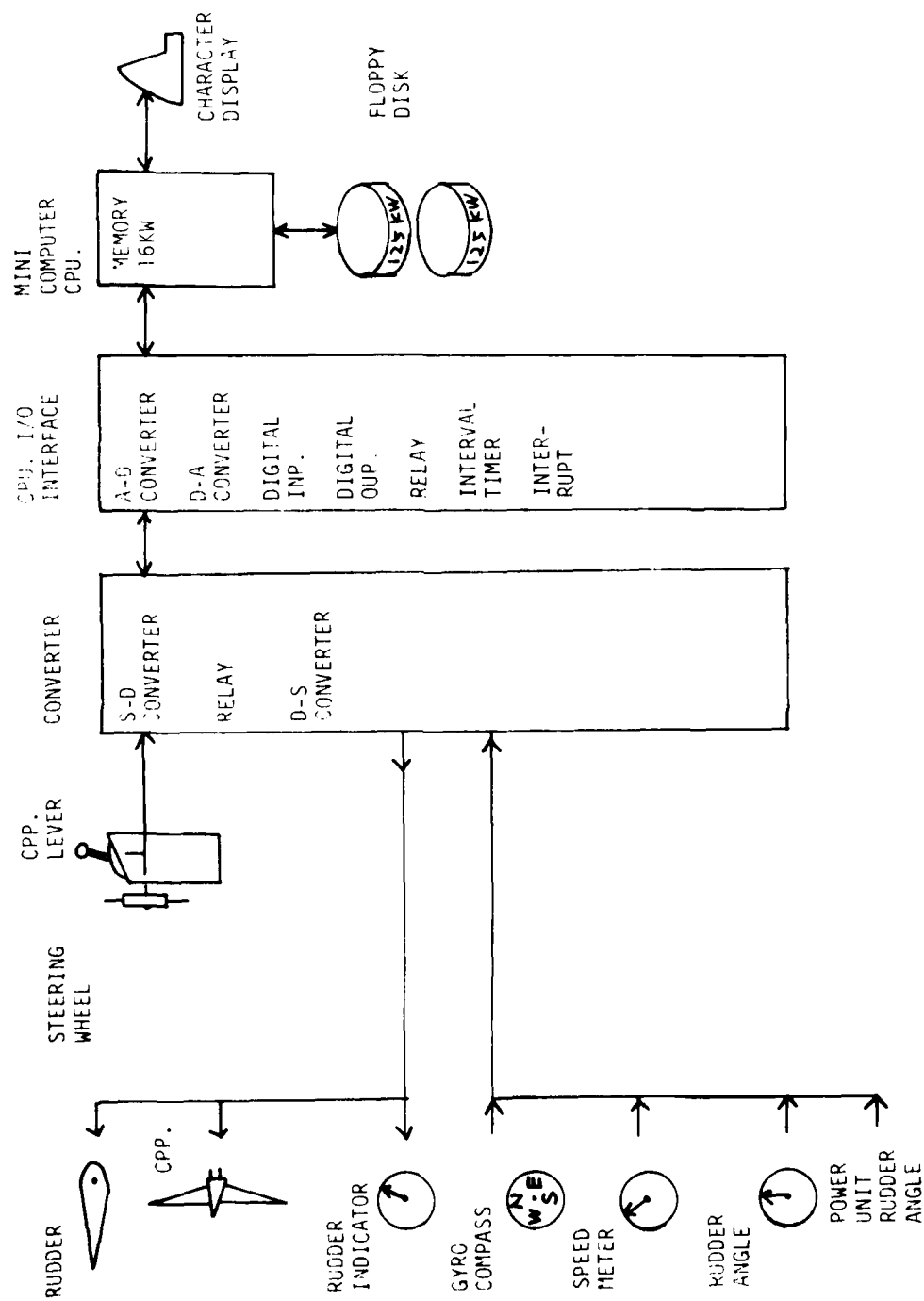


Figure 3. Composition of Maneuverability Transducer

, maneuverability of original ship is changed apparently to other ships.

The device consists of following five parts; (see Fig.3)

- 1) signal converters(change-over switch, input interface and output interface): to transfer signals from/to onboard instruments and switch on/off the device
- 2) CPU interfaces(A-D converter, D-D converter, relay and interval timer): to connect signal converters to digital computer
- 3) mini-computer(CPU memory 16kw): to calculate for changing ship maneuverability, read in input signals from input interface and write out output signals to output interface
- 4) external store(floppy disk, memory capacity 125kw\*2): to store transducing programs and measured data of ship motions
- 5) character display: device for conversation with computer, that is to say, key-board for input to computer and characters on Braun tube for output from computer

#### MATHEMATICAL MODEL OF YAW MOTION FOR TRANSDUCE

In time of transduce for ship yaw motion, a simple mathematical model is preferable, but it have to represent reasonably the motion in ship handling. For this purpose Nomoto's rudder-to-yaw response equation is sufficient. The equation is described with non-dimensional steering quality characteristics  $K'$ ,  $T'$ ,  $T'_2$  and  $T'_3$

$$T'_1 T'_2 \left( \frac{L}{V} \right)^2 \ddot{\psi} + (T'_1 + T'_2) \left( \frac{L}{V} \right) \dot{\psi} + \psi = K' \left( \frac{V}{L} \right) \delta + K' T'_3 \dot{\delta} \quad (1)$$

where  $L$  is ship length,  $V$  is ship speed,  $\psi$  is yaw angle,  $\delta$  is rudder deflection and  $\dot{\cdot}$  is time differential<sup>(5)</sup>. The Eq.(1) is not reasonable to a whole extent of yaw motion. But this equation is applicable to course-keeping motion and small alter course steering motion without speed change.

In case of steering motion with long period, the Eq.(1) is transferred to first order linear approximated equation (2) with  $K'$  and  $T'$ .

$$T' \left( \frac{L}{V} \right) \dot{\psi} + \psi = K' \left( \frac{V}{L} \right) \delta \quad (2)$$

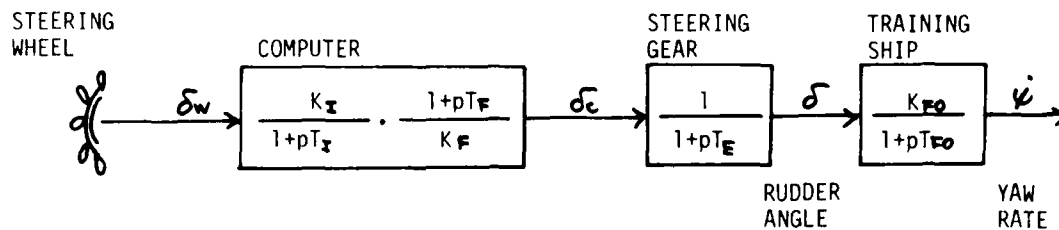
This equation is a reasonable mathematical model for slow varying motion at constant speed.

In this paper a small training ship is employed to change ship maneuverability. The small TS is easily disturbed by wind and wave. Therefore mock ship's motion transduced by this device are not always described with the second order equation (1), so that the rigorous mathematical model is not necessary in use. Moreover steering quality indices  $K'$  and  $T'$  are easily comprehensible by ship operator and derived easily from zig-zag maneuvering test. So first order approximated equation (2) is adopted in this paper.

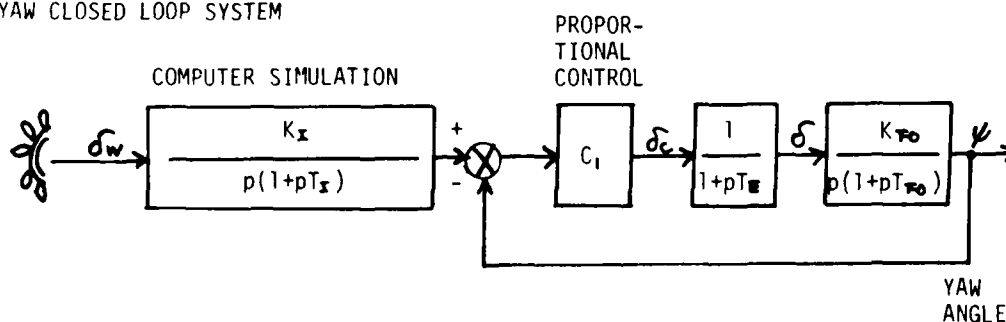
#### TRANSDUCE SYSTEM

Rewriting first order equation (2) in transfer function as rudder-to-yaw rate response, following Eq.(3) is obtained.

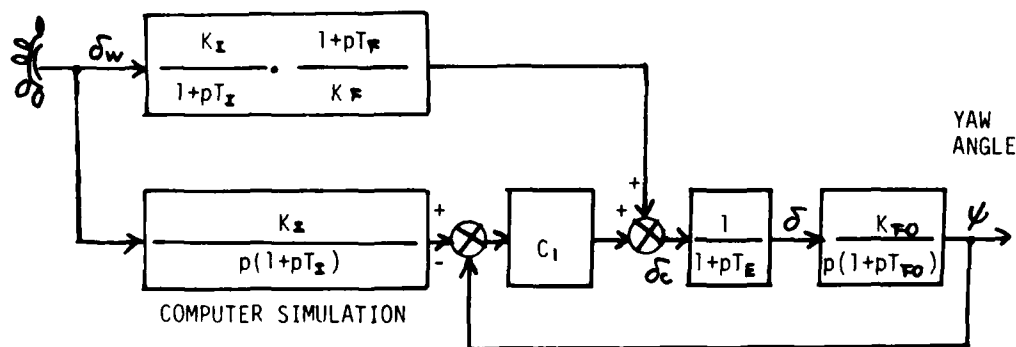
a) YAW OPEN LOOP SYSTEM



b) YAW CLOSED LOOP SYSTEM



c) YAW MODIFIED CLOSED LOOP SYSTEM



$K_x, T_x$  : Intended steering quality indices of mock ship  
 $K_f, T_f$  : Estimated steering quality indices of Training Ship  
 $K_{po}, T_{po}$  : Actual steering quality indices of Training Ship  
 $p$  : Complex Number  $\alpha + j\omega$   
 $\delta_w$  : Rudder angle ordered by Steering Wheel  
 $\delta_c$  : Rudder angle ordered by Computer  
 $\delta$  : Actual rudder deflection

Figure 4. Block Diagram of Transduce system for Yaw Motion

$$Y_s(p) = \frac{\mathcal{L}[\dot{\psi}(t)]}{\mathcal{L}[\delta(t)]} = \frac{K}{1+pT} \quad (3)$$

where  $\mathcal{L}[\ ]$  is Laplace's transform,  $p$  is complex number  $\alpha + j\omega$ ,  $K = K'(V/L)$ ,  $T = T'(L/V)$  and  $t$  is time. A basic idea of changing ship's maneuverability is started from Eq.(3). Namely the transfer function of TS combines cascadedly a transfer function of an element (computer) to a transfer function of another ship. This cascade method is a simplest means to identify the total ship system with mock ship. But considering the disturbance of wind and wave, there is limit of changing the characteristics. To extend its limit, a feed-back control system of yaw angle is considered in this paper.

Three kinds of transduce system as follows are conducted (see Fig.4)

**YAW OPEN SYSTEM.** This transduce system consists in direct application of mentioned basic idea. The cascade combination can eliminate the original transfer function of TS and newly produces mock ship's transfer function. Accordingly the movement of steering wheel gives only one input to the computer and the computer output signal drives the steering gear without feed-back of yaw motion.

When the steering motion of TS is described by the first order response equation, its transfer function is assumed to be  $Y_{F0} = K_{F0}/(1 + pT_{F0})$ , where the steering quality indices of TS are  $K_{F0}$  and  $T_{F0}$ . Moreover the transfer function of a mock ship is assumed to be  $Y_1 = K_1/(1 + pT_1)$ , where  $K_1$  and  $T_1$  are the steering quality indices of the mock ship. The transfer function of cascade combined element (computer) is

$$Y_c(p) = \frac{1 + pT_{F0}}{K_{F0}} \frac{K_1}{1 + pT_1} \quad (4)$$

The first term of right hand side in Eq.(4) is a factor eliminating the characteristics of TS and the second term is a factor newly producing the characteristics of a mock ship. Therefore the total transfer function of TS is cascade combination of  $Y_c$  with  $Y_{F0}$ , so that  $Y_c \cdot Y_{F0}$  is equal to  $Y_1$  which is the transfer function of a mock ship. This  $Y_c$  is a transfer function of the computer, so that computer programs carry out the operation of following differential equation

$$T_1 \frac{d\delta_c}{dt} + \delta_c = \frac{K_1}{K_{F0}} (\delta_w + T_{F0} \frac{d\delta_w}{dt}) \quad (5)$$

where  $\delta_w$  is a rudder angle of steering wheel (computer input) and  $\delta_c$  is a rudder angle ordered to steering gear by computer (computer output). As a matter of fact, the steering quality indices  $K_1, T_1, K_{F0}, T_{F0}$  vary with ship speed, then Eq.(5) is rewritten with non-dimensional steering quality indices as

$$T'_1 \frac{d\delta_c}{dt} + \frac{V}{L} \delta_c = \frac{K'_1}{K'_{F0}} \frac{L_F}{L_1} (\frac{V}{L_1} \delta_w + T'_{F0} \frac{L_F}{L_1} \frac{d\delta_w}{dt}) \quad (6)$$

where  $L_F$  and  $L_1$  are ship length of TS and the mock ship respectively and ship speed  $V$  is treated as the same for two ships.

In this OPEN SYSTEM accuracy for the steering quality indices  $K'_{F0}$ ,  $T'_{F0}$  of TS is necessary. But in the case where estimated figures  $K'_F$ ,  $T'_F$  are different from true characteristics  $K'_{F0}$ ,  $T'_{F0}$ , the transfer function of total ship system is

$$\begin{aligned} Y(p) = \frac{\mathcal{L}[\dot{\psi}(t)]}{\mathcal{L}[\delta_w(t)]} &= \left( \frac{1+pT_F}{K_F} \frac{K_I}{1+pT_I} \right) \frac{K_{F0}}{1+pT_{F0}} \frac{1}{1+pT_E} \\ &= \left( \frac{K_{F0}}{K_F} \frac{1+pT_F}{1+pT_{F0}} \right) \frac{K_I}{1+pT_I} \frac{1}{1+pT_E} \end{aligned} \quad (7)$$

This transfer function leads a different second order equation of ship motion from a intended mock ship.

YAW CLOSED SYSTEM. This system requires a real time simulation of mock ship's yaw motion responded to steering wheel movement. The motion of TS is controlled automatically by computer following the target of simulated motion. The target motion may be yaw rate or yaw angle.

In the case of yaw rate target, transfer function of ship total system is

$$\begin{aligned} Y_{\dot{\psi}}(p) = \frac{\mathcal{L}[\dot{\psi}(t)]}{\mathcal{L}[\delta_w(t)]} &= \frac{K_I}{1+pT_I} \frac{1}{1+pT_E} \frac{1+pT_E}{1 + \frac{1}{C_2 K_{F0}} + p \frac{T_{F0} + T_E}{C_2 K_{F0}} + p^2 \frac{T_{F0} T_E}{C_2 K_{F0}}} \\ &= \frac{K_I}{1+pT_I} \frac{1}{1+pT_E} \begin{cases} 1 & : p \rightarrow 0, C_2 K_{F0} \gg 1 \\ \frac{C_2 K_{F0}}{p T_{F0}} & : p \rightarrow \infty \end{cases} \end{aligned} \quad (8)$$

where  $C_2$  is a proportional factor for yaw rate errors of auto-pilot and  $T_E$  is a time constant of steering gear.

In case of yaw angle target, transfer function of ship total system is

$$\begin{aligned} Y_{\psi}(p) = \frac{\mathcal{L}[\psi(t)]}{\mathcal{L}[\delta_w(t)]} &= \frac{K_I}{1+pT_I} \frac{1}{1+pT_E} \frac{1+pT_E}{1+p \frac{1}{C_1 K_{F0}} + p^2 \frac{T_{F0} + T_E}{C_1 K_{F0}} + p^3 \frac{T_{F0} T_E}{C_1 K_{F0}}} \\ &= \frac{K_I}{1+pT_I} \frac{1}{1+pT_E} \begin{cases} 1 & : p \rightarrow 0 \\ \frac{C_1 K_{F0}}{p^2 T_{F0}} & : p \rightarrow \infty \end{cases} \end{aligned} \quad (9)$$

where  $C_1$  is a proportional factor for yaw angle error of auto-pilot.

In each cases there is phase lag of response on TS. These phase lag do not lead the ship motion correctly to intended one especially at high frequency range. In selection of these two target systems, the

yaw rate target system is preferable due to be less phase lag at high frequency range. But in this paper the yaw angle target system is adopted because of absence of yaw rate pick-up device.

YAW MODIFIED SYSTEM. Before-mentioned both systems have weak points; for OPEN SYSTEM, it is disturbance by wind and wave, for CLOSED SYSTEM, phase lag at high frequency range. Overcoming these defects and making the best use of advantage of two systems, YAW MODIFIED SYSTEM which combines YAW CLOSED SYSTEM with YAW OPEN SYSTEM is introduced; OPEN SYSTEM orders rudder deflection producing a mock ship yaw motion and on the other hand CLOSED SYSTEM corrects the error of yaw motion due to OPEN SYSTEM. When ship motion is nearly equal to intended mock ship motion, CLOSED SYSTEM part is almost useless and orders small rudder deflection to correct the course in this YAW MODIFIED SYSTEM. Transfer function of this system

$$\begin{aligned}
 Y_{\psi}(p) &= \frac{\mathcal{L}[\dot{\psi}(t)]}{\mathcal{L}[\delta_w(t)]} = \frac{K_I}{1+pT_I} \cdot \frac{1}{1+pT_E} \cdot \frac{C_I + p \frac{1}{K_F} (1+pT_F)}{\frac{C_I}{1+pT_E} + p \frac{1}{K_{F0}} (1+pT_{F0})} \\
 &= \frac{K_I}{1+pT_I} \cdot \frac{1}{1+pT_E} \begin{cases} 1 & : p \rightarrow 0 \\ \frac{T_F K_{F0}}{K_F T_{F0}} & : p \rightarrow \infty \end{cases} \quad (10)
 \end{aligned}$$

Comparing Eq.(10) with Eq.(9), it is clear that MODIFIED SYSTEM is superior to CLOSED SYSTEM at high frequency range.

#### EXPERIMENTS OF CHANGING YAW MOTION

In order to find the limit of performance of the device and transduce system, maneuvering experiments following sequent right/left turning motion with small rudder deflection, must be carried out. Because ship handling operation by this device aims mainly to the training of alter course/course keeping, and turning motion with large rudder deflection is performed easily even under the disturbance by wind and wave. Then frequency response maneuvering tests or zig-zag maneuvering tests are considered. In this paper well known zig-zag maneuvering tests are chosen and especially 5° Z test are conducted for the limit-study.

The intended mock ships are common cargo ships of 1,000—10,000GT : ship length Lpp are 60—150m, steering quality indices K', T' are both 1—2 (Table 1) and Fig.5 shows a block diagram of conducted experiments. Most of testing conditions are sea state 4 which are not ideal test condition for experiments. Ship speed in experiments set about 9 knots of stand by engine speed, 250rpm and CPP blades angle 20 deg.

#### EXPERIMENTAL RESULTS OF CHANGING SHIP YAW MOTION

Valuation of yaw motion changed by transducer must be made how approximately the device can imitate the intended mock ship motion and how much figures input data take to realize intended motion. In this paper the valuation of yaw motion is based on K-T analysis which is proposed by Nomoto and is widely accepted.

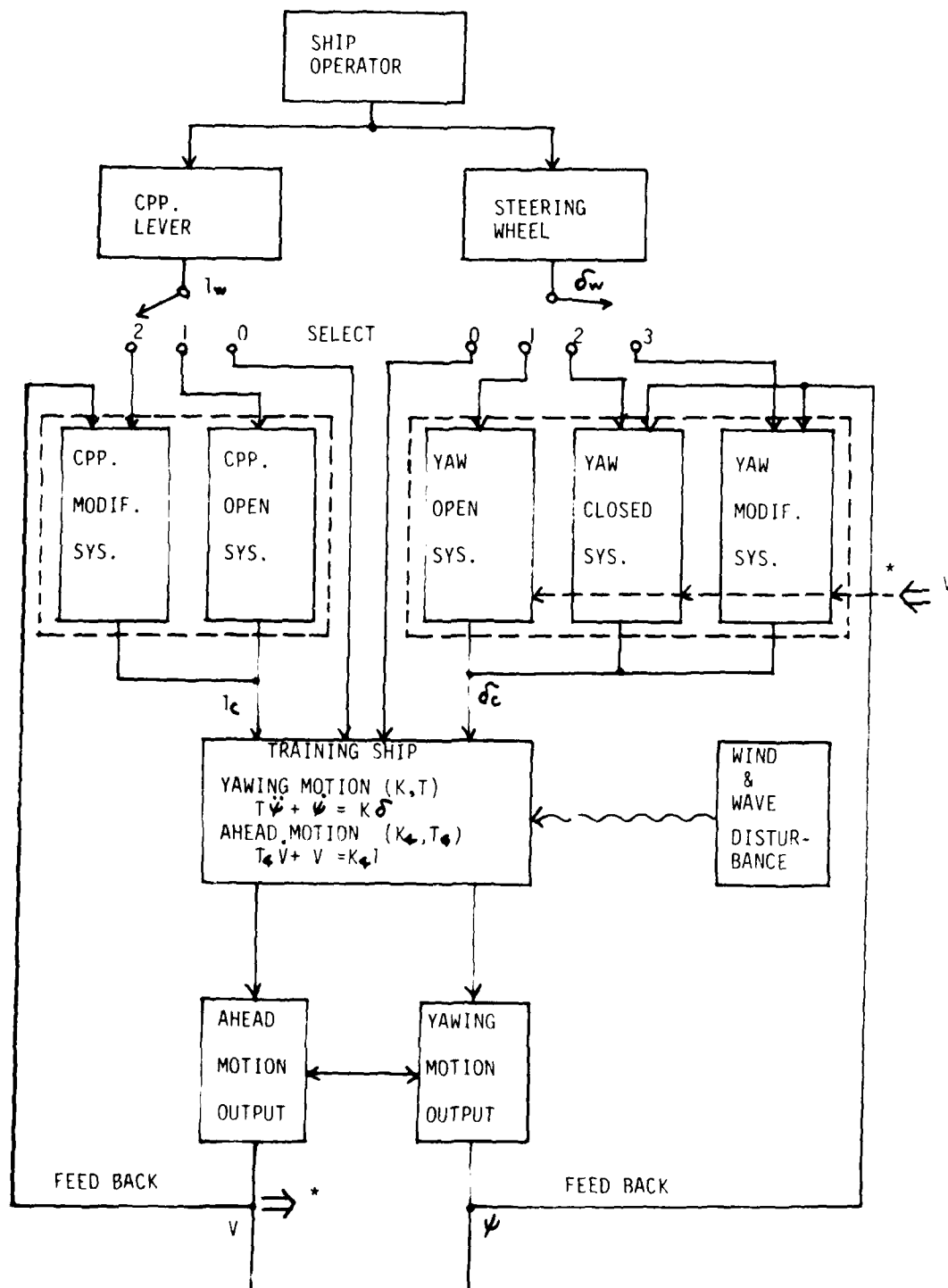


Figure 5. Block Diagram of Tansduce Tests

Original steering quality indices of TS affect the mock ship motion through the assumed indices in OPEN SYSTEM and through response lag to target motion in CLOSED/MODIFIED SYSTEM. The analysed K,T results of Z tests on TS in Fig.6 show that TS is a stable, quick turn and quick response ship. But her characteristics vary largely according to intensity of motion and have non-linearity which is an important characteristic affecting on mock ship motion with large motion changing especially for OPEN SYSTEM.

Table 2. Steering Quality Indices of Model Ships

MODEL	LENGTH (CM)	$K'_1$	$T'_1$	$K'_1 T'_1$	$K'_1 T'_1$
A-1	50	1.41	2.0	2.82	1.0
A-2	50	1.41	1.5	2.12	1.0
A-3	50	1.41	1.0	1.41	1.0
B-1	100	1.41	1.0	1.41	1.0
B-2	100	1.41	1.5	2.12	1.0
B-3	100	1.41	1.0	1.41	1.0
B-4	100	1.00	1.0	1.00	1.0
B-5	100	2.00	2.0	4.00	4.0
C-1	150	1.41	1.0	1.41	1.0
C-2	150	1.41	1.5	2.12	1.0
C-3	150	1.41	1.0	1.41	1.0

SHIP SPEED  $V=9Kt$

$K'_1, T'_1$ : NON-DIMENSIONAL STEERING QUALITY  
INDICES OF MOCK SHIP

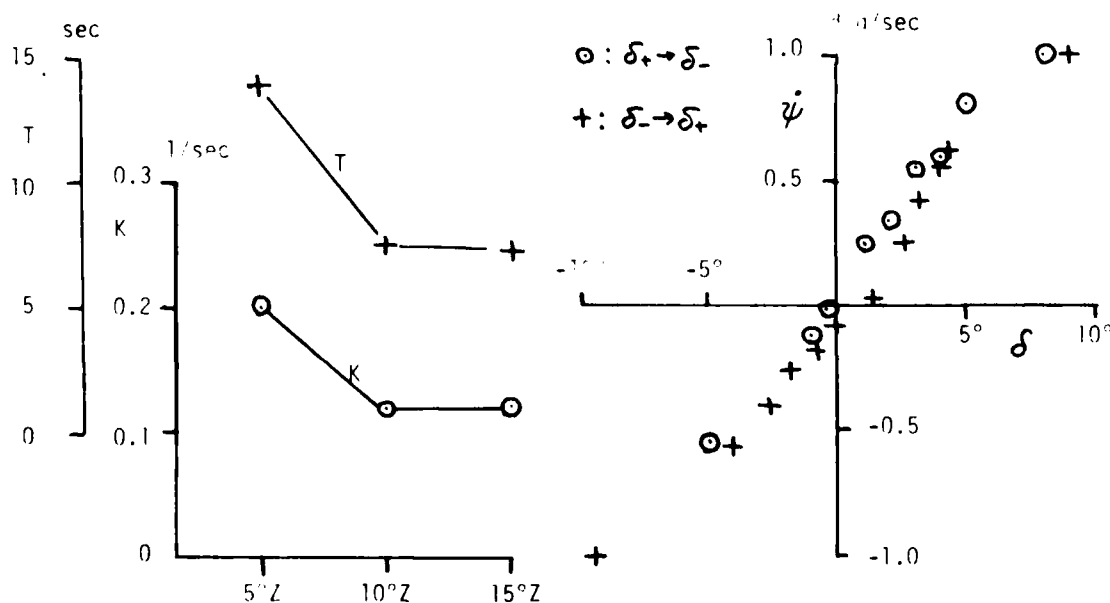


Figure 6. Z Test and Spiral Test Results of TS FUKAE-MARU ( $V=9$  knots)



Experimental Results on OPEN SYSTEM. An example of time histories on this transduce system is shown in Fig.7. In this example the length of mock ship is 100m, steering quality indices intended are  $K_I=0.063$  (1/sec) and  $T_I=44.7$ (sec), steering quality indices realized are  $K=0.21$  (1/sec) and  $T=98.0$ (sec) under the conditions, that is, ship speed of 9 knots and estimated steering quality indices of TS  $K'_F=0.102$ (sec) and  $T'_F=4.85$ (sec). Z test results of this system are shown in Fig.8 where ordinates are realized  $K, T$  and abscisas are intended  $K_I, T_I$ . Fig. 8 shows clearly the effect of estimated steering quality indices  $K_F, T_F$  of TS on realized  $K, T$ . Good estimation leads to good agreement between realized  $K, T$  and intended  $K_I, T_I$ . From the test results it is said that 5° Z tests can be carried out on mock ship of 50—100m Lpp and not on 150m Lpp.

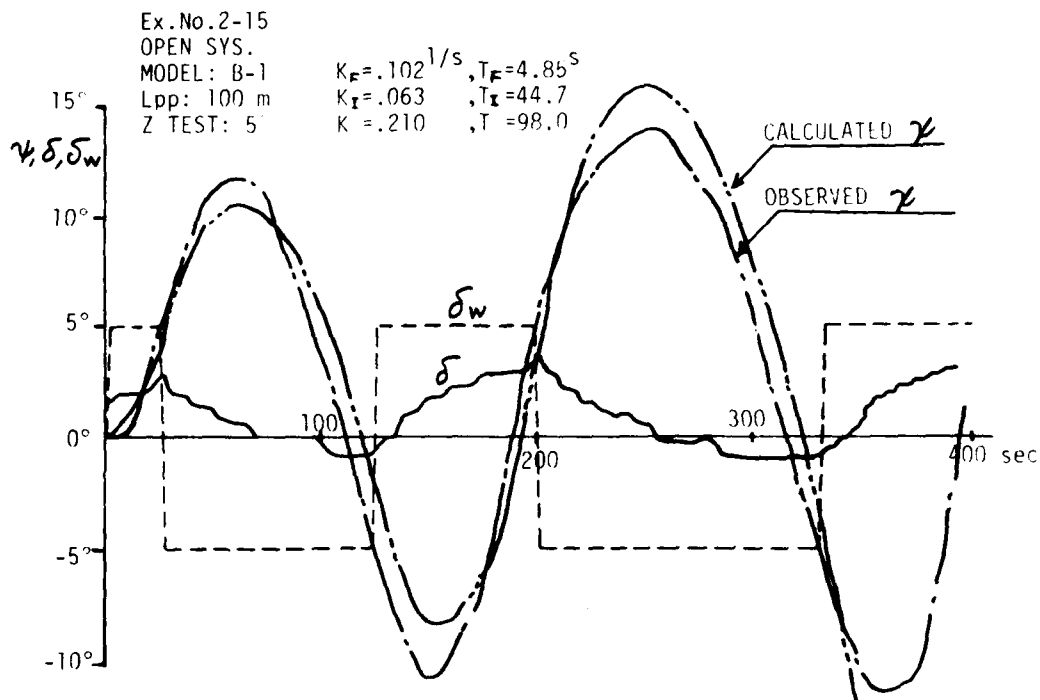


Figure 7. Time Histories of YAW OPEN SYSTEM (Lpp=100m, 5° Z Test)

Experimental Results on CLOSED SYSTEM. An example of time histories on this transduce system is shown in Fig.9. The example shows that the resultant yawing motion  $\psi$  follows target  $\psi_r$  which is calculated by using steering quality indices of intended ship  $K_I, T_I$  and steering wheel movements. Although target movement  $\psi_r$  is smooth, realized movement  $\psi$  is waved by disturbance. 5° Z test results are shown in Fig.10. In this system realized  $K$  are nearly equal to intended  $K_I$  and realized  $T$  are larger than intended  $T_I$  by about 25 sec. This shows the large effect of phase lag in the ship control system at high frequency motion.

Experimental Results on MODIFIED SYSTEM. An example of time histories of this system is shown in Fig.11. In the system, proportional

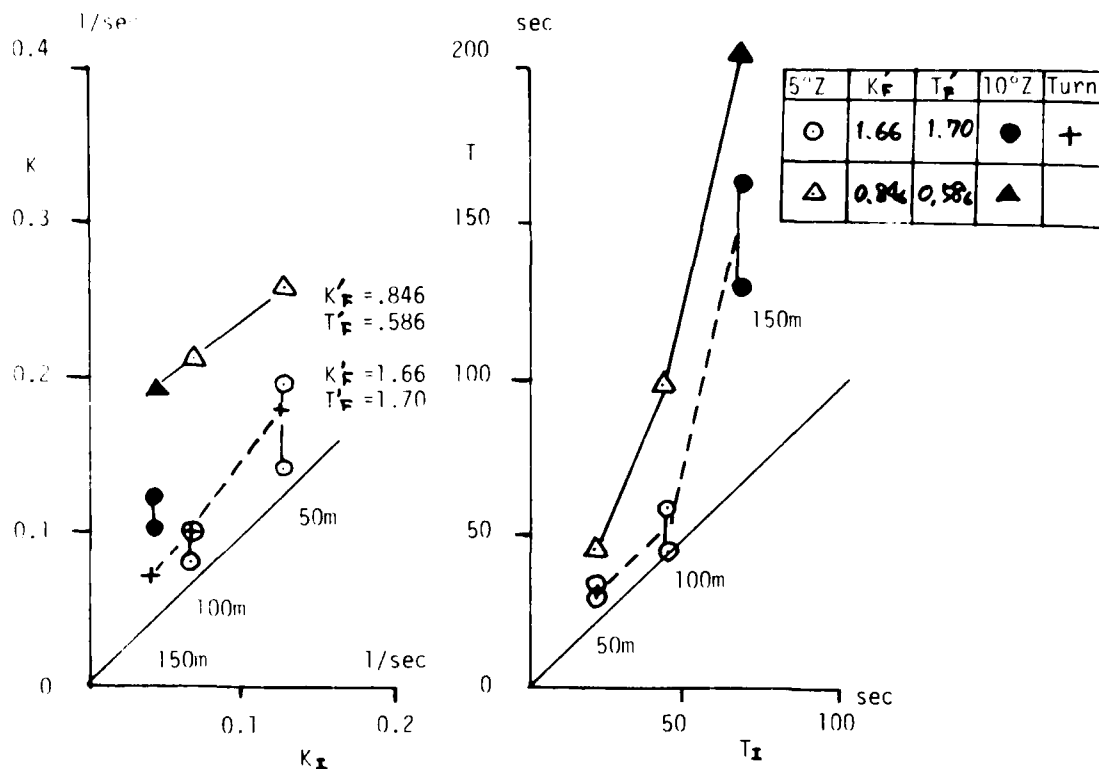


Figure 8. Effects of  $K_F, T_F$  on Z Test Results of YAW OPEN SYSTEM

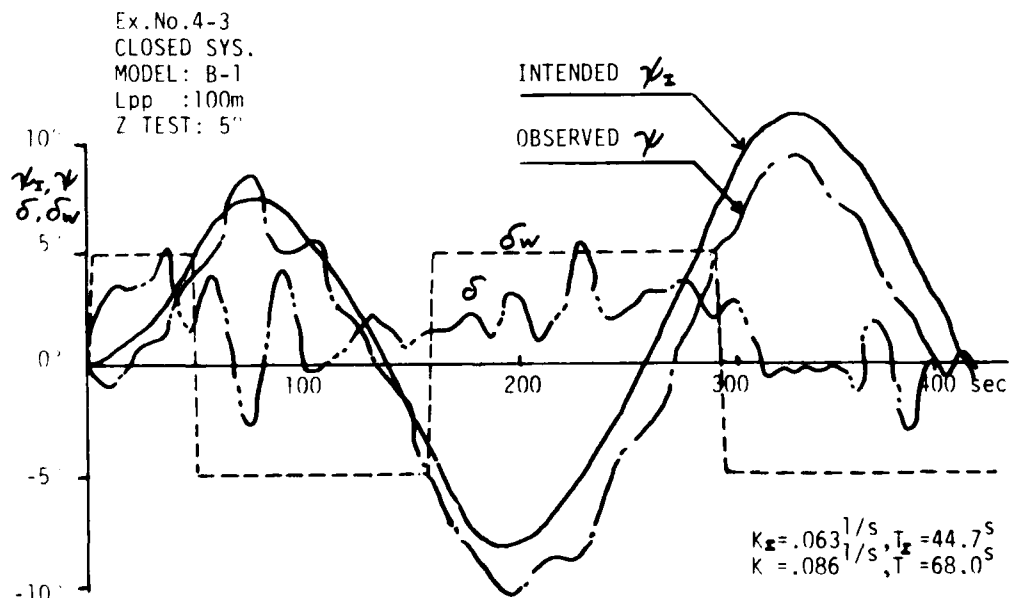


Figure 9. Time Histories of YAW CLOSED SYSTEM (Lpp=100m, 5°Z Test)

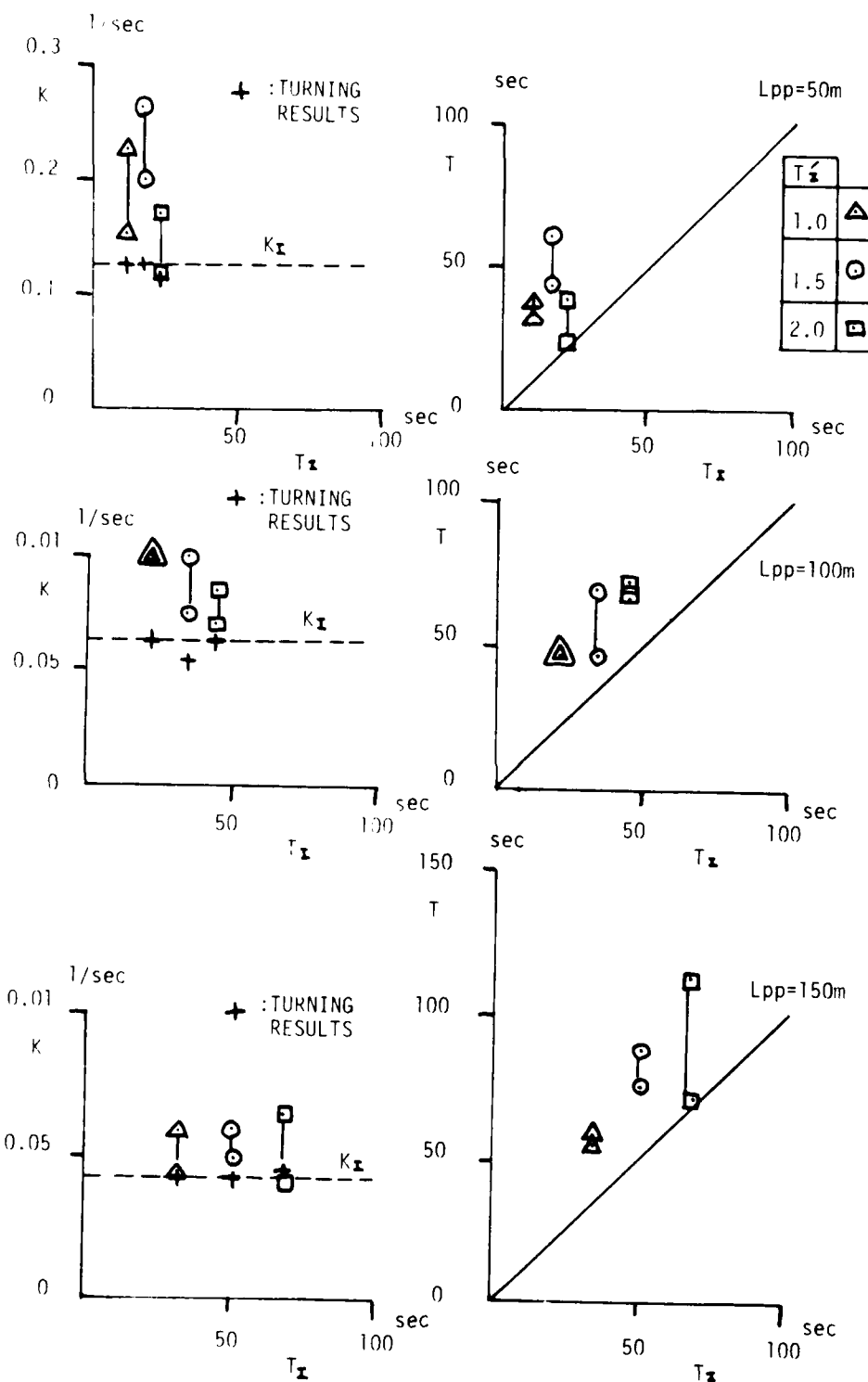


Figure 10. Effects of  $T'_x$  Variation on 5° Z Test Results of YAW CLOSED SYSTEM

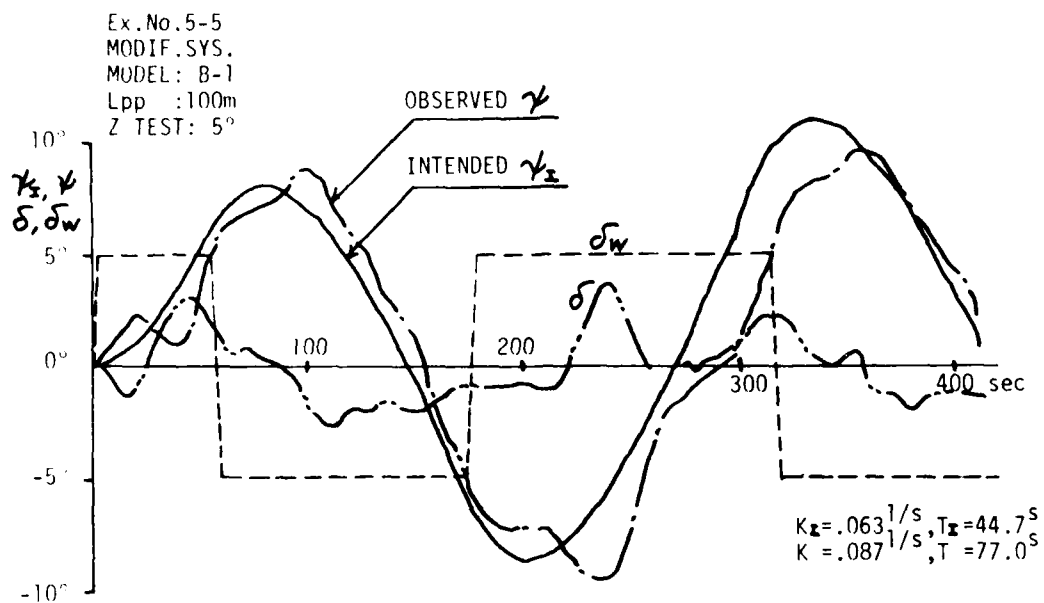


Figure 11. Time Histories of YAW MODIFIED SYSTEM (Lpp=100m, 5° Z Test)

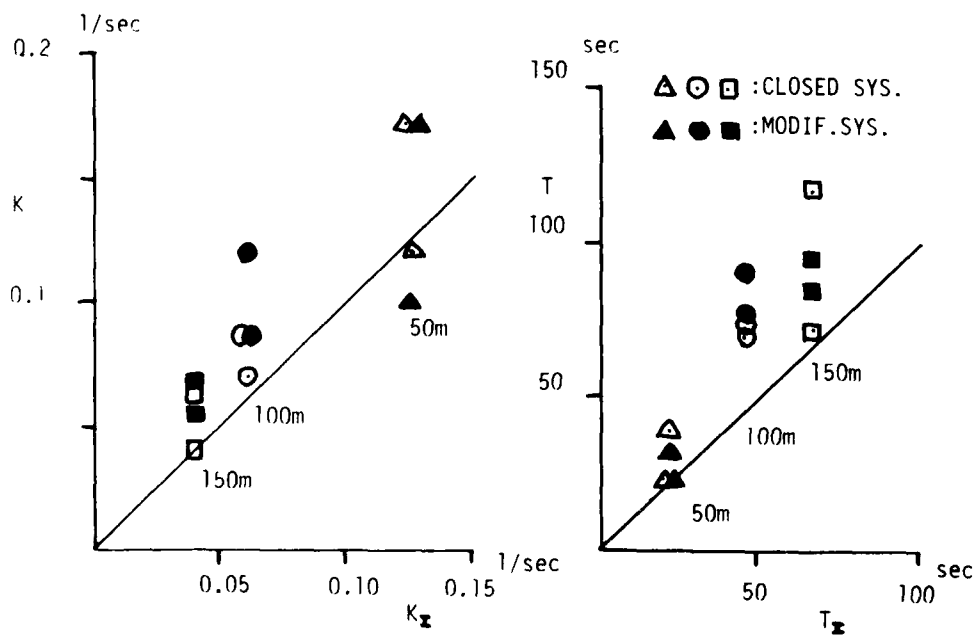


Figure 12. Comparison of 5° Z Test results between CLOSED SYSTEM and MODIFIED SYSTEM ( $K'_z = 1.41$ ,  $T'_z = 2.0$ )

factor  $C_1$  is not necessary to be larger than in CLOSED SYSTEM, therefore the factor is adopted to be 1.0 rather than 2.0 in CLOSED SYSTEM. In the experiments the effectiveness of MODIFIED SYSTEM are not shown because of test conditions of sea state 4. The results of MODIFIED SYSTEM are compared with the results of CLOSED SYSTEM in Fig.12.

#### LIMIT OF CHANGING YAW MOTION

There are limits of changing yaw motion on each transduce system because 5° Z test can not be carried out on 150m Lpp mock ship by OPEN SYSTEM and because the motion of the small mock ship can not be realized by CLOSED SYSTEM concerning phase lag of TS.

Limit of OPEN SYSTEM. In this system rudder deflection in transduce mode are usually small, so that the effect of disturbance from wind and wave may induce larger motion than the rudder deflection in the transduce mode. Sometimes it is difficult to carry out 5° Z test. From the test results the enable limit of 5° Z test is shown in Fig.13. This limit may be deduced by reform of minimum level of effective rudder deflection and rate of rudder deflection.

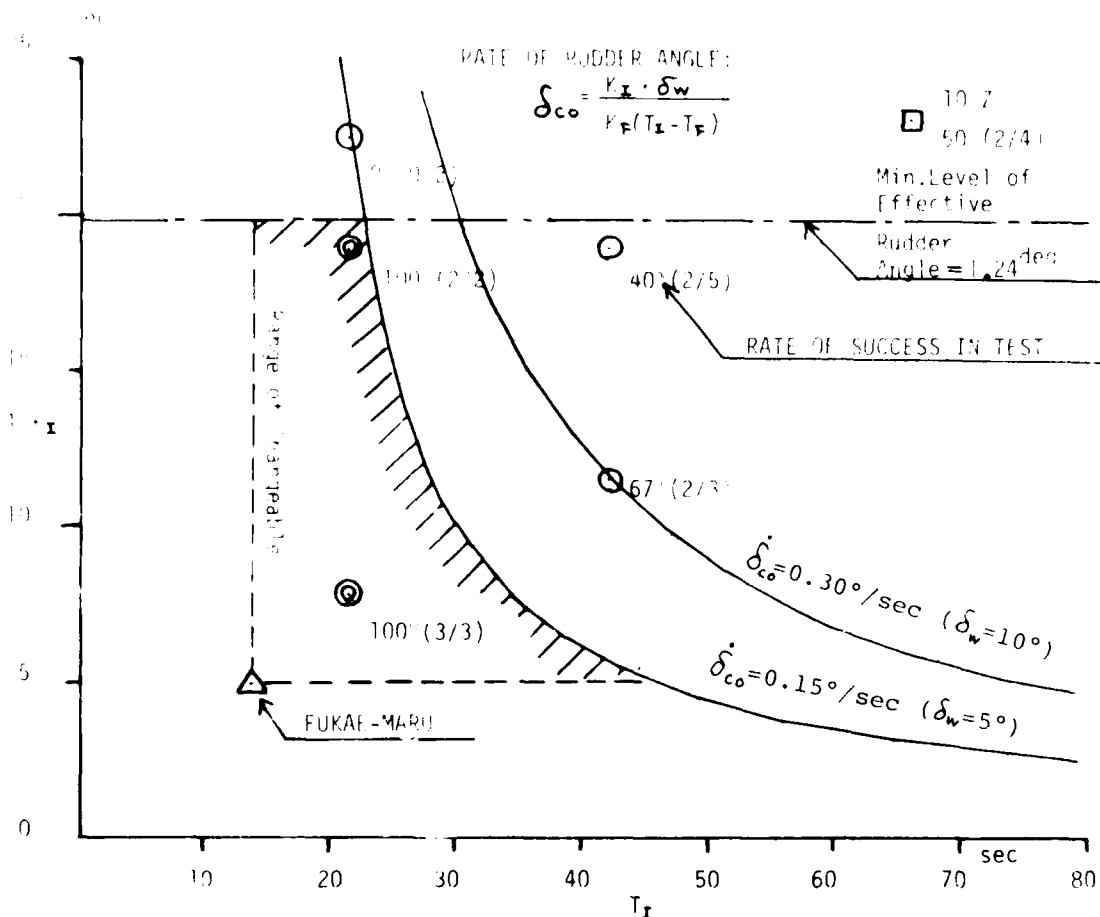


Figure 13. Transduce Criteria on YAW OPEN SYSTEM (5° Z Test)

Limit of CLOSED SYSTEM. Almost all mock ships except quicker response and turn ship than TS can carry out 5° Z test by CLOSED SYSTEM. Fig.14 illustrates correlation between realized steering quality indices  $K_r, T_r$  and input steering quality indices  $K_i, T_i$  as the result of simulation of this CLOSED SYSTEM. It is said from the simulation results that the quicker response motion which time constant is less than about 10 sec is not realized by this system. On the other hand the 5° Z experiment (see Fig.12) shows that minimum value of realized time constant may be about 25 sec on this system. Further in course keeping steering motion, it is important problem for CLOSED SYSTEM that ship's movement does not respond adequately to rudder movement at the high frequency range.

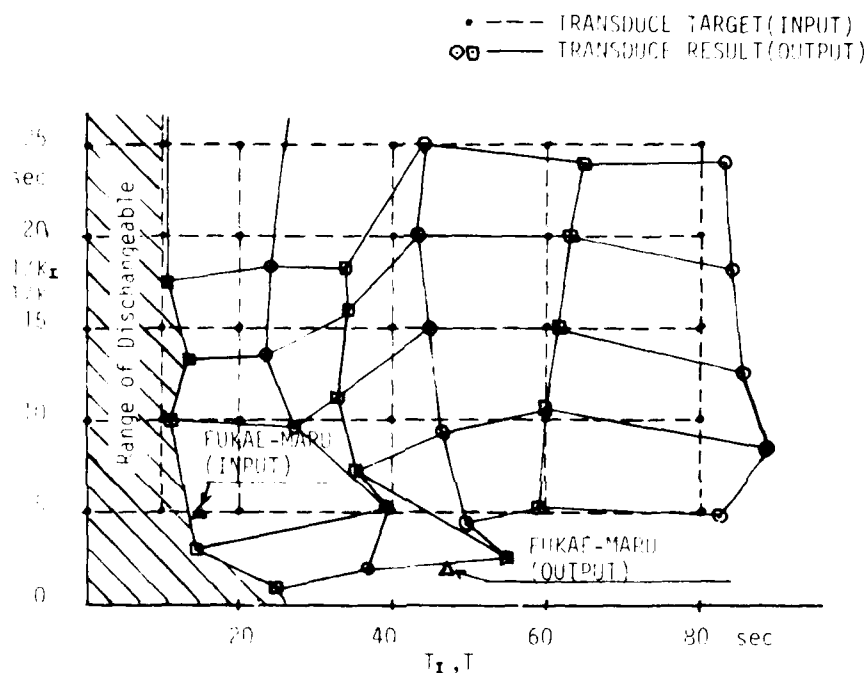


Figure 14. Transduce Criteria on YAW CLOSED SYSTEM (5° Z Test)

Limit of MODIFIED SYSTEM. There is not notable difference in test results between MODIFIED SYSTEM and CLOSED SYSTEM. Therefore limit of changing yaw motion may be the same. But in course keeping motion this system is better than CLOSED SYSTEM because of phase compensation.

#### MATHEMATICAL MODEL OF AHEAD MOTION FOR TRANSDUCE

Controlling ship speed with propeller in ship handling, main operations are acceleration and deceleration in ahead motion. Especially it is important for ship operator to decelerate ahead motion avoiding collision to other ship or wharf. Only accelerated and decelerated ahead motion is considered in this paper. Mathematical model for these ahead motion controlled by propeller are published in recent

Figure 4.2 shows the setpoint and the estimated low frequency position during a setpoint change of approximately 50 meters sideways. The curve shows a constant translation speed with a smooth acceleration and retardation.

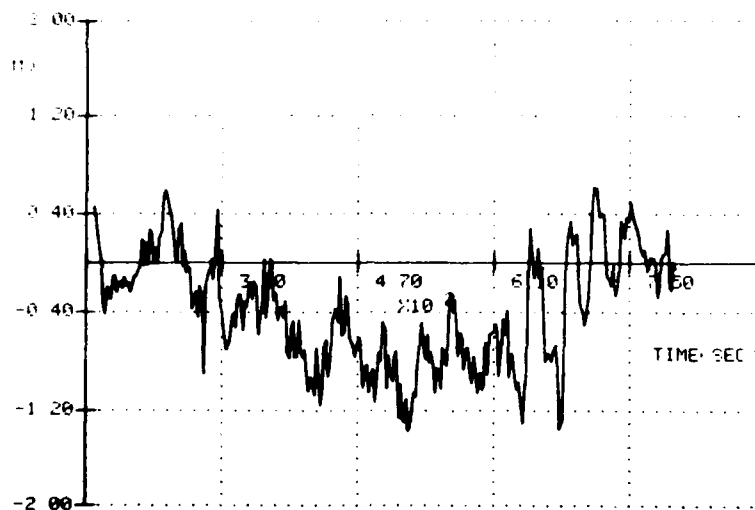


Figure 4.3

In figure 4.3 the estimation error or innovation process for the Y-direction is plotted. It will normally indicate the measurement noise. During the maneuver, however, there can in addition be seen a growth to a significant negative value. The reason is most likely to be a little difference between the model computed thrust and the obtained thrust while moving.

The heading stabilization during this maneuver is shown in figure 4.4. The maximum deviation is about 0.8 degrees. The one curve shows the heading estimate and the other the measurement. Notice the resolution of the gyro compass reading.

#### 4.2 M/V Capalonga

Registered: During diving operation at the Brent oil field in the North Sea.

Vessel: Diving support and fire fighting, displacement 5700 tons

Pos.ref.syst: Taut wire

Conditions: wind: 25 kt  
current: 1.0 kt  
waves: ca 8 feet  
depth: 120 m

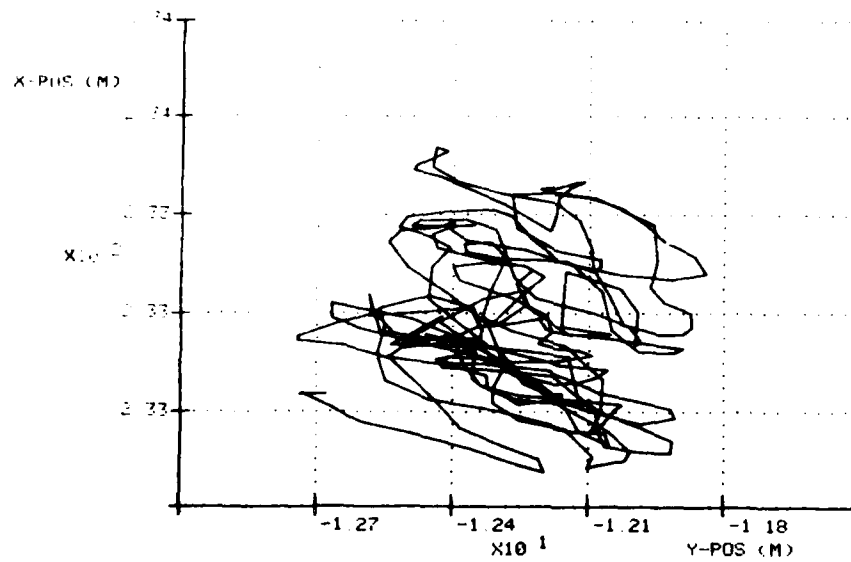


Figure 4.1

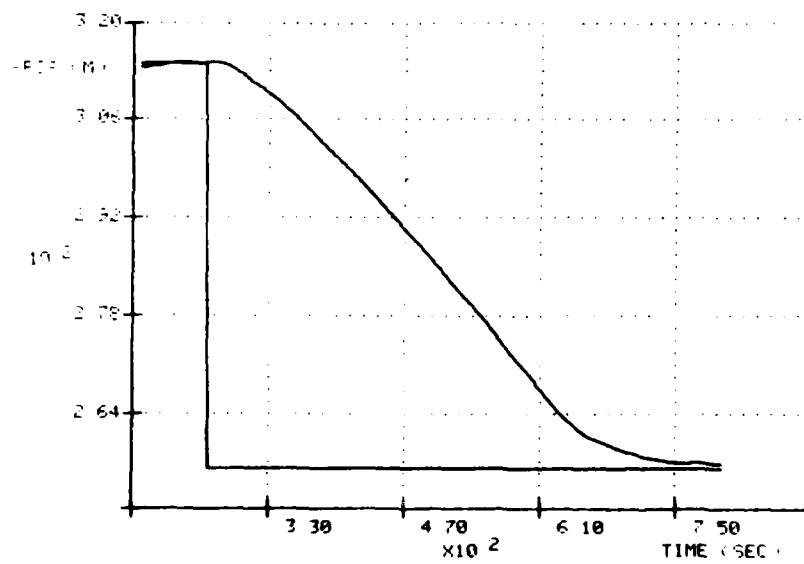


Figure 4.2



3.2.2 Optimal control feedback and thruster allocation. From the model of vessel behaviour and environmental states one can now extract the information necessary to compute a proper set of forces and moment. This is done by exactly compensating the wind forces (feed forward) and exactly compensating the computed current forces. Thereafter the estimated values of vessel's position, heading and speeds are used to stabilize movements and keep the position as close as possible to the wanted value (setpoint).

The selection of feedback variables is done with proper consideration of the desired bandwidth of the control system, and at the same time one must assure that the system is at least critically damped.

The computed force- and moment demand from the control feedback routine has to be converted into setpoints for propeller rpm, pitch and azimuth angle. Since there always is an upper limit for rpm, pitch angle and possibly also azimuth, and there often is an upper limit for the total power consumption onboard, such a module will be complicated. Depending on the thruster configuration one can have so many control signals available that these are not uniquely determined from the force- and moment demand. To solve the problem the thruster control is regarded as an optimization task where the most powersaving combination of setpoints is computed.

During this operation the interaction between current and thrusters, and to some extent also the interaction between thrust and hull is taken care of and compensated for. This is to assure similar behaviour irrespective of current speed and direction relative to vessel.

It should now be clear that such an estimator-based control system needs a verification of the parameters used in the different models. During sea trials the parameters will be tuned until the whole system reacts properly.

#### 4. SYSTEM PERFORMANCE

In the following the system performance is presented by a number of figures. These figures are based on data registrations on board several vessels, some of them showing the vessel in normal operation using dynamic positioning. Others are recorded during the DP sea trial and tuning period.

##### 4.1 M/V GC 308

Registered: During sea trials, off Holland

Vessel: Split type barge, displacement 2200 tons

Pos.ref.syst: Artemis short range (microwave).

Conditions: wind: ca 10 kt  
current: ca 0.5 kt  
waves: zero

Figure 4.1 shows a xy-plot of the position estimates over a period of approximately 25 minutes of positioning. The maximum deviation during this period is about 60 cm. The figure shows pure control deviation due to no primary wave motion. The two axes indicate the distances in x- and y-direction from the reference transponder.

velocity in the three horizontal degrees of freedom (surge, sway and yaw), and the input forces, the estimator predicts the state vector one time step ahead.

We also realize that the measurements of position and heading will only serve as a correction for the model output by an update of the estimates through the elements in the Kalman filter gain matrix denoted K. This implies that the estimator output is the base for computation of feedback forces. Thus we avoid the problems related to the derivation of the measurement signals.

To avoid modulation of the thruster setpoints as a function of the first order wave induced motions, these oscillatory components of the vessel motions are modelled in a high frequency vessel model, in the diagram denoted as wave model. This model is simply a set of harmonic oscillators with adaptive centerfrequencies due to the fact that the vessel will oscillate with a frequency close to the wave frequency.

The following differential equation describes the high frequency model of vessel behaviour:

$$\begin{aligned}\ddot{\underline{X}}_H &= -W^2 \cdot \underline{X}_H + \underline{V}_{1H} \\ \dot{\underline{W}} &= \underline{V}_{2H}\end{aligned}$$

where:  $\underline{X}_H$  - high frequency state vector (wave induced component)

$W$  - angular frequency matrix of high frequency motion

$\underline{w}$  - angular frequency vector

$\underline{V}_{1H}$

$\underline{V}_{2H}$  - white process noise with zero mean

$\dot{\phantom{x}}$  - time derivation

The model is forced to follow the measurements, and the model output is added to the low frequency estimate before comparing this with the measurements. By this technique we obtain the correct figures of the innovation process - which is the difference between measured and predicted position - for proper state corrections.

The integral feedback of the PID-controller is taken care of by an environmental estimator or a current model. The output from this model is a force vector representing all the stationary unknown forces acting on the vessel, plus effects from unmodelled or uncorrectly modelled phenomena. As can be seen from the block diagram, the current is updated from the innovation process, which means that a small part of the difference between vessel and model behaviour gives rise to a change in the estimated current. The current estimate will mainly be the sum of the real sea current and mean wave drift forces. Thus we have established an equivalent current in magnitude and direction, and because the model is supplied with information about the relationship between the resulting force and the angle of attack, we can turn the vessel with a high speed without a transient drift-off in position.

We also realize that a total blocking of the position measurements for a period, no longer will cause a breakdown of the control function. The control feedback forces are based on estimates and the only effect will be a slow drift-off in position as the accuracy of the estimates decrease due to no corrections from the measurements.

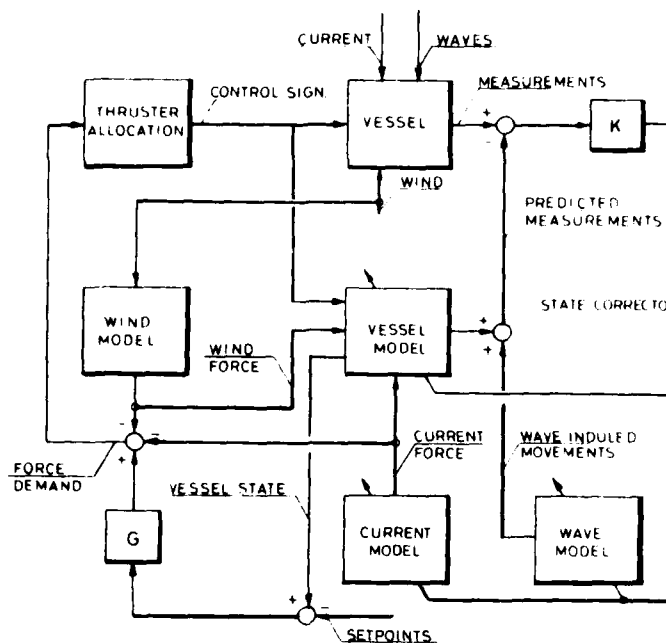


Figure 3.2

3.2.1 Vessel estimator. From the earlier mentioned problems related to a conventional PID-concept, we realize that a way of improving the DP-system performance is through better knowledge of vessel dynamics. This information is implemented in the system by a so-called vessel estimator, which is a mathematical model of the vessel behaviour, based on Newton's laws. Inputs to this model are all the known forces acting on the vessel - wind forces, current and wave forces and thruster forces.

This low frequency vessel model is described by the following vector differential equation:

$$M \ddot{\underline{X}}_L = -D \cdot (\dot{\underline{X}}_L - \underline{U}_c) \cdot |\dot{\underline{X}}_L - \underline{U}_c| + \underline{F}_w + \underline{F}_t + \underline{V}_L$$

where:  $\underline{X}_L$  - low frequency state vector  
 $\underline{U}_c$  - current speed vector  
 $M$  - total mass and moment of inertia matrix  
 $D$  - drag coefficient matrix  
 $\underline{F}_w$  - wind force and moment vector  
 $\underline{F}_t$  - thrust force and moment vector  
 $\dot{\phantom{x}}$  - time derivation  
 $\underline{V}_L$  - white process noise with zero mean

Based on the current system state vector, which consists of the position and

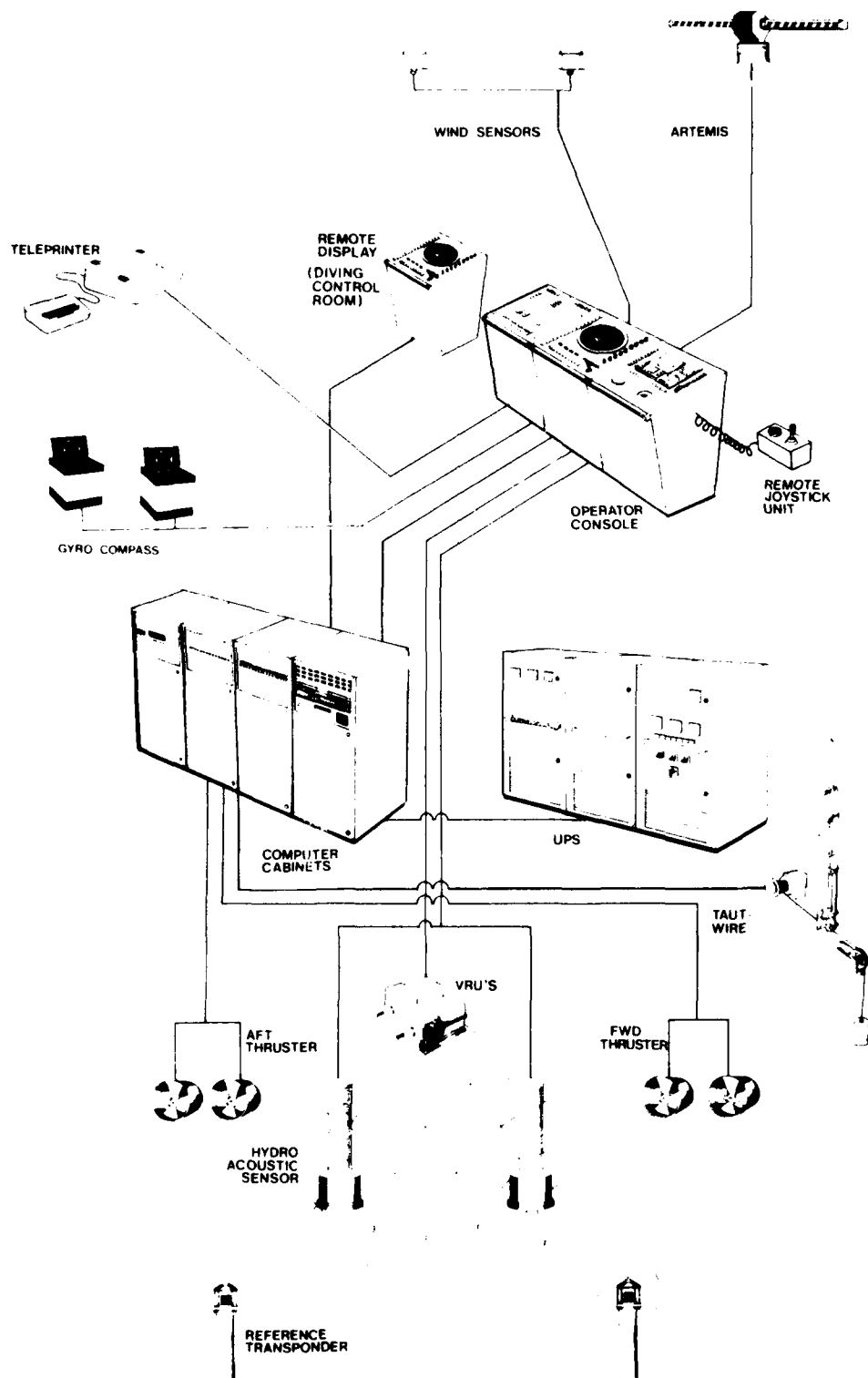


Figure 3.1

The vessel response due to 1. order wave forces will introduce an oscillatory component in the measurements. (This effect is not related to the actual reference system). The component has to be removed from the measurement, because it is impossible to compensate for these forces. A so-called notch-filter has been used for this purpose, but it seems to be difficult to suppress the oscillations effectively without removing necessary information from the measurement. The consequence is that the setpoint signals to the thrusters will be modulated with a frequency close to the dominating wave frequency, and the result will be more thruster wear and higher power consumption.

The integral feedback from a PID-controller shall compensate for stationary unknown forces acting on the vessel. These will be current forces and mean wave drift forces because they are normally not measured. This integral contribution needs relatively long time to stabilize, and heading changes have to be done at a very slow rate to prevent transient deviations in position.

In view of the above mentioned it is obvious that the system performance can be improved, especially for the situations described. We also see a growing demand for safety, flexibility and easy operation, which is taken into account when developing the system.

### 3. SYSTEM DESCRIPTION

#### 3.1 System Components

The components of a dynamic positioning system will roughly spoken be the same independent of the chosen control strategy. Figure 3.1 shows a system where the most important components are duplicated.

The operator's console together with a printer are placed in the wheelhouse. These give the operator total control of the system via buttons/lamps, a tactic display and printed messages.

The computers are supplied with stabilized power from UPS's (Uninterruptible Power Supply).

System inputs come from:

- wind sensor, wind speed and direction
- VRU, vertical reference unit
- gyro compass, heading reference
- different position reference systems:
  - Super short baseline hydroacoustic systems
  - Microwave surface reference systems
  - Radionavigation systems
  - Taut wire systems
  - Inertial navigation systems

System outputs are control signals to thrusters/propellers: pitch, rpm, azimuth.

#### 3.2 Control System Concept

Figure 3.2 shows a block scheme of the control system strategy including the Kalman filter.

## MODERN CONTROL THEORY FOR DYNAMIC POSITIONING OF VESSELS

by Olav D. Ropstad  
A/S KONGSBERG VAPENFABRIKK  
KONGSBERG, NORWAY

### ABSTRACT

The present range of ALBATROSS dynamic positioning systems from A/S KONGSBERG VAPENFABRIKK is based on the use of modern control theory and Kalman filtering, in order to give smooth optimal control to offshore work vessels using a variety of measurement systems.

The control system principles are presented in the paper together with the system performance on board several vessels using different measurements systems.

The paper also deals with an extension to the system providing mooring assisted DP. This combination system has a great potential for providing stable positioning in deep water as well as under severe weather conditions. The anchor parameters are estimated on-line to avoid complex and costly measurement techniques.

### 1. INTRODUCTION

The term dynamic positioning (DP) may be defined as: "The technique of maintaining the position and heading of a floating vessel by means of active thrust controlled by a computer".

During the last decade the field of operation for dynamic positioning systems has developed rapidly. It has often come up to be the best solution and for some applications the only one, especially in offshore oil field operations, where mooring is unpractical or prohibited due to underwater pipes and installations. The demand for accuracy, safety and flexibility is great when tasks as diving support, fire fighting and drilling are to be carried out. The experiences up to now show some basic problems related to earlier DP-systems. Based on these facts a new generation of DP-systems was developed, using optimal control theory and Kalman filtering.

### 2. WHY THE NEED FOR A NEW GENERATION?

Earlier generations of DP-systems have been based on conventional PID-controllers (Proportional + Integral + Derivative feedback). This means that the control feedback is computed from both the instantaneous position deviation, the integral of this deviation over time, and the change of deviation (speed). This concept has showed up some serious handicaps and the total availability has for some applications been insufficient.

Due to the demand for accuracy, the most commonly used technique for measuring the position is based on hydroacoustics. The great disadvantage with these position reference systems are the sensitivity to acoustic noise and air bubbles in the signal transmission line. Blocking of measurements in 20-40% of operation time may occur. The blocking may be fatal because a PID-controller will not function during the period without position reference. In addition the noisy signals create a big problem. Derivation of the signals is necessary to get a figure of the speed, which is used to compute a proper derivative feedback force for stabilization of the vessel.

- (2) Kawasaki Aircraft Mfg Division, "Variable Stability Airplane", KAWASAKI Technical Review, No.65, Dec.1977
- (3) S. Matora and T. Koyama, "On an Improvement of the Maneuverability of Ships by means of Automatic Steering", J. of the Society of Naval Architects of Japan, No.116, Dec. 1964
- (4) K. Karasuno, N. Kasuya and H. Nakao, "on Availability of Yaw-Rate Wheel System in Maneuvering Ships", Review of Kobe University of Mercantile Marine, Part 2, No.24, Oct. 1976
- (5) K. Nomoto, A. Murase and H. Tatano, "Utilities of Free-running Models in Ship Maneuverability Reseaches", Part 1, Part 2, J. of the Society of Naval Architects of Japan, No.109, No.110, June, 1961, Dec. 1961
- (6) The Shipbuilding Reseach Association of Japan SR-151, "Study of Ship Control System for Maneuvering", No.247, No.265, 1976, 1977
- (7) H. Tani and M. Enokida, "A Practical Method of Analysing the Acceleration and Deceleration of Ships", J. of Japan Institute of Navigation, Vol.54, Dec. 1970

$K_4, T_4$  from experimentally observed data, following equation (16) integrated Eq.(13) by time is used.

$$T_4 [V]_0^t + \int_0^t V dt = K_4 \int_0^t l_w dt + C \quad (16)$$

where  $V$  and  $l_w$  are considered the displacements from initial values of  $V$  and  $l_w$ , because of getting reasonable analyses data.

Examples comparing analysed ship motion with observed motion are shown in Fig.16. Analyses results of  $K_{4F}, T_{4F}$  of original TS are shown in Fig.17 and the results of  $K_4, T_4$  of the mock ships in Fig.18 where  $T_{4I}$  is for the intended,  $T_4$  and  $K_4$  are for the observed and  $K_{4I}$  is constant for all experiments. Symbols  $\circ, \Delta$  are OPEN SYSTEM results and symbols  $\bullet, \blacktriangle$  are MODIFIED SYSTEM results. MODIFIED SYSTEM shows the results of  $K_4 \approx K_{4I}, T_4 \approx T_{4I}$ . On the other hand  $K_4, T_4$  obtained from observed motion by OPEN SYSTEM are not same with intended  $K_{4I}, T_{4I}$ . But ship speed control of ahead motion by the device with OPEN/MODIFIED SYSTEM is usable.

#### CONCLUSIONS

This paper deals with the outline of the performance of the device which changes 360GT training ship to larger ship in motion apparently. Mathematical models of ship motion are first order linear equations

$$T \ddot{\psi} + \dot{\psi} = K \delta \quad \text{and} \quad T_4 \dot{V} + V = K_4 l$$

and transduce systems to control the ship are OPEN SYSTEM, CLOSED SYSTEM AND MODIFIED SYSTEM.

Following conclusions are derived from experiments

- 1) YAW OPEN SYSTEM can produce certainly mock ship motion with  $K_4=0.05-0.2$  (1/sec),  $T=10-60$  (sec) at ship speed 9 knots. Mock ship motion due to this system are affected strongly by disturbance of wind and wave, so reproduction of the motion is uncertain in rough environment.
- 2) YAW CLOSED SYSTEM can produce mock ship motion with  $1/K \geq 5$  sec,  $T \geq 10$  sec. But there are some problems of response characteristics in course keeping steering.
- 3) The effect of YAW MODIFIED SYSTEM is the same as YAW CLOSED SYSTEM. But it is expected for YAW MODIFIED SYSTEM to operate well in course keeping steering.
- 4) Transition of heading angle are natural in YAW OPEN SYSTEM and waved in other two system. Causes of the waving are disturbance due to wind and wave and one degree of sensibility for heading angle in device.
- 5) CPP MODIFIED SYSTEM is better than CPP OPEN SYSTEM in reproduction.
- 6) CPP MODIFIED SYSTEM is useful in dealing with speed drop due to steering and turning.

#### REFERENCES

- (1) K. Karasuno and S. Matsuki, "Design of Device for Changing Ship's Maneuverability on Trainging Ship FUKAE-MARU", Review of Kobe University of Mercantile Marine, Part 2, No.20, Jan. 1973



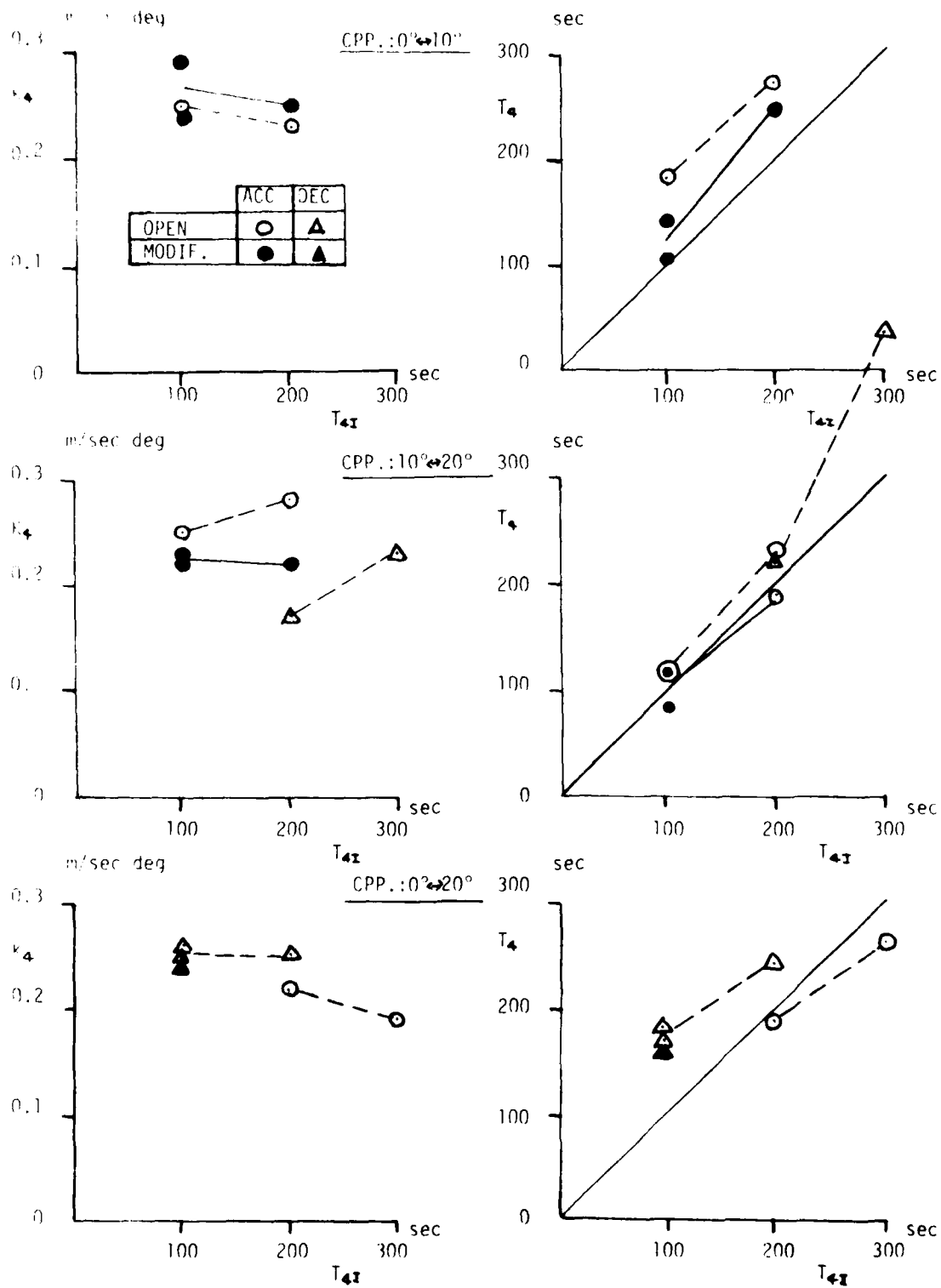


Figure 18. Comparison of Test Results between CPP OPEN SYSTEM and MODIFIED SYSTEM with Variation  $T_{4I}$

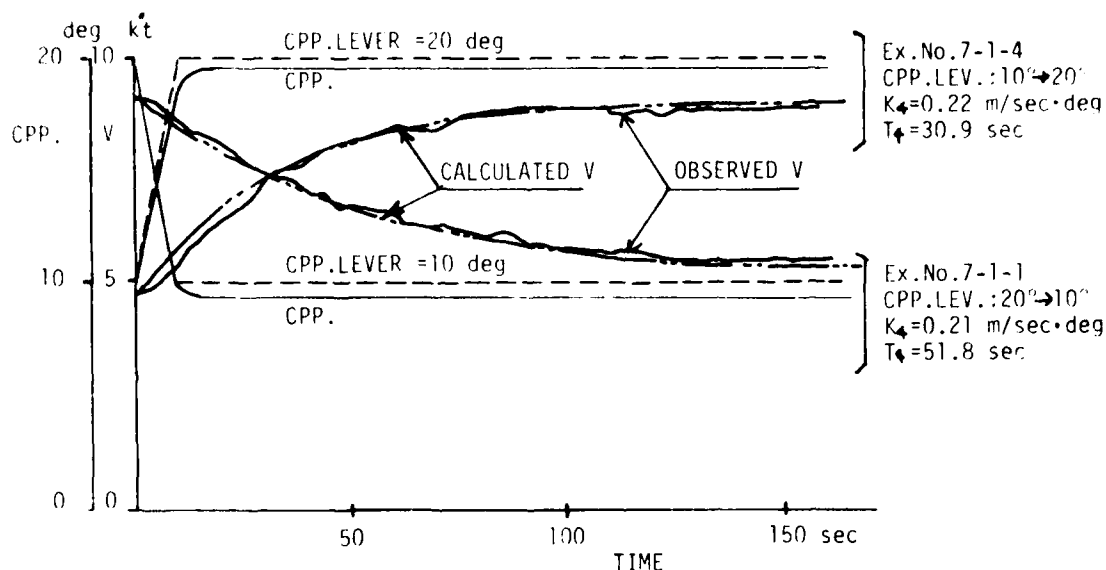


Figure 16. Time Histories of Ahead Motion on TS.FUKAE-MARU

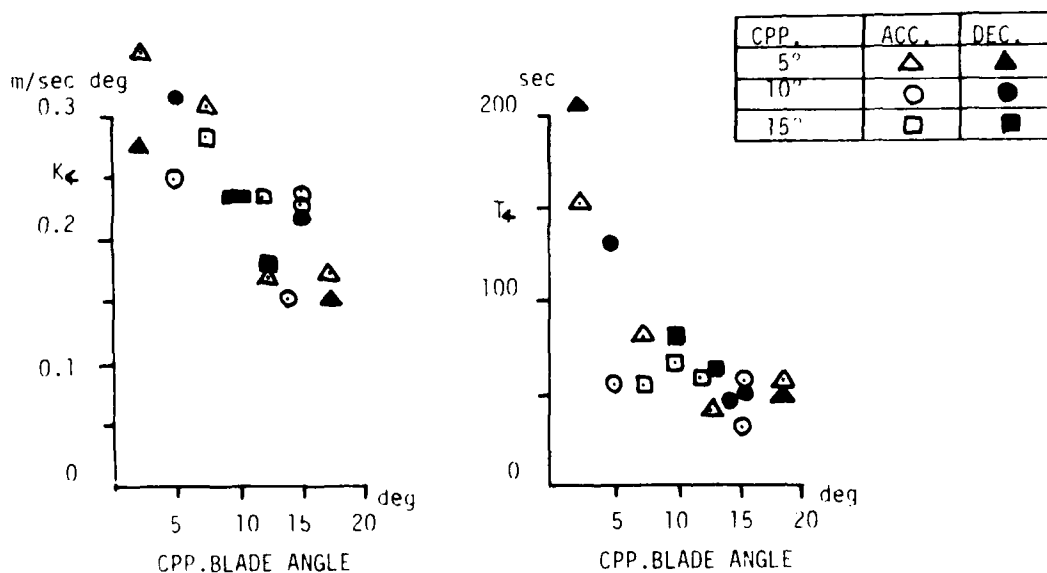


Figure 17. Test Results of Ahead Motion on TS.FUKAE-MARU

#### ANALYSIS OF SHIP AHEAD MOTION AND TEST RESULTS

(7). A general method to analyse ahead motion is not formularized yet. It is necessary to discuss what are the preferable elements describing ship ahead motion. In this paper from the point of view of control engineering it is assumed that response characteristics of ship speed  $V$  to CPP control lever blade angle  $l_w$  may be described by a gain constant  $K_4$  and a time constant  $T_4$  in Eq.(13). In analysis of

$$Y_c(p) = \frac{\mathcal{L}[l_c(t)]}{\mathcal{L}[l_w(t)]} = \frac{1 + p T_{4F}}{1 + p T_{4I}} \quad (15)$$

where input to computer is CPP control lever blade angle  $l_w$ , output from computer is ordered blade angle  $l_c$ ,  $T_{4F}$  is estimated time constant of ahead motion of TS and  $T_{4I}$  is time constant of ahead motion of intended mock ship.

**CPP MODIFIED SYSTEM.** OPEN SYSTEM can not realize speed drop due to steering and turning. It can be realized by CLOSED SYSTEM or MODIFIED SYSTEM like yaw motion. CLOSED SYSTEM in ahead motion needs the difficult selection of proportional factor and bang-bang control, so MODIFIED SYSTEM with retouch of OPEN SYSTEM may be better than COSED SYSTEM only.

#### EXPERIMENTS OF CHANGING AHEAD MOTION

In ahead motion test, operation of CPP control lever is varied discontinuously as stop engine(CPP control lever blade angle:  $0^\circ$ ), slow ahead( $10^\circ$ ) and full ahead( $20^\circ$ ) successively without rudder deflection. Intended mock ships are general cargo ships or tankers and their time constants of ahead motion are 100sec, 200sec and 300sec. In OPEN SYSTEM estimated time constant  $T_{4F}$  is 25sec at CPP blade angle  $20^\circ$  (see Fig.17). In MODIFIED SYSTEM proportional factor  $C_1$  assumes  $5^\circ\text{sec/m}$ . Example of time histories on OPEN/MODIFIED SYSTEM are shown in Fig.15.

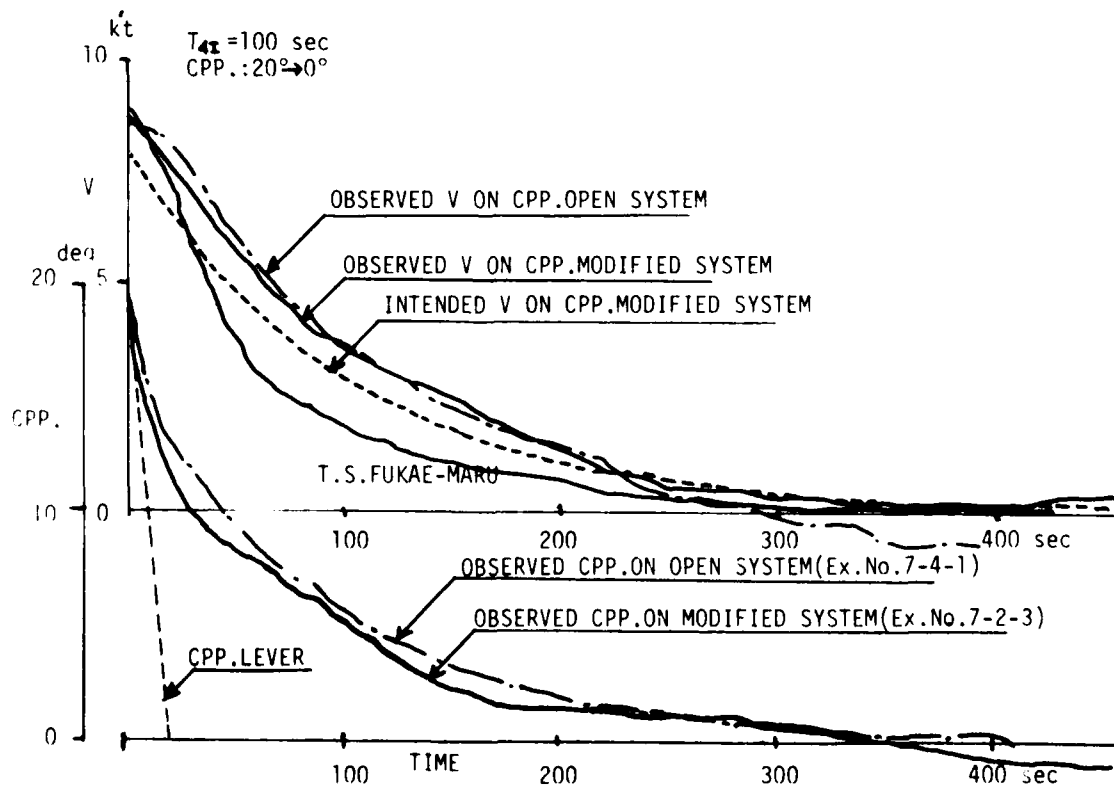


Figure 15. Comparison of Time Histories between CPP OPEN/MODIFIED SYS.

papers and some of them describe ship ahead motion well<sup>(6)</sup>. But as they are too complicated to analyse the phenomena of ahead motion, the simplest mathematical model is adopted in this paper to comprehend ahead motion easily.

In general, considering speed drop due to steering and turning of ship, accelerated and decelerated ahead motion under ahead propelled condition may be described reasonably with following equation (11) even in large change of propeller revolution<sup>(6)</sup>.

$$\dot{V} + a_{vv} V^2 + a_{rr} \dot{\psi}^2 + a_{\delta\delta} V^2 \delta^2 = a_{nn} n^2 + a_{nv} n V \quad ; \quad n \geq 0 \quad (11)$$

Rewriting Eq.(11) under the conception of quasi-linear theory, Eq.(12) is obtained if steering and turning are negligible<sup>(6)</sup>.

$$T_4 (V_o, n_o) \dot{V} + V = K_4 (V_o, n_o) n \quad ; \quad n \geq 0 \quad (12)$$

where  $n$  is propeller revolution per sec,  $V$  is ship speed. It shows that  $T_4$  is time constant of ahead motion and  $K_4$  is gain constant of ahead motion. This equation of motion is accepted in this paper.

The training ship equips with CPP, so that ahead motion is controlled by blade angle  $l$  of CPP instead of propeller revolution  $n$  in Eq.(12). Because of proportional relationship between  $n$  and  $l$ , so Eq.(12) is rewritten as following Eq.(13)

$$T_4 (V_o, l_o) \dot{V} + V = K_4 (V_o, l_o) l \quad ; \quad l \geq 0 \quad (13)$$

Eq.(13) is a first order linear equation and same type as yaw motion. This equation is used in OPEN SYSTEM and CLOSED SYSTEM on ahead transduce motion. Considering speed drop due to steering and turning, a following equation must be used only in CLOSED SYSTEM

$$T_4 (V_o, l_o) \dot{V} + V + c_r \dot{\psi}^2 + c_\delta V^2 \delta^2 = K_4 (V_o, l_o) l \quad ; \quad l \geq 0 \quad (14)$$

#### TRANSDUCE SYSTEM OF AHEAD MOTION

Although ship speed is controlled not only by propeller characteristics but governed partly by main engine dynamic characteristics, a mock element of main engine characteristics is not considered in this paper. A basic transduce system of OPEN SYSTEM is same as yaw motion. OPEN SYSTEM on ahead motion requires adequately large CPP blades angle for mock ahead motion unlike yaw motion, so the mock motion is not strongly affected by disturbance from wind and wave. On the other hand the MODIFIED SYSTEM is useful to feed-back control of steering and turning.

CPP OPEN SYSTEM. Transfer function in computer is following Eq.(15), because of identifying mock ship's speed at steady state with TS's speed.

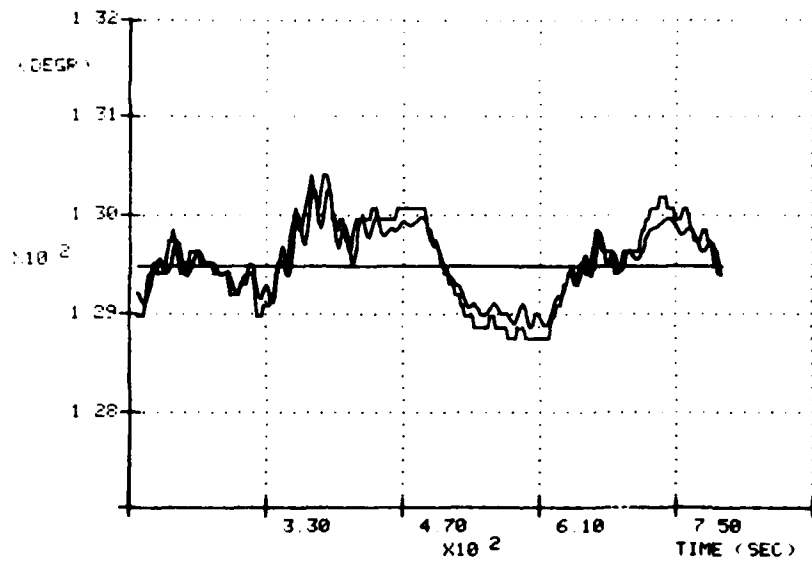


Figure 4.4

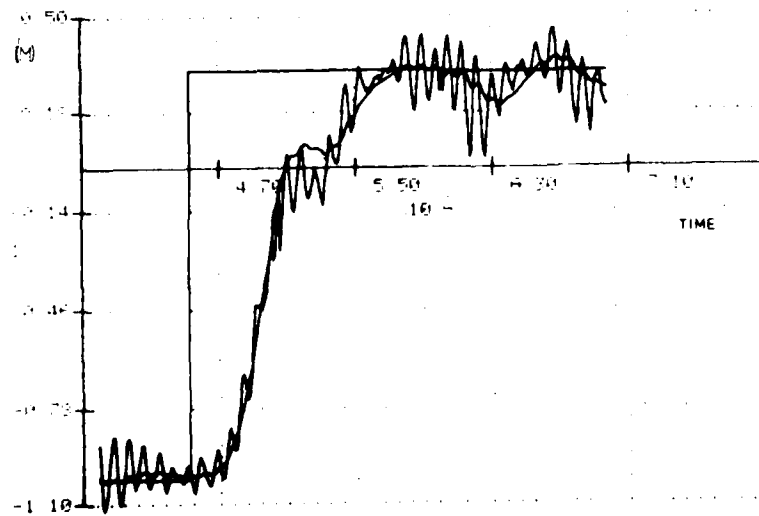


Figure 4.5

Figure 4.5 shows a sideways setpoint change of approx. 13 m. The curves represent the setpoint, the estimate and the measured position. Notice the oscillatory measurement. This is a typical noise picture for taut wire measurements. The noise has the same frequency as the dominating wave frequency and is caused by the wave forces acting on the wire. Note that the measurements from the taut wire system are angle measurements of the wire deviations from the vertical axis. The water depth is used to calculate the horizontal deviation in meters.

#### 4.3 M/V Seaway Eagle

Registrations: During operation at the Ekofisk-Emden gas pipeline in the North Sea.

Vessel: Diving support, 2000 tons

Pos.ref.syst: Simrad hydroacoustic (super short baseline).

Conditions: wind: 40-50 kt  
 current: ca 1.5 kt  
 waves: 15-20 feet  
 depth: 70-80 m

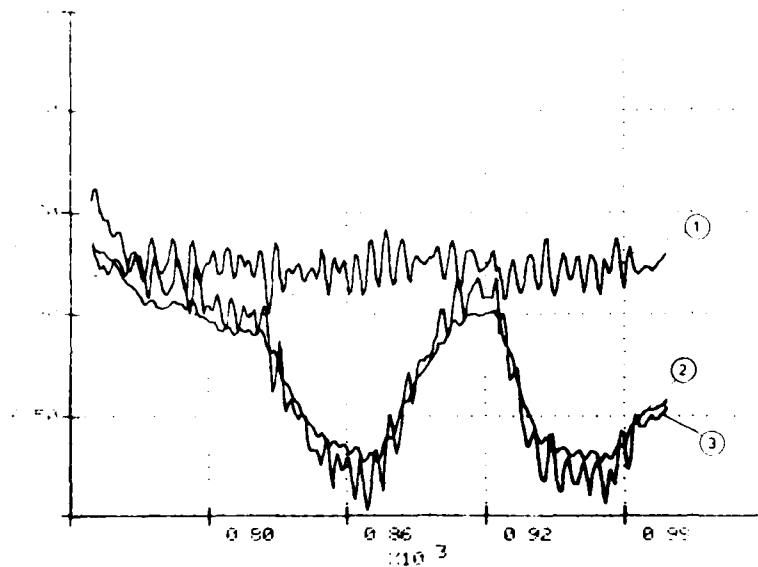


Figure 4.6

Figure 4.6 shows measured vessel heading (curve 3), low frequency estimate (curve 2) and first order heading motion due to waves (period approx. 5-7 sec.). Note that the high frequency estimate has a zero mean. Estimated heading variation is within approx.  $\pm 1.5$  degree. Note also the effectiveness of the filter in removing the first order yaw component.

Registrations: Tests off Haugesund, Norway

Conditions: wind: 15 kt  
current: 0.3 kt  
waves: 2-3 feet  
depth: 85 m

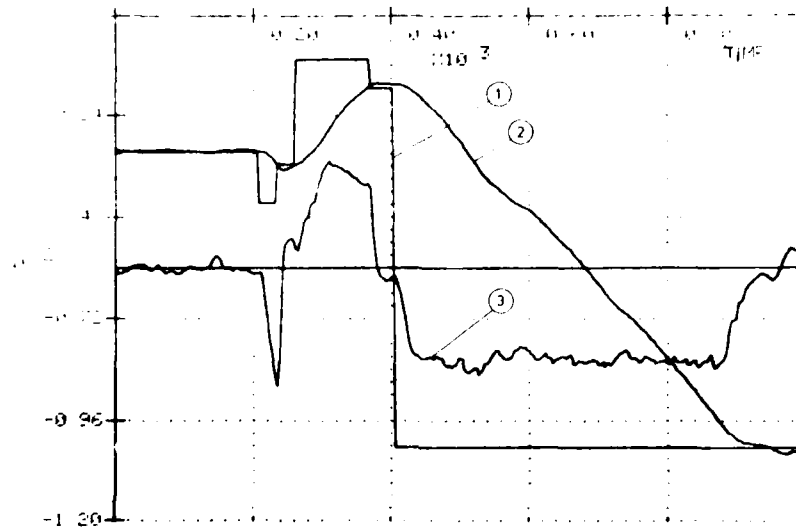


Figure 4.7

The vertical axis of figure 4.7 indicates x-position in meters for curve 1 and 2, which indicate position setpoint and estimate. Note that 5 changes of setpoint were made during this test, and not all were allowed to be completed before a new setpoint was initiated. The test indicates the dynamics of change of position setpoint. The velocity estimate is shown in curve 3. Notice the zero velocity at the leftmost part of the curve representing normal positioning, and the constant speed of approx. 1 kt during the last setpoint change.

Figure 4.8 shows the estimation error (residual) for the hydroacoustic measurement during the translation in the latter part of figure 4.7, ending at the limit of the HPR range. This can be seen in figure 4.8 as increasing measurement noise as the distance from the transponder is increased. Note the sequence marked, which represents measurement blocking.

Figure 4.9 shows thruster pitch variation during 200 sec. of positioning. The "steps" in plot, represent a deadband programmed into the software. Notice that the deadband is operative up to seconds. Essentially no activity in the wave frequency is observed.

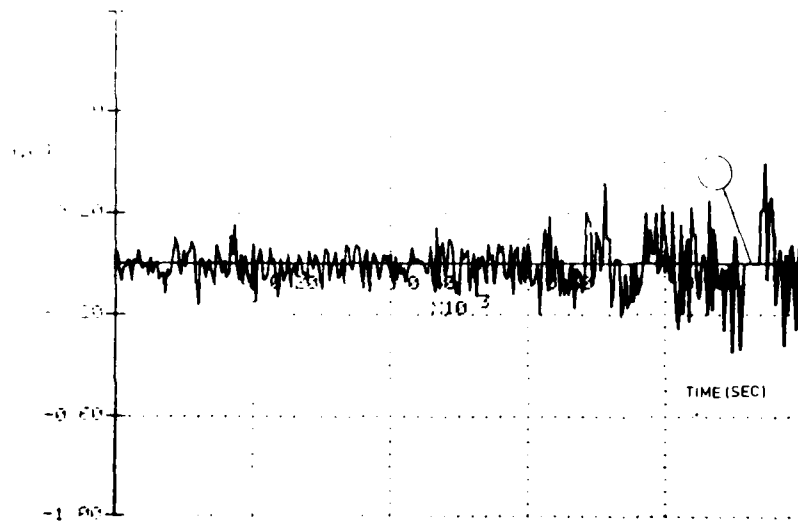


Figure 4.8

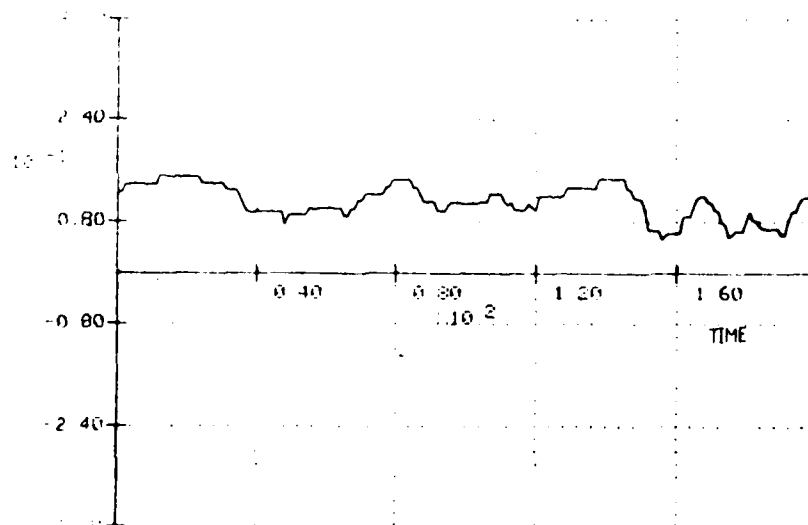


Figure 4.9



## 5. DP ASSISTED MOORING

Deep water mooring of greater work vessels may represent a problem. Oscillations with amplitudes of 15-20 m may occur, and these oscillations are very slowly attenuated because of the small damping forces in the system. A DP system working together with anchors can prevent oscillations or at least attenuate them quickly.

The time-consuming task of moving on anchors will be more or less eliminated by the flexibility of the DP system. Under severe weather conditions a combination system with DP and one or more anchors provides a great potential for safety and stable positioning.

The concept of a combined DP- and mooring system is shown in figure 5.1. The mooring submodule is designed as an extension to the normal DP system and may be switched on and off as anchors are used or not.

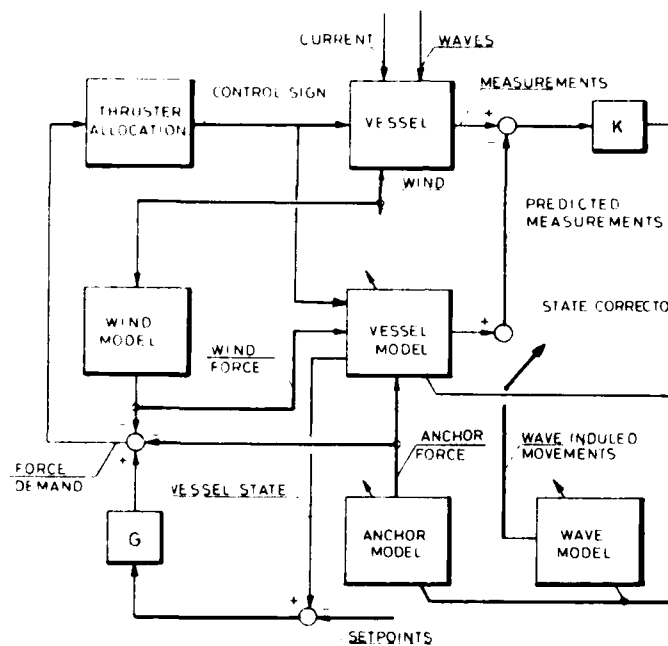


Figure 5.1

The dynamics of a moored vessel may be modelled as an equivalent mass-spring system with small attenuation. The main effect on the mass-spring equivalent of introducing the combination with DP, is that the damping in the system will be considerably increased. The equation for the anchor model will be:

$$M \cdot \ddot{X}_L = -K_a (X_L - X_a) + F_{ao}$$

where:  $M$  - total mass and moment of inertia matrix

$K_a$  - spring constant matrix

$F_{ao}$  - bias excitation vector

$X_L$  - vessel state vector

$X_a$  - equilibrium state vector

$\dot{\phantom{x}}$  - time derivation

With respect to figure 5.1 we see that the current estimator is replaced by an anchor model. To be able to calculate the correct anchor force acting on the vessel we have to estimate the bias excitations and spring constants for the actual three degrees of freedom. Since the estimator is unable to differentiate between the current force and the bias excitation, the latter is chosen to constitute the environmental estimator for the combined system, estimating an equivalent anchor bias. The spring constants are estimated on the base of the oscillation periods. Notice that the wave filter is disabled due to the difficulties in deriving the first order wave motion from the total motion.

The combination system is not yet implemented and tested in practice, but the laboratory simulations that are carried out are promising. We believe that this system will be very useful as offshore activity moves into areas of greater water depth and rougher weather conditions.

#### CONCLUSION.

The experience with our system concept after the first year of operation is satisfying. The system seems to work properly with respect to wave motion filtering, measurement system handling and precise positioning.

We feel that the system so far constitutes a good base for exacting control tasks in combination with a DP system. Challenging tasks we see coming in the near future are water monitor stabilization, vertical motion compensation of heavy crane loads and active anchor winch control.

THE DESIGN AND SIMULATION OF NAVIGATION  
AND  
SHIP CONTROL ALGORITHMS FOR A MINESWEEPER

by J.R. Moon  
and J.R.E. Thomas  
Ferranti Computer Systems Ltd

ABSTRACT

In minesweeping operations it is necessary for the vessel to be able to follow as closely as possible a pre-defined path. This paper describes algorithms, devised and implemented for a shipboard computer system, to accurately estimate the position and velocity of the vessel and to steer it along geographically-defined paths. The navigation system inputs are provided from radio navigation aids or from radar measurements of buoys at geographically known positions. The ship control algorithms are designed to bring the vessel onto the optimum track and to maintain the track in all reasonable conditions of wind and tide. This paper describes the analysis and simulation of the system.

INTRODUCTION

This paper describes work sponsored by the Ministry of Defence on the development of ship navigation and control algorithms for the Brecon class of mine countermeasures vessels, the first of which is due to go into service with the RN during 1979. These vessels can perform either a minesweeping or a minehunting role, and in both roles there is a requirement to be able to steer accurately along a geographically-defined line or series of lines. The algorithms for achieving this objective are implemented in a mini-computer (Ferranti FM1600B) which also performs many other functions principally connected with the display and recording of operational information and the operation of a minehunting sonar. The overall computer system is known as MCMV CAAIS (Mine Counter Measures Vessel Computer Aided Action Information System).

The navigation and control system divides functionally into two distinct sub-systems:

- (a) Own Ship Tracking - defined as the task of finding the vessel's position with respect to the optimum track (i.e. the desired line) and its velocity components.
- (b) Ship Control - the task of directing the ship onto the optimum track and maintaining it there.

The hardware interfaces, illustrated in figure 1, consist of navigational inputs from radio-navigation aids (Decca QM14 and Hifix 6) and from the surveillance radar, ship's log and compass data, and outputs to the autopilot, an operator's display and a helmsman's meter. The autopilot control is rotated via a stepper motor driven at 4Hz. The helmsman's meter indicates the across-track error and can be used to assist manual steering of the ship when not under automatic control.

OWN SHIP TRACKING SUBSYSTEM

There are three possible inputs of navigation data to the system and these are described below in order of accuracy.

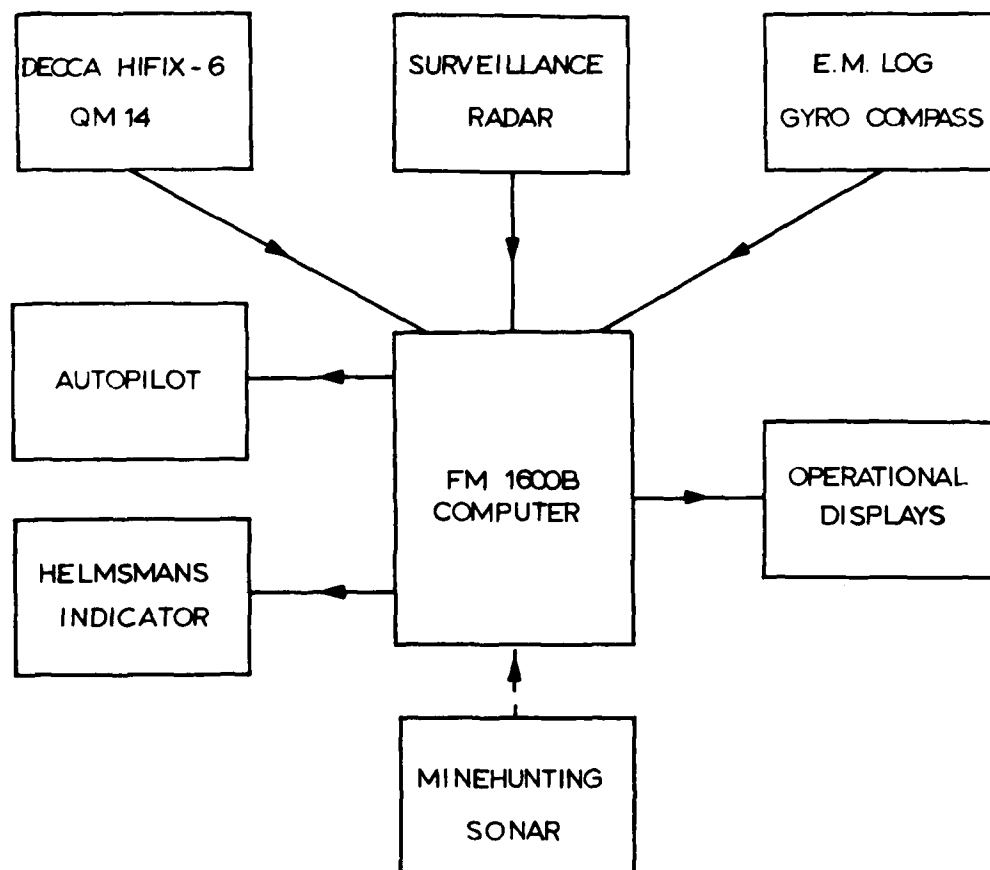


Figure 1. MCMV CAAIS Overall System Diagram

## Decca Hifix 6

This radio positioning system operates in the band 2-5MHz and is based on relative phase measurements from a master and two or more slave stations located ashore. The phase-locked transmitters each radiate at a different multiple of a fundamental frequency and, with the location of each transmitting station held within the computer, geographical fixes are derived from the hyperbolic lines of position (LOPs) output from the on-board receiver. The maximum operational range is of the order 100 to 200km and the achievable accuracy can be within 10m depending on geographical and atmospheric conditions.

## Radar Measurements of Buoys

In this mode a chain of up to 9 buoys are laid at geographically-known positions adjacent to the area to be swept and range R and bearing  $\theta$  measurements from the surveillance radar are used to give the ship's position relative to the buoys. The short-scope buoys are held under tension to restrict their movement from the nominal positions. The radar (Type 1006) has a rotation period of 2.5 seconds and, having a short pulse length and high PRF, is capable of giving positional measurements to within a few tens of metres. The plot extraction process is performed automatically by the computer system.

## Decca Navigator QM14

The principles of the operation of this device are very similar to those described for Hifix, however the long wavelength of the fundamental frequency ( $\sim 15\text{KHz}$ ) limits the maximum accuracy to a few tens of metres, and this figure can be degraded by an order of magnitude or more in the worst combinations of atmospheric and geographical conditions. For this reason it is only feasible to use QM14 measurements for ship control in the most favourable conditions although the own-ship tracking subsystem will continue to provide positional and velocity estimates in all circumstances.

## Own Ship Tracking

The own ship tracking is performed in cartesian coordinates, and the quantities that we wish to estimate are contained in the state vector  $X = (x, \dot{x}, y, \dot{y})$ . A Kalman filter is capable of providing a minimum variance estimate of this state vector, and is in fact very well suited to this problem since the dynamics of the situation are well defined - we know the ship is trying to travel in a straight line and, in addition, reasonable estimates can be made of the variances associated with the basic navigation measurements. This algorithm is recursive in that, following a position measurement, an updated estimate of the state vector is produced from a linear combination of that measurement and a prediction based on the state after the previous measurement:

$$\hat{X}_{k+1} = X'_{k+1} + K_{k+1} (Y_{k+1} - M_{k+1} X'_{k+1})$$

where

$$X'_{k+1} = \Phi_k \hat{X}_k$$

is the state vector at the current measurement time predicted from the last estimate  $\hat{X}_k$  via the state transition matrix  $\Phi_k$ .  $Y_{k+1}$  is the quantity measured and  $M_{k+1}$  specifies its relationship with the ship state  $X'_{k+1}$ , thus  $M_{k+1} X'_{k+1}$  can be regarded as the predicted measurement.  $K_{k+1}$  is the matrix of optimum position and velocity weighting factors (gains) and is derived from the condition that it should minimise the covariance matrix of the best estimate  $\hat{X}_{k+1}$ . The details of the derivation are given in (1) and are briefly summarised below.

The covariance matrix of the predicted state  $P'_{k+1}$  is calculated from the covariance matrix of the last best estimate  $\hat{P}_k$  by

$$P'_{k+1} = \Phi_k \hat{P}_k \Phi_k^T + G_k Q_k G_k^T,$$

where  $Q_k$  is the covariance matrix of the plant noise and  $G_k$  specifies its effect on the state vector. The gain matrix is then given by

$$K_{k+1} = P'_{k+1} M_{k+1}^T [M_{k+1} P'_{k+1} M_{k+1}^T + R_{k+1}]^{-1}$$

where  $R_{k+1}$  is the covariance matrix of the measurements. The covariance matrix of the current best estimate can be shown to be

$$\hat{P}_{k+1} = (I - K_{k+1} M_{k+1}) P'_{k+1}$$

The above equations constitute one complete cycle of the filter described in general terms; the specific forms of the matrices used in this application will now be derived.

The assumed dynamics of the ship are that only a random acceleration (plant noise) perturbs its motion from a straight line so that the true ship motion is assumed to be given by

$$X_{k+1} = \Phi_k X_k + G_k a_k$$

where

$$\Phi_k = \begin{bmatrix} 1 & \Delta T & 0 & 0 \\ 0 & 1 & 0 & 0 \\ 0 & 0 & 1 & \Delta T \\ 0 & 0 & 0 & 1 \end{bmatrix},$$

$$G_k = \begin{bmatrix} \frac{1}{2} \Delta T^2 & 0 \\ \Delta T & 0 \\ 0 & \frac{1}{2} \Delta T^2 \\ 0 & \Delta T \end{bmatrix}$$

and  $a_k$  is a random acceleration of variance  $\sigma_a^2$  which is assumed to be constant for  $\Delta T$ , the time elapsed since the last measurement. The measurements of xy position obtained from the radar or the radio-navigation aids can be written as

$$Y_{k+1} = M_{k+1} X_{k+1} + N_{k+1},$$

where

$$M_{k+1} = \begin{bmatrix} 1 & 0 & 0 & 0 \\ 0 & 0 & 1 & 0 \end{bmatrix}$$

and  $N_{k+1}$  is the vector of measurement noise with covariance matrix

$$R_{k+1} = \begin{bmatrix} \sigma_x^2 & \sigma_{xy}^2 \\ \sigma_{xy}^2 & \sigma_y^2 \end{bmatrix}.$$

In the case of range and bearing measurements from the radar this can be expressed as

$$R_{k+1} = \begin{bmatrix} \sigma_R^2 \sin^2 B + R^2 \sigma_B^2 \cos^2 B & \frac{1}{2} \sin(2B) (\sigma_R^2 - R^2 \sigma_B^2) \\ \frac{1}{2} \sin(2B) (\sigma_R^2 - R^2 \sigma_B^2) & \sigma_R^2 \cos^2 B + R^2 \sigma_B^2 \sin^2 B \end{bmatrix}$$

When LOPs are available from the radio-navigation equipment, an xy measurement is obtained at 2½ second intervals by performing a minimum variance fit to all the available LOPs. This algorithm also provides an estimate of the elements in  $R_{k+1}$ .

One method of simplifying the above equations is the commonly-used device of decoupling the coordinates. If the off-diagonal terms in the measurement covariance matrix  $R_{k+1}$  are assumed zero then the equations reduce to two entirely independent filters for estimating  $(x, \dot{x})$  and  $(y, \dot{y})$ . The amount of computation is reduced by a factor of three, but clearly the implications needed investigating. It can be shown that no bias errors are introduced in the estimate of the state vector by this approximation, but the uncertainty associated with the estimate will increase. However tests have shown (e.g. figure 2) that the degradation in performance is, in practice, fairly minimal and that, for a minesweeping scenario, the only effect of note is an increase in the variance of the velocity estimate following a turn. This change though is not significant compared with the effects caused by different methods of handling own ship turns. The method we chose uses a higher value of plant noise when the ship is not travelling along a straight leg of an optimum track. This simple approach is possible since operator inputs inform the system when an optimum track is being followed.

During straight legs the filter output will reduce the measurement standard deviation by an asymptotic factor of 4. Figure 2 illustrates how the position output variances will reduce with increasing number of measurements and also shows how little the decoupling assumption degrades performance. The averages of ten simulation runs (with different random noise seeds) are shown for a case where the measured bearing of the buoy was around 45 degrees (i.e. maximum XY covariance) and the range about 3000m.

Typically an optimum track for minesweeping will consist of a number of linked straight legs with angles between the legs not exceeding  $30^\circ$  and figure 3 shows that the plant-noise switching technique described above will keep the velocity errors to within 1 knot during such a turn.

#### Treatment of Compass Bias

When radar measurements of buoys are being used as navigational inputs the largest potential source of inaccuracy is due to the compass (used to convert radar bearings relative to ship's head to true bearing) which can have errors up to 2½ degrees following a  $180^\circ$  turn. The principle components of this error are:

- (a) errors due to drift - typical time constants greater than 2 days
- (b) errors following sustained turns - time constants around 90 minutes.

These errors are sufficiently slowly varying to be regarded as biases as far as the own ship tracking is concerned. There are other higher frequency errors present but they are of little concern as they are substantially attenuated by the low-pass filtering effect of the Kalman algorithm.

One approach to this problem would be to ignore the bearing measurements altogether and just use the range inputs to provide the updates of own ship's position, however this would only give acceptable solutions in certain geometries. A more satisfactory approach is to try and estimate the bias error as part of the own ship tracking filter and, since the bias error will affect measurements of own ship position based on different buoys in different ways, then it is intuitively apparent that the information for providing an estimate of the bias is available. The usual method of correcting Kalman filter outputs for measurement biases is to augment the state vector with elements to represent them, but this inevitably increases the complexity of the filter processing. A modification of this technique has been suggested by Friedland (2,3) who, by partitioning the augmented state vector and the associated covariance

- x OUTPUT OF FILTER USING FULL MEASUREMENT COVARIANCE MATRIX
- o OUTPUT OF FILTER USING ONLY THE TWO DIAGONAL TERMS
- M INPUT MEASUREMENT STANDARD DEVIATION

(MEASUREMENT PARAMETERS  $\sigma_R = 40.0$  FEET  $\sigma_B = 0.2$  DEGREES)

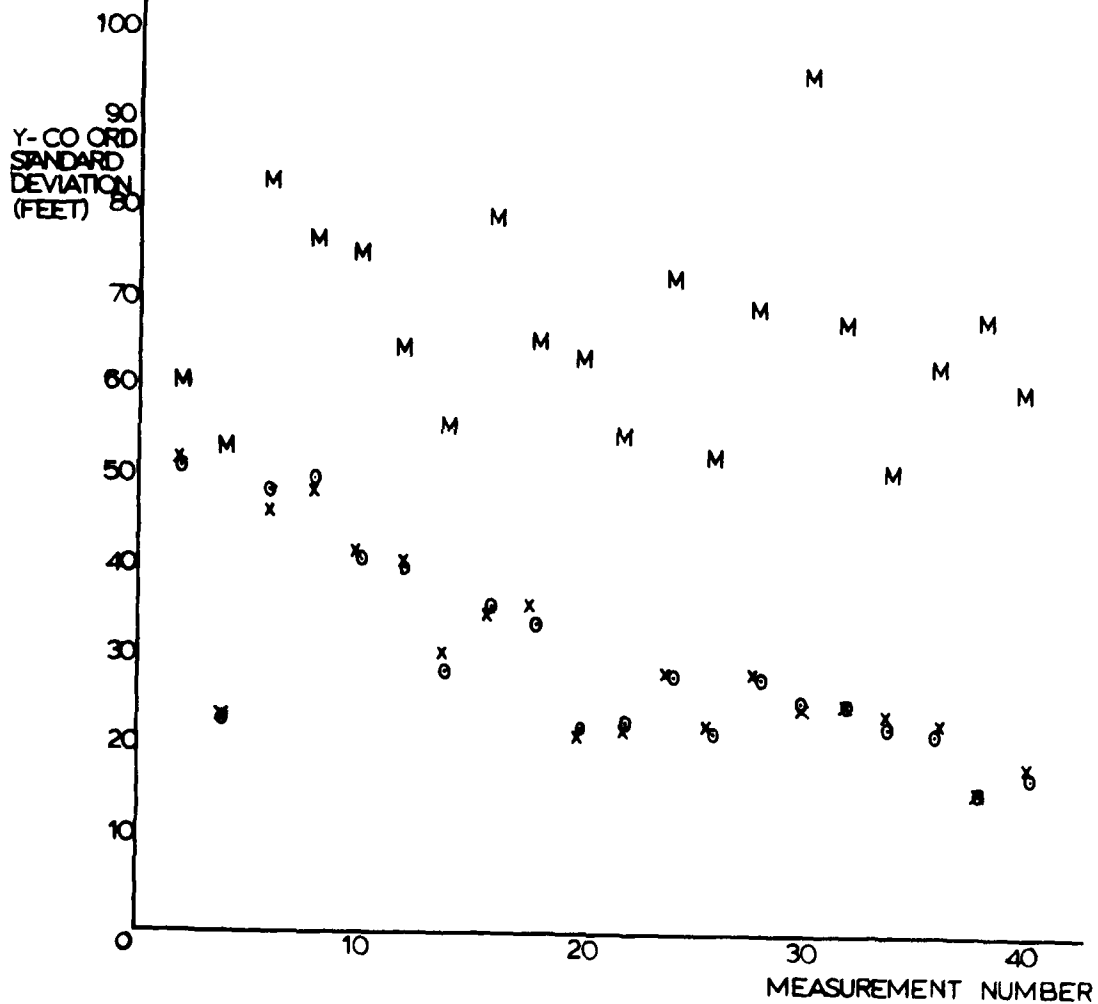


Figure 2. Variance reduction due to Kalman Filter



The ship, initially travelling along the X axis, turned through  $30^\circ$  with a radius of turn = 300 yards at a speed of 6 knots. The new plant noise was switched in for a time given by:

$\frac{\text{Dog leg angle turned through}}{\text{Nominal rate of turn of ship}}$  (secs), in this case about 60 seconds.

0 Plant noise unchanged at turn  $= 0.0009(\text{Ft}^2/\text{Sec}^4)$

X Plant noise  $= 0.1(\text{Ft}^2/\text{Sec}^4)$  at turn

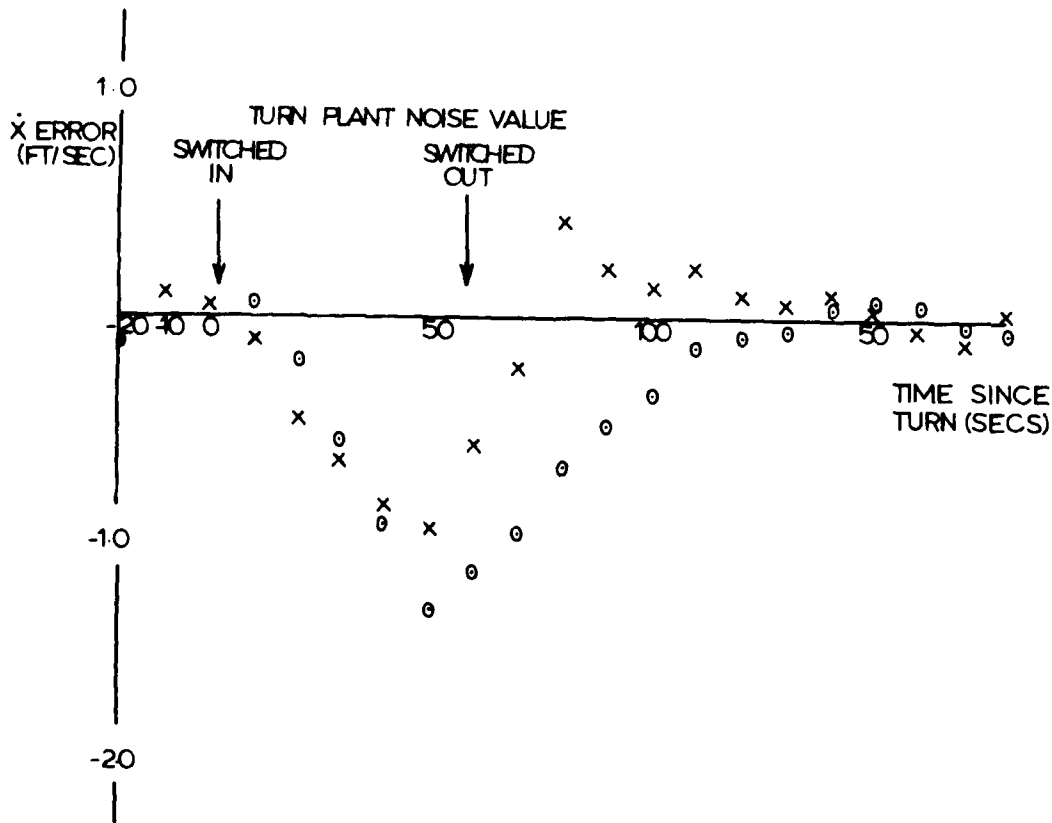


Figure 3. Velocity Errors from Ship Tracking Filter During  $30^\circ$  Turn.

matrices, was able to show that, with some generally justifiable approximations, the bias errors can be estimated recursively by a set of update equations running in parallel to the normal Kalman filter update equations. This method gives a considerable saving in computing resources in comparison with the straightforward augmented matrix approach.

When used in conjunction with the decoupled ship tracking filter the set of parallel equations assumes the simple form shown in figure 4; those illustrated are for the X coordinate and exactly similar equations are used independently in the Y coordinate. The effectiveness of this bias filter in a variety of geometrical situations is illustrated in figure 5.

#### SHIP CONTROL SUBSYSTEM

The requirement for the ship control subsystem was that it should be capable of bringing the ship onto an optimum track and of guiding the ship along that track to within a given accuracy. The control was to be applied via an existing interface between the computer and the set-heading input of the autopilot. This interface allowed the computer to change the autopilot heading in  $\frac{1}{2}^\circ$  steps through a stepper motor.

The information available from the own ship tracking filter comprises an estimate of the ship state vector and a tidal stream estimate derived indirectly from the state vector and the log and compass inputs. The ship state vector is rotated to give the off-track distance (p) and its first derivative ( $\dot{p}$ ).

#### Course Correction Algorithm

The simplest course correction algorithm capable of driving p to zero in the steady state is a proportional plus integral controller with the off track distance p as its input i.e.

$$\theta = k_1 p + k_2 \int p \, dt,$$

where  $\theta$  is the correction to the autopilot set heading and  $k_1, k_2$  are constants. In the steady state, the integral term provides a constant heading correction that is needed to offset the effect of tidal stream.

This algorithm is most suited to the regulator function of keeping the ship on the optimum track. When used in automatic track changing, the integral term can produce a substantial overshoot if the initial ship's position gives a large value of p, and when a significant tidal stream is present a prolonged period of overshoot may be necessary to build up the required heading offset.

An alternative course correction algorithm can be derived from the ship tracking filter outputs. Consider the vector diagram of figure 6. If the ship is off-track p metres with a heading vector  $\underline{H}$  (magnitude given by the log) and a true course  $C$ , then  $\alpha$  is the heading required to make the new course of the ship align with the optimum track angle plus the off-track proportional angle. If it is assumed that the ship maintains a constant speed through the water then

$$\alpha = k_1 p + \sin^{-1} \left\{ \frac{t}{s} \sin \theta \right\},$$

where the terminology is defined in figure 6.

### Current Forces

The force on the ship due to the velocity  $U$  relative to the water has the components  $X_H$  and  $Y_H$  in x- and y-direction respectively, while the moment is  $N_H$ .

$X_H$ ,  $Y_H$  and  $N_H$  are given by:

$$\begin{aligned} X_H &= \frac{1}{2} \rho U^2 L T C_{XH}(\beta) \\ Y_H &= \frac{1}{2} \rho U^2 L T C_{YH}(\beta) \\ N_H &= \frac{1}{2} \rho U^2 L T C_{NH}(\beta) \end{aligned} \quad (1)$$

The values of the coefficients  $C_{XH}$ ,  $C_{YH}$  and  $C_{NH}$  as functions of  $\beta$  have been determined experimentally for a hull form of a similar vessel. The values are shown in figure 2.

### Wind Forces

The force on the ship due to the wind speed  $V_W$ , has the components  $X_W$  and  $Y_W$  in x- and y direction respectively, while the moment is  $N_W$ .

$X_W$ ,  $Y_W$ , and  $N_W$  are given by:

$$\begin{aligned} X_W &= \frac{1}{2} \rho_a V_W^2 A_W C_{XW}(\psi_W - \psi) \\ Y_W &= \frac{1}{2} \rho_a V_W^2 A_W C_{YW}(\psi_W - \psi) \\ N_W &= \frac{1}{2} \rho_a V_W^2 A_W L C_{NW}(\psi_W - \psi) \end{aligned} \quad (2)$$

The estimated values of the coefficients  $C_{XW}$ ,  $C_{YW}$  and  $C_{NW}$  as functions of  $(\psi_W - \psi)$  are given in figure 3.

### Total External Forces and Required Restoring Forces

For a current speed  $V_C = 3$  kts and a wind speed  $V_W = 30$  kts the total external forces  $X_{ext}$  and  $Y_{ext}$  and the moment  $N_{ext}$  acting on the vessel were calculated.

$$\begin{aligned} X_{ext} &= X_H + X_W \\ Y_{ext} &= Y_H + Y_W \\ N_{ext} &= N_H + N_W \end{aligned} \quad (3)$$

The next step was to calculate the forces in longitudinal direction and in lateral direction at 18.34 m forward of the centre of gravity and at 21.0 m aft of the centre of gravity, to make equilibrium with the external forces. Those points corresponded with the planned locations of the thrust units.

The angle between wind and current direction  $(\psi_W - \psi_C)$  was varied between 0 and 180° with steps of 10° and the relative current direction  $(\psi_C - \psi)$  between 0 and 360°, also with steps of 10°.

Results of the calculations of the total external forces are shown in figure 4, but only for the lateral  $Y_{ext}$ . An example of the required restoring forces in

longitudinal and lateral direction is shown in figure 5. The most favourable heading for which the total lateral force is minimal coincides with the heading for which the forward lateral force is zero.

The most favourable headings and the required restoring force in longitudinal and lateral direction have been plotted as a function of the angle between wind and current  $(\psi_W - \psi_C)$  in figure 6. The required restoring forces in longitudinal and lateral direction forward and aft for 20° deviation from the most favourable heading as a function of  $(\psi_W - \psi_C)$ , are shown in figure 7.

The next step was to determine the available thrust.

A firm design requirement was the capability to remain at a fixed position under external disturbances from wind, current and waves. This "hovering"-capability is necessary to be able to investigate mine-like objects with the mine-hunting sonar and in case of a mine to neutralize the mine. As the first part of the study, the required thrust fore and aft was determined to be able to hover the design external disturbances.

Another requirement was the reduction of the ship's complement as much as possible. This lead to the study of an integrated control system, both an integrated manual and an automatic control system.

For the necessary simulation studies, model test were carried out at the Bassin d'Essais des Carènes in Paris, whilst computer simulation studies were carried out by TNO-Institute for Mechanical Constructions (TNO-IWECO) in Delft.

### 3. THRUSTER SIZING

In the preliminary design phase, the wind and current forces were estimated, the wind speed being 30 knots and the current speed 3 knots, while the relative wind and current directions were varied.

The heading of the ship, called the "favourable heading", for which minimal lateral thrust fore and aft is required to maintain position was calculated for different combinations of wind and current direction.

To maintain position and heading between e.g.  $45^\circ$  at both sides of this course, the required thrust was found 90 kN fore and 65 kN aft.

The calculation procedure is explained in the following paragraphs.

#### Definitions

The current and wind speed and direction are defined relative to a fixed orthogonal axes system  $0 x_0 y_0 z_0$  as shown in figure 1.

The ship has a heading  $\psi$  and a velocity  $U$  relative to the water. The axis system  $CGxyz$  has its origin in the ship's centre of gravity  $CG$ .

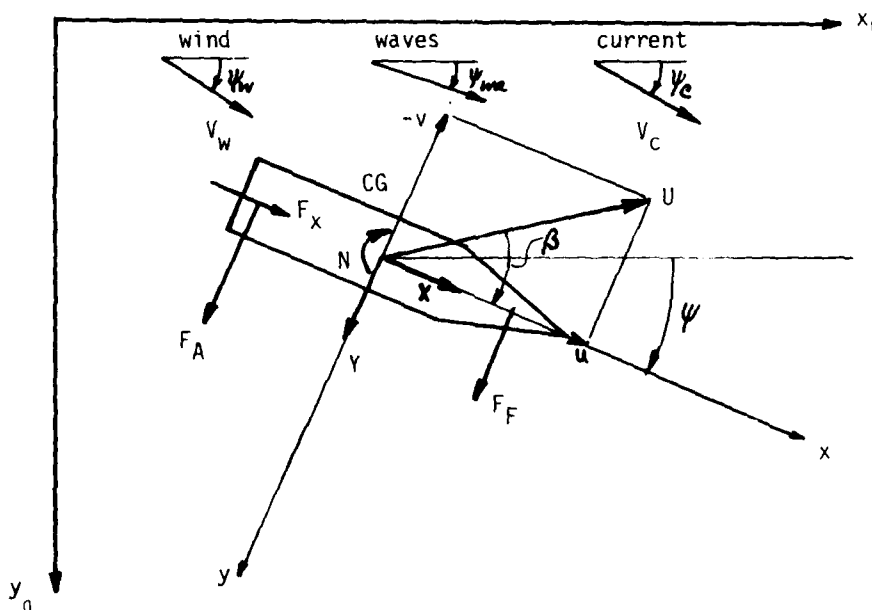


Figure 1: Axes systems and definitions

# AUTOMATIC AND MANUAL CONTROL OF THE "TRIPARTITE" MINEHUNTER IN THE HOVER AND TRACK-KEEPING MODES - A PRELIMINARY DESIGN STUDY

by A.W. Brink  
TNO-Institute for Mechanical Constructions, Delft, The Netherlands  
and A.M. Stuurman  
Royal Netherlands Navy, The Hague, The Netherlands

## 1. ABSTRACT

In a joint venture the French, Belgium, and Netherlands Navies have designed a mine-hunter and the proto-type is now under construction at a French Naval Dock-yard.

Precision-manoeuving was a firm design requirement. To achieve at the design goals, a thruster sizing study was carried out to establish the required thruster sizes.

Automatic and manual control in the hover-mode (hovering means position keeping) were studied to compare the positioning accuracies in both cases and to establish the need for an automatic position keeping system. Subjects of all three navies performed a one week simulation exercise to define the precision in the hovering mode under manual control. These subjects were experienced mine-hunter officers. Their scores were significantly inferior to the score under automatic control, which led to the incorporation of an automatic control system in the design. A further advantage is that automatic control saves man power, in the sense that people can do additional jobs, while the automatic controller steers the ship.

Results of static and dynamic simulations are presented together with the comparison between automatic and manual control.

Finally the automatic track-keeping control system will be described and some simulation results of track-keeping under various external influences (wind, sea and current conditions) will be given.

## 2. INTRODUCTION

In a joint venture, the French, Belgium and Netherlands Navies have designed a mine-hunter with France as pilot nation.

For some particulars of the design: see table 1.

Table 1: General data of "Tripartite" mine hunter.

<u>Ship</u>	
Length overall	51.0 m
Length between perpendiculars	46.5 m
Beam	8.9 m
Draught (forward)	2.3 m
Draught (aft)	2.6 m
Wind area - lateral	285.5 m <sup>2</sup>
Displacement	490 tons
Centre of gravity - fwd. of aft perpendicular	21.93 m
- above baseline	3.65 m
<u>Thrust units</u>	
- Active rudders (2): combinations of rudder and ducted propeller	- 21.0 m
- Bow thruster: Y-configuration. Direction of flow controlled by valve	18.34 m

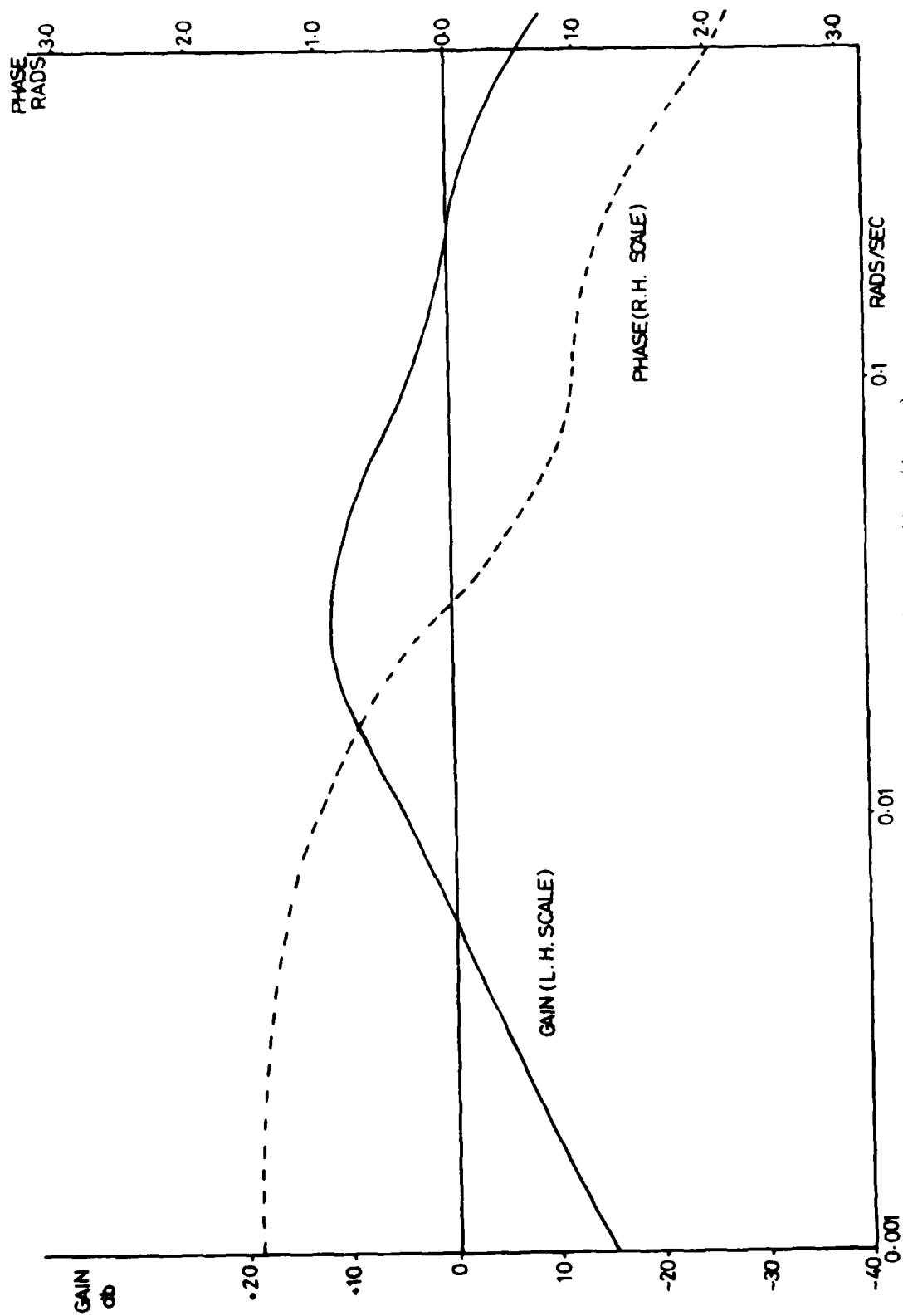


Figure 12. Track to Heading Transfer Function  $G_{th}$  (feet/degree)

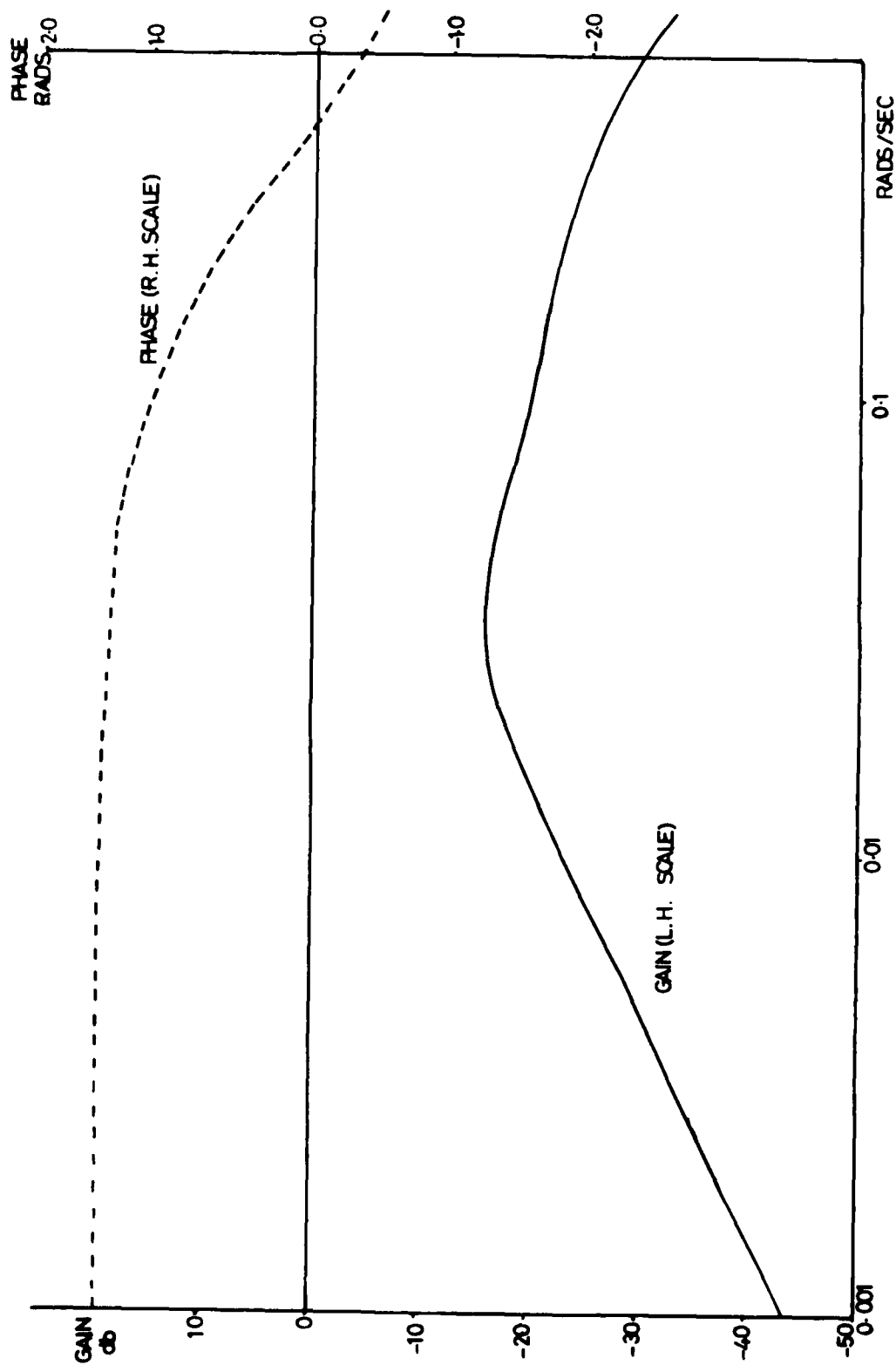


Figure 11. Heading to Track Transfer Function  $G_{ht}$  (degrees/foot)

The Bode plots of these transfer functions are shown in figures 11 and 12 for a ship speed of 5 knots. These indicate that the coupling between heading disturbances and track deviation is weak, with a peak value in the 0.01 - 0.1 rad/sec band, but the heading deviations caused by track disturbances is more significant with the maximum amplitude also occurring in the 0.01 - 0.1 rad/sec band; this will imply increased rudder activity in rough seas.

Further analytical and simulation work is in progress to examine the performance of the system in specific sea states and wind conditions, and to quantify the rudder activity in these conditions.

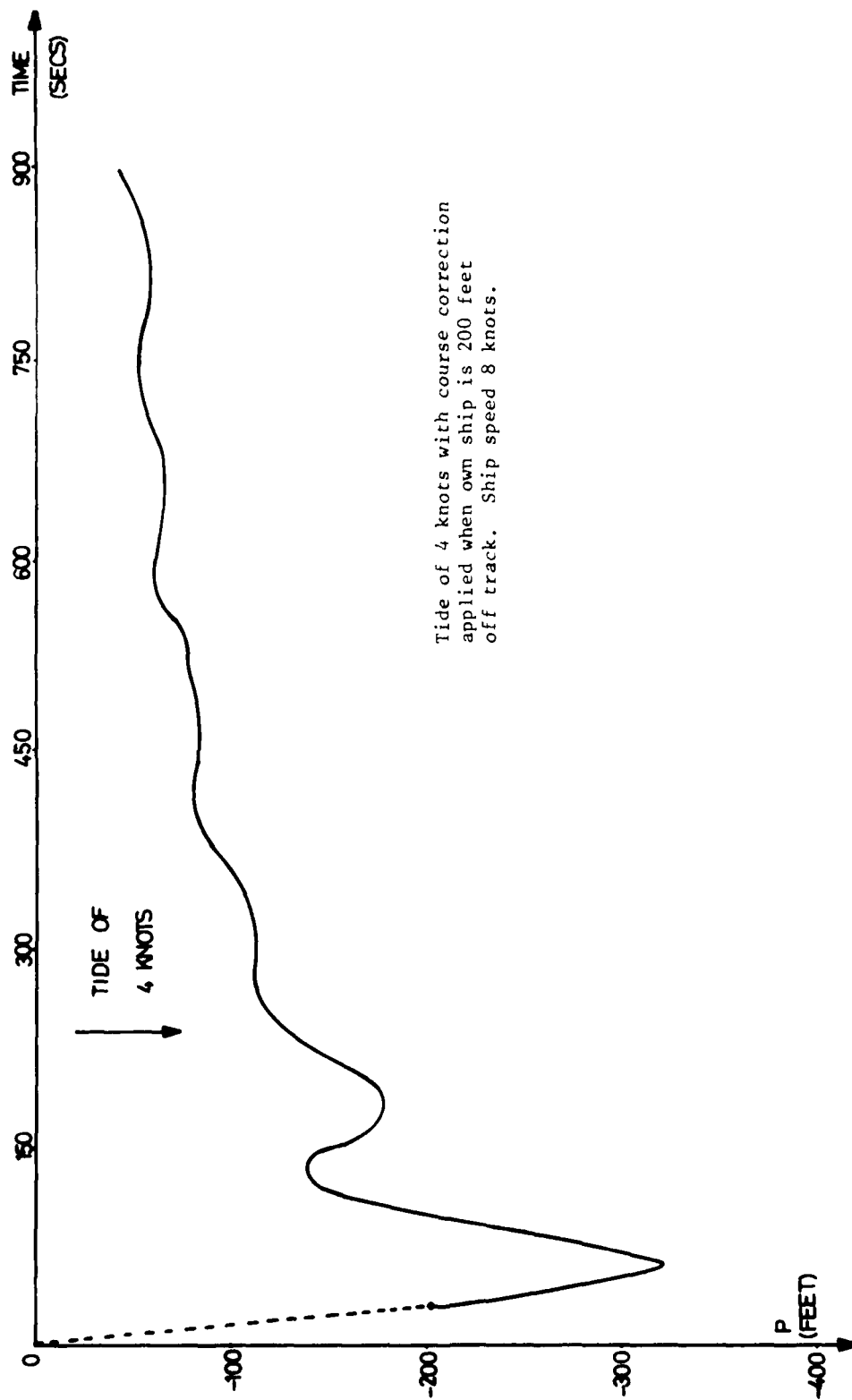
#### ACKNOWLEDGEMENTS

Thanks are due to the Ministry of Defence (Procurement Executive) for permission to publish this work. The authors also gratefully acknowledge the assistance of other members (and ex-members) of the Ferranti System Problem Analysis group especially Mr. A.J. Dick, for his contributions to the compass bias problem, and Miss H. Allington who has skillfully manipulated the simulation program. We would also like to thank Dr. S.J. Wright of the CAAIS MCMV project team for many useful discussions.

#### REFERENCES

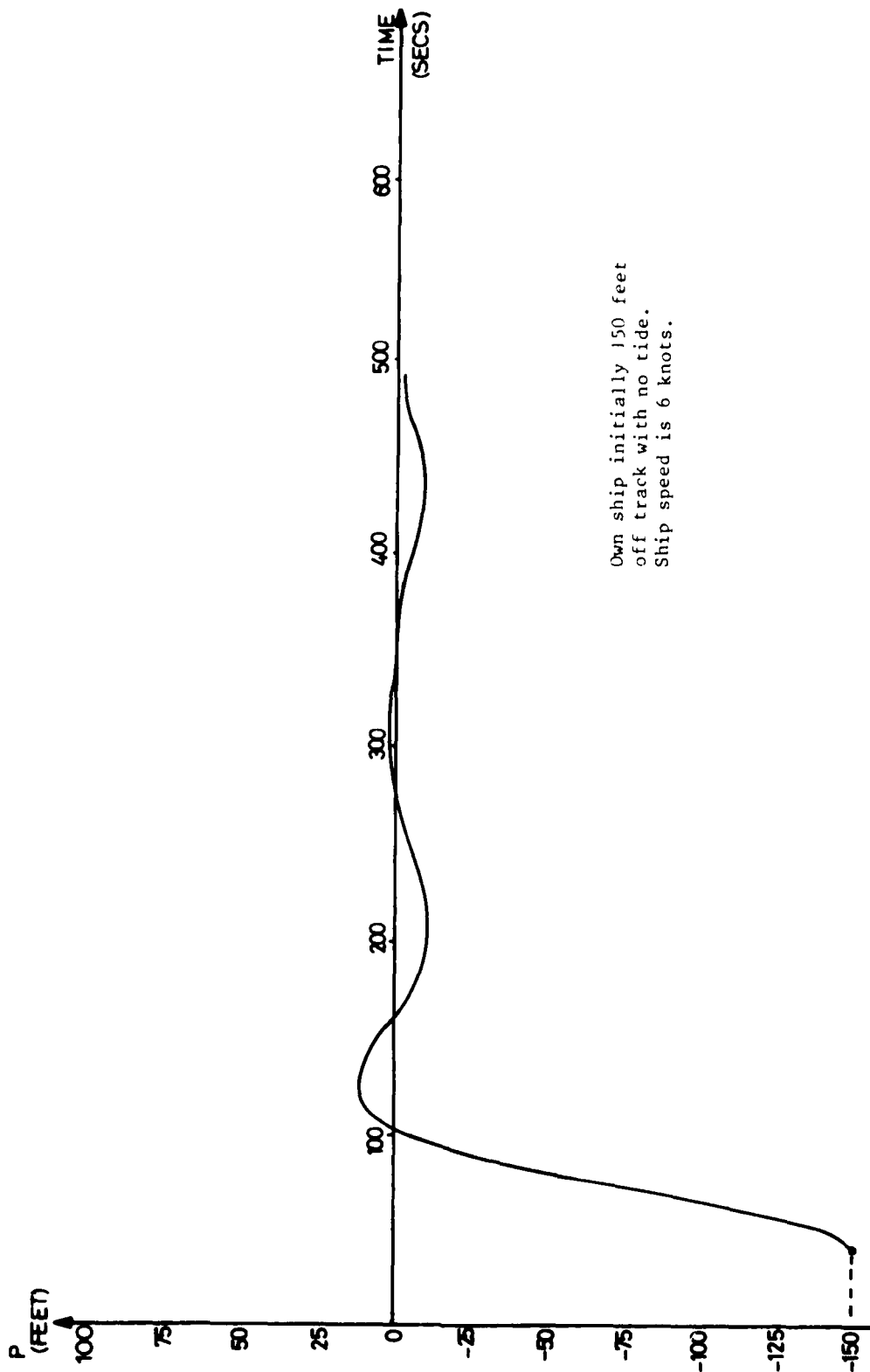
- (1) P.M. Barham and D.E. Humphries, "Derivation of Kalman Filtering Equations from Elementary Statistical Principles", AGARD publication AGARDograph 139, 1970, p 43-49.
- (2) B. Friedland, "Treatment of Bias in Recursive Filtering" IEEE Transactions on Automatic Control, Vol AC-14, 1969, p 359-367.
- (3) B. Friedland, "Recursive Filtering in the Presence of Biases with Irreducible Uncertainty" IEEE Transactions on Automated Control, Vol AC-21, 1976, p 789-790.





Tide of 4 knots with course correction applied when own ship is 200 feet off track. Ship speed 8 knots.

Figure 10. Coming Onto Track with 4 Knot Tide



81 2-15

Figure 9. Coming Onto Track With Zero Tide

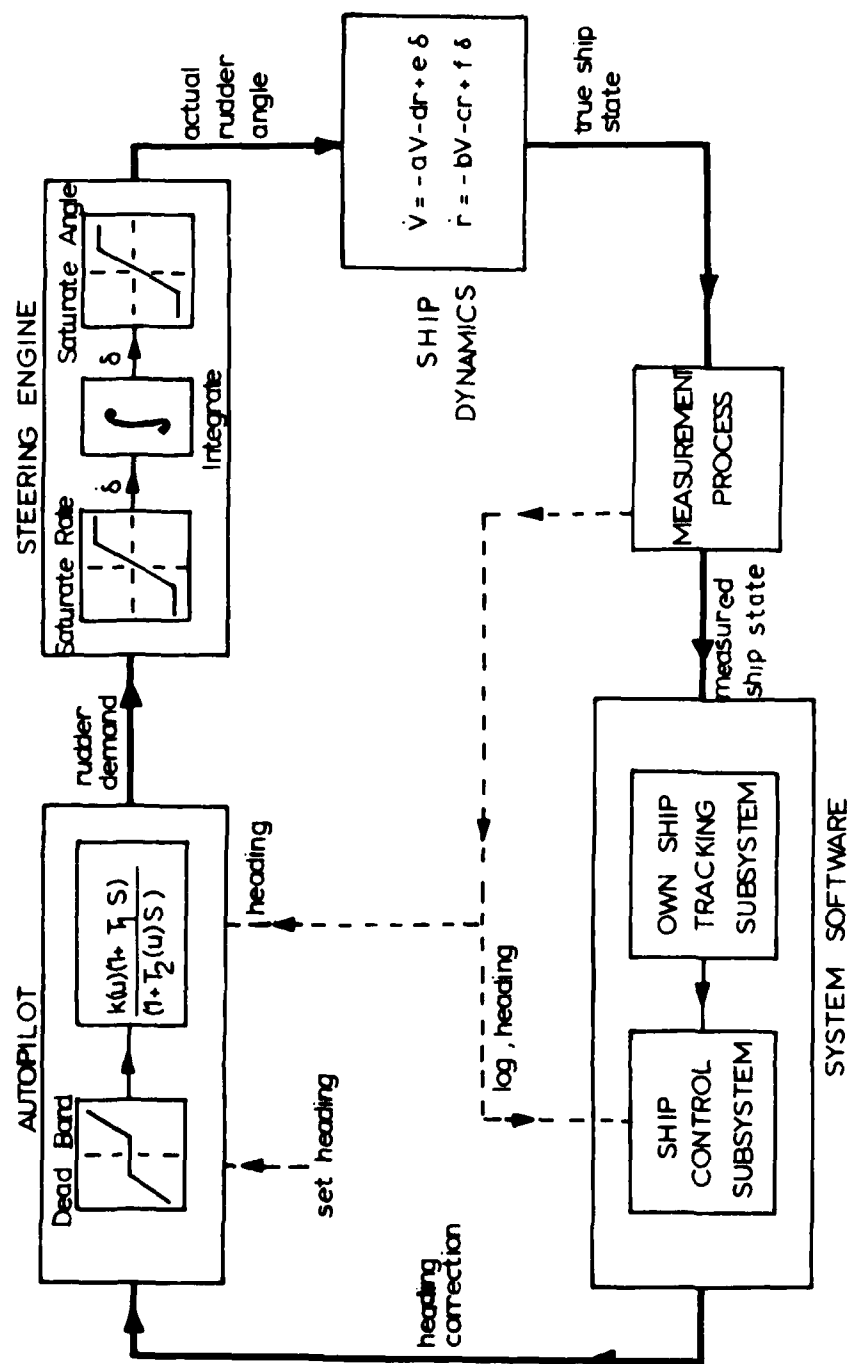
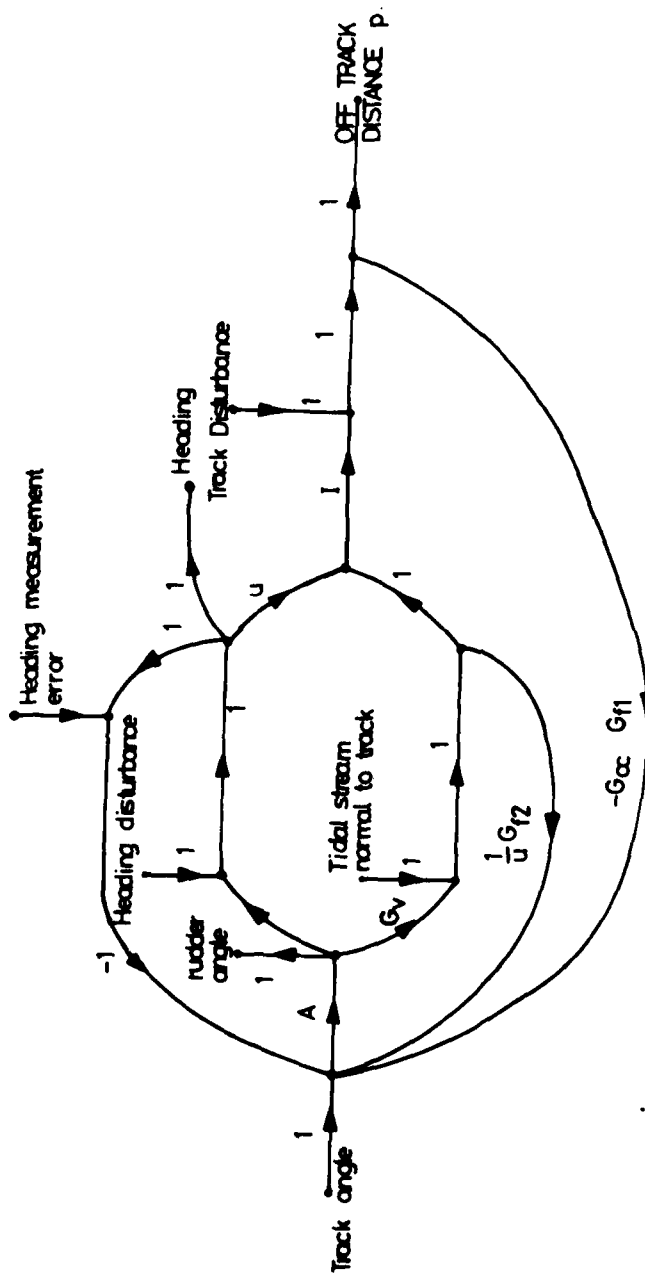


Figure 8. Block Diagram of Simulation Model



The transfer functions of each path represent:

- $A$  = Autopilot (rudder demand/heading error)
- $G_h$  = Ship heading/rudder angle
- $G_v$  = Ship sway velocity/rudder angle
- $I$  = Integrator

- $U$  = Ship speed through the water
- $G_{f1}, G_{f2}$  = Own ship tracking filter
- $G_{cc}$  = Course correction algorithm

Figure 7. Signal Flow Graph of System

Although this form of heading correction is capable of bringing the ship onto track in a tide with little or no overshoot, it does rely on an accurate estimate of the tide (or tide-equivalent effects) to achieve a zero steady state value of  $p$ , and, since no position feedback is used in the tide estimating algorithm, an open loop path exists. The final form of the course correction algorithm, which has been implemented, is a combination of the above two methods. If the proportional term is set to zero, then the angle  $\alpha$  is the steady-state heading correction to account for tidal stream. This can then be added to the first algorithm to give the corrected heading demand as:

$$\theta = \alpha + k_1 p + k_2 \int p \, dt.$$

#### Analysis and Simulation

The analysis of the system and calculation of the algorithm parameters was based on a simplified linear model with small angles assumed. This is summarized in the signal flow graph of figure 7. The other design tool developed was a digital simulation of the system that included mathematical models of the major components of the overall control system that are outside the computer, namely the sensors, the autopilot, the steering engine, the rudder and finally the ship itself. The mathematical description of these components is indicated in figure 8.

Another important feature of the simulation is that it has been constructed around the actual system software, rather than just the algorithms. This approach ensures that the software is rigorously exercised under realistic conditions and that effects due to quantisation errors in the implementation were not masked. Both the simulation and the system software are written in CORAL 66 to run on FMI600B machines.

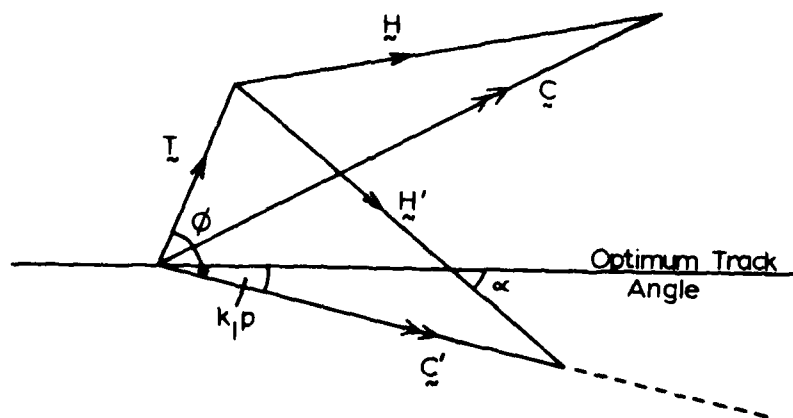
Figures 9 and 10 are simulation results illustrating the performance of the system at bringing the ship onto track in (a) zero tide and (b) 4 knot tide conditions when own ship's speed was 8 knots. The slight oscillations coming onto track are due to lags in the ship tracking filter, and the slight oscillation around  $p = 0$  when the optimum track has been achieved is due to a dead band built into the  $k_1 p$  term (for  $p$  less than 10 feet) in order to minimise rudder activity.

Once the initial design of the course correction algorithm had been established, the simulation was used to confirm that the linear analysis was a reasonable approximation to the system. The analysis was then extended to assess the magnitude of the coupling between the heading control loop and the track-keeping control loop, and to investigate the effects of random disturbances on the overall system. The coupling between ship heading disturbances and the resultant track deviations is represented by the transfer function  $G_{ht}$ , which can be found by applying Mason's theorems to the signal flow graph:

$$G_{ht} = \frac{-G_{cc} A G_h}{1 + A(G_h - G_{f2} G_v / U + G_{f1} G_{cc} I(G_h U + G_v))}$$

In a similar way the coupling between disturbances on the ships track and the resultant heading disturbances is characterised by the transfer function

$$G_{th} = \frac{I(U - 2A G_v)}{1 + A(G_h - G_{f2} G_v / U + G_{f1} G_{cc} I(G_h U + G_v))}$$



$\vec{H}$  = heading vector,  $S = |\vec{H}|$   
 $\vec{H}'$  = new heading vector  
 $\vec{C}$  = course vector  
 $\vec{C}'$  = new course vector  
 $\vec{T}$  = tidal stream vector,  $t = |\vec{T}|$   
 $\alpha$  = heading demand relative to optimum track  
 $k_1p$  = proportional off-track correction

$$\frac{\sin(\alpha - k_1p)}{t} = \frac{\sin \phi}{S}$$

$$\alpha = k_1p + \sin^{-1} \left\{ \frac{t}{S} \sin \phi \right\}$$

Figure 6. Course Correction Algorithm Using Tide Estimate

- 1- TRACKING 2 BUOYS,  $\sigma_R = 40\text{ft}$ ,  $R = 3000\text{ft}$ , PLANT NOISE =  $0.006\text{ft}^2/\text{sec}^4$
- 2- AS 1, EXCEPT TRACKING 3 BUOYS
- 3- AS 1, EXCEPT  $\sigma_R = 10\text{ft}$
- 4- AS 1, EXCEPT  $R = 900\text{ft}$

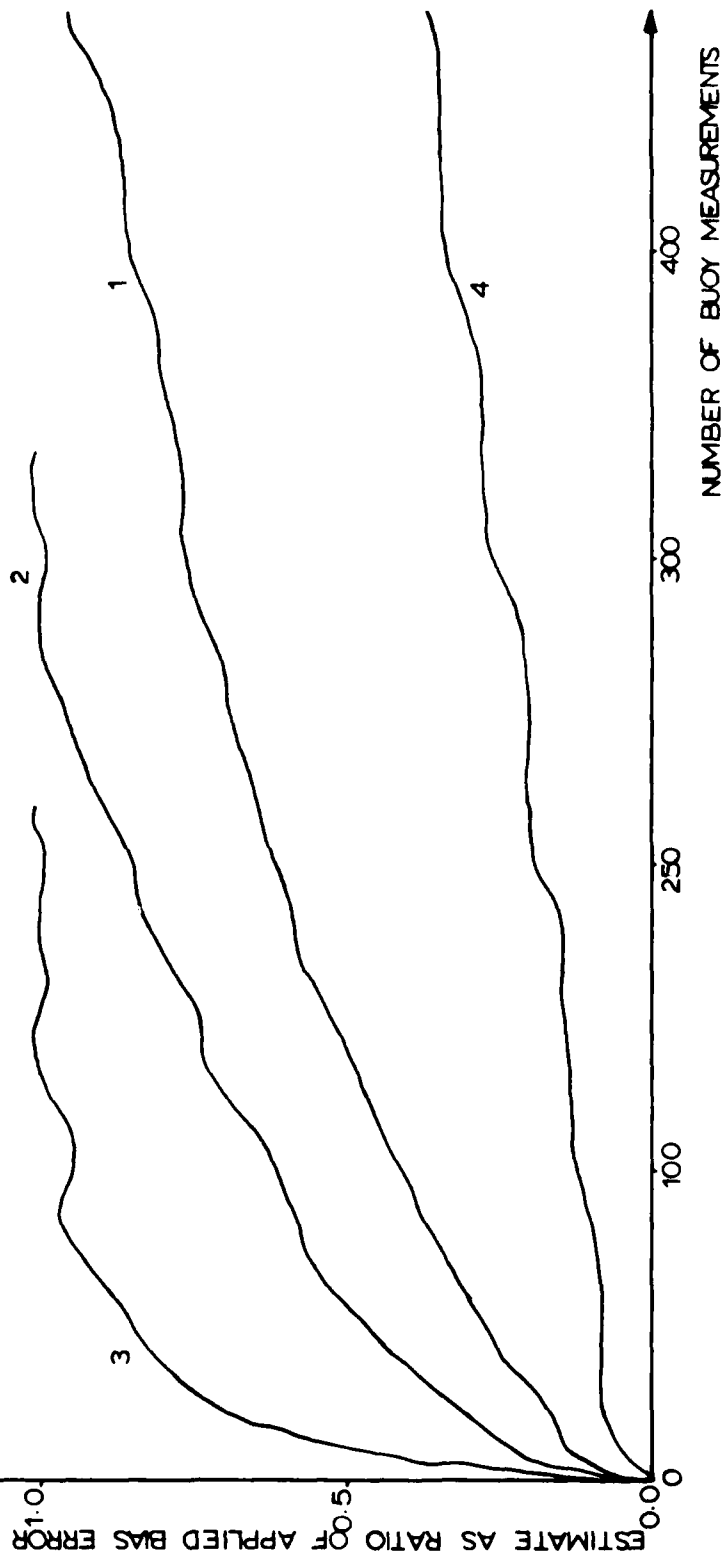
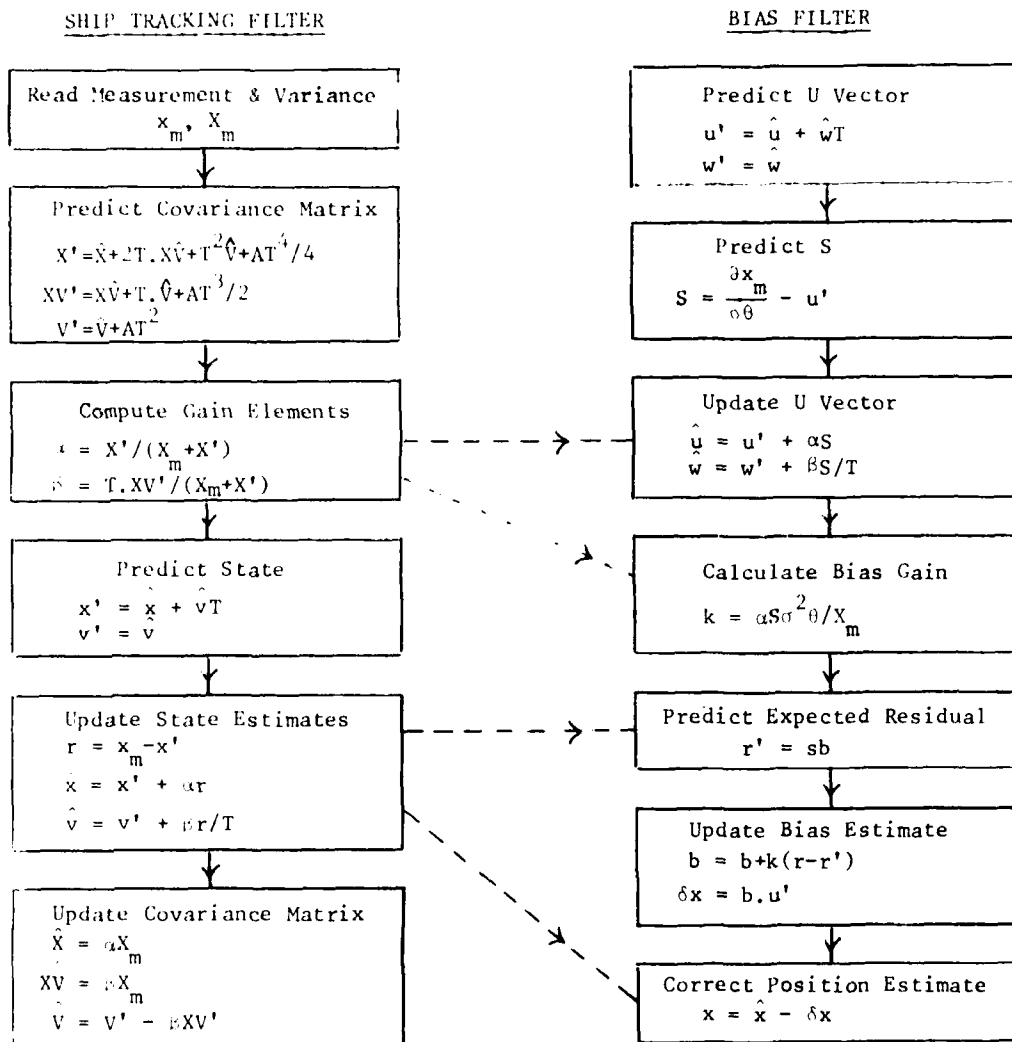


Figure 5. Initialisation of Bias Error in Various Geometries



**Notation**

$x, v$  are ship's position and velocity i.e. the state vector elements  
 $X, V, XV$  are the associated variances and covariance,  $A$  is the plant noise  
 $x_m, X_m, T$  are the measurement, measurement variance and measurement interval  
 $u, w$  are partial derivatives of the position and velocity with respect to the bearing bias  
 $s$  is the partial derivative of the measurement residual  $r$  w.r.t. bias.

Figure 4. Parallel Filter Scheme for Compass Bias Estimation



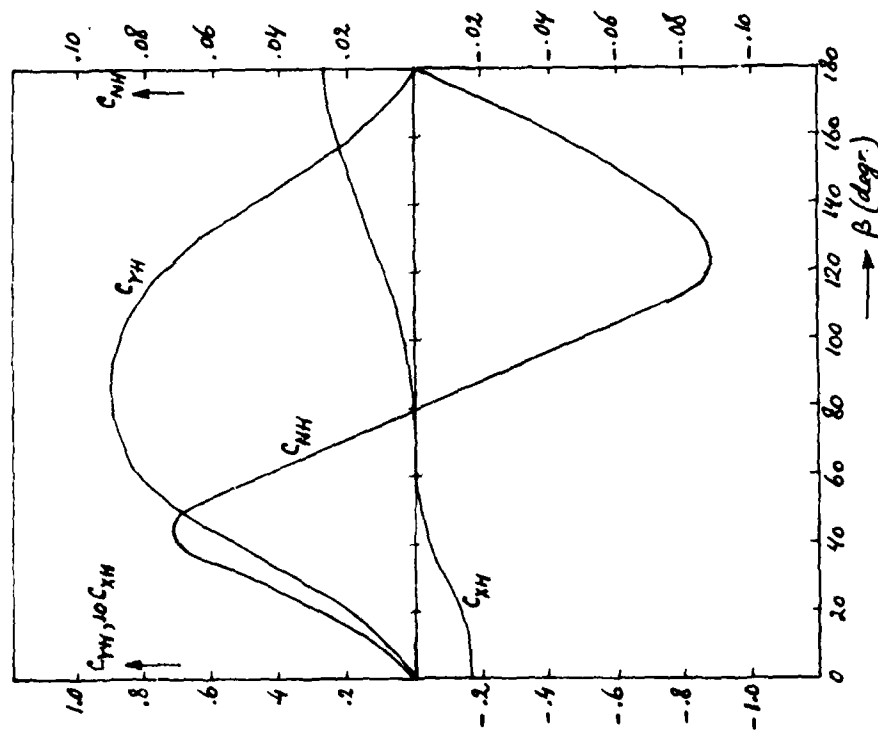


Figure 2: Hull coefficients as function of the drift angle.

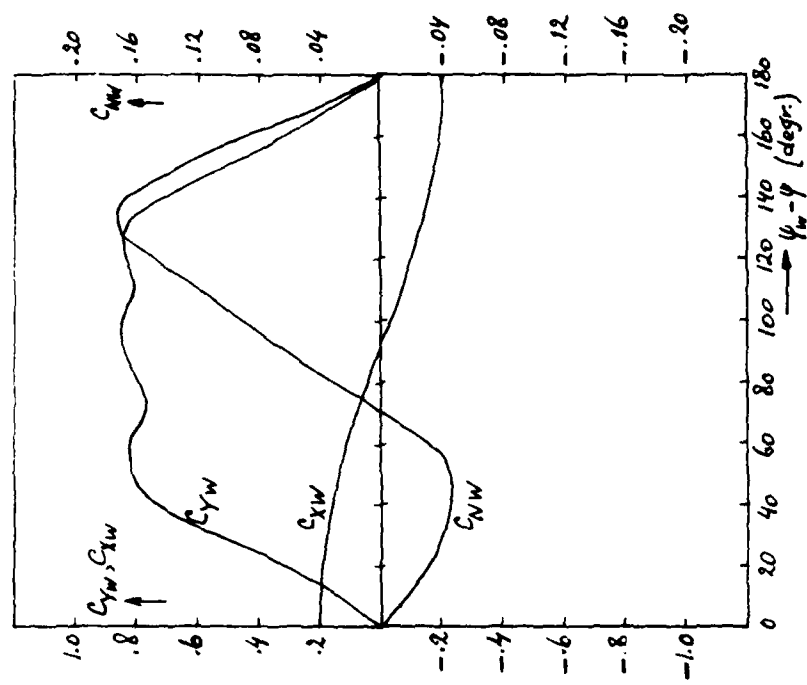


Figure 3: Wind coefficients as function of the relative wind direction.

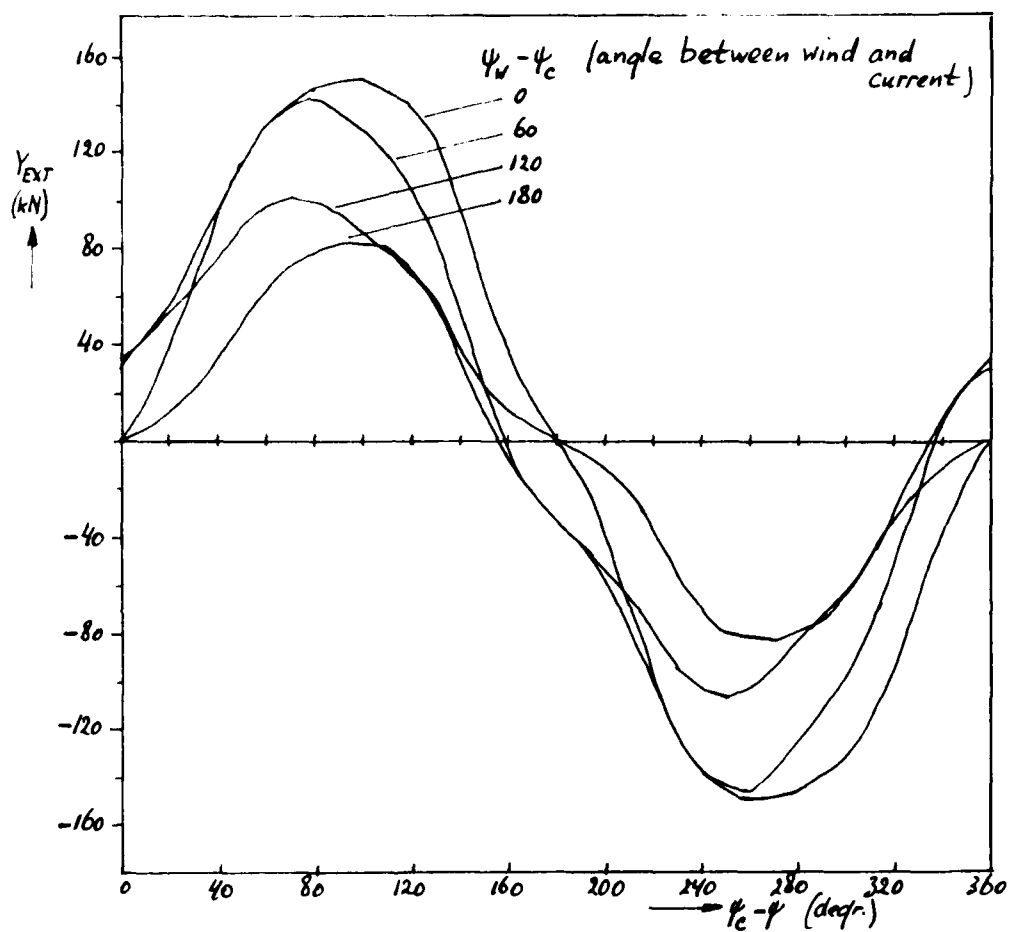


Figure 4: Total external force  $Y_{EXT}$  as function of the relative current angle.

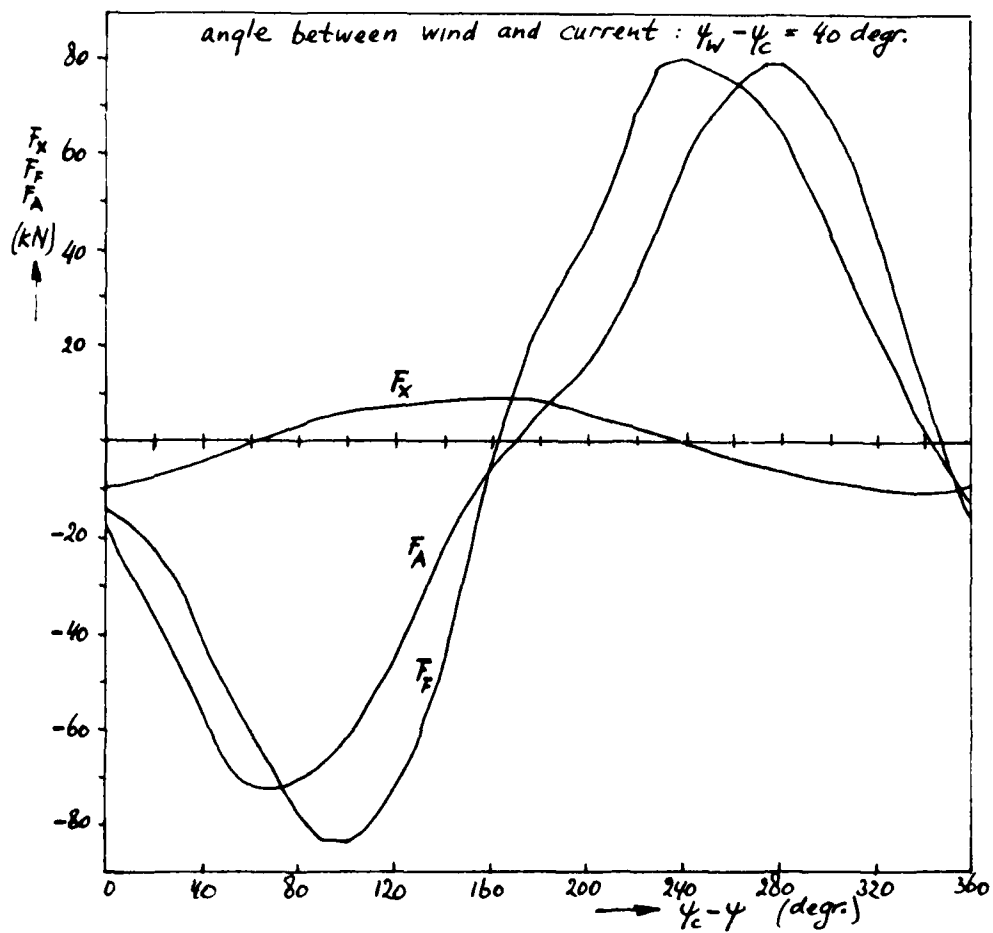


Figure 5: Restoring forces as function of the relative current angle.

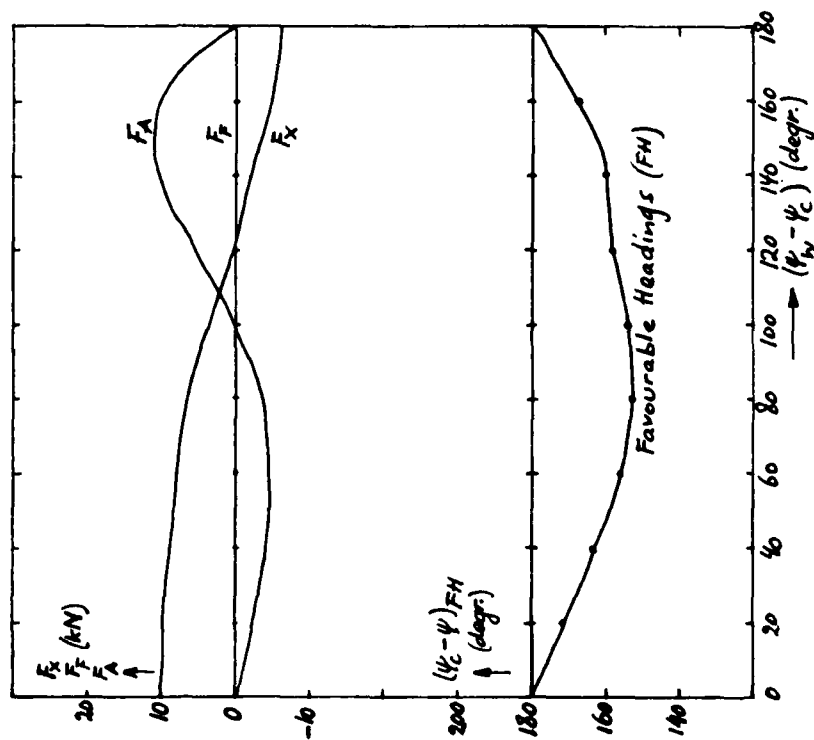


Figure 6: Favourable headings and required restoring forces.

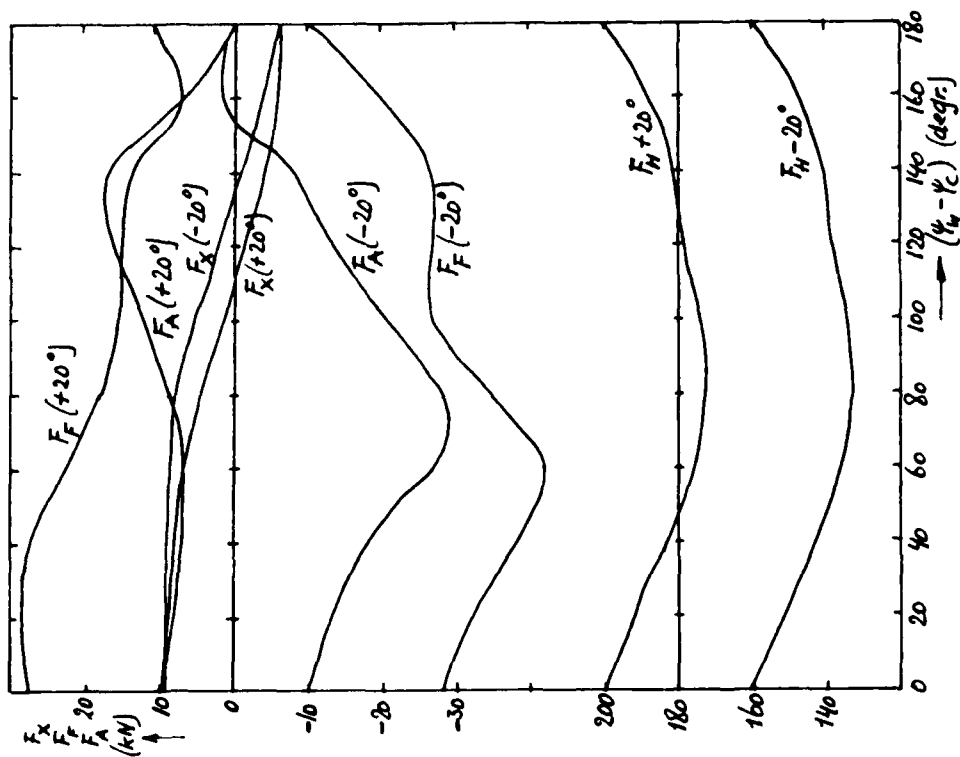


Figure 7: Favourable headings  $+20^\circ$  and required restoring forces.

### Available Restoring Forces

Two alternative thrust unit configurations were investigated. The first one being a combination of two active rudders in the aft section of the vessel and a bow thruster, the second one being two propellers in combination with two conventional rudders.

**Active Rudder Force.** The forces acting on an active rudder can be divided into two parts, being the ducted propeller and the rudder. It is assumed that the units are outside the wake area of the ship.

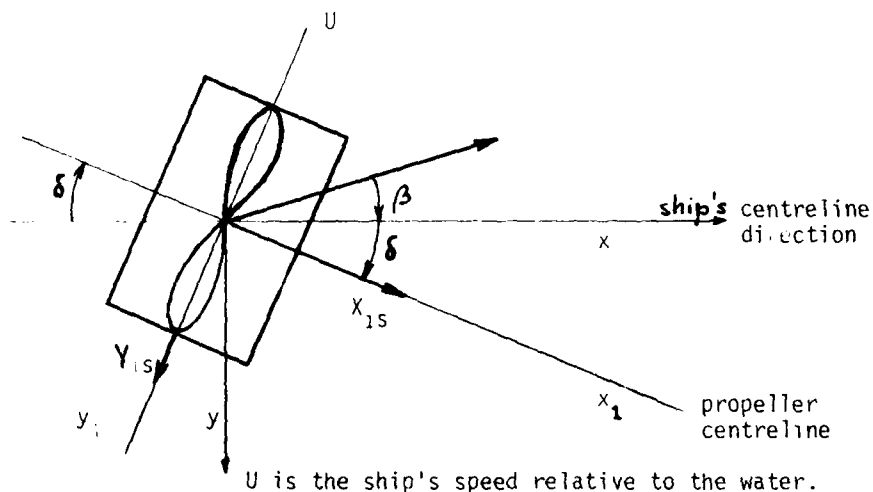


Figure 8: Axes systems of the ducted propeller.

The forces in x- and y direction are, as can be seen in figure 8:

$$X_s = X_{1s} \cos \delta - Y_{1s} \sin \delta$$

$$Y_s = X_{1s} \sin \delta + Y_{1s} \cos \delta$$

The forces  $X_{1s}$ ,  $Y_{1s}$  are functions of the propeller rpm, rudder angle  $\delta$  and velocity  $U$ .

### Bow Thruster Forces.

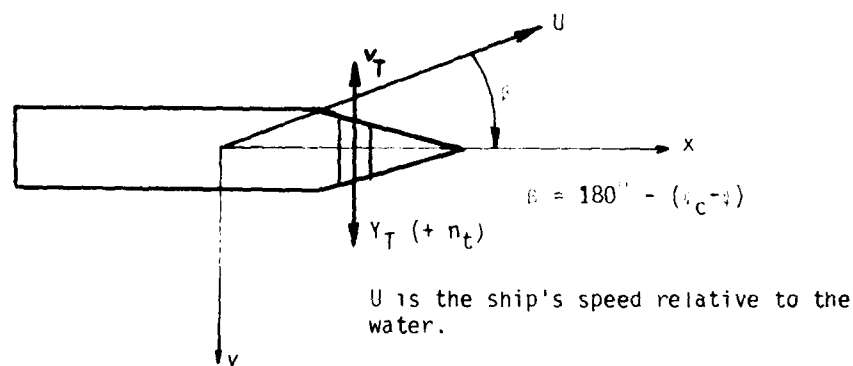


Figure 9: Nomenclature of the bow thruster.

The bow thruster force was assumed to:

$$Y_T = (\text{sign } n_t) \left[ 0.415 \cdot n_t \cdot D_t^2 - C_t U^2 \right] - C_{tR} B U^2$$

$$C_t = 780 \quad \text{with} \quad C_{tR} = 8300 \quad \text{when} \quad (\text{sign } n_t)B \geq 0$$

$$C_t = 0 \quad \text{with} \quad C_{tR} = 0 \quad \text{when} \quad (\text{sign } n_t)B < 0$$

Propeller and Conventional Rudder Forces. Propeller and rudder are in the wake of the ship and the rudder is in the slipstream of the propeller. The forces of both propellers acting on the ship in x direction are (forces of both propellers in y direction cancel each other):

$$X_S = 2(1 - 0.2)S = 1.6 S$$

where S is the thrust per propeller.

#### Positioning Capabilities

With the known characteristics of the thrust units the positioning capabilities were calculated. At first only the bow thruster capabilities were investigated, secondly the aft thruster capabilities and finally the combination of bow and aft thrusters.

Bow Thruster. For the most favourable headings the required thrust at the bow was zero. The nominal required thrust for headings at  $20^\circ$  on both sides of the most favourable heading is given in figure 10. In this figure also the available nominal thrust for two cases (0.8 tonf and 1.5 tonf) is shown.

In figure 11 the areas, where the lateral thrust at the bow of 0.8 and 1.5 tonf was sufficient to make position and heading keeping possible, are given in terms of off-sets from the most favourable headings as a function of the angle between wind and current direction. These areas thus apply only to the forward thruster.

Active Rudders. In figure 12 the area's, where the thrust generated by the specified active rudders at the stern was sufficient to make position and heading keeping possible, are given in terms of off-sets from the most favourable headings as a function of the angle between wind and current direction. These areas thus apply only to the active rudders.

Two areas can be distinguished: an area with propeller rpm ahead and an area with rpm astern.

Propellers and Conventional Rudders. The combination of propellers and conventional rudders was found to be inferior to the alternative configuration of active rudders and bow thruster.

Active Rudders and Bow Thrusters. Position and heading keeping is limited by bow thruster, as well as for 0.8 tonf as for 1.5 tonf.

For a bow thruster with a minimal thrust of 1 tonf and specified active rudders, the positioning and heading keeping areas were also calculated, see figure 13. In this graph also the rudder angle, relative rudder angle and the longitudinal thrust force per active rudder have been plotted. Moreover, the thrust force for which cavitation of the propeller is expected at the corresponding relative rudder angle, is shown. Cavitation data were supplied by the Netherlands Ship Model Basin, Wageningen.

## 4. SIMULATION MODEL

### Introduction

Figure 14 shows a block-diagram of the simulation model.

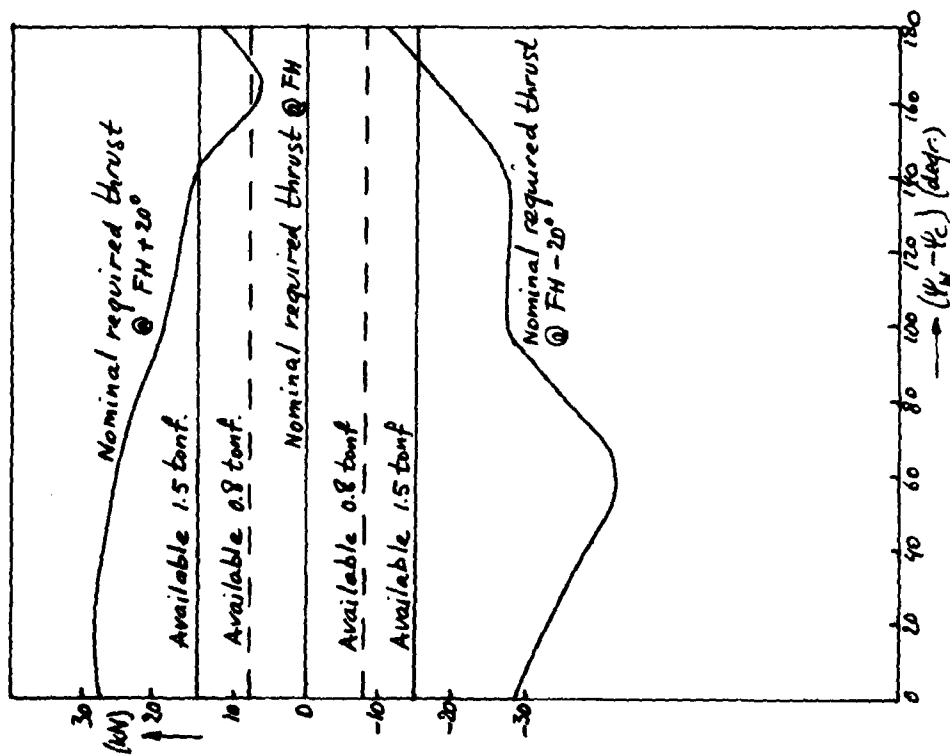


Figure 10: Available and nominal required thrust for the favourable headings and  $FH \pm 20^\circ$  for the bow thruster.

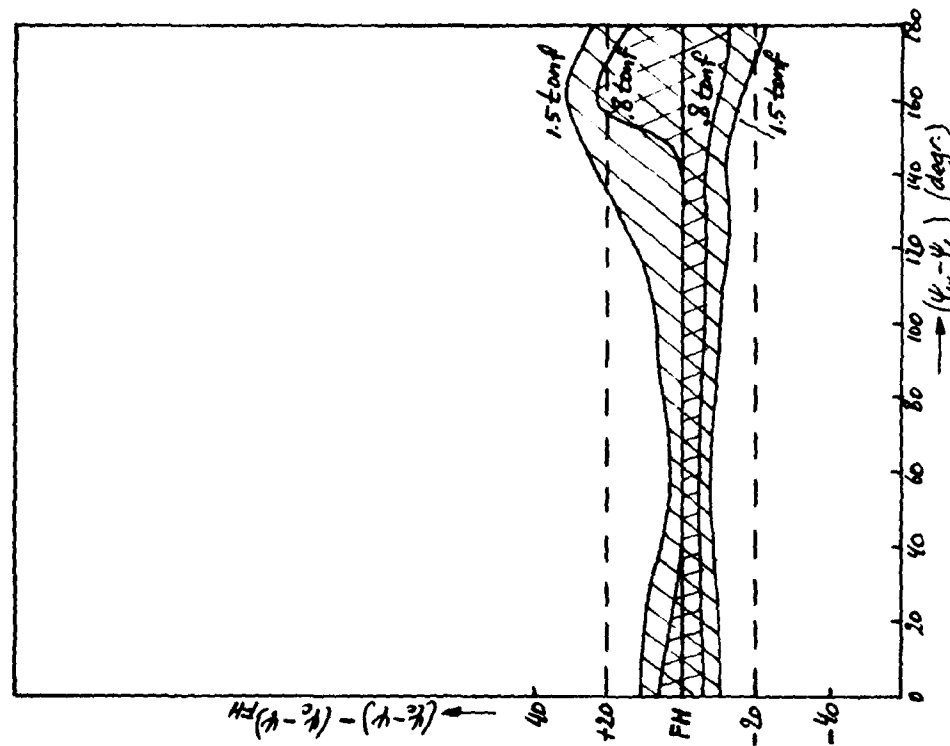


Figure 11: Possible equilibrium area's for the bow thruster.

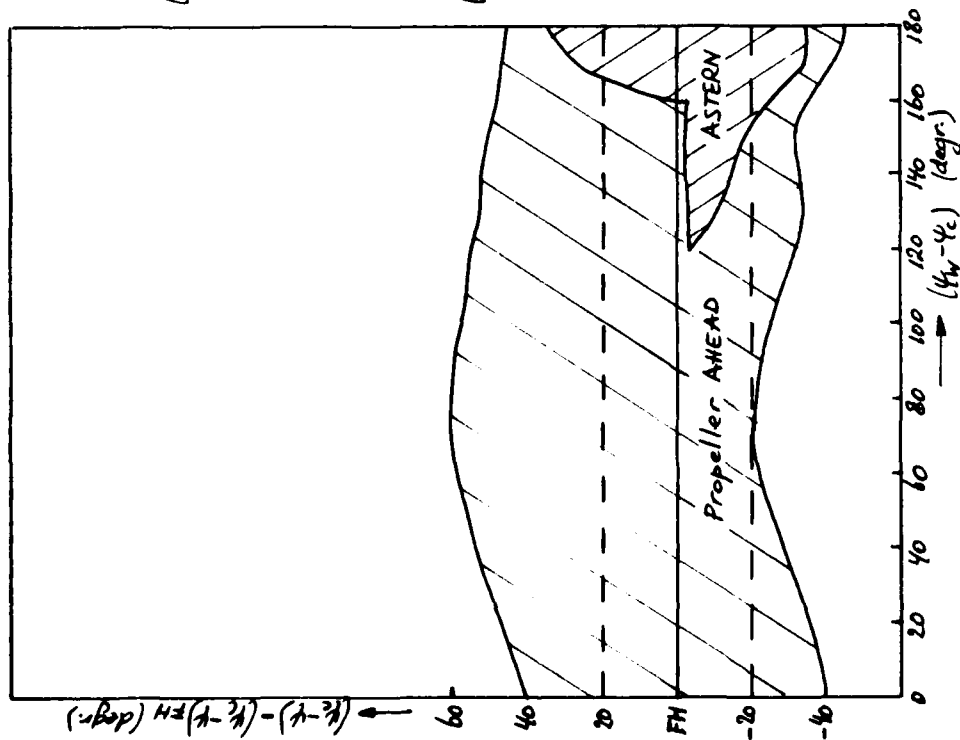


Figure 12: Possible equilibrium area's for active rudders.

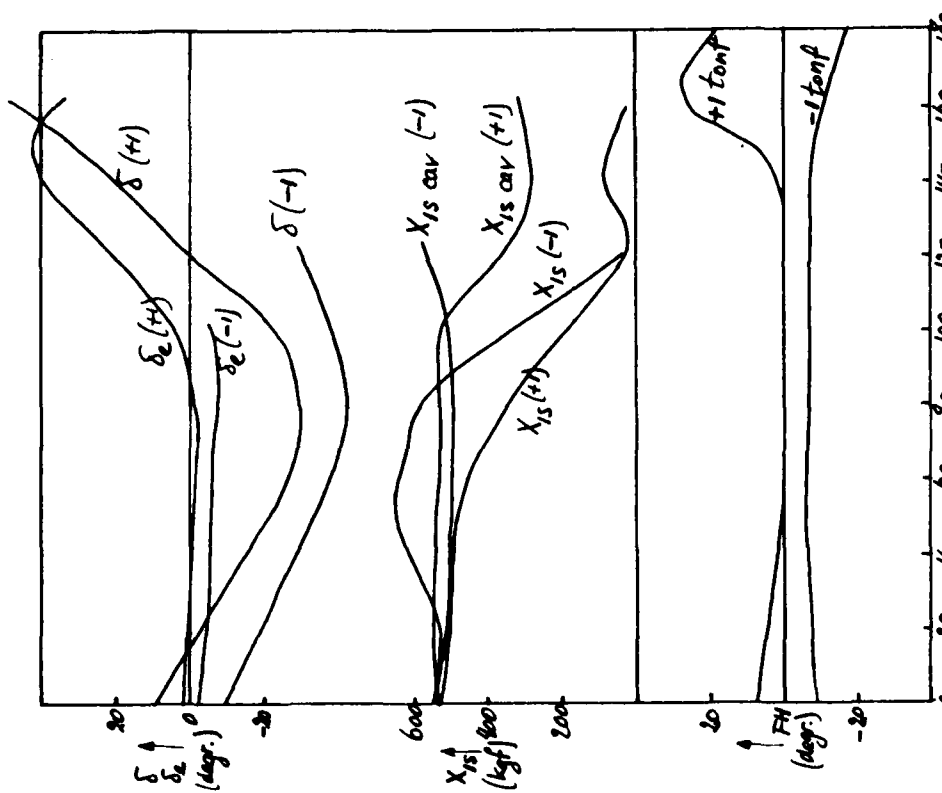
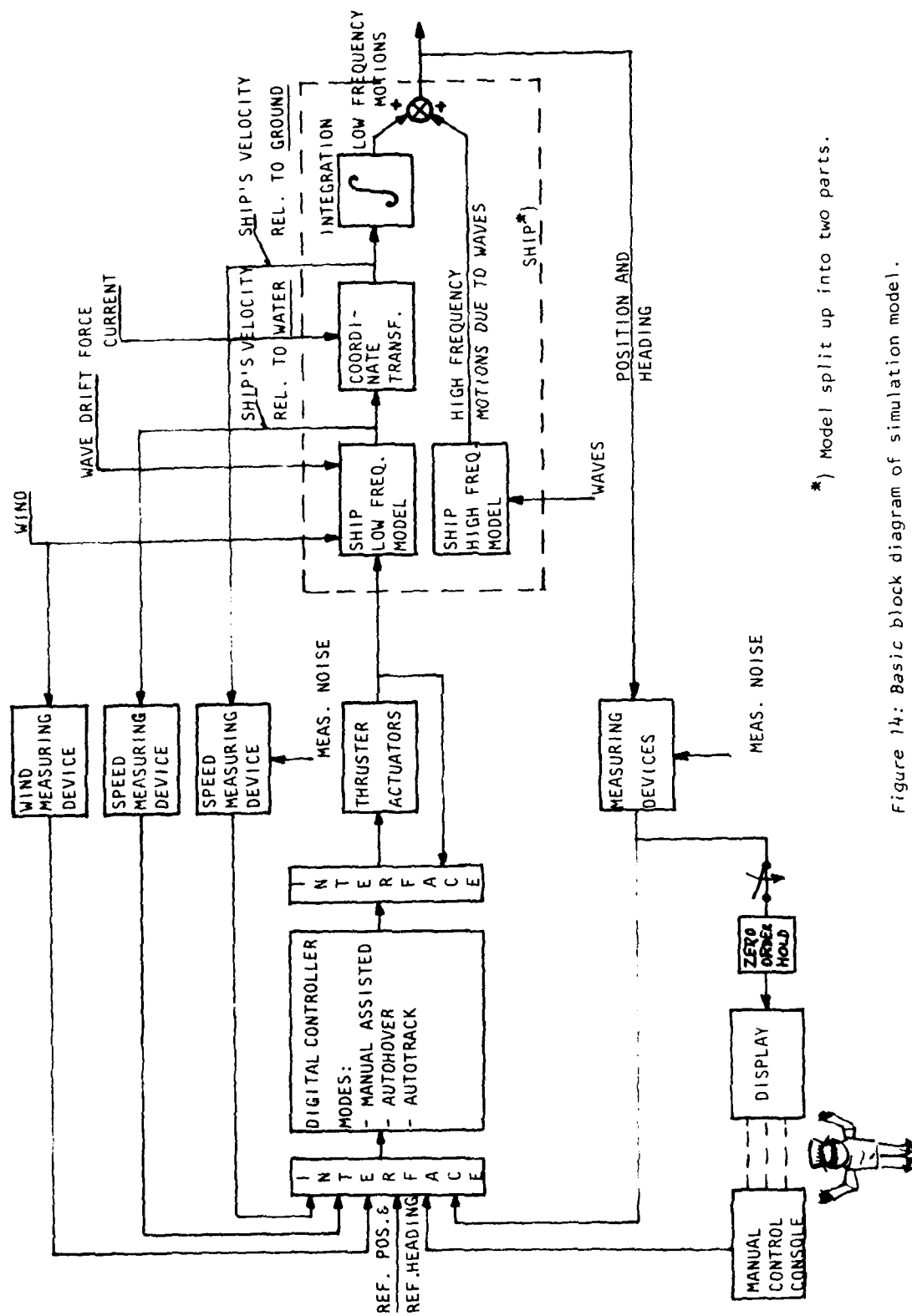


Figure 13: Possible equilibrium area's for a bow thruster of 1 tonf and active rudders; rudder angle; effective rudder angle; active rudder force in  $x_1$ -direction.





\*') Model split up into two parts.

Figure 14: Basic block diagram of simulation model.

The following components are part of the process: the vessel and the thrust units. The environment of wind, waves and current are the external disturbances. The process is controlled by a digital control system.

#### Mathematical Model of the Vessel

The block diagram shows two vessel models, a low frequency model and a high frequency model. During the simulation, the low frequency model is used. The high frequency model is used off-line to compute the effects due the waves. Only the results of these calculations are used on-line: the wave induced motions are superimposed on the low frequency motions, while the second order wave drift forces are introduced as external disturbances in the low frequency vessel model.

The low frequency model is explained below in more detail: Usually three coupled equations are taken into account, describing the motions in horizontal plane: longitudinal and lateral translation and rotation about the vertical axis. These equations are non-linear, however, the hydrodynamic coefficients are constant and not dependent on frequency. These coefficients were obtained from model tests, executed by the French "Bassin des Carènes". Once all forces and moments, acting on the vessel, are known, the acceleration of the vessel can be computed and subsequently the velocity, which is the velocity relative to water. By co-ordinate transformation and introduction of the ocean current, the velocity relative to earth is found. From that the position in earth fixed co-ordinates is computed. The vessel's heading is computed by direct integration (twice) of the yawing acceleration.

To obtain the total position and heading information, the high frequency wave induced motions have to be added.

#### Model of the Thrust Units

The model of the thrust units can be divided into two parts. The first part describes the response of the thrust units to command input signals, which are generated by the control computer.

The second part models the thrust, generated by the thrust units, taking into account interaction effects, and inflow velocity due to the vessel motions relative to the water. The necessary data were also obtained from model tests executed by the French "Bassin des Carènes". It is considered very important to take these effects into account in the simulation, because the performance of the thrust units may be significantly different from the open water performance, due to the presence of the hull and interaction between units.

#### Model of the Environment

Wind. At any given instant in time the wind speed can be regarded as being the sum of the mean wind speed taken over a suitable period and a superimposed gust component. The gust can be described as a random phenomenon of which the variations follow the Gaussian probability distribution. The same applies to the wind direction.

To simulate these random variations in speed and direction, the corresponding power spectra are modeled by means of shaping filters with inputs from white noise generators. The power spectra data are obtained from literature. Once the instantaneous windspeed and -direction are known, the windforces and moment are calculated, making use of coefficients derived from literature. A realistic wind simulation is of great importance in case of automatic control.

Waves. The effects of the waves (wave induced motions and wave drift forces) are computed off-line using special computer programmes.

The "high frequency" motions induced by the waves are oscillatory motions with zero and with frequencies equal to the wave frequencies (roughly between .05 Hz and .35 Hz). At the same time the vessel drifts off its position as the result of the second-order wave drift force.

To calculate the motions in 6 degrees of freedom, linear coupled equations of motions are used of which the coefficients are frequency-dependent. As a result, transfer functions in regular waves and motion spectra in irregular waves are obtained.

Also the mean wave driftforces and moment in regular and irregular waves are computed.

For simulation purpose, time series are needed of both the wave motions and the wave driftforces and moment in irregular waves.

Programmes are available, which convert the motion transfer functions into time series, for a given wave spectrum and which generate time series of the drift forces and moment, on the basis of the mean drift forces and moment in regular waves.

On-line, the wave induced motions are superimposed on the calculated low frequency position and heading, while the wave driftforces and moment are introduced at external disturbances, in the same way as the wind.

Simulation of the wave driftforces and moment, as they vary with time, is very important. This is because the natural frequency of the controlled vessel is in the frequency range of the driftforces, which may lead to relatively large excursions from the average position. This phenomenon must be observed during the simulation in order to take the proper measures.

Current. The (ocean) current comes only into play - as far as the vessel is concerned - when the velocity relative to water is converted into velocity relative to ground.

The accompanying forces are part of the total hydrodynamic forces, because the vessel's velocity relative to the water includes the current velocity.

## 5. STATION KEEPING

### General

The decision to incorporate an automatic controller for station keeping or "hovering" was to be based on a comparison of the hovering accuracy under manual and automatic control.

The task in both modes was:

Take and keep the entire ship between the two circles around the minelike object with radii 100 m and 200 m, thus c. of g. of the ship between a radius of 120 m and of 180 m, as indicated in figure 15, heading equal to the favourable heading. Starting point was at a distance of 240 m from the object, ground speed 3 kts, heading equal to the favourable heading.

The manual control simulation tests were performed by 9 officers of three navies. The simulation program was executed by each officer three times; each run had a duration of 20 minutes.

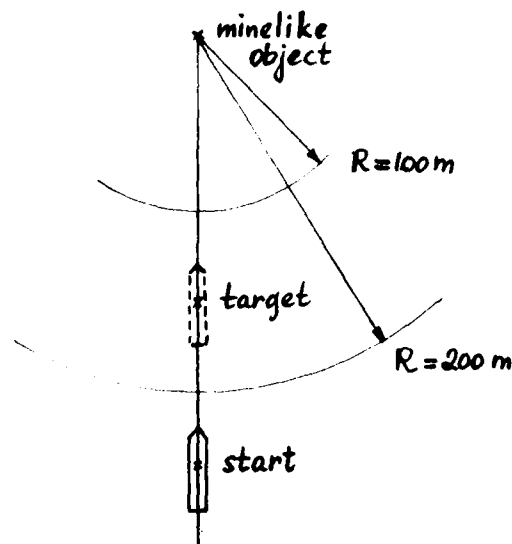


Figure 15: Task description.

The performance of the system with automatic control and of the system with human operator control were evaluated, using the following outputs after each run:

1. Time on target:

The time that the centre of gravity of the ship is in a sector originating from the object with an apex of 30 degrees and the bisectre parallel to the favourable heading and the distance from the c. of g. to the object  $R$  is  $120\text{ m} \leq R \leq 180\text{ m}$ , and the heading deviation from the favourable heading is less than or equal to 15 degrees (see figure 16).

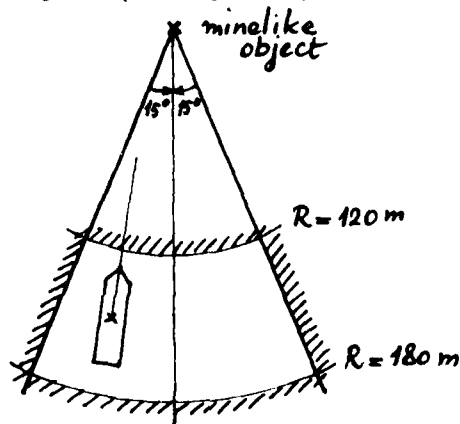


Figure 16: Time on target. The distance  $R$  to the object is determined for the ship's centre of gravity.

2. The number of times that the sonar base (coinciding with the c. of g.) crosses the circle with radius 120 m around the object (danger zone), and the minimum distance to the object.

3. Histograms, mean and mean square of:
  - distance to the object
  - heading deviation from the favourable heading
  - rudder angle
  - rpm of active rudders
  - total power consumption
  - net thrust of bow thruster.
4. The mean and mean square of:
  - the position of the manual control knobs - in case of manual control;
  - the control commands of rudder angle, rpm of active rudders,
  - rpm of bow thruster, valve opening of bow thruster - in case of automatic control.

#### The Manual Control System

The manual control system considered here is a system where certain functions are performed by the computer to lighten the task of the human operator. A block diagram of the manual control system is presented in figure 17. The operator uses the position- and heading information from the display to determine the setting of the controls of the system. Every two seconds the ship's position and heading is updated; in the position information the measurement error is present. The controls are a yawing knob (the position represents a demanded turning moment) and a joystick (the position represents a demanded force ahead or astern and to the left or to the right). From the position of the controls the computer calculates the required thrust of the bow thruster in direction and magnitude and the required rudder angle and rpm of the active rudders.

In these calculations information of the sonar doppler is used to adjust the rudder angle. After the demanded rudder angle and the thrust of the active rudders have been calculated, the computer checks if this thrust is below the thrust at cavitation inception in this situation; if not, the demanded thrust is taken to be the thrust at cavitation inception. This is the systems noise reduction feature, which feature was based on preliminary data obtained from the Netherlands Ship Model Basin in Wageningen.

Finally, the power demand is checked, based on the calculated demanded active rudder thrust, bow thruster rpm and the present power consumption. This power limitation feature will reduce the demanded rpm of the active rudders - if the total power consumption should exceed the available power -, in such a way that the bow thruster will always have the demanded power available.

#### The Automatic Control System

General. The system, which is used during automatic hovering includes a measurement system and a control system. A schematic diagram is presented in figure 18. In the first part of the control system, the thrust and moment, which are required to hold position, are calculated. The force and moment due to wind are taken into account ("wind feed forward"-control).

In the second part the commands are calculated, which are sent to the actuators (active rudders and bow thruster). That part is also used in the manual control system.

Once a set point (position and heading) has been defined, the automatic control system keeps the ship at that point. The operator may, however, choose to adjust the position and/or heading set point. Once he has validated the adjustment, the actual set point is changed smoothly.

#### Digital Control System

- 1) First, the signals are passed through low-pass filters to filter out high frequency components.
- 2) Then the position- and heading rate-limited command-signals are calculated and the position error and heading error signals.

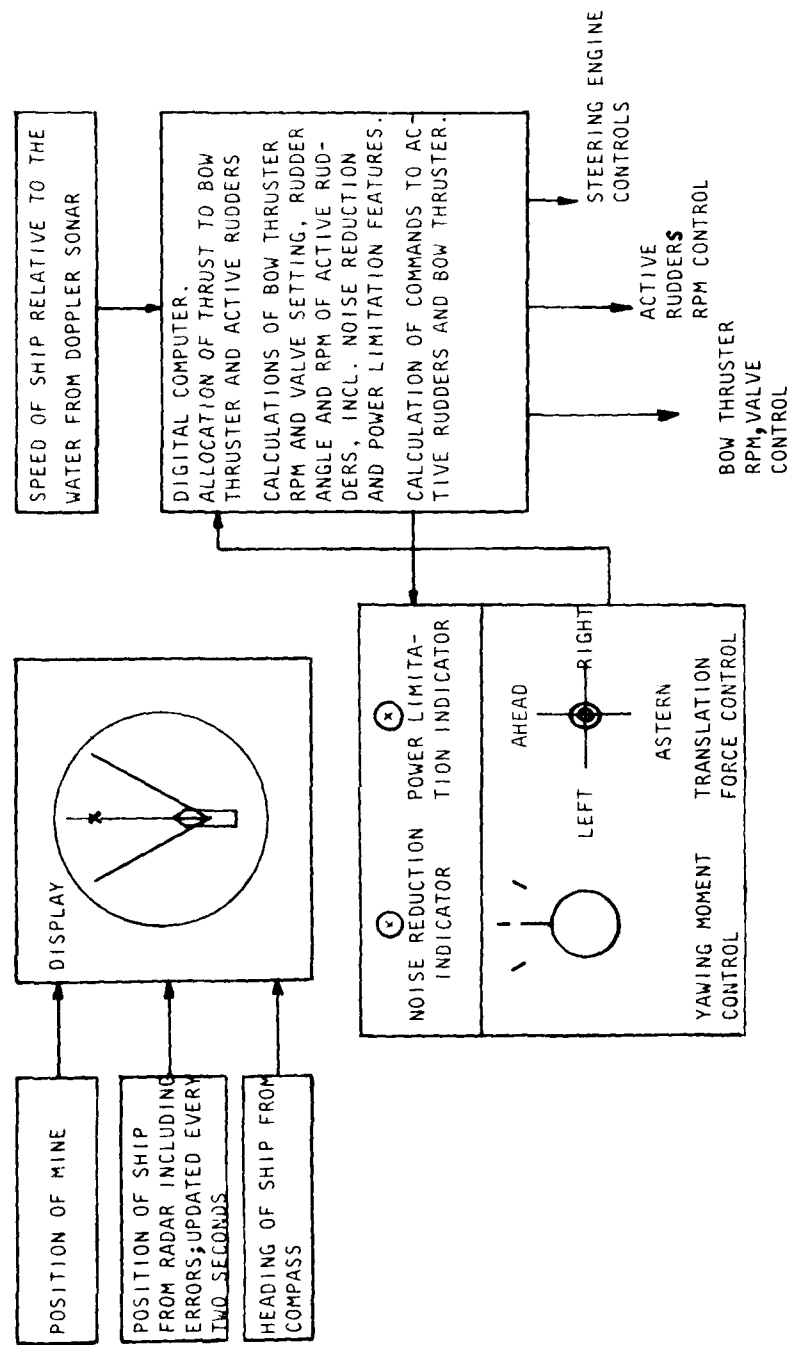


Figure 17: Block diagram of manual control system.

AD-A159 082

PROCEEDINGS OF THE SHIP CONTROL SYSTEMS SYMPOSIUM (5TH)

244

HELD AT U S NAVAL... (U) DAVID W TAYLOR NAVAL SHIP

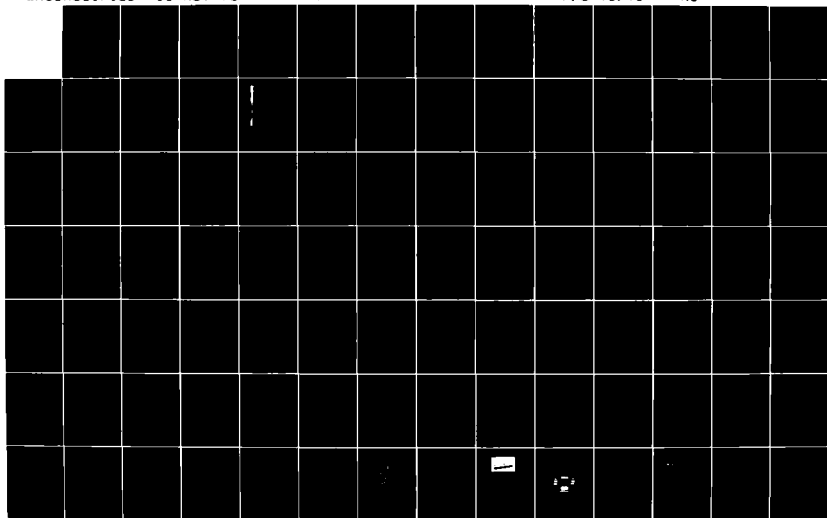
RESEARCH AND DEVELOPMENT CENTER ANN... P MARTIN ET AL.

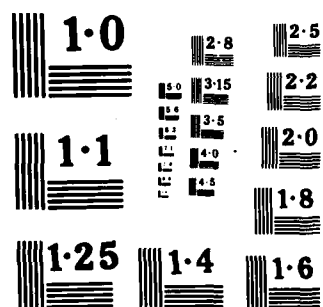
UNCLASSIFIED

03 NOV 78

F/G 13/10

NL









The rate-limited command signals are calculated as follows:

In case the operator changes the set point and validates the set point adjustment, the new set point is compared with the old one.

As long as the difference exceeds a threshold-value, the set point is updated at a constant rate. In this way any set point change is processed very smoothly.

- 3) Next, the demanded thrust and moment are calculated, taking into account the position or heading error itself, the rate of change of the error and the time-integral of the error. This type of control is commonly known as PID-control. It should be noted that all individual contributions are limited, as well as the total value.

For the rate of change of the position-error ( in longitudinal and lateral direction) the ground speed signals, as measured by the Doppler-sonar, are used. In case the integral value of the ship's lateral motion exceeds a threshold value, the heading set point is changed by a few degrees to a maximum of  $5^{\circ}$  or  $7.5^{\circ}$  dependent on the weather conditions. The heading set point change makes the ship move in lateral direction. This procedure should keep the lateral motion of the ship within reasonable limits.

- 4) The demanded thrust and moment are corrected for the wind force and moment: Using the measured wind speed and - direction signals, the wind force and moment acting on the ship are calculated. By subtracting the wind force and moment from the demanded thrust, as defined under 3), the influence of the wind is counteracted in advance. This procedure is called wind feed forward control.
- 5) Once the net demanded thrust and moment are known, the command signals are calculated, which determine the setting of the active rudders (angle and rpm) and of the bow thruster (valve opening and rpm). In these calculations information of the doppler-sonar is used to adjust the angle of the active rudders. This is done because the force developed by the active rudders is also a function of the velocity of the vessel relative to the water. Finally, the command signals are checked by the noise reduction and power limitation features.

#### Comparison of Manual and Automatic Control by Means of Simulation

The following simulation program was carried out to compare the manual with the automatic control system:

Table 2: Simulation program - Weather conditions.

TEST No.	WIND	WAVES	CURRENT
	SPEED/DIRECTION	STATE/DIRECTION	SPEED/DIRECTION
1.	no wind	no waves	no current
2.	Beaufort 5 mean 20 kts/ $180^{\circ}$	Sea state 3/ $150^{\circ}$	no current
3.	Beaufort 5 mean 20 kts/ $233^{\circ}$	Sea state 3/ $240^{\circ}$	2 kts/ $153^{\circ}$
4.	Beaufort 5 mean 20 kts/ $327^{\circ}$	Sea state 3/ $330^{\circ}$	2 kts/ $167^{\circ}$
5.	Beaufort 7 mean 30 kts/ $233^{\circ}$	Sea state 5/ $240^{\circ}$	3 kts/ $153^{\circ}$
6.	Beaufort 7 mean 30 kts/ $327^{\circ}$	Sea state 5/ $330^{\circ}$	3 kts/ $167^{\circ}$
NOTE: A direction of $180^{\circ}$ means: on the bow; $150^{\circ}$ means $30^{\circ}$ off bow, etc..			

Both windspeed and -direction signals included gusts. The sea state was defined by means of a modified Pierson-Moskowitz wave spectrum:

- sea state 3: significant wave height 1.5 m, mean wave period 4 s;
- sea state 5: significant wave height 3.0 m, mean wave period 7 s.

The comparison was made on the basis of statistical data, see the figures 19 - 23, and of recordings. Samples of recordings of tests 2 and 6 are given in the figures 27 - 30.

Distance to the Object. The "ideal" distance to the object is 150 m. Figure 19 shows that the ACS holds the ship closer to the ideal position than the manually controlled runs. This figure applies only to the mean value. Typical examples for the various test situations are given in the figures 24 - 26. These histograms illustrate that also the variation of the distance to the object is quite different for almost all tests. It is worthwhile, in this respect, to note the number of crossings of the danger circle and the minimum distance to the object, see figures 22 and 23. The ACS keeps the vessel away from the danger zone, while under manual control the danger zone is entered.

Time on target: From figure 21 it can be seen that the ACS scores better. The ACS score can never be 1200 sec., since the starting position is 240 m, outside the required zone.

Heading relative to the favourable heading: From figure 20 it can be seen that the ACS keeps the heading closer to the favourable heading. It should be noted, that the operators in the manual mode can choose, during the run, a favourable heading which is different from the initial one. The same applies to the ACS if the operator selects the so-called "coupling feature", the ACS adjusts its favourable or reference heading dependent on the lateral motion of the ship. This feature was selected during tests 2, 5 and 6.

From the individual recordings-examples are given in the figures 27 - 30 - it is concluded that the position is more stable in the case of the ACS. The heading is the most critical parameter to control, which task depends very much on the environmental conditions. This applies to both systems.

It should be noted that manual control recordings show on channel 5, 6 and 7 the control stick positions (longitudinal and lateral) and control knob position, respectively. The automatic control recordings present on the same channels the rps and valve opening of the bow thruster and rps of active rudders, respectively.

In conclusion the following can be said:

- As far as position keeping is concerned, the automatic control systems shows much better performance.

A very important point is that, during the tests, the ship under automatic control never crossed the danger circle, which is in contrast with the manually controlled vessel, see figure 22. Consequently, the minimum distance to the object was much smaller for the manually controlled vessel.

During the experiments the human operator had to pay full attention to the handling of the vessel. It is clear that, if the operating officer of the vessel under real conditions has any additional task, the performance will be much less. The performance will also depend on the type of display.

Although the automatic control system must be monitored, the officer will be able to carry out additional tasks, if necessary, during most of the time.

- Another important aspect is that the study of the manual control had the objective to compare the performance with the automatic control only. No general conclusions can be drawn on the performance of the manually controlled vessel, because only a limited number of situations have been tested.

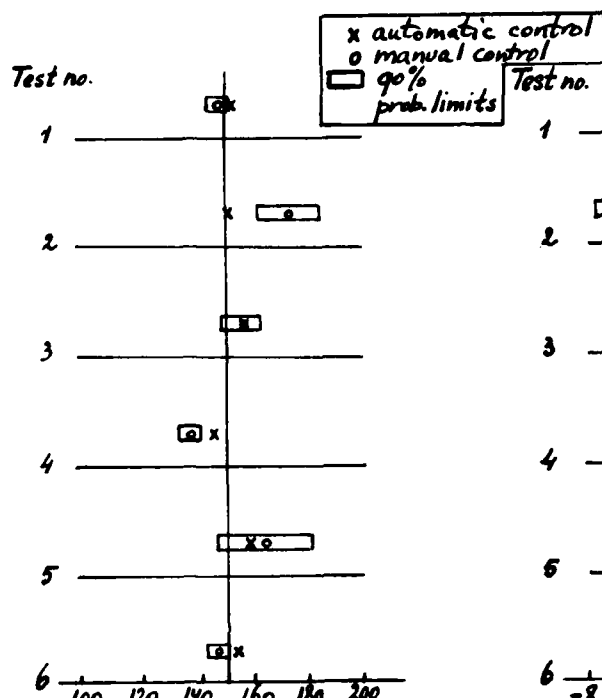


Figure 19: Mean values of the mean distance to the object (meters).

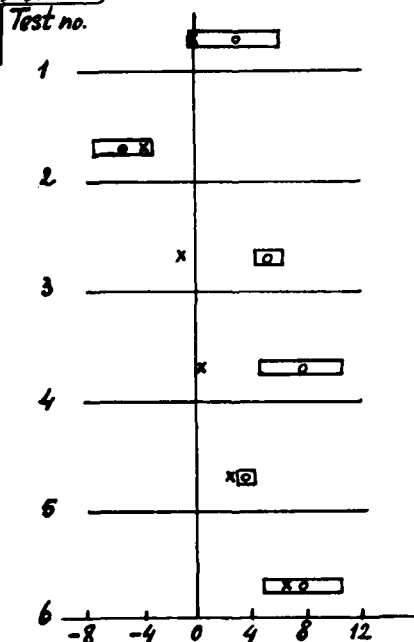


Figure 20: Mean values of the mean heading relative to favourable heading (degrees).

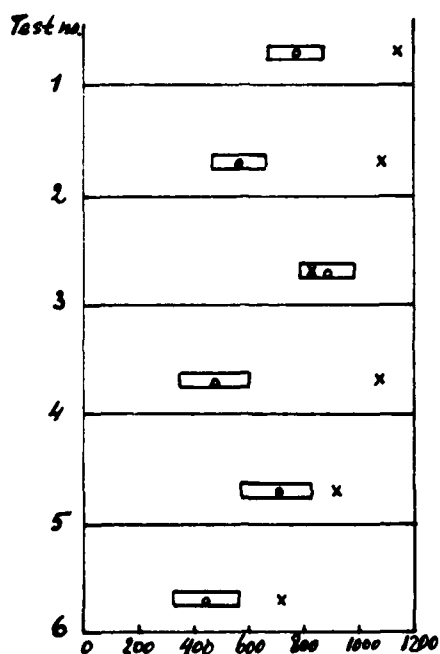


Figure 21: Mean time on target (seconds).

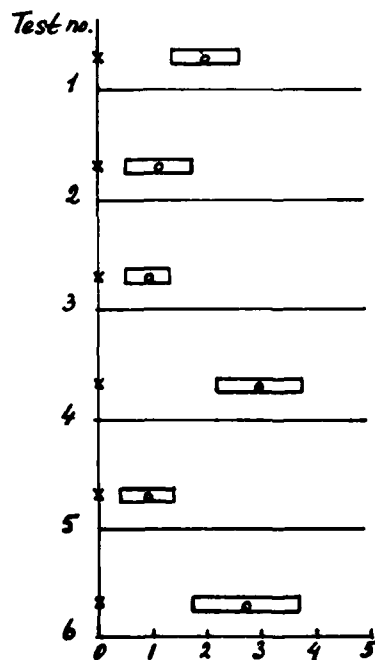


Figure 22: Mean values of the number of crossings of the danger circle.

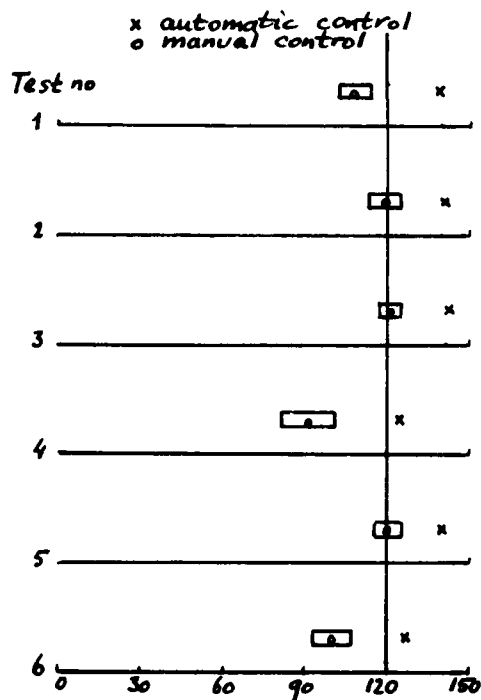


Figure 23: Mean values of the minimum distance to the object (meters)

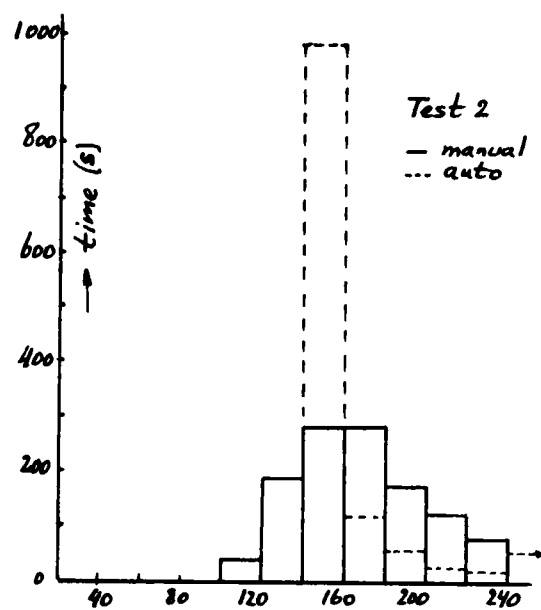


Figure 24: Histogram of the distance to the object (meters) - average of all operators.

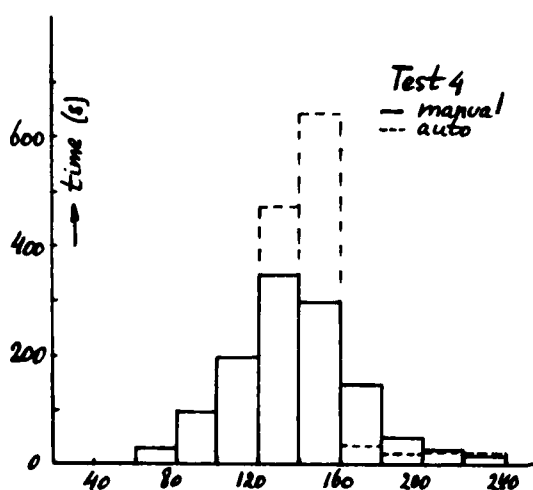


Figure 25: Histogram of the distance to the object (meters) - average of all operators.

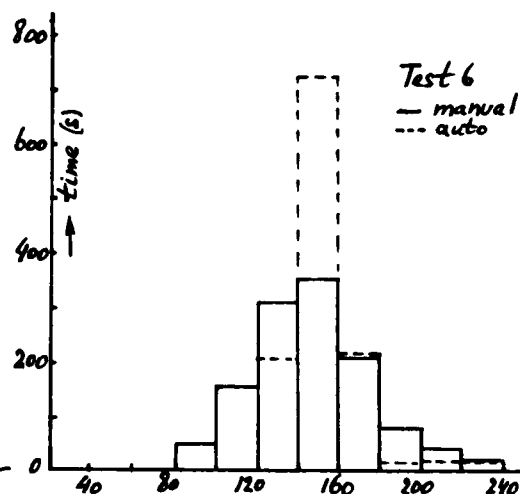
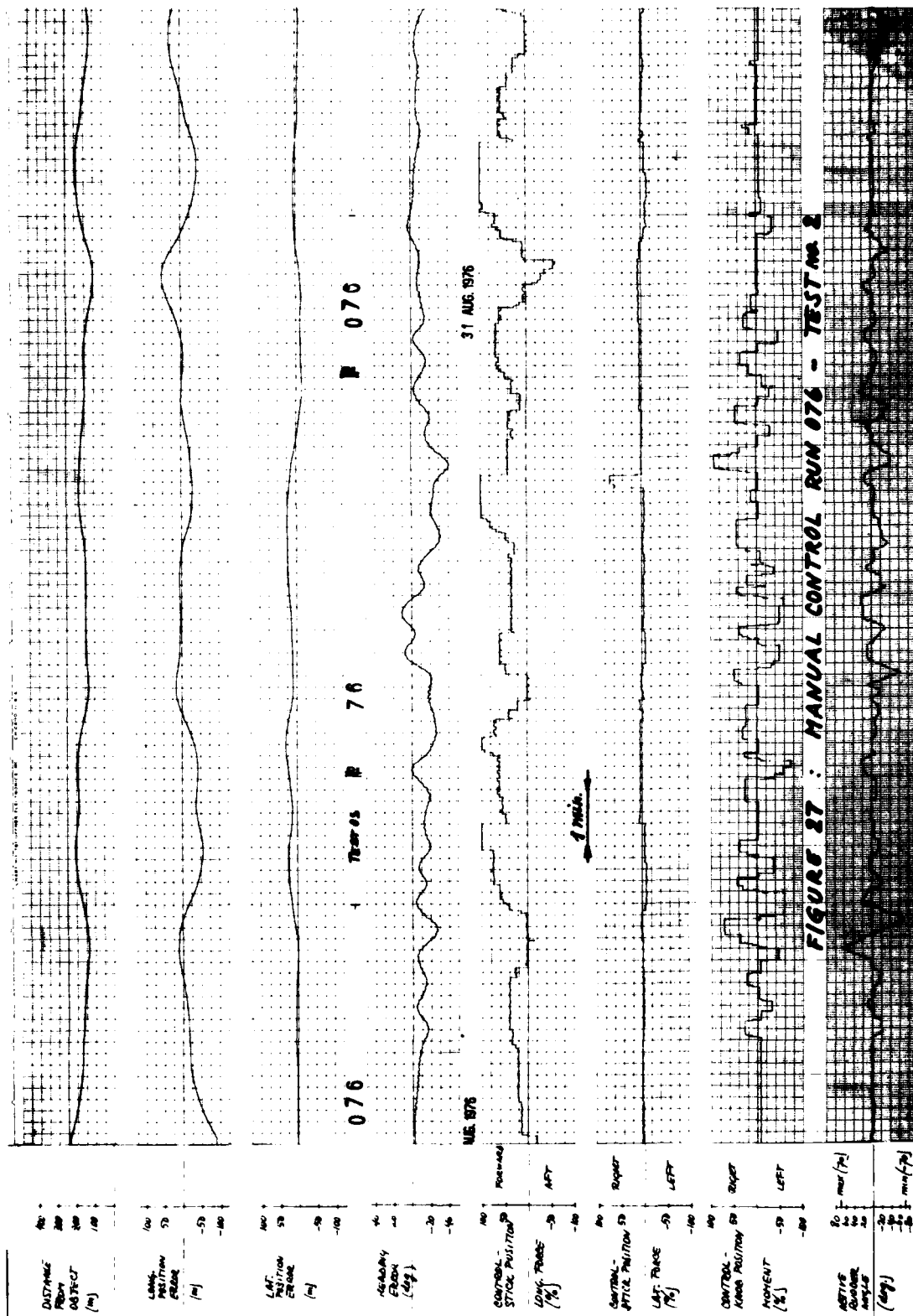


Figure 26: Histogram of the distance to the object (meters) - average of all operators.



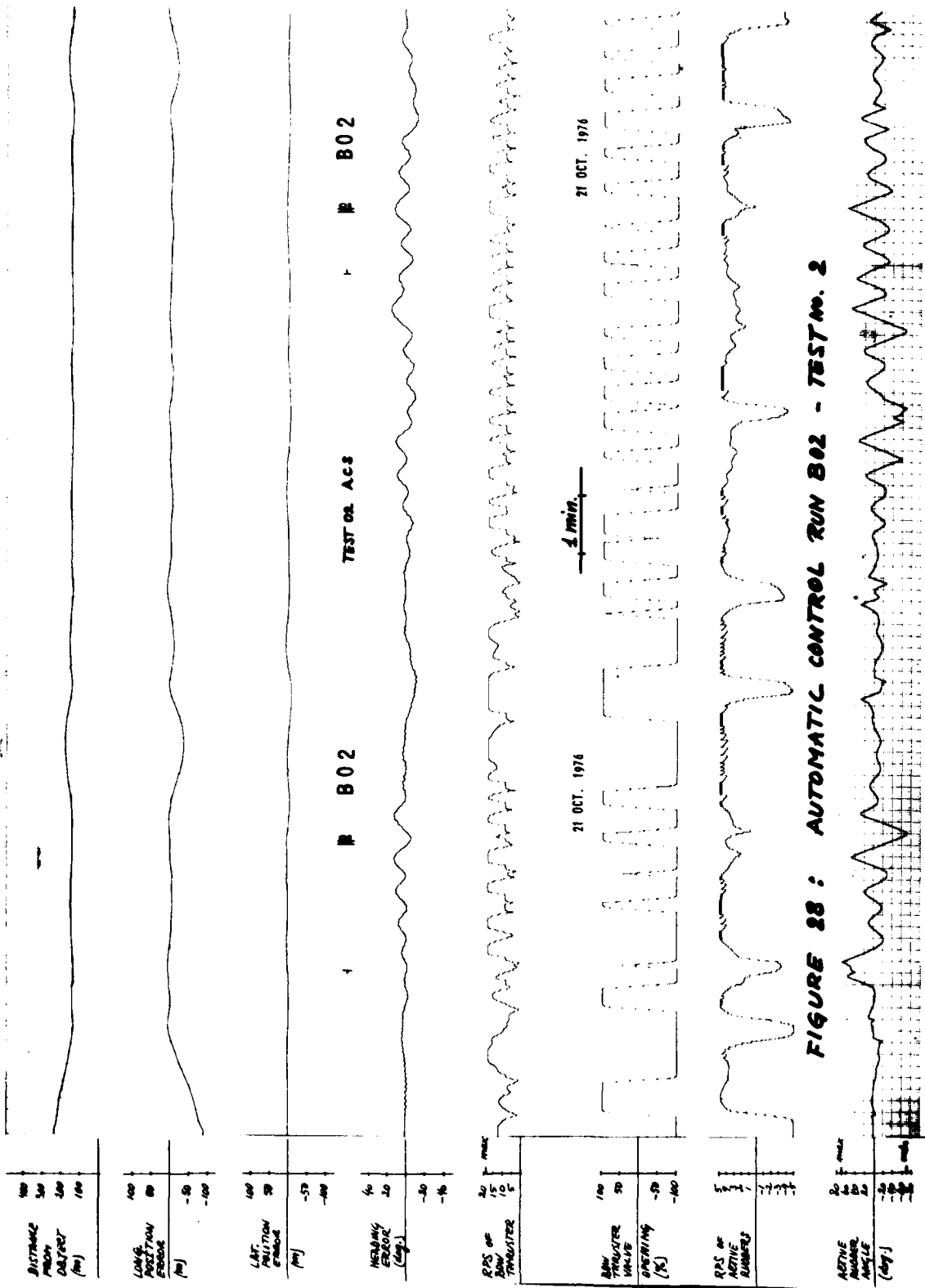
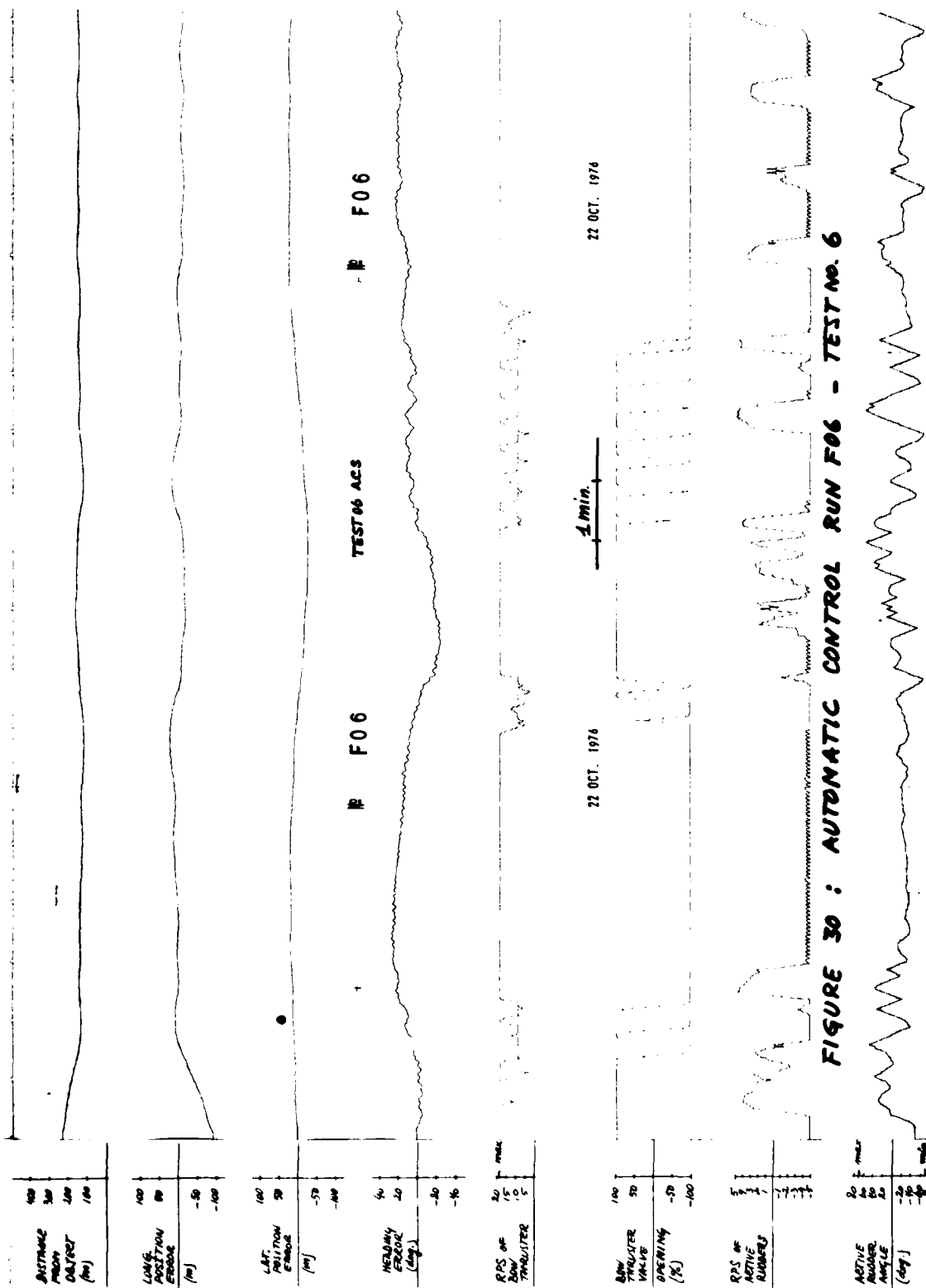


FIGURE 28 : AUTOMATIC CONTROL RUN B02 - TEST No. 2







- The same applies, to a smaller extent, to the automatic controlled vessel.
- The automatic control system design, being preliminary, should be further improved. The heading control channel shows periodic oscillations, which should be avoided.

## 6. AUTOMATIC TRACKKEEPING

### Introduction

As part of the design and development of the Tripartite minehunter also a simulation study has been carried out of the vessel in the automatic trackkeeping mode.

The objective was the development of the automatic trackkeeping control system, while intercepting and following a predetermined track under varying weather conditions and at different speeds.

The trackkeeping requirements were such that under normal conditions - wind-velocity up to 20 kts, sea state 3, current velocity 2 kts - trackkeeping should be better than 20 meters ( $2\sigma$ -value). Under more severe conditions - wind-velocity up to 30 kts, sea state 5, current-velocity 3 kts - trackkeeping accuracy should be better than 40 meters ( $2\sigma$ -value). Vessel speed relative to the water between 2 kts and 7 kts with corresponding groundspeed between 1 kts and 5 kts. Maximum drift or crabangle during trackkeeping should be about  $15^\circ$ .

The bow thruster should not be used. Only the two active rudders should be used, with a maximum allowable rudder angle of  $\pm 35$  degrees, instead of  $\pm 70^\circ$  during station keeping.

### Automatic Trackkeeping Control System

Figure 31 shows how the signals, which are received from the measuring devices, are handled. These signals are position and heading and the speed relative to water and ground from the Doppler Sonar. The windmeter signals are not processed in this mode of operation.

The control system has three channels, the "path-channel", the "heading channel" and the "speed channel". In the "path-channel", the desired track intercept angle or crab angle  $\xi$  is calculated, while in the "heading channel" the rudder angle command is calculated, as a function of the heading error  $e_\psi$  and of the intercept or crab-angle  $\xi$ . In the "speed-channel" the rpm of the active rudders is controlled as a function of the speed error.

Path-channel. The actual position of the vessel, as measured by the radar, is filtered by low pass-filters and compared with the reference track in order to deduce the cross track error.

In the case the desired or reference track is changed, the rate-of-change is limited by the command-rate limit feature. In this way the new reference track is approached smoothly.

Also the measured ground speed component perpendicular to the track is used in the path control channel.

The path controller is basically a PID-controller, although the derivative control is based on the measurement of the groundspeed itself, instead of taking the derivative of the cross-track error. In addition, all contributions can be limited by choosing an appropriate limit-level.

The angle  $\xi$  is subsequently introduced into the heading control channel.

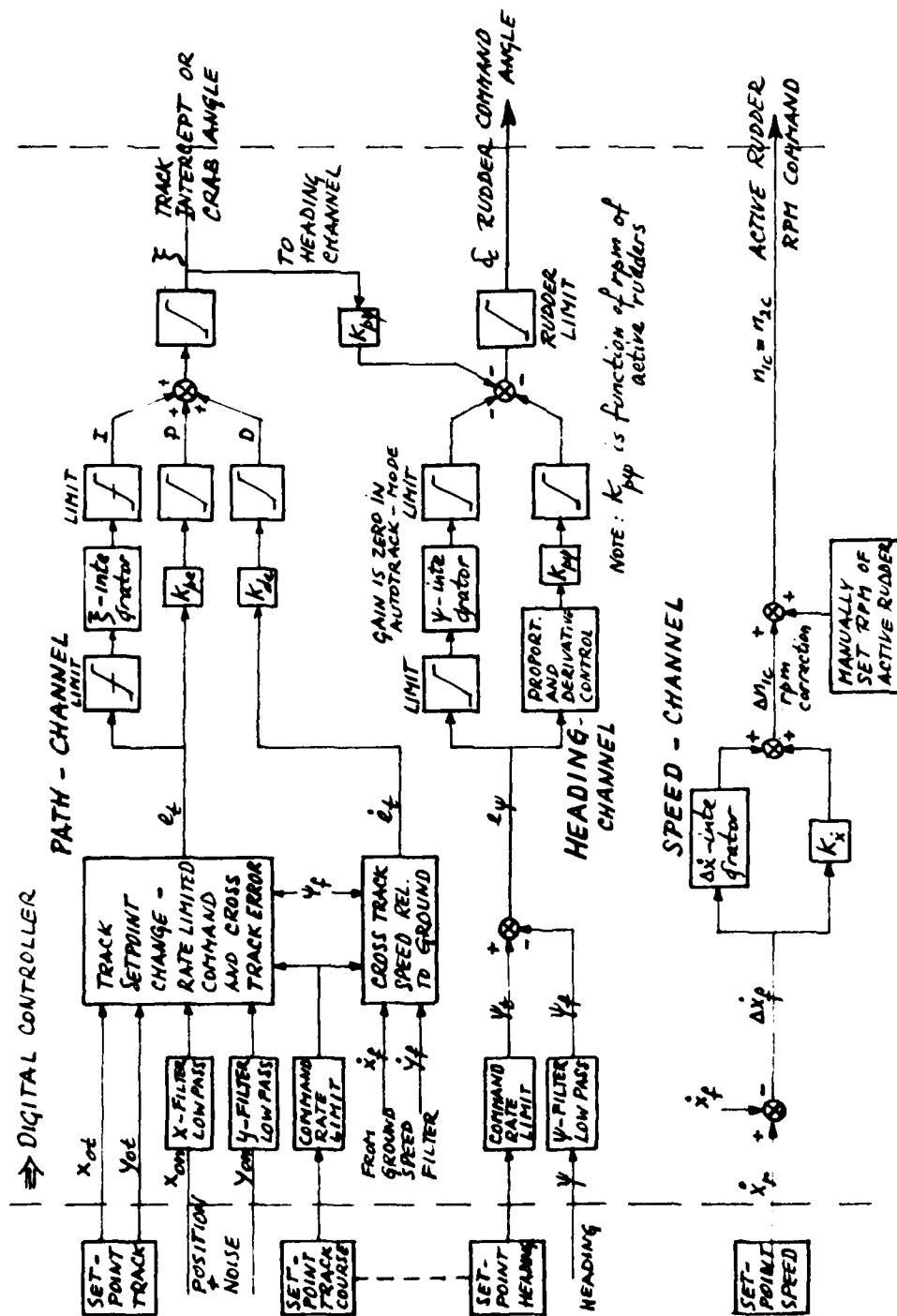


Figure 31: The automatic control system - AUTOTRACK mode.

Heading-channel. The heading- or course-channel includes the components of a conventional autopilot.

The filtered compass heading signal is compared with the heading set point to obtain the heading error  $e_\psi$ . In the AUTOTRACK-mode, the set point heading is identical to the track course set point.

The heading error is processed via a second-order Proportional-Derivative controller, while the integral control gain is put equal to zero in the AUTOTRACK-mode.

This is done because it should be possible to deviate from the desired heading to allow for a crab-angle in case of crosswind or -current.

The output of the PD-controller is a rudder command angle. At that point, the command angle is corrected as a function of the path error. This correction is equal to the intercept- or crab-angle  $\xi$ , multiplied by the proportional gain coefficient  $K_{p_\psi}$ .

Thus we have:

$$\text{Rudder command angle } \delta_c(z) = -K_{p_\psi} [D(z) * E_\psi(z) + \xi(z)]$$

in which

$K_{p_\psi}$  = proportional gain coefficient

$z$  = z-transform operator

$D(z)$  = second order derivative transfer function

$\delta_c(z)$  is the z-transform of  $\delta_c$ ,  $E_\psi(z)$  of  $e_\psi$ ,  $\xi(z)$  of  $\xi$ .

Based on preliminary simulation runs, it was decided to adjust the heading proportional gain coefficient  $K_{p_\psi}$  automatically as a function of the rpm-setting of the active rudders.

The reason for this was that the rudder efficiency largely depends on the rpm, because of the fact that the direction of the thrust is coupled with the rudder angle. So the moment due to rudder is -apart from the rudder angle itself- a function of the thrust and of the velocity relative to the water.

Speed-channel. The speed controller keeps the vessel on the average at the prescribed groundspeed, as measured by the Doppler Sonar. The rpm of the active rudders is adjusted as a function of the groundspeed error and of the integral of the error.

#### The Simulation Programme

The programme was set up to establish the track intercepting and track following capabilities of the vessel under varying conditions:

Table 3: Trackkeeping simulation program.

Test series	Weather conditions	Objective
1	calm (no wind, no waves, no current)	- system stability - response to track set point commands
2	2 kts-current from ahead or astern; 1 kts-current from abeam	- system stability - integral action of path control channel
3	waves: sea state 3 and 5, from different directions	- effect of high frequency wave induced motions on rudder motions - effect of low frequency wave drift forces on trackkeeping performance

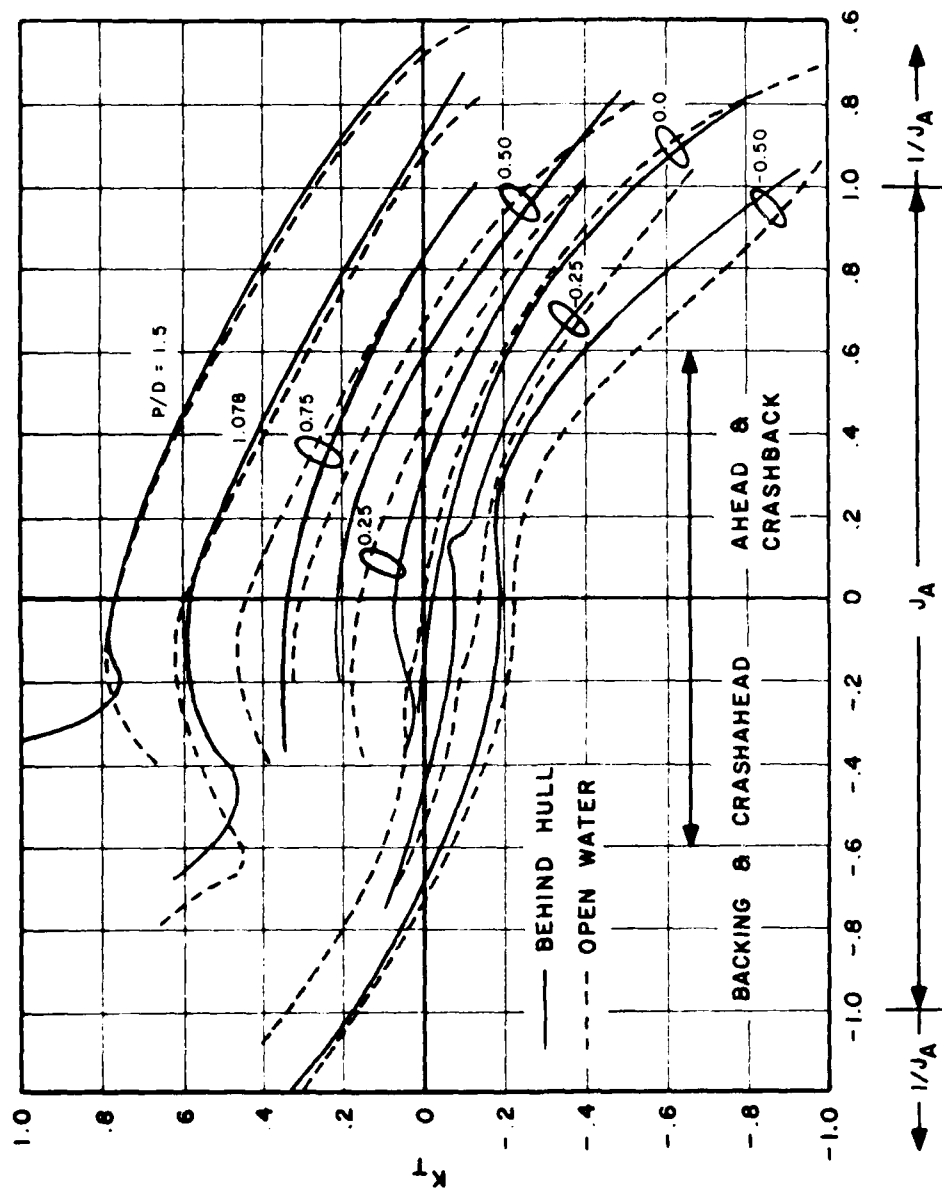


Figure 3. Propeller Open Water and Behind-The-Hull Experimental Thrust Coefficient Data

transient loads in the propulsion system but still provide protection against excessive load levels.

Only two functions are provided by the integrated throttle control system, namely: scheduling of gas turbine power lever angle and propeller pitch ratio for any bridge throttle lever position and limiting of gas turbine power lever angle in response to an achieved propeller pitch ratio. This limiter is designed to limit transients by restricting throttle position at low pitch ratios, thus preventing throttle commands that are excessive (in terms of peak speeds, torques or thrusts) for any particular pitch ratio.

Throttle Control, Power Lever Angle/Pitch Ratio Scheduler. The steady-state schedule between bridge throttle lever (BTL) position and the ordered power lever angle (PLA) and pitch ratio (PR) is shown in figure 2. This schedule was used in the simulation to order a pitch ratio and a power lever angle for any bridge throttle command. For the case of one engine operation the ordered PLA and PR are in accordance with this schedule; for twin engine operation each engine receives an identical PLA command according to the schedule.

The PLA/PR limiter shown in dashed lines is a propulsion maneuvering transient limiter which is inactive in normal steady-state operation since the PLA steady-state schedule is always below the PLA/PR limiter characteristics as shown in figure 2.

Power Lever Angle/Pitch Ratio Limiter. The PLA/PR limiter can be summarized as follows: The limiter schedule of figure 2 is used to limit the power lever angle (PLA) as a function of pitch ratio during propulsion maneuvering transients. Its function is to restrict PLA commands to any region below the limiter characteristic regardless of the commanded PLA at the throttle. Thus, for decreasing pitch ratio, hence decreasing propeller torque, the allowable PLA decreases reaching a minimum at zero pitch ratio.

In the simulation, instantaneous pitch ratio is compared against the PLA/PR limiter schedule. If the commanded PLA exceeds the allowed value (according to the limiter schedule) then PLA follows the schedule and the limiter is considered "active". If commanded PLA falls below the schedule for any pitch ratio the limiter has no effect and the limiter is considered "inactive".

Propulsion control systems in this simulation were limited to those discussed as part of the gas turbine and integrated throttle control systems. Thus, a propeller speed governing system was not implemented as part of this simulation because it is not involved in the reversing dynamics investigation.

The primary objective in this simulation was an investigation of transient loads and system responses during the most severe ship maneuvers such as those encountered in crashback (reversing from one or two engine full ahead to full astern) and crashahead (acceleration from one or two engines full astern to full ahead).

#### PROPELLER AND HULL MODEL TEST RESULTS

For each fixed pitch ratio, experimental model test measurements were taken for various ship and propeller speeds. Wake fraction data was computed by the thrust identity method from the open water and behind-the-hull data of figure 3. Thus, the propeller thrust coeffi-

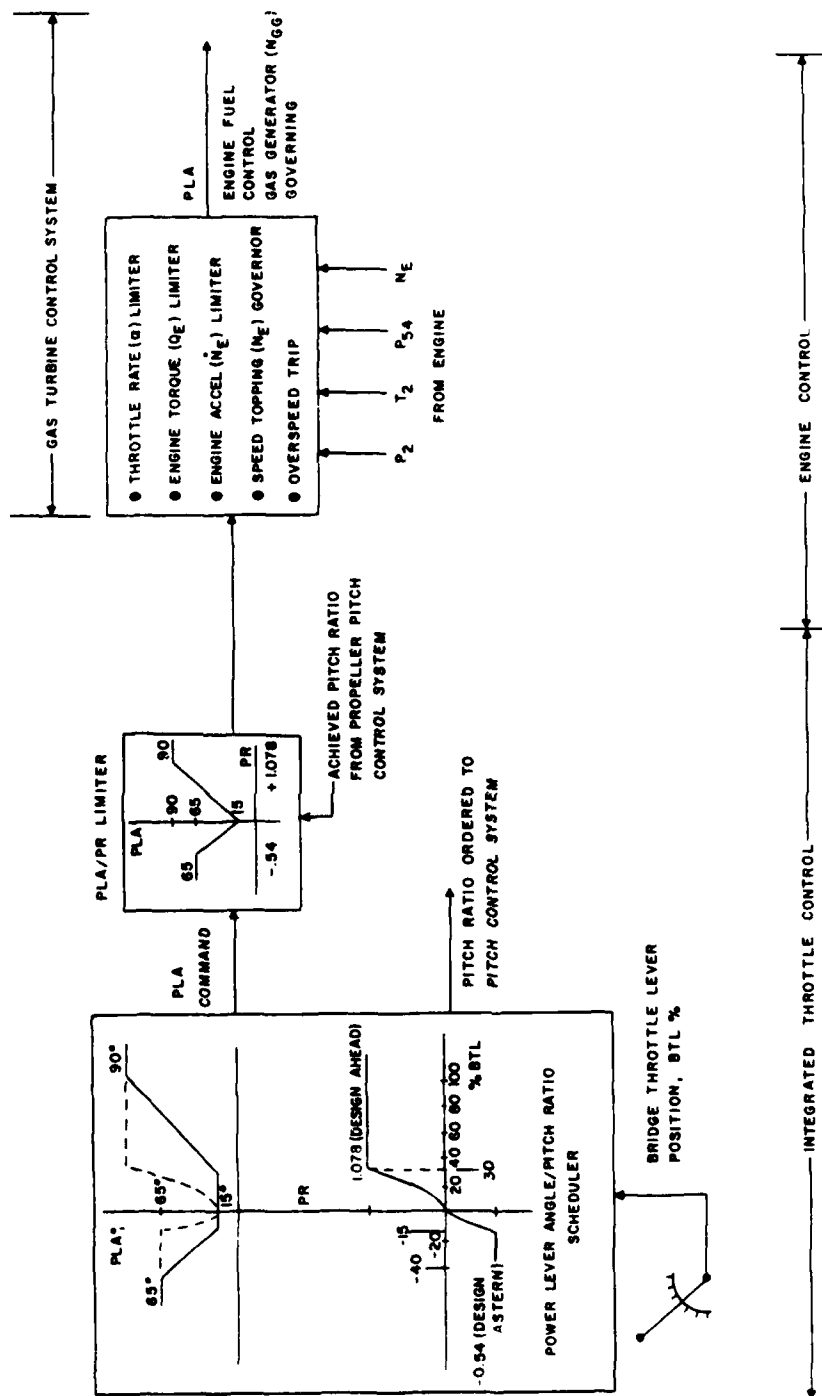


Figure 2. Overall Propulsion Control System

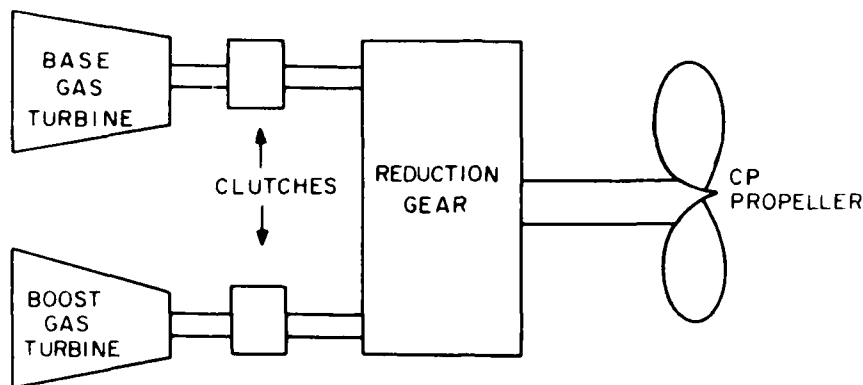


Figure 1. Propulsion System for CPP Study Ship

#### Gas Turbine Controls

Throttle Rate Limiter. Irrespective of the rate of change of commanded throttle position the rate of change of the actual throttle position fed to the fuel control system was limited to 22.5°/sec for engine acceleration and 89°/sec for engine deceleration.

Engine Torque Limiter. An engine torque computer continuously calculates engine shaft torque from the following variables:

P <sub>54</sub>	power turbine inlet pressure
P <sub>2</sub>	compressor inlet pressure
T <sub>2</sub>	compressor inlet temperature
N <sub>E</sub>	engine speed

The control system was designed to prevent the engine from developing a torque more than 6% to 8% above a preset limit. The engine torque limits in this simulation (referred to the engine shaft) are 42,000 lb-ft for a single engine/shaft and 36,000 lb-ft for each engine in a twin engine/shaft mode.

Engine Acceleration Limiter. The engine acceleration was limited to a rate of change of 200 RPM/sec on engine speed N<sub>E</sub>.

Engine Overspeed Limits. Two overspeed limits on engine speed, N<sub>E</sub>, are provided. The topping governor implements a fuel decrease when the engine speed exceeds the topping governor reference speed, N<sub>E</sub> = 3672 RPM and a fast-acting solenoid valve completely shuts off fuel when an engine speed of 3960 RPM is exceeded.

Engine Governing System. The engine throttle command (PLA) is translated to percent demanded core speed (%N<sub>CG</sub>) which is an input to the fuel control system. A closed loop control maintains the speed of the gas generator (N<sub>CG</sub>) at the demanded value. The free turbine speed or engine speed (N<sub>E</sub>) is determined by a balance between power produced by the gas generator and the power consumed by the load. All of the gas turbine controls are implemented via a reduction in the actual throttle position (PLA) fed to the fuel control system.

#### Integrated Throttle Control

The integrated throttle control for this simulation was designed with the utmost simplicity so as not to obscure the interpretation of



Digital computer simulations for crashback and crashahead maneuvers were conducted with a complete dynamic model of the LM2500 engine and propulsion control system. This control system was designed to limit peak propulsion loads to safe levels for all conditions.

This paper discusses the experimental propeller data and its incorporation into the simulation. Results of the simulation for crashback and crashahead maneuvers include ship and propeller speeds, head reach, shaft and blade spindle torques, shaft thrusts and other engine and ship parameters as a function of time for various control system conditions. Evaluation is made on the effect of wake and thrust deduction fraction data in correctly predicting transmission and propeller loads. Peak system loads for these reversing simulations are tabulated for various conditions and the cause-effect relationship of control actions to load levels and stopping performance is discussed.

#### STUDY SHIP CHARACTERISTICS

The study ship used in these simulations is a hypothetical Navy frigate used in previous simulations with the exception that the propeller has been changed slightly, together with changes in the wake and thrust deduction fractions which were determined from experimental model tests.

The ship characteristics are summarized below: <sup>(1)</sup>

length overall, ft	440
full-load displacement, long tons	about 4000
propulsion plant	COGAG CPP, single screw
base turbine rating, hp	up to 25,000
boost turbine rating, hp	25,000
reduction gear ratio, $k_g$	14.0
propeller number of blades	5
propeller diameter, ft	15.0
propeller pitch ratio at 0.7 radius	1.078
propeller expanded area ratio	0.826

The ship weight  $W$  including 8% entrained water is  $W = (1.08)(4000 \text{ tons})$  (2240 lb/ton) =  $9.68 \times 10^6 \text{ lb}$ .

Total ahead ship resistance  $R_T$  is the same as Reference 1. Astern resistance is 1.9 times the ahead resistance for any ship speed from zero to 15 knots astern.

#### PROPULSION SYSTEM

The COGAG propulsion system with two gas turbines driving a single CP propeller through a reduction gear is shown in figure 1. Propeller, hull and propulsion system equations are summarized in Appendix A with a nomenclature list presented in Appendix B.

The ship propulsion control system (shown in figure 2 for one engine only) is composed of two major subsystems: the gas turbine control system which is an integral part of the LM2500 gas turbine engine and an integrated throttle control system.

REVERSING DYNAMICS OF A GAS TURBINE SHIP  
WITH CONTROLLABLE-PITCH PROPELLER

by C. Joseph Rubis  
and Thurman R. Harper  
Propulsion Dynamics, Inc.

ABSTRACT

A reversing dynamics and control simulation of a single screw controllable-pitch propeller frigate study ship driven by two General Electric LM2500 gas turbine engines is described. Results of the research effort include behind-the-hull model tests of a controllable-pitch propeller under all maneuvering conditions. Model test results with wake and thrust deduction fractions during maneuvering were used in the digital computer simulations to determine drive train and propeller loads and ship performance during crashback and crashahead maneuvers.

INTRODUCTION

Reversing of gas turbine controllable-pitch propeller (CPP) ships presents new problems not usually encountered with steam turbines. With a gas turbine, reversing power equal to maximum ahead power is available; the free turbine rotor typically has a much lower moment of inertia than the low pressure/reversing rotor of a steam turbine and very rapid accelerations (e.g., on the order of 6 seconds from idling to full power) are possible. In addition, during CPP reversal the propeller is unloaded as the propeller blades pass through a region of low pitch ratio. And, as with steam turbines, gas turbine torque increases with decreasing speed so that in the vicinity of zero shaft RPM very large engine torques are possible unless the throttle is constrained. During crashback maneuvers, especially from full power, very large peak negative thrust transients in the vicinity of twice the maximum ahead condition can be developed along with blade spindle torque peaks more than twice the maximum ahead condition. For crash-ahead, from a maximum backing condition or for any rapid acceleration maneuver, very large engine and shaft torques as well as large peak blade spindle torques and propeller thrusts are developed. For gas turbine CP propeller ships it is essential that the propulsion control system provide transient limiting controls to ensure safe propulsion system operating conditions for any throttle command.

A reversing dynamics and control simulation of a single screw controllable-pitch propeller frigate study ship driven by two General Electric LM2500 gas turbine engines is described in this paper. This simulation is a continuing phase of Navy propulsion dynamics and control research for gas turbine ships. Results of the reversing research effort include behind-the-hull propeller model tests for crashback and crashahead maneuvers on a frigate hull conducted in the model basin at the David Taylor Naval Ship Research and Development Center. Results of these model tests were then incorporated into the reversing dynamics simulations to improve prediction of drive train, propeller and ship loads and responses during crashback and crashahead maneuvers.

$\delta$	drift angle
$\delta_a$	active rudder angle
$\rho, \rho_a$	density of (sea) water and air, resp.
$\psi$	ship's heading
$\psi_c, \psi_w, \psi_{wa}$	direction of current, wind, waves, resp.

#### Indices

A	aft
a	air
c	current or command
d	derivative
ext	external
F	fore
FH	favourable heading
f	filtered
H	hull
n	noise
p	proportional
r	reference
s	propeller ( of active rudder or conventional)
T,t	(bow) thruster
t	track
W,w	wind
wa	waves

## 7. CONCLUSIONS

In the preliminary design phase of the "Tripartite"-minehunter, the thruster sizing and manual versus automatic control have been studied by means of simulation.

The thruster sizes to meet the design requirements have been determined. The basic configuration of the control system has been defined of both the "hover"-mode and the autotrack-mode. This will be used as a starting point for the detailed design studies by the autopilot manufacturer. In this way the autopilot settings can be defined, before going out to sea.

This will shorten the first-of-type sea trials considerably.

Also, this total-system simulation set-up will be used to familiarize and train the operators, so to shorten work-up periods.

To establish the final configuration of both control systems, follow-up studies are necessary with respect to:

- final design and evaluation of manual and automatic control system including the definitive incorporation of the noise reduction feature, and of the power limitation feature,
- incorporation of definitive data of the ship's hull and of the bow thruster and active rudders in the simulation model,
- configuration of controls and display,
- performance degradation due to failure of components,
- direct manual control, in case of computer failure,
- method to determine the favourable heading for station keeping,
- testing of prototype hardware.

## 8. ACKNOWLEDGEMENT

The authors thank the French, Belgium and Netherlands Navy authorities for their permission to publish these study results.

We are grateful to Mr. J.B. van den Brug and W.R. van Wijk of TNO-IWECO for their contribution to the studies.

Last but not least, we thank Mr. A.J. Bekendam for his part in the project, being the realisation of the simulation computer program.

## 9. LIST OF SYMBOLS

$A_w$	lateral wind area
$C_{XH}, C_{YH}, C_{NH}$	hull coefficients
$C_{XW}, C_{YW}, C_{NW}$	wind coefficients
$D_t$	bow thruster diameter
$F_X, F_A, F_F$	required restoring forces: in longitudinal direction ( $F_X$ ), in lateral direction at the stern ( $F_A$ ) and at the bow ( $F_F$ ).
$L$	ship's length
$n$	rpm or rps of thrusters (active rudders or bow thruster)
$T$	ship's draught
$u, v, r$	ship's speed rel. to water: in longitudinal direction, in lateral direction, about ship's vertical axis
$U$	ship's velocity rel. to water
$V_c, V_w$	current velocity, wind velocity, resp.
$X, Y, N$	forces and moment acting on ship: in longitudinal, in lateral direction, about ship's vertical axis. resp.

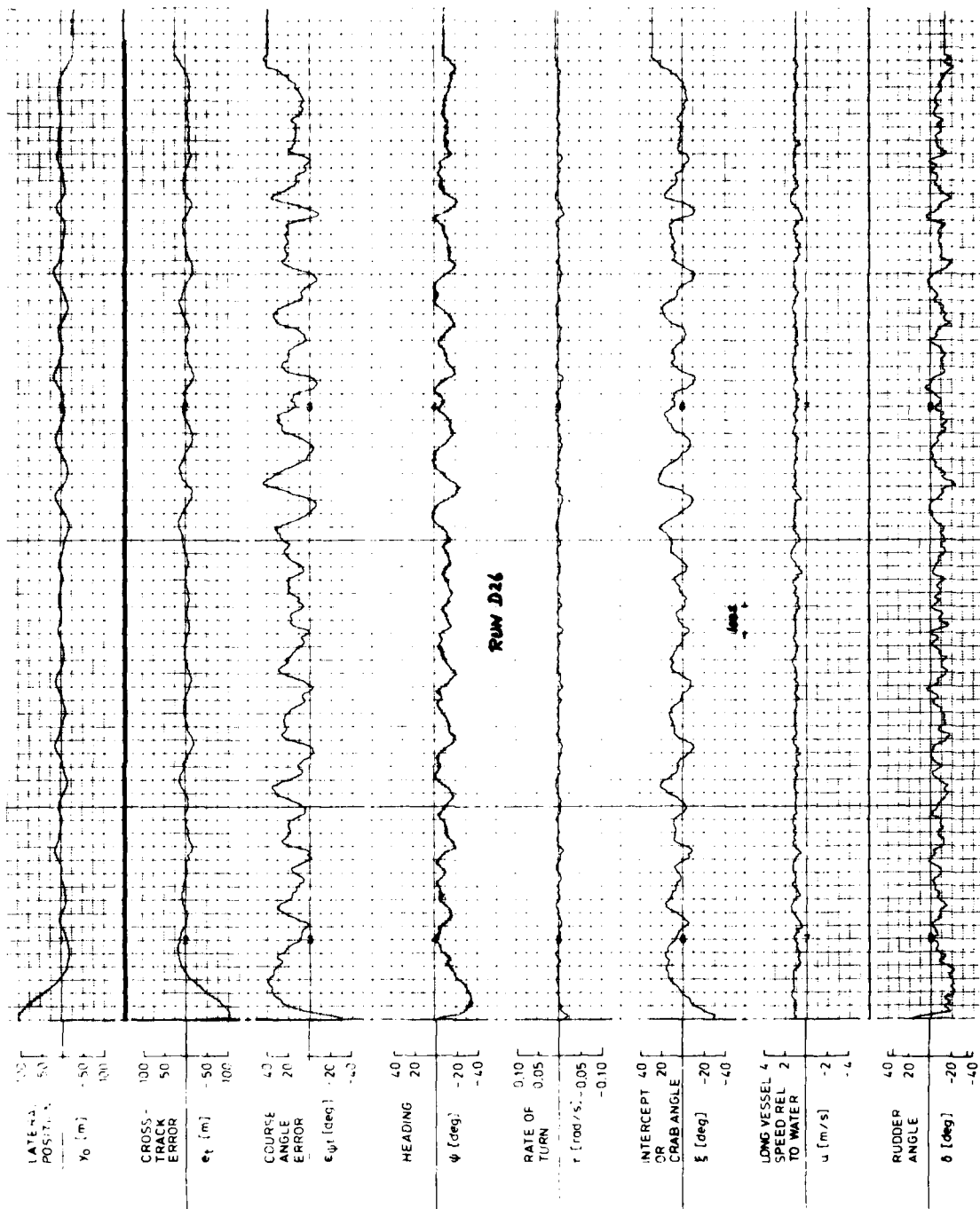


Figure 35: Test series 6 - wind, waves and current - RUN D 26. Average groundspeed: 2 kts.

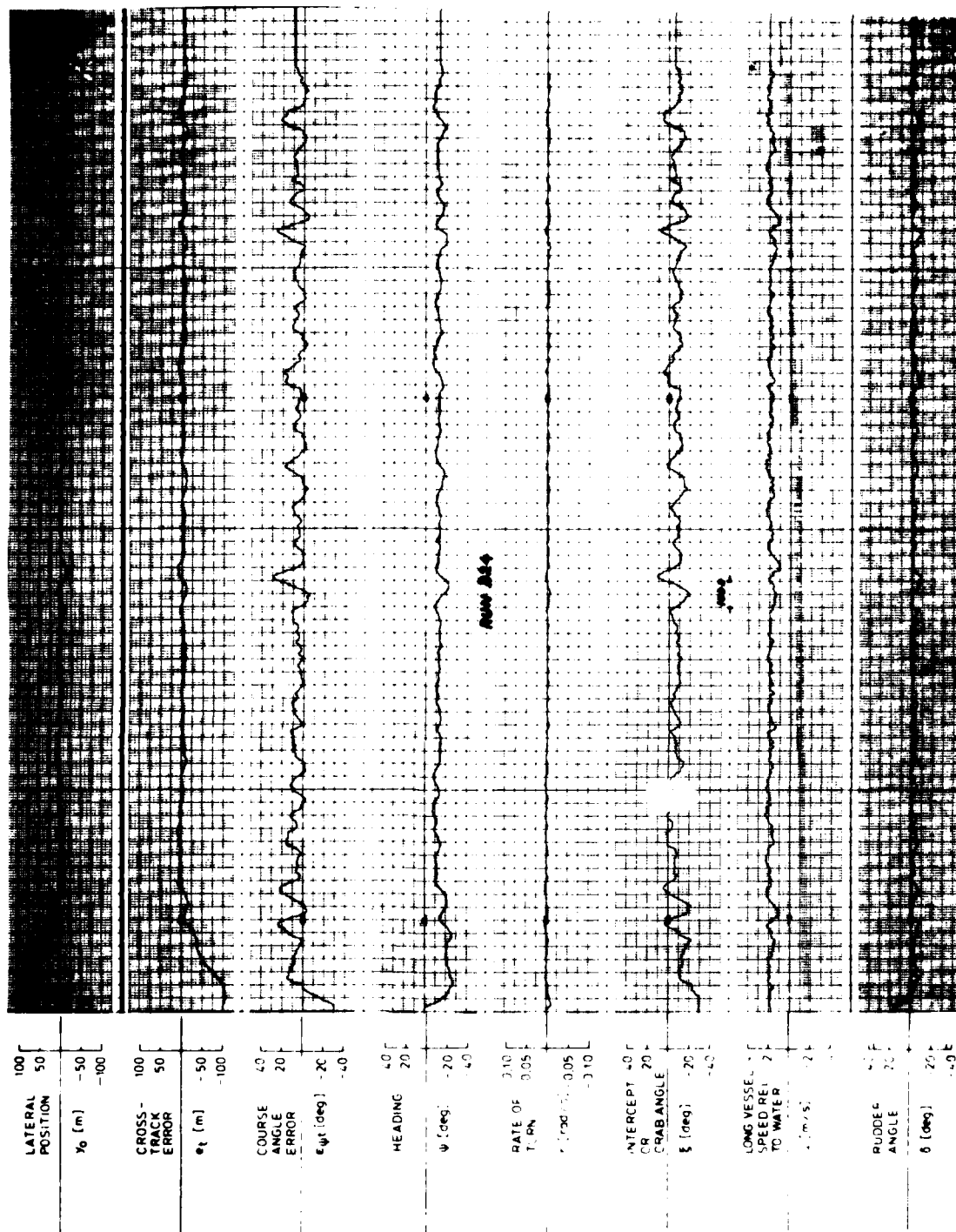


Figure 34: Test series 6 - wind, waves and current - RUN D 24. Average groundspeed: 2 kts.

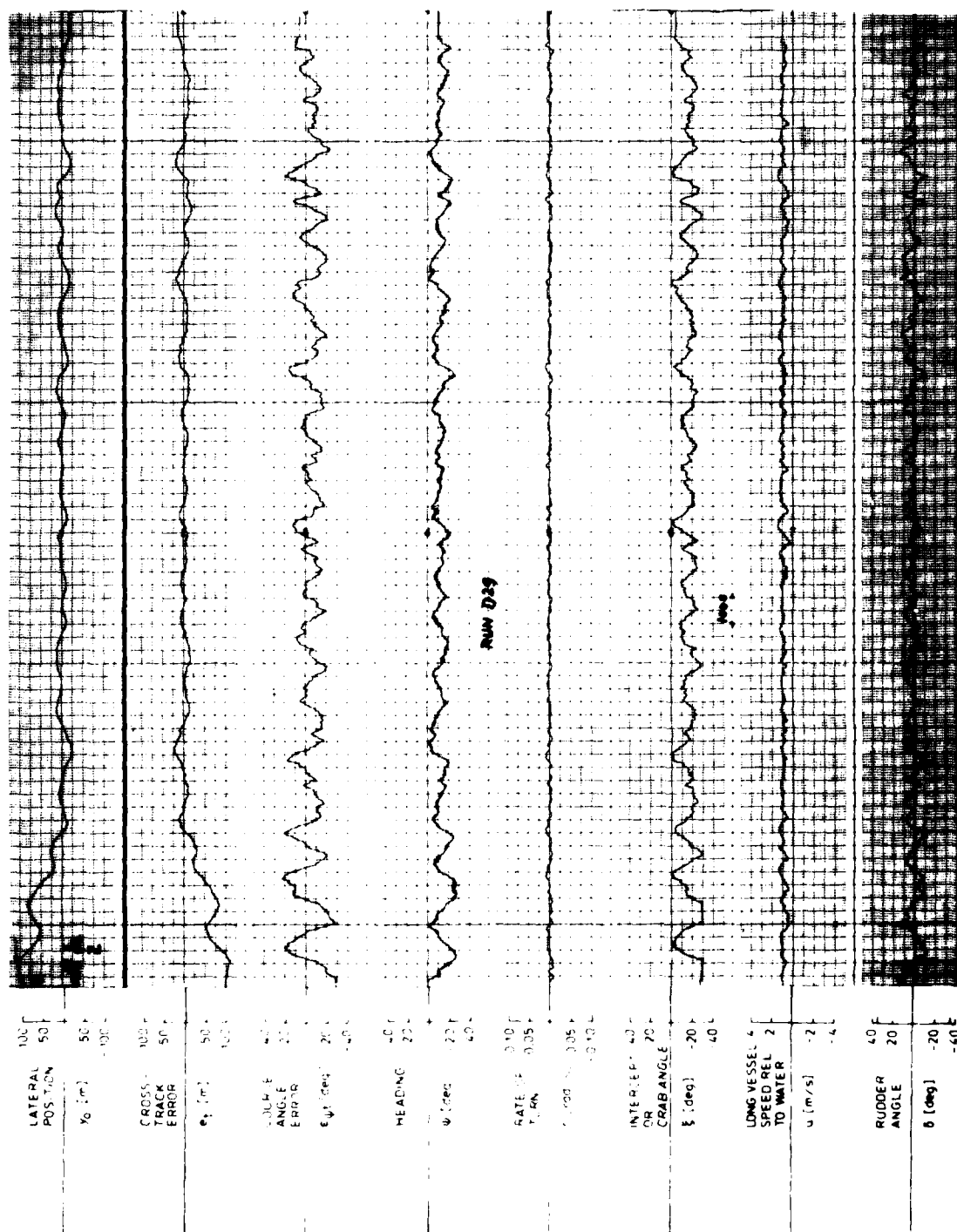


Figure 33: Test series 5 - wind and waves - RUN D 29. Average groundspeed: 2 kts.

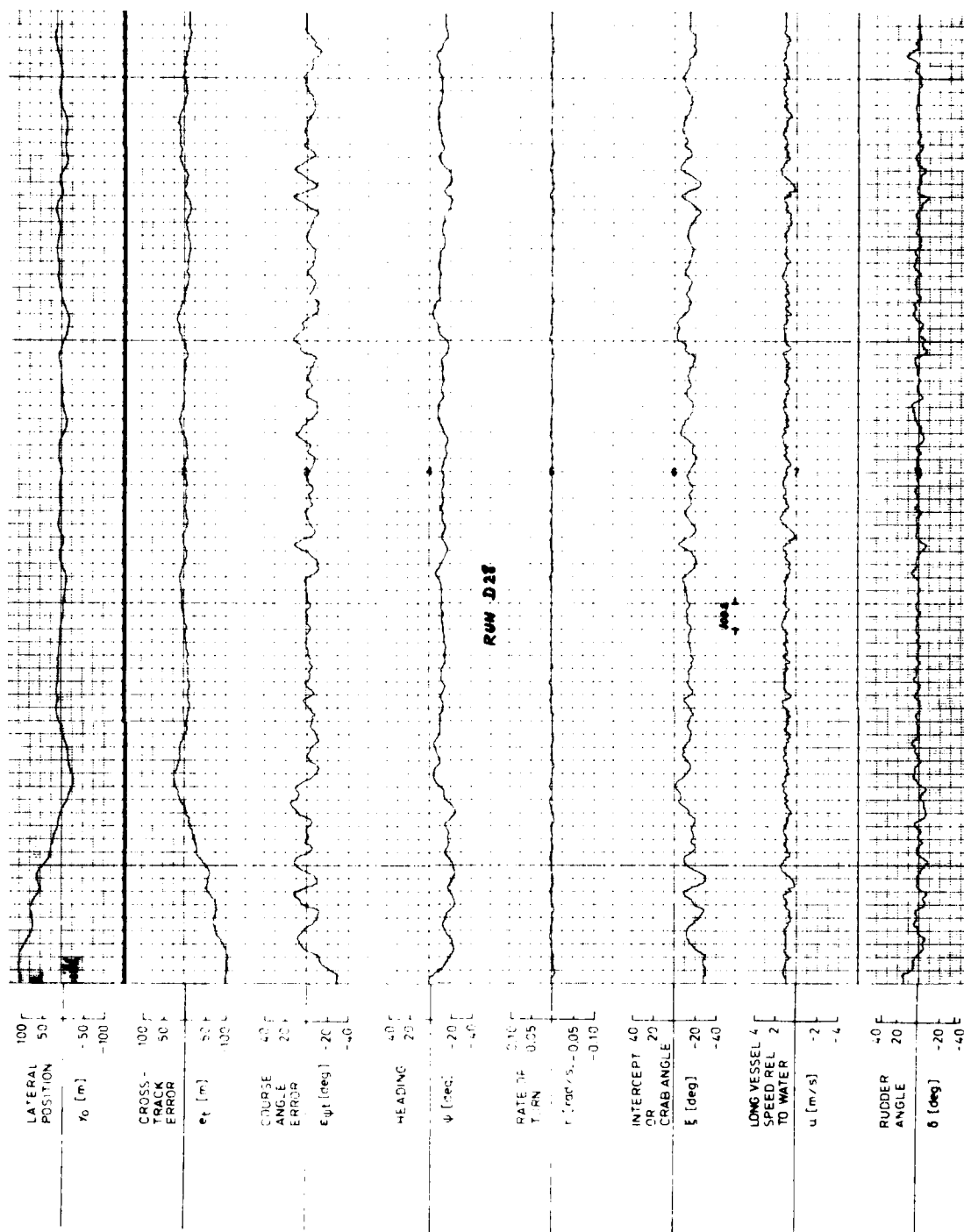


Figure 32: Test series 5 - wind and waves - RUN D 28. Average groundspeed: 2kts.



Table 4: Weather conditions

Table 4: Weather conditions								
RUN NUMBER	TEST SERIES	WEATHER CONDITIONS						AVERAGE LONG. GROUND- SPEED (m/s)
		WIND		WAVES				
		MEAN SPEED (m/s)	MEAN DIRECTION (deg)	SIGN. HEIGHT (m)	DIRECTION (deg)	SPEED (m/s)	DIRECTION (deg)	
D28	5	10.29	160	1.5	150	-	-	1.0
D29	5	15.43	160	3.0	150	-	-	
D24	6	10.29	180	1.5	150	1.03	150	
D26	6	15.43	180	1.5	150	.52	90	
NOTE: A direction of 180° means: on the bow; 160° means: 20° off bow etc...								

NOTE: A direction of 180° means: on the bow; 160° means: 20° off bow etc..

TABLE 5: Performance index and mean square values of contributing parameter.

RUN NUMBER	TEST SERIES	PERFORMANCE INDEX	MEAN SQUARE VALUES			ACTIVE RUDDER ANGLE (deg <sup>2</sup> )
			CROSS TRACK ERROR (m <sup>2</sup> )	COURSE ANGLE ERROR (deg <sup>2</sup> )		
D28	5	1066	383	46		11
D29	5	1311	818	122		31
D24	6	773	484	92		13
D26	6	1932	315	397		102

Table 3 (con'd)

Test series	Weather conditions	Objective
4	wind: 20 kts- and 30 kts-gusty wind from different directions	- effect of wind on trackkeeping performance
5	wind (20 kts- and 30 kts-) and waves (sea state 3 and 5) from different directions.	- trackkeeping performance
6	wind and waves, according to 5, and current from different directions	- trackkeeping performance - influence of current

### Results of the Simulation

Figures 32 through 35 present a sample of all runs. The time-series show eight of the most important system parameters. Two runs from test series 5 have been selected here, both at a relatively low forward speed of 2 kts. Weather conditions were normal and more severe, respectively. The weather conditions can be found in detail in Table 4. Differences between the two runs can be found in the rudder angle and course angle error-signals. The crosstrack error is within the required accuracy. The other two runs are from test series 6, which included current. Weather conditions during Run D 24 were normal, while during Run D 26 the mean wind speed was 30 kts. See also Table 4 for details. Run D 24 was quiet, Run D 26 needed more rudder angle, while the course angle error was significantly worse. The trackkeeping accuracy was good in both cases. The results have also been analysed using a special programme, which calculates a performance index:

$$C = \frac{1}{T} \int_0^T (e_t^2 + \lambda_{\psi t} e_{\psi t}^2 + \lambda_{\delta} \delta^2) dt$$

in which

$e_t$  is the crosstrack error

$e_{\psi t}$  is the course angle error, being the algebraic sum of the heading error  $e_{\psi}$  and crab angle  $\xi$

$\delta$  is the rudder angle of the active rudders

$\lambda_{\psi t}$  and  $\lambda_{\delta}$  are weighing factors (chosen values 2.0 and 8.0, respectively)

Table 5 presents these values for the four selected runs. Although the initial crosstrack error - typically 100 m - influences the scoring unfavourable, the scoring takes into account the speed of interception, which is also a factor to be considered.

The examples presented here were all at relatively low forward speed and corresponding rpm. The runs made at higher speed showed, in general, better or equal performance with less rudder activity.

Based on this preliminary design study, the tentative conclusion was drawn, that trackkeeping was feasible and that the requirements could be met.

The control system coefficients were chosen, as to keep the necessary adjustments at a minimum: A calm weather-setting was specified (1) and a normal setting, to be used under all conditions without current (2). With current, the proportional gainfactor  $K_{pe}$  was increased (3). During actual operation, the appropriate setting must be chosen.

cient data (where  $K_T$  is defined by  $K_T = T/\rho n^2 D^4$ ) in terms of  $J_A = \frac{V}{nD}$  for various pitch ratios was used only to obtain  $w_T$  which is shown plotted in figure 4. In all the experimental data for both wake and thrust deduction fractions  $n > 0$ , hence only two quadrants of data are needed, i.e.,  $\pm J_A$  corresponding to  $\pm V$ . The other variable is pitch ratio where a positive or negative pitch ratio is analogous to a positive or negative  $n$ .

The wake and thrust deduction factors are computed from  $(1 - w_T) = J/J_A$  (where  $J = V_A/nD$ ) and  $(1 - t) = (R_T + F)/T$  respectively with  $t$  shown in figure 5 versus  $J_A$ . The resistance  $R_T$  is the towed resistance of the hull with no propeller attached,  $T$  is the measured propeller (behind-the-hull) thrust during the model tests and  $F$  is a force supplied by the carriage to the model. The force  $F$  was varied by adjusting carriage speed to produce steady-state equilibrium ( $F = 0$ ), overpowered ( $+F$ , opposing  $T$ ) or underpowered ( $-F$ , aiding  $T$ ) conditions.

#### CRASHBACK SIMULATIONS

From maximum ahead speed or some intermediate speed, the bridge throttle is set to full astern (a fraction of full ahead power). The power lever angle, PLA, is ordered to an idling fuel rate of about  $15^\circ$  (for each engine if two engines are used) and gas turbine fuel reduction begins immediately and reaches the ordered idling value in less than 5 seconds. Coincident with the ordered reduction in PLA, the pitch control system is ordered to a pitch ratio of  $-0.54$  (one-half the design ahead pitch ratio of  $1.078$ ). Pitch ratio reduction begins immediately at a rate determined by the chosen pitch stroke time  $\tau$ . The pitch stroke time is the time required to change pitch ratio from design ahead ( $+1.078$ ) to design astern ( $-0.54$ ). A pitch stroke time of 30 seconds was used in these simulations. When the decreasing pitch ratio reaches zero, the PLA is commanded to the maximum astern position ( $PLA = 65^\circ$ ) and an increase in fuel flow to the gas turbine(s) begins, reaching the final value in about 10 seconds. The pitch ratio continues decreasing until a value of  $-0.54$  is reached; the pitch ratio is then kept at this value for the remainder of the crashback maneuver. After the PLA is advanced to the astern position, the turbine fuel, torque and speed increase, reaching their final values with the ship moving astern. The steady-state astern speed for the maximum astern throttle position is about  $V_{Max\ Astern} \approx 1/2 V_{Max\ Ahead}$ .

The sequence of events, causes and effects, during a typical crash reversal are as follows (see figure 6):

#### Fuel-to-Idle Phase

Following the command to idle the engine(s), a rapid fuel decrease occurs resulting in a rapid decrease in engine torque since engine torque follows fuel rate. The rapid decrease in engine torque delivered to the propeller shaft,  $Q_d$ , causes  $Q_d$  to be less than the propeller torque  $Q$  resulting in the rapid decrease in the propeller speed  $N$ . The propeller torque  $Q$  is also falling rapidly due to a combination of the decreasing pitch ratio ( $C_Q$  or  $K_Q$  and  $Q$  are both proportional to pitch ratio) and decreasing  $N$ , but still  $Q_d < Q$  during the fuel-to-idle phase. Another rapidly decreasing parameter is the propeller thrust  $T$  which falls rapidly from a large positive value to some value near zero. This rapid thrust decrease is due primarily to decreased  $N$  and secondarily to a decrease in pitch ratio. Because of its large inertia the ship decreases little in speed. From the definition of advance coefficient,  $J = V(1 - w)/nD$ , it is apparent that  $J$  will increase during

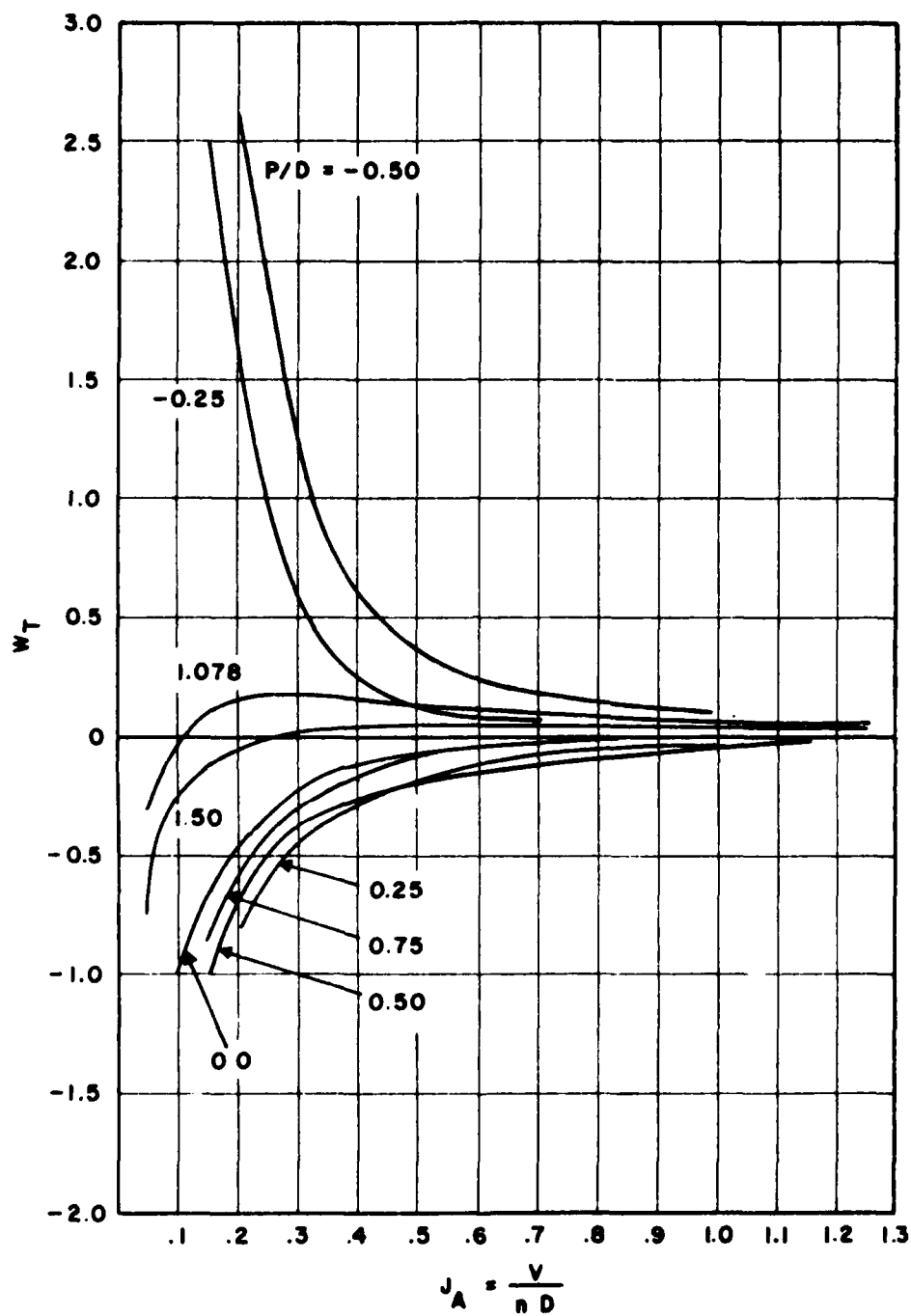


Figure 4. Experimental Wake Fraction for Various Propeller Pitch Ratios Computed from Thrust Identity Behind Single Screw Model Hull

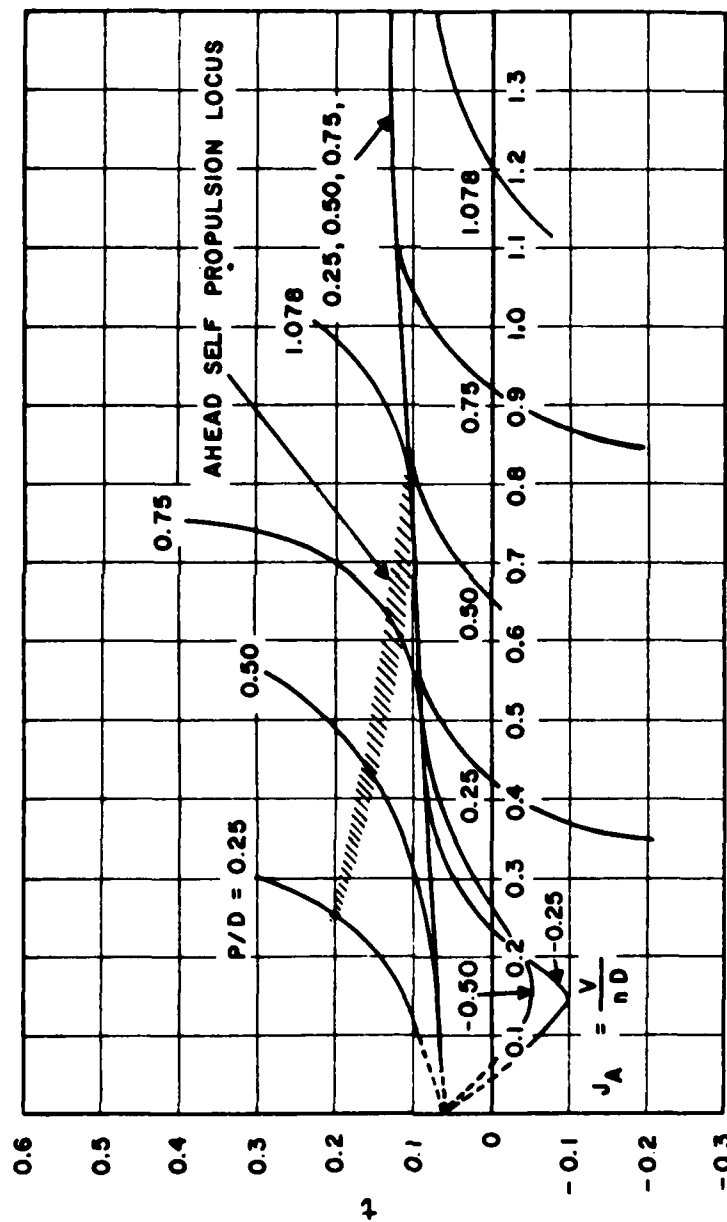


Figure 5. Experimental Thrust Deduction Fraction for Various Propeller Pitch Ratios Computed from Overload Thrust Measurements Behind Single Screw Model Hull

this phase because the percentage decrease in  $n$  is greater than that of  $V$ .

During the fuel-to-idle phase there are no peak values encountered in the parameters  $N$ ,  $Q_d$ ,  $Q_B$  or  $T$ .

#### Fuel-at-Idle Phase

During the fuel-at-idle phase, engine torque  $Q_E$  and torque delivered to the propeller,  $Q_d$ , stop decreasing and reach a minimum value. In fact,  $Q_d$  can go slightly negative due to the rapid fuel reduction and remaining high engine speed. At some time during this phase  $Q_d = Q$ , i.e., the deceleration of  $N$  becomes zero. Then  $N$  begins to accelerate when  $Q_d > Q$ . The increasing propeller speed peaks and again begins decelerating as the magnitudes of  $Q_d$  and  $Q$  interchange. The magnitude of the  $N$  peak is determined by the difference in magnitudes of  $Q_d$  and  $Q$ . In turn, the magnitude of  $Q_d$  is proportional to the idling fuel rate while the magnitude of propeller torque  $Q$  depends on  $N$  and the pitch ratio. This peak in  $N$  occurring during the fuel-at-idle phase is the typical propeller speed-up (or water turbine) phenomenon noted in controllable-pitch propeller propulsion plants caused by the decreasing pitch ratio of the watermilling propeller. This speed peaking tendency even with the engine fuel at idle illustrates the need to cut engine fuel rapidly to a low idling level. The blade spindle torque peak ( $Q_B$  is proportional to  $N^2$ ) typically coincides with this speed peak in  $N$ .

Propeller thrust  $T$  can have one or more peaks, occurring at different times. These peaks generally differ in magnitude and occur when the  $|n^2 K_T|$  (or equivalently  $|C_T(V_A^2 + n^2 D^2)|$ ) product is a maximum. By coincidence the peak or peaks could occur when  $|C_T|$  is a maximum, but this is not the general case. The thrust peak or peaks usually occur in the region between a small positive ahead pitch ratio and a negative pitch ratio at design astern. Additionally, the time at which the propeller thrust peak(s) occurs extend from the engine-at-idling phase over into the engine reacceleration phase of the crashback maneuver. For example, one thrust peak can occur during idling and another peak of equal or greater magnitude may occur during engine reacceleration.

In the engine-at-idling phase both engine and propeller torques are at a minimum because of the engine idling fuel rate; hence no engine or shaft torque peaks are possible.

Thus, the three propulsion system parameters which could become excessively high during the engine-at-idle phase of a crashback maneuver are  $N$ ,  $T$  and  $Q_B$ . These must be maintained within acceptable bounds by proper control system design.

#### Engine Reacceleration Phase

Engine reacceleration is typically timed to occur when the decreasing pitch ratio passes through zero. A scheduled fuel increase taking about 10 seconds to reach the commanded fuel rate is begun when pitch ratio becomes zero. Usually  $N$  is below its peak value and decreasing rapidly at the beginning of engine reacceleration. During the engine reacceleration phase propeller shaft torque  $Q_d$  can reach an excessively high peak unless constrained by the control system. Thus, the engine power lever angle PLA must be limited by the control system because the decreasing pitch ratio is still near zero and the propeller cannot absorb sufficient torque to prevent overspeed with a rapidly increasing engine fuel rate. Consequently, the control system is designed (in

this case with a PLA/PR limiter) to prevent the application of large PLA under conditions of low pitch ratio. In addition, very large engine and shaft peak torques can be developed at the end of the reacceleration phase as the fuel rate reaches its final level requiring, therefore, an engine torque limiting control (for high commanded PLA). Furthermore, the maximum allowable PLA for reverse is set below the maximum ahead PLA condition.

In summary, during the engine reacceleration phase of a crashback maneuver the critical parameters that must be limited by the control system are  $N$  and  $Q_d$  (and correspondingly  $N_E$ ,  $Q_E$  on the engine side of the reduction gear). As previously noted, propeller peak thrust can occur either during the idling or reacceleration phase. This peak thrust which is inversely related to pitch stroke time  $\tau$  is potentially one of the most serious stress problems in the ship propulsion drive system. Since the thrust is negative and possibly exceeds ahead thrust, the thrust bearing must withstand large bidirectional transient loads.

A twin engine crashback time history showing several important parameters for constant  $w = .050$ ,  $t = .100$  is shown in figures 6,a and 6,b. A locus of transient modified advance coefficient and modified thrust coefficient as the pitch ratio varies with time during the same crashback maneuver is shown in figure 6,c. The points at which the two propeller thrust peaks occur are also shown on the same figure. Note that in these figures an assumed constant  $w$  and  $t$  were used, with the open water propeller data of figures A-1 and A-2.

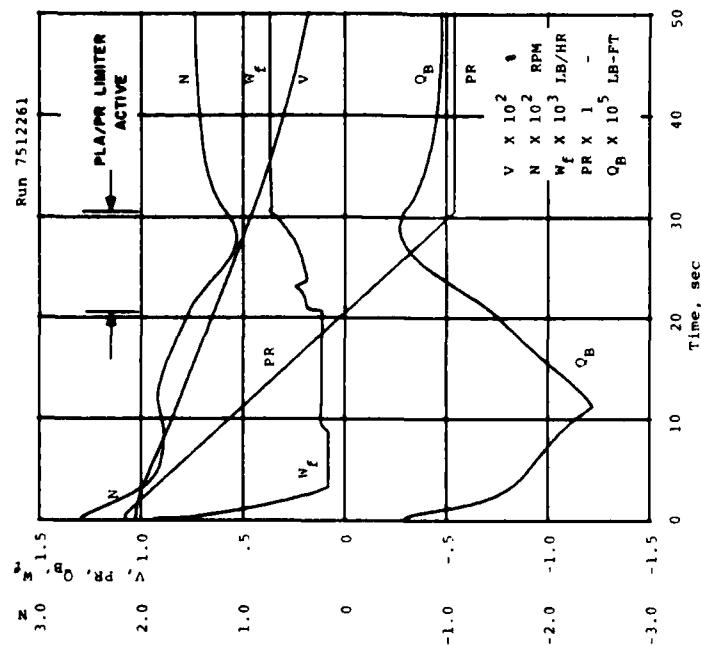
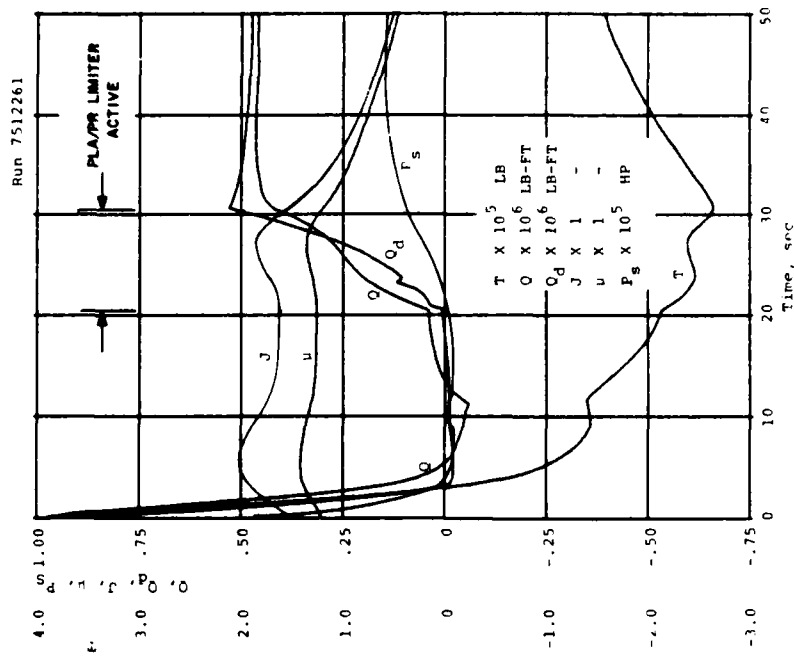
Behind-the-hull experimental propeller data (from figure 3) converted to the forms of figures A-1 and A-2 was also used in crashback and crashahead simulations to compare with the open water propeller simulations. In using behind-the-hull propeller data, the corrections for wake and thrust deduction fraction as indicated in the propulsion equations of appendix A are no longer needed since they are implicit in the data. Thus, for example an effective propeller thrust coefficient  $K_R$  can be derived.<sup>(2)</sup> In these simulations the use of wake and thrust deduction is cumbersome except for the most simple assumptions on wake and thrust deduction when open water propeller data is used. As an example, figure 6,d shows the transient behavior of  $t$  during a crashback maneuver where behind-the-hull propeller data was used with  $t$  computed from instantaneous values of  $K_R$  and  $K_T$ .

The effect of pitch stroke time  $\tau$ , on various ship performance parameters was also investigated for crashback from maximum ahead and constant  $w = .050$ ,  $t = .100$ . These results showing the sensitivity of ship stopping time and distance as well as the largest peaks encountered for  $T$ ,  $Q_B$  and  $N$  during the crashback transient for various  $\tau$  are shown in figure 7.

## SUMMARY AND CONCLUSIONS

### Effect of Steady-State and Transient Wake Fraction on Performance Predictions

Experimental model tests on a controllable-pitch propeller behind a frigate type hull were conducted for various pitch ratios and a range of advance coefficients. The experimental behind-the-hull results were incorporated into the simulations together with idealized wake fraction behavior introduced by a parametric variation of the wake fraction magnitude. Results of these simulations in the prediction of peak transmission loads and ship maneuvering characteristics were compared.





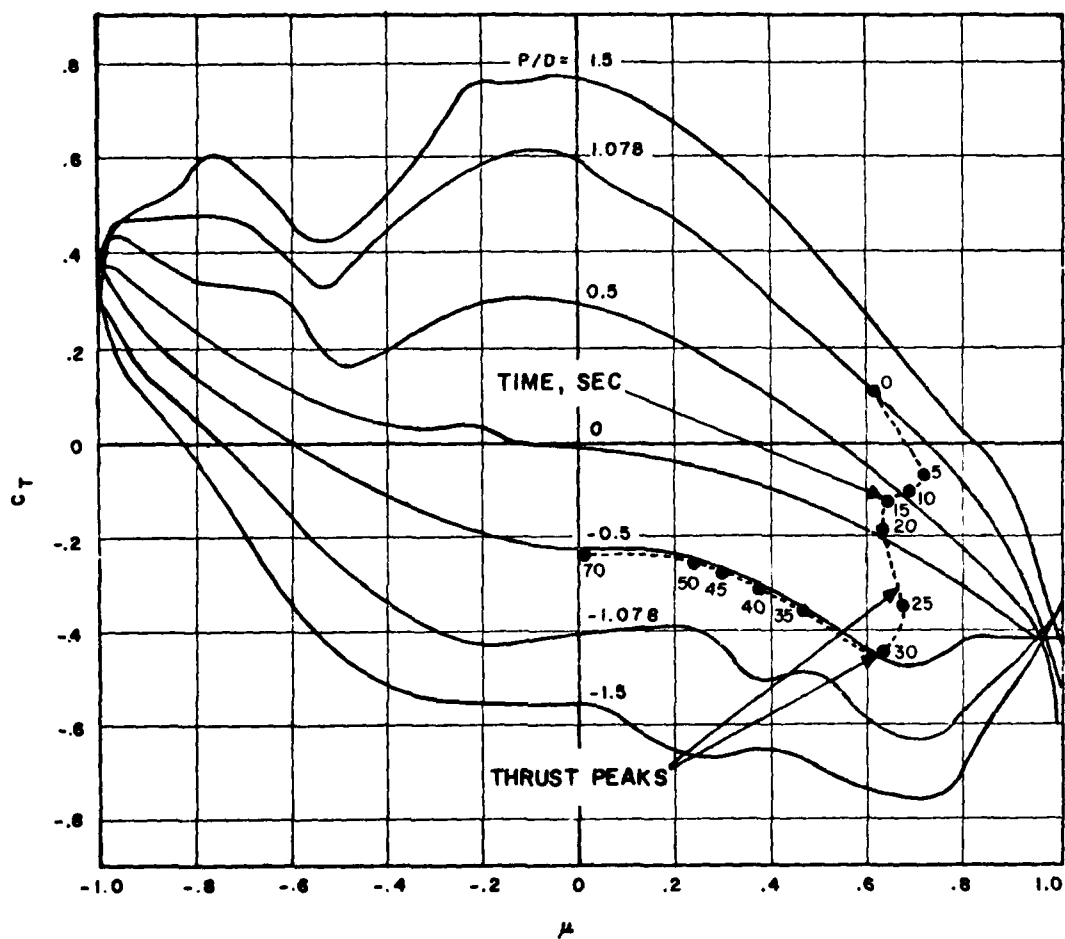


Figure 6,c. Locus of Transient Modified Advance and Thrust Coefficients for Crashback from Maximum Ahead (7512261)

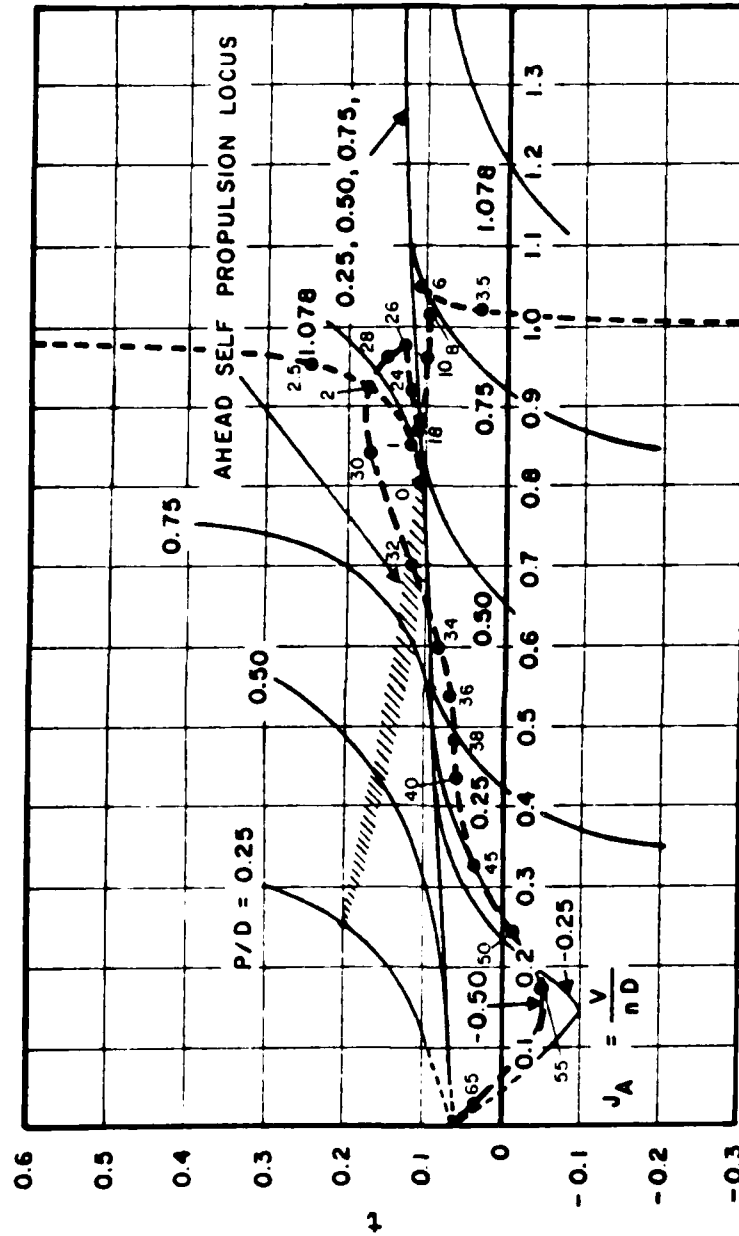


Figure 6,d. Thrust Deduction Fraction Locus  
During Crashback from Full Ahead  
from Behind-the-Hull Data  
(Constant  $w = 0.05$ , Run 7602241)

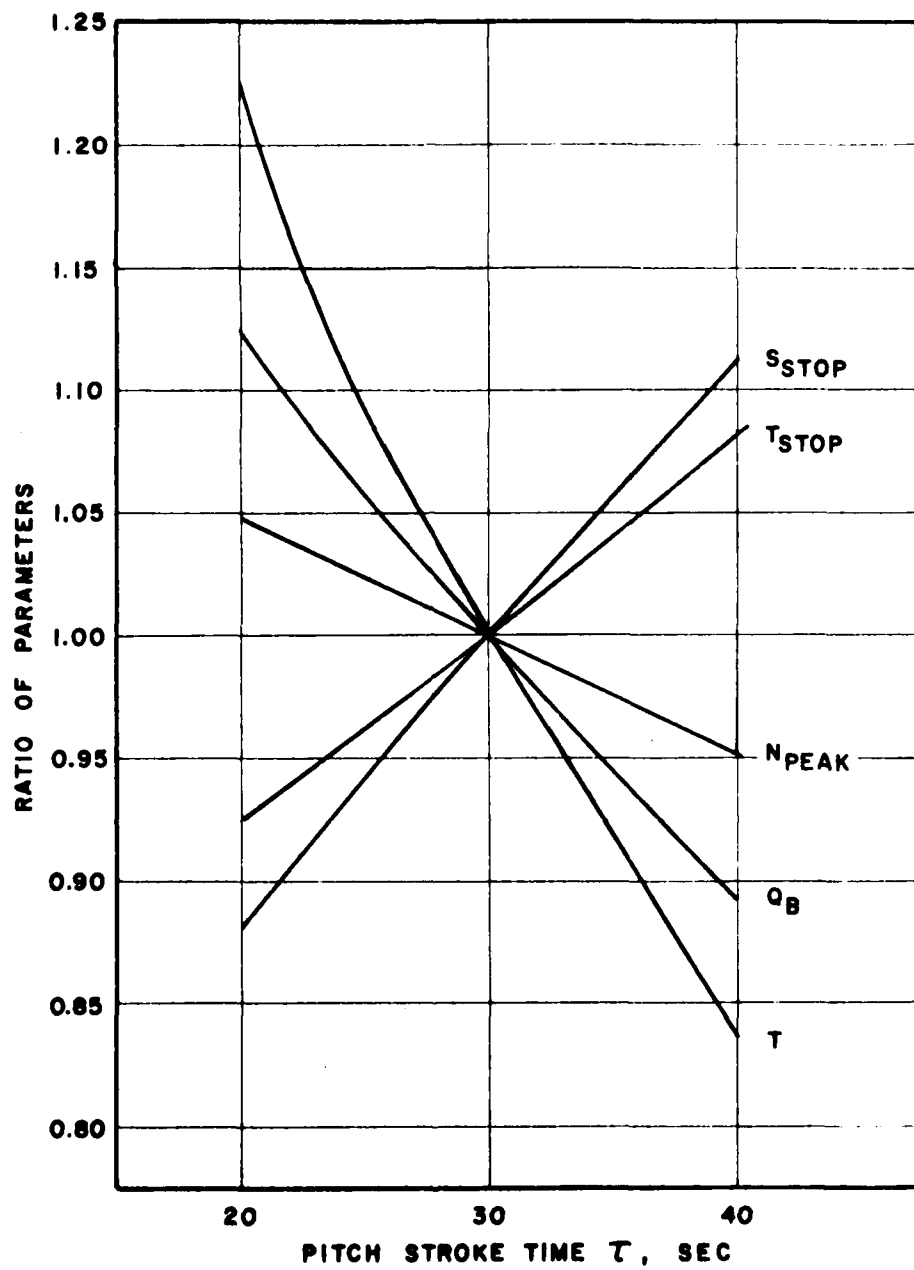


Figure 7. Effect of Pitch Stroke Time (Parameter Ratios)  
for Crashback from Maximum Ahead  
( $w$  and  $t$  Constant)

During crashback from full ahead, the magnitudes of the five parameters,  $N$ ,  $T$ ,  $Q_B$ ,  $T_{STOP}$  and  $S_{STOP}$  were all essentially linearly proportional to wake fraction when the wake fraction in the simulation is assumed constant during the maneuver. Under such conditions a +100% change in wake fraction (from  $w = 0.05$  to  $0.100$ ) caused the following percentage changes in these parameters (at their peak values for  $N$ ,  $T$ ,  $Q_B$ ):

$$\frac{\Delta N}{N} = -3.9\% \quad \frac{\Delta T_{STOP}}{T_{STOP}} = +2.2\%$$

$$\frac{\Delta T}{T} = -2.0\% \quad \frac{\Delta S_{STOP}}{S_{STOP}} = +3.4\%$$

$$\frac{\Delta Q_B}{Q_B} = -7.8\%$$

Transient wake fraction data can be an input into ship propulsion dynamics simulations in the form of behind-the-hull propeller data tested over the anticipated range of  $J_A$  with no need to utilize a wake fraction. Wake fraction is cumbersome to compute and use in simulations because of its asymptotic behavior as  $V$  or  $J_A$  approach zero. In most cases ship maneuvering simulations must rely on open water propeller data with only crude estimates of wake fraction.

When ship propulsion dynamics and control simulations are conducted to evaluate propulsion control system approaches, steady-state wake fraction data is adequate, but when comparing simulations against full scale trials, behind-the-hull propeller test data becomes important if good correlations are expected.

Along with the experimental wake fraction model tests, the thrust deduction fraction was determined for the same frigate model hull and propeller for various pitch ratios and powering conditions to obtain the thrust deduction fraction under overload situations off the self propulsion point encountered during acceleration and deceleration. The experimental thrust deduction fraction data and idealized parametric thrust deduction fraction data were used in the simulations. Results of these simulations in the prediction of peak transmission loads and ship maneuvering characteristics were compared. All the simulations of transient thrust deduction fraction  $t$  with both idealized and experimental data were conducted using the method of an effective behind-the-hull propeller thrust coefficient  $K_R$ . This technique eliminates the need for  $t$  in simulating the crashback transient time history.

The effect of thrust deduction fraction was determined during crashback from full ahead on the five parameters  $N$ ,  $T$ ,  $Q_B$ ,  $T_{STOP}$  and  $S_{STOP}$  for  $t$  constant during the crashback. The sensitivity to a 100% change in  $t$  ( $t = 0.100$  to  $0.200$ ) was:

$$\frac{\Delta N}{N} = -1.5\% \quad \frac{\Delta T_{STOP}}{T_{STOP}} = +7.6\%$$

$$\frac{\Delta T}{T} = +3.4\% \quad \frac{\Delta S_{STOP}}{S_{STOP}} = +3.2\%$$

$$\frac{\Delta Q_B}{Q_B} = -2.9\%$$

The above results which seem to indicate a negligible effect of  $w$  and  $t$  on these variables are deceptive. In cases where experimental transient wake fraction was employed, errors in  $w$  on the order of 300% during transients are not uncommon. The extremely complex transient behavior of both  $w$  and  $t$  during crashback or crashahead maneuvers resulting in part from the definitions of  $w$  and  $t$  makes their use impractical in such simulations. If the simulations require the additional accuracy then behind-the-hull propeller data should be used with no need to define the  $w$  and  $t$  transient behavior.

During crashback maneuvers with a CP propeller ship, severe transmission and propeller loads are possible unless limited by the propulsion control system. In the early phase of a crashback with the engine(s) at idle, the propeller can experience negative thrust peaks much larger than the maximum ahead condition, the propeller speed increases as propeller pitch decreases, and the propeller blade spindle torque reaches peaks several times the maximum ahead value. Peak shaft torques and thrusts during the fuel-at-idle phase are not affected by engine torque or PLA limits, but rather determined by pitch stroke time,  $\tau$ , propeller and ship speeds. The greatest effect on peak negative propeller thrust is that due to pitch stroke time,  $\tau$ , where for example, a decrease in  $\tau$  from 30 seconds to 20 seconds increases peak negative thrust by more than 22% while decreasing the stopping distance by less than 12%. For decreasing  $\tau$ , the peak blade spindle torque increases greatly. A possible tradeoff is to increase  $\tau$ , thus decreasing the peak propeller loads, then after the largest peak loads have occurred, apply greater astern engine power during the rest of the crashback maneuver until the ship is stopped. During the engine reacceleration phase with the ship still moving ahead and with negative pitch engine torque limiting and PLA/PR limiting must be employed.

Crashahead, which is forward acceleration of a backing ship represents probably the most severe potential transient loads. For example, with each of two engines limited to about 70% of full power, the controlled crashahead produced a peak propeller thrust 24% above the maximum ahead condition; with the engine torque limiter and PLA/PR limiter disabled and the same ahead engine power this percentage would have increased to 69%. Thus, the control system design is very important in limiting peak loads during crashahead.

Computer simulations are now in world-wide use for the prediction of peak engine, propeller, and transmission loads together with ship performance during the development of propulsion control system designs. The areas of uncertainty are mainly those of hydrodynamics concerned with hull, propeller and hull/propeller interactions. Considerable work has already been accomplished in the prediction of peak propulsion loads and propulsion performance simulations while the area of propulsion control system design and specification is still undergoing a continuing evolution.

## APPENDIX A - PROPULSION SYSTEM MODEL

The propeller data used in this simulation is represented in terms of the modified advance coefficient  $\mu$ . The definition of propeller modified advance coefficient and propeller thrust and torque coefficients is given below.

$$\mu = \frac{V_A}{\sqrt{V_A^2 + n^2 D^2}} \quad (\text{modified advance coefficient})$$

$$C_T = \frac{T}{\rho D^2 (V_A^2 + n^2 D^2)} \quad (\text{modified thrust coefficient})$$

$$C_Q = \frac{Q}{\rho D^3 (V_A^2 + n^2 D^2)} \quad (\text{modified torque coefficient})$$

where  $D$  is the propeller diameter,  $\rho$  is water mass density,  $n$  is propeller rotational speed and  $V_A$  the propeller speed of advance given by  $V_A = V(1 - w)$ .

Spindle torque on a controllable-pitch propeller is the torque acting to turn each blade on its axis. This torque caused by hydrodynamic and centrifugal forces must be opposed under steady-state conditions and at times exceeded by the propeller blade hydraulic system when the propeller pitch is changing. The blade spindle torque  $Q_B$  is given by the sum of the hydrodynamic,  $Q_{BH}$ , and centrifugal,  $Q_{BC}$ , components

$$Q_{BH} = C_{BH} \rho D^3 (V_A^2 + n^2 D^2) \quad (\text{hydrodynamic component of blade spindle torque})$$

$$Q_{BC} = K_{BC} \rho_B n^2 D^5 \quad (\text{centrifugal component of blade spindle torque})$$

The hydrodynamic spindle torque coefficient  $C_{BH}$  is a function of both the propeller pitch ratio and modified advance coefficient, whereas the centrifugal coefficient  $K_{BC}$  depends only on the pitch ratio. In the  $Q_{BC}$  equation,  $\rho_B$  is the blade material mass density.

Figures A-1 and A-2 show "four quadrant" thrust and torque coefficient open-water model test data in modified form for a controllable-pitch propeller. This five-bladed propeller has an expanded area ratio of 0.826 and a pitch ratio of 1.078 at 0.7 radius. Its characteristics are very similar to propeller model 4402 discussed in reference 1.

The CP propeller ship propulsion dynamics equations with no turning are given below in terms of the propeller modified coefficients. These equations do not include engine dynamics or propulsion control system models.

$$m \frac{dV}{dt} = C_T \rho D^2 (V_A^2 + n^2 D^2) (1 - t) - R_T \quad (\text{thrust equation})$$

$$2\pi I \frac{dn}{dt} = k_g (Q_{E_{\text{base}}} + Q_{E_{\text{boost}}}) - Q_f - C_Q \rho D^3 (V_A^2 + n^2 D^2) \quad (\text{torque equation})$$

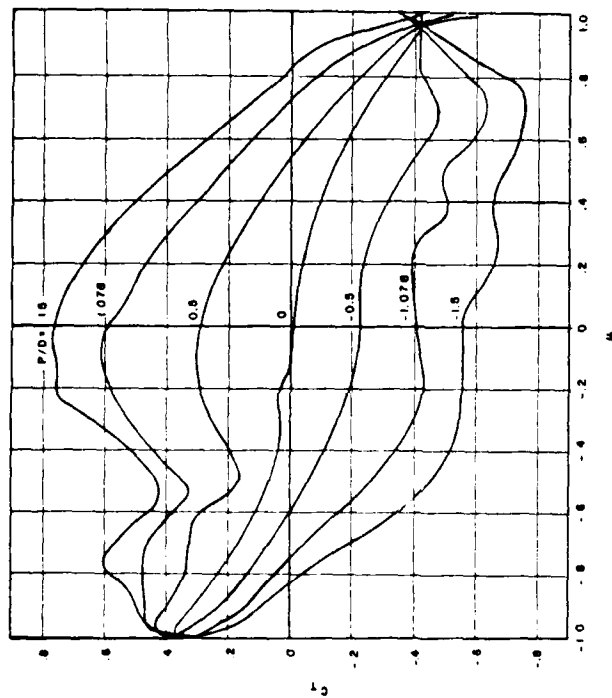


Figure A-1. CP Propeller Modified Thrust Coefficient Versus Modified Advance Coefficient  $\mu$  for Various Pitch Ratios

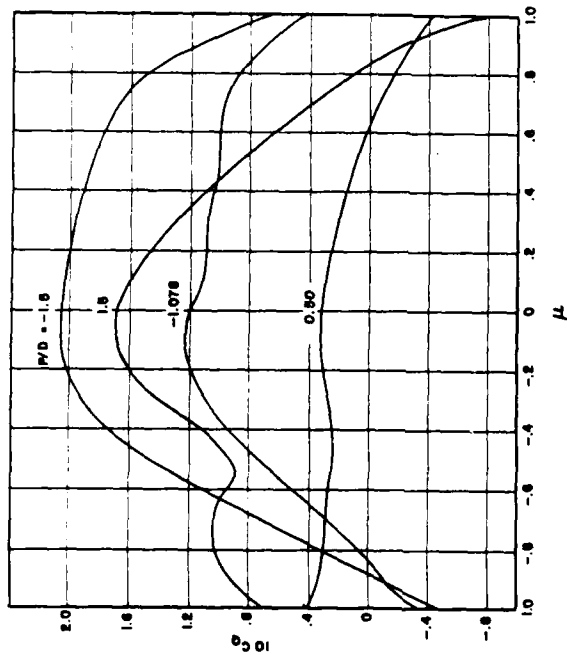


Figure A-2. CP Propeller Modified Torque Coefficient Versus Modified Advance Coefficient  $\mu$  for Various Pitch Ratios

$$PR = PR_i + \left( \frac{PR_T}{\tau} \right) t \quad (\text{pitch ratio equation})$$

These equations together with the engine dynamics and control system simulation comprise the digital computer simulation. Nonlinear functions such as the propeller coefficients and ship resistance are stored as computer look-up tables.

Propeller open-water thrust is corrected by the thrust deduction factor  $(1 - t)$ , note that everywhere else  $t$  is time. The instantaneous pitch ratio  $PR$  varies with time from an initial pitch ratio  $PR_i$ , taking  $\tau$  seconds to change a total amount  $PR_T$  (total pitch ratio change from design ahead to design astern). In this simulation  $\tau = 30.0$  seconds and  $PR_T = 1.618$ .

Engine torque  $Q_E$  is obtained by a dynamic simulation of the gas turbine engine. The gas turbine engine simulation solves a number of differential equations relating gas flows, temperatures and pressures within the engine to the speed of the two rotating engine components, namely the turbine-compressor rotor and the power turbine rotor. The power (free) turbine is aerodynamically coupled to the gas generator.

The drive train moment of inertia including 25% for propeller entrained water referred to propeller speed is  $9.8 \times 10^4$  lb-ft-sec<sup>2</sup> for one engine and  $10.92 \times 10^4$  lb-ft-sec<sup>2</sup> for two engines; ship mass  $m$  is that corresponding to  $W = 9.68 \times 10^6$ . These values together with the drive train frictional torque  $Q_f$  are the same as those of reference 1.

#### APPENDIX B - NOMENCLATURE

BTL	Bridge throttle lever position
CPP	Controllable-pitch propeller
$C_{BH}$	Propeller modified hydrodynamic spindle torque coefficient
COGAG	Combined gas turbine and gas turbine propulsion plant
$C_Q$	Propeller modified torque coefficient
$C_T$	Propeller modified thrust coefficient
$D$	Propeller diameter
$F$	Carriage force
$J$	Propeller advance coefficient
$J_A$	Propeller apparent advance coefficient
$K_{BC}$	Propeller centrifugal spindle torque coefficient
$K_g$	Reduction gear ratio
$K_Q$	Propeller torque coefficient
$K_R$	Effective propeller thrust coefficient
$K_T$	Propeller thrust coefficient
$m$	Ship mass
$N$	Propeller speed, rpm
$n$	Propeller speed, rps
$N_{GG}$	Gas generator speed
$N_P$	Power turbine speed



In phase 3 the fuel flow is again lowered to a value below the idle point. Now the braking action of the propeller is transformed by the thyristor-set driving the gas turbine with constant frequency at minimum speed. Because the level of braking power determined by the fuel flow is constant, this means a hyperbolic increase of braking torque for the propeller with decreasing speed. This is a very effective way to reduce the propeller speed in the 4th quadrant of the torque-speed-diagram.

After 32 seconds the propeller passes through speed zero and in phase 4 is accelerated with a fuel flow profile for maximum temperature at the turbine entry to stationary operation in the 3rd quadrant, until the ship is dead in the water. This happens after 354 seconds and a stopping distance of a little more than 1 nm.

Fig. (7) shows the torque-speed-diagram and the lines of operation for gas turbine and propeller. In the vicinity of propeller speed zero it is necessary to limit the braking torque by a fast thyristor governor to an acceptable value determined by shafting and couplings. According to informations from manufacturers this seems to be no problem for modern power electronics.

To demonstrate the result of including all formerly described physical effects within the turbomachines and the heat exchanger, Fig. (8) compares cases a. and d. during the first minute of a crash-stop-maneuvre. The initial fuel flow pattern is the same. An interesting feature is the reduction of braking power during phases 1 and 3, which is caused by the additional heat release of the turbo-machines and heat exchanger, thus retarding the efficiency of the fuel flow pattern. Fig. (9) shows the same comparison in the torque-speed-diagram.

It is obvious that serious misinterpretations will happen for this gas-turbine's short-time-behaviour, when only quasi-static modelling for the cycle dynamics is used.

To which extent will the computed stopping ability of the ship be influenced by the gasturbine model complexity? This point is of special interest to the naval architect as well as to the propulsion

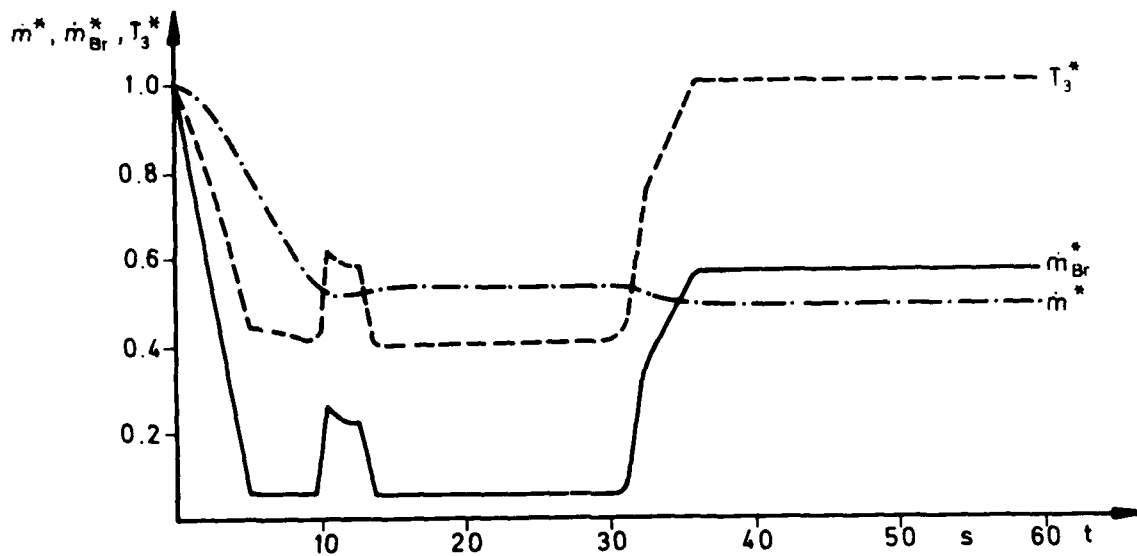


Figure 6 Related mass flow, fuel flow and turbine entry temperature during crash-stop (case a)

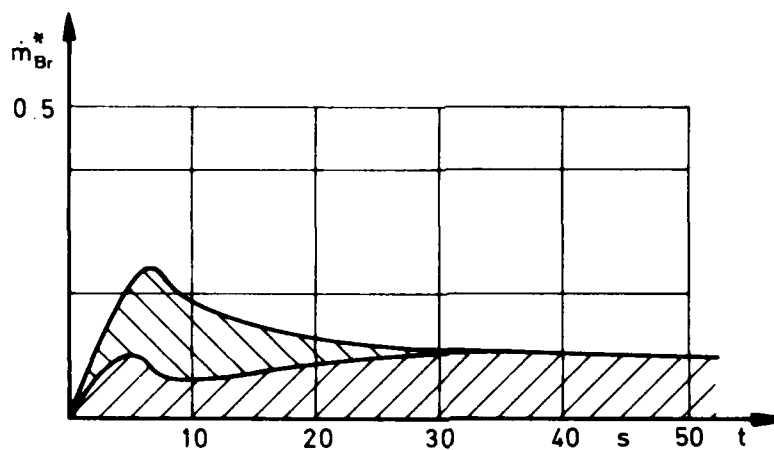


Figure 4 Excess fuel flow during acceleration

≡ fuel used for acceleration of plant  
 ≡ fuel used for temperature increase of recuperator material

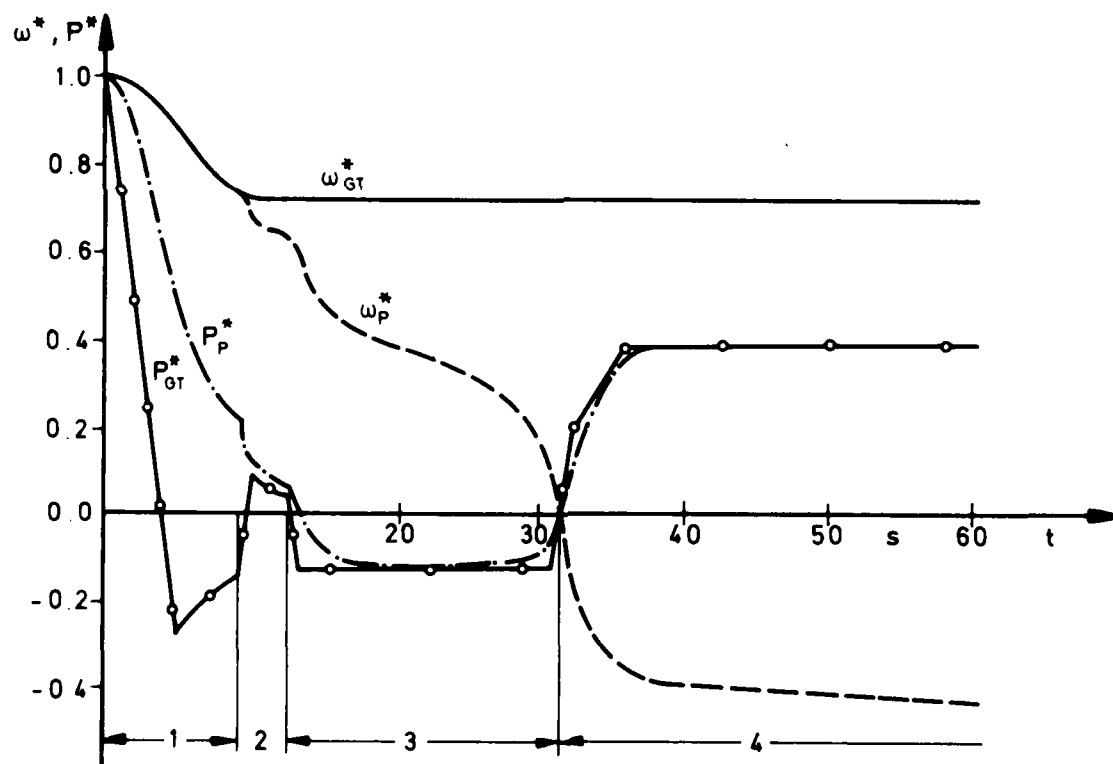


Figure 5 Speed and power transients for gasturbine and propeller during crash-stop (case a)

in this case they happen to level out each other after 30 seconds of acceleration.

#### Computed Crash-Stop Maneuvres

To compare the influence of different refinements within the gas turbine model the engine- and ship dynamics were computed for

- a. gas turbine without thermal storage effects (quasi-stationary behaviour)
- b. gas turbine with heat storage in turbo-machine parts (diabatic process)
- c. heat storage only in the recuperator
- d. regard of all storage effects in the gas-turbine-cycle.

The ship assumed is a modern, 4th generation single shaft container ship. The dynamic response of the 6-bladed propeller is calculated by use of the Wageningen-Fourier-Coefficients (8) for torque and thrust. Wake- and thrust-deduction-factor are considered to be constant, while the ship's resistance was reckoned by using the towing tank curve.

Fig. (5) shows the path for gas turbine- and propeller-speed and -power for case a. During phase 1 fuel flow is rapidly decreased to a value well below the idle-point. This causes the propeller to transfer power via the propeller-motor acting then as a generator and the generator acting as a motor to drive the compressor. It is an inherent advantage of the single shaft gas turbine, that it is able to absorb a certain amount of braking power by reducing fuel flow below the idle line.

When after approximately 10 seconds the gasturbine's speed reaches the compressor performance limit, the synchronous coupling of generator and motor must be released. With a short power burst caused by the according fuel flow pattern shown in Fig. (6) the gas turbine speed is stabilised to the minimum allowable rpm for stall-free operation. This is phase 2 of the manœuvre.

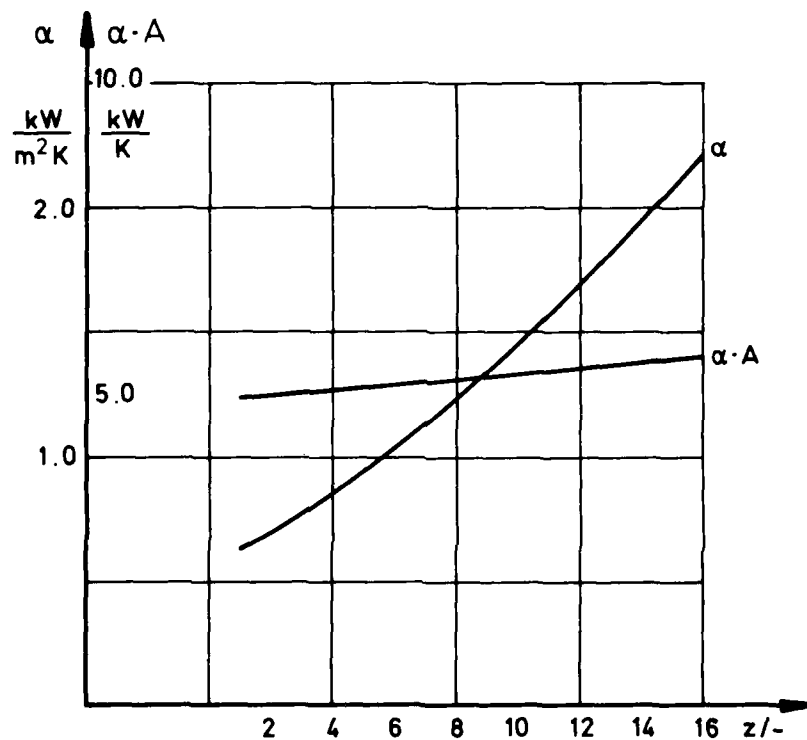


Figure 3 Heat transfer conditions of a single-shaft-gt compressor at service rating

Z No. of stages

are determined. Afterwards the change of state is corrected for the diabatic process. This is repeated to improve accuracy. The procedure converges quickly.

Fig. (3) shows the heat-transfer-coefficient and the even more important product of  $\alpha$  by the heat-transfer-area for the compressor of a single shaft heavy duty gas turbine running at nominal point. While the value of  $\alpha$  changes from compressor-entry to -exit by roughly 4, the product is nearly constant because of the change of heat-transfer-area across the stages. The same is true for the turbine, where at the entry  $\alpha$  is high and the area is small, while a low value of  $\alpha$  and a high value of A correspond at the exit.

#### Dynamic behaviour of the recuperator

For heavy duty gas turbines of moderate temperature and pressure level the integration of a heat-exchanger is necessary to obtain a satisfactory sfc. In this study a modern plate-fin-counter-flow recuperator was incorporated. The dynamics of this component are described by a set of three differential equations (2), each one representing either the time-dependent change of air-, wall- and gas-temperature along the flow path. For the solution a proposal was used, by which for a small intersection of the heat-exchanger the recuperator is represented by a regenerator with very small switching time. This method is characterized by good convergence and small computation time (7) and therefore is well accustomed for a digital simulation model.

The result of the recuperator within the cycle is demonstrated by Fig. (4), which shows the excess fuel flow profile for an acceleration from idle to full power. Heat storage is only considered for the recuperator. During the first 30 seconds, nearly 50 percent of the excess fuel is consumed by heating up the heat exchanger material.

After this period the effect vanishes, though the acceleration is not terminated. This is due to the fact, that the acceleration proceeds along the line of maximum turbine-entry-temperature. That means decreasing turbine-exit-temperature with growing power output. Therefore the mean temperature level on the heat-exchanger is decreasing, while it is increasing on the air-side. As both changes are retarded,

## Effect of heat storage in turbo machines

During a transient the change of local temperature within the stages will cause an intense heat transfer between the fluid and the material of blading, stator and rotor. To include the heat exchange into a mathematical model for the gas turbine's dynamic behaviour it is necessary to abolish the assumption of adiabatic change of condition of state and to accept the realistic diabatic process.

The law of energy conservation for non-steady conditions leads to

$$\alpha A (T_{\text{Mat}} - T_G) = m_G c_p \left( w \frac{\partial T_G}{\partial t} + \frac{\partial T_G}{\partial t} \right) \quad (15)$$

$$\alpha A (T_{\text{Mat}} - T_G) = - m_{\text{Mat}} c_{\text{Mat}} \frac{T_{\text{Mat}}}{t} \quad (16)$$

for a single stage of a turbo machine.

This model only includes the effect of heat transfer between material and gas flow, but excludes the complicated process of heat conduction within the sophisticated mechanical components of the engine. This seems to be appropriate, because our aim was to develop a model for project studies, during which the otherwise necessary knowledge of the complete engine mechanical lay out normally has not yet been obtained. As this is also relevant for the heat-transfer-input data, a reckoning method to derive these from similar engines already in operation was included. It is described in (2).

Solution of Eq. (15) and (16) for a time-intervall  $\Delta t$  gives the amount of transferred heat. By that the polytropic exponent for pressure- and temperature -change within the stage and the thermodynamic state at the stage-outlet can be defined. Because these coupled differential equotations are to be solved for each stage, the momentary state of flow, which is affecting the heat exchange, must be known. The solution is obtained by iteration. For the first step the state-change is computed by assuming adiabatic behaviour, using Eq. (3) - (6). With these values for temperature and pressure, the actual Reynolds- and Prandtl-Number for the stage and the resulting heat-transfer-coefficient

$$\alpha = \frac{\lambda}{l} a R_e^b \text{Pr}^c \quad (17)$$

In recent publications (e.g. (3)) such quasi-stationary models have been used to full extent. In order to assume the magnitude of transient thermodynamical and aerodynamical effects on the dynamic response, the necessary computer program was adapted to these questions.

#### Effect of mass storage in turbo machines

While the existence of unsteady flow is tantamount for the function of a turbomachine (otherwise in a real stage with a limited number of blades no energy could be transferred; see (4)), the addition of time dependent disturbances is not yet possible even in by far more sophisticated flow models as used here. Therefore only a rough assumption is possible, whether this effect has to be taken into account or not.

The change of mass within a limited volume is described by

$$\frac{d}{dt} m_{1,2} = \dot{m}_1 - \dot{m}_2 \quad (13)$$

when using average values of temperature and pressure along the flow path. Eq. (13) leads to Eq. (14) by adaption of the gas law.

$$\frac{d}{dt} m_{1,2} = \dot{m}_{1,2} = V_{1,2} \left( \frac{1}{RT_{1,2}} \dot{P}_{1,2} - \frac{P_{1,2}}{RT_{1,2}^2} \dot{T}_{1,2} \right) \quad (14)$$

The solution of this differential equation can be obtained for appropriate assumptions for the different turbo-machinery-volumes.

The complete equations may be taken from (2). They led to the conclusion, that in open cycle gas turbines the effect of mass storage on the pressure and temperature rise under transient condition within the turbomachine components may be neglected because of the small component-volumes in modern gas turbine applications. This coincides with (5) for jet engines and with (6) for closed cycle gas turbines.



are used, which are derived from the Euler-Equation for axial stages assuming rotational flow symmetry. The meridian flow plane is considered to be representative for the flow between hub and tip.

When solving the quasi-stationary problem, the computation of the following 8 unknowns for the gas turbine

$$\dot{m}; \pi_V; \epsilon; T_3; \eta_{V,S}; \eta_{T,S}; \omega; \frac{d\omega}{dt}$$

is necessary.

Beneath Eq. (1) we use the fuel flow as the control variable

$$\dot{m}_{Br} = f(t) \quad (6),$$

and further on

$$T_3 = f(\dot{m}_{Br}, \dot{m}, \omega) \quad (7),$$

$$\pi_V = f(\dot{m}, \omega) \quad (8),$$

$$\epsilon = f(\pi_V, T_3, \dot{m}) \quad (9),$$

$$\eta_{V,S} = f(\dot{m}, \omega) \quad (10),$$

and

$$\eta_{T,S} = f(T_3, \dot{m}, \omega) \quad (11).$$

If no storage effects within the turbomachine are taken into account, the mass flow balance between compressor and turbine is further added (Eq. 12).

$$\dot{m}_V = \dot{m}_T \quad (12)$$

Eq. (6) - (11) are fully described in (2).

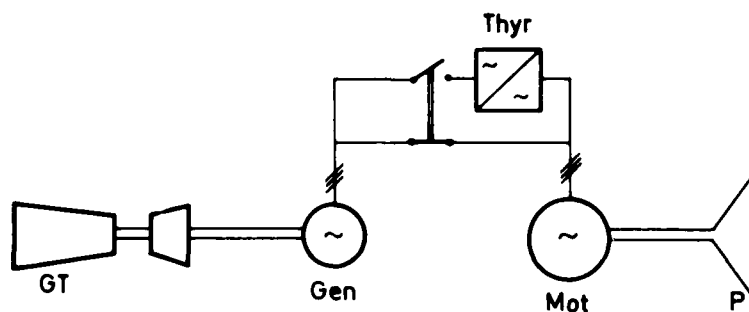


Figure 1 Gasturboelectric propulsion plant with single-shaft-gasturbine and fixed pitch propeller

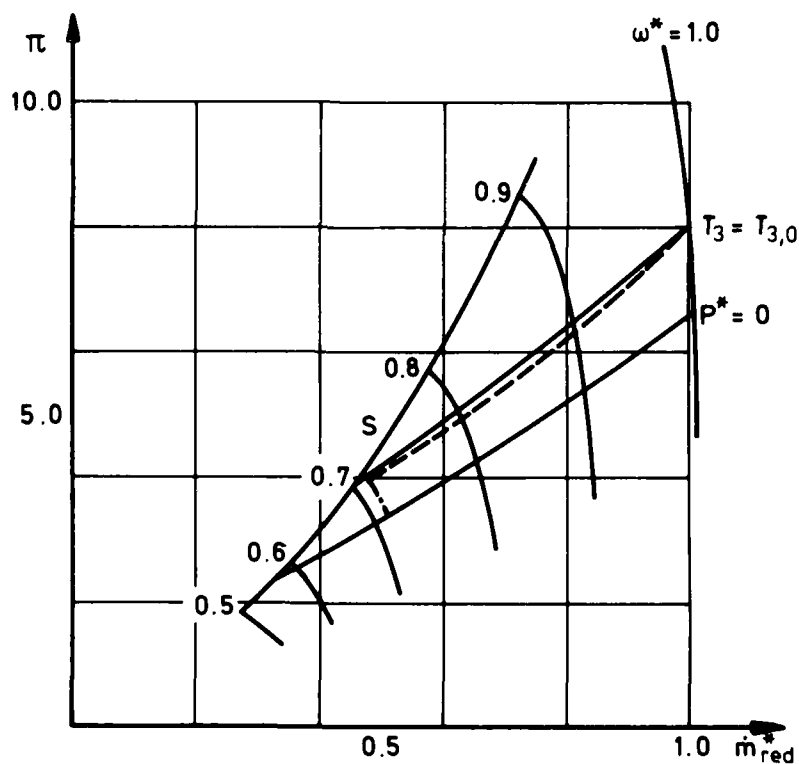


Figure 2 Steady-state operationline within the compressor chart (variable geometry compressor)

S	Surge line	--	G.T. operation with variable speed (f.p. prop. load curve)
$T_3$	Turbine entry temperature	---	G.T. operation with constant speed
$P^* = 0$	Idle line		

propeller rpm is obtained via the thyristor set. (Fig. 1 and 2).

#### Dynamic behaviour

Special consideration was paid to the transient behaviour of this type of plant because of the implication of ship's safety.

Eq. (1)

$$\Theta \frac{d\omega}{dt} = Q_{GT} - Q_p \quad (1)$$

describes the dynamic response of the rotating elements, while Eq. (2)

$$m_s \frac{dv_s}{dt} = T_p - R_s \quad (2)$$

represents the response of the ship to a variation of thrust or speed. As the gas turbine dynamics were topic of this research work, the electrical components were simplified by considering them to be without transient effects except their moment of inertia.

The momentary gas turbine net torque as the difference between the turbine gross torque and the compressor torque including auxiliary drives is computed by taking into account the momentary mass flow, fuel and speed of the gas turbine components.

When reducing the problem to the quasi-stationary level, the thermodynamic and aerodynamic operation points are obtained by stage-stacking the characteristics of the components.

For the compressor and the turbine Eq. (3), (4) and (5)

$$\lambda^* = \frac{2}{\lambda_o} + (1 - \frac{2}{\lambda_o}) \varphi^* \quad (3),$$

$$\gamma^* = (1 + \frac{2}{\lambda_o} - \frac{2}{\lambda_o} \varphi^*) \varphi^* \quad (4),$$

$$\varphi^* = \dot{m}^* \frac{P_o}{P} \left(\frac{T}{T_o}\right)^{0.5} \frac{1}{\omega} \left(\frac{T}{T_o}\right)^{0.5} \quad (5)$$

## INTRODUCTION

Gasturboelectric propulsion developed during recent years as an alternative to conventional plants. The advantages result from the characteristics of the modern open cycle marine gas turbine in connection with the electric propulsion plant. Because the gas turbine uses no sea-water as heat sink, the prime mover may be accommodated independently from the propeller shafting, e.g. in the upper works of a ship, while the conventional engine room, which then only contains the electric propulsion motor, can be reduced in size.

To counteract the high specific cost of the electrical components it is desirable to use mechanical elements of the greatest possible simplicity. These are a single shaft gas turbine and a fixed pitch propeller. As this research project was performed within the frame work of Sonderforschungsbereich 98, Technische Universität Hannover, with the general theme of "Safety and Economics of fast and/or big Merchant Ships", only propulsion plants of high power output were taken into account. This leads to an ac-propulsion plant consisting out of a synchronous generator and for example a synchronous propeller motor. As the fixed pitch propeller requires variable speed including reversal when manouvering, the synchronous generator must operate either with variable speed too, or a thyristor set must be used to generate variable frequency ac according to the propeller load curve.

In order to minimize the amount of this thyristor set and therefore the additional cost, we examined the non-transient part load behaviour of a single shaft gas turbine driving a fixed pitch propeller with variable speed. The results as discussed in (1) were encouraging. Because the lower load limit for the synchronous operation of gas turbine and propeller is fixed by the compressor surge line, it is advisable to use variable geometry stages at the compressor entry to reduce the necessary thyristor power. The "electrically geared" operation is possible between approximately  $1/3$  po' and full power, resulting in a by far better part load sfc than the constant rpm-operation of the gas turbine. Below this lower load limit the gas turbine runs with constant speed, while the further reduction of

TRANSIENT BEHAVIOUR OF GASTURBO-ELECTRIC  
PROPULSION PLANT WITH SINGLE SHAFT GAS-  
TURBINE AND FIXED PITCH PROPELLER

BY DR.-ING. ECKHARD ROHKAMM  
BLOHM + VOSS AG  
GERMANY

ABSTRACT

System dynamics of a gasturboelectric propulsion plant with single shaft gasturbine, ac-synchronnous generator and -propellermotor driving a fixed pitch propeller are examined.

The fixed pitch propeller requires the gasturbine to run with variable rpm between nominal load and lower load limit caused by the compressor stall line. Below this limit the propeller motor is connected to the gasturbine-generator-set then running with constant rpm by means of a thyristor set.

Special attention is paid to gasturbine dynamics. Various gasturbine simulation models with or without regard of mass- and heat-storage within the turbomachines and the dynamic response of a recuperator are compared in their influence on a container ship's stopping characteristics. While the engine behaviour is strongly affected by storage effects, the effect on ship's dynamics is small.

Stopping ability of this ship is comparable to similar craft with conventional plants. In case of the gasturboelectric system it can be further improved by various means, which are discussed.

P/D,PR	Propeller pitch ratio
PLA	Gas turbine power lever angle
P <sub>S</sub>	Shaft horsepower
P <sub>2</sub>	Compressor inlet pressure
P <sub>54</sub>	Power turbine inlet pressure
Q	Propeller torque
Q <sub>B</sub>	Propeller spindle torque
Q <sub>BC</sub>	Propeller centrifugal spindle torque
Q <sub>BH</sub>	Propeller hydrodynamic spindle torque
Q <sub>d</sub>	Engine torque developed on propeller shaft
Q <sub>E</sub>	Power turbine torque
R <sub>T</sub>	Total ship resistance
S	Head reach
T	Propeller open-water thrust
t	Thrust deduction fraction or time
T <sub>2</sub>	Compressor inlet temperature
V	Ship speed
V <sub>A</sub>	Propeller speed of advance
W	Ship weight
w	Wake fraction
W <sub>f</sub>	Engine fuel flow rate
α	Generalized gas turbine power lever angle
U	Propeller modified advance coefficient
ρ	Water mass density
ρ <sub>B</sub>	Propeller blade mass density
τ	Propeller pitch stroke time

#### REFERENCES

- (1) C. J. Rubis, "Acceleration and Steady-State Propulsion Dynamics of a Gas Turbine Ship with Controllable-Pitch Propeller," SNAME Transactions, Vol. 80, 1972.
- (2) SV. AA. Harvald, "Wake and Thrust Deduction at Extreme Propeller Loadings," NR61, 1967, Publication of the Swedish State Shipbuilding Experimental Tank.

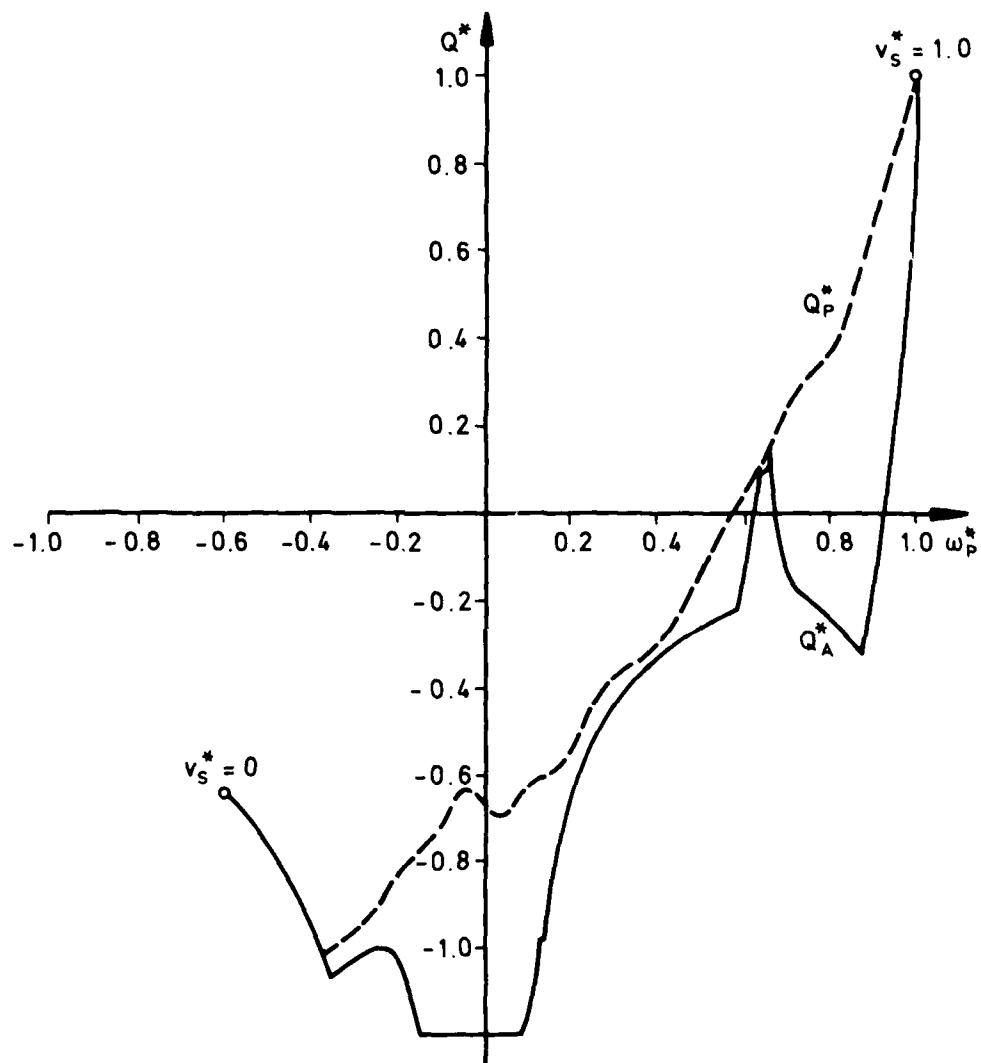


Figure 7 Torque-speed-transients during crash-stop  
(case a)

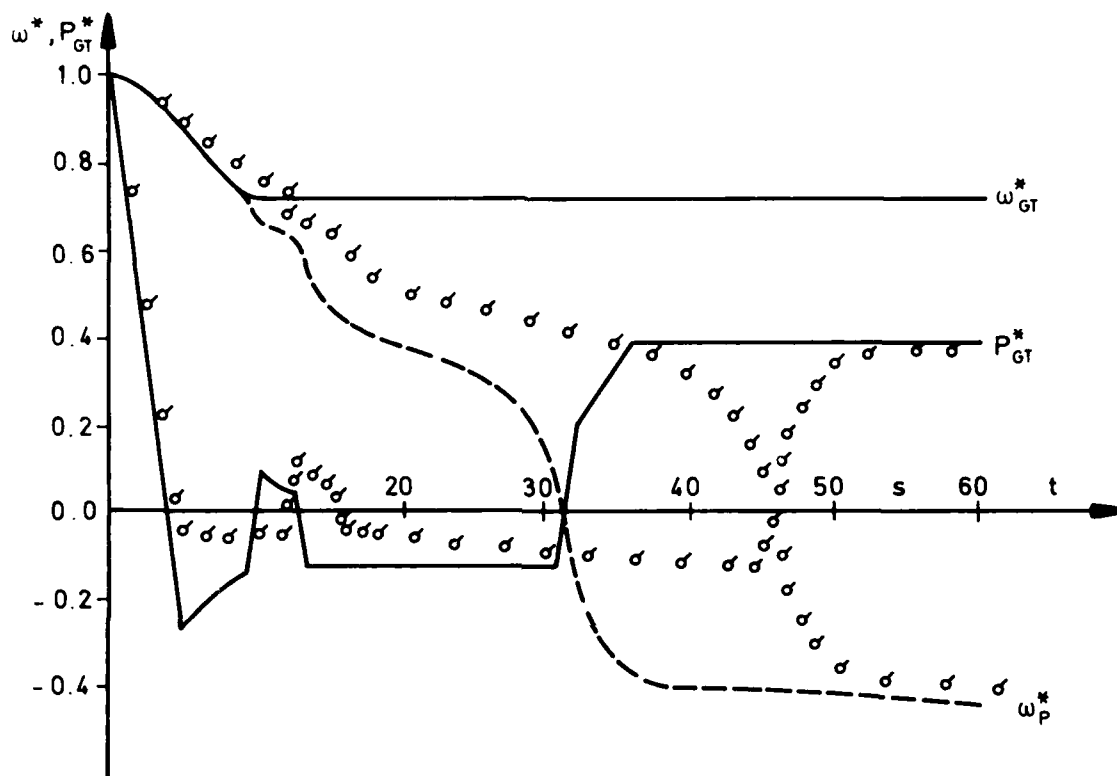


Figure 8 Speed and power transients during crash-stop

— } case a  
 - - - }  
 σ case d



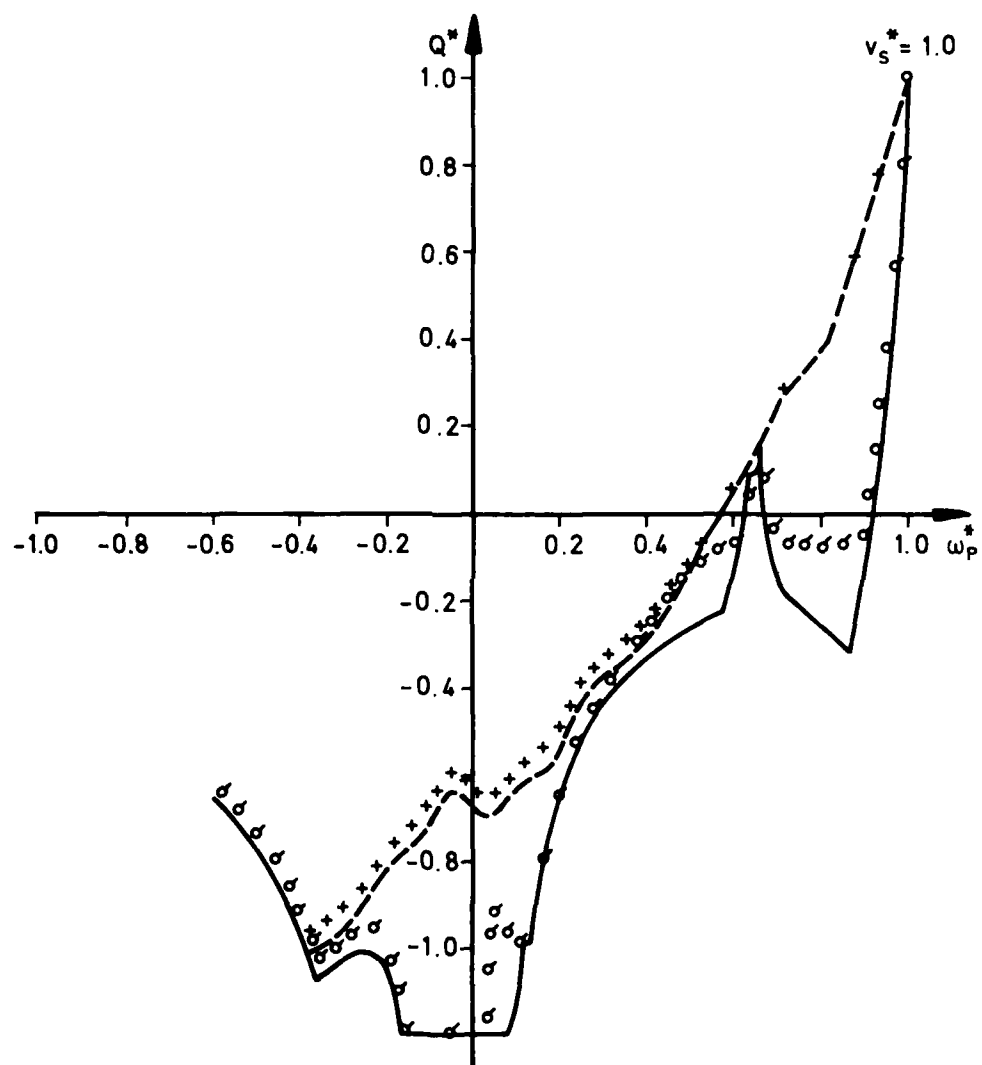


Figure 9 Torque-speed-transient during crash-stop

—	gas turbine	} case a
---	propeller	
o	gas turbine	} case d
+	propeller	

plant project engineer when studying system dynamics in an early stage of design.

Fig. (10) gives reason to the assumption, that as was to be expected, ships dynamics are only slightly affected by including storage effects in the gas turbine cycle. The band width between case a. and case d. is well below 10 % of related speed or stopping time. This margin is smaller than by considering or neglecting propeller cavitation or variation of wake- and thrust deduction factors.

What is the potential for further improvement of the ship's stopping characteristics? As shown in (2), various methods were discussed. Increasing the fuel flow slope at the beginning of manoeuvre as well as further reduction of the lower fuel limit in phases 1 and 3 improve stopping way and -time only insignificantly. On the other hand a too low fuel flow must be avoided to ensure safe operation of the combustion chambers during this critical period. Flame out on this occasion could spell disaster and really "ruin your entire day!"

The best method is to enlarge the thyristor set and therefore enable the gas turbine to operate at an increased value of speed. That means a greater astern power and a sizable cutdown in stopping distance. The interaction between astern power and stopping distance may be extracted from Fig. (11).

#### CONCLUSION

The propulsion of modern merchant-ships with gasturboelectric plants using a single shaft gas turbine and fixed pitch propeller seems to be possible. By incorporation of well proven aerodynamical methods as variable geometry stages within the compressor, the necessary amount of thyristor power can be reduced.

The transient behaviour of this plant and the associated ship-dynamics indicate, that safe operation of ship and plant also when considering crash stop manoeuvres is obtainable. The influence of more or less sophisticated gas turbine models is small on the computed stopping characteristics of the ship, but is great in its effect on the result for the dynamic performance of the gas turbine, especially during the first seconds. The design of control methods for such a plant should be based on an extensive mathematical model including storage effects.

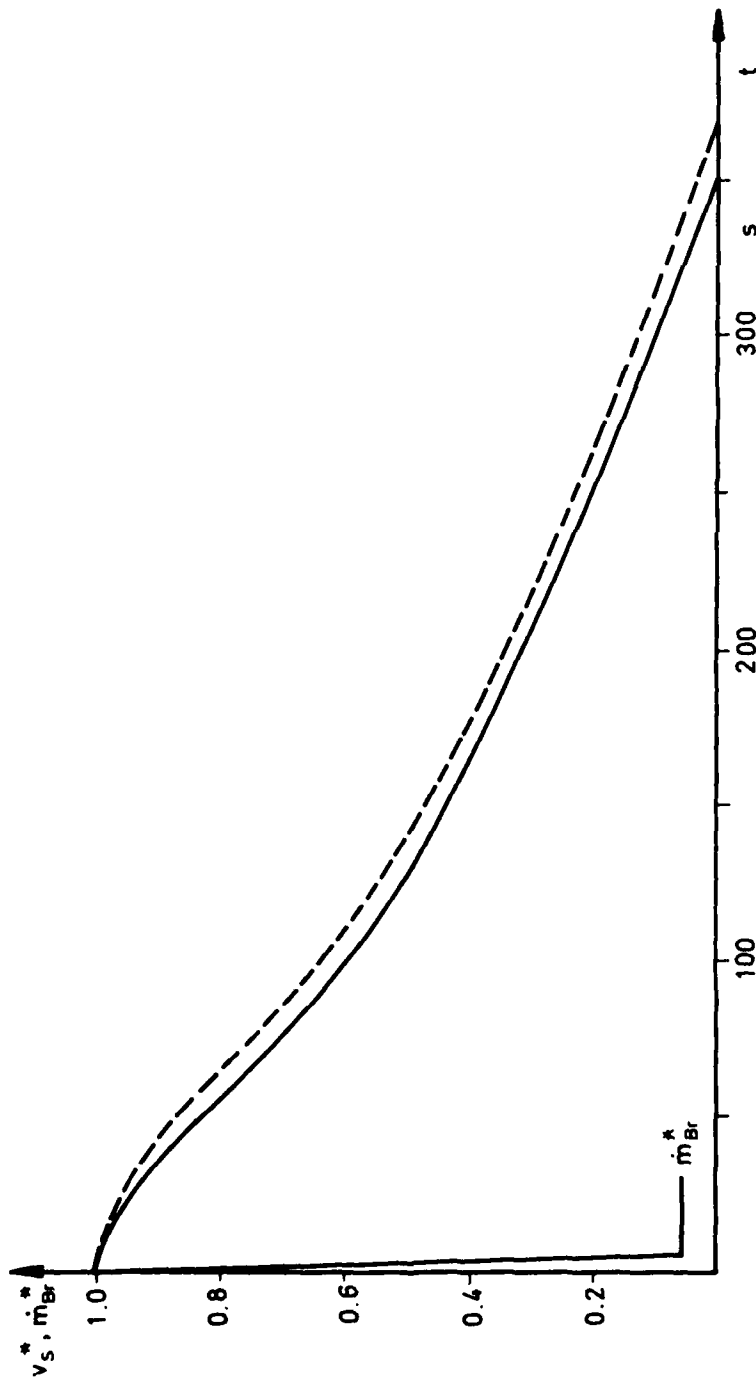


Figure 10 Stopping distance for crash-stop

$\nabla$  43000 ts  
 $P_0$  26 MW  
 $V_0$  25 Kts

— gas turbine simulation case a  
 --- gas turbine simulation case d

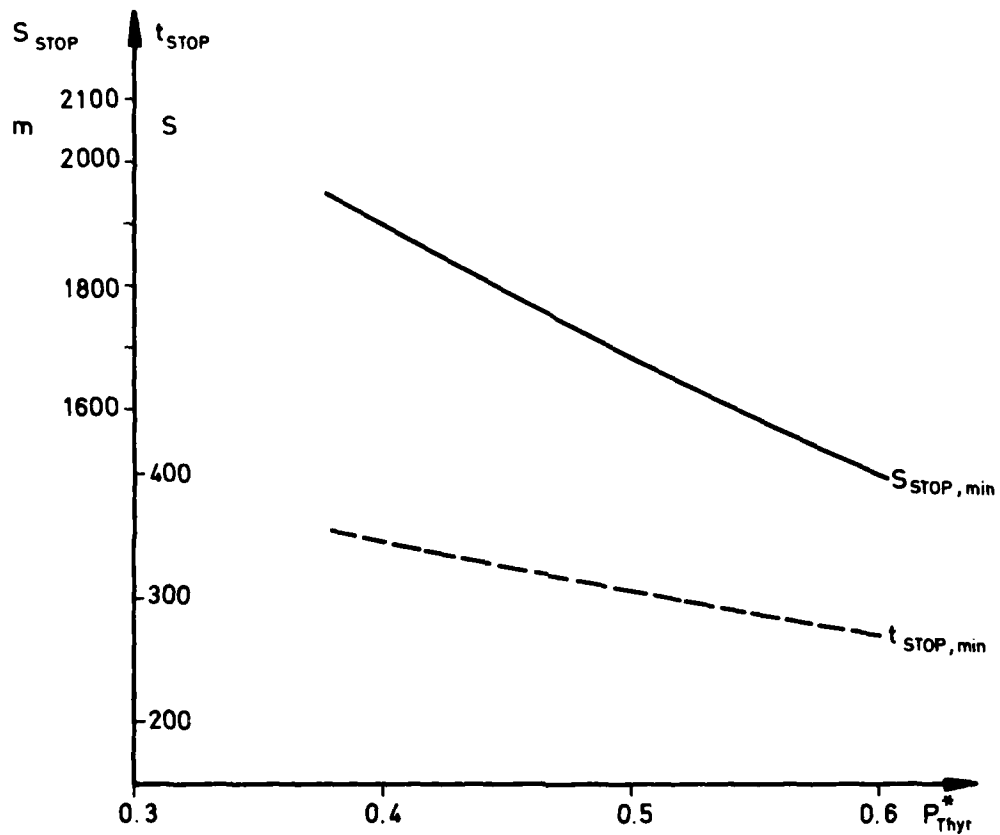


Figure 11 Stopping distance and -time for variation of Thyristor power

The necessary thyristor power for the propulsion plant cannot be fixed only reflecting the stationary part load demand. It is necessary to include propulsion dynamics for the correct dimensioning.

It is an advantage of this plant, that only by variation of the thyristor size without any change at gas turbine, electrical machines and propeller the ship's crash-stop-performance may be improved, thus giving the design-engineer an additional degree of freedom for the development of advanced surface ships.

#### ACKNOWLEDGEMENT

This project was sponsored by Deutsche Forschungsgemeinschaft within the framework of Sonderforschungsbereich 98 "Schiffstechnik und Schiffbau" at the Technische Universität Hannover/Institut für Schiffshilfsmaschinen.

#### REFERENCES

- (1) Rohkamm, E.: "Gasturboelektrische Propellerantriebe mit Einwellengasturbine"  
Hansa 113 (1976), Nr. 23
- (2) Rohkamm, E.: "Dynamisches Verhalten gasturboelektrischer Propellerantriebe mit Einwellengasturbine und Festpropeller"  
Dissertation TU Hannover, 1977
- (3) Venturini, G.: "Dynamics of Naval Propulsion Gas Turbine"  
4. Ship Control Systems Symposium,  
Den Haag, 1975
- (4) Bammert, K.: "Zur Entwicklung von stationären Axialverdichtern mit großem Schluckvermögen und hohen Druckverhältnissen"  
GHH-MAN-Renk-Symposium, Leningrad,  
Juni 1972 (Vortrag)
- (5) Bauernfeind, K.: "Die Berechnung des Übergangsverhaltens von Turbo-Strahltriebwerken unter Berücksichtigung des instationären Verhaltens der Komponenten"  
Luftfahrttechnik-Raumfahrttechnik 14,  
(1968), Nr. 5
- (6) Krey, G.: "Das dynamische Verhalten von einwelligen geschlossenen Gasturbinen"  
Dissertation TU Hannover (1974)
- (7) Dolezal, R.: "Iterationsfreies Verfahren für die Simulation großer Zustandsänderungen bei komplexen, nichtlinearen Systemen mit verteilten Parametern wie mehrstufige Überhitzer"  
BWK 28 (1976), Nr. 1

(8) Dien, R.:  
Prien, J.:

"Die rechnerische Ermittlung von Stopp-  
manövern auf Schiffen mit Propelleran-  
trieb"  
Schiff und Hafen 25 (1973), Nr. 8

# Nomenclature

$a, b, c,$	constants
$A$	Area
$c_p$	specific heat at constant pressure
$c$	specific heat
$m$	mass flow
$m$	mass
$l$	length
$P$	power
$Q$	torque
$R$	resistance
$R$	gas constant
$t$	time
$T$	thrust
$T$	temperature
$V$	volume
$w$	velocity
$x$	axial coordinate
$\alpha$	heat transfer coefficient
$\epsilon$	relative pressure loss
$\eta$	efficiency
$\theta$	polar moment of inertia
$\lambda$	heat conduction coefficient
$\lambda$	work number
$\pi$	pressure ratio
$\phi$	flow number
$\psi$	pressure number
$\omega$	angular velocity



Subscripts

Br	fuel
G	gas
GT	gas turbine
Mat	material
O	design point
P	propeller
red	corrected
s	isentropic
S	ship
T	turbine
1, 2	entry, visit
V	compressor
*	related

GAS-TURBINE SIMULATION TECHNIQUE FOR SHIP  
PROPULSION DYNAMICS AND CONTROL STUDIES

by Thomas L. Bowen  
David W. Taylor Naval Ship Research and Development Center  
Annapolis, Maryland

ABSTRACT

A gas-turbine simulation technique for ship propulsion dynamics and control studies is discussed. A review of existing generalized gas-turbine simulations indicates previous efforts have concentrated on aircraft engine configurations and few existing simulations have the capability for calculating transient performance. Marine engines of current interest are free-power-turbine gas-turbines having either single-spool or dual-spool gas generators. The mathematical techniques used to model the compressor, burner, turbine, engine load and fuel control are summarized. A modified Newton-Raphson convergence technique is used for solution convergence. Component maps, design constants, and fuel control characteristics for General Electric's LM2500 marine gas turbine are used to demonstrate this technique. Typical results are shown for steady-state and transient performance calculations.

INTRODUCTION

The purpose of this paper is to discuss a generalized gas-turbine simulation technique for ship propulsion dynamics and control studies. The inherent advantage of a generalized approach is its adaptability to solving a variety of complex control problems. The large inventory of advanced surface ships and gas-turbine propulsion systems being investigated, developed, or deployed by the U. S. Navy suggests numerous applications and a genuine need for a gas-turbine simulation similar to the one described in this paper. As the mission requirements of advanced naval vehicles become more and more demanding, dynamic considerations will play a greater role in the early stages of platform design and development. This gas-turbine simulation technique is envisioned as fulfilling a need during preliminary evaluations when expensive, complex performance decks provided by engine manufacturers can be traded for a simpler, faster and cheaper model that gives good results. A gas-turbine simulation provided by the manufacturer for a specific marine gas-turbine is typically a large, complex computer program developed from an existing aircraft engine simulation. Usually, rotor acceleration is the only dynamic affect incorporated in the simulation rendering it incapable of predicting certain transient behavior accurately. There can be several disadvantages associated with using these programs. Time-consuming gas-turbine calculations, which do not significantly affect ship dynamics, and obsolete solution convergence techniques lead to expensive computation costs. Since each engine manufacturer uses its own preferred approach to writing gas-turbine simulations, other users must repeat a learning process before using each manufacturer's simulation. And since customer users are not always involved in the development of these simulations, troubleshooting day-to-day problems or modifying the simulation to investigate new ideas becomes difficult. It is apparent from past experience

that an alternative approach to simulating dynamics of marine gas turbines is needed.

#### BACKGROUND

Gas-turbine simulation techniques that have been used for several years in the aircraft industry could be applied to naval engineering problems involving propulsion dynamics and control. Several existing computer programs for calculating steady-state and transient performance of gas turbines provide an information base for development of a generalized, flexible, and efficient simulation. Details pertaining to these existing computer programs are summarized in Table 1.

Table 1. Generalized Gas-Turbine Simulations for Digital Computers

Computer Code	Date	Developed by	Engine Configurations			Capabilities	
			Turbo-fan	Turbo-jet	Turbo-shaft	Steady-state	Transients
SMOTE	1967	AFAPL	X			X	
GENENG	1972	NASA LeRC	X	X		X	
GENENG II	1972	NASA LeRC	X			X	
NEPCOMP	1974	NADC	X	X	X	X	
DYNGEN	1975	NASA LeRC	X	X		X	X
NNEP	1975	NADC/NASA	X	X	X	X	

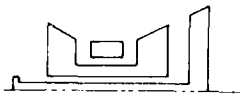
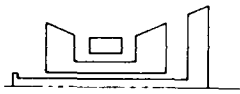

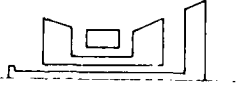




The SMOTE (1), (2) computer code was developed in 1967 by the Turbine Engine Division of the U. S. Air Force Aero Propulsion Laboratory (AFAPL), Wright-Patterson AFB, Ohio. This simulation is capable of calculating steady-state design and off-design performance of a two-spool turbofan engine. GENENG (3) was developed in 1972 by NASA's Lewis Research Center (LeRC), Cleveland, Ohio, to improve the versatility of SMOTE. Steady-state design and off-design performance of one- and two-spool turbojets can be calculated as well as the two-spool turbofan with the GENENG simulation. The GENENG II (4) computer program, a derivative of GENENG, calculates steady-state performance of two- or three-spool turbofan engines with as many as three nozzles. NEPCOMP (5) was developed in 1974 by the Naval Air Development Center (NADC), Warminster, Pennsylvania. The exceptional flexibility of the NEPCOMP simulation provides for calculation of steady-state performance of gas-turbine engines with multispools, including turbojets and turbofans (with mixed or separate flow streams) and turboshafts, as well as ramjets. The DYNGEN (6) computer code was developed in 1975 by NASA LeRC. DYNGEN has the combined capabilities of GENENG and GENENG II for calculating steady-state performance of one- and two-spool turbojet engines or two- and three-spool turbofan engines. To these capabilities have been added the further capability for calculating transient performance. NNEP (7), the newest member in this family of generalized gas-turbine simulations, was jointly developed in 1975 by NADC and NASA LeRC. The NNEP computer code is capable of simulating steady-state design and off-design performance of almost any conceivable turbine engine configuration. It is a derivative of the NEPCOMP computer code and uses stacked component maps and multiple flow paths to simulate variable cycle engines with variable component geometry. This brief review of existing gas-turbine simulations has shown that previous efforts have concentrated on turbofan and turbojet engine configurations, and few existing simulations have the capability for calculating transient performance. Therefore, considerable modifications

to an existing computer program would be necessary before it could be used to simulate transient performance of marine gas turbines.

#### MARINE GAS-TURBINE CONFIGURATIONS

Although the gas-turbine has been applied to a variety of advanced surface ships having many machinery arrangements, the engines have remained simple cycle gas-turbines. Table 2 lists some propulsion gas-turbines in the 2400 to 32000 kW power range. These gas-turbines are either currently installed aboard a U. S. Navy ship or potential candidates for future applications. Included in Table 2 is a schematic drawing of the engine configurations. All of these engines are free-power-turbine gas-turbines, and most have single-shaft gas generators (i.e. one compressor and one turbine in the engine core). A higher output power class of marine gas turbines having dual-shaft gas generators is being developed. Therefore, a generalized gas turbine simulation should have the capability to simulate both engine configurations if it is going to satisfy current near-term needs. Another important group of marine gas-turbines is single-shaft engines used for electric power generation. This engine configuration is easily simulated using a single-shaft gas generator directly coupled to the electrical machinery.

Table 2. Marine Gas-Turbines for Naval Ship Applications

Gas Turbine Make & Model	Rated Power & Speed	Engine Configuration	Naval Ship Applications
General Electric T-64	2400 kW 1000 r.p.m.		Semi-Submerged Platform "Kaimalino"
AVCO Lycoming TF-40	2500 kW 15400 r.p.m.		Amphibious Assault Landing Crafts
Garrett 990	3800 kW 3600 r.p.m.		Future Ships
Detroit Diesel Allison 570K	4000 kW 11500 r.p.m.		Future Ships
General Electric LM1500	10400 kW 5500 r.p.m.		AGEH Experimental Hydrofoil PG-84 Patrol Gunboats
General Electric LM2500	16000 kW 3600 r.p.m.		DD 963 Destroyers FFG-7 Destroyers PHM-1 Hydrofoils
Pratt & Whitney FT-9	24600 kW 4000 r.p.m.		Future Ships
General Electric LM5000	32000 kW 4000 r.p.m.		Future Ships

SHIPCON performs the following control functions:

- start/stop/stand by routines (automatic, remote or local manual control as required)
- presentation of operational parameters
- alarm functions (static and dynamic alarm limits)
- safety actions
- remote control of propulsion machinery
- remote control of systems
- condition monitoring (i.e. processing and presentation of data onboard for short term trend developments as well as recording and storage of data for further processing in SHORCON).
- independent back-up systems (conventional techniques)

To obtain the best system reliability, resistance to ship environment, weight volume and human engineering we have decided to employ the following devices as building bricks of SHIPCON:

- high quality analogue sensors
- micro computers
- alpha numeric displays
- semigraphic colour monitors
- magnetic tape

A typical SHIPCON structure is shown very simplified in principle on Fig. 1.

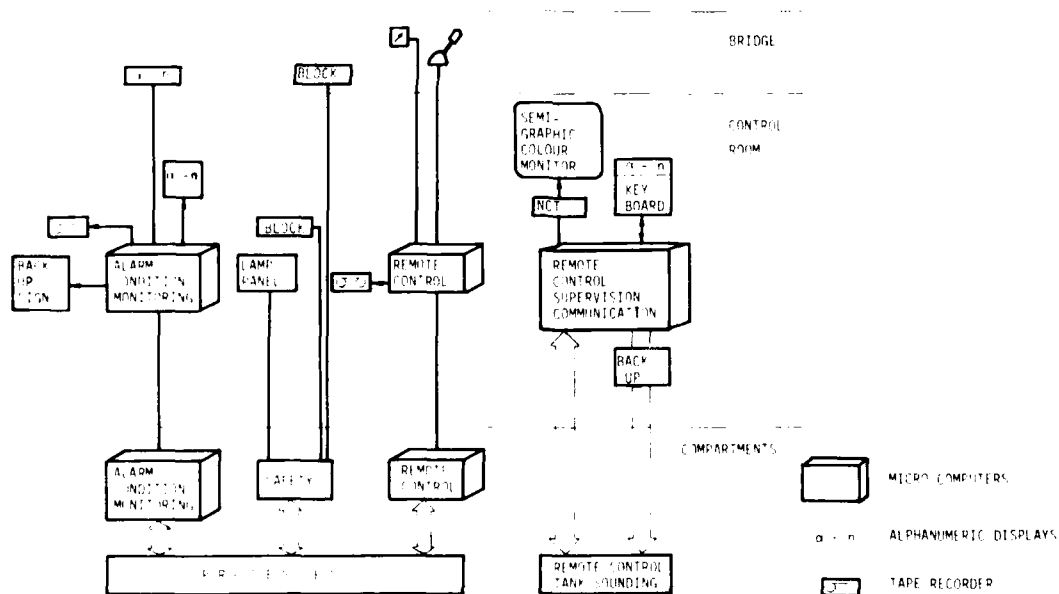


Figure 1. Typical SHIPCON Structure.

ment system as well as formulating requirements for an improved system with the overall governing aim of

#### IMPROVING SHIP AVAILABILITY

To achieve this it is obviously necessary to reduce the number, extension and frequency of programmed maintenance activities as well as trying to reduce the chances of unpredictable disturbances and break-downs.

This is the well known dilemma of striking the balance between hours at sea and hours at yard, in other words how to do the minimum amount of maintenance to achieve the required availability. It became obvious that the following measures would be necessary:

- To design the systems themselves as simple as possible to reduce the potential of disturbances.
- To install some kind of control and supervision system which would:

contain sufficient protection and safety devices.

provide the crew with better and more relevant information of the operational conditions of the machinery systems.

provide the management system ashore with information that could be processed in such a manner that maintenance activities could be predicted as well as intercepting developments leading towards otherwise unpredictable disturbances and breakdowns.

And last but not least the important requirement that the control systems themselves should not require additional specialist people onboard and mean an additional maintenance load.

#### DEFINITION OF THE SHIPCON/SHORCON CONCEPT

SHIPCON and SHORCON are complementary systems which together constitute a complete package for control and monitoring of the ship technical systems onboard as well as providing facilities for long term monitoring and administration ashore.

SHIPCON is short for SHIPBORNE CONTROL  
SHORCON is short for SHOREBASED CONTROL

SHIPCON is an integrated and computerbased shipborne control and monitoring system for ship technical functions. It comprises control objects such as

- propulsion engines
- transmission systems
- propeller systems
- electrical generating systems
- auxiliary systems in connection with prime movers and generators
- auxiliary systems associated with the hotel functions of the ship
- fire detection and extinguishing systems
- bilge, trim and compensating systems
- fuel transfer and sounding systems

NEW SHIP TECHNICAL CONTROL SYSTEMS FOR  
THE ROYAL NORWEGIAN NAVY

by Øystein Rønning, The Royal Norwegian Navy  
and Eivind Engebretsen, The Ship Research Institute of Norway

ABSTRACT

In 1975, the Royal Norwegian Navy entered an extensive new construction program. In this connection it was necessary to decide the future policy of machinery control techniques. Working groups consisting of members from the Naval Material Command, Norway, and the Ship Research Institute of Norway have developed a new operational management system including Condition Monitoring concepts and Data Techniques.

The system consists of two basic parts, the shipborne system (SHIPCON) and the shorebased system (SHORCON). The principles have up to now been applied to various projects, of which details of two are given.

The system is based upon micro-computer techniques and data storage on magnetic tape for Condition Monitoring - and Pattern Recognition processing ashore. Efficient man-machine communication has been accomplished by means of alpha numeric displays and graphic color monitors.

For the first project it was necessary to keep weight and volume of the control equipment at an absolute minimum. Due to high speed, light weight, 4-stroke engines, condition monitoring data cannot always be accomplished by direct measurements. Methods for indirect establishment of parameter values are therefore introduced. Additional data processing onboard is provided for special monitoring of certain short trend condition developments.

For the second project, graphic color screen monitoring methods are utilized for supervision of remote controlled systems.

INTRODUCTION

Around the mid-seventies, the Ship Research Institute of Norway (NSFI) was engaged by the Royal Norwegian Navy for participation in various projects with the main target of determining principles for the future use of control and instrumentation techniques in the Navy. The background for this was that the Navy at this time entered an extensive new construction program.

The staff requirements for these ships called for a minimization of the complement as well as the highest possible ship availability. At the same time it was felt among people responsible for the logistic support functions ashore that the existing technical management system could be improved.

A study was therefore carried out analyzing the existing manage-

configuration will be needed in the future. So far, rotor dynamics and control volume storage of mass and energy are the only transient effects included in the gas-turbine simulation. Heat exchange between gas and engine materials, compressor and turbine blade tip clearance changes, and fuel droplet combustion lags were neglected, but may be necessary requirements of a good marine gas-turbine simulation. It is believed there exists numerous applications and a genuine need for a gas-turbine simulation technique such as the one described in this paper. Continuing effort will depend upon the identification of a sufficient number of specific applications to warrant further development of this analytical tool.

#### TECHNICAL REFERENCES

- (1) McKinney, J. S., "Simulation of Turbofan Engine - Part I. Description of Method and Balancing Technique," AFAPL-TR-67-125-PT-1 (Nov 1967)
- (2) McKinney, J. S., "Simulation of Turbofan Engine - Part II. User's Manual and Computer Program Listing," AFAPL-TR-67-125-PT-2 (Nov 1967)
- (3) Koenig, R. W., and L. H. Fishbach, "GENENG - A Program for Calculating Design and Off-Design Performance for Turbojet and Turbofan Engines," NASA TN D-6552 (Feb 1972)
- (4) Fishbach, L. H., and R. W. Koenig, "GENENG II - A Program for Calculating Design and Off-Design Performance of Two- and Three-Spool Turbofans with as Many as Three Nozzles," NASA TN D-6553 (Feb 1972)
- (5) Caddy, M. J., and S. R. Shapiro, "NEPCOMP - The Navy Engine Performance Program," ASME 74-GT-83 (Apr 1974)
- (6) Sellers, J. F., and C. J. Daniele, "DYNGEN - A Program for Calculating Steady-State and Transient Performance of Turbojet and Turbofan Engines," NASA TN D-7901 (Apr 1975)
- (7) Fishbach, L. H., and M. J. Caddy, "NNEP - The Navy-NASA Engine Program," NASA TM X-71857 (Dec 1975)
- (8) Rubis, C. J., "Acceleration and Steady-State Propulsion Dynamics of a Gas Turbine Ship with Controllable-Pitch Propeller," in Transactions SNAME, Vol 80 (1972)
- (9) Rubis, C. J., and T. R. Harper, "Reversing Dynamics of a Gas Turbine Ship with Controllable-Pitch Propeller," Fifth Ship Control Systems Symposium (Nov 1978)
- (10) Thomson, B., "Basic Transient Effects of Aero Gas Turbines," in Power Plant Controls for Aero-Gas Turbine Engines, AGARD-CP-151 (Feb 1975)



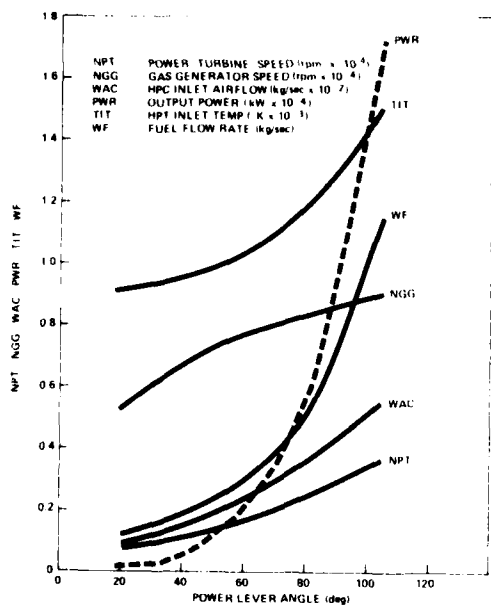


Figure 7. Steady-State Design and Off-Design Performance

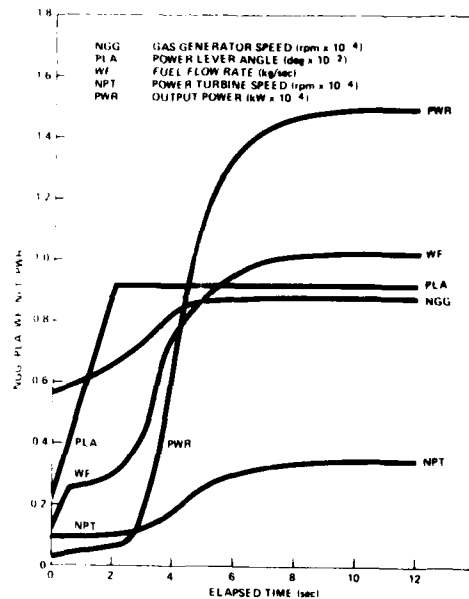


Figure 8. Typical Engine Acceleration (Idle to Full Power)

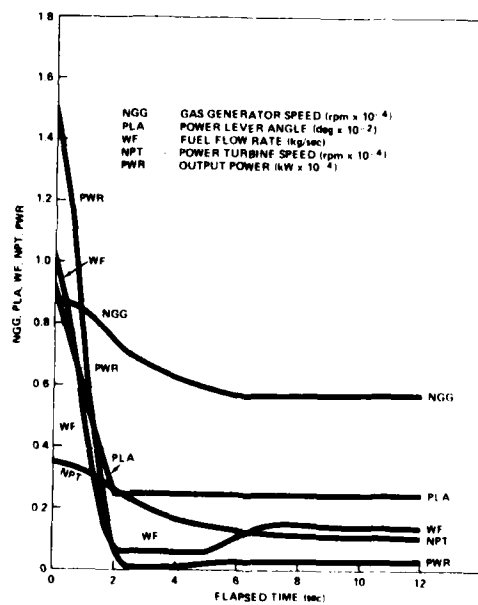


Figure 9. Typical Engine Deceleration (Full Power to Idle)

where X refers to an independent variable, E refers to an error, and EB refers to a base error. For solution convergence the errors  $E_i$  should approximate zero and therefore should be dropped from the above equation. The unknowns  $dx_j$  are determined by using a matrix elimination method and then used to correct the initial guesses for the independent variables. The new guesses become:

$$X_j = XB_j + dx_j \quad [21]$$

where XB refers to the previous guesses. Since the performance calculations are nonlinear functions, it is necessary to repeat the process several times before all base errors approach negligible values.

## RESULTS

A dynamic gas-turbine simulation using these generalized techniques has been developed in the Gas Turbines Branch at David W. Taylor Naval Ship Research and Development Center (DTNSRDC). To date only the single-spool engine configuration option has been included. The component maps, design constants, and fuel-control characteristics for General Electric's LM2500 marine gas turbine were input to the simulation. The results presented in this paper are typical examples of steady-state design and off-design performance, engine acceleration from idle to full power, and engine deceleration from full power to idle. Steady-state results are shown in Figure 7 as a function of power level angle. A given power lever angle corresponds to a constant demanded gas generator speed. Fuel flow rate is fixed by the fuel-metering valve in the fuel control. Other operating conditions shown in Figure 7 include engine output power, HPT inlet temperature, HPC inlet airflow, and power turbine speed. An engine acceleration is simulated by quickly increasing the power level angle from an idle setting to the full power setting. The transient results shown in Figure 8 were generated by a two-second ramp disturbance of the power lever. The response of gas generator speed and fuel flowrate is limited by the protective acceleration schedule used in the fuel control. The gas generator rotor accelerates from idle to final demanded speed in about six seconds. Due to the larger inertia, the free-power-turbine requires about 10 seconds to accelerate to final speed. Engine output power is plotted in Figure 8 as a function of elapsed time. An engine deceleration is simulated by quickly decreasing the power lever angle from the full power setting to the idle setting. A two-second ramp disturbance of the power lever is used again to generate the transient results shown in Figure 9. Steady-state and transient results obtained with this simulation have been compared with results obtained from the engine manufacturer's simulation and with existing experimental data. The comparisons made between the two simulations demonstrated that good results could be obtained using the simpler generalized approach to modeling gas turbines. In generating the transient data used in these comparisons, the DTNSRDC simulation consumed 1/3 less computer time than was used by the engine manufacturer's simulation. Improvements to the current version of the DTNSRDC simulation could be made to further reduce execution time.

## CONCLUDING REMARKS

The investigation of generalized simulation techniques has demonstrated a newer, more flexible and more efficient approach for simulating the dynamics of marine gas turbines. The scope of this investigation has been limited to simulating only the single-spool engine configuration. However, a capability for simulating a dual-spool engine

This convergence technique has been shown to converge faster, with higher stability and reliability than the classical nested loop method. To use this convergence technique, an equal number of independent variables and error tests must be programmed into the simulation. Seven independent variables can be identified for the single-spool engine configuration and its fuel control; these include:

- HPC - HPT rotational speed
- HPC exit pressure
- Burner exit pressure
- Burner exit temperature
- HPT exit pressure
- FPT rotational speed
- Fuel-metering valve position

The seven error tests generated by the performance calculations are mismatched:

- HPC and HPT power
- mass flow rates at station 3
- mass flow rates at station 4
- Guessed and calculated burner exit temperature
- mass flow rates at station 5
- FPT power and engine load
- servo fluid flow rate ( $\epsilon_3$ ) and derivative of valve position

A total of ten independent variables and error tests apply to the dual-spool engine configuration and its fuel control. The additional independent variables are:

- LPC-LPT rotational speed
- LPC exit pressure
- LPT exit pressure

and the additional error tests are mismatched:

- LPC and LPT power
- mass flow rates at station 2.5
- mass flow rates at station 4.5

The solution convergence technique is the same for both steady-state and transient performance calculations. Accumulation of mass, accumulation of energy, and rotor acceleration are absent under steady-state conditions. Therefore, the time derivatives of pressure, internal energy, and rotor speed in the dynamic equations are set equal to zero during steady-state performance calculations. During transients, however, the error calculations account for storage of mass and energy and for rotor acceleration. With initial guesses for the independent variables a first pass through the performance calculations is made to determine values of base errors. Succeeding passes are made, perturbing one independent variable by a small amount during each pass. In the process the change of each error "i" due to the small perturbation of each independent variable "j" is computed and used as the coefficients in a set of simultaneous equations:

$$dE_i = \sum \left( \frac{\partial E_i}{\partial X_j} \right) dX_j = E_i - EB_i \quad [20]$$

$$\dot{Q} = \frac{60 k_p W}{2 \pi N} \quad [15]$$

the dynamic power balance for each rotor of the gas generator is:

$$(W_t - W_c) = \frac{1}{k_p} \left( \frac{2\pi}{60} \right)^2 I.N. \frac{dN}{dt} \quad [16]$$

and the dynamic power balance for the free-power-turbine rotor is:

$$(W_t - W_{load}) = \frac{1}{k_p} \left( \frac{2\pi}{60} \right)^2 I.N. \frac{dN}{dt} \quad [17]$$

Disagreement between transient engine test data and simulation results have been experienced when using simple computer models based on normal steady-state component performance and rotor dynamics. Although rotor inertias may account for most of the system's stored energy, other transient mechanisms in the components are important. Since the gas-turbine engine is a series of physical volumes, accumulation of mass and energy may occur in its components during a transient. The differential equations used in DYNGEN (6) assume that storage of mass and energy occur isentropically. The accumulation of mass within a control volume is given by the expression:

$$\frac{dM}{dt} = (\dot{m}_{in} - \dot{m}_{ex}) = \frac{V}{RT} \left( \frac{dP}{dt} \right) \quad [18]$$

and accumulation of energy, which is the product of specific internal energy and stored mass, is given by the expression:

$$\frac{d(uM)}{dt} = \dot{m}_{in} h_{in} - \dot{m}_{ex} h_{ex} - u (\dot{m}_{in} - \dot{m}_{ex}) - \frac{PV}{RT} \left( \frac{du}{dt} \right) \quad [19]$$

A more accurate approach would have temperature as a derivative of time also. Other transient mechanisms include heat exchange between gas and engine materials, compressor and turbine blade tip clearance changes, and fuel droplet combustion lags (10). Neglecting the heat transfer in the engine simulation can lead to predicted acceleration rates some 20 to 30% faster than observed during transient engine tests. Methods for predicting transient tip clearances and their associated effects on component performance can be found in the literature. Fuel droplet combustion lags range from 20 to 80 milliseconds, depending upon the type of burner. It remains to be determined which transient engine effects have a significant impact on gas-turbine-ship dynamics.

#### Solution Convergence Technique

An iterative approach is required to balance the performance characteristics of the various engine components. Solution convergence techniques involve initial guesses for independent variables from which the performance calculations are made. Since the initial guesses are only approximations, errors result in the form of mismatched flow rates, pressures, temperatures, rotational speeds, or powers between components; and an iterative scheme is used to adjust the independent variables until all errors are negligible. Since its first application to gas-turbine modeling nearly a decade ago the Newton-Raphson convergence technique has become a popular iteration scheme for balancing computerized engine performance calculations. The Newton-Raphson convergence technique is used in several general-purpose, multiconfiguration, engine simulations including those shown earlier in Table 1.

inputs to the fuel-control model include power level angle (PLA), gas generator speed (NGG), compressor inlet temperature (CIT), and compressor discharge pressure (CDP). The primary disturbance during a transient is a change in PLA as a function of time. When a difference between demanded and sensed gas generator speed exists, an error signal causes a change in fuel flowrate that will produce the demanded NGG. The NGG and CDP inputs are already independent variables in the compressor model, and CIT is usually assumed to be constant. These three parameters are used in the fuel-control model to establish the maximum allowable fuel flow rate based on the acceleration schedule. The minimum allowable fuel flow rate or deceleration schedule may be some fraction of the acceleration schedule. With an equation for the inverse fuel metering valve schedule, the maximum and minimum fuel flow rates are converted to maximum and minimum fuel metering valve positions. The error signals generated in the fuel-control model correspond to servo fluid flow rates in the hydromechanical fuel control. Integration of the final error signal gives fuel metering valve position which is checked against the upper and lower limits established by the acceleration and deceleration schedules. During steady-state operation or for small PLA disturbances, the fuel metering valve position is controlled by the speed error. For large PLA disturbances the fuel-metering valve position is limited by the acceleration or deceleration schedule. The fuel-metering valve position is selected as the independent variable in the fuel-control model. Valve position is used to calculate servo fluid flow rates. The calculated value of  $\epsilon_3$  should equal the derivative w.r.t. time of valve position,  $X$ . With an equation for fuel-metering valve schedule, valve position is converted to the fuel flow rate supplied to the gas-turbine engine.

Two feedback loops in the fuel-control model provide stability during transients. Feedback of fuel-metering valve position and feedback of gas generator rotor acceleration are used to control servo fluid flow rates. Flexibility in obtaining the desired fuel-control response is provided by several transfer functions in the fuel-control model. Errors between sensed and demanded NGG are converted to servo fluid flow rates by the K3 transfer function. The K4 transfer function may range in value from 0 to 1.0 and is used to adjust the amount of acceleration feedback. Similarly, the K5 transfer function is used to adjust the amount of valve position feedback. The K7 transfer function is used in the fuel-control model to limit the absolute value of servo fluid flow rate and is therefore referred to as a rate limiter. The K6 and K8 transfer functions may be used to scale the acceleration and deceleration schedules, respectively. The primary transfer functions affecting the stability and response of the fuel control are K3, K4, and K5, while the other transfer functions provide additional options for obtaining desired results. Under normal circumstances K6 and K8 would have values of unity, and K7 would have a value too large to affect results.

#### Dynamic Equations

The momentum balance for rotating machinery states that any excess torque provided by either turbine will produce rotor acceleration. Therefore:

$$\frac{dN}{dt} = \frac{60}{2\pi I} \cdot \Delta Q \quad [14]$$

Since torque, speed, and power are related by the expression:

$$h_{ex} = (\dot{m}_{in} h_{in} - \dot{m}_{in} \Delta h + \dot{m}_{bl} h_{bl}) / (\dot{m}_{in} + \dot{m}_{bl}) \quad [12]$$

Exit temperature is calculated using a curve-fitted polynomial equation for temperature of combustion products as a function of  $h_{ex}$  and  $FAR_{ex}$ .

#### Engine Load

One approach to modeling the propeller load on the free-power-turbine utilizes the thrust and torque characteristics of a particular propeller given as a function of propeller speed of advance and the propeller shaft's rotational speed. For a controllable-pitch propeller thrust and torque also depend upon a variable pitch-to-diameter ratio. Thus, the total number of independent variables in the simulation will increase, and certain characteristics of the ship's hull and propulsion drive train must be modeled when taking this approach. Other technical papers (8), (9) have discussed this approach in more detail. Since the scope of this paper deals primarily with gas-turbine dynamics, a simpler approach to modeling the load is sufficient to demonstrate this technique. The power absorbed by the load is a function of rotational speed cubed:

$$W_{load} = W^* (N_{FPT}/N^*)^3 \quad [13]$$

where  $W^*$  and  $N^*$  define a reference point on the curve such as the design output power and rotational speed of the free-power-turbine. This cubic load curve was used to generate the results shown in this paper, with the understanding that it does not account for the effect of ship's inertia on the free-power-turbine response during transients.

#### Fuel Control

For shipboard main propulsion the output power of the free-power-turbine can be indirectly controlled by maintaining a constant gas generator speed for a given power lever position. By advancing the power lever, a higher gas generator speed is selected and the gas-turbine engine accelerates to a higher output power. During transients protective acceleration and deceleration schedules in the fuel control limit the fuel flow rate independently of demanded gas generator speed. Figure 6 is a block diagram of the fuel-control model. Note the four

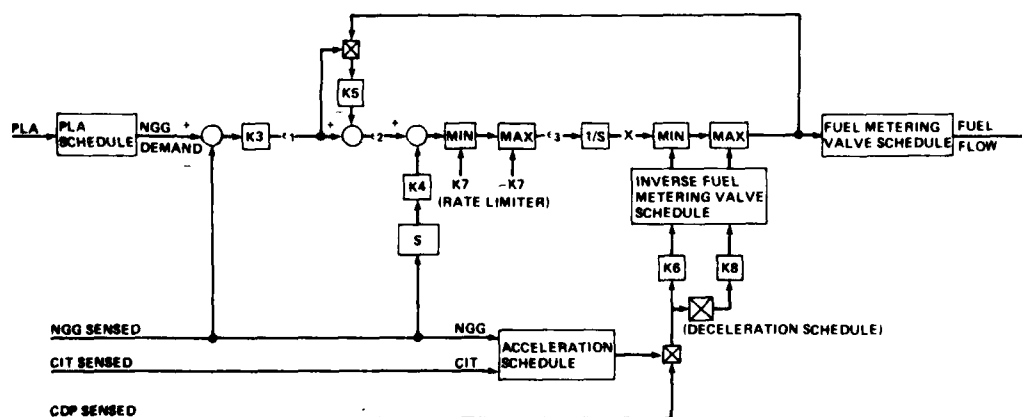


Figure 6. Flow Chart for Fuel-Control Model

$$h_p = (h_A - h_A^0 + LHV \cdot b \cdot FAR) / (1 + FAR) + h_p^0 \quad [7]$$

where FAR is the fuel-to-air mass ratio ( $\dot{m}_f/\dot{m}_A$ ). Exit temperature is calculated using a curve-fitted polynomial equation for temperature of combustion products as a function of  $h_p$  and FAR. The burner exit mass flow rate is the sum of air and fuel flow rates.

#### Turbines

Turbine exit pressure and rotational speed are selected as independent variables in the turbine model. Performance characteristics (i.e. flow function and enthalpy function) of a high-pressure turbine are plotted in Figures 4 and 5, respectively, as a bivariate function

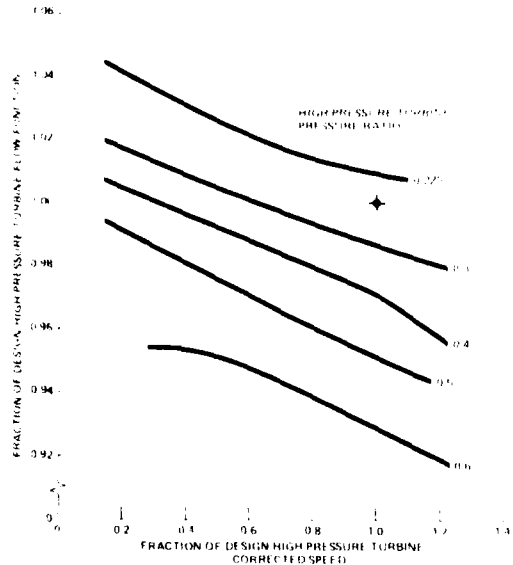


Figure 4. High-Pressure Turbine Flow Function as a Function of Corrected Speed and Pressure Ratio

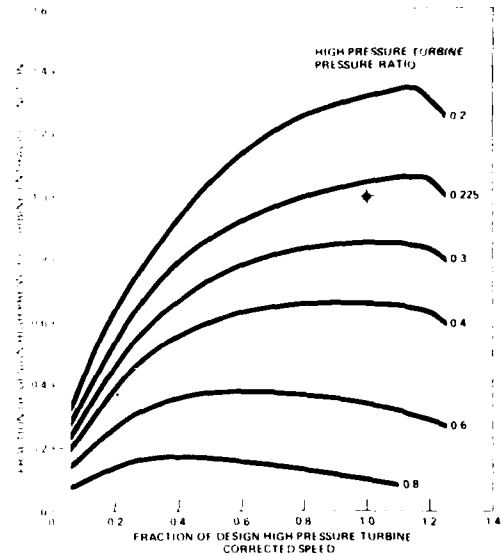


Figure 5. High-Pressure Turbine Enthalpy Function as a Function of Corrected Speed and Pressure Ratio

of pressure ratio and corrected speed. Calculation of the inlet mass flow rate is based on the definition of turbine flow function:

$$\text{turbine flow function} = \dot{m}_{in} \sqrt{T_{in}/P_{in}} \quad [8]$$

and the enthalpy drop across the turbine is determined from the definition of turbine enthalpy function:

$$\text{turbine enthalpy function} = \Delta h/T_{in} \quad [9]$$

The turbine power is then calculated:

$$W_t = J \dot{m}_{in} \Delta h/k_p \quad [10]$$

The turbine exit mass flow rate is the sum of any cooling bleed air and the inlet mass flow rate. Taking into account this mixing of gas streams, the exit conditions of the turbine are:

$$FAR_{ex} = FAR_{in} / [1 + (FAR_{in} + 1) (\dot{m}_{bl} + \dot{m}_{in})] \quad [11]$$

and compressor efficiency is used to calculate actual CET:

$$T_{ex} \text{ (actual)} = (T_{ex} \text{ isentropic} - T_{in.})/\eta_c + T_{in.} \quad [3]$$

The compressor power is then calculated:

$$W_c = J \dot{m}_a (h_{ex} - h_{in.})/k_p \quad [4]$$

In order to calculate air flow rate at the compressor exit, knowledge of the compressor's parasitic air streams is required. The majority of the bleed air may go to cool hot parts in the engine, while the remaining bleed air may go to satisfy external needs or may be lost overboard.

#### Burner

The burner's exit pressure and exit temperature are selected as independent variables in the burner model. The pressure drop through the burner is assumed proportional to dynamic pressure; thus, the burner inlet airflow can be expressed as:

$$\dot{m}_a = k_b / P_{in.} (P_{ex} - P_{in.})/T_{in.} \quad [5]$$

where  $k_b$  is the pressure loss coefficient. As shown in Figure 3, burner efficiency is tabulated as a bivariate function of its temperature rise and inlet pressure. In this case the highest efficiency

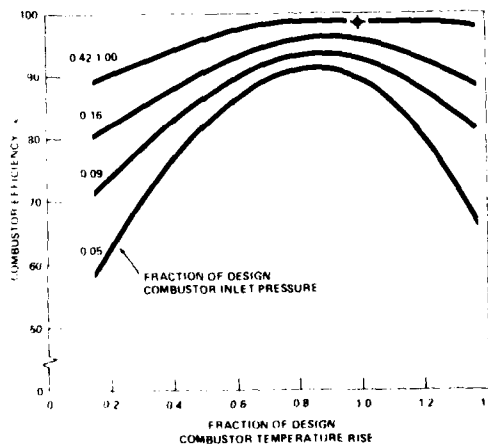


Figure 3. Combustor Efficiency as a Function of Temperature Rise and Inlet Pressure

curve applies to burner inlet pressures equal to or greater than 42% of the design point inlet pressure. The energy balance for the combustion process is:

$$\dot{m}_a (h_a - h_a^\circ) + \dot{m}_f (h_f - h_f^\circ) + FHV \eta_b \dot{m}_f = (\dot{m}_a + \dot{m}_f) (h_p - h_p^\circ) \quad [6]$$

where the superscripted enthalpies refer to a standard state of 25°C. Assuming the ambient temperature of the fuel is approximately 25°C, the  $(h_f - h_f^\circ)$  term can be neglected. Solving for the enthalpy of combustion products at the burner exit gives:



In the dual-spool configuration, additional station numbers are used in the gas generator at intracompressor and intraturbine locations.

#### ANALYTICAL APPROACH

##### Compressors

Compressor discharge pressure, CDP, and rotational speed are selected as independent variables in the compressor model. Performance characteristics of the compressor are represented graphically by using the parameters: pressure ratio, percent corrected speed, corrected airflow, and efficiency. Figure 2 is a typical plot of pressure ratio versus corrected airflow for lines of constant percent corrected speed. The compressor efficiency contours are omitted in this figure. The

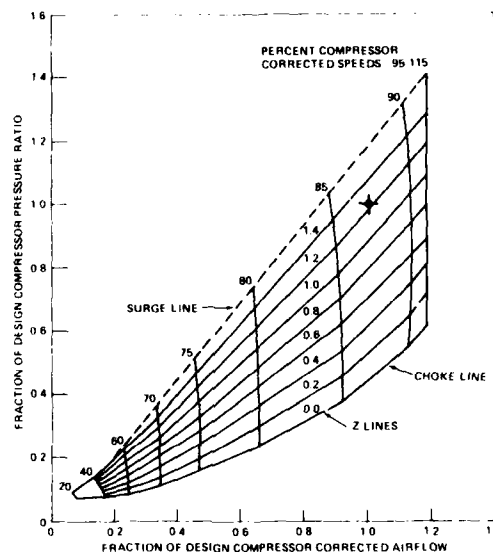


Figure 2. Compressor Performance Characteristics

percent corrected speed lines are bounded by the compressor's surge and choke lines. Due to the narrow spread of data at low corrected speeds, a pressure ratio parameter,  $Z$ , is often used to facilitate the tabulation of compressor performance data. This parameter divides each corrected speed line into an equal number of segments. At the intersection of each corrected speed line and  $Z$  line, values for corrected airflow and efficiency are tabulated. Specifying CDP and rotational speed defines an operating point on the compressor map, and by interpolation of the tabulated performance data a corresponding value for corrected airflow and efficiency is obtained. Calculation of airflow rate of the compressor inlet is based on the definition of corrected airflow:

$$\text{corrected airflow} = \frac{\dot{m}_a \sqrt{T_{in.}/T_o}}{P_{in.}/P_o} \quad [1]$$

The isentropic compressor exit temperature, CET, is calculated from the pressure ratio:

$$T_{ex} \text{ (isentropic)} = T_{in.} (P_{ex}/P_{in.})^{\frac{\gamma-1}{\gamma}} - 1 \quad [2]$$

Once the configuration options have been identified, a system of numbered stations is derived designating common locations throughout the engine configurations. There are probably as many different numbering systems as there are gas turbine manufacturers, which can cause confusion when comparing performance data for several gas turbines. In a generalized simulation the numbering system must provide for the consistent definition of locations regardless of differences in engine configuration. Figure 1 illustrates such a system for free-power turbines having either single-spool or dual-spool gas generator. The station numbers common to both configurations are:

- 0 - reference conditions
- 1 - inlet/engine interface
- 2 - first compressor inlet
- 3 - last compressor discharge
- 4 - burner discharge
- 5 - gas generator discharge
- 6 - free-power-turbine discharge
- 8 - exhaust conditions

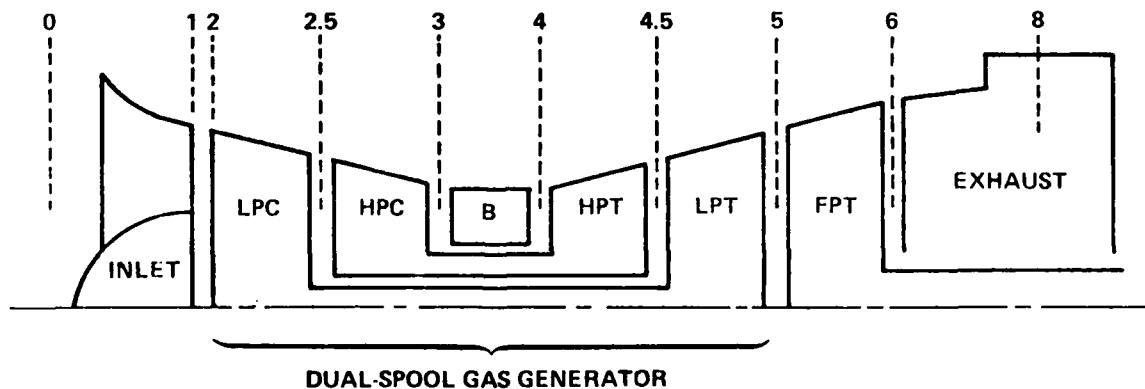
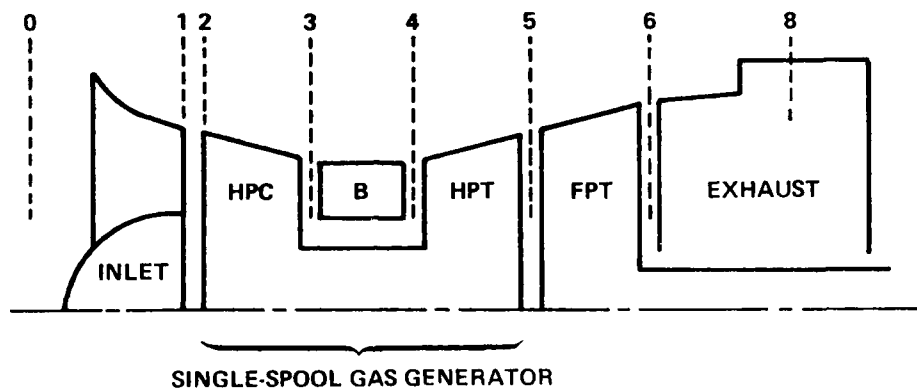


Figure 1. Marine Gas-Turbine Engine Configurations

SHORCON is a more extensive concept than a condition monitoring system in the traditional sense.

It is a common designation for a computerbased system of programmes, the output of which provides a tool for efficient maintenance strategy.

SHORCON combines the two principally different maintenance strategies:

- periodic maintenance, i.e. mean time between failure (MTBF) based on statistics
- condition monitoring based on calculation of the various components ability to perform its intended function.

Figure 2. shows the main structure of SHORCON.

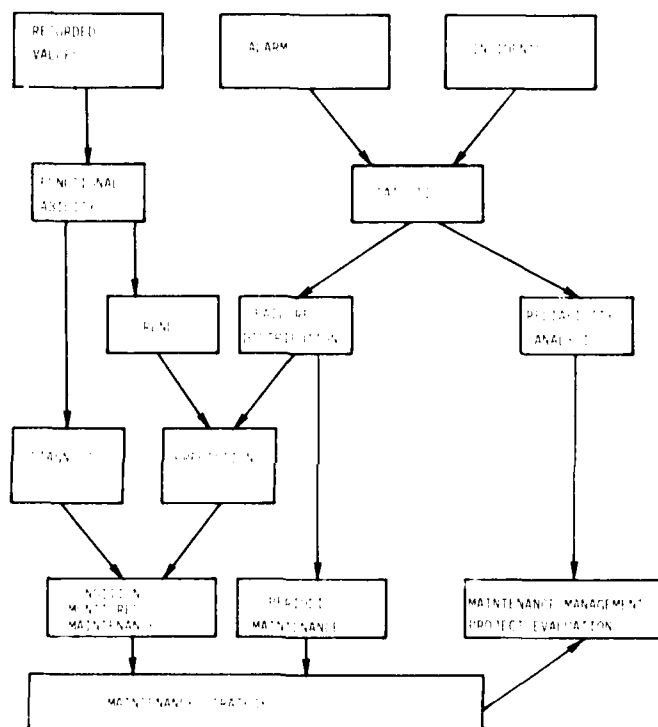


Figure 2. SHORCON Main Structure.

The input to SHORCON originates from SHIPCON by:

- automatic recording of a set of measured parameters on magnetic tape during certain stable operating conditions
- automatic recording of alarm conditions on magnetic tape
- automatic information of safeguard actions recorded on magnetic tape
- manual report forms.

Various important data-sets are continuously stored on a RAM memory. For certain alarms or safeguard actions taking place the data

sets are dumped on magnetic tape thus providing a recorded history of the situation for a time interval of some minutes preceeding the alarm or safeguard action.

Completed cassettes are delivered to the administration ashore and the content transferred to the central computer where the SHORCON data processing takes place.

Associated with the central computer is also a data storage where information about machinery performance, maintenance and disturbances is accumulated on a magnetic tape station. The SHORCON machinery configuration is shown on Fig. 3.

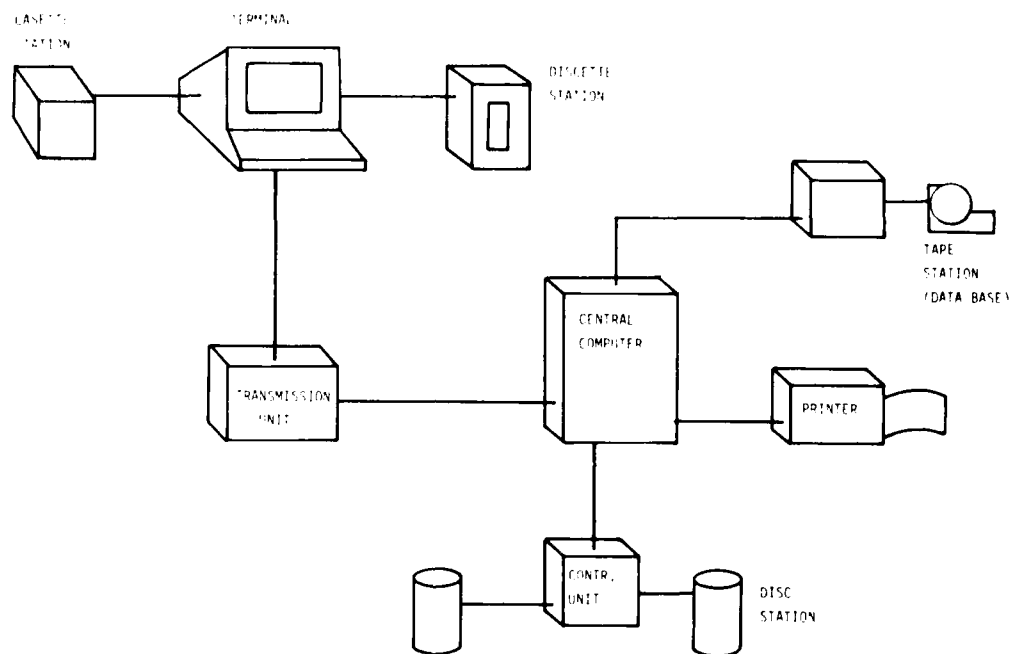


Figure 3. SHORCON Machinery Configuration.

SHORCON works by means of the following measures:

- prediction
- statistics
- reliability analysis (prepared)
- diagnosis, pattern recognition

Prediction is based on the establishment of certain mathematical functions or condition parameters. Examples of such parameters, and how they are calculated in SHIPCON and SHORCON are shown in the following table 1.

PARAMETER	INPUT VALUES	FUNCTIONS	PROCESSED IN	
			SHIPCON	SHORCON
SHAFT HP SHP	n: rpm I: torque I: fuel rack	$f_1(n, I)$ $f_2(n, I)$	x	
SPEC. FUEL CONSUMPTION b.	B: measured value $t_b$ : temp H: calorific value	$b = f(B, t_b, H)$	x	
HEAT LOAD I	N: engine power n: rpm $t_m$ : temp. air manifold $P_m$ : manifold press. $\Delta t_e$ : temp. rise across engine $t_1$ : temp. compressor intake	$I = f(N, n, t_m, P_m, \Delta t_e, t_1)$  (Will be modified when more exact parameter estimation data are available)	x	y

Table 1. SHIPCON/SHORCON: Examples of Data Processing.

The parameters are used to calculate the functional ability of components or engine sub-systems and indicate this as a percentage of the ability of a new identical component or system. The models used are considering the operational condition such that the established functional ability is independent upon load.

The functional ability in itself provides important information to the operators. However, if the functional ability is plotted as a function of time, it is possible to predict the time where the performance reaches a lower limiting value.

Incidents like damages and maintenance actions will cause discontinuities in the plot. From these it is possible to appreciate the seriousness of various types of damages and the quality of maintenance actions.

Statistics. Statistic information used in SHORCON is

- hours of operation
- operational profile
- type number and distribution of incidents

The present system is summing up incidents within groups to establish statistical values of MTBF. However, the system is prepared for performing reliability analysis and parameters are sampled for this purpose.

Diagnosis, pattern recognition. A conventional alarm system only indicates the effect of a fault condition on a single measured parameter. It gives no information about the cause of the failure. The system gives response orientated messages. This is sufficient as far as unique cause/effect connections are concerned. In more complex machinery systems however, fault conditions can manifest themselves by

disturbances in other parts of the system. A number of fault conditions can thus be detected contemporarily.

The diagnostic system of SHORCON is based on a number of recordable effects of fault conditions in the complete system. An identification of a fault pattern is accomplished before a cause orientated message is given. The SHORCON diagnosis is accomplished by selecting the most probable fault pattern of a number of predefined patterns.

The probable types of failures are described as vectors composed of modified condition parameters. If a set of condition parameters are recorded, these can define a measured vector. By comparison of the measured vector with the predefined fault vectors, the case which gives the smallest vector difference indicates the most probable failure or failure development.

The vector matrix and the vector comparison are illustrated in Fig. 4.

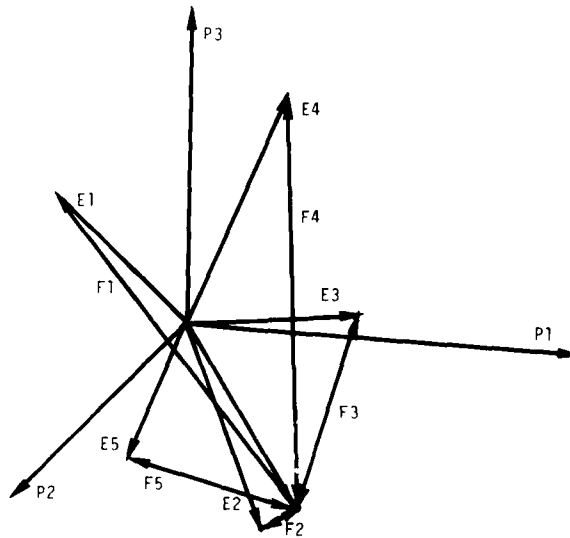


Figure 4. Diagnosis Predefined Fault Vectors.  
Calculation of Vector Difference.

The SHORCON program structure consists of the following 12 main programmes:

- |        |  |
|--------|--|
| ADMIN  | is an administrative routine which calls the other main programs based on the operator run-options.                                    |
| CASIN  | performs reading in and checking measured parameters as to parameter quality and instrument failure of data recorded on magnetic tape. |
| MANIN  | performs similar reading in of manually recorded data.   |
| DISCOP | performs reading and writing to and from disk file.  |

TRUSTI accumulates alarms, safeguard actions, damage incidents, maintenance in separate sub-systems.

CALCO calculation of condition parameters.

SYSOR time of measurements and events are established and numbers of measurements in each time interval between events are calculated.

WEPAR calculation of mean values of condition parameters over a defined period of time.

LINOR organization of condition parameters in line sequential order.

DIABLO diagnostisation of fault conditions.

ANCON prediction by calculation of slopes of trend lines until intersection with limit value. If no trend is found prediction is based on statistics (MTBF).

HARCO provides print outs.

The resulting printout from SHORCON in the format it will be presented to the maintenance personell is shown in Fig. 5.

TILSTANDSUTVIKLING OG PREDIKSJON							
MOTOR: SB TURTALL: 1850							
PARAMETER	TILSTANDSUTVIKLING				PREDIKSJON		
	TREND	VAR	SPRANGAVVIK(X)		DY TIL FEILSANS		
	%/100DT	±, %	SKADE	VEDL.	10%	50%	
IMM. TURTALL	-8.00	0.80	0.00	0.00	1998.00	3600.00	*
IEFF. MIDDELYRK.	6.00	0.43	0.00	0.00	429.80	481.80	
IAKSELEFFEKT	-42.00	0.44	0.00	23.87	401.10	410.70	
IARMEBELASTN.	1.00	0.09	0.00	0.64	1098.00	1800.00	*
ISPES. GO. FORBR.	-5.00	0.19	0.00	0.00	591.60	806.80	
ITRK. E.GO. FILT.	0.00	0.00	0.00	0.00	598.00	800.00	*
IV.GR. HT. PUMPER	0.00	0.00	0.00	0.00	598.00	800.00	*
ILUFTOVERSKUDD	0.00	0.00	0.00	0.00	598.00	800.00	*
ILADER TURTALL	0.00	0.00	0.00	0.00	1998.00	3600.00	*
ITMP. EKS.E.SYL.	-5.00	0.19	0.00	0.00	584.80	793.20	
ITRK. LADELIFT	0.00	0.00	0.00	0.00	598.00	800.00	*
IV.GR. KOMPRESSOR	0.00	0.00	0.00	0.00	598.00	800.00	*
IV.GR. TURBIN	0.00	0.08	0.00	0.00	598.00	800.00	*
IK-VERDI LUFTKJ.	0.00	0.00	0.00	0.00	1998.00	3600.00	*
ID.TRK. LUFTKJ.	-16.00	0.18	0.00	0.00	1998.00	3600.00	*
ID.TRK. MOTOR	0.00	0.00	0.00	0.00	1998.00	3600.00	*
ITRK.E. EKSOSTURBIN	0.00	0.00	0.00	0.00	1998.00	3600.00	*
ILUFTOVERSKUDD	0.00	0.00	0.00	0.00	1998.00	3600.00	*
ILADER TURTALL	0.00	0.00	0.00	0.00	1998.00	3600.00	*
ITMP. EKS.E.SYL.	43.00	0.27	0.00	0.00	498.00	600.00	*
ITRK. LADELIFT	-11.00	0.14	0.00	0.00	407.30	422.00	
IARMEBELASTN.	0.00	0.00	0.00	0.00	1998.00	3600.00	
ISPES. GO. FORBR.	6.00	0.43	0.00	0.00	429.80	481.80	
ILUFTOVERSKUDD	-5.00	0.19	0.00	0.00	591.60	806.80	
ILADER TURTALL	0.00	0.00	0.00	0.00	598.00	800.00	

\* PREDIKSJON BASERT PÅ MIDLERE TID MELLOM FEIL.

Figure 5. Examples of Printout from SHORCON.

We shall below give some details about two of the projects which, for the time being, we will refer to as "The small Vessel Project" and "The Large Vessel Project".

#### THE SMALL VESSEL PROJECT

This was the first project to be undertaken, and the overall aim of it was to:

- increase the ship reliability and availability
- reduce number of crew members
- develop the preventive maintenance system into a predictive system.

Based upon a preliminary evaluation performed by naval personnel, it was fairly early decided that the control and instrumentation system in this case would have to include:

- A system for "prechecks" and "ready-to-start" functions for the main engines.
- A system for performing the necessary starting sequences for the main engines.
- A supervision system performing necessary safety actions as well as giving the necessary warnings and alarms for safe operation of all machinery.
- A condition monitoring system for supplying data suitable for advanced, shore processed, predictive maintenance.
- A display and presentation system for bridge, control room and local engine stands.
- Supervision of remote control system.
- Supervision and control of electric power supply and auxiliaries.
- A fire detection system.

The system would of course also have to satisfy all usual military standards concerning environmental requirements such as shocks, vibrations, EMI etc.

The Navy placed a previously built vessel at disposal in order to install a prototype control and instrumentation system. This prototype installation will be delivered primo October 1978.

#### Machinery Details

These vessels are supplied with two propulsion engines type: MTU 16V 538. The engines are manufactured by MOTOREN- UND TURBINEN-UNION, Friedrichshafen GmbH in Germany. Some general engine data are:

Number of pistons	V16
Engine weight (including accessories)	6200 kg (13 700 lbs)
Max. continuous load	3300 HP
Max. continuous RPM	1845 RPM
Max. permissible load	3600 HP/2 hrs.
Max. permissible RPM	1900 RPM/2 hrs.



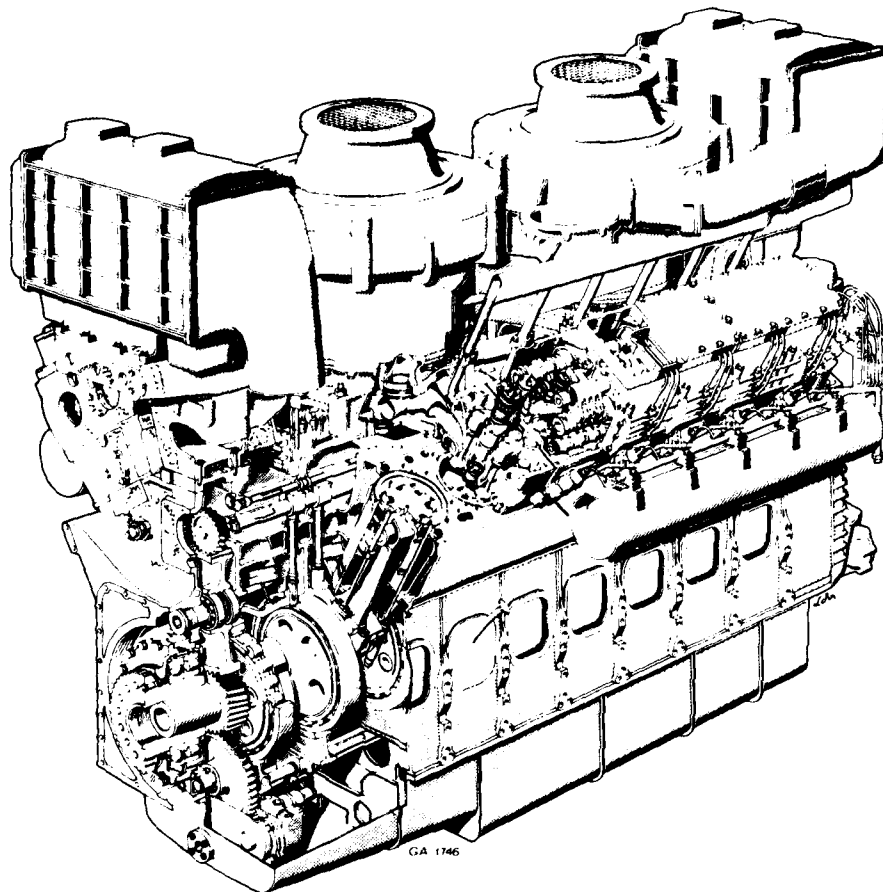


Figure 6. MTU Engine Type 16V 538.

The prototype vessel is supplied with 2 auxiliary engines of make MWM, each rated for 80 kVA. The auxiliary engines are automatically starting and synchronizing on the main switchboard.

#### General Description of the Control and Instrumentation System.

During the projecting phase several alternative principle systems were considered, and it was decided to go for a system based upon micro computer technology having operationally distributed CPU's. It was required that the digital control system for security reasons should have a certain back up based upon conventional technology.

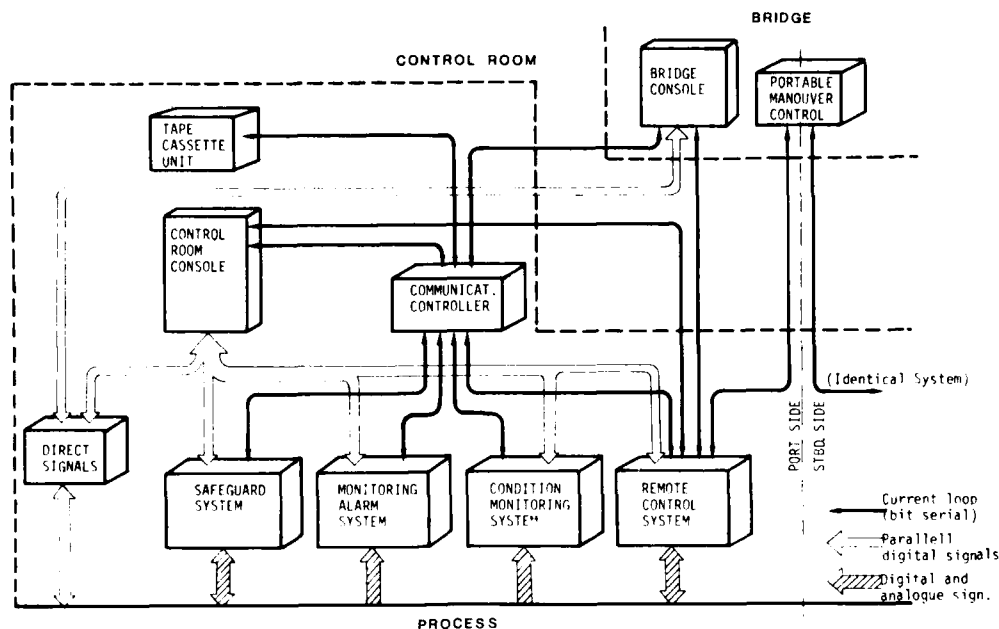


Figure 7. Configuration of "Small Vessel" Control and Instrumentation System.

The configuration shown in figure 7. was found to give a satisfactory level of independency and redundancy. Communication with the process is taken care of by 4 separate processors, i.e. for the safeguard system, the monitoring alarm system, the condition monitoring system and the remote control system. A communication controller is in charge of the various data presentation features. Information is presented on a 12x40 character alpha numeric display in the control room and a single line display on the bridge. Data for condition monitoring as well as certain alarm data are fed to the tape cassette unit for later processing. Certain safety functions are obtained by a completely separate system feeding direct signals to a separate set of alarm lamps on the control room console. This system also supplies certain signals to the bridge console. The two main engines have separate control and instrumentation systems. Certain interconnections are, however, possible in case of failures in one of the systems.

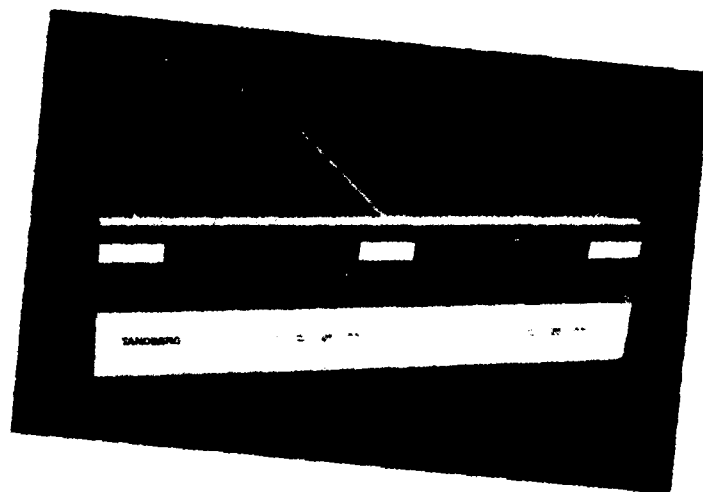


Figure 8. Tape Cassette Unit.

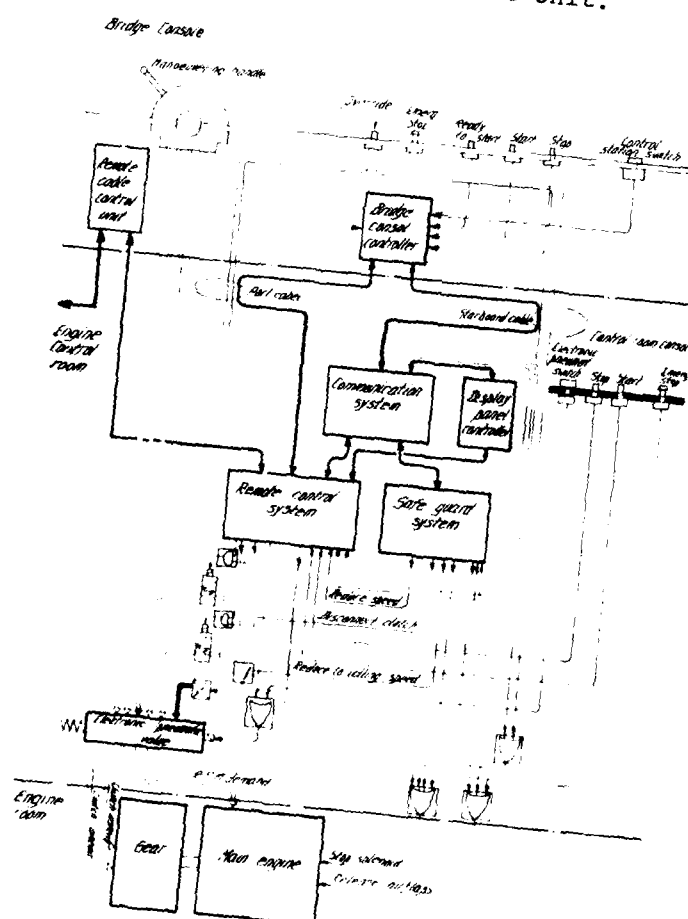


Figure 9. Arrangement for Remote Control of Engine and Gear.

Operation of the machinery is not dependent upon the control and instrumentation system. In case of a complete break-down, the engines can still be operated by conventional means. An example of how this has been arranged for the bridge remote control system is shown on figure 9. The electrical control system has a high degree of duplication such as separate cable lanes, duplicated electronic systems, etc. In addition to this, the manoeuvring system also utilizes the conventional pneumatic signal transmission which can be put in operation either manually or automatically, if electrical control should fail.

It is believed that certain recurring breakdowns have been due to hard manoeuvring of the engine. The pneumatic system has direct control of the engine load while the electronic system (which normally will be used) prevents the engines from being loaded beyond a preset value until normal engine temperatures are reached. The electronic system is also supplied with load increase/ decrease programs in order to obtain correct run-up and run-down procedures.

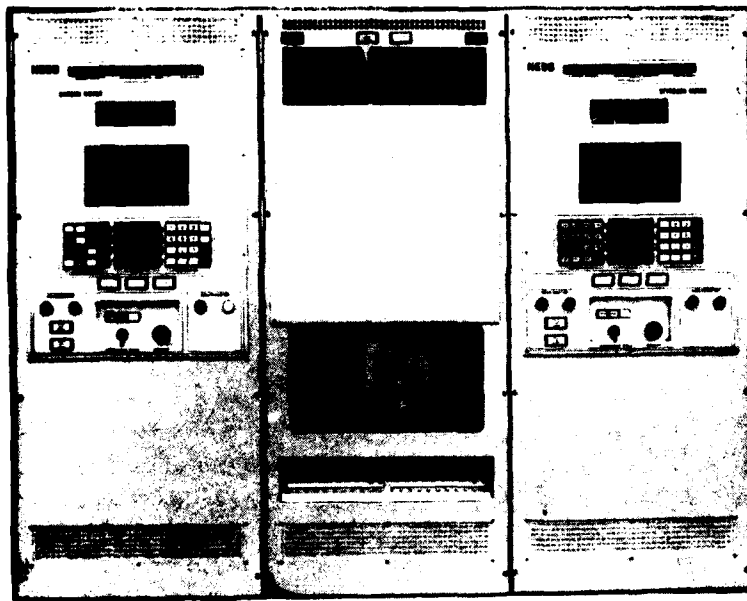


Figure 10. "Small Vessel Project". Control Room Console.

A picture of the control room console is given in figure 10. It shows the control systems for the two engines. The top part of the centre section will contain the tape cassette unit. The lower part contains power supplies, telephones, etc.

It will be impossible to describe the control and instrumentation system in detail in a short paper. We will therefore leave the general description and concentrate on a few points of more general interest.

Interplay with Shorebased Condition Monitoring system. This feature refers to data recording on magnetic tape and has already been described in some detail.

Short Trend Condition Monitoring System. The vessel is also supplied with an on-line short trend condition monitoring system. Information from this can be obtained either by calling up certain data in the system, or an alarm will automatically be given if certain limit values are exceeded. The following is included:

- Calculation of shaft horse power.
- Relating pump index to engine output.
- Relating fuel oil flow to engine output.
- Relating pressure rise across turbocharger compressor to turbocharger RPM.
- Relating turbocharger RPM to fuel oil consumption.
- Calculating air flow.
- Relating air flow to engine speed.
- Relating pressure drop across air cooler to air flow.
- Relating scavenging air pressure to air flow and engine output.
- Relating exhaust gas temperature to engine output.

Estimation of Thermal Load. The Navy has previously experienced a number of breakdowns of the cylinder covers. This is assumed to be due to excessive thermal stresses, particularly during accelerations and decelerations. For reasons of mechanical strength, no type of temperature sensor can be introduced in the cylinder cover. The thermal load is therefore estimated by means of the following formula:

$$t_v = K_1 + K_2 \frac{N^a \cdot T_1^b}{L^c}$$

where:

$t_v$	=	metal temperature
$K_1, K_2, a, b, c$	=	constants
$N$	=	engine revolutions
$T_1$	=	temp. air receiver
$L$	=	air throughput

This model is referring to steady state conditions, but will give valuable information concerning permissible engine maneuverability. The reliability of the mathematical model has been tested by introducing three thermometers into a test cylinder cover fitted to an engine on the test stand. Figure 11. shows the cylinder cover and positions for the introduced thermo-elements.

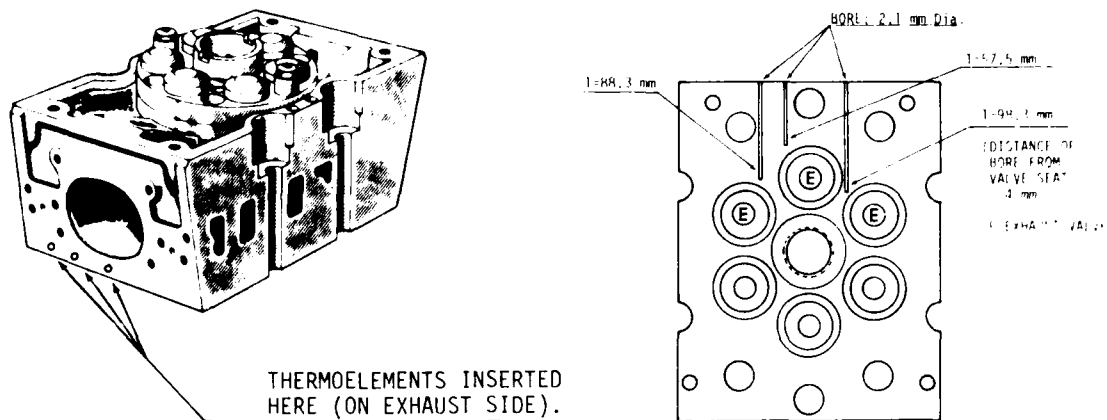


Figure 11. Installation of Thermoelements in Test Cylinder Cover.

Floating Alarm Limits. The operational profile of these vessels shows great variations, and it is desirable to supply the engines with floating alarm limits for parameters which are dependant on engine RPM.

As an example figure 12 shows the variation of the main lub. oil pressure as a function of the RPM. The "stair case curve" shows the variation of the alarm limit.

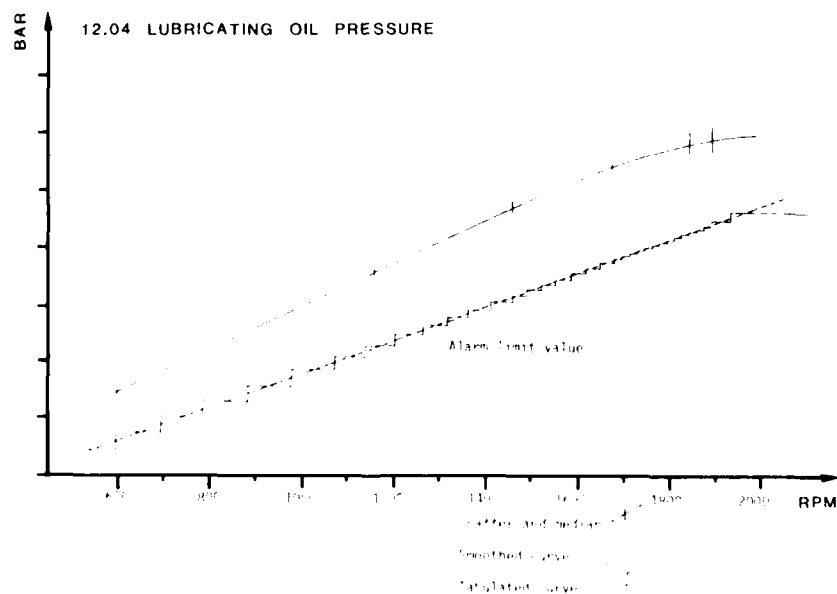


Figure 12. Floating Alarm Limit for L.O. Pressure.

Figure 13 shows the signal combination in the system. Alarm will be given both in the control room and on the bridge if the floating alarm limit is exceeded. If the oil pressure should fall below a fixed limit, a new and higher degree alarm will occur. It should also be mentioned that for further oil pressure reductions the separate safeguard system will be activated.

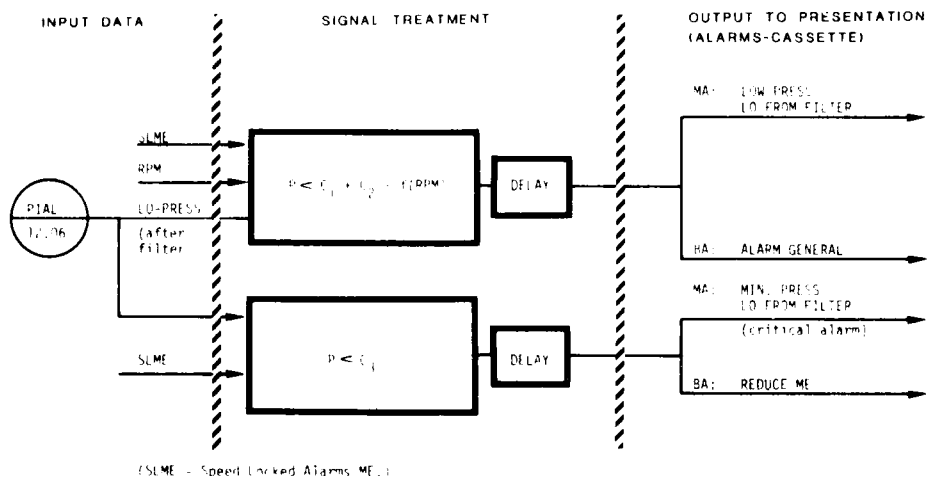


Figure 13. Signal Combination for L.O. Alarm Circuit.

The significance of the symbol SLME (Speed Locked Monitoring) is that all alarm or safety actions are to be blocked when the engine is at stand still due to an ordered stop.

Add Info feature. The system is supplied with a push-button called "Add Info". When certain alarms are occurring and this push-button is pressed, the system will display values of parameters which must have influence on the alarm situation. This will assist the operator in quickly localizing the fault causing the alarm.

Portable Cable Control Unit (PCC). From the operational side it has been expressed the desire for being able to control the vessel from a portable station. A device which is shown on figure 14 has therefore been designed. It is connected to the control system by means of a flexible cable. It enables full control of the main engines as well as full rudder control.

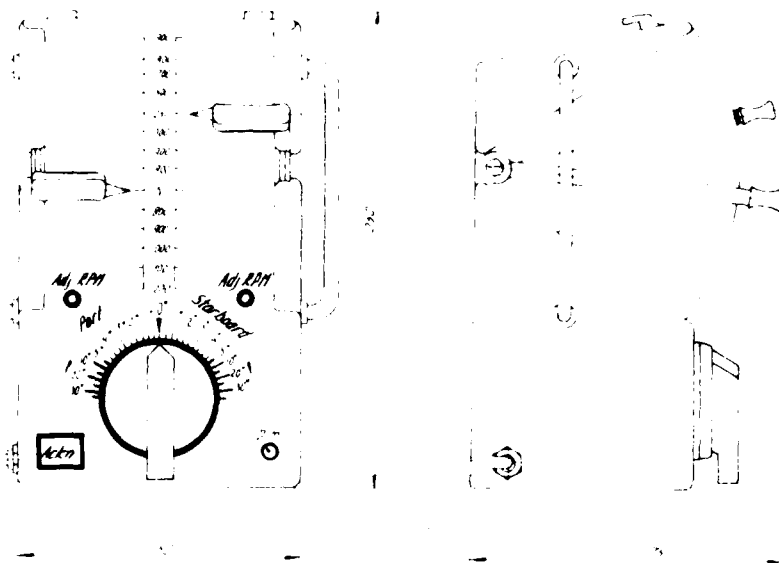


Figure 14. Portable Cable Control Unit.

#### THE LARGE VESSEL PROJECT

In the beginning of 1977, construction started on a larger vessel, and it was desired that also this ship should be equipped with modern control and instrumentation systems. Although a decision to this effect had to be made late in the projecting phase, this was to a great extent possible. The present machinery control and instrumentation system follows the same lines as previously have been described for the "Small Vessel Project". Micro computer techniques are adopted and machinery data will be processed in the SHORCON system, as described earlier. The engine supervision system, including the necessary back-up, cassette unit etc., is shown on the left hand side of figure 15. The substation processor U is continuously communicating with the master processor M.

The "Large Vessel" is supplied with a rather complex set of systems for bunkering and power supply. In addition, the ship also has a comprehensive trim and ballast system giving a large number of tanks for oils as well as for sea water. These systems are to be remotely operated from the machinery control room. The systems are so that with a conventional control and supervision system it had to be assumed that the load on the operator would have been substantial.

In order to improve the working situation as much as possible for the operator, it was decided that control of the various systems should be supervised by means of semi-graphic diagrams displayed on a colour television monitor. This method had previously been investigated, and proved to give a very satisfactory communication between the operator and the process.



AD-A159 082

PROCEEDINGS OF THE SHIP CONTROL SYSTEMS SYMPOSIUM (5TH)  
HELD AT U S NAVAL... (U) DAVID W TAYLOR NAVAL SHIP  
RESEARCH AND DEVELOPMENT CENTER ANN... P MARTIN ET AL.

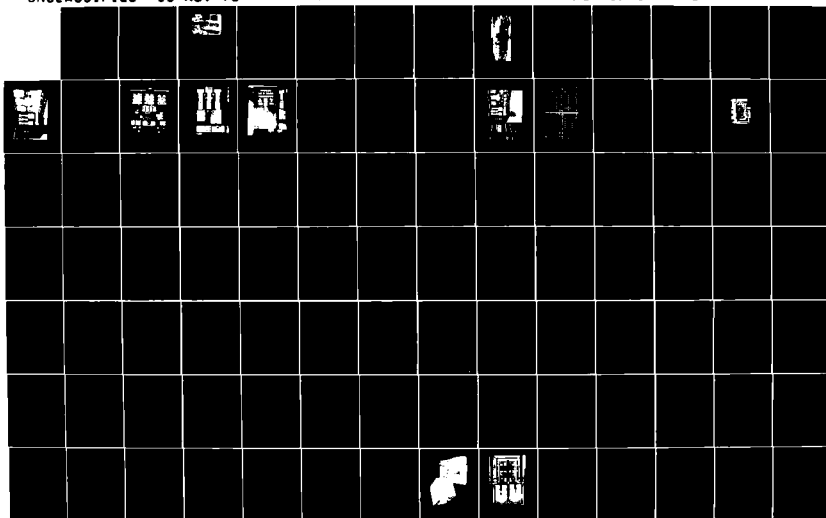
3/4

UNCLASSIFIED

03 NOV 78

F/G 13/10

NL



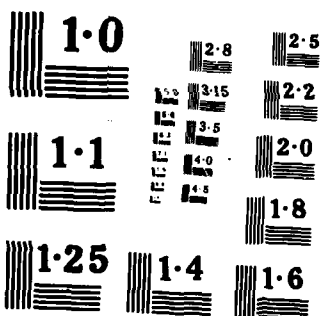






Figure 16. Control Desk with Colour Monitor during Installation.

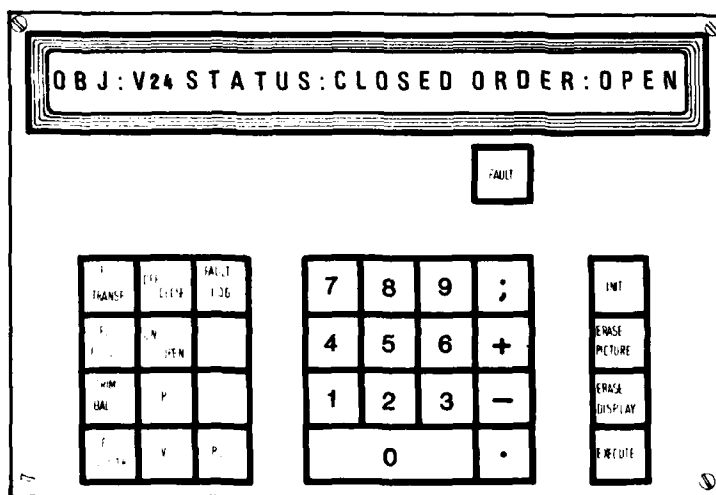


Figure 17. Keyboard for Valve and Pump Operation.

The keyboard is supplied with a one line alpha numeric screen acting as a separate signal device for valve and pump operation.

The introduction of a colour TV screen is to some extent regarded as an experiment. The system has therefore up to now only been supplied with 4 different pictures. Drawings of two of these, i.e. the Bunkering System and the Electrical Power Main Distribution System are shown on figures 18 and 19. The pictures are fully dynamic in so far as open valves and lines under pressure are indicated with green colour, while closed valves and nonpressurized lines are shown with red colour. The amount of tank filling is indicated by filling the tank symbol partly with a colour representing the filling liquid (i.e. brown colour for fuel oil). The exact filling is indicated by means of a two-digit number in each tank, indicating the filling in percent. During a period of filling or emptying a tank, the number and the colour filling of the symbol will vary continuously.

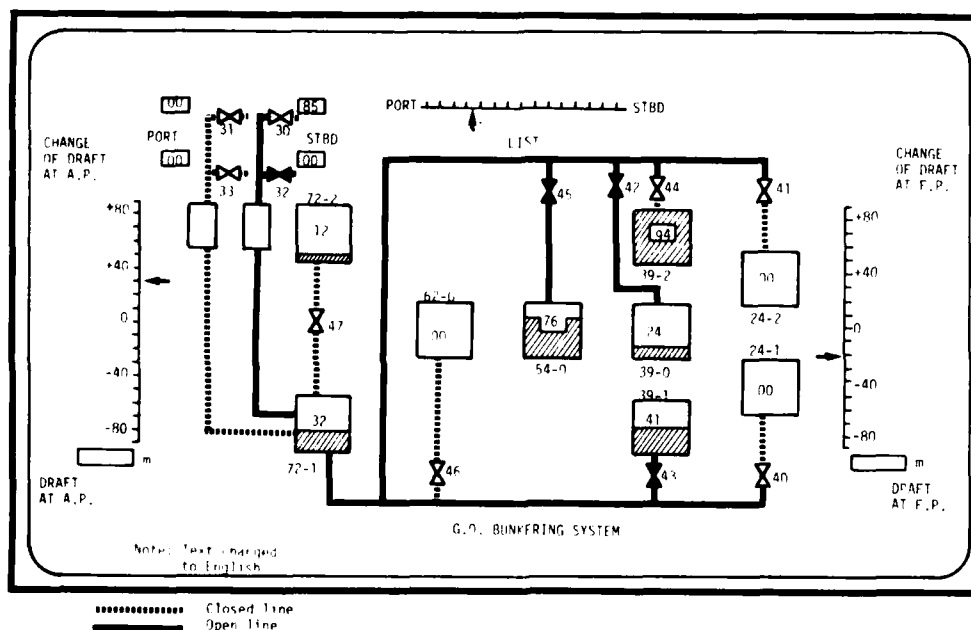


Figure 18. Colour Screen Picture showing Bunkering System.

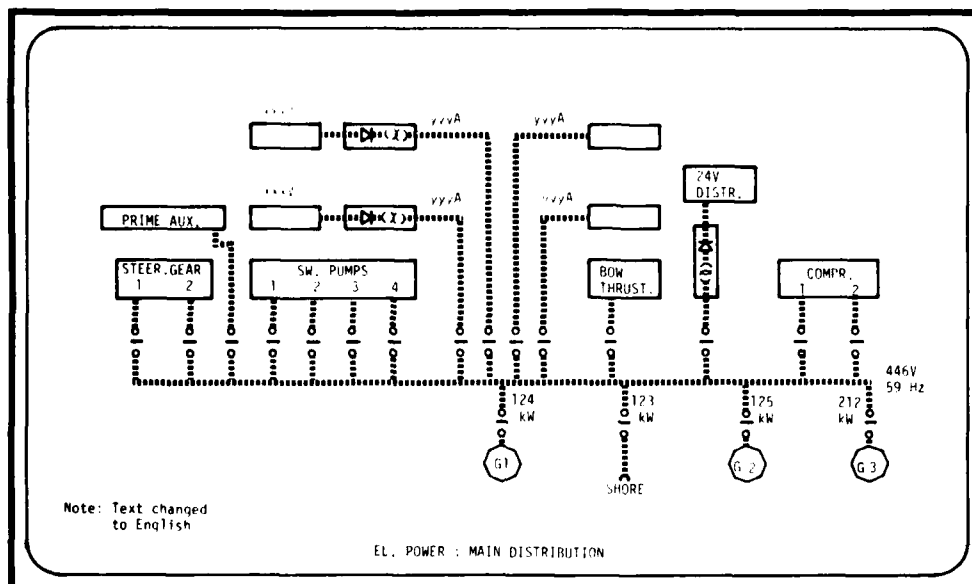


Figure 19. Colour Screen Picture showing Electrical Power Main Distribution.

Since the various tank systems are used for trimming the ship, scales are included at the top and each side of the screen showing list and trim. These scales are of course also fully dynamic.

The picture showing the Electrical Power Main Distribution is coded in the same way as the other diagrams, i.e. green colour indicating voltage on, while red colour indicates voltage off.

#### SOME THOUGHTS ABOUT FUTURE CONTROL AND INSTRUMENTATION TECHNIQUES ON SHIPS

Compared to the conventional control and instrumentation techniques which have been used throughout the 1960's and 1970's, modern systems can represent very powerful tools, which are able to perform tasks which would have been considered unrealistic only a few years ago. Although we certainly will see great developments within the measuring techniques, we still believe that the treatment of instrument signals will show some of the most interesting developments.

Systems with logical signal treatment and floating limit values depending upon the operating conditions will be very much more usual than today. Methods involving "parameter estimation" will also be more commonly adopted when it is desirable to read on-line parameter values which cannot be measured directly.

Standard alarm systems will only give information about a faults action on one or more parameters, and will normally not give any information of the original cause of the alarm. It is expected that in the near future on-line "diagnosis systems" may to some extent replace the conventional alarm systems. In these systems parameter values relevant

to the fault information are compared, and the actual cause of the alarm is calculated.

Systems for condition monitoring are also expected to be more common in the near future. Such systems have already been used for several years, and a certain amount of experience has been collected. Manual systems have not fulfilled the original expectations. They are partly too inaccurate and partly too complex to use. Computer-based condition monitoring systems have been more successful, but also in this case it is expected that a higher degree of perfectioning may be obtained when better mathematical models and measuring techniques are available.

We also think that the concept of on-line short trend condition monitoring will be of great interest in the future. We are here considering cases where no limiting values are exceeded, but where combinations of parameter readings indicate fault situations which quickly may develop into objectionable situations.

Machinery systems are becoming more and more complex. So are also the control and supervision systems necessary to serve them. The aspect of Human Engineering is therefore becoming more and more vital. It is not uncommonly believed that this is the area where some of the greatest winnings may be earned.

Most of the features described above are included in the prototype control and instrumentation systems recently installed in vessels of the Royal Norwegian Navy. The Navy will now operate these vessels for periods to come, and it is important that experience and practical know-how about their functioning are collected and systematically analysed. As a result of this work it will be possible for the Navy to establish a well balanced level for the control and instrumentation techniques which are practical for the purpose, and which can be expected to stand up to the required standard for the nearest years ahead.

THE DEVELOPMENT OF A MACHINERY CONTROL AND  
SURVEILLANCE SYSTEM FOR A MINE COUNTER MEASURES VESSEL

by Terrence G Turner Vosper Thornycroft (UK) Ltd  
and Roy R Cummings Ministry of Defence (PE)  
Copyright Vosper Thornycroft (UK) Ltd

ABSTRACT

This paper describes the unique requirements and the development of an integrated machinery control and surveillance system for a new class of Mine Counter Measures Vessel for the Royal Navy. The project is being undertaken by the Controls Division of Vosper Thornycroft (UK) Ltd under a Ministry of Defence contract.

The system provides remote control and surveillance for the ship's machinery which includes two main propulsion diesel engines driving fixed pitch propellers, with a third diesel engine coupled to a pulse generator and four variable swash hydraulic pumps. These pumps can be operated to power the main propeller shafts, a bow thruster water pump and deck machinery.

The control system is electronic and employs DC position servo loops. A comprehensive interlock logic system ensures optimum machinery control, performance and safety of operating modes.

INTRODUCTION

The following paper discusses the progress of a specialised machinery control system from the placement of an initial development contract in 1971 to the present day. This system has been custom designed for a class of glass reinforced plastic Mine Counter Measures Vessels, presently being built by Vosper Thornycroft (UK) Ltd for the Royal Navy (see figure 1). The design, development and build contract were placed by the Ministry of Defence (PE) with the Controls Division of Vosper Thornycroft (UK) Ltd which is now a member of British Shipbuilders. At the time of placing the contract the Controls Division had a number of years proven experience in the field of machinery control, and remains today an autonomous division of Vosper Thornycroft (UK) Ltd. This group, as a whole, enjoys a world wide reputation for the design and construction of fast warships ranging from patrol craft to high performance frigates.

Initial work on the system development was concentrated on the design and prototype testing of a diesel engine proportional lever and actuator package, which would be compatible with the envisaged control philosophy for the ship. In 1973 the results of this preliminary development were incorporated by the MOD(PE) into a statement of requirements for a complete machinery control and surveillance system. The system ultimately produced has sometimes been described as a "ship mobility system" and is the result of the very closest collaboration between MOD(PE), Vosper Thornycroft Controls Division and the major machinery sub-contractors associated with the ship project. Presently standard production sets of control





Figure 1. Mine Counter Measures Vessel (Artist's Impression)

equipment are either under construction or have been delivered, and a joint trials programme is in progress, using the first production set of control equipment at a purpose built, shore-based, machinery test facility.

A significant feature of the project has been the extensive use of computer simulation both to achieve an optimum performance design for the control system itself, and in the development of a dynamic shaft loading system for the machinery of the Shore Test Facility.

The authors would like to take this opportunity of firstly, acknowledging the help received from their colleagues in the preparation of this paper and secondly, to state that, due to the unique nature of the Mine Countermeasures Vessel's requirements, the control solution and technology employed do not necessarily reflect the general policies of the MOD(PE) or Vosper Thornycroft (UK) Ltd.

The various constraints and requirements which were placed on the control system design will now be described. These constitute the "Control Problem". The methods of meeting these stipulations and their incorporation into the design will then be described. This constitutes the "Control Solution".

#### CONTROL PROBLEM

The task undertaken by VTC was to design, develop and build an electronic machinery control and surveillance system to unite a defined package of:-

- (i) hull + propellers
- (ii) main machinery
- (iii) machinery configuration
- (iv) machinery control console
- (v) operating requirements
- (vi) physical constraints

into a three man operated ship control system.

#### Hull and Propellers

The first of the constraints (item (i) above) were major inputs to the initial ship performance computer simulation which is discussed later. This simulation predicted critical parameters to be met by the machinery control system, in order to ensure that the required ship performance characteristics were achieved.

#### Main Machinery

The second factor ((ii) above) is the main machinery. The equipments to be used were defined before the control system design started and their performance specifications had been agreed and included in the initial computer simulation. However, in many instances, including the main engines, development of the hardware was to progress in parallel with design and build of the control system. Timescale and cost considerations precluded the building of

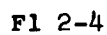


Figure 2. MCMV Main Drive System

a prototype control system and the first set of equipment was built to production standards for the previously mentioned shore Test Facility, at which a complete ship's main machinery package was to be proved. It was therefore imperative that parameter and even mode changes could be accommodated during its design, build and test stages with minimum disruption. This flexibility has been achieved by following a strictly functional approach to the circuits and their packaging.

#### Machinery Configuration

Item (iii) on the list of constraints is the machinery configuration, which is unique to the class of vessel. The control tasks to be undertaken are described with the machinery as follows:-

- (a) The main propulsion is given by two Paxman Deltic type diesel engines (see figure 2). These drive fixed pitch propellers through reversing gearboxes. The control system is required to start, stop and survey the engines, engage forward and reverse clutches, exercise governor control and ensure power limitations of components are not exceeded. All these operations are to be performed remotely by the control system mounted in the Ship Control Centre. Once running, engine and clutch control is to be in response to single 100% ahead to 100% astern levers for each engine, either from levers mounted in the ship control centre or from levers mounted on the bridge. All "on machinery" control actuators are to be capable of local operation should the control system fail.
- (b) A third deltic type engine is fitted and is called the Auxiliary Engine (see figure 3). This drives either an electrical pulse generator or 4 variable swash hydraulic pumps. The hydraulic system into which these pumps drive can be valved to power a number of fixed swash hydraulic motors viz:-
  - (i) Pump one powers either a deck winch or the bow thruster.
  - (ii) Pump two powers either a deck winch or a motor contained within the starboard main engine gear box. This latter motor may be engaged remotely via its own clutch, whilst the propulsion engine is declutched, and provides a slow speed drive capability.
  - (iii) Pump three drives either a deck winch or the bow thruster (both pumps one and three are required for full bow thrust power).
  - (iv) Pump four is dedicated to the port main shaft slow speed drive.

The selection of the main hydraulic system is the only major operation on the plant that has to be performed locally in the engine spaces. No requirement for remote control was seen at the initial ship design stage, and none has been given in the interests of simplicity, reliability and cheapness. Although valve control is not remote, the

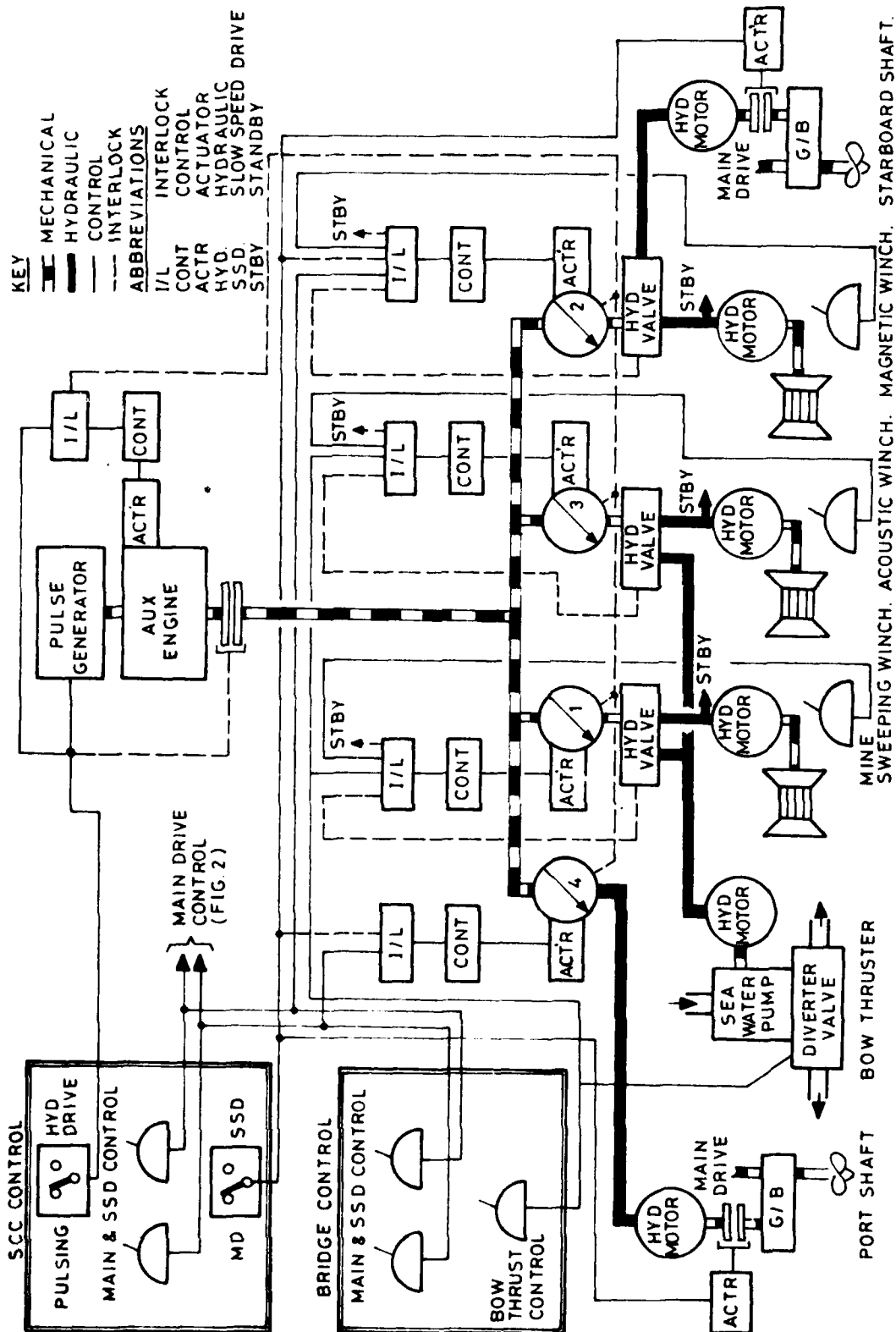


Figure 3. MCMV Hydraulic Drive System

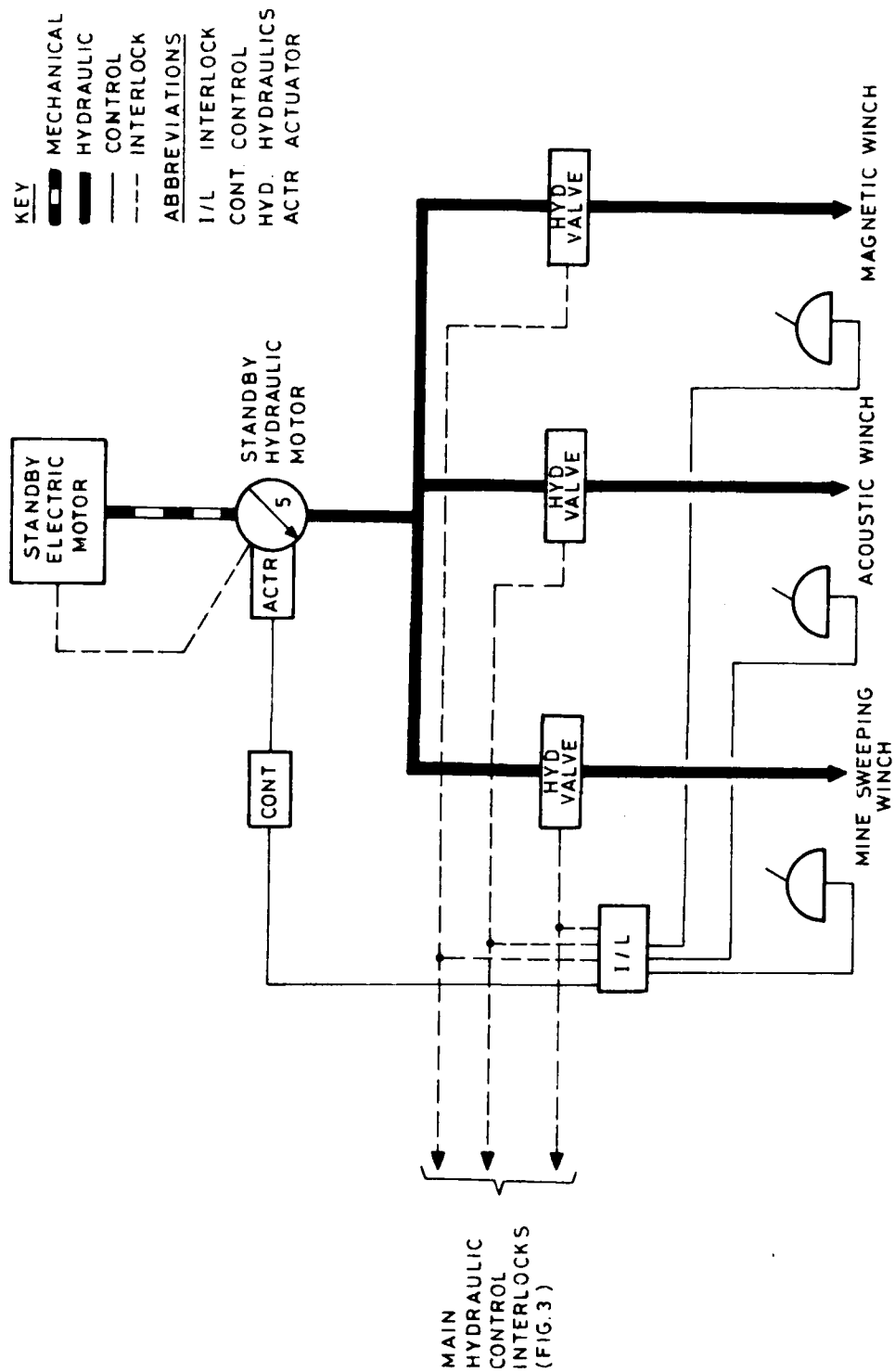


Figure 4. MCMV Standby Hydraulic System

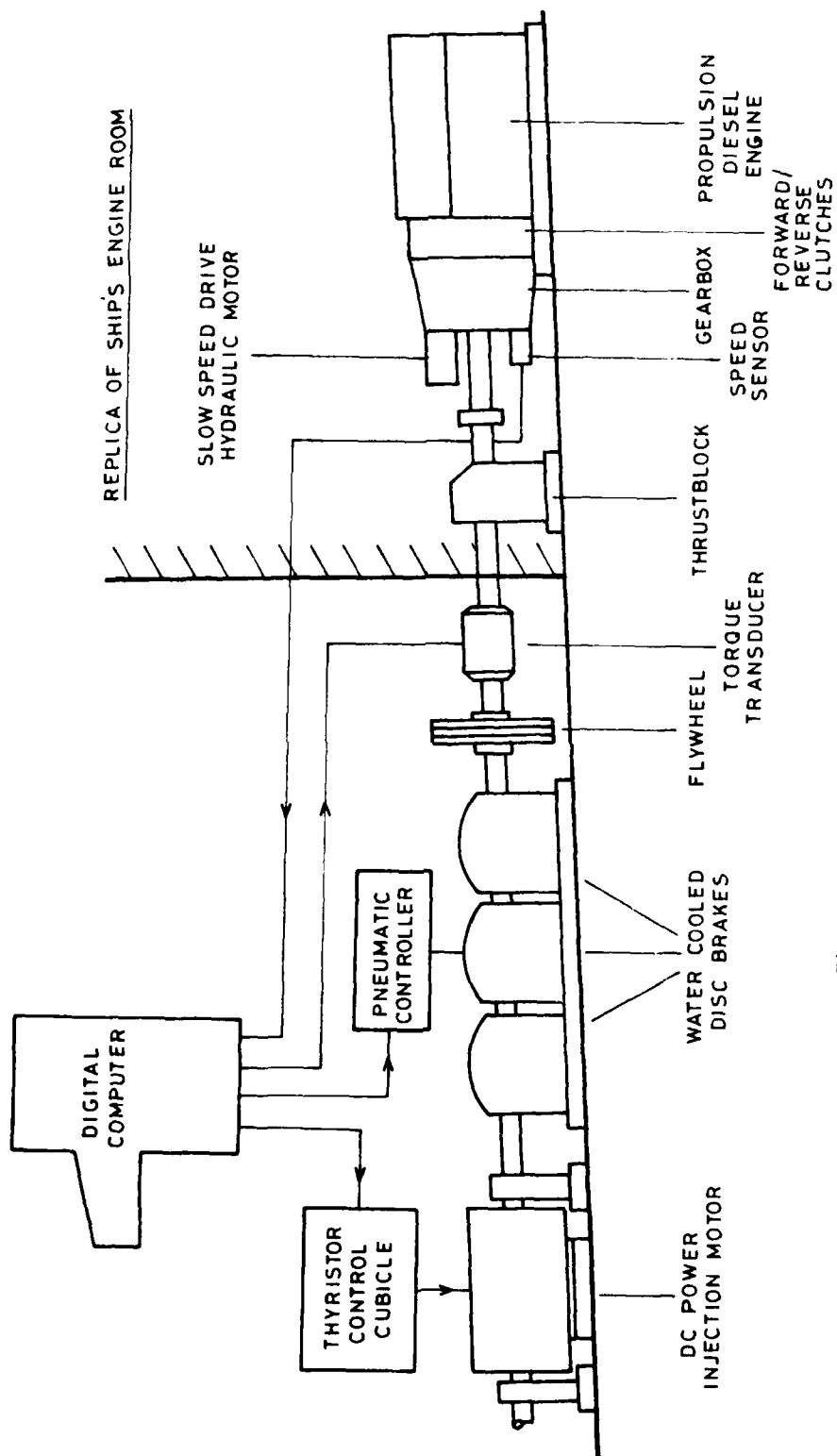


Figure 12. NCMV Shore Based Test Facility  
Schematic Layout of One Shaft Set

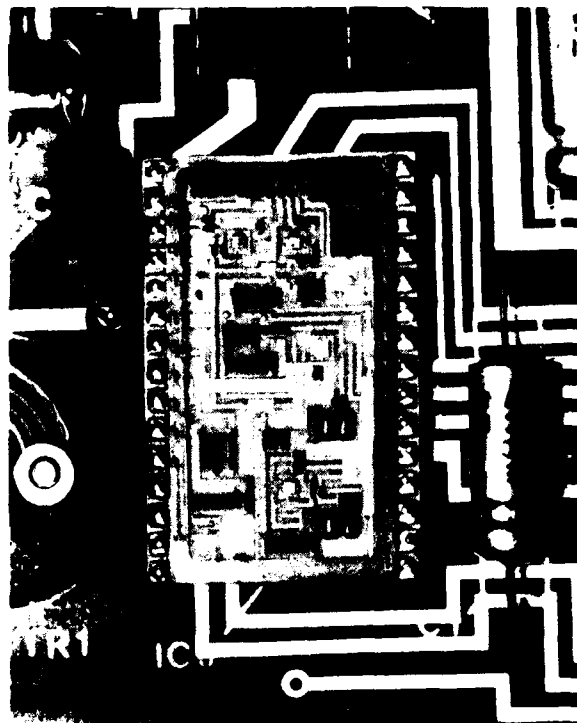


Figure 11. Hybrid Microcircuit



particular mode of control is displayed by a sequence of light emitting diodes and any failure to achieve control can be traced immediately to a loss of a particular signal. To further aid location each surveillance channel logic module within the Logic Rack and each sensor amplifier in the machinery space cubicles, carries a light emitting diode to indicate when it is in the alarm condition. As each logic module is clearly labelled with the parameter which it monitors, interpretation of the light indicators makes it possible to rapidly pinpoint a potential failure to a specific aspect of the plant.

At least one of each type of electronic module is fitted as a spare within the "Logic Rack", and as a first step a module associated with a failed feature of the Control System can be rapidly exchanged. Whilst the repair by replacement approach is generally effective in dealing with faults in the digital areas of the system it is not always successful with analogue circuitry and for this reason a full built in test position is provided for the major type of analogue module - the Control Servo Amplifiers.

This test position enables a suspected faulty unit to be exercised in its various operating modes and also permits limited resetting up to be carried out. Also provided within the built in test facility is a general purpose digital multimeter which can be used for either general monitoring of test points provided on the front panel of each module, or switched to read essential services such as power rail voltages and earth leakage resistance.

#### Special Design Requirements

Running through all aspects of the control system design were a number of features which are very specific to the requirements of an MCMV. Each is touched upon very briefly in this paper but each, of course, has had a significant influence on the ultimate design solution chosen.

##### (a) Reduction of Magnetic Signature

Very close material control was necessary to ensure that the system as a whole was kept below a target magnetic permeability figure. This involved the use throughout of austenitic stainless steel and other non-magnetic metals for all fastenings and mechanical parts, and in some cases necessitated the modification of proprietary components to reduce magnetic content. Items such as relays, solenoids and meters were naturally avoided wherever possible but, where their use was essential, compensation coils have been developed to cancel the induced field and compensation magnets have been fitted to cancel permanent fields.

##### (b) Low susceptibility to, and low emission of Electro-Magnetic Radiation

The decision to employ a DC System significantly reduced the potential problems in this area but nevertheless extensive use has been made throughout the design of suppression diodes, power line filtering, signal line pull-up resistors and the avoidance of unterminated signal lines. In addition, bearing in mind the non-conductive

visual indication to a continuous one. Figure 5 shows the layout of the SCC Console which is in three sections mounted in a wrap round configuration. The panel on the right contains all the main machinery control gauges and indicators, the centre panel is associated with the ships auxiliary machinery and that on the left with Nuclear Biological and Chemical and Defence indications. The sloping portion of the desk contains all the machinery controls and communications facilities. The desk is extremely compact being only 1.5m long 1.6m high and 0.5m deep from the front edge of the desk to the rear panel, and the panel layout, which was devised by the Ministry of Defence, provides a clear visual presentation of the machinery configuration. Referring to the machinery control indication panel (see figure 6) the Port and Starboard main engines may be seen with their respective gauges and annunciators, driving through forward and reverse clutches to the propellers represented by the digital shaft speed displays. In the centre is the third or auxiliary diesel engine providing drive to either the pulse generator or the four hydraulic pumps. Hydraulic system valve states are indicated and the operator is provided with a continuous indication of which pump is providing power to which service. On the right is the instrumentation for the electrically driven standby hydraulic pump, which can be switched in to provide emergency power for the recovery of gear etc in the event of the auxiliary engine not being available. A full test of the warning and alarm lamps is provided for each section of the console.

As an example of the operation of the control and interlock system it is of interest to consider the sequence of operation in an extreme manoeuvre such as the crash stop from full ahead. The engine control levers will be thrown by the operator from the full ahead to the full astern position, the engine actuators will move the engine governor at a controlled rate from the full ahead setting to the forward clutch engagement set point. At this position the actuators will be held by an interlock derived from propeller shaft speed which will continue until the propeller speed has dropped to a speed low enough to keep power dissipation during clutch engagement at an acceptable level. The interlock having been released the actuator moves through the idle condition to the astern clutch engagement point. Here there is a further pause until astern clutch engagement is achieved following which the actuator continues to the engine full astern setting. The computer simulation demonstrated that the above sequence of operation offered the shortest stopping distance commensurate with the avoidance of excessive energy dissipation in the clutches or stalling of the engines, however flexibility remains within the control system to alter the clutch engagement and disengagement points if slight variations are found to be beneficial in practise.

#### Design for Ease of Servicing

A significant feature of the design of the "Logic Rack" is the provision of the Sequence Panels shown in figure 10. The inherently digital nature of the interlocking system makes it possible to display the signal states of the system in a logical manner.

Advantage has been taken of this fact by providing a display sequence for each of the major control facilities, Engine Starting and Stopping, Main Drive, Slow Speed Drive, Control of Bow Thruster and Control of each of the three Deck Winches. Each of the prerequisite functional or interlock conditions to achieve a

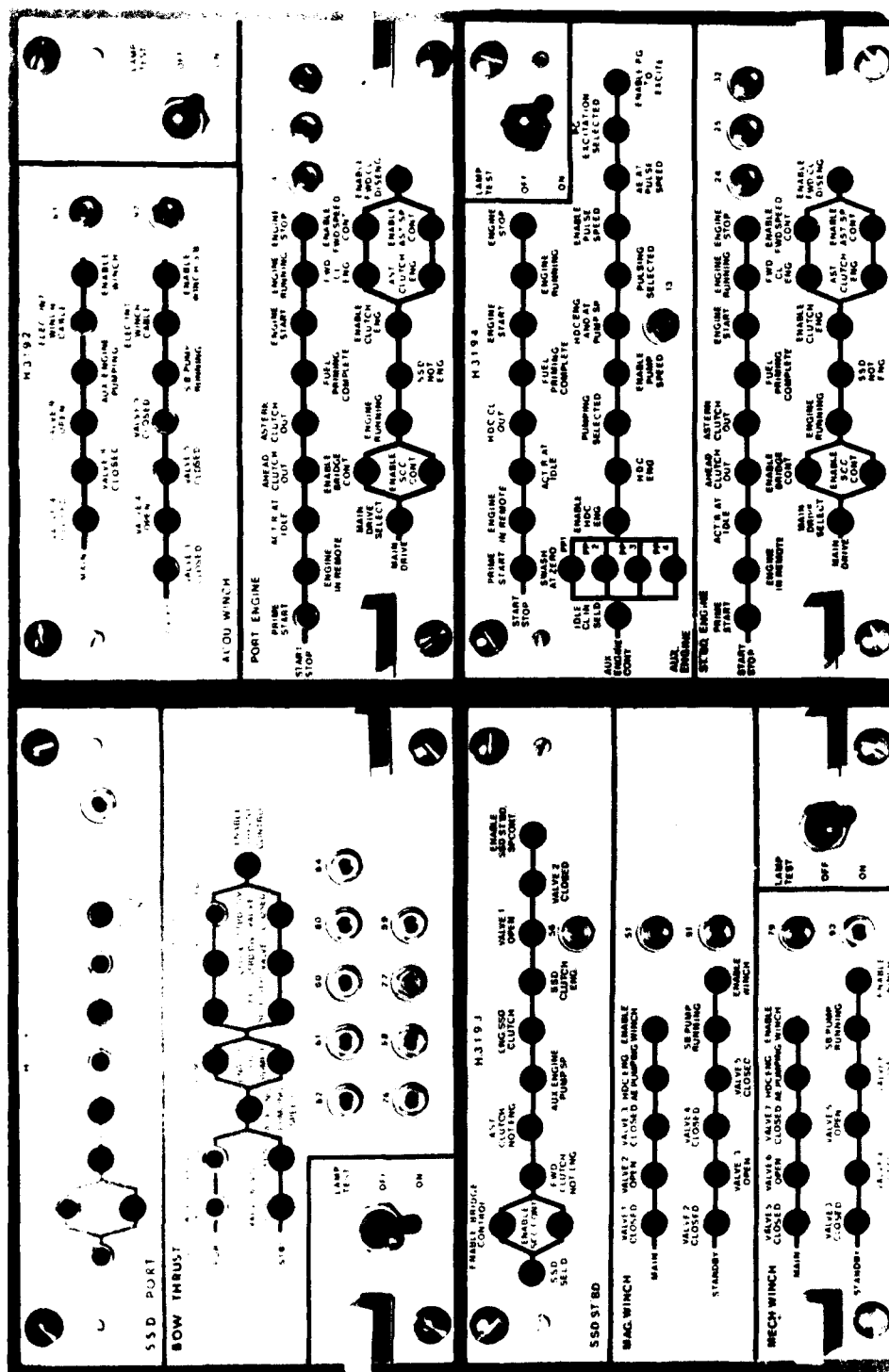


Figure 10. Sequence Indication Panels

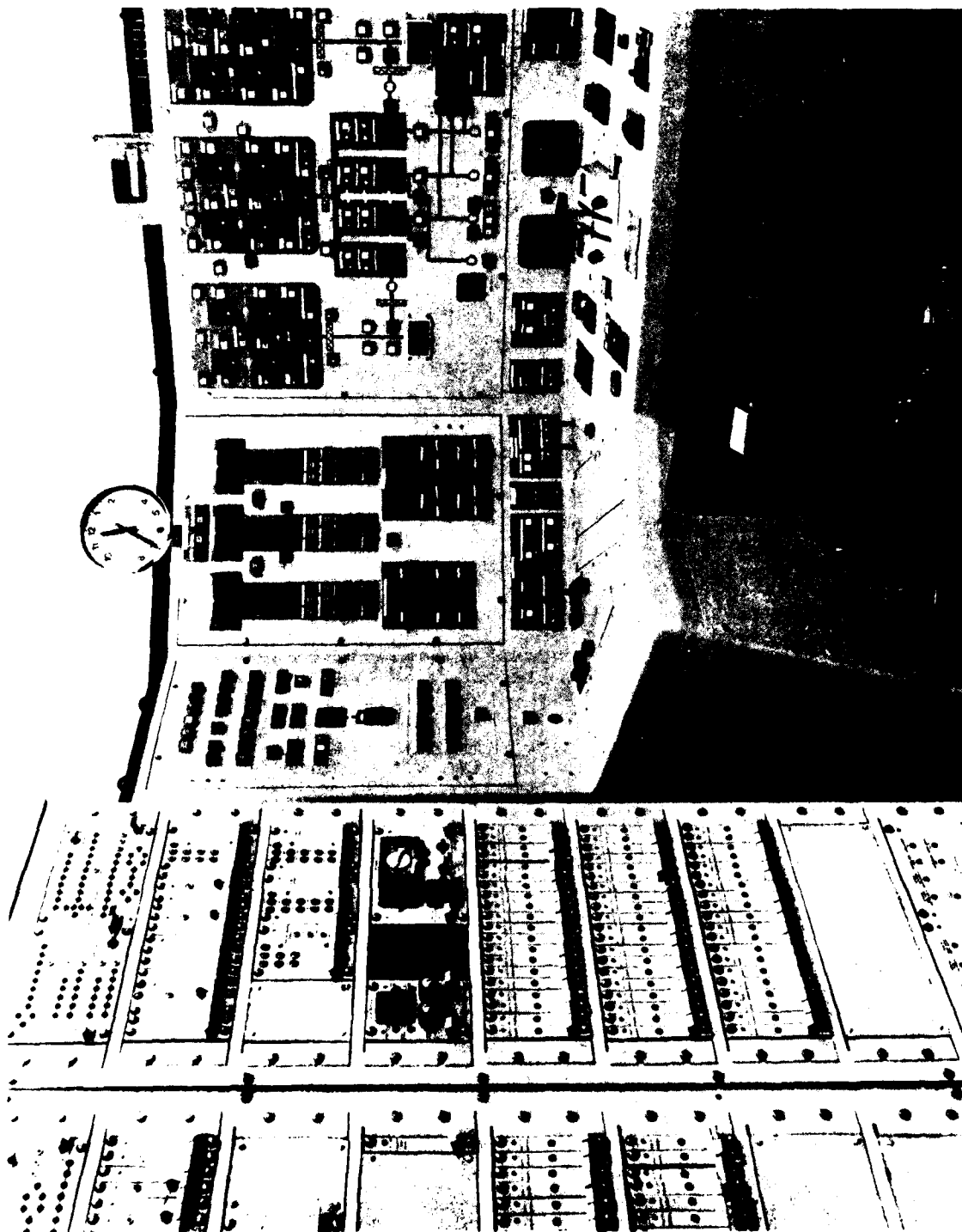


Figure 9. Machinery Control Console and Logic Rack

Control of the diesel engines is achieved by movement of the engine governors and of the hydraulic pumps by angular displacement of the swash plate. In both cases the operation is rotational making possible the adoption of a common actuator design. The one fundamental difference between actuators for the two functions is that the engine actuator has a fail set facility whereas the hydraulic pump actuator fails to zero. Both types of actuator incorporate a manual override control.

#### Surveillance

Having provided the operator with a precise and responsive method of controlling the machinery it was next necessary to turn attention to considerations of machinery state surveillance and safety. The machinery configuration of the Brecon class MCMV, which has been described above, is exceptionally complex, not only because the main propeller shafts can be controlled in either a main drive or slow speed drive mode, but also because hydraulic pumps may be switched to provide power for a variety of different services. A comprehensive interlocking system is therefore necessary to safeguard plant and ensure that inadmissible machinery configurations are prevented. To this end some 146 channels of fixed surveillance are provided gathering data from the following sources:

- Pressure transducers
- Resistance thermometer detections
- Thermocouples
- Pressure switches
- Contract operations of various types.

Signal conditioning circuits for the pressure transducers, resistance thermometers and thermocouples are housed in ten similar electronic cubicles which are distributed throughout the ships machinery spaces to reduce, as far as possible, the signal path length between a sensor and its associated conditioning amplifier. The amplifiers are housed in individual "plug in" modules, and each cubicle has a total capacity of 19 modules. Because of the more hostile environment in the machinery spaces, particular emphasis has been placed on the robustness of construction. The cubicles are totally enclosed with drip proof access doors to the amplifiers and cable chambers, and the amplifiers themselves employ a hybrid microcircuit to contain all but the adjustable or non critical elements of the circuit. Each channel is capable of providing both an analogue output and an alarm signal which can be preset to any desired point within the analogue range. Signals from the surveillance cubicles are fed to a control electronics unit, known as the "Logic Rack", which is mounted adjacent to the Control Console in the Ship Control Centre (see figure 9). Here further signal processing takes place to provide, as required, direct inhibition of machinery operation, and/or indication at the SCC Console of machinery states of readiness or failure. The electronics to achieve this is housed in functional "plug in" modules. Indication of warnings or alarms is given on the Control Console by means of flashing annunciators which may be accepted by the operator via integral pushbuttons. Alarms which are here defined as indications that a shutdown has occurred, may be accepted by the operator at his discretion but cannot be removed except by removal of the alarm condition itself. Warnings are similarly accepted manually, but reset automatically once the fault condition is removed or reverts to normal. Acceptance of an alarm or warning silences the audible indication of the occurrence and changes the "flashing"

## THE CONTROL SOLUTION

### Simulation

A primary requirement of the project was the conduct of a Computer Simulation to investigate the predicted ship performance and to recommend an optimum control solution for each of the primary roles of the new vessel:

- (a) Patrolling and Cruising
- (b) Minesweeping
- (c) Minehunting

The initial simulation work was carried out by the Marine Industries Centre at Newcastle and particular emphasis was placed on such features as the rate and timing of engine clutch engagements for optimum manoeuvring control, the rate of application of hydraulic pump swash for best performance with minimum transient load and the investigation of bow thruster performance. This work resulted in the presentation of reports during 1974 which confirmed a ship performance within the design requirements and defined the essential responses of the machinery control system. With the progress of development there have been inevitable changes to some parameters of both the hull and machinery, and in 1977 the simulation was transferred to Vosper Thornycroft's own powerful in house hybrid computer facility. This provided the design team and the Ministry of Defence with continuous access to a fully up to date simulation for the analysis of plant behaviour as practical data became available. The technique of maintaining a continuously up to date simulation throughout the life of a project is now fundamental to the Vosper Thornycroft approach to Ship Control System design. This has already proved invaluable on other projects for the rapid and cost effective solution of unforeseen aspects of plant behaviour, which may not become evident until the sea trials stage.

### Proportional Lever Control

The fundamental requirement of the control system was for a proportional lever control of all major machinery functions, Propeller Shaft Main and Slow Speed Drive Modes, Bow Thruster and Deck Winches. To this end a common design philosophy was pursued for a control lever mechanism, a servo control amplifier and a rotating shaft actuator. In the initial stages an ac servo was considered as this was felt to offer advantages from the point of view of reduced magnetic fields. However this was discarded at an early stage because of limited torque and the risk of electromagnetic radiation from such a system. The final Statement of Requirements specified a totally DC operated system and consequently a DC position servo incorporating rate feedback was developed for the ship system. This solution offers precise control in terms of both positional and rate response with a relatively high torque for a compact physical size. Although the DC torque motor and rate feedback tachometer inevitably incorporate permanent magnets, components employing toroidal magnets were chosen which have exceptionally high performance characteristics and generate an inherently low level of stray field.

the main electrical switchboard which is placed adjacent to the control console). Air conditioning, main seawater, high pressure air, refrigeration, fuel transfer and sewage systems are monitored and, where required, controlled on this panel.

- (c) The final section (figure 8) provides surveillance of the remaining equipments and parameters viz:- converted electrical supplies, flood level alarms, air filtration units, machinery ventilation, firefighting and fire detection systems and finally engine exhaust stack temperatures. As can be seen from the figures of the console layout, standard broadcast and communication equipment is also incorporated.

#### Operating Requirements

Stipulation number (v) for the control system is the defined operating requirements. Single lever bridge control of the main shafts was a major requirement, thus both bridge and ship control centre levers require to operate either main engine gearbox clutches and governors or the hydraulic pump swash plates on the slow speed drive hydraulic system. All surveillance is to be undertaken by one man in the ship control centre, who has a roving watchkeeper providing assistance in hydraulic valve selection etc. The console operator is also the control system maintainer. To meet this requirement sufficient fault finding equipment is necessary, which together with presentation of failure modes, must allow fast diagnosis of faults to the level suitable for onboard repair.

#### Physical Constraints

The final factors (Item (vi)) are the physical constraints. The general requirements for this type of vessel of minimum magnetic signature, size and weight had to be met. The ship design was such that the equipment had to fit a small, specified space which allowed only front access.

Finally the system is required to work from a 24 volt DC, battery backed supply.

The next section of the paper will discuss the control solution to the above problem and will be followed by a situation report on development to date.

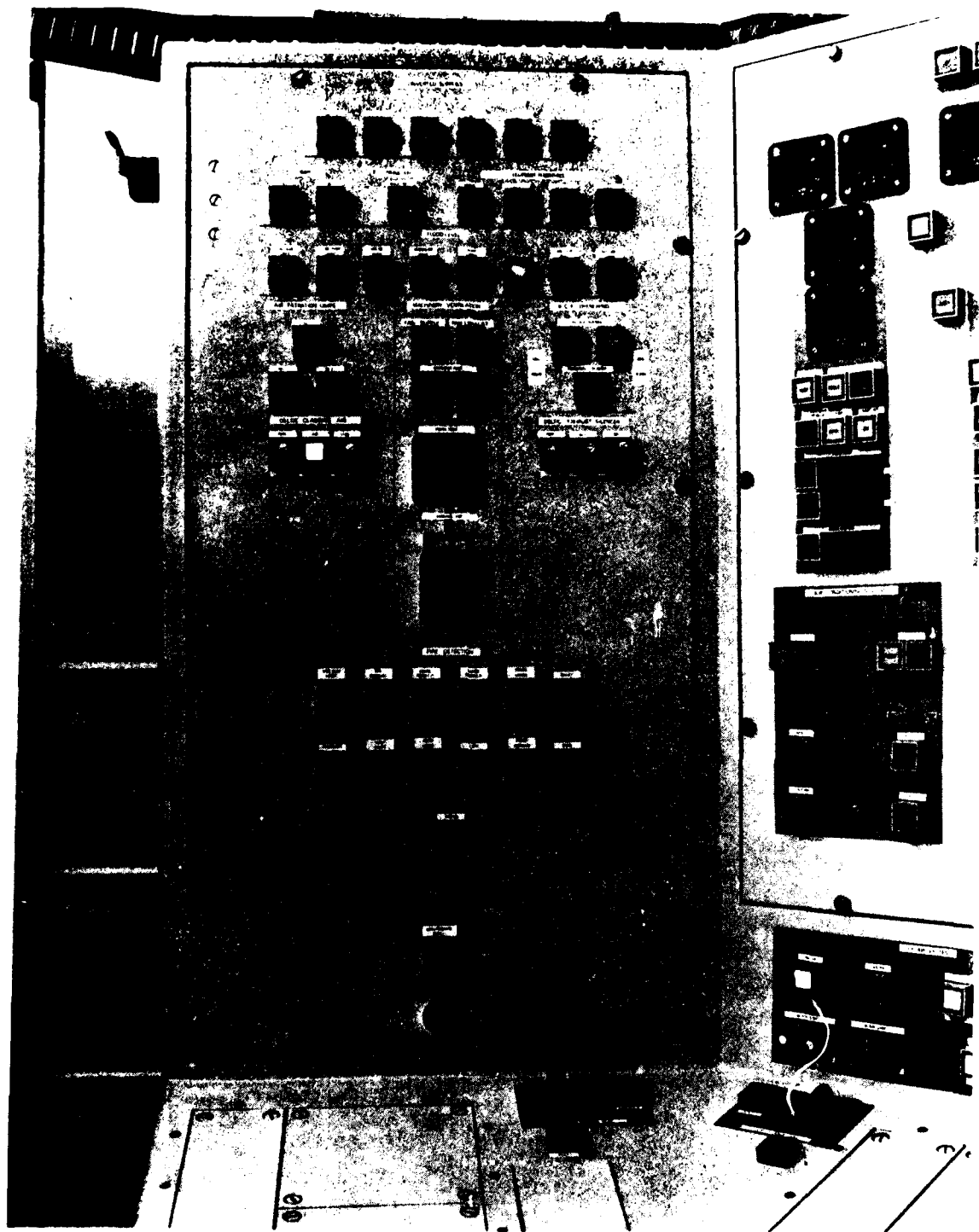


Figure 8. Misc. Surveillance Panel



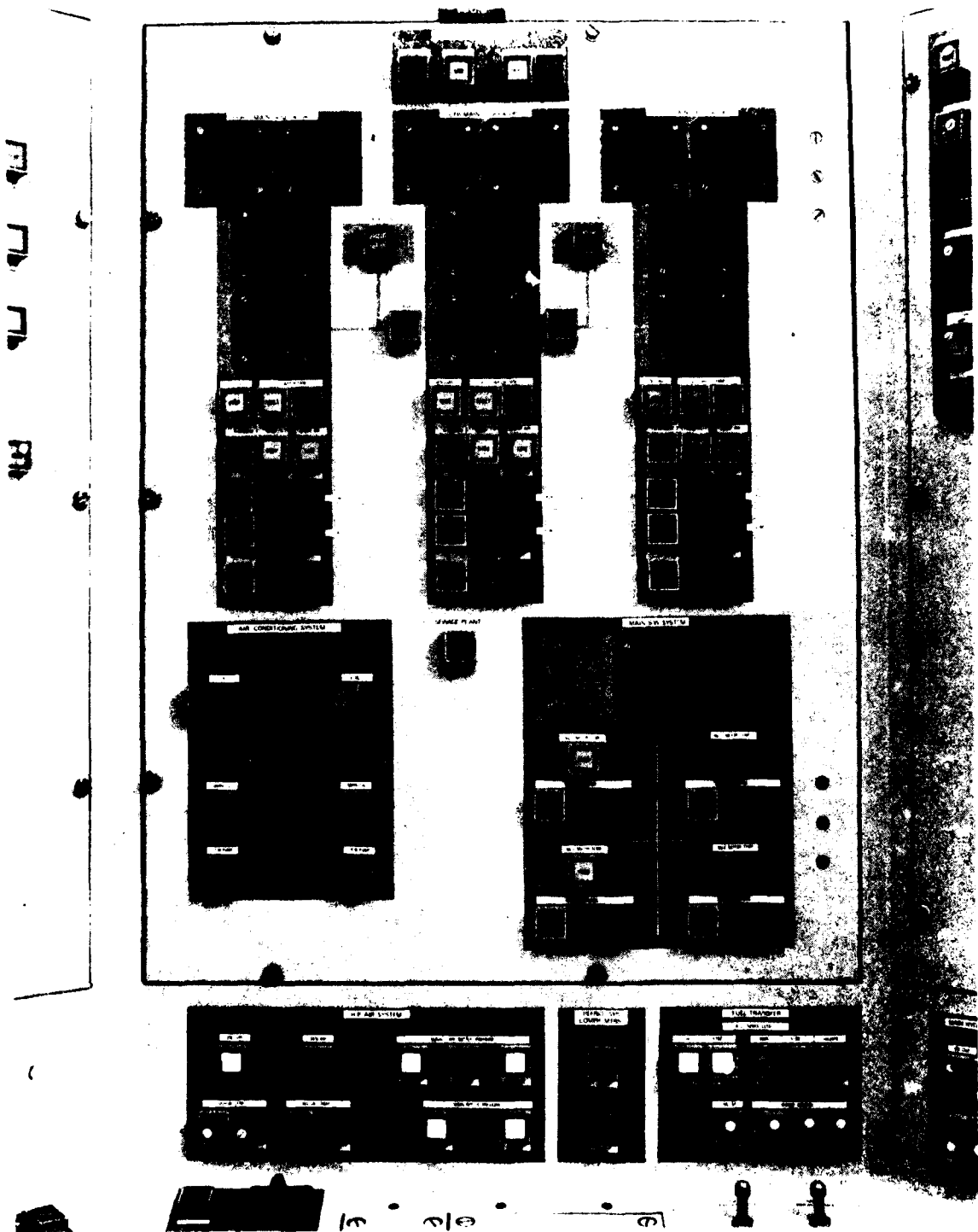


Figure 7. Auxiliary Machinery Panel

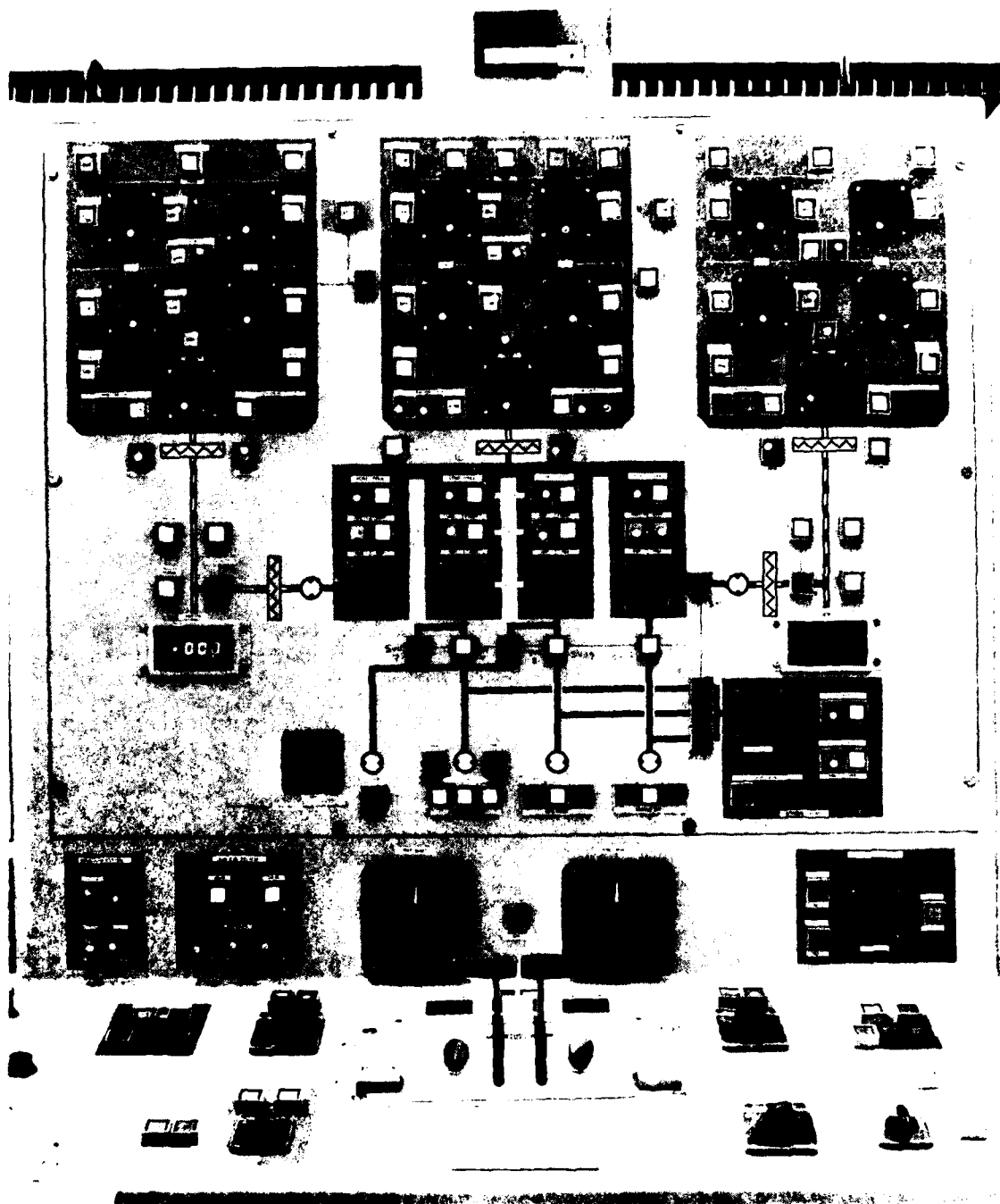


Figure 6. Main Machinery Panel

positions of all valves are automatically monitored and are an important input to the interlocks in the control system. These interlocks ensure that the hydraulic system is correctly set up, before operation in the selected mode is effected.

- (c) A fifth, electrically drive hydraulic pump is fitted as a standby, should the auxiliary engine pumps not be available, and can be selected to drive any one of the three deck winches. See figure 4.

The control requirements of the hydraulic system described above are as follows:- initially it must remotely start the auxiliary engine and ensure that it runs at a set pumping speed. Engagement of the clutch giving drive to the pumps is only to be allowed when all the swash plates of the pumps are set to zero. Should the hydraulic valves be correctly set, remote control of the swash plates is to be automatically enabled and effected from;

- (a) the dedicated remote deck position for each of the winches;
- (b) the Bridge for the bow thruster;
- (c) either the main propulsion single lever controls in the ship control centre, or those in the bridge, for the slow speed drive motors.

Additionally the control system is required to impose maximum swash limits on the pumps and to reduce them automatically depending on which load they are supplying, to prevent the power limitations on particular equipments being exceeded. Similarly remote start/stop and surveillance of the standby pump is needed, with swash control automatically enabled from the selected winch control position.

#### Machinery Control Console

Item (iv) on the list of constraints is the machinery control console (see figure 5), whose layout and scope was defined by MOD(PE). This prerequisite was necessary to incorporate the many control and surveillance functions for auxiliary systems not included in the main machinery control package contracted to Vosper Thornycroft. The control system design was influenced by these auxiliary requirements in that surveillance electronics and control wiring had to be provided. Included in this brief description of the console, the auxiliary machinery requiring control or surveillance will be mentioned.

- (a) Main machinery panel (figure 6). As well as providing all remote control and surveillance of the 3 deltic type diesel engines and the main hydraulic system which will be described in detail later, the auxiliary seawater system pumps, steering system motors and main propulsion mode selection controls are contained on this panel. Throughout the console control of auxiliary systems, where provided, is limited to start/stop functions.
- (b) The centre section (figure 7) of the console provides control and surveillance of the three main diesel generators (paralleling and loading of them is performed on



Figure 5. Machinery Control Console

nature of the ship itself, particular attention has been paid to earth bonding and the skin integrity of electronic cubicles.

(c) Reduction of Weight and Volume

In the interests of reducing weight and volume, and also because they offer greater reliability, hybrid micro-circuits were used wherever this was economically viable. Their use in the signal conditioning amplifiers for the surveillance system has already been mentioned and they have also been included in the surveillance logic modules and the servo amplifiers. In all a total of seven types of purpose built hybrids are employed in the design and figure 11 shows a typical example. The picture is taken with the lid removed and shows such features as the individual integrated circuit chips, capacitors and resistive ink resistors. These resistors are laser trimmed to achieve the required resistance value.

The Shore Test Facility

In conclusion the Shore Based Test Facility is briefly described. This facility has been constructed to enable the detailed study of the ship's machinery and control system. As an adjunct to the original control simulation a simulation study was also undertaken to define a suitable equipment package for the dynamic loading of the ships propeller shafts to enable fully realistic, "straight line" ship manoeuvres to be conducted with the test facility. The results of this study recommended the use of pneumatically operated disc brakes for basic shaft loading, backed up by powerful thyristor controlled DC motors to provide simulated power injection from the propellers and to continuously trim the load setting. The loading loop is closed by means of a torque transducer positioned between the ships engines and the load and a general purpose digital computer fed with the ship performance profile. A fully fitted ships engine room section is included as part of the test facility and all machinery is controlled by the control system developed for the ship. A general layout of the test facility is shown in figure 12 in which the major features such as the disc brakes and power injection motors are shown.

At the present time the trials programme is in progress at the Shore Test Facility which has already resulted in minor parameter changes to the control system. These have arisen from the verification of uncertain predictions of machinery performance. No major changes to the control system have been found necessary. The second set of control equipment has been delivered for installation in the first ship of the class, having been satisfactorily tested as a system in the Vosper Thornycroft factory. All future systems will be similarly tested, however electro-magnetic compatibility, environmental and shock "type testing" was additionally carried out on the second system with satisfactory results.

## MARINE GAS TURBINE HEALTH/PERFORMANCE MONITORING

by Robert J.C. Harris  
and Geoffrey Keating  
Decca Radar Co. Limited

### GENERAL

The use of marinised aero derived gas turbines for main propulsion power for Naval vessels is now well established. The reasons for this are well known, but one of the main aspects is the ease of surveillance, control and maintenance particularly when related to manpower and man capabilities. The Royal Netherlands Navy realised at an early stage of future manpower difficulties and this is reflected in their decision regarding new vessels. (1)

Parallel with the appearance of the marine gas turbine came advanced techniques in surveillance and maintenance and the philosophy of maintenance by replacement, so enabling the warship to have preferably 100% power source available. Routine exchange of engines was scheduled for approximately 4000 running hours and it is comparatively easy to see, from both the operational and economic point of view, the benefits of being able to decide whether this time scale is the correct moment for exchange or whether an attitude of 'leave well alone' could be adopted.

There are, in principle, two areas to obtain an indication of the gas turbine health or condition:-

- a) The "gaspath" of air and exhaust gases through the engine.
- b) The construction which means the pure mechanical parts, i.e. bearings, blades etc.

The construction can be covered by equipment such as vibration, temperature and pressure sensors etc., and the gaspath by performance monitoring. The thermodynamic process is an excellent means of obtaining an insight into the health of the engine but it is essential to have good information and trend analysis to determine the process.

The objective of performance monitoring is to be able to measure the behaviour of a gas turbine in a sufficiently meaningful way that deterioration requiring corrective action can be detected early enough to prevent excessive fuel consumption or costly breakdowns.

A key factor in applying trend analysis to engine performance is the high degree of repeatability of information. The output of trend analysis is then two fold:-

- a) Prediction of time failure caused by progressive deterioration.
- b) Early detection of mechanical discrepancies.

In the Royal Netherlands Navy ships, the main monitoring, surveillance and recording of all machinery parameters is carried out by the Decca ISIS 300

equipment. (2) Consideration was initially given to carrying out the trend analysis manually, using routine data logged by this main equipment but it was soon appreciated that this was impossible to carry out successfully in a warship operational configuration, and computer based equipment using the data obtained from the main ISIS 300 equipment was finally chosen.

With guidance from the engine manufacturer, Rolls Royce Ltd., the equipment has been developed to monitor the performance of the Olympus and Tyne gas turbine on warships of the Royal Netherlands Navy.

#### METHODS OF PERFORMANCE MONITORING

All methods of performance monitoring rely upon the measurement of a number of key parameters. It is not usually necessary to measure all of the many parameters which it is possible to measure since most causes of deterioration produce inter-linked changes in parameters. The key parameters recommended by Rolls Royce are as follows:-

##### Speeds

L.P. compressor speed	n
H.P. compressor speed	n

##### Pressures

Absolute Atmospheric Pressure	$P_0$
Absolute Air Intake Pressure	$P_1$
H.P. Compressor Delivery Pressure	$P_3$
Power Turbine Entry Pressure	$P_6$

##### Temperatures

Air Intake Temperature	$T_1$
Power Turbine Entry Temperature	$T_6$

##### Miscellaneous Parameters

Fuel Flow	Q
Power Output	B
Gas Generator vibration	$V_1$
Power Turbine vibration	$V_2$

#### PROBLEMS ENCOUNTERED IN PERFORMANCE MONITORING

The reason for this inclusion of atmospheric temperature and pressure in the above list brings the first problem to be encountered when monitoring gas turbines. In essence a gas turbine is a thermodynamic heat engine and as such, is affected appreciably by changes in atmospheric temperature and pressure in the same way that the classical Carnot engines output depends on the sink temperature and pressure. It is therefore necessary to distinguish between changes in the values of parameters caused solely by changes in ambient conditions and changes in the values of parameters caused by genuine deterioration. To enable this distinction to be made, all parameters that are affected by changes in ambient conditions are corrected to a fixed ambient temperature and pressure known as Standard Day Conditions. Although these corrections can be performed manually, not all parameters are corrected in the same way which leaves room for mistakes to be made. It is

obviously much more satisfactory for the monitoring equipment to apply the appropriate formula to each parameter to convert them to Standard Day Conditions.

For industrial gas turbines which are normally operated very close to full power output the variations in parameters caused by intentional changes in power output are very small and can easily be compensated for. In marine useage the problem is much more difficult, since engines may be run at power levels down to 25% of full output power. The key parameters vary enormously over this range in a very non linear way. Clearly some means has to be found of correcting the parameters for the effects of reduced power operation and relating the results to some standard bench marks against which comparison of performance can be made.

#### METHOD OF PERFORMANCE MONITORING USED IN THE EQUIPMENT BEING DESCRIBED

In the equipment being considered, a further normalisation process is incorporated to allow for variations of key parameters over the range 25% to full output power.

Two different methods are commonly used. One is based on the engine pressure ratio and the other is based on the L.P. compressor speed. Rolls Royce recommend the latter method and the equipment described followed the Rolls Royce recommendation.

In essence a series of graphs of the variation of each of the key parameters with L.P. compressor speed  $n_1$ , is used to compensate for the non linear variations of the key parameters over the range 25% to full output power. To facilitate performance comparison a set of values of L.P. compressor speed  $n_1$ , is used to represent bench marks. Performance can be checked at each of these bench marks to see if deterioration has taken place since the engine was installed.

The equipment uses a set of values of key parameters for each of the standard values of L.P. compressor speed  $n_1$ . When a reading of performance is taken, the two standard values of  $n_1$  lying immediately above and below the parameter valued at the time of measurement, are identified. The stored values of the key parameters at these standard points are then used to calculate by interpolation the variations in the key parameters which would be observed if the measurement had taken place at the nearest standard value. These variations are then added algebraically to the measured values of the key parameters corrected for Standard Day Conditions.

By this means a set of corrected data is available for the nearest standard bench mark to the actual operating condition. This set of data can be compared with the stored data for this particular standard bench mark so that a valid measure of deterioration is obtained. This method ensures that the problems of comparing 'apples with pears' which would occur if the two sets of data were compared at different operating conditions, are completely overcome.

An important practical point is that it is not necessary to try to operate the gas turbine at exactly a standard value of L.P. compressor speed  $n_1$  to obtain a valid measurement. Any operating condition will automatically be corrected to one of the standard values of  $n_1$  so that a valid comparison is made. This considerably simplifies the task of obtaining valid performance checks.

#### THE ACCURACY REQUIRED FOR THE MEASUREMENT OF KEY PARAMETERS

Because the objective of performance monitoring is to detect small amounts of deterioration, it is necessary that the repeatability of the measurement of the key parameters is high. Since some of the key parameter values measured are used to normalize other key parameters to Standard Conditions, these normalizing parameters must be measured with considerable precision.



The normalizing parameters are Absolute Inlet Pressure  $P_1$ , Absolute Inlet Temperature  $T_1$  and L.P. Compressor Speed  $n_1$ .

A complication arises in that the Absolute Inlet Pressure  $P_1$  must be corrected for the dynamic head caused by the fast air flow. To do this accurately requires the Absolute Atmospheric Pressure  $P_0$  to be measured so that the dynamic head which is a function of both  $P_0$  and  $n_1$ , can be calculated.

The equipment described monitors the performance of four gas turbines, two Tyne and two Olympus. Highly accurate pressure transducers are very expensive, so that the following method is used to obtain accurate measurements at reasonable cost. Two very accurate pressure transducers are used to measure absolute atmospheric pressure and their outputs are averaged. These transducers are separately vented to the atmosphere on the upper superstructure of the ship on the Port and Starboard sides. This provides compensation for errors caused by prevailing winds.

The Absolute Inlet Pressure  $P_1$  for each gas turbine is obtained from a set of four differential pressure transducers which are vented to the same points as the Port and Starboard atmospheric pressure transducers. The appropriate differential pressure is subtracted from the accurate atmospheric pressure reading to obtain accurate absolute inlet pressures. The span of the differential pressure transducers is approximately 60 millibars so that a 1% measurement still enables the absolute inlet pressure to be measured to better than one millibar. In this way four results accurate to 0.1% are obtained from four transducers whose accuracy is only 1%.

The inlet temperature can be measured accurately by the use of a standard platinum resistance thermometer having a resistance of 100 ohms at  $0^\circ\text{C}$  and a fundamental interval of 38.5 ohms.

The L.P. compressor speed cannot easily be measured accurately. The standard instrumentation fitted to the gas turbines consists of an A.C. tachogenerator whose output is monitored by a rectifier moving coil meter. The obstacles to accurate measurement using this technique include the temperature coefficient of the rectifier diodes and the rather indeterminate loading imposed on the tachogenerator caused by the connection of remote instrumentation.

More accurate results can be obtained by measuring the frequency or the period of the S.C. tachogenerator output. A problem with a direct measurement of frequency is that the tachogenerators are joined to the turbines such that the frequency is in the region 40 to 50 Hertz. This means that cycles of output must be counted for twenty seconds to achieve an accuracy of 0.1%. Obviously if the speed varies during the time interval the average is obtained. Two consecutive samples are needed to determine whether the L.P. compressor is accelerating or whether the speed is reasonably steady. The update time is far too long.

The usual way of overcoming this problem is to measure the period of the waveform and calculate the reciprocal to find the frequency and hence the speed. This method, whilst overcoming the low data rate problem encountered in a direct frequency measurement has the disadvantage that it is more readily upset by noise and waveform distortion.

The equipment being described uses a newer technique which has been made cost effective by the rapid developments in integrated circuits which have taken place. A phase lock loop is used to synchronise an oscillation at exactly 64 times the tachogenerator frequency. The frequency of the oscillator can then be measured accurately with a short update time. The flywheel effect of the phase lock loop time constants make the results much more immune to interference than the period measuring technique. For simplicity, a precision frequency to analogue converter is used to provide an output which is scaled by precision resistors to the parti-

cular values required by the gear reactions between the compressors and the tachogenerator. Eight standard phase lock loop modules are used in conjunction with scaling resistors contained on plug in modules. There is one type of scaling modules for a Tyne gas turbine and one for an Olympus gas turbine.

By the above technique, the compressor speeds can be measured to within 0.1% over a wide range of ambient temperature and tachogenerator loadings.

It has been shown that all the normalising parameters can be measured with the considerable provision necessary for meaningful Engine Performance Monitoring

#### INTERFACE WITH ISIS-300

Signals are obtained from the duplicate printer output terminals available in the ISIS-300 equipment. These are of the form TIME, ADDRESS and DATA. These signals are equipped with line-driving circuits so that the information can be transmitted over reasonable distances (up to 100 metres).

The first part of the interface comprises standard ISIS signal-receiving circuits. These are fast trigger circuits with high input impedance and noise immunity and are well proven on ISIS-300 peripherals. The high noise immunity is obtained by building in considerable hysteresis.

Since the output from ISIS-300 takes the form of serial pulse trains, the next requirement is for a counter or register to total the pulse count in a channel period. A further counter keeps track of the channel number by totalling the address pulses. This counter is used to select the data for the relevant group of channels.

The parallel output of this data register has added to it the decimal point position and minus sign information to produce a 16-bit word for each channel.

A microprocessor is used to control the storage and subsequent manipulation of these 16-bit words, which contain the value of each channel. Each scan is stored in the microprocessor random access memory and overwrites the readings of the previous scan. In this manner, information is continuously available.

The microprocessor is programmed to convert the parameters into standard day conditions which are similarly stored and updated, and also translates the output data into ASC 11 code character by character and adds the necessary spaces between channels. At the end of each line of channel values a carriage return/line feed command (in ASC 11) is inserted. This ensures compatibility with the chosen display unit

#### DISPLAYS

Display of data can be by means of various proprietary units, such as visual displays, tapes, printers, etc. For the application under discussion a printer is used and is arranged for compatibility with computer output interfaces such as current loop or V24. The interface is serial to reduce connections and operates on characters coded in ACS 11.

Read out parameters are in three selected modes:-

- a) Uncorrected reading as measured.
- b) Corrected reading to standard day conditions.
- c) Percentage and arithmetic difference plus or minus from baseline.

It is suggested that, to facilitate comparison from day to day, percentage differences are corrected to fixed l.p. compressor speeds. A range of say 10 fixed speeds would be used, spaced throughout the operating range and any reading would be corrected to the nearest fixed speed by linear interpolation.

#### FURTHER OUTPUTS REQUIRED FOR PERFORMANCE MONITORING

It will be recalled that one of the purposes of Performance Monitoring was to determine when maintenance was required without costly inspections which involve stripping down the gas turbine. To assist in the prediction of essential maintenance, it is necessary to keep a record of the running hours of the gas turbines. In particular the blades of the turbine are subjected to strong centrifugal force whilst being at the same time subjected to high temperatures. Under these arduous conditions, the blades gradually stretch or creep until they are in danger of touching the fixed casing of the gas turbine. When this happens, they must be replaced before actual contact and ensuing damage takes place.

This blade creep is a function of turbine speed, gas temperature and time. Generally the turbine speed and gas temperature are related and it is sufficient to monitor gas temperature and time. The power turbine entry temperature  $T_6$  is monitored and is divided into a number of bands. The running hours in each temperature band are logged. A life factor for each temperature band which experience has shown to be appropriate, is used to multiply the actual running hours to produce a figure of equivalent running hours. In addition, an allowance of half an equivalent running hour is added for each time the gas turbine is started. By the means, a total of hours of effective use is obtained which enables maintenance to be properly scheduled.

The actual running hours in each temperature band are logged so that a check can be made on the appropriateness of the life factors used.

Metalurgists of gas turbine manufacturers are continually researching new improved alloys for the manufacture of turbine blades. Whenever new materials are introduced adjustment to the life factors will probably be necessary. At first the life factors will be based on rather scant data but gradually sufficient hours of operation will have accrued to enable more precise life factors to be calculated.

The logging of actual running hours in each temperature band provide the vital feedback to the manufacturer to enable him to correct his estimates of engine life and thus safely lengthen the intervals between overhauls.

#### REFERENCES

- (1) Paper given by Capt. P. van Staalduinen, Royal Netherlands Navy to Gas Turbine Conference and Products Show, Philadelphia - March 1977
- (2) Paper by Robert J.C. Harris and Peter T.C. Wilkinson, Ship Control Symposium - Bath 1972

## DEVELOPMENTS IN MARINE GAS TURBINE CONDITION MONITORING SYSTEMS

by Floyd Foltz, Jr.  
Hamilton Test Systems, Inc.  
United Technologies

### ABSTRACT

Developments have been made in systems that determine the performance and health of gas turbine propulsion systems. The primary objective of the Condition Monitoring System (CMS) is "On-Condition" maintenance: diagnosing maintenance requirements that may be eminent, and determining how much more running time is available before the maintenance should be performed.

Computer data processing, data storage methods, data compression, analysis techniques, and man-machine interfaces are reviewed.

Also discussed is how sensor errors can be detected and not interpreted as turbine degradation.

The increased availability of reliable, computer-compatible Automatic Spectral Analysis equipment and its effects upon gas turbine diagnostics is considered.

The paper concludes with a consideration that the CMS is ready for integration with a marine gas turbine station control system.

### CMS DESIGN CONSIDERATIONS

#### "On-Condition" Maintenance

The purpose of the CMS is to permit shipboard "On-Condition" gas turbine maintenance; gas turbine maintenance planned according to actual need rather than a pre-determined calendar schedule.

The "On-Condition" maintenance concept has significant advantages: early detection of impending gas turbine faults, prediction of "running time allowed" before the problem is serious enough to require gas turbine shutdown, prevention of forced shutdowns, improved operational readiness, maintenance actions performed only in the appropriate section of the gas turbine, and reduced maintenance costs.

#### Operator Interface

The most important CMS design guideline is consideration of the shipboard operator. Since the CMS is a powerful analytic tool, there can be a tendency to forget the importance of human engineering for the shipboard operator's role; the analytic capability of the CMS is then overstressed with complex operational procedures and lengthy data reports.

The CMS must be designed for simple operation. Its messages must direct the operator to specific operational or maintenance actions. He should not be burdened with lengthy start-up or re-load procedures, nor should he be required to interpret data or perform off-line calculations from lengthy data reports. He must be made to feel "part-of-the-system", and trained to continually understand the relative health of his gas turbines.

## Background

The CMS discussed in this paper is based primarily upon the FT9 Marine Engine Program, a current NAVSEA Research and Development Program conducted by Pratt & Whitney Aircraft (P&WA) Group of United Technologies for developing a 30-40,000 horsepower gas turbine and related systems.

Hamilton Standard Division (HSD) of United Technologies is responsible for the design and fabrication of the FT9 CMS. HSD has also designed Diagnostic and Condition Monitor Systems for Airborne and Commercial ground-based gas turbines.

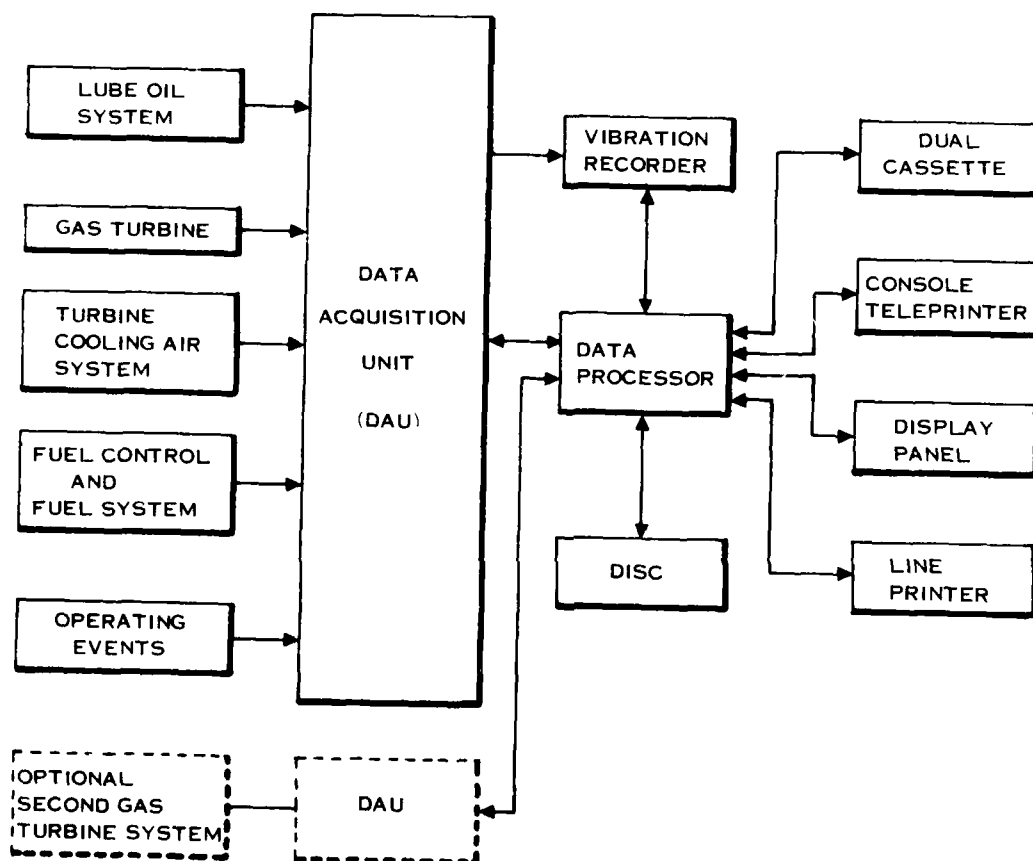
In defining the initial FT9 program requirements, NAVSEA recognized the need to make the "On-Condition" maintenance philosophy a part of the procurement specifications. As a result, all major gas turbine components are modular, and field replaceable. CMS requirements were also considered. Sensors dedicated to the CMS were included in the design of the turbine to expand the diagnostic capabilities of the CMS beyond what was available in other gas turbine types.

The comprehensive data base available in the CMS led to many optional software programs to provide the turbine performance engineers with on-line, realtime performance calculations during gas turbine endurance tests.

## CMS CONFIGURATION

### Block Diagram

A block diagram of the CMS is shown in Figure 1. The CMS is a complete diagnostic system; in addition to the gas turbine, it also monitors: the cooling air system; lubrication oil system; the fuel conditioning and fuel control system; ambient operating pressure, temperature, and humidity; and operating condition events.



H8-343

FIGURE 1 CMS BLOCK DIAGRAM

## Sensors

With the exception of the turbine gas path pressure sensors, all sensors are state-of-the-art, and chosen for their reliability.

Pressure Sensors - The gas path pressure transducers are a critical part of the turbine fault analysis and must be accurate and repeatable since minor variations in pressure can be indicative of impending changes in turbine health. The CMS uses vibrating cylinder pressure transducers manufactured by Hamilton Standard. These transducer types are used in applications requiring high accuracy and repeatability.

The sensing element of the pressure sensor consists of two concentric, closed-end cylinders--a vibrating inner one and a protective outer one. These cylinders are joined together at one end by an electron beam weld, and they are free at the other end. A reference vacuum is automatically created between the cylinder walls during the welding operation. This assembly is referenced in Figure 2 as the "pressure chamber".

Extending from the sensor base is a magnetic structure referenced in Figure 2 as the "spoolbody assembly". This supports the electromagnetic coil and pole-pieces that magnetically excite the thin-walled inner cylinder of the pressure chamber assembly. Also included is the pick-off coil for the detection of cylinder vibratory amplitude and frequency. The open end (welded end) of the pressure chamber assembly is physically assembled over the magnetic structure and firmly clamped to the spoolbody base which is drilled and ported so that the gas, whose pressure is to be measured, will find its way into the annular cavity between the vibrating inner cylinder and the spoolbody assembly. (Reference Figure 2)

When a pneumatic pressure is introduced into the annular cavity between the spoolbody and the vibrating cylinder, the wall elements of the cylinder are tensioned by the pressure forces attempting to elongate the cylinder and increase its circumference. This causes the cylinder natural frequency to increase. The pick-off coil detects the cylinder vibratory motion and frequency and instantly relays this information to the sensor amplifier-limiter combination. This new, increased frequency is then fed back to the drive coil so as to produce a reinforcing magnetic force pulse at the proper frequency. The sensor output is a frequency signal that is a function of the input pressure.

The frequency output signal is a function of the vibrating cylinder material itself, and the pressure and temperature of the environment surrounding the vibrating cylinder.

The material of the cylinder is the key to the transducers basic stability; frequency and temperature outputs are processed to determine the correct pressure input. The CMS processor stores the coefficients of the pressure versus frequency and temperature equations to provide accuracies in the order of  $\pm 0.01\%$  through computer sensor compensation techniques.

Sensor compensation centers around the calibration of the sensor non-linear output and adjustment of the output for density/temperature effects so as to achieve the required high accuracy. Because of the latter effects, an analog temperature sensor was designed into the spoolbody assembly to monitor sensor (and, therefore, internal gas) temperature.

The sensor compensation is rather long and involved, and it requires the closed solution of polynomial equations and a linear interpolation. An exact solution could be obtained by solving all pressure equations and curve fitting the resulting pressure points with respect to temperature. Fortunately, the effect of temperature on gas density and sensor frequency is fairly linear, so the use of a more complex

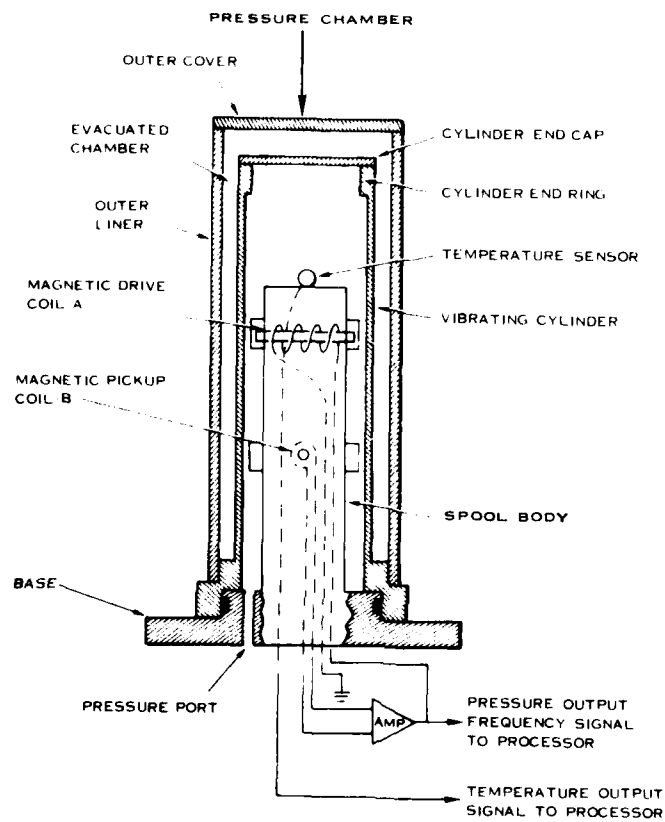


FIGURE 2 VIBRATING CYLINDER PRESSURE TRANSDUCER



compensation method was unwarranted.

#### Data Acquisition Unit

The Data Acquisition Unit (DAU) can sample 256 parameters per second. Each parameter is sampled 1 to 8 times per second depending upon its importance. Accurate data is a must for proper fault analysis; the DAU calibrates every channel each second to determine any changes from nominal of the channel gain and offset. If any changes occur, the data value passed through the channel is then adjusted accordingly.

All data is formatted in either a 12 or 16 bit word, depending upon parameter accuracy requirements.

#### Data Processor

The Data Processor is the AN/UYK-20(V), with 64K words of memory, using CMS-2M language and all associated software peripherals. The processor is configured to process data from an optional, second gas turbine.

#### Disc

The Singer militarized CL107B disc, with a 16 million bit capacity, uses a rotating disc memory constructed in a hermetically sealed enclosure. The disc is classified as a high reliability system and does not require any preventative maintenance.

#### Vibration Recorder

The Data Processor initiates the operation of the analog vibration recorder if the gas turbine vibration exceeds certain levels. A manual mode is also provided.

#### Console Teleprinter

A militarized Kleinschmidt model 7302 teleprinter is the device used by the operator to communicate with the CMS. All automatic messages are outputted on the teleprinter.

#### Display Panel

The Operator Display Panel provides engineering unit display and updates of any CMS parameter requested by the operator. The panel also includes 6 meters for analog readout of gas turbine vibration levels.

#### Dual Cassette

The Dual Cassette is used to initially load the CMS Software programs. Data can also be manually or automatically placed on cassette by the Processor for turbine history information.

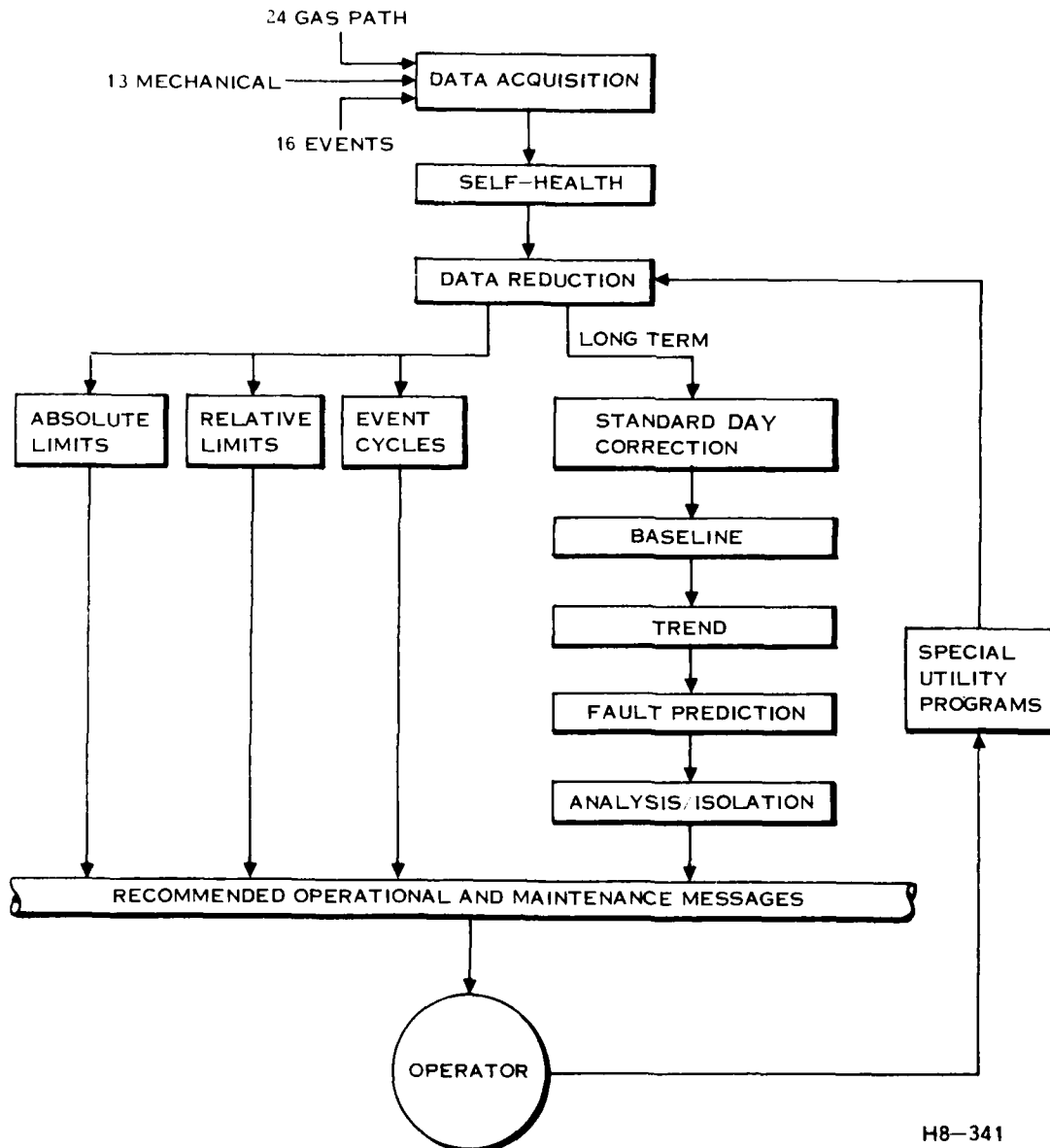
#### Line Printer

During the development tests, the line printer is used for data dumps and gas turbine performance calculations; it is not necessary for shipboard application.

### FUNCTIONAL DESCRIPTION

Many different software programs are needed to convert the raw data obtained from the gas turbine into correct operational and maintenance messages.

Figure 3 is a simplified flow diagram of the major functional elements of the CMS software. The following sections will explain the role of each of the functional elements.



H8-341

FIGURE 3 CMS FLOW DIAGRAM

The root square locus technique<sup>7</sup> is used to select an appropriate value for  $\xi$ . For each possible value of  $\xi$ , there exists a corresponding optimal feedback gain matrix  $G^*$ , and a closed loop system matrix  $A_{CL}$  which specifies the closed loop dynamics according to

$$\dot{x} = A_{CL}x \quad (12)$$

where, from equations (3) and (7),

$$A_{CL} = A - BG^* \quad (13)$$

One may therefore gain an impression of the behaviour of the closed loop system by examining the locus of eigenvalues of  $A_{CL}$  as  $\xi$  is varied. The movement of the roll, sway and yaw eigenvalues as a function of  $\xi$  is depicted in Fig. 3. For  $\xi \ll 1$ , the open and closed loop eigenvalues coincide, except for the unstable eigenvalue which is reflected about the imaginary axis. As  $\xi$  increases, the closed loop eigenvalues move further into the left half plane because the feedback gains become larger. Since the roll mode shows a tendency to become less stable as  $\xi$  increases, one should not choose  $\xi$  too large. For  $\xi = 0.001$ , the roll mode is well damped, indicating that this is a good value to choose. The corresponding feedback gain matrix  $G^*$  is presented in Table II, along with the closed loop eigenvalues. Unfortunately, one of these eigenvalues is very small, so that this mode will dominate the transient response after a few seconds, resulting in a sluggish response. This can be counteracted by modifying  $G^*$  or by weighting roll angle more heavily in the performance index. Either approach results in a slight departure from the desired optimality criterion. After a sensitivity study of the effect of each feedback gain, it was decided to increase the roll angle to rudder feedback gain  $g_{23}$  by twenty percent. The resulting closed loop eigenvalues of this modified optimal controller are presented in Table II. The smallest eigenvalue has become much more negative and coupled with the next smallest eigenvalue. The other eigenvalues are practically unchanged, suggesting that the performance of the modified optimal controller is very close to optimal.

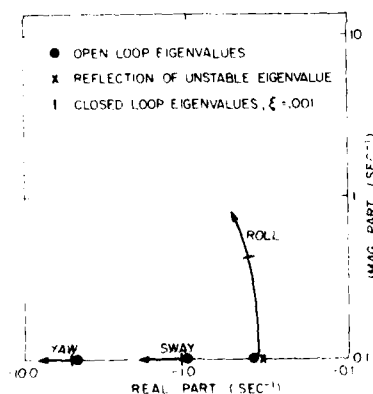


Figure 3. Closed Loop Eigenvalues as a Function of  $\xi$

The specification which is to be met is the following:

"In a beam sea, with a significant wave height of 10.0 ft., the lateral acceleration experienced in the wheelhouse must be less than 0.05g rms at a speed of 50 kt. This criterion must be achieved without foil cavitation and without placing excessive demands on the hydraulic system."

The control system designer must determine J so as to satisfy this specification. Obviously, J must include a term which represents the wheelhouse lateral acceleration  $a_{wh}$ , where

$$a_{wh} = a_{cm} + x_s \ddot{r} - z_s \ddot{p} \quad (8)$$

and the lateral acceleration at the centre of mass is

$$a_{cm} = \ddot{v} + U r + g \phi \quad (9)$$

If  $\dot{v}$ ,  $\dot{r}$  and  $\dot{p}$  are expressed in terms of the state variables using equation (3), then  $a_{wh}^2$  may be written as

$$a_{wh}^2 = x' Q x \quad (10)$$

and therefore the minimization of J will tend to minimize the mean square value of  $a_{wh}$ .

In the absence of cavitation, stall or ventilation, any level of stabilization or ride quality can be achieved if sufficient hydraulic power is available. Unfortunately, hydraulic power is limited, and it is required for longitudinal control and maneuvering as well as lateral control. Therefore a tradeoff is necessary between the ride quality and the hydraulic power consumption. This is reflected in the performance index by including the  $u'Ru$  term.

From Reference 6, the hydraulic power is proportional to the rms control surface rates:

$$\text{Power} = (\dot{\delta}_A)_{\text{rms}} + \kappa (\dot{\delta}_R)_{\text{rms}}$$

where the weighting factor  $\kappa$  is taken as unity for this example. Since a rate command controller has been assumed, it is valid, if the actuator dynamics are fast enough, to approximate the hydraulic power by using  $\dot{\delta}_{AC}$  and  $\dot{\delta}_{RC}$  in place of  $\dot{\delta}_A$  and  $\dot{\delta}_R$  in the above expression, so that  $u'Ru$  represents the mean square hydraulic power required by the control system. Finally, in order to trade off ride quality and hydraulic power consumption, a weighting factor  $\xi$  is included in the performance index. Consequently, the performance index used in this application is

$$J = \frac{1}{2} \int_0^\infty [ \xi a_{wh}^2 + (\dot{\delta}_{AC}^2 + \dot{\delta}_{RC}^2) ] dt, \quad \xi > 0 \quad (11)$$

It remains only to specify  $\xi$  before  $G^*$  can be determined.

vergence associated with the roll mode. Therefore an automatic control system is mandatory for foilborne operation.

## CONTROL SYSTEM DESIGN AND SIMULATION

### Derivation of the Optimal Control Law

Given the state equation (3), it is up to the designer to derive a control law which achieves the desired levels of closed loop stability and performance. The use of modern control theory guarantees that for small perturbations about the reference condition at constant speed in a calm sea, the closed loop system will be stable. In addition, one may address the performance specifications directly by choosing feedback gains which are optimal in some well-defined sense. The optimal feedback gains will be those which minimize the value of the quadratic performance index

$$J = \frac{1}{2} \int_0^{\infty} [x'Qx + u'Ru]dt \quad (6)$$

For the problem under consideration, the use of this performance index yields a constant gain control law which is a linear combination of the states; i.e.,

$$u = -G^*x \quad (7)$$

where the optimal feedback gain matrix  $G^*$  is constant. Fig. 2 is a block diagram of the resulting closed loop system. The existence and uniqueness of  $G^*$  are guaranteed by the theory under certain restrictions on the state weighting matrix  $Q$  and the input weighting matrix  $R$ . These restrictions are satisfied in the present application. The details of the theory may be found in References 3 and 4. Computer programs are presented in Reference 5 for determining  $G^*$  once  $Q$  and  $R$  are specified by the control system designer. Note that if the feedback gains vary significantly with ship speed, several  $G^*$  matrices will have to be stored in an on-board computer.

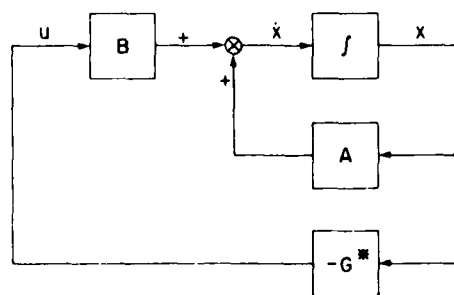


Figure 2. Closed Loop Block Diagram

$$\begin{aligned}
\text{yaw: } & N_v \dot{v} + N_v v + (N_p^* - I_{xz}) \dot{p} + N_p p + N_{\dot{\phi}} \dot{\phi} + (N_r^* + I_{zz}) \dot{r} \\
& + N_r r + N_{\delta_R}^{\ddot{}} \ddot{\delta}_R + N_{\delta_R}^{\dot{}} \dot{\delta}_R + N_{\delta_R} \delta_R + N_{\delta_A}^{\ddot{}} \ddot{\delta}_A + N_{\delta_A}^{\dot{}} \dot{\delta}_A + N_{\delta_A} \delta_A = 0
\end{aligned}
\tag{2c}$$

The coefficients  $Y_i$ ,  $K_i$  and  $N_i$ , called stability derivatives, are derived in Appendix A. These linearized equations give results accurate enough for engineering purposes over a surprisingly wide range of applications, including stability and control response. However, they are not valid when cavitation or ventilation effects are significant.

In order to utilize modern control theory, it is necessary to reformulate equations (2a-c) as a first order matrix differential equation, known as the state equation:

$$\dot{x} = Ax + Bu \tag{3}$$

The system matrix  $A$  and input matrix  $B$  are constant. The stability of small perturbations about the reference condition is indicated by the eigenvalues of  $A$ . The elements of  $x$  are the system states and the elements of  $u$  are the control inputs. These vectors are taken to be

$$x = [v \ p \ \phi \ r \ \delta_A \ \delta_R \ \dot{\delta}_A \ \dot{\delta}_R] \tag{4a}$$

$$u = [\dot{\delta}_{AC} \ \dot{\delta}_{RC}] \tag{4b}$$

The inputs are the commanded aileron rate  $\dot{\delta}_{AC}$  and the commanded rudder rate  $\dot{\delta}_{RC}$ . The use of a rate command control system, rather than position command, simplifies the formulation of the control problem because the control surface rates can be related to the hydraulic power required by the control system. The actual aileron and rudder rates are related to the commanded rates by

$$\tau_A \dot{\delta}_A + \delta_A = \dot{\delta}_{AC} \tag{5a}$$

$$\tau_R \dot{\delta}_R + \delta_R = \dot{\delta}_{RC} \tag{5b}$$

That is, the aileron and rudder actuator dynamics are modelled as first order lags of time constants  $\tau_A$  sec. and  $\tau_R$  sec. respectively.

A particular hydrofoil ship is now chosen for the purpose of presenting a design example. The leading particulars are presented in Table I. The assumed speed is 50 kt. This ship is purely hypothetical, and does not correspond to any current vehicle. The resulting numerical values of the  $A$  and  $B$  matrices are given in Table II, along with the eigenvalues of  $A$ . The single positive eigenvalue is indicative of a di-

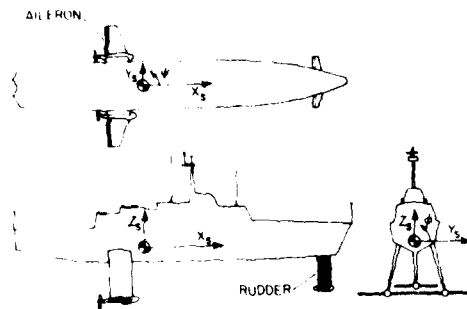


Figure 1. Axis System

$$\text{sway: } m(\dot{v} + Ur + g\phi) = Y \quad (1a)$$

$$\text{roll: } I_{xx}\dot{p} - I_{xz}\dot{r} = K \quad (1b)$$

$$\text{yaw: } I_{zz}\dot{r} - I_{xz}\dot{p} = N \quad (1c)$$

where the side force  $Y$  and moments  $K$  and  $N$  are functions of the sway velocity  $v$ , roll rate  $p$ , roll angle  $\phi$ , yaw rate  $r$ , aileron deflection  $\delta_A$ , rudder deflection  $\delta_R$  and their time derivatives. By expanding  $Y$ ,  $K$  and  $N$  in Taylor series and deleting all terms higher than first order, the linearized equations of motion are obtained:

$$\begin{aligned} \text{sway: } & (m + Y_v)\dot{v} + Y_v v + Y_p\dot{p} + Y_p p + (Y_\phi + mg)\phi + Y_r\dot{r} \\ & + (Y_r + mU)r + Y_{\delta_R}\ddot{\delta}_R + Y_{\delta_R}\dot{\delta}_R + Y_{\delta_R}\delta_R \\ & + Y_{\delta_A}\ddot{\delta}_A + Y_{\delta_A}\dot{\delta}_A + Y_{\delta_A}\delta_A = 0 \end{aligned} \quad (2a)$$

$$\begin{aligned} \text{roll: } & K_v\dot{v} + K_v v + (K_p + I_{xx})\dot{p} + K_p p + K_\phi\phi + (K_r - I_{xz})\dot{r} \\ & + K_r r + K_{\delta_R}\ddot{\delta}_R + K_{\delta_R}\dot{\delta}_R + K_{\delta_R}\delta_R + K_{\delta_A}\ddot{\delta}_A + K_{\delta_A}\dot{\delta}_A + K_{\delta_A}\delta_A = 0 \end{aligned} \quad (2b)$$

marine vehicles. Automatic control for motion stabilization and acceptable ride quality is a particularly important technology for hydrofoil ships with fully submerged foil systems. These vehicles are inherently dynamically unstable and must often operate in an adverse seaway environment.

A mathematical model of hydrofoil ship lateral dynamics is developed below. The purpose of this paper is to employ the model in the design of a lateral control system for a conceptual hydrofoil ship and to simulate the resulting closed loop system in a seaway. The performance objectives of satisfactory ride quality and minimal hydraulic power consumption may be expressed mathematically in a performance index, and consequently the optimal control law may be most easily derived using modern control theory.

The question of optimality arises in all engineering design problems. In the realm of modern control theory, optimality is precisely defined by a mathematical formulation known as the performance index. It is very important for the designer to select an appropriate performance index for his problem. If this is done, the control system can be expected to provide the best compromise over all possible variations of the design parameters. However, for some variations in parameters, so-called suboptimal controllers may actually provide better performance. It is important, therefore, to simulate the closed loop system for a number of parameter variations during the design phase.

Hsu<sup>1</sup> has applied modern control theory to the design of a controller for hydrofoil longitudinal dynamics. His performance index incorporates vertical acceleration, as a function of frequency, and hydraulic power. A number of iterations are necessary to adjust the many weighting factors in the performance index. In the present work, only one weighting factor is used, and it can be determined easily.

Because control laws derived using modern control theory employ many feedbacks, they may not be practical. This leads naturally to the consideration of a suboptimal controller which employs fewer feedbacks. As a final step, the analysis is extended to include the effect of uncertainty in the sensor measurements, and a Kalman filter is designed to generate the estimates of the state variables required by the control system.

#### THE MATHEMATICAL MODEL

It is assumed that the foil system is a canard arrangement with the main foil, an inverted 'n', aft of the centre of mass. The bow foil is an inverted 'T'. This configuration is displayed in Fig. 1, together with the associated axis system. The axes used in this analysis are stability axes<sup>2</sup>, with the  $x_s$  axis initially aligned with the ship velocity vector. Thereafter, the axes move with the ship during a disturbance. The ship is considered to be in the foilborne mode at all times.

The control surfaces are also shown in Fig. 1. The rudder is the all-moving bow strut, and the ailerons are the portions of the main foil flap which are outboard of the struts.

Given only small perturbations about the reference condition of rectilinear motion at constant speed, the longitudinal and lateral equations of motion decouple. The lateral equations may then be written as follows:



$x$	state vector
$x_s$	x coordinate
$y$	output vector
$y_s$	y coordinate
$z$	measurement vector
$z_s$	z coordinate
$E$	plant noise covariance matrix
$\Sigma$	summation
$Q$	sensor noise covariance matrix
$\phi$	roll angle
$\psi$	heading angle
$\rho$	density of sea water
$\delta$	control surface deflection
$\tau$	time constant
$\xi$	weighting factor in J
$\omega$	natural frequency
$\gamma$	white plant noise
$\theta$	white sensor noise
$\eta$	wave height
$( )_1$	refers to seaway model
$(\dot{\phantom{a}})$	first time derivative
$(\ddot{\phantom{a}})$	second time derivative
$( )_A$	pertaining to the ailerons
$( )_R$	pertaining to the rudder
$( )'$	matrix transpose
$( )_C$	commanded variable
$( )^*$	optimal matrix
$(\hat{\phantom{a}})$	estimated value

#### INTRODUCTION

The Defence Research Establishment Atlantic (DREA) is engaged in research in control systems for conventional naval ships and advanced

$N_W$	yawing moment applied by the seaway
$N_\beta$	$\partial N / \partial \beta$ , where $\beta$ is any state variable
$P$	state covariance matrix
$Q$	state weighting matrix
$R$	input weighting matrix
$S$	foil or strut area
$S_e$	Sears function
$S_{KK}$	power spectral density of roll moment
$S_{WW}$	power spectral density of wave orbital velocity
$S_{YY}$	power spectral density of side force
$S_{\eta\eta}$	power spectral density of wave height
$U$	ship speed
$W$	wave orbital velocity
$Y$	side force
$Y_W$	side force applied by the seaway
$Y_\beta$	$\partial Y / \partial \beta$ , where $\beta$ is any state variable
$a_{wh}$	lateral acceleration at the wheelhouse
$a_{cm}$	lateral acceleration at the centre of mass
$c$	chord length
$g$	acceleration due to gravity
$g_{ij}$	the $(i,j)$ th element of $G$
$h$	foil operating depth
$j$	square root of $-1$
$k$	wave number
$m$	ship mass
$p$	roll rate
$r$	yaw rate
$t$	time
$u$	input vector
$v$	sway velocity

## OPTIMAL CONTROL OF HYDROFOIL SHIP LATERAL DYNAMICS

by P. H. Whyte

### ABSTRACT

A linear mathematical model of the lateral dynamics of a foilborne vessel equipped with a fully submerged hydrofoil system is developed. As such a vessel is inherently dynamically unstable it requires an automatic control system to provide motion stabilization. Using the techniques of modern control theory, an optimal controller is designed for a hypothetical ship moving through beam seas at a speed of 50 knots. The performance index used in this application is a functional of both the lateral acceleration experienced in the wheelhouse and the hydraulic power required by the actuators.

Because of the large number of feedbacks required, an optimal controller may not be practical. This leads to the consideration of an adequate suboptimal controller which employs a reduced number of feedbacks. The performance of the final design is evaluated in beam seas using a time domain simulation. As a final step, the analysis is extended to include the effect of uncertainty in the sensor measurements, and a Kalman filter is designed to generate the estimates of the state variables required by the control system.

### NOTATION

A	system matrix
$A_{CL}$	closed loop system matrix
B	input matrix
C	output matrix
$C_{L1}$	lift coefficient
G	feedback gain matrix
H	Kalman filter gain matrix
$I_{ij}$	moment or product of inertia
J	performance index
K	rolling moment
$K_w$	rolling moment applied by the seaway
$K_\beta$	$\delta K / \delta \beta$ , where $\beta$ is any state variable
L	plant noise gain matrix
N	yawing moment

### EXPERIENCE-TO-DATE

The FT9 CMS has over 1000 hours of operation with gas turbines in the present program. P&WA's documented conclusions indicate that the unit is easy to operate, is a help rather than a burden to engine operating personnel, and provides data accuracies comparable to a typically high accuracy test stand data system. The overall system will make "on-condition" maintenance a reality for Navy gas turbine powered ships.

Hamilton Standard's experiences with airborne gas turbines and industrial gas turbines also indicate that the techniques used for fault analysis and prognostication are conclusive<sup>2</sup>. The sensor correction technique has also been verified in data taken from over 200 gas turbines.

### THE FUTURE

Gas Turbine Condition Monitoring Systems are finally gaining the confidence of gas turbine operators. The fears of poor sensor reliability, doubts about analytic techniques, and concerns for loss of man-in-the-loop functions are gradually being overcome. The passive role that the CMS has played in the operation, maintenance and performance of gas turbine engines in the past will change. The next function for the CMS to incorporate is to utilize the information in gas turbine Station Control Systems.

The CMS programs outlined in this paper complement the requirements of the Control System--together they will provide the technology for a system that would meet the goals of improved readiness, efficient fuel consumption, and low maintainability costs.

### References

- (1) ASME 74-GT-62, 1974, "Parameter Selection for Multiple Fault Diagnostics of Gas Turbine Engines" by Louis A. Urban, Hamilton Standard Division
- (2) Sven-Goran Danielsson. Scandinavian Airlines "Gas Path Analysis applied to Pre and Post Overhaul Testing of JT9D Turbofan Engine" Society of Automotive Engineers, Inc. 770993, 1977

Prognosis is now performed by linear extrapolation of the actual points in the history file to some pre-selected time in the future, usually 10-30 days.

The diagnosis and fault isolation, highly simplified in Figure 4, is then performed using each of the performance parameter values determined via the Influence Coefficient Matrix, and results in maintenance message to the operator.

The importance of the number of gas path sensors incorporated in the design of the gas turbine is also illustrated by the Influence Coefficient Matrix. The larger the number of parameters that can be measured, the larger the number of performance parameters that can be deduced, the finer the degree of isolation to the problem within the gas turbine.

Sensor Correction Technique - Gross sensor failures can be detected by self-health programs. These are generally high/low range checks. Sensor non-repeatability, or drift, that is in the order of one or two percent can falsely be interpreted as gas turbine performance degradation if not properly handled. To evaluate the effects of this sensor non-repeatability, the Gas Path Analysis program also uses a technique where measured parameters are passed through a Sensor Integrity Matrix, whose coefficients are derived from the coefficients used in the Gas Path Analysis Influence Coefficient Matrix. Thus performance parameters are calculated using only that portion of the measured parameter which is judged to be attributed to changes in gas turbine performance.

Vibration - The CMS utilizes vibration information in determining maintenance decisions. Typically, vibration information is passed through 2 or 3 band pass filters to provide a degree of selectivity on the frequency content of the measured vibration signal. It is expected that recent improvements in Spectral Analysis equipment with computer compatible output formats will greatly improve the information available to the gas turbine performance engineer. Spectral lines can be stored, and compared in real-time for evaluating changes in the amplitude of each frequency line. Hamilton Standard is presently using this technique in a heavy industrial machine diagnostic application.

Utility Programs - Various utility programs are available to the operator. During development and turbine endurance tests, additional utility programs for the turbine engineer are also available. Examples of the programs are:

- Data dumps to either printer or cassette
- Total data frame printout
- Lock-out of any software program
- Complete Turbine Performance Reports
- Files and logs dumps to printer
- Manual input for changing fuel type
- Display of any parameter
- Continual printout of any parameter(s)
- Automatic program "on-line" after power outage
- Operator comments to event logs

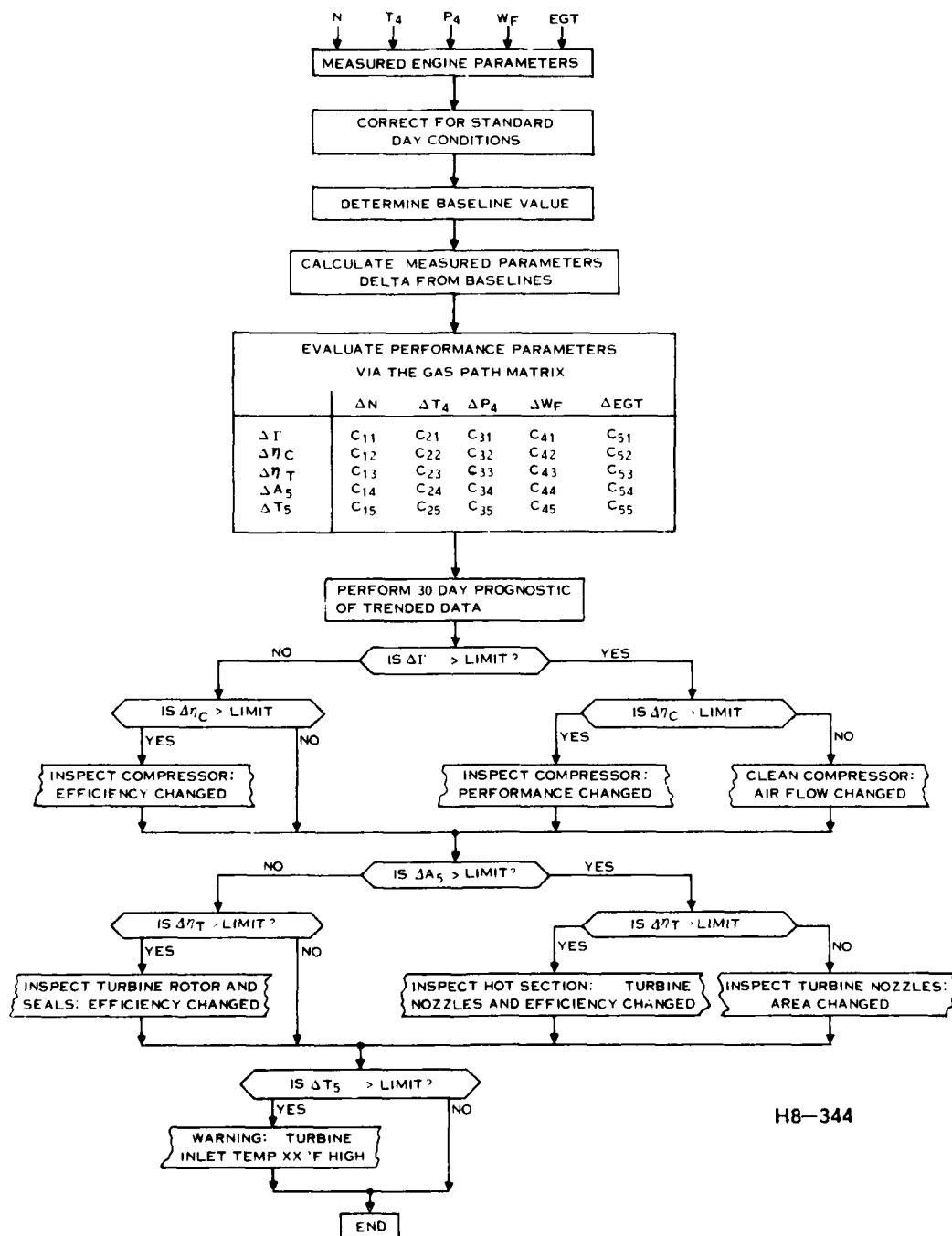


FIGURE 4 SIMPLIFIED GAS PATH ANALYSIS FLOW DIAGRAM

### Gas Turbine Analysis - Steady State

Steady-state analysis of gas turbine performance requires a high degree of sophistication to allow fault prediction and isolation of the correct problem. To correctly identify faults, the CMS must be capable of determining the values of gas path performance parameters which cannot be measured directly (efficiencies of all turbine stages, air flow, effective nozzle area, degree of compressor fouling, turbine inlet temperature). The CMS must determine these non-measurable performance parameters from parameters that can be measured--pressures, temperatures, speeds, fuel flow.

This section describes some of the programs that are required for steady-state analysis of the gas turbine.

Standard Day Corrections - Since the steady-state analysis is based upon comparing changes to an initial condition, the CMS, by sensing the ambient air temperature and pressure, converts all turbine data to static conditions on a standard day at sea level.

Baseline - The CMS automatically records and stores the initial baseline characteristics of the gas turbine. It is from this baseline that all subsequent changes are measured. The CMS also can adjust the baseline to account for changes due to subsequent maintenance actions.

Gas Path Analysis and Fault Isolation - The key to correct fault prognosis and fault isolation is the Gas Path Analysis Program.

Various programs are in use, each of which varies in approach and complexity. The program chosen as a descriptive example is the Gas Path Analysis by Influence Coefficient Matrix<sup>1</sup> and described in Figure 4. It is used by Hamilton Standard for both airborne and ground based gas turbines.

The measured gas turbine parameters, after correction for standard day, are compared to their baseline value to determine the change in the measured parameter. Each of the non-measurable performance parameters is now calculated via the Gas Path Influence Coefficients for the particular set of measurable parameters.

For example, the change in compressor efficiency is:

$$\Delta\eta_c = C_{12}\Delta N + C_{22}\Delta T_4 + C_{32}\Delta P_4 + C_{42}\Delta W_f + C_{52}\Delta EGT$$

This calculation is performed typically every half hour, and all values of the non-measurable performance data are stored in the disc history files, and used for diagnostics and prognostics. ( $C_{12}$ ,  $C_{22}$ , etc. are constants derived from the gas turbine thermodynamic equations).

### Self-Health

A Self-Health program is mandatory for preventing unnecessary "false-alarms" from defeating the purpose of the CMS. The multiplexer, gain conditioning, and A/D circuits within the Data Acquisition Unit are self-calibrating with each data sample. Sensor values are not only checked for open and short circuit values, but cross-checked with other gas turbine parameters through complementary logic.

A software "data point editor" edits any data point whose value departs rather drastically from the value of the preceding sample. Since it is not known if the new data point when sampled, is valid or not, the data point editor acts as a first-order digital lag circuit. It effectively smooths the parameters value until the next data sample can be examined. If the value repeats, and appears authentic, the editor allows the data point to "lag" up to its correct value.

### Data Reduction

The gas turbine has varied operational characteristics with many different steady-state operational points. To satisfy analysis requirements for all conditions, the data is presented in three basic forms.

The prime data sampling rate for each parameter is 1 to 8 times per second depending upon its criticality. This data, once approved by the self-health checks, is passed directly to certain software programs that are used for instant analysis of gas turbine conditions.

For software programs that are used to analyze short-term changes in gas turbine performance, the data is averaged for 30 seconds, every two minutes.

For software programs that are used to analyze long-term trends in performance, only the 30 second average data representing the most stable gas turbine condition within the last 30 minutes is used.

### Gas Turbine Analysis - Transient/Cycles

There are three major programs that are used to evaluate the gas turbine performance in the transient and repetitive cycle condition.

Absolute Limits - This program notifies the operator of any condition requiring immediate operational corrective action due to exceedance of a prime gas turbine parameter's absolute limit, such as an over-speed condition, an over-temperature condition.

The program will also notify the operator of maximum values obtained, the duration of the over-limit condition, and any recommended maintenance actions, if the condition was severe.

Relative Limits - There are gas turbine operating conditions where a parameter is not exceeding its absolute limit, but may exceed a relative limit set for that particular operating condition, and the operator should be notified. For example, if the Vane Angle value for a given power setting exceeds its Relative Limit, the operator will be notified of the value of exceedance and the recommended maintenance action.

Event Cycles - Event cycles are recorded and programmed to predict faults. For example, if the number of chips in the oil exceeds a predetermined count, or if the gas turbine has been operating in a manner that causes the low cycle fatigue count to become excessive, the operator will be notified of the event and the corrective maintenance action.



The fact that the optimal control law required modification does not negate the value of the approach. In practice, considerable modification, or 'tuning', would be required during implementation anyway. The final modified optimal controller is derived very quickly by executing two short computer programs. If classical design techniques had been used for this complex multi-variable system, the design would have taken much longer. Furthermore, there is no guarantee that the classically-designed controller is optimal or even near-optimal in any sense.

#### Selection of a Practical Suboptimal Control Law

There are sixteen feedback gains in the optimal control law. For reasons of simplicity and reliability, it is desirable to reduce this number, so long as the resulting controller will perform in a near-optimal manner. A practical suboptimal controller is therefore sought. The procedure to realize this controller is not unique, and a number of good suboptimal designs can probably be found. For this application, the suboptimal controller is derived from the optimal controller in the following manner:

- (i) Set  $g_{11} = 0$  (no  $v$  feedback to ailerons)
- (ii) Set  $g_{18} = g_{27} = 0$  (no cross coupling between control surface rates)
- (iii) Set  $g_{16} = g_{25} = 0$  (no cross coupling between control surface deflections)
- (iv) Assume that the actuator dynamics are fast enough so that  $\dot{\delta}_{AC} = \dot{\delta}_A$  and  $\dot{\delta}_{RC} = \dot{\delta}_R$ . Then the control laws may be written as

$$(1 + g_{17})\dot{\delta}_{AC} = -g_{12}p - g_{13}\phi - g_{14}r - g_{15}\delta_A \quad (14a)$$

$$(1 + g_{28})\dot{\delta}_{RC} = -g_{21}v - g_{22}p - g_{23}\phi - g_{24}r - g_{26}\delta_R \quad (14b)$$

and solved for  $\dot{\delta}_{AC}$  and  $\dot{\delta}_{RC}$ . The resulting suboptimal control law is given in Table II as matrix  $G$ . Seven of the original sixteen feedbacks have been eliminated.

As an initial check on the performance of the suboptimal controller, the transient response to an initial roll angle is computed for calm seas. This simulation is useful to verify that the control system gives a smooth, stable response without excessive control surface deflections. The roll, yaw, aileron and rudder time histories are displayed in Fig. 4 for an initial roll angle of 0.17 rad. The controller appears to be functioning as desired, because in order to counteract the lateral acceleration caused by the initial roll angle, the control system commands a coordinated turn. The aileron and rudder deflections required to accomplish this are not excessive. In Fig. 5, the transient response of the modified optimal controller is presented. A comparison of Figs. 4 and 5 shows that the suboptimal response is slightly less damped, but the two systems are very similar. Thus the above methodology leads to reasonable closed loop transients for the modified optimal and suboptimal controllers. This having been established, it remains to verify the performance by simulation in a seaway.

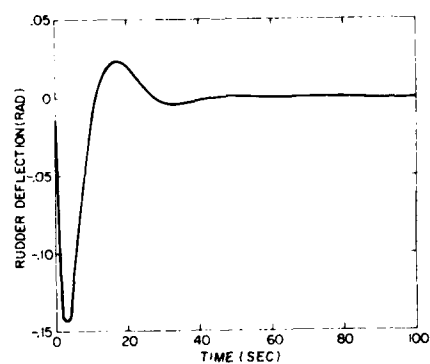
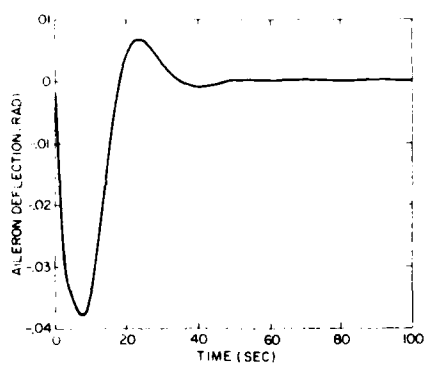
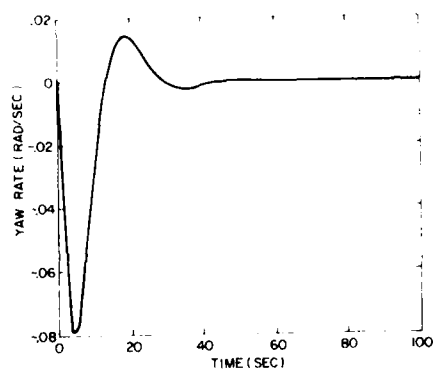
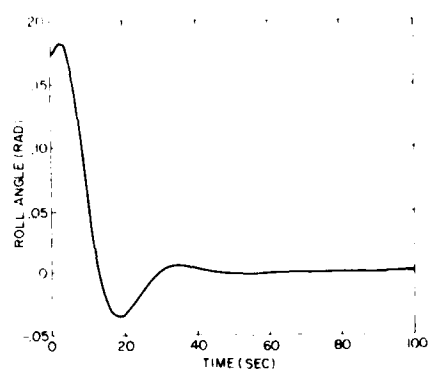
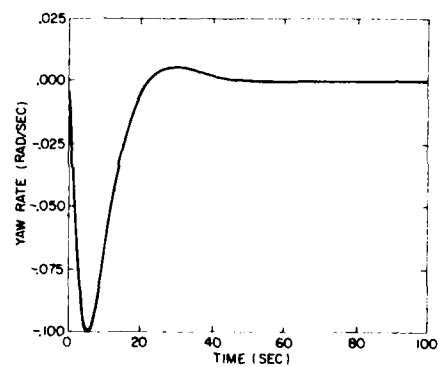
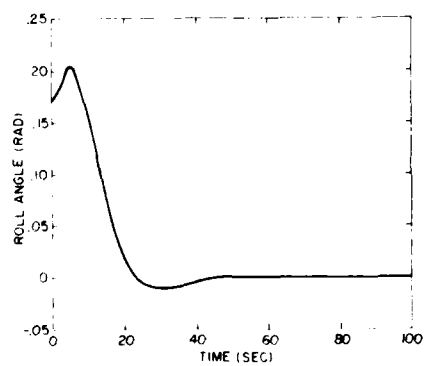


Figure 4. Response of Suboptimal Controller



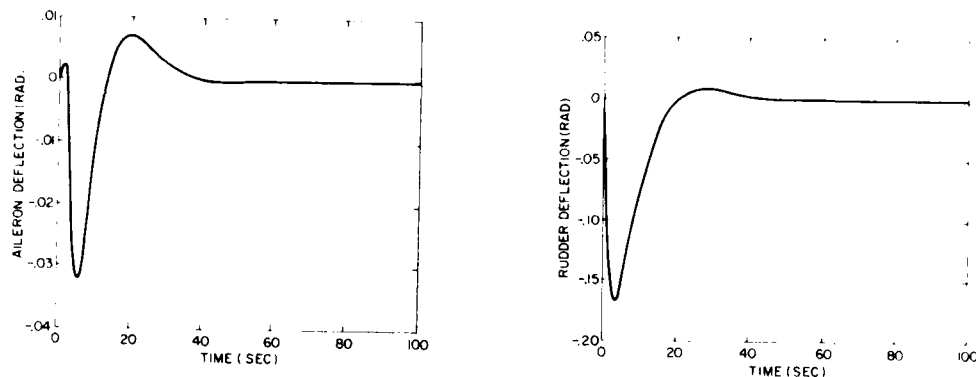


Figure 5. Response of Modified Optimal Controller

#### Derivation of the Seaway Model

In many control system applications, the design is considered to be complete once the transient response of the closed loop system to deterministic initial conditions and forcing functions (such as steps and ramps) is deemed to be acceptable. Historically, this approach has led to many successful designs, usually when any random disturbances are quite small. Unfortunately, a ship at sea is subject to random disturbances of considerable magnitude. The prudent designer must therefore simulate the ship motion in a seaway so as to obtain a realistic appraisal of the performance of his control system.

The simulation approach adopted herein is to use stochastic control theory and model the wave forcing functions as the outputs of a linear system driven by white noise. This approach is chosen purely on theoretical grounds, in order to illustrate how the methodology of modern control theory may be applied to the present problem. It is recognized that actual design applications require more sophisticated simulations, and indeed a non-linear time domain simulation of the seaway is under development at DREA. It should be noted, however, that linear techniques have been applied with considerable success to predict the seaway-induced motions of both displacement ships and hydrofoils<sup>8</sup>.

The wave-induced forces and moments depend on the wave elevation  $\eta$  and the wave orbital velocity  $W$ . Both are assumed to be stationary, ergodic, zero-mean stochastic processes defined by their power spectral densities  $S_{\eta\eta}$  and  $S_{WW}$ , where

$$S_{WW}(\omega) = \omega^2 e^{-kh} \cdot S_{\eta\eta}(\omega) \quad (15)$$

Assuming that the wave-induced forces and moments are transmitted to the ship through variations in wave orbital velocity, thus changing the angle of attack of the foils and struts, the side force and rolling moment in beam seas may be expressed as

$$Y_W = - \frac{1}{2m} \rho U W \sum (S C_{L\alpha} \cos ky_s)_{\text{struts}} \quad (16a)$$

$$K_W = - \frac{1}{2I_{xx}} \rho U W \left[ \sum (y_s S C_{L\alpha} S_e \sin ky_s)_{\text{foils}} \right. \\ \left. - \sum (z_s S C_{L\alpha} \cos ky_s)_{\text{struts}} \right] \quad (16b)$$

These formulae are derived in Appendix B, based on equations from Reference 8. The yawing moment is considered to be negligible. Because  $Y_W$  and  $K_W$  are linear in  $W$ , they are themselves random variables whose power spectral densities may be computed, once the power spectral density for  $W$  is specified. For a 7.0 ft. foil depth, and a significant wave height of 10.0 ft.,  $S_{WW}$  is assumed to be the spectrum shown in Fig. 6. The resulting spectra  $S_{YY}$  and  $S_{KK}$  are represented in Fig. 7 by solid lines. The objective is to find a linear system

$$\dot{x}_1 = A_1 x_1 + L_1 \gamma \quad (17)$$

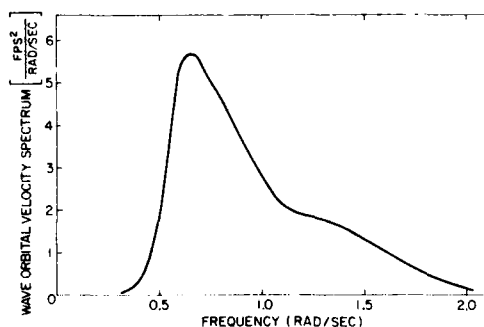


Figure 6. Power Spectral Density of Wave Orbital Velocity

such that, for driving white noise  $\gamma$  whose covariance  $E$  is unity, the power spectral densities of two of the elements of  $x_1$  are identical to those derived from equation (16). These two states are therefore statistically identical to  $Y_W$  and  $K_W$ . The system defined by equation (17) may then be combined with the state equation, equation (3), resulting in the augmented state equation

$$\begin{bmatrix} \dot{x} \\ \dot{x}_1 \end{bmatrix} = \begin{bmatrix} A & A_{12} \\ 0 & A_1 \end{bmatrix} \begin{bmatrix} x \\ x_1 \end{bmatrix} + \begin{bmatrix} B \\ 0 \end{bmatrix} u + \begin{bmatrix} 0 \\ L_1 \end{bmatrix} \gamma \quad (18)$$

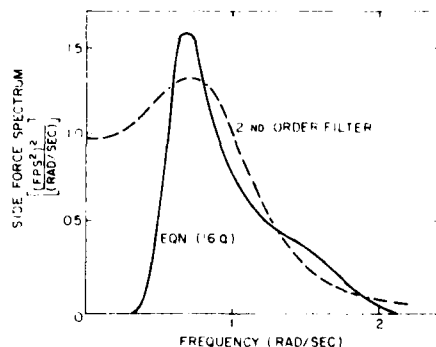


Figure 7a. Power Spectral

Density of Side Force

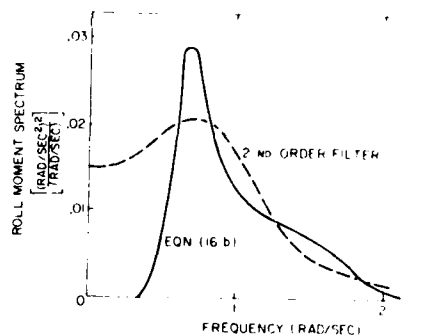


Figure 7b. Power Spectral

Density of Roll Moment

The elements of matrix  $A_{12}$ , which couples equations (3) and (17), are obtained by replacing the right hand side of equations (2a-c) with  $Y_w$ ,  $K_w$  and zero, respectively, before they are reformulated as the state equation. In the sequel, equation (18) will be expressed as

$$\dot{x} = Ax + Bu + Ly \quad (19)$$

where it is understood that  $x$  is larger than eight dimensions by virtue of the inclusion of  $x_1$ . A block diagram of this system is presented in Fig. 8. It should be noted that none of the elements of  $x_1$  will be fed back, so that the elements of  $G^*$  or  $G$  corresponding to  $x_1$  are set to zero.

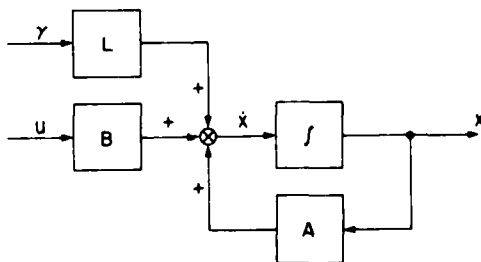


Figure 8. System Block Diagram, Including Seaway Terms

Unfortunately, a prohibitive number of additional states are required to match  $S_{YY}$  and  $S_{KK}$  exactly. This number can be drastically reduced if one is content to closely approximate these spectra only in the frequency range of most interest. This frequency range is found by computing the frequency response of the principal variable of interest, wheelhouse lateral acceleration. In the frequency domain, equations (2a-c) are a set of coupled linear algebraic equations whose unknowns are the real and imaginary parts of  $v$ ,  $\phi$ ,  $r$ ,  $\delta_A$  and  $\delta_R$ . By including a sinusoidal wave forcing function in these equations, the unknowns can be determined as a function of frequency. The frequency responses of  $v$ ,  $\phi$ ,  $r$ ,  $\delta_A$  and  $\delta_R$ , together with equations (8) and (9) are then used to obtain the frequency response of  $a_{wh}$ . The result, shown in Fig. 9, suggests that the ship responds most readily to frequencies from 0.8 rps to 5.0 rps. However, wave excitation frequencies do not exceed about 2.0 rps, so only the range 0.8 - 2.0 rps need be considered. This range can be adequately represented by incorporating the three additional states  $Y_W$ ,  $\dot{Y}_W$  and  $K_W$  into the state equation, as follows.

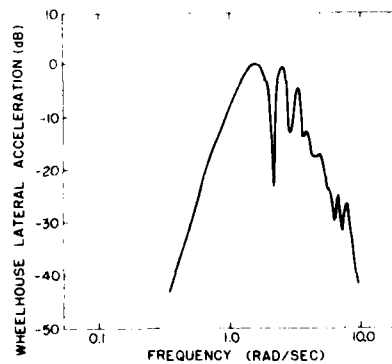


Figure 9. Frequency Response of Wheelhouse Lateral Acceleration

If  $Y_W$  is taken as the output of a second order filter driven by white noise, the gain, damping ratio and natural frequency of the filter can be adjusted so that the spectrum of  $Y_W$  is given by the dotted line in Fig. 7. Multiplication of the  $Y_W$  signal by a constant gives the  $K_W$  spectrum, also shown as a dotted line in Fig. 7. Both these spectra adequately approximate those given by equation (16) in the desired frequency range. The  $A_1$  and  $L_1$  matrices which result from this approach are given in Table II, for  $x_1 = [Y_W \dot{Y}_W K_W]'$ .

There are some major simplifications in the above analysis. A nonlinear disturbance has been modelled as linear. This step is unavoidable if any progress is to be made in the analysis. In addition, the colorations in the random process have not been modelled exactly. As Fig. 7 shows,  $Y_W$  and  $K_W$  have actually been whitened slightly. This

is not too serious, since the gross discrepancies occur away from the frequencies of most interest. Besides, if a Kalman filter is employed, broadening the wave input 'noise' may help to avoid divergence problems<sup>3</sup>.

As a check on the validity of the second order filter approach, the power spectral density of wheelhouse lateral acceleration is computed using this model and compared with the power spectral density obtained using equation (16). This comparison is shown in Fig. 10. The correlation is surprisingly good, considering the simplicity of the model.

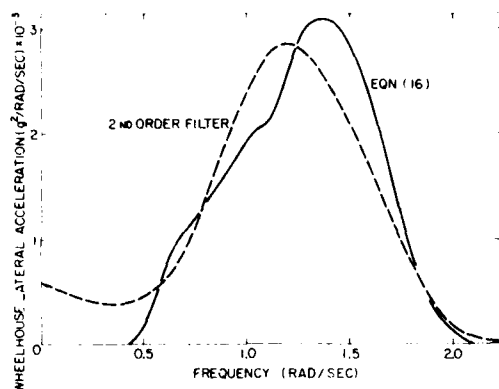


Figure 10. Power Spectral Density of Wheelhouse Lateral Acceleration

#### Simulation of Suboptimal and Modified Optimal Controllers

Once the mathematical model of the seaway is incorporated into the state equation, it is a simple matter to simulate any closed loop system and obtain both typical time histories and rms motions for the steady state. For any feedback gain matrix  $G$ , the closed loop dynamics are described by

$$\dot{x} = A_{CL}x + Ly \quad (20a)$$

$$A_{CL} = A - BG \quad (20b)$$

and  $P$ , the steady state covariance matrix of the state, is the solution of<sup>3</sup>

$$A_{CL}P + PA_{CL}' + L \Sigma L' = 0 \quad (21)$$

The square roots of the diagonal elements of  $P$  are the steady state rms values of the elements of  $x$ .

In Fig. 11, time histories of wheelhouse lateral acceleration, aileron deflection and rudder deflection are presented for the sub-optimal and modified optimal controllers. These time histories are in response to identical initial conditions and white noise sequences, so they are directly comparable. The results show that these two controllers are very similar in performance. This is borne out by the rms

motions presented in the second and third columns of Table III. The rms motions obtained using the optimal controller are also shown in Table III. The single small eigenvalue for this system results in some large excursions in the states, particularly roll angle. This is due, of course, to the low weighting of roll angle in the performance index. The gain change resulting in the modified optimal controller cures this problem and reduces wheelhouse lateral acceleration at a cost of higher rms values of  $\delta_A$  and  $\delta_R$ ; i.e., higher power consumption.

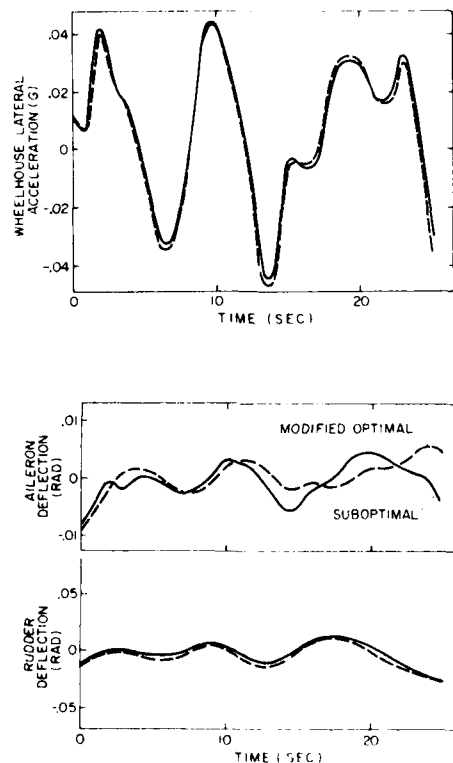


Figure 11. Time Domain Simulation of Suboptimal and Modified Optimal Controllers

The rms values of  $a_{wh}$  presented in Table III are all well below the specified 0.05g limit. This suggests that more lateral acceleration can be tolerated, with an accompanying reduction in hydraulic control power. This effect of such a tradeoff can be conveniently assessed if desired by reducing the value of  $\xi$  in the performance index, deriving new  $G^*$  and  $G$  matrices, and simulating the resulting closed loop system.



If one knew the control surface deflection limit for cavitation-free operation, one could check this specification as well. Assume, for example, that control surface deflections of 0.17 rad. will cause cavitation at a speed of 50 knots, and that half of the available deflection is allocated to lateral control. The remainder is required for maneuvering and longitudinal control. If the maximum allowable control deflection of 0.085 rad. for lateral control is presumed to occur once in ten aileron or rudder motion cycles, the allowable rms control surface deflection is 0.035 rad. if a Rayleigh probability distribution of deflection angles is presumed. Therefore the specification for cavitation-free operation may be interpreted to mean an rms aileron and rudder deflection limit of 0.035 rad. As Table III demonstrates, this specification is easily met by the suboptimal and modified optimal controllers, but not by the optimal controller.

If the specification on cavitation-free operation had not been met, it would have been necessary to redesign  $G^*$  and hence  $G$  by reducing the value of  $\xi$  in the performance index  $J$ . This results in smaller feedback gains, smaller control surface deflections and larger values of  $a_{wh}$ .

One may or may not be able to satisfy the specifications on  $a_{wh}$ ,  $\delta_A$  and  $\delta_R$  simultaneously, depending on the foil system.

If all the state variables required by the suboptimal control system can be measured exactly, the design is now complete and the suboptimal controller can be implemented. Of course, if every state variable in equation (4a) is measured, one may implement the modified optimal controller. This may not be practical, although the modified optimal controller is to be preferred over the suboptimal controller. The solution is to generate an estimate of the complete state vector based on the available measurements. In the happy case where the measurements are very accurate, a minimal order observer can be employed to do this. However, the performance of such an observer is very poor when the measurements are corrupted by sensor noise, as is so often the case in practice. When sensor noise is significant, the designer must resort to a Kalman filter for state estimation.

#### KALMAN FILTER DESIGN AND SIMULATION

Naval shipboard equipment must often operate in a severe environment. Vibrations due to hull slamming, for example, or 'crosstalk' from the electronic systems in close proximity, definitely affect performance. For a foilborne ship moving at high speed in heavy seas, one may expect that the relatively high encounter frequency with the waves would aggravate this problem. Physical sensors will generate noise outputs in this situation, and the realistic control system designer will want to counteract this measurement uncertainty so as to retain acceptable performance. The most common, practical method for estimating the system states in the presence of uncertainty is the well-known Kalman filter.

In this section, a Kalman filter is designed to generate the optimal estimate  $\hat{x}$  of  $x$ . This estimate may then be fed back to control the ship according to

$$u = -G\hat{x} \quad (22)$$

The Kalman filter and the control law are together referred to as the compensator. Because of the Separation Theorem, each may be designed separately. By specifying  $L$ , the driving noise gain matrix, and  $Q$ , the

sensor noise covariance matrix, one may derive the Kalman filter gain matrix  $H^*$  in much the same manner as the feedback gain matrix  $G^*$  was determined after specifying  $Q$  and  $R^4$ .

This analysis assumes that only  $p$ ,  $\phi$ ,  $r$ ,  $\delta_A$  and  $\delta_R$  are measured. These states are the elements of the output vector  $y$ , where

$$y = Cx \quad (23)$$

The measurements  $z$  are assumed to be corrupted by white sensor noise  $\theta$ :

$$z = Cx + \theta \quad (24)$$

where the sensor noise covariance matrix  $\theta$ , presented in Table II, is based on data from Reference 9. The state estimate  $\hat{x}$  is generated from  $z$  according to the matrix differential equation

$$\dot{\hat{x}} = A\hat{x} + Bu + H^*(z - C\hat{x}) \quad (25)$$

where  $H^*$  is given by

$$H^* = PC\theta^{-1} \quad (26)$$

and  $P$  is the solution of

$$PA + A'P + LEL' - PC'\theta^{-1}CP = 0 \quad (27)$$

Although  $H^*$  may be generated off-line, the dynamics of the estimation process require that, in addition to the feedback gain matrix  $G$ , the matrices  $A$ ,  $B$ ,  $C$  and  $H^*$  must be stored in the on-board control computer. If estimation were not required, only  $G$  would have to be stored. Thus the use of a Kalman filter leads to significant increases in computer memory size. Moreover, a number of these matrices, corresponding to different ship speeds, may have to be stored. It is important to keep these hardware and software constraints in mind during the design phase.

Although the driving noise gain matrix  $L$  has been specified above, it is to the designer's advantage to modify it by introducing some 'fake' driving noise before the Kalman filter is derived<sup>3</sup>. This tends to compensate for modelling errors in the equations of motion. Unfortunately, there is no systematic method for the selection of the elements of  $L$ . As in the selection of  $Q$  and  $R$ , physical intuition is of great importance. The driving noise gain matrix selected for this application is presented in Table II, along with the resulting optimal filter gain matrix  $H^*$ . This matrix, together with the modified optimal gain matrix  $G$  and the  $A$ ,  $B$  and  $C$  matrices completely defines the compensator structure.

The same seaway model derived above is used to simulate the performance of the filter-controller combination. The time histories displayed in Fig. 12 show that use of the Kalman filter has apparently resulted in reduced wheelhouse lateral acceleration compared to Fig. 11, at a cost of increased aileron and rudder deflections, and increased hydraulic power consumption. These results are borne out by the steady state rms values presented in Table III.

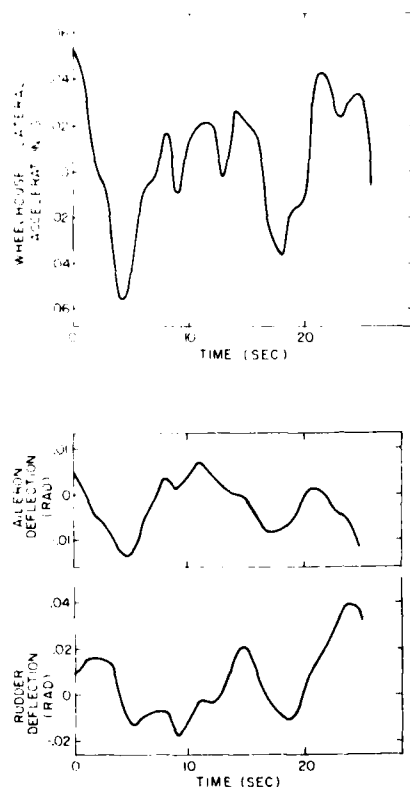


Figure 12. Time Domain Simulation of Kalman Filter Plus Modified Optimal Controller

#### CONCLUDING REMARKS

A mathematical model of the lateral dynamics of a hydrofoil ship equipped with fully submerged foils is presented. The open loop system is inherently unstable and requires an automatic control system to provide stability and an acceptable level of ride quality. This paper presents a methodology based on modern control theory for the design of the necessary control system. An advantage of this approach is that the closed loop performance, expressed in terms of ride quality and hydraulic power consumption, may be explicitly specified by the performance index.

The methodology of stochastic control theory has been employed to provide a quick preliminary assessment of the behaviour of the closed loop system in waves. The results indicate that the controllers appear

to be functioning as desired. This analysis has been extended to include the situation where sensor noise is significant, or all the feedbacks cannot be measured. Kalman filter design has been discussed and the filter-controller combination has been simulated in a seaway.

#### REFERENCES

- (1) Hsu, S.K.: "Application for Optimal Control Theory to a Large Hydrofoil Craft", Proceedings of the IV Ship Control Systems Symposium, October 1975.
- (2) Etkin, B.: Dynamics of Atmospheric Flight, John Wiley and Sons, 1972.
- (3) Athans, M.: "The Role and Use of the Stochastic Linear-Quadratic-Gaussian Problem in Control System Design", IEEE Transactions on Automatic Control, Vol. AC-16, December 1971.
- (4) Kwakernaak, H. and Sivan, R.: Linear Optimal Control Systems, John Wiley and Sons, 1972.
- (5) Sandell, N.R. and Athans, M.: "Manual of Fortran Computer Subroutines for Linear, Quadratic, Gaussian Designs", MIT Press, 1974.
- (6) Remington, P.J. and Bender, E.K.: "Hydrofoil Design for Minimum Control Power", Bolt Beranek and Newman, Inc., Report 2511, 1973.
- (7) Rynaski, E.G.: "Optimal Helicopter Station Keeping", IEEE Transactions on Automatic Control, Vol. AC-11, July 1966.
- (8) Schmitke, R.T.: "Prediction of Wave-Induced Motions for Hullborne Hydrofoils", AIAA Journal of Hydronautics, July 1977.
- (9) Elliott, J.R.: "NASA's Advanced Control Law Program for the F-8 Digital Fly-by-Wire Aircraft", IEEE Transactions on Automatic Control, Vol. AC-22, October 1977.
- (10) Jones, E.A., Eames, M.C. and Davis, B.V.: "The Prediction of Flap-Controlled Hydrofoil Ship Steady State Performance", DREA TM/75/A, September 1975.
- (11) Schmitke, R.T.: "Prediction of Pitch and Heave Motions of Hullborne Hydrofoil Vessels", DREA Report 74/2, January 1974.
- (12) Abramson, H.N. et al: "Hydroelasticity with Special Reference to Hydrofoil Craft", DTNSRDC Report 2557, September 1967.

#### APPENDIX "A"

##### DERIVATION OF THE STABILITY DERIVATIVES

Consider an arbitrary hydrofoil or strut of dihedral angle  $\Gamma$  and sweep angle  $\Lambda$ . The lift may be expressed as

$$L = L_{NC} + L_C \quad (A1)$$

where the subscripts NC and C denote noncirculatory and circulatory lift respectively. The sweep angle correction is assumed to be included in  $C_{L\alpha}$ , which is computed in the manner of Reference 10. The moment developed by this foil or strut is, from Reference 11,

$$M = - L_{NC}s - L_C x_s - m_v \left(\frac{C}{4}\right) (Ur + \frac{3}{8} \dot{r}) \quad (A2)$$

where:

$m_v$  is the virtual mass

$c$  is the chord length

$s$  is the x coordinate of the mid chord

$(x_s, y_s, z_s)$  are the coordinates of the centre of lift

Resolving the lift and moment into sway, roll and yaw components gives

$$Y = - L \sin \Gamma \quad (A3)$$

$$K = L(y_s \cos \Gamma + z_s \sin \Gamma) \quad (A4)$$

$$N = M \sin \Gamma \quad (A5)$$

The evaluation of  $L_{NC}$  and  $L_C$  is carried out in Reference 12, and referred to an inertial frame. If these results are referred to stability axes, they may be expressed as

$$L_{NC} = m_v [(\dot{s}r + \dot{v}) \sin \Gamma - (y_s \cos \Gamma + z_s \sin \Gamma) \dot{p}] \quad (A6)$$

$$L_C = \frac{1}{2} \rho U^2 C_{L\alpha} \{[(s - \frac{c}{4})r + v] \sin \Gamma - (y_s \cos \Gamma + z_s \sin \Gamma) p\} - \frac{\partial L}{\partial h} y \phi \quad (A7)$$

Equations (A1), (A2), (A6) and (A7) are substituted into equations (A3), (A4) and (A5). Then Y, K and N are differentiated with respect to each motion variable and the results are summed over all struts and foils to produce the following stability derivatives:

$$Y_v^* = \Sigma (m_v \sin^2 \Gamma)$$

$$Y_v = \frac{1}{2} \rho U^2 \Sigma (C_{L\alpha} \sin^2 \Gamma)$$

$$Y_p^* = - \Sigma [m_v (y_s \cot \Gamma + z_s) \sin^2 \Gamma]$$

$$Y_p = - \frac{1}{2} \rho U \Sigma [SC_{L\alpha} (y_s \cot \Gamma + z_s) \sin^2 \Gamma]$$

$$Y_{\dot{\Gamma}} = - \frac{1}{2} \rho U^2 \Sigma (y_s SC_{Lh} \sin \Gamma)$$

$$Y_r^* = \Sigma (m_v s \sin^2 \Gamma)$$

$$Y_r = \frac{1}{2} \rho U \Sigma [SC_{L\alpha} (s - c/4) \sin^2 \Gamma]$$

$$K_v^* = - \Sigma [m_v (y_s \cot \Gamma + z_s) \sin^2 \Gamma]$$

$$K_v = - \frac{1}{2} \rho U \Sigma [SC_{L\alpha} (y_s \cot \Gamma + z_s) \sin^2 \Gamma]$$

$$K_p^* = \Sigma [m_v (y_s \cot \Gamma + z_s)^2 \sin^2 \Gamma]$$

$$K_p = \frac{1}{2} \rho U \Sigma [SC_{L\alpha} (y_s \cot \Gamma + z_s)^2 \sin^2 \Gamma]$$

$$K_{\dot{\Gamma}} = \frac{1}{2} \rho U^2 \Sigma [y_s SC_{Lh} (y_s \cot \Gamma + z_s) \sin \Gamma]$$

$$K_r^* = - \Sigma [m_v s (y_s \cot \Gamma + z_s) \sin^2 \Gamma]$$

$$K_r = - \frac{1}{2} \rho U \Sigma [SC_{L\alpha} (s - c/4) (y_s \cot \Gamma + z_s) \sin^2 \Gamma]$$

$$N_v^* = \Sigma (m_v s \sin^2 \Gamma)$$

$$N_v = \frac{1}{2} \rho U \Sigma (x_s SC_{L\alpha} \sin^2 \Gamma)$$

$$N_p^* = - \Sigma [m_v s (y_s \cot \Gamma + z_s) \sin^2 \Gamma]$$

$$N_p = - \frac{1}{2} \rho U \Sigma [x_s SC_{L\alpha} (y_s \cot \Gamma + z_s) \sin^2 \Gamma]$$

$$N_{\dot{\Gamma}} = - \frac{1}{2} \rho U^2 \Sigma (x_s y_s SC_{Lh} \sin \Gamma)$$

$$N_r^* = \Sigma [m_v (s' + c^2/32) \sin^2 \Gamma]$$

$$N_r = \Sigma \{ [\frac{1}{2} \rho U x_s SC_{L\alpha} (s - c/4) + m_v U c/4] \sin^2 \Gamma \}$$

The stability derivatives with respect to the control variables are given below. Control deflection is defined to be positive when a positive moment results.

the ship that is in error of decreasing 'command' authority but increasing 'control' authority. The operator of a MM can take control of its equipment, if necessary, but control can be passed on to its SCU by the PCU only if the PCU and SCU control levers are aligned. The transfer of control between MMIs is supervised by the SCU, the Bridge and SCC being connected to each SCU by point-to-point buses. In this way control can be transferred between Bridge and SCU or between SCC and SCU if either the Bridge or MM are unavailable due to action or fire damage.

The size of the SCU MMIs will depend upon the ship in which the system is to be fitted. For the purposes of evaluation a relatively complex panel was decided upon; with the possibility of blanking off areas to get operator reaction during hardware evaluation in the National Gas Turbine Establishment's (NGTE's) facility (described in reference 1).

Dedicated point-to-point data buses have been selected to transmit primary surveillance and control data between individual control units and MMIs. A separate ship data bus is used to transmit secondary surveillance data from the propulsion system and also data from the various auxiliary systems to the SCC.

#### Reference Control System

The control and surveillance system for the reference ship is defined in the first-level functional diagram in Figure 4. Figure 5 shows, as an example of the

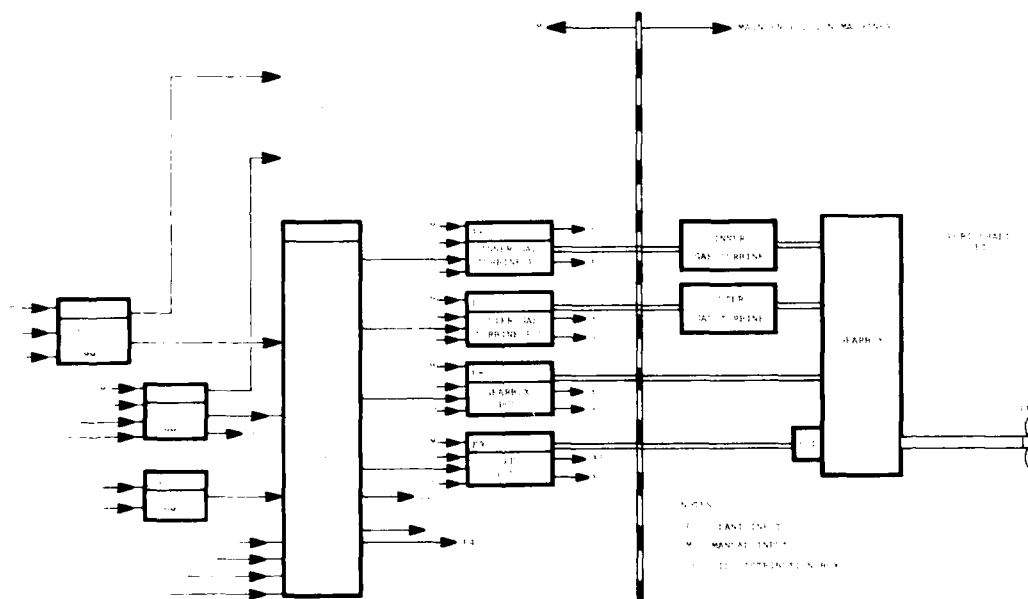


Figure 4. Reference Control System (First Level)

second level, the functional diagram of an SCU. Figure 6 shows the functional diagram for the engine power control function of an SCU (i.e. function F5.2 in Figure 5) and is thus an example of the third level. The fourth level is illustrated in Figure 7 which shows the SCU's engine power integral control (i.e. function 5.2.1 in Figure 6). At this last level the input/output control signals can be identified as can the major control systems settings.

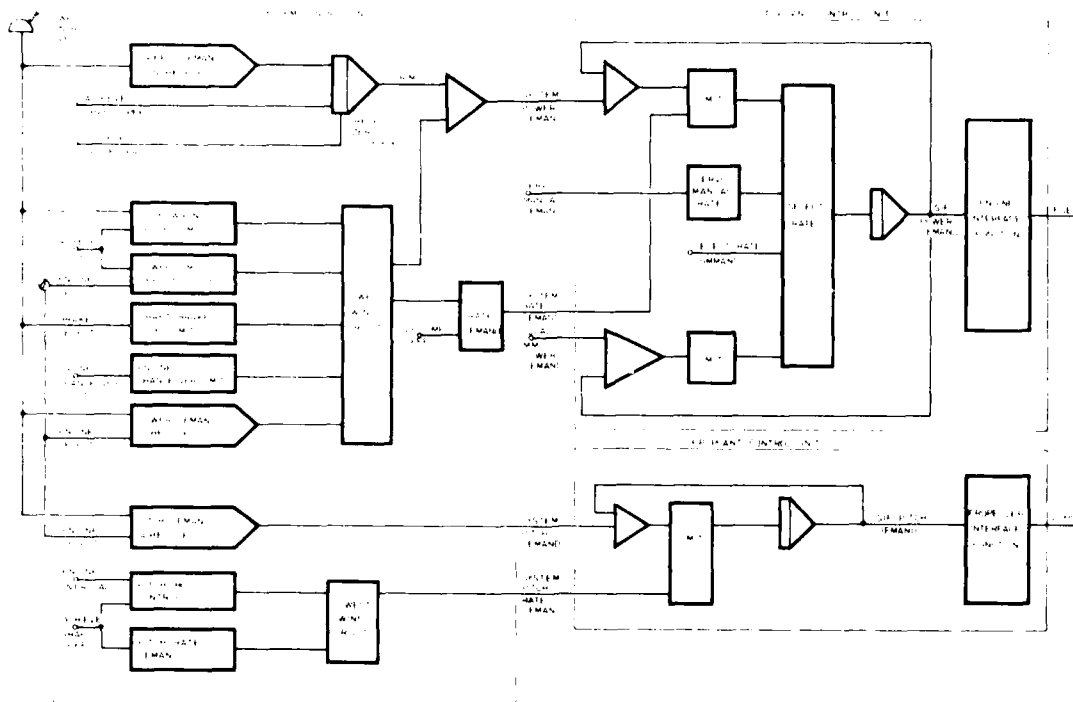


Figure 3. Power/Pitch Control System

- SMIA gas turbine controlled by LP compressor speed demand rather than fuel actuator position.

Even with the above differences from present generation identified, the structure of the functional description is such that the third-level, and in some cases the fourth-level, diagrams can be the same for present and new systems. This allows the diagrams to be used, say, in the production of statements of requirements at an early stage in the ship design before commitment to particular schedules and control settings is made.

#### Servo Manual Control

Following recent ship philosophy, servo manual control at the SCU was adopted. The reference control system provides hard-wired connection between "inching" buttons on the SCU panel into each of the PCUs, by-passing their respective SCU. Direct connection to the PCUs allows for failure of the respective SCU or data bus but retains protected control of the plant by the PCU. It was decided that failure of a PCU would require reversion to emergency hand control of the plant, rather than having servo-manual input directly to the plant actuators.

#### Man Machine Interfaces (MMIs)

MMIs are used in the reference control system at each of the following locations:

- Bridge
- SCC
- SCU of each shaft set
- Each PCU



In addition, the structure of the system was to be organised such that individual control units could be used in different types of ships with possibly different machinery configurations.

As noted in the paper by Reeves and Spencer (reference 4), the system design had to be progressed even though some of the Machinery Control and Surveillance Research Programme items were not completed, but we are confident that the flexibility of the reference control systems design will cater for any foreseeable change which future research might recommend.

#### Plant Control Units (PCUs)

The development of the reference control system coincided with the development of the SMLA gas turbine's on-plant controls by Rolls-Royce. Because of this a joint YARD/Rolls-Royce/MOD(PE) team was established to define the SMLA's PCU requirements and that PCU was then used as a model for the other main machinery PCUs.

Each PCU performs the on-plant closed loop control and protection functions, start/stop sequencing and provides an interface with the rest of the system. In addition it conditions plant data (including generation of alarms and warnings against pre-set datum levels) and interfaces with the propulsion machinery and ship data buses to transmit this information to its SCU and to the SCC respectively.

The definition of control and protection functions should take account of the essential levels of system reliability to be achieved. A study was instigated by MOD(PE) to define such reliability levels and apply them to particular items of ship plant. As a result of this study a method, utilising failure analysis techniques, was established for specifying the functional and reliability requirements for the PCUs (reference 6). The required protection functions and the plant failure probabilities are derived from a fault and failure mode effects analysis. "Fail dangerous" probability and "spurious trip" probability estimates are made and these are used in conjunction with the plant failure probability to produce failure predictions which can be compared with the level of acceptable risk.

#### System Control Units (SCUs)

SCUs are located in the main machinery space in the vicinity of their propulsion system. Their purpose is to co-ordinate the individual PCUs and, at the time of writing, a simulation study had begun to evaluate the system control philosophies adopted for the SCU. Their prime function is to co-ordinate propeller pitch and engine power throughout the ship operating range and to control engine changeovers. In addition the SCU's power and pitch programmes must take cognisance of different ship operating conditions, such as single or twin engine drive, single shaft operation and ship action power profiles.

A schematic diagram of the power/pitch control system of the reference ship is shown in Figure 3. The most significant differences between this system and that of the Type 42 class (i.e. present generation system) are:

- Open loop control of engine power at the system level (i.e. no proportional control based on shaft speed) except for a limited authority slow acting integral channel whose output is set to zero during manoeuvring.
- Different engine power programmes depending on ship operating mode.
- Discrete levels of pitch rate demand as opposed to pitch rate demand being a continuous function of propeller shaft speed.
- Astern pitch schedules adjusted such that full pitch does not occur at very low engine power.

Figure 1 (a)

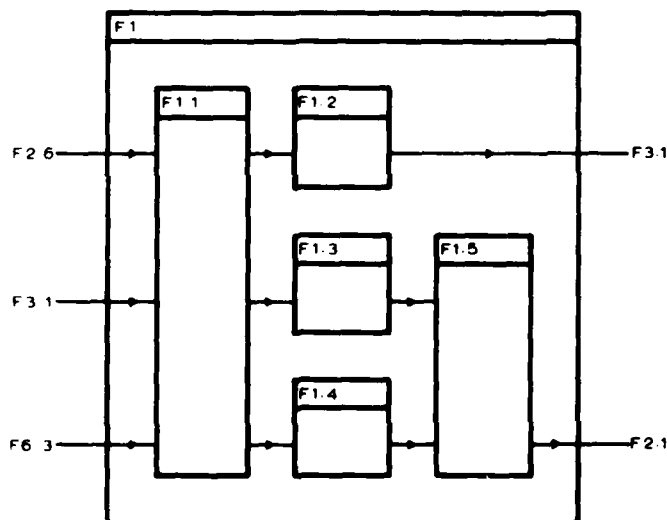
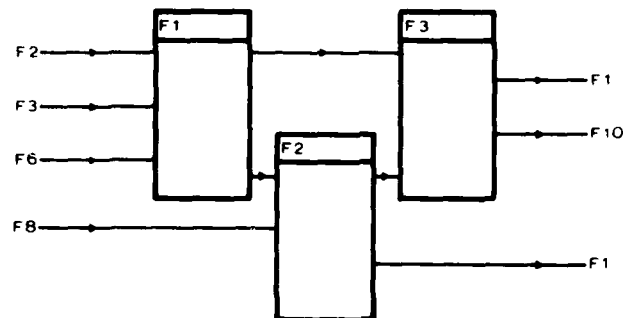


Figure 2 (b)

Figure 2. Development Documentation System

#### DEFINITION OF CONTROL AND SURVEILLANCE FUNCTIONS

##### Operational Features

The distributed control concept described earlier has been followed. However, some fundamental decisions had to be taken in order that a fully integrated system could be specified; the most important of these are:

- Control features in each PCU.
- Control features in each SCU.
- Scope of each MMI.
- Hierarchy of control authority of the MMIs.
- Communication of data between control units and MMIs.

At the outset it was agreed that should digitally based technology be selected then its power should be utilised to increase flexibility, invulnerability, etc, but that the complexity of the control algorithms should, if anything, be simpler than in say the Type 42 class based upon recent operational experience with those systems.

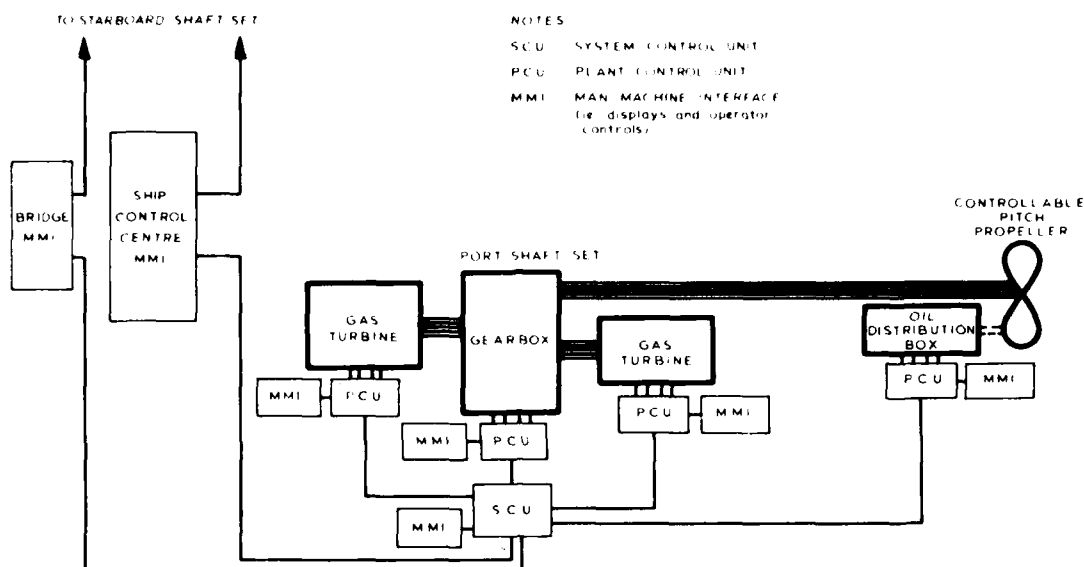


Figure 1. Reference Control System.

The design of SCU and Bridge equipment and layout has been deemed worthy of a separate intensive study. It has involved identification and analysis of command, operator and maintainer requirements. Within this integrated 'MI' activity, the propulsion MMIs have received full consideration. The task of identifying their requirements for the reference ship and possible variants is therefore reduced to being one of detail.

#### FUNCTIONAL DOCUMENTATION

Functional documentation has been used for some time in the specification and design of weapon systems and a similar approach was adopted in the derivation of control and surveillance requirements for future generation warships.

The documentation method adopted uses a 'top down' approach and defines the control and surveillance functions to be carried out by the systems. The emphasis is on 'function' and not on description of hardware components or technology of implementation. System definition follows the Development Documentation System (DDS) methodology, in spirit, if not in absolute detail. The DDS method comprises functional blocks with functional interconnections and is illustrated in Figure 2.

In developing the reference control system four functional levels were used, the highest, or first, level defining the system's overall structure, the lowest, or fourth, level defining individual control and surveillance signals. (It should be noted that the connections between the functional blocks on the diagram are identified at the same level as the blocks themselves. The interconnections are functional only and do not necessarily indicate direct physical links between the blocks.) The first level is the master level and each block of this level is defined by a sequential number (F1, F2, etc, as illustrated by Figure 2a). Each subsequent level is a logical expansion of the preceding level. For instance, the second level is used to show in more detail the functions specified in each individual first-level block. The second-level blocks are identified by an additional decimal number (F1.1, F1.2, etc, as shown in Figure 2b).

determine the certain or highly probable factors involved and hence the most likely ship, machinery fit and configuration. Thus, the plan needs to define a presumed 'reference ship'. The functions required of the controls and surveillance system of the reference ship can then be defined in relation to the degree of automation that is most likely to be required. Following this, options for the reference ship itself, and ship variants to cover the range of ship types originally predicted or known, must be dealt with to complete the plan.

#### Equipment Implications

The effectiveness of designing the controls system from a functional viewpoint becomes even greater if the equipments and subsystems of the reference ship's control system design can be conveniently, inexpensively and rapidly modified to suit the requirements of another ship. This is achievable for future systems as will be shown later. In fact, this flexible characteristic is desirable in its own right for any specific ship. The aim of the plan, therefore, is that design and development can proceed for the reference ship without significant waste of resources even if a new ship is approved elsewhere in the range and with non-favourite equipment options. This implies maximum standardisation of system component parts.

#### Vessels Considered

The range of conventional surface warships within which choices for future Royal Navy vessels are likely to be made was foreseen as embracing patrol craft and cruisers and spanning displacements of, say, 1000 to 10 000 tonnes. Within this range the reference ship was identified as having the role of a destroyer, displacing about 4500 tonnes, and as being fitted with a twin shaft, gas turbine propulsion system driving controllable pitch propellers.

#### Controls Configuration and Characteristics

The results of the Machinery Control and Surveillance Research Programme (reference 4) suggest a distributed control system with a maximum delegation of function down the system. It follows that it is a distributed hardware concept as opposed to the centralised concept of present systems in which most of the electronics are sited in the Ship Control Centre (SCC). Thus, the reference control system, illustrated in Figure 1, has a Plant Control Unit (PCU) for each element of the propulsion system. These PCUs are capable of local operation through their own Man Machine Interfaces (MMIs) or as a co-ordinated shaft set under the control of a System Control Unit (SCU). In turn, the behaviour of an SCU is controlled from its own MMI or by either the SCC or Bridge MMIs as desired. The separate links to each SCU from the SCC and Bridge are run by different routes to increase invulnerability. The facility to run a shaft from its SCU, or constituent plants from their PCUs, enables the propulsion system to be operated under many damage or fault conditions, albeit in degraded mode and with more men. In addition, this facility enables each propulsion plant to be run independently of the SCC for diagnosis and testing. The distribution of the hardware not only increases invulnerability to damage but also affords reductions in ship installation problems, because the PCUs will generally be built and tested with the parent equipment at the manufacturers. Of more importance, the reference control system can provide the flexibility necessary to cater for a wide range of different ship propulsion systems.

The flexibility that is required can be achieved by defining the functions required in each of the control units and MMIs and then separating as far as possible the electronics and software fulfilling these individual functions. Thus changes to one function have no, or little, effect on other functions, whether these changes arise for technical or operational reasons. The aspects which cannot be easily changed are sensors and actuators fitted as part of a plant. In the design of the independent pieces of plant, therefore, care has to be taken to foresee future ship configurations in which the plant could possibly be fitted so that provision can be made for the most demanding case.

## FUTURE PROPULSION CONTROL SYSTEMS FUNCTIONAL REQUIREMENTS

by Collier French  
Ministry of Defence (P.E.), Bath, U.K.  
and Alexander M. Dorrian  
Y-ARD Ltd., Glasgow, U.K.

### ABSTRACT

The ability to determine rapidly, and with high confidence, the proper control equipment that should be fitted to a new ship at a stipulated date has at least two major benefits. Firstly, it provides information for better decisions to be made on a proposed ship and, secondly, it shortens controls development programmes. For this ability to be attained, a well-supported strategy is needed for identifying what the controls are to do and then specifying the optimum control system composed of the maximum amount of well or fully developed, modern sub-systems and components.

This paper is concerned with the "what to do" aspect of the process, namely, the rapid derivation of a proper statement of the functional requirements.

### INTRODUCTION

In the context of this paper the control system is taken as being all control and surveillance hardware plus any associated computer software and the men involved in the system's operation and maintenance. The design approach described herein is aimed at any nominated surface warship of conventional type, but it will also be helpful for more unusual craft. The technological and design details of the engineering implementation of the required functions are dealt with elsewhere in companion papers (references 1, 2, and 3).

### BACKGROUND

#### Major Design Factors

For very practical and well known reasons, the types and configurations of propulsion system plants for a ship are very limited and, for a nominated new ship, the decisions about these will usually have been made before controls design commences. Nevertheless, even with such initial plant constraints, optimum controls design depends essentially on a 'top down' approach. Ship level features - such as ship roles and functions, survival or invulnerability requirements, manning policy, etc - must be correctly translated and traded-off in the early stages of design to derive eventually the functions and characteristics that the engineering systems, including their operators and maintainers, are to provide and to have, respectively. The interim level of the process is the consideration of major interface features concerning operating, displaying, data transmitting and communicating.

#### Requirements of the Design Method

A plan for the rapid derivation of the functional requirements for the control and surveillance system of any single type of ship in a given range requires to be comprehensive yet concise and flexible. It must certainly provide fully for the most likely ship and be almost as sound for the less likely, but entirely possible, ship choice within the range. Therefore the plan needs to comprehend the likely range of ships and options within which a Naval Staff Target or Requirement may arise, to

Copyright © Controller, HMSO, London, 1978.

Table 3. RMS Motions in the Seaway

	Optimal Control (Perfect Measurements)	Modified Optimal (Perfect Measurements)	Suboptimal Control (Perfect Measurements)	Modified Optimal (Noisy Measurements)
$a_{wh}$ (g)	.0201	.0180	.0209	.0160
$v$ (fps)	3.77	.358	.496	1.34
$\dot{\theta}$ (rad)	.356	.0464	.0365	.0294
$r$ (rps)	.135	.0194	.0133	.0161
$\delta_A$ (rad)	.0233	.00585	.00799	.00869
$\delta_R$ (rad)	.2064	.0285	.0210	.0247
$\dot{\delta}_A$ (rps)	.00157	.00169	.00257	.00352
$\dot{\delta}_R$ (rps)	.00527	.00645	.00612	.00989

Kalman Filter Gain Matrix H\*

-.176	-13.2	-8.87	-30.50	179.
.0186	.809	.653	1.81	-2.10
.00486	.603	.168	.429	-1.88
.0261	1.12	1.01	3.01	-7.05
.00325	.129	.136	.488	-1.31
-.00419	-.626	-.352	-1.45	18.7
.0101	.323	.333	.854	-.525
.0113	.398	.386	1.04	-1.09
.170	5.87	9.67	36.2	-171.
2.32	106.	88.5	261.	-632.
-.0222	-.765	-1.26	-4.72	22.4

Seaway Model System Matrix A

0.00	1.00	0.00
-1.00	-1.00	0.00
0.00	-0.130	0.00

Seaway Model Driving Noise Vector L<sub>1</sub>

0.00
1.00
0.00

Eigenvalues

	Open Loop	Closed Loop (Optimal)	Closed Loop (Modified Optimal)	Closed Loop (Suboptimal)
Ship Dynamics	.355	-.425 + .437j	-.442 + .408j	-.412 + .481j
	-.390	-.425 - .437j	-.442 - .408j	-.412 - .481j
	-1.04	-1.21	-1.18	-1.26
	-4.86	-5.08	-5.08	-5.10
Actuator Dynamics	0.	-.00118	-.117 + .0967j	-.111 + .194j
	0.	-.240	-.117 - .0967j	-.111 - .194j
	-8.00	-7.99	-7.99	-7.08
	-12.0	-11.9	-11.9	-11.5

State Weighting Matrix Q

.078	27.2	.151	-3.98	-11.6	.128	-.0866	.0138
27.2	9529.	52.9	-1395.	-4074.	44.7	-30.3	4.84
.151	52.9	.294	-7.75	-22.6	.248	-.168	.0269
-3.98	-1395.	-7.75	204.	596.	-6.54	4.44	-.709
-11.6	-4074.	-22.6	596.	1742.	-19.1	13.0	-2.07
.128	44.7	.248	-6.54	-19.1	.209	-.142	.0227
-.0866	-30.3	-.168	4.44	13.0	-.142	.0964	-.0154
.0138	4.84	.0269	-.709	-2.07	.0227	-.0154	.00246

Input Weighting Matrix R

1.00	0.
0.	1.00

Optimal Feedback Gain Matrix G\*

-.000414	-.290	.162	.197	.418	.204	.0338	.0250
-.0107	.284	.661	.759	.207	.858	.0158	.111

Suboptimal Feedback Gain Matrix G

0.	-.281	.156	.191	.404	0.	0.	0.
-.010	.256	.595	.683	0.	.772	0.	0.

Plant Noise Gain Vector L

.00100	.0100	.00110	.0110	.000900	.000800	.00900	.00800
.0	1.00	.0					

Sensor Noise Covariance Matrix  $\Theta$

.0005	0.	0.	0.	0.
0.	.000003	0.	0.	0.
0.	0.	.000002	0.	0.
0.	0.	0.	.0000009	0.
0.	0.	0.	0.	.000001



Table 2. Matrices and Eigenvalues Associated with the Problem

System Matrix A

-1.346	.638	-29.5	-79.9	-4.23	7.41	-.0315	1.43
-.0325	-4.89	.101	.594	1.89	.594	.014	.115
0.	1.00	0.	0.	0.	0.	0.	0.
-.00256	-.0807	-.00727	-.696	.0201	.493	.000149	.0972
0.	0.	0.	0.	0.	0.	1.00	0.
0.	0.	0.	0.	0.	0.	0.	1.00
0.	0.	0.	0.	0.	0.	-12.0	0.
0.	0.	0.	0.	0.	0.	0.	-8.00

Input Matrix B

0.	.930
0.	.0746
0.	0.
0.	.0597
0.	0.
0.	0.
-12.0	0.
0.	-8.00

Output Matrix C

0.	1.00	0.	0.	0.	0.	0.	0.
0.	0.	1.00	0.	0.	0.	0.	0.
0.	0.	0.	1.00	0.	0.	0.	0.
0.	0.	0.	0.	1.00	0.	0.	0.
0.	0.	0.	0.	0.	1.00	0.	0.

$$N_W = - \frac{1}{2I_{zz}} \rho U W \sum (x_s SC_{L\alpha} e^{jky_s})_{\text{struts}} \quad (B6)$$

Consider  $e^{jky_s} = \cos ky_s + j \sin ky_s$ . Because the  $x_s z_s$  plane is a plane of symmetry, the  $\sin ky_s$  terms will disappear. In the expression  $jy_s e^{jky_s}$ , the odd function is  $jy_s \cos ky_s$ , so it will disappear from  $K_W$  after summation. The equations may then be written as

$$Y_W = - \frac{1}{2m} \rho U W \sum (SC_{L\alpha} \cos ky_s)_{\text{struts}} \quad (B7)$$

$$K_W = - \frac{1}{2I_{xx}} \rho U W [\sum (y_s SC_{L\alpha} \sin ky_s)_{\text{foils}} - \sum (z_s SC_{L\alpha} \cos ky_s)_{\text{struts}}] \quad (B8)$$

$$N_W = - \frac{1}{2I_{zz}} \rho U W \sum (x_s SC_{L\alpha} \cos ky_s)_{\text{struts}} \quad (B9)$$

For the ship under consideration, the numerical expressions are

$$Y_W = - [.414 \cos(.418\omega^2) + .125]W \quad (B10)$$

$$K_W = - [.340 \sin(.661\omega^2) + .028 \sin(.151\omega^2) + .050 \cos(.418\omega^2) + .016]W \quad (B11)$$

$$N_W = [.006 \cos(.418\omega^2) - .007]W \quad (B12)$$

Since  $N_W$  is an order of magnitude smaller than the smallest terms in  $Y_W$  and  $K_W$ ,  $N_W$  is neglected in the analysis.

Table 1. Leading Particulars

All up weight	400 tons
Length between perpendiculars	152.5 ft.
Roll radius of gyration	13.1 ft.
Yaw radius of gyration	39.4 ft.
Cross product of inertia	0.
Foil base length	112.5 ft.
Bow foil/aft foil area ratio	21/79
Foil operating depth	7.0 ft.
Foil dihedral	0.
Foil lift coefficient	0.18
Flap chord ratio	0.25
Aileron actuator time constant	0.08 sec.
Rudder actuator time constant	0.13 sec.

$$T_1 = -\frac{1}{3}(2 + p_a^2)\sqrt{1 - p_a^2} + p_a \cos^{-1} p_a$$

$$T_4 = -\cos^{-1} p_a + p_a \sqrt{1 - p_a^2}$$

$$T_7 = -(\frac{1}{8} + p_a^2)\cos^{-1} p_a + \frac{1}{8}p_a(7 + 2p_a^2)\sqrt{1 - p_a^2}$$

$$T_8 = -\frac{1}{3}(1 + 2p_a^2)\sqrt{1 - p_a^2} + p_a \cos^{-1} p_a$$

$$T_{10} = \sqrt{1 - p_a^2} + \cos^{-1} p_a$$

$$T_{11} = \cos^{-1} p_a(1 - 2p_a) + (2 - p_a)\sqrt{1 - p_a^2}$$

where  $p_a$  is the distance from the aileron hinge line to mid chord, divided by the semi-chord.

#### APPENDIX "B"

##### DERIVATION OF THE WAVE FORCING FUNCTIONS

Including only forces due to orbital velocity, the side force, rolling moment and yawing moment are, with  $W = \omega e^{-kh}$ :

$$Y_W = -\frac{1}{2m}\rho U W \Sigma [SC_{L\alpha} S_e \cdot e^{jky_s} \sin \Gamma (\sin \Gamma + j \cos \Gamma)]_{\text{struts}} \quad (B1)$$

$$K_W = \frac{1}{2I_{xx}}\rho U W \Sigma [SC_{L\alpha} S_e \cdot e^{jky_s} (y_s \cos \Gamma + z_s \sin \Gamma) \cdot (\sin \Gamma + j \cos \Gamma)]_{\text{foils and struts}} \quad (B2)$$

$$N_W = -\frac{1}{2I_{zz}}\rho U W \Sigma [x_s SC_{L\alpha} S_e \cdot e^{jky_s} \sin \Gamma (\sin \Gamma + j \cos \Gamma)]_{\text{struts}} \quad (B3)$$

For the struts, the Sears function  $S_e$  is taken as unity because of the low aspect ratios involved. For the foils, only the real part of  $S_e$  is included.

If the struts are assumed to be vertical ( $\Gamma = \frac{\pi}{2}$ ) and the foils have no dihedral, the above equations reduce to

$$Y_W = -\frac{1}{2m}\rho U W \Sigma (SC_{L\alpha} e^{jky_s})_{\text{struts}} \quad (B4)$$

$$K_W = \frac{1}{2I_{xx}}\rho U W [\Sigma (y_s SC_{L\alpha} S_e \cdot j e^{jky_s})_{\text{foils}} + \Sigma (z_s SC_{L\alpha} e^{jky_s})_{\text{struts}}] \quad (B5)$$

$$Y_{\delta R}'' = - \frac{1}{4} m_{VR} c_R$$

$$Y_{\delta R}' = - m_{VR} U - \frac{1}{4} \rho U S_R C_{L\alpha R} c_R$$

$$Y_{\delta R} = - \frac{1}{2} \rho U^2 S_R C_{L\alpha R}$$

$$Y_{\delta A}'' = - \frac{1}{4} \rho b_A T_1 c_A^3 \sin \Gamma_A$$

$$Y_{\delta A}' = - \frac{1}{2} \rho U b_A c_A^2 (T_4 - \frac{1}{2\pi} C_{L\alpha A} T_{11}) \sin \Gamma_A$$

$$Y_{\delta A} = \rho U^2 b_A c_A C_{L\alpha A} e_\beta \sin \Gamma_A$$

$$K_{\delta R}'' = - Y_{\delta R}'' \cdot z_R$$

$$K_{\delta R}' = - Y_{\delta R}' \cdot z_R$$

$$K_{\delta R} = - Y_{\delta R} \cdot z_R$$

$$K_{\delta A}'' = \frac{1}{4} \rho b_A T_1 c_A^3 (y_A \cos \Gamma_A + z_A \sin \Gamma_A)$$

$$K_{\delta A}' = \frac{1}{2} \rho U b_A c_A^2 (T_4 - \frac{1}{2\pi} C_{L\alpha A} T_{11}) (y_A \cos \Gamma_A + z_A \sin \Gamma_A)$$

$$K_{\delta A} = - \rho U^2 b_A c_A C_{L\alpha A} e_\beta (y_A \cos \Gamma_A + z_A \sin \Gamma_A)$$

$$N_{\delta R}'' = Y_{\delta R}'' \cdot s_R + \frac{1}{32} m_{VR} c_R^2$$

$$N_{\delta R}' = - m_{VR} U (s_R - \frac{c_R}{4}) - \frac{1}{4} \rho U C_{L\alpha R} S_R c_R x_R$$

$$N_{\delta R} = Y_{\delta R} \cdot x_R$$

$$N_{\delta A}'' = Y_{\delta A}'' \cdot s_A + \frac{1}{8} \rho b_A c_A^4 (T_7 + p_a T_1) \sin \Gamma_A$$

$$N_{\delta A}' = \frac{1}{2} \rho U b_A c_A^2 [- T_4 s_A + \frac{1}{2\pi} C_{L\alpha A} T_{11} x_A - \frac{c_A}{2} (T_1 - T_8 - p_a T_4 + \frac{1}{2} T_{11})] \sin \Gamma_A$$

$$N_{\delta A} = Y_{\delta A} \cdot x_A - \frac{1}{2} \rho U^2 b_A c_A^2 (T_4 + T_{10}) \sin \Gamma_A$$

The  $T_i$  used in the above expressions are reproduced below from Reference 11:

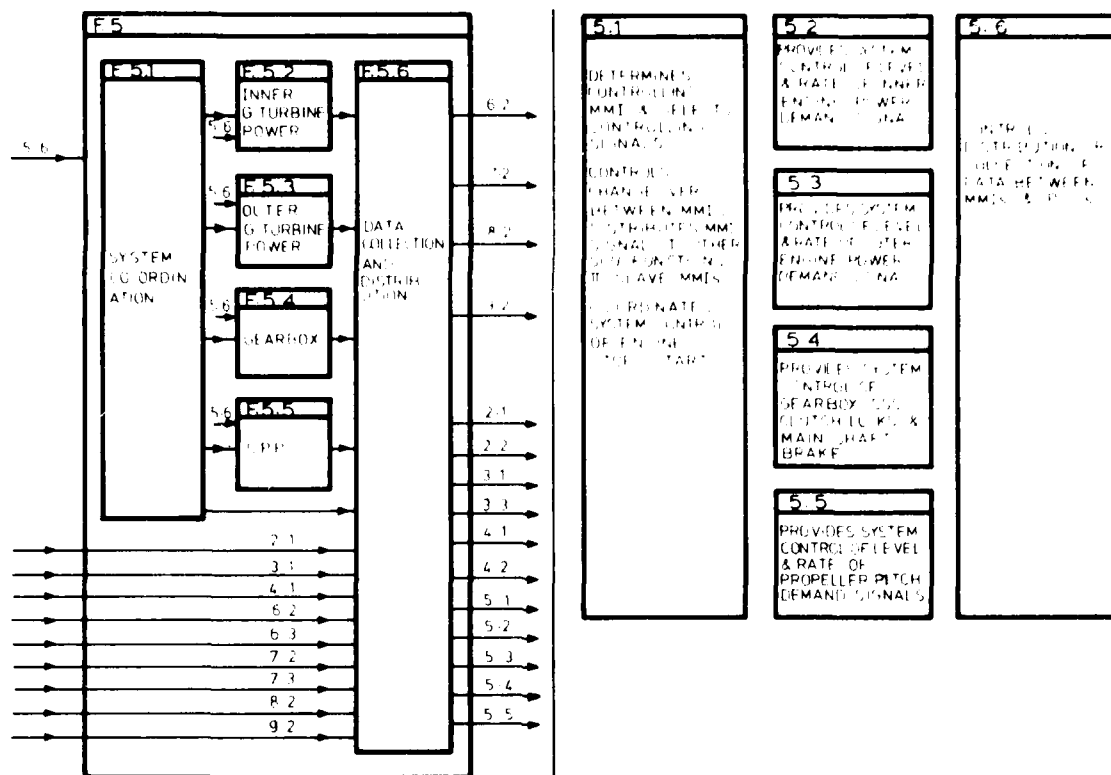


Figure 5. Reference Control System (Second Level)  
System Control Unit

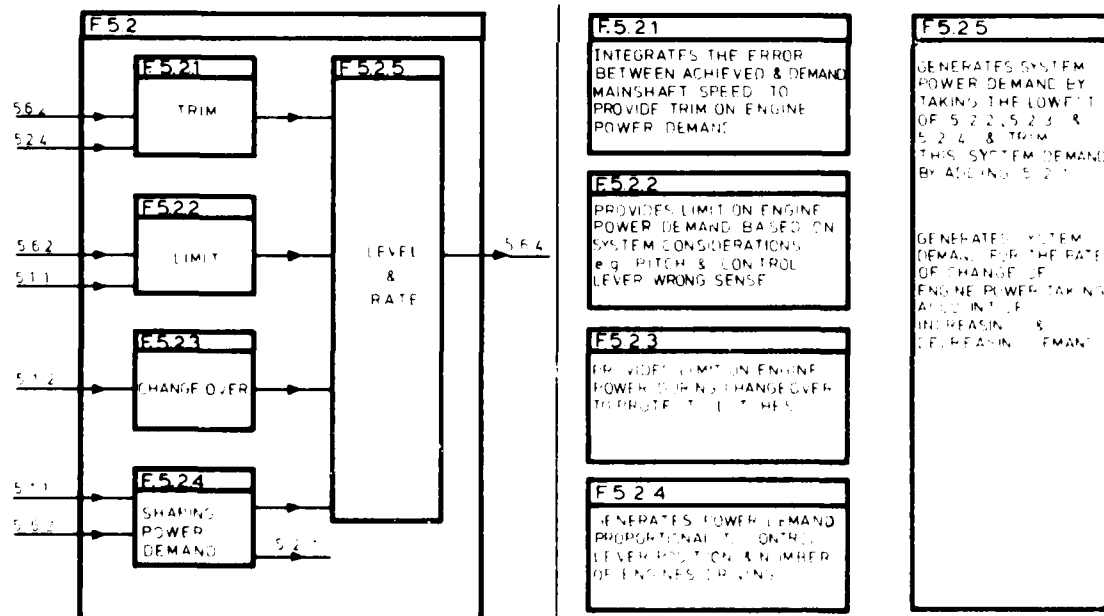


Figure 6. Reference Control System (Third Level)  
SCU - Inner Engine System Power Control

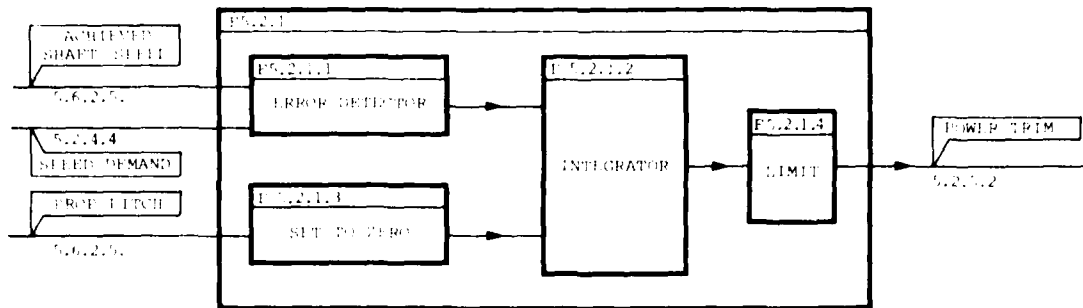


Figure 7. Reference Control System (Fourth Level)  
SCU - Engine Power Integral Control

#### Desirable Level of Functional Diagrams

Our experience is that the area of greatest debate in specifying a new control and surveillance system is that of the scope of the MMIs and in particular the individual parameters to be displayed upon them. This particular study has been no different and we have found that, while the control system definitions remained largely unchanged during the latter part of the study, the individual MMI surveillance parameters changed as the study progressed.

We had initially taken the functional diagrams to the fourth level for the control units and the MMIs. We now consider that fourth-level functional diagrams are very worthwhile, but that the third level is sufficient for MMIs when backed up by appropriate tables of surveillance information.

#### REFERENCE DOCUMENT

The foregoing reference control system design was established as part of a "Reference Document" which defines the system in functional terms, allowing the control and surveillance system configuration to be hardware independent and to be specified purely from ship operational and propulsion plant requirements. Because the control system definition is dependent on ship and machinery configuration then, provided sufficient options are covered in the Reference Document, it is possible to readily produce the controls configuration for a particular ship fit from it.

The reference ship for which the preceding controls definition was evolved was thought to resemble closely the next most likely ship fit. The fact that the reference ship was also in the mid-range of the ship types considered to be feasible in the future, was an added attribute. The actual range of ship fits considered in the Reference Document is shown in Table 1.

In developing the Reference Document the approach was to fully progress the design for the reference ship and to test the sensitivity of this design to the differing control requirements of the alternative machinery types and the individual MMI requirements of the different ship roles. In addition, within each machinery type, the control functions were defined so that, where possible, hardware components or software modules could be common in different parts of the system e.g. control schedules or limit schedules. The definition of the controls and surveillance for alternative ship fits was taken to the third level in the functional diagrams.

The Reference Document is structured such that the decision for the control philosophies, functions and surveillance configurations is recorded in a manner compatible with the functional diagrams. It provides a means, therefore, to rapidly define a control and surveillance system for a wide variety of ship fits.

Table 1. Selection of Machinery Configurations

Ship Role	Configuration	Description	Selected on Control Basis	Selected on MM Basis	Comment
Cruiser	COGAG	One SMIA & One Olympus per shaft: Two shaft sets : CPP	No	Yes	Assume Olympus PCU same as SMIA in future
Destroyer	COGAG	Two SMIA per shaft : Two shaft sets : CPP	Yes	Yes	Reference ship
Destroyer	COGAG	Two SMIA per shaft : Two shaft sets : reversing gearbox	Yes	No	Selected as option to reference ship to examine reversing gearbox
Frigate	CONAG	Three SMIA into combining gearbox with two CP propellers	Yes	Yes	Examine effects of multiple GT into combining gearbox
Frigate	CONAG	Two Diesels per shaft : Two shaft sets : CPP	Yes	No	Selected to examine load sharing requirements
Frigate	COGOG	One SMIA & One Diesel per shaft : Two shaft sets : CPP	Yes	No	Selected to examine COGOG control requirements
Corvette/ Patrol Craft	COGOG	One SMIA & One Diesel into combining gearbox with two CP propellers	Yes	Yes	Selected to examine independent pitch with diesel also small craft MM

## APPLICATIONS

## The Reference Controls System Demonstrator

In advance of a new ship requirement, it was decided to design and procure the reference control system in a demonstrator form for evaluation as a complete system at a centre to be specially set up at NGTE for this purpose. At this centre the propulsion machinery and hydrodynamic effects are to be simulated by digital computer equipment to interface the reference control system for real time operation. The evaluation centre will be used to validate the equipment interfaces and system performance of the reference control and surveillance system, to develop operator strategies, to evolve maintenance and servicing procedures, etc.

For the 'demonstrator' system to be developed a statement of requirements was needed so that project definition studies could be let to possible contractors. The functional definition of the 'demonstrator' system was able to be completed quickly because the "reference" system was fully defined. In fact the only major differences were in the number and scope of the MMIs.

It took three weeks to produce the 'demonstrator' system's statements of requirements and the majority of this time was spent in discussion of contractual aspects.

It is interesting to note that, although the statement of requirements was structured in functional terms, the contractors responding to it unilaterally selected the use of digital based control hardware.

## Next New Construction Ship

Some significantly different ship configuration proposals are expected in the future but even though these could possibly have different main propulsion machinery it is anticipated that the controls and surveillance definition of the "reference" system should apply. The reference ship provisions are ideal in kind, and more than adequate in timescale, for application to the next warship project.

#### ACKNOWLEDGEMENT

The encouragement given by Director General, Ships, and by the directors of YARD Limited is gratefully acknowledged, as is the generous assistance of the authors' colleagues. Where opinions are expressed they are those of the authors and not necessarily those of H.M. Government.

#### REFERENCES

- (1) Lt.Cdr. J. Steinhausen and J.N. Orton, "A Structural Approach to Man-Machinery Interface Design for Machinery Control", Fifth Ship Control Systems Symposium, Annapolis, USA, October 1978.
- (2) I.W. Pirie and J.B. McHale, "Evaluation of Digital Technology for use in Naval Propulsion Control Systems", Ibid.
- (3) Lt.Cdr. R. Whalley and B. Gladman, "The Formulation of a Computer Policy for Real-Time Shipborne Digital Systems", Ibid.
- (4) Capt. P. Reeves and J.B. Spencer, "Ship Automation in the Royal Navy", Ibid.
- (5) A. Duberley and I.W. Pirie, "An Evaluation Facility for Machinery Control, Surveillance and Display Systems", Ibid.
- (6) J.B. Willcox, I.A. Watson and P.J. Tharratt, "The Role of Reliability in establishing Plant Control and Surveillance Requirements for Warships", National Reliability Conference, University of Nottingham, U.K., September 1977.



AN ANALOGUE PRESENT, A DIGITAL FUTURE  
FOR MARINE PROPULSION CONTROL?

by N.D. Probert B.Sc.  
Hawker Siddeley Dynamics Engineering

SYNOPSIS

The level of automation in Marine Propulsion Control Systems is increasing continually to meet modern operational requirements. The vast majority of electronic propulsion control systems at present in service use analogue circuit techniques. The introduction of the microprocessor, however, has made the use of digital technology a viable possibility.

This paper describes the development of analogue systems designed by Hawker Siddeley Dynamics Engineering Limited; from the original system built for the Type 21 frigate and Type 42 destroyer for the Royal Navy, to the latest systems built for the Niels Juel Class of Corvettes for the Royal Danish Navy. The advantages inherent in the concept of functional control zones, first applied to the Danish Corvette, are illustrated with regard to fundamental control system requirements.

The concept of a distributed control system, using 'on-plant' controllers, is outlined. The relative merits are discussed with respect to both analogue and digital implementation. It is shown that the use of distributed, microprocessor-based plant control units linked by serial data links results in a significant increase in system survivability under battle damage. Various control system configurations are considered, the use of a System Control Unit to co-ordinate the Plant Control Units is shown to provide a worthwhile reduction in the complexity of the data network.

It is emphasised that this paper represents the personal views of its author, and does not necessarily reflect either the opinion or the policy of Hawker Siddeley Dynamics Engineering Limited.

## 1. PROPULSION CONTROL SYSTEMS

### THE NEED FOR AUTOMATION

The degree of automation in the modern warship is increasing steadily to keep pace with changing operational requirements and the performance characteristics of the latest propulsion machinery.

- Two major factors are responsible for the increase in automation,
- The remote operation of major controls has become a necessity with the advent of nuclear, biological and chemical warfare and the resultant need to provide a protected area for ships personnel. The concept of a ship control centre (SCC) arose directly from this; sited below decks and fitted with control and surveillance equipment.
  - Automation has allowed the increased performance available with the use of aero-derived gas turbines and controllable pitch propellers to be utilised to the fullest extent.

### Propulsion Control System Requirements

The principal task of a propulsion control system (PCS) is the co-ordination of the various items of propulsion machinery to provide the desired ship performance, whilst including safeguards to prevent unsafe operation or allow machinery stress limitations to be exceeded. The PCS must programme engine power and propeller pitch in response to operator demands, and in addition start and stop power plants, and control the changeover from one driving mode to another.

Within this broad objective the design of a PCS is subject to a number of practical and often conflicting constraints:-

- The need for high system integrity; i.e. ability to survive partial system or plant failure.
- The need to provide a system which is reliable and simple to operate, together with the need for rapid fault diagnosis and ease of maintenance should a failure occur.
- The need to minimise space and weight.
- The need to provide flexibility and ease of modification to allow for changes in machinery fit, or in requirements.

### Technological Advances in Electronics

The implementation of a comprehensive and reliable propulsion control and surveillance system has been made possible by dramatic advances in electronic technology.

The earliest systems for remote operation of major controls used pneumatics; These systems were generally remote manual rather than fully automatic. The decision to use electronics in place of pneumatics involved a radical change in the concept of ship propulsion control.

In 1967 Hawker Siddeley Dynamics Engineering Limited began the development of the first electronic PCS for the Royal Navy to be fitted to a gas turbine powered warship. The object of this paper is to describe the development of this system into the present generation of analogue control systems and to outline possible future developments concomitant with the introduction of microprocessors and serial data links.

## 2. FUNCTION APPROACH

### ANALOGUE PAST - MODULAR APPROACH

The first electronic propulsion controls designed by HSDE were for the Type 21 frigate and Type 42 destroyer for the Royal Navy. The first system, fitted to HMS AMAZON the first of class Type 21 frigate, was commissioned in 1974. In this, and in its other applications, the HSDE system has provided 16 ship-years of reliable sea service.

Experience gained with this system in service allowed certain refinements to be made. However, whilst incorporating improvements in technology, the basic design philosophy of the system remained unchanged. Thus, certain inherent disadvantages remained which could not be eradicated simply by a change in technology, requiring instead a change in fundamental thinking.

The first generation of control systems were based upon a range of standard modules derived from proven items already employed in industrial control applications. The modules comprise up to seven analogue printed circuit cards (approximately 80mm by 80mm): each module containing specific types and groups of components; such as amplifiers, voltage controlled oscillators or stepper motor drives. A typical module is shown in Figure 1.

The modules are used as building blocks to construct the required control functions. To this end, a number of modules, usually six are plugged into a hard-wired chassis. In addition mini-modules, containing passive components, are fitted to the chassis to tailor the standard modules to specific tasks. The object being to create a range of ship independent modules, each application being catered for by specific mini-modules. Figure 2 shows a console during build; fitted with semi-complete chassis.

When this system was first conceived there existed a considerable degree of doubt concerning the reliability of electronics, especially in the harsh environment prevalent in a warship. The use of proven modules eliminated much of the risk related to the electronics itself, and allowed greater consideration to be given to the overall problem of introducing an automated propulsion control system.

This system has proved to be reliable and effective, and is said to be generally well-liked by its

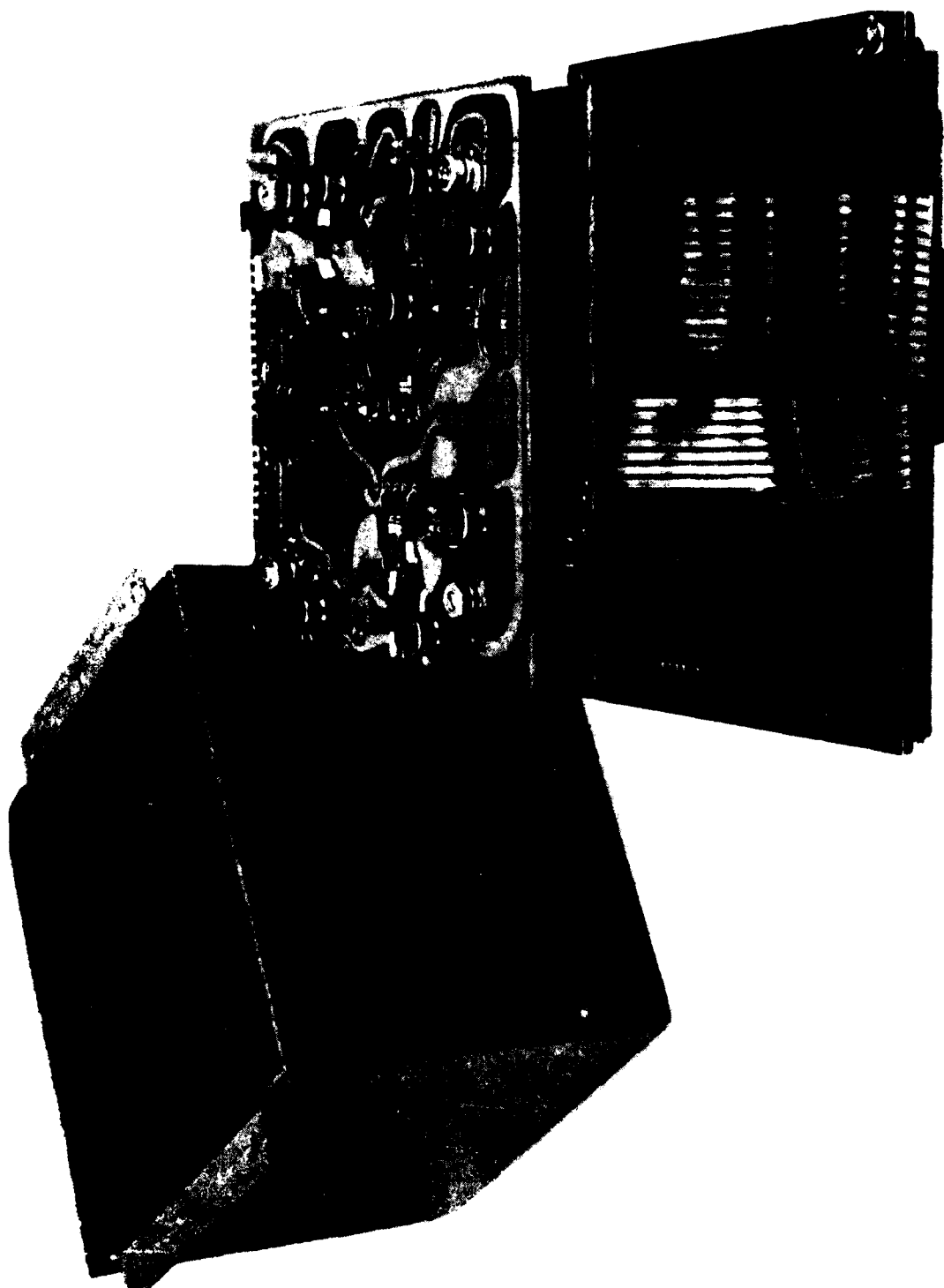


Figure 1: A Typical Module, showing constructional details

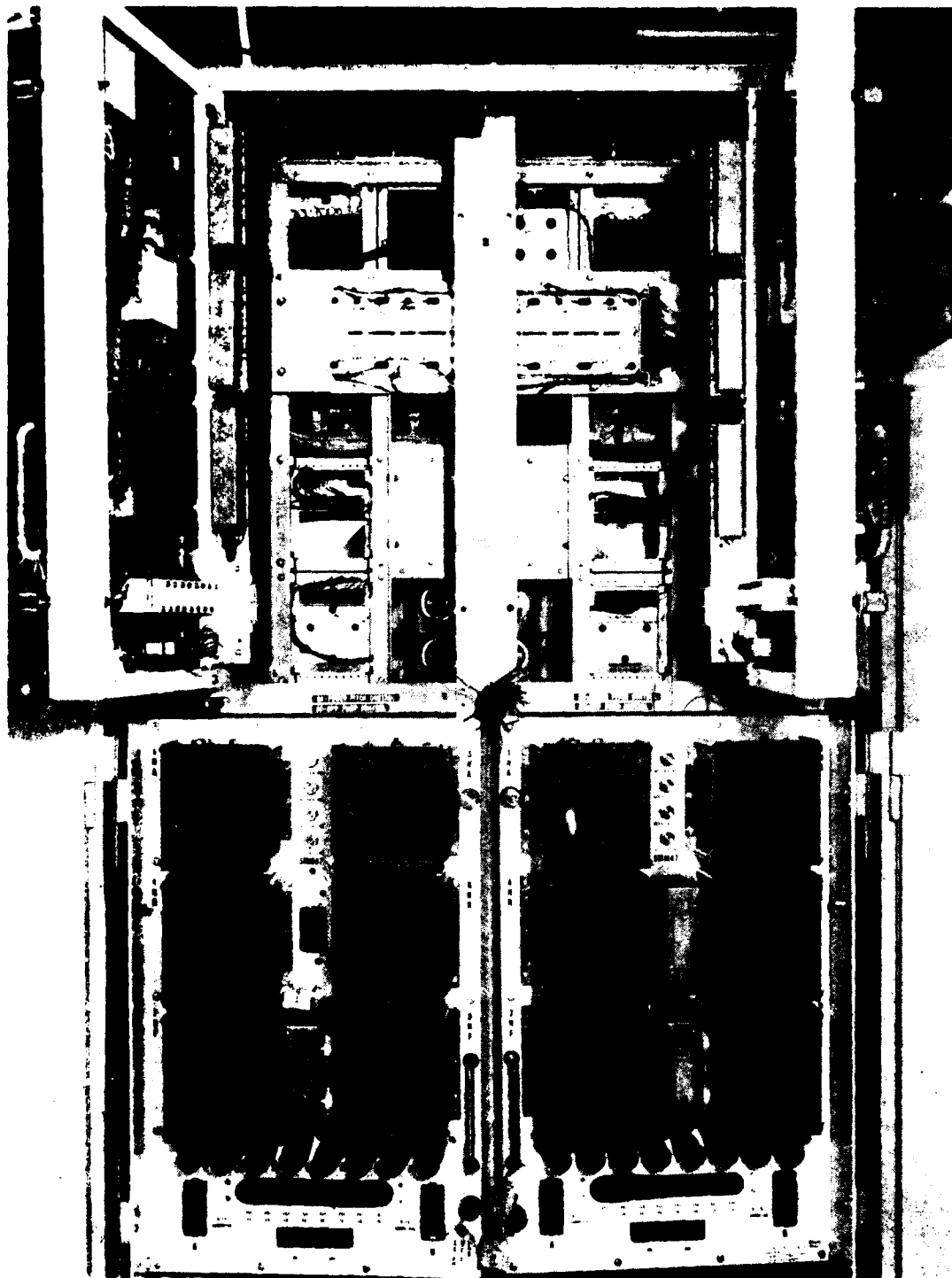


Figure 2: Rear View of Control Console during  
build, showing chassis

operators. However, the system does have drawbacks in the important areas of integrity and maintainability. These will be outlined more fully when compared to the present analogue systems.

#### ANALOGUE PRESENT - FUNCTIONAL APPROACH

Drawing on experience gained with their first propulsion control systems, HSDE undertook an exhaustive study into the likely future developments of marine control systems. The study reverted to basic principles, consideration being given to the functions required of the control system and to the parameters the system might control to implement these functions. Two major conclusions resulted from this study: firstly, the functional hardware equivalence in the system design; and secondly, the concept of a distributed control system.

#### Functional Control Zones

The main propulsion machinery for a typical naval application may be divided into three sub-systems:-

- Power plant
- Couplings
- Propeller

The propulsion control system provides control signals to each of these sub-systems to co-ordinate the application of power and pitch (when a controllable pitch propeller is fitted) in response to operator demands whilst maintaining the machinery within its design limitations.

Whatever machinery configuration is considered there are only a limited number of parameters upon which the propulsion control system can act to implement the desired control functions.

- Engine power level
- Rate of change of engine power level
- Coupling states
- Propeller pitch angle
- Rate of change of propeller pitch angle

The latter two assume a controllable pitch propeller. Figure 3 shows the main functional zones of a typical Naval application and indicates the parameters which can be controlled.

The identification of functional zones within the propulsion machinery leads to the concept of propulsion control system which is functionally distributed. The control system ceases to be a unit in which the control algorithms are implemented as a homogeneous function, instead the system is divided into functional zones each having authority over one sub-system of the propulsion machinery. Each zone is isolated from the other zones as far as possible.

There are, thus, three functional zones:-

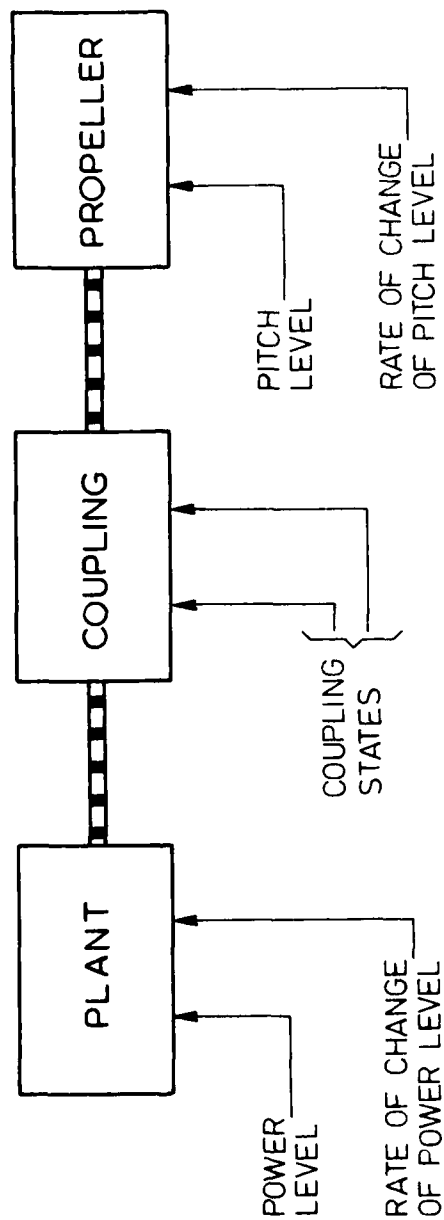


Figure 3: Function Control Zones

- Engine power : To provide a demanded power level and rate of change of power level.
- : To provide for engine starting and stopping.
- Coupling : To control their engagement and disengagement in response to system requirements.
- Propeller Pitch : To provide a demanded propeller pitch angle and rate of change of pitch angle.

Each sub-system controller is responsible for maintaining its sub-system within safe operational limits.

Each zone controls both steady-state and transient operation. The steady running control is organised as the main forward control path which may be modified by transient and limiting functions. The steady-running control is implemented in the simplest possible manner to increase reliability. Operation of the ship is possible if the steady-running control is functioning even if failures occur in the transient or limiting functions; although the introduction of extra operator procedures may prove necessary.

It is a major design objective that each shaft set of machinery be controlled by a single Power Control Lever (PCL) such that shaft speed is approximately linear with PCL position. To achieve this aim the forward control paths of both the Engine Power Zone and the Propeller Pitch Zone must implement the following functions:-

- Shaping function : provides a non-linear characteristic to generate an engine or pitch demand as a function of system demand. The demand to the engine may be in the form of throttle angle, fuel, speed etc. but the shaping function for both the engine and the propeller pitch is set such that the overall steady-state system demand to achieved shaft speed characteristic is maintained.
- Level and Rate Generator : operation of the PCL allows the output of the shaping function to be set anywhere within its range of values. However, the level of the demand and the rate of change of that demand must be controlled as a function of various plant parameters to ensure that design limits are not exceeded. The Level and Rate Generators provide means whereby the output of the shaping function may be modified by the transient and limiting functions.

The transient and limiting functions interface with the plant parameters to modify the forward control path demand during engine changeovers and manoeuvring; Figure 4 shows typical control functions.

#### Advantages of Functional Approach

Irrespective of the technology used, a system designed along the lines outlined above has a number of advantages over the previous



	Volume	Session	Page
Whyte, P. H. D.R.E.A. (Canada)	2	F2	3-1
Williams, K. E. MARA-TIME Marine Serv Corp.	5	Q1	1-1
Williams, V. E. National Maritime Research Center	1	C	1-1
Wolford, J. C. Naval Weapons Support Center	5	R	1-1
Zuidweg, J. Royal Netherlands Naval College (Neth)	3	J1	4-1

	Volume	Session	Page
van Amerongen, J. Delft Univ of Technology (Neth)	3	J2	4-1
van Dam, J. Royal Netherlands Naval College (Neth)	3	J1	4-1
van de Linde, J. G. C., RADM Chairman, Session Q1 Royal Netherlands Navy (Neth)			
van Nauta Lemke, H. Chairman, Session P Delft Univ (Neth)	3	J2	4-1
Verhage, W., LCDR Chairman, Session D The Royal Netherlands Naval College (Neth)			
Verlo, G. Det Norske Veritas 'Norway)	3	J1	2-1
Volta, E. Laboratoria per l'Automazione Navale (Italy)	4	P	4-1
Ware, J. Operations Research, Inc.	1	C	4-1
Whalen, J. Operations Research, Inc.	4	O2	2-1
Whalley, R., LCDR, RN Ministry of Defence (UK)	3	H	3-1
Wheatley, S. Chairman, Session N Natl Maritime Res Center			
Wheeler, D. J. Rolls Royce (UK)	1	B	2-1
Whitesel, H. K. David W. Taylor Naval Ship R&D Center	4	O2	3-1

AD-A159 082

PROCEEDINGS OF THE SHIP CONTROL SYSTEMS SYMPOSIUM (5TH)

4/4

HELD AT U S NAVAL... (U) DAVID W TAYLOR NAVAL SHIP

RESEARCH AND DEVELOPMENT CENTER ANN... P MARTIN ET AL.

UNCLASSIFIED

03 NOV 78

F/G 13/10

NL

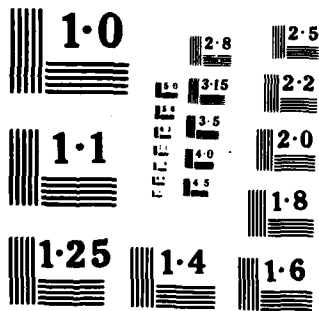
END

DATE

ENTER

11 85

DT



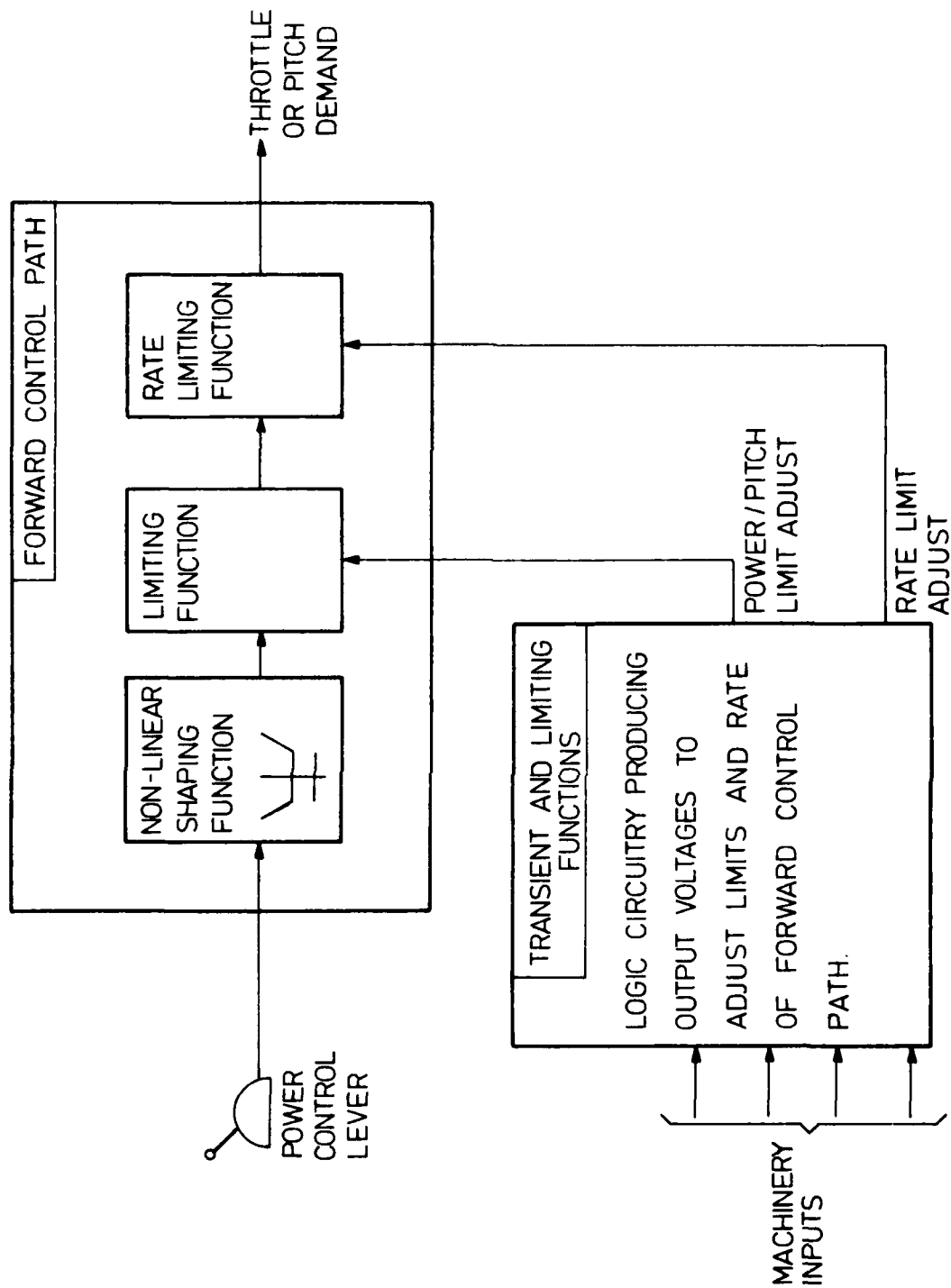


Figure 4: The Forward Control Path and its Modifying Functions

modular approach.

### Integrity

Integrity is a measure of the ability of the ship to continue functioning in the event of a partial plant or system failure. With the modular system adopted in the past the PCS is not sub-divided according to the machinery zones, thus, a fault occurring in, for example, the main gas turbine control may be found to be caused by any of a number of modules. Conversely, the failure of a single module can result in faulty control of more than one item of plant.

A control system sub-divided in accordance with the functional zones of the propulsion machinery obviates this problem to a large extent. All the control for, say, the port main gas turbine are located in three, or possibly four, printed circuit cards: one card provides the forward control path, one the transient and limiting functions and the other control start/stop sequencing. It follows, therefore, that should a fault occur in the controller for one particular zone, the other functional zones are able to continue operation due to this functional isolation.

In addition, should a fault occur in the limiting or start/stop cards, these may be removed from the system, and operation can continue using the forward control path alone; albeit with the introduction of extra operator procedures. This may not seem a significant advantage at first sight. However, the electronics themselves are generally reliable, failures are far more likely to occur in the transducers sending information back to the PCS, or in the wires used to transmit this information. A transducer failure could result in incorrect operation of the PCS; all inputs from machinery, however, are via the transient and limiting card. Hence, removal of this card isolates the PCS from the machinery and any faults therein. The ship may thus be kept operational whilst repairs are performed.

### Maintainance and Fault Diagnosis

Together with the increase in system integrity achieved by the adoption of the functional design approach is a reduction in related problems of maintainance and fault diagnosis. A problem occurring in for example, the pitch system can be quickly identified as only a limited number of cards relate to the pitch control zone. In addition, by grouping the cards according to their functional zones the operation of the system becomes clear to those who have to work with it, Figure 5 shows how a typical control system could be arranged.

### Flexibility

The isolation of the functional control zones has the added advantage of increasing the flexibility of the control system. A specific control zone can be modified to allow for a change in operational

1. Gas Turbine Power Demand
2. Diesel Speed Demand
3. Pitch Demand
4. Gas Turbine Limiting
5. Diesel Limiting
6. Pitch Limiting
7. Gas Turbine Start/Stop
8. Gas Turbine Start Interlocks
9. Diesel Start Interlocks
10. Clutch Selection
11. Demodulator Gain (4 Channel)
12. Dual Demodulator
13. Motor Drive
14. Dual Speed Probe
15. Current Driver
16. Power Supply
17. Integrity Monitor
18. Gas Turbine Actuator
19. Gas Turbine Engine Controller
20. Diesel On Engine Controller
21. Power Control Lever

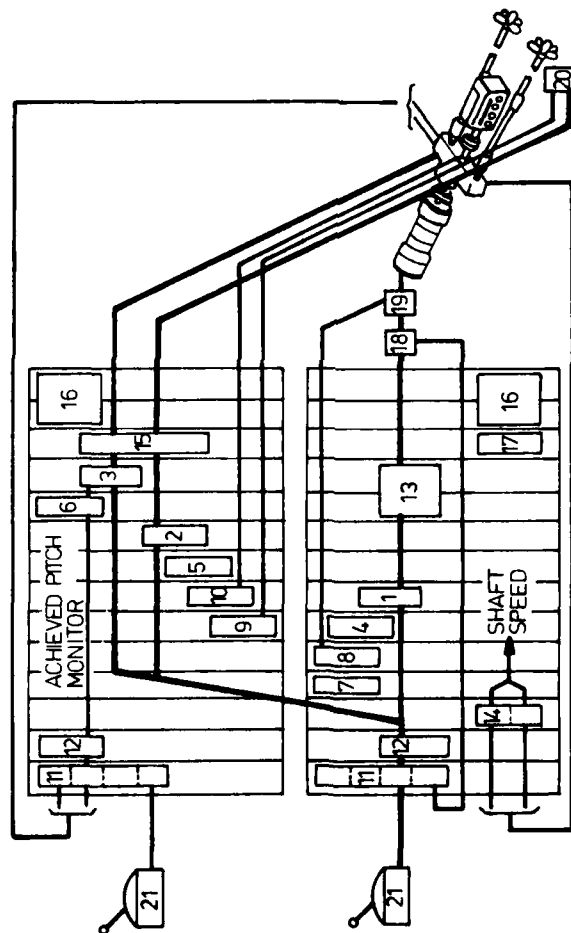


Figure 5: Typical Schematic Arrangement of Propulsion Control System for CODOG

requirements or machinery whilst no other control zone is affected.

#### Practical Application of Functional Approach

The functional-to-hardware design concept was used by HSDE Ltd. for their propulsion control system fitted to the Niels Juel Class of Corvettes for the Royal Danish Navy: Figure 7 shows the completed unit. The system consists of printed circuit cards, as shown in Figure 6, housed in three standard 19 inch racks. Interconnection between cards is via back-plane wiring as can be seen in Figure 8. All signals into and out of the PCS are routed through a filter and suppression unit; the top left hand unit in Figure 7.

The adoption of a racking system led to savings both in cost and in weight. Trials have shown the effectiveness of the design approach, in that faults are quickly identified and modifications easily introduced.

#### CONTROL SYSTEM CONFIGURATION

The choice of control system configuration allows a multitude of possibilities within the following two extremes:-

- A single, centralised control system, incorporating the controllers for each of the machinery sub-systems; with local plant actuators to provide the requisite output power. This arrangement is outlined in block diagram form in Figure 9.
- A totally distributed control system, consisting of remote machinery control positions connected to Plant Control Units (PCU) mounted on or near to machinery they control, Figure 10 shows a distributed system in block diagram form. The PCU has as its input a demand from the remote PCL, and contains within it both the steady-running and transient control functions relating to that item of plant.

As with the concept of functional control zones, certain characteristics of a distributed system may be stated, irrespective of the technology chosen to implement them.

Concentration of all plant controllers within a small area, as in a centralised system, renders such a system highly susceptible to battle damage. Geographical distribution of the plant controllers reduces the likelihood of total system failure due to battle damage, although the multiplicity of inter-connecting wires is still an area of vulnerability. The increase in the survivability of the ship as a whole is the main advantage achieved by the adoption of a distributed control system utilising on-plant controllers.

In addition to the reduction of vulnerability a distributed system is highly flexible, since the plant controllers are isolated one from another. Similarly, the identification of a plant controller to each major item of plant eases fault diagnosis and maintenance problems.



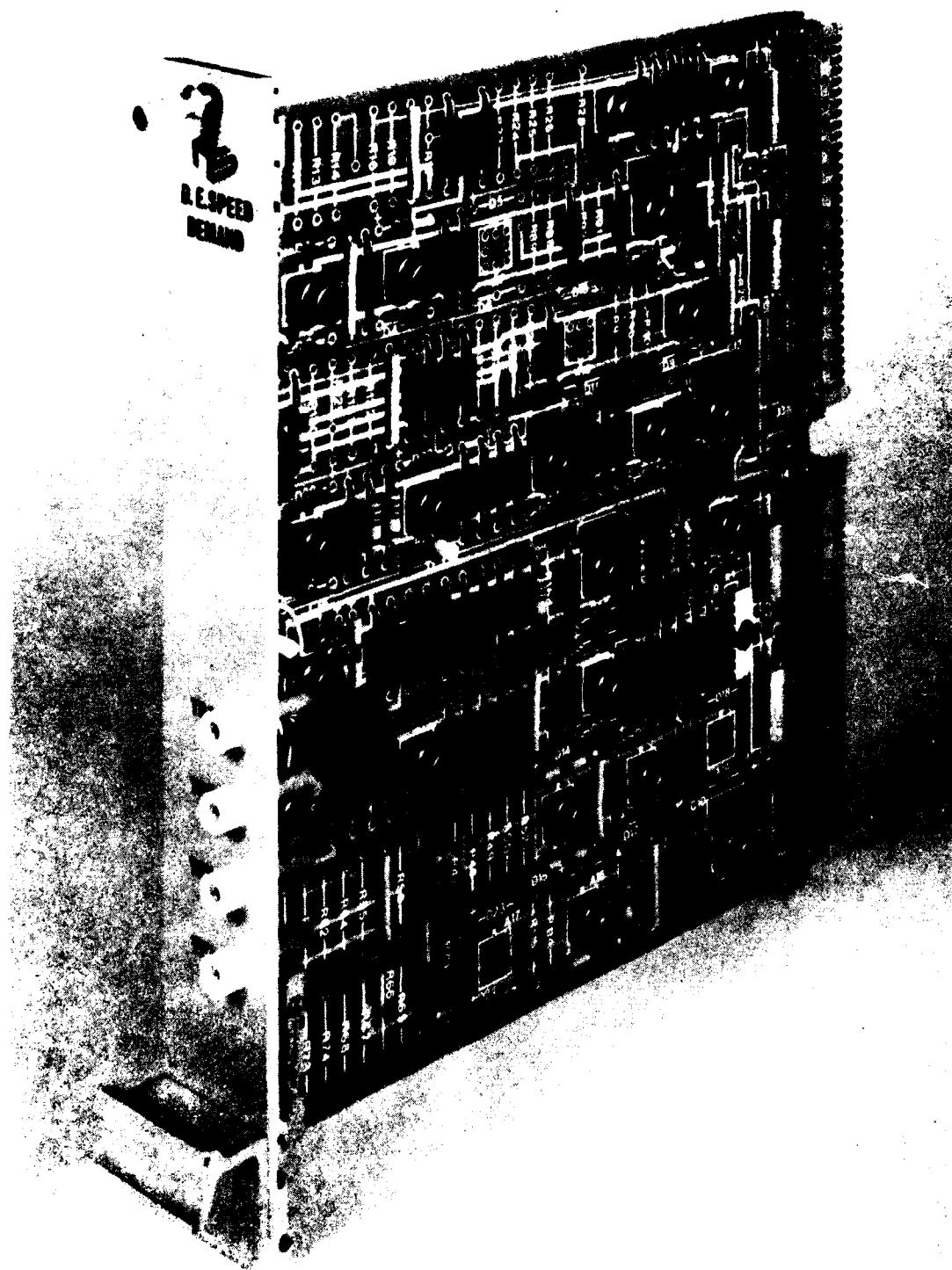


Figure 6: A Printed Circuit Card as used  
on the Danish Corvette

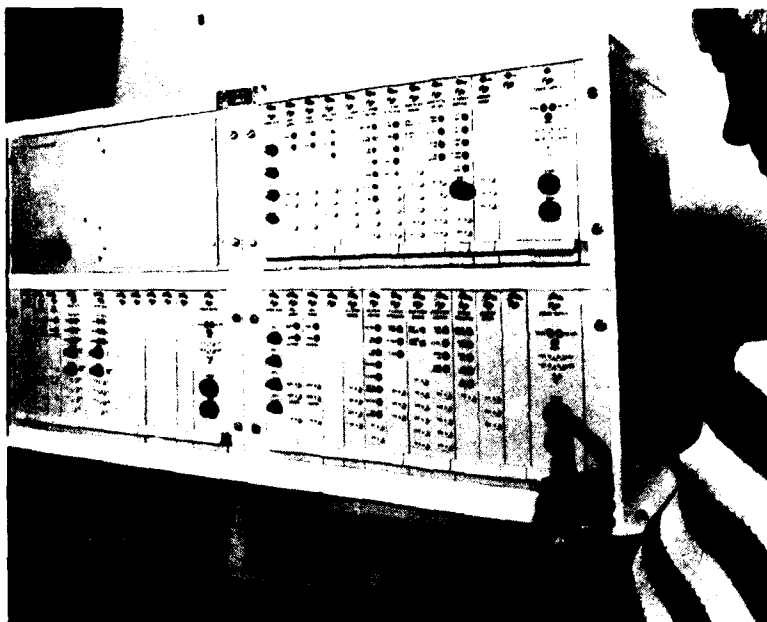


Figure 7: The Propulsion Control System  
Supplied for the Danish Corvette

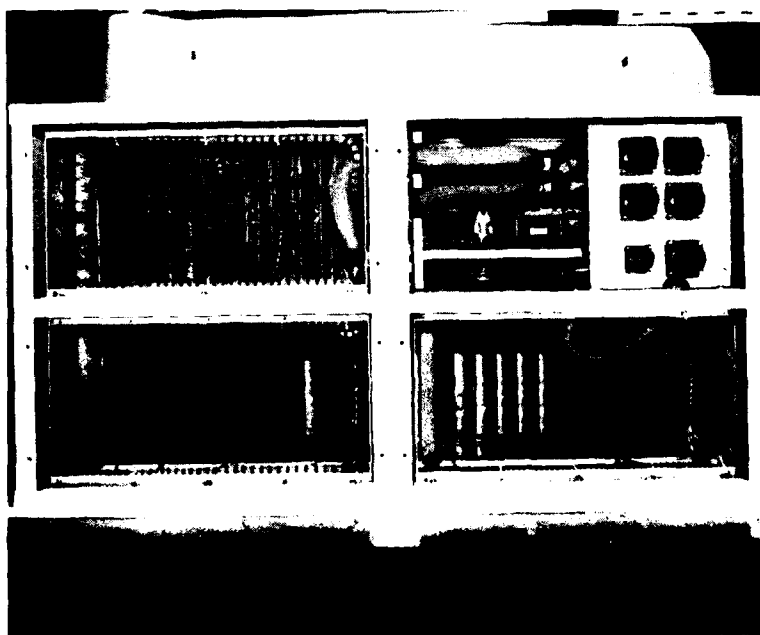


Figure 8: Rear View of Propulsion Control  
System showing Back-plane Wiring

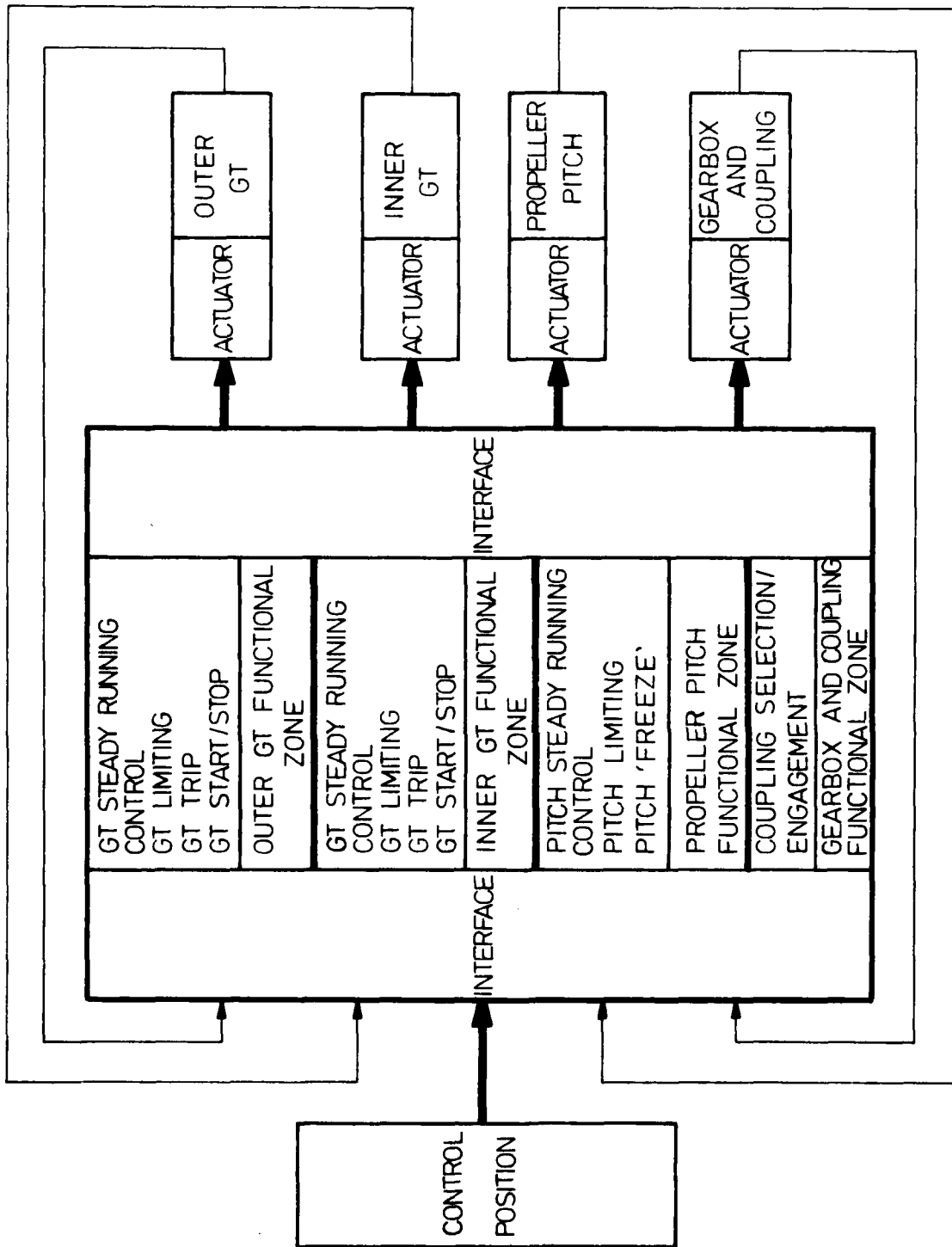


Figure 9: Schematic Representation of a Centralised Control System

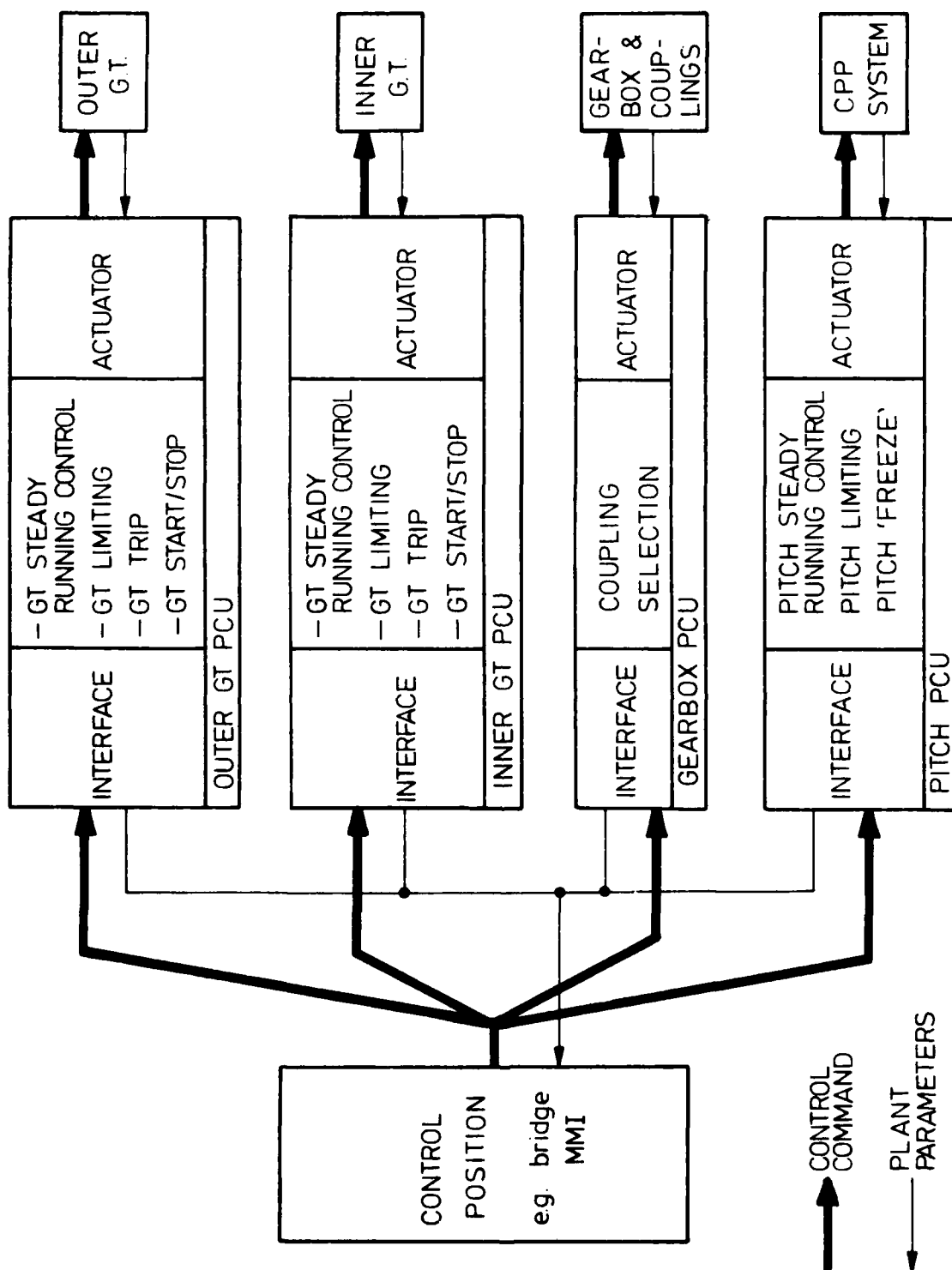


Figure 10: Schematic Representation of a Distributed Control System

There are, however, disadvantages inherent in this configuration: such as the difficulty of setting-up and optimising geographically separate controllers. In addition, extra design constraints are necessary as the environment within the machinery spaces is harsher than that found in the S.C.C. (Ship Control Centre). Equipment has to be sealed against the environment to prevent the ingress of dirt and moisture. This demands careful design if forced cooling is to be avoided. Shock and vibration criteria are also more severe in the machinery spaces, requiring anti-shock mounting and a rigid assembly.

The advantages of a distributed system tend to be outweighed by the practical disadvantages of implementation when an analogue implementation is considered. Many of the advantages inherent in a distributed system may be achieved in a functionally sub-divided centralised control system; flexibility, ease of maintenance and fault diagnosis and high system integrity, for example.

Thus, it can be said, that for the present a centralised control system based upon the functional zones of the propulsion machinery offers the best solution to problem of propulsion control system design. However, whilst improvements in analogue technology will lead to a simplification of the electronic circuitry required, reducing the component count and increasing reliability, future major advances in propulsion control systems will revolve around digital designs using the computing power of microprocessors.

### 3. DIGITAL FUTURE

#### DIGITAL TECHNOLOGY

The continuing trend towards miniaturisation of electronic components has reduced the size and component count of electronic control systems. With the introduction of Large Scale Integration (LSI) techniques the number of components used in a chip has increased manyfold, and has allowed the development of microprocessors which have the processing capability of early computers at a fraction of the size.

Microprocessors are already used in many industrial applications, increased flexibility and reliability being obvious advantages. On board ship microprocessors make distributed control systems a viable possibility by allowing processing power to be dispersed to 'on-plant' controllers. In addition, communication between the various microprocessor-based controllers can utilise serial data links (SDL). The microprocessor controls the distribution of data along the SDL; converting 8-bit or 16-bit parallel words into serial form for transmission, etc. The use of a SDL allows a dramatic reduction in the amount of wiring required - with a great saving in both cost and weight - and also allows duplication to increase the system integrity.

## Advantages of Microprocessor Based System

A microprocessor-based distributed system has the following advantages, in addition to those common to any distributed system, which offset many of the aforementioned disadvantages:-

- Common hardware : the microprocessor, its store and interfaces will be the same for a range of applications. The software contained in the microprocessor and its store will be specific to each application, however certain elements of the software will also be common; such as the programmes controlling the use of the data highway or those generating arithmetic functions.
- Flexibility : the nature of the system ensures that much of the hardware is ship independent. If a modular approach to software construction operation and testing (MASCOT) is adopted, then much of the software is also application independent. Also modifications and additional control functions or sequences can usually be introduced without hardware changes.
- Health and Trend Monitoring : health monitoring and long term trend analysis can be readily incorporated into the system, making use of the spare computing power available at the PCU's. This facility can be used to predict major plant failures.
- Auto-test : whilst automatic fault diagnosis and self repair remain within the realms of science fiction, the spare processing power available can be used for routine automatic testing and to assist in fault diagnosis. This possibly is one of the major advantages offered by a microprocessor-based system. Assuming a policy of 'Repair by Exchange' is adopted, then the system must identify which item the maintainer must replace to allow continued operation in order that a satisfactorily low Mean Time To Repair (MTTR) may be achieved. It is becoming recognised that present automated systems largely absolve the operator from decision making and hence reduce job satisfaction. At the same time, however, highly trained personnel are required should a fault occur. The discrepancy existing between the skills required for routine observation and those required for fault diagnosis and repair is a common problem in automated systems. The aim of the microprocessor-based system must be to reduce the skill required for fault diagnosis by inclusion of automatic test routines, thus obviating the need for highly trained technical operators.
- Reduced cabling requirement : as stated previously, the introduction of microprocessors allows the use of Serial Data Links. The SDL can be used to replace with a single multi-core wire all the wiring previously necessary to link the SCC with the plant. This allows a considerable saving in both weight and cost. More importantly, however, duplication or even triplication is a possibility. If the SDL are routed via geographical separate paths then the likelihood of system failure due to battle damage is substantially reduced.

## Distributed System Configuration

The fully distributed system outlined in Figure 10 is not representative of a typical Naval application. A more likely configuration

is shown in Figure 11; each shaft set comprising two engine PCU's, one gearbox PCU and one CPP PCU. Both shafts sets are controlled from either the SCC, the Bridge or the Operations Room. In addition, certain parameters, such as achieved pitch must be transmitted from one PCU to another. From Figure 11 it can be seen that the number of point-to-point links provide an unacceptable penalty. There are two solutions to this problem;

- The use of some form of adaptive routing to reduce the number of SDL required.
- The introduction of a centralised system control unit to co-ordinate the operation of the PCU's.

#### Adaptive Routing

Adaptive Routing Packet Switching (ARPS) is a name given to a method of communication between 'intelligent' sub-systems connected in a network rather than by point-to-point links. Each sub-system requiring access to the communications system has a node, or Highway Access Unit (HAU), consisting of serial communication interfaces linked to the microprocessor. The nodes are connected by SDL so as to provide a number of alternate routes between any two nodes that need to communicate. Each node possesses a table that defines the preferred routing to a particular node. The system is adaptive in that should failure of a particular link be detected the system alters the route table at each node to avoid its use.

The information to be transmitted is first converted from parallel to serial form. The message controller located in the HAU adds to this data an envelope of priority and check bits together with details of the final address, it then dispatches the envelope along the first leg of the preferred route.

On reaching its destination, the message is decoded, converted back to parallel form and is received by the acceptor microprocessor. If confirmation of correct receipt is not received within a specified time, diagnostic and re-routing procedures are initiated. The operation of ARPS is shown schematically in Figure 13.

#### System Control Unit

An alternative solution to the use of adaptive routing package switching is the introduction of a System Control Unit (SCU) as shown in Figure 12. In its simplest form the SCU controls the distribution of control signals and plant information throughout the system; however, the SCU can also contain control functions to co-ordinate the operation of the individual PCU's. The introduction of the SCU introduces a vulnerable element into the system; should the SCU fail all remote operation using the microprocessor system is rendered inoperative. Duplication of the SCU is not considered practical; partly due to cost, partly due to the difficulties that arise during changeover from one unit to its replacement. Provision must be made for extensive

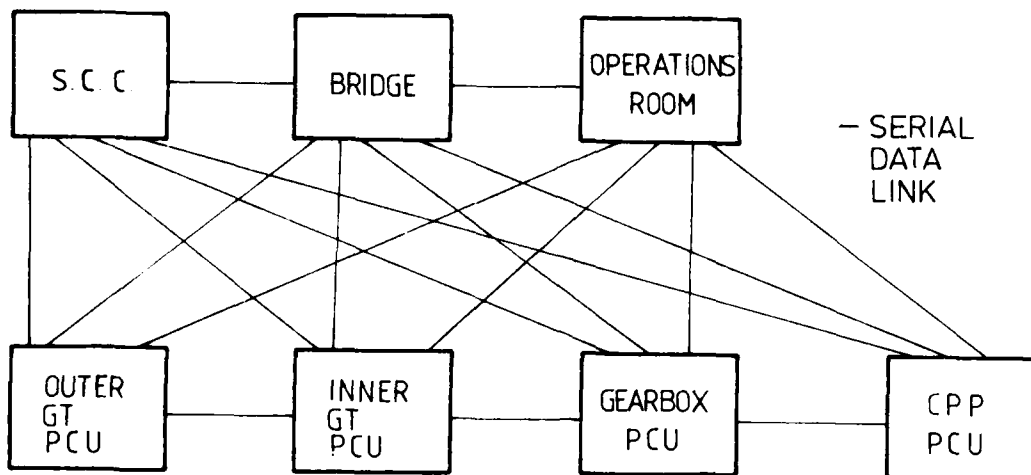


Figure 11: Communications Network required for a typical fully distributed system

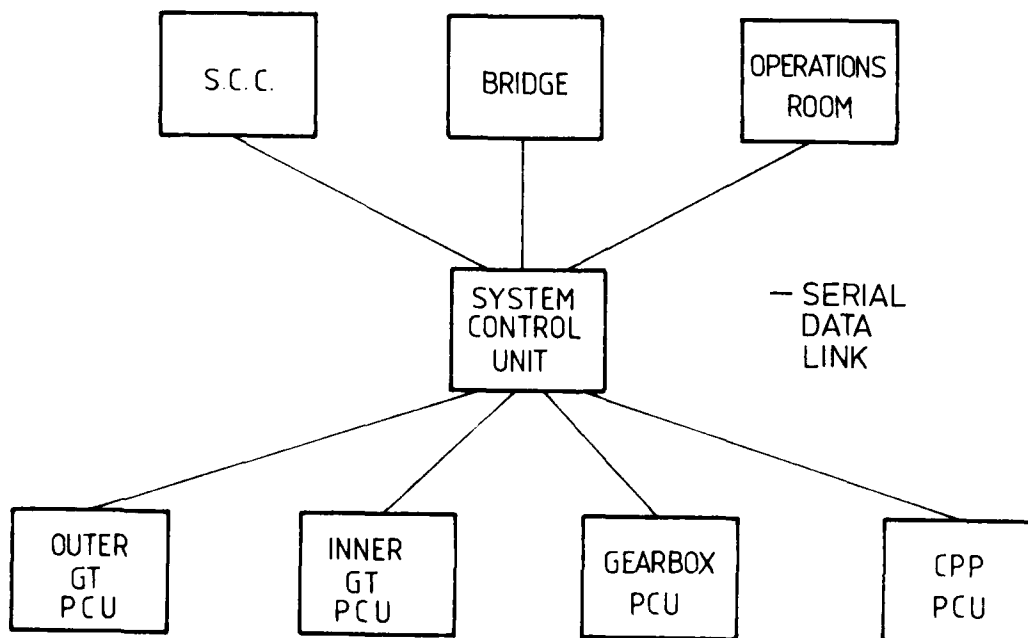


Figure 12: Communications Network for distributed system incorporating a System Control Unit



The engine will continue running at its previously selected condition, and control of the engine can be achieved using the manual reversion capability provided on the throttle valve.

Thus it can be seen that a very comprehensive safety system exists which takes all necessary action to protect the engine in the event of a control failure, but at the same time maintains the maximum use of remaining control functions.

The safety circuits were designed following a failure modes and effects analysis. Associated reliability analyses are discussed in the next section.

#### RELIABILITY

The reliability analysis of electronic systems is normally carried out by assessing the circuits on a component by component basis, using data from a standard source, and takes into account the operating temperature, the utilization of the equipment and include an allowance for joints, wiring, maintenance damage etc. For gas turbine engine control systems this approach has been found by experience to give a very realistic reliability figure for the overall equipment.

A preliminary calculation (6) for the electronic control gives the total failure rate to be 150 failures per  $10^6$  hours. However, it should be noted that the number of failures resulting in a throttle freeze and subsequent reversion to manual engine control would be much less than this figure.

A reliability estimate for the hydraulic system, based largely on field service figures for similar equipment, including the pump, hydromechanical governor, pressure drop unit, throttle and stepper motor gives a figure of 50 failures per  $10^6$  hours.

The overall figure for the system of 200 failures per million hours gives a Mean Time Between Confirmed Defects of 5000 hours, which for a gas turbine powered ship would probably represent about 2 years service at sea. This is considered to be a very acceptable figure, contributing towards an excellent system availability.

#### MAINTAINABILITY

Considering the hydraulic system first, marine engine control systems have an advantage over their aircraft counterparts in that they do not need to be integrated to the same extent to save space and weight. This gives improved accessibility and allows piece part replacement.

A high standard of maintainability of the electronic control unit is achieved by means of the modular constructional techniques used, and by means of built in fault diagnostic displays and purpose built test equipment.

The construction of the unit is illustrated in prototype form in Fig.5.

The unit is rack mounted on a sliding frame, which allows the whole unit to be withdrawn from the cubicle and rotated to gain access to the rear connections.

Each board (23 total) is removable for repair, by unscrewing the fixing at the top.

If, however, the  $N_3$  (control) channel has failed, as detected by the circuit in the upper part of the diagram, the " $N_3$  control failed" signal is passed onto the Supervisory Logic which decides what action to take.

#### Supervisory Logic

Inputs from all the other safety circuits in the system are also passed onto the Supervisory Logic, the output of which can take one of three states, depending on circumstances, as follows:-

##### a) Ready To Start Signal

This is for indication only and will not actually inhibit an engine start. The signal is on when:-

- All trip channels are clear
- There are no safety circuit failures
- The shut off valve is open
- The throttle position  $\theta_A$  is at minimum

##### b) Control Failed Signal

This is again indication only for faults which, although giving degraded control are not serious enough to need a throttle freeze.

Examples of these are:-

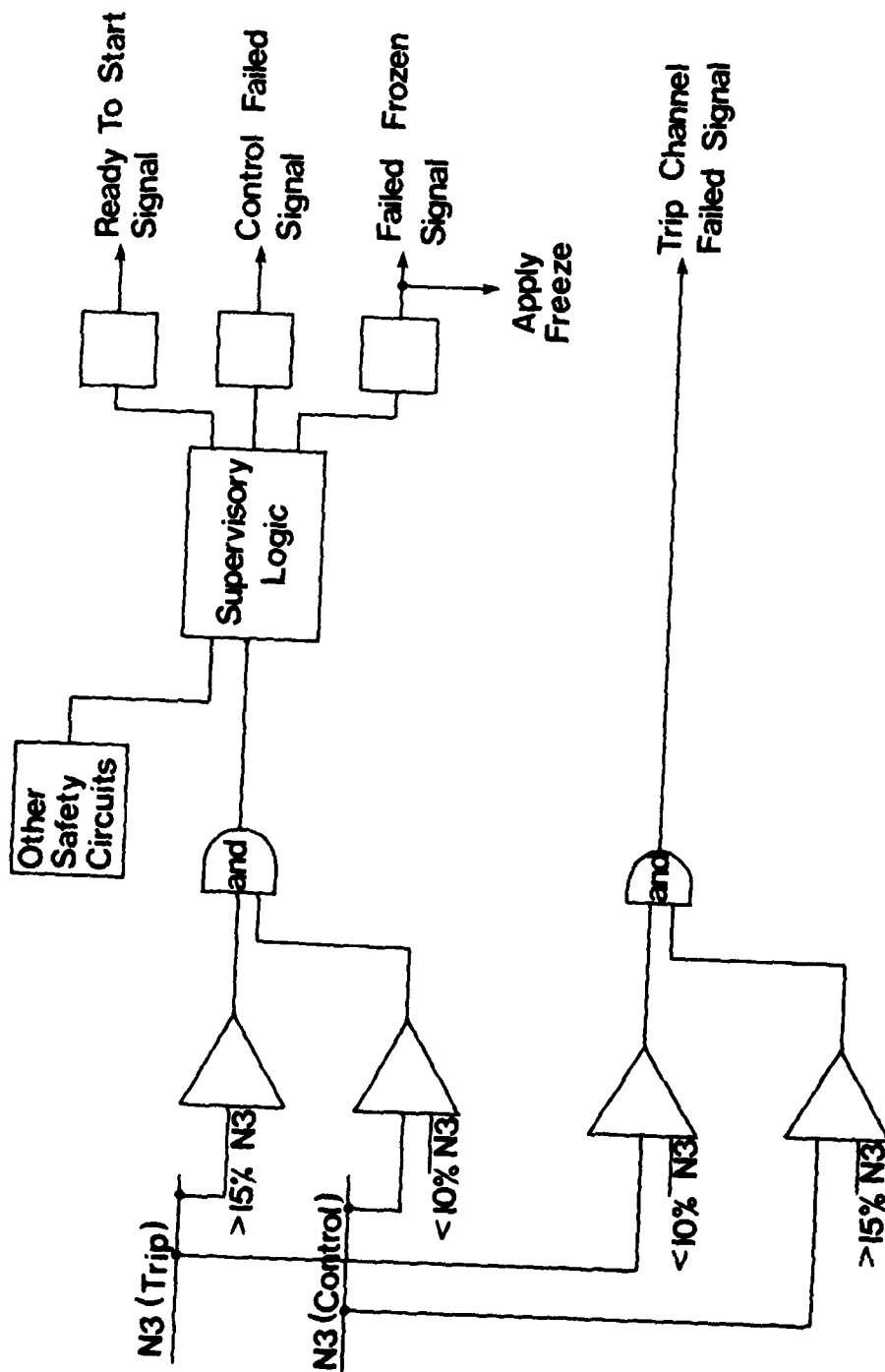
- $T_1$  bias failed
- $N_3$  control failed
- $T_6$  control failed
- Minor supply rail failure
- $N_1$  limit failed
- Flow schedules failed
- HP7 failed

##### c) Apply Freeze Signal

In this case, the control failed indication is given, also a Failed Frozen indication is given and a freeze signal is applied to the stepper motor drive circuits.

Failure in this category are:-

- Error amplifiers failed
- Integrator failed
- Supply rails failed
- Throttle position signal  $\theta_A$  outside limits
- Power Demand signal failed
- Stepper motor or drive circuit failed



G 3-9

Example of Safety Circuitry

Fig. 4

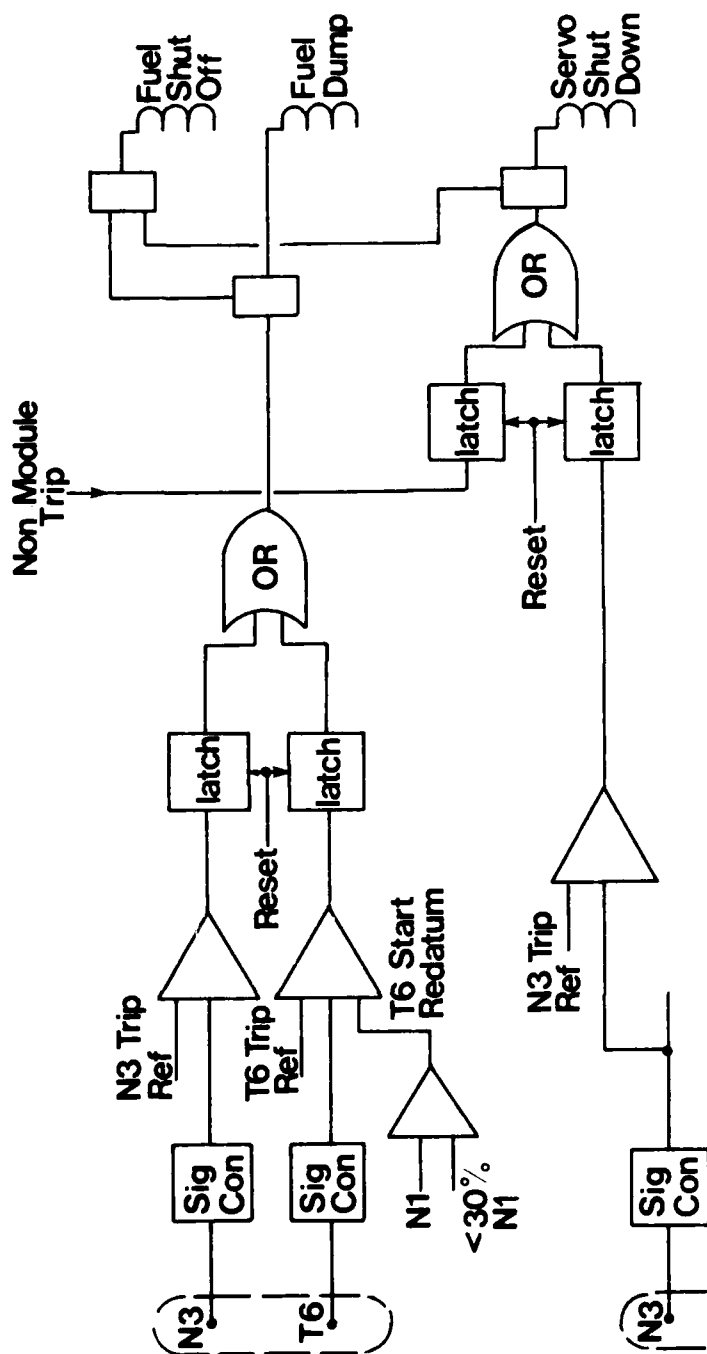


Fig. 3

## Trip Channels

Gas generator overspeed is catered for by the top speed limiter on N1 with duplicated N1 transducers. Power Turbine overspeed is catered for by the N3 limiter in the main control and a separate overspeed trip circuit which is described in more detail below.

Engine stall or flameout during power changes are catered for by the acceleration and deceleration schedules provided.

In the event of failure of the HP7 transducer which is used to generate the acceleration schedule, accelerations are automatically controlled at a safe rate by means of a back up acceleration control (see Fig. 1). The integrator input is limited to a constant low value, thus a steadily increasing Slave Datum signal at the integrator output is produced and the engine follows this demand due to the action of the inner  $N_1$  closed loop control.

Engine overtemperature is catered for by the T6 limiter plus a separate trip circuit similar to the N3 trip.

Unscheduled shutdown and power changes are avoided by the comprehensive safety circuitry built into the control together with the inherent fail frozen capability of the stepper motor interface.

Maintenance of set conditions is assured by the use of isochronous governing. Any desired power level can be accurately held for as long as required.

#### Trip Channel

The separate overspeed and overtemperature trip channels are shown in Fig.3, which will shut the engine down if triggered. In the case of N3, one of the trip circuits uses the same transducer as the main control, and the second trip circuit has its own independent transducer.

In the case of  $T_6$ , this channel has its own thermocouples independent of the main control. A redatum facility is provided to avoid unwanted trips during start up. A facility for incorporating an external trip signal is also included, and each trip channel has its own test and reset circuit to prove its operation during routine maintenance.

#### Safety Circuits

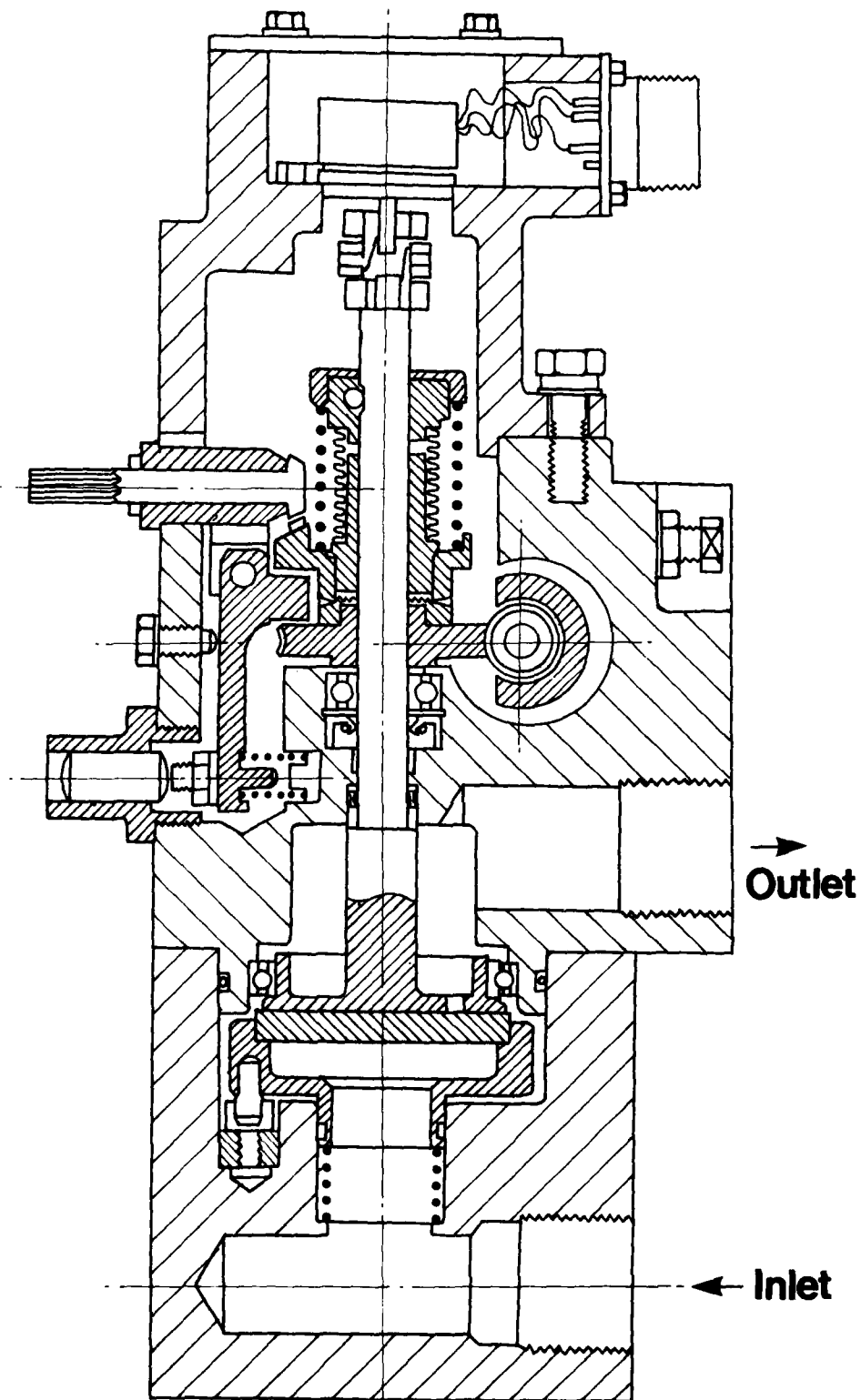
Comprehensive circuits are incorporated to monitor the transducers and control functions and to initiate the most appropriate action in each case such as indication only, reversion to a degraded control mode, or freezing the throttle and allowing the engine to be controlled manually.

One example of the type of safety circuits included is shown in Fig.4. Here the signals derived from the two  $N_3$  transducers are being compared. The predominant failure mode of these is open circuit, thus the signal would drop to zero. The lower part of the diagram shows comparators being used to check the trip channel transducer:-

thus if  $N_3$  (control)  $> 15\%$  AND

$N_3$  (trip)  $< 10\%$ , then  $N_3$  (trip) must have failed.

Indication of this fault is given, but the engine running is not affected in this case.



**Face Throttle with Manual Reversion**

**Fig. 2**

The variable delivery capability means that the pumps have a reduced power consumption, lower fuel temperature and less wear at part loaded conditions.

Special materials have been incorporated to give a long life capability with low lubricity fuels and salt water contamination. The pump includes a hydromechanical governor. This is driven by the engine HP spool on a common shaft with the fuel pump, and is situated in the same housing, thus providing  $N_2$  speed limiting in the event of electronic control failure.

The current control system on Rolls Royce marine engines is essentially a pressure control system. In arriving at the SMIA control a number of schemes were evaluated including controlling pump servo pressure, pump flow using a turbine flowmeter and flow by means of a throttle valve with a controlled pressure drop. The last of these approaches was finally adopted following detailed studies as it provided the required flow control, fail frozen capability and simple manual reversion.

For these reasons a new face throttle design is being used for the SMIA. Details are shown in fig 2. Throttling takes place at two flat surfaces which are pressure loaded to prevent silting up which is possible in valves with small working clearances. This enables materials to be used which are hard and corrosion resistant. The moving valve plate is rotated by a stepper motor via a worm and wheel, the latter being mounted concentrically with the throttle shaft. Position is sensed by a plastic film potentiometer and fed back to the electronic control unit. This type of transducer has been chosen as being reliable and requiring only simple signal conditioning circuitry.

#### Manual Reversion

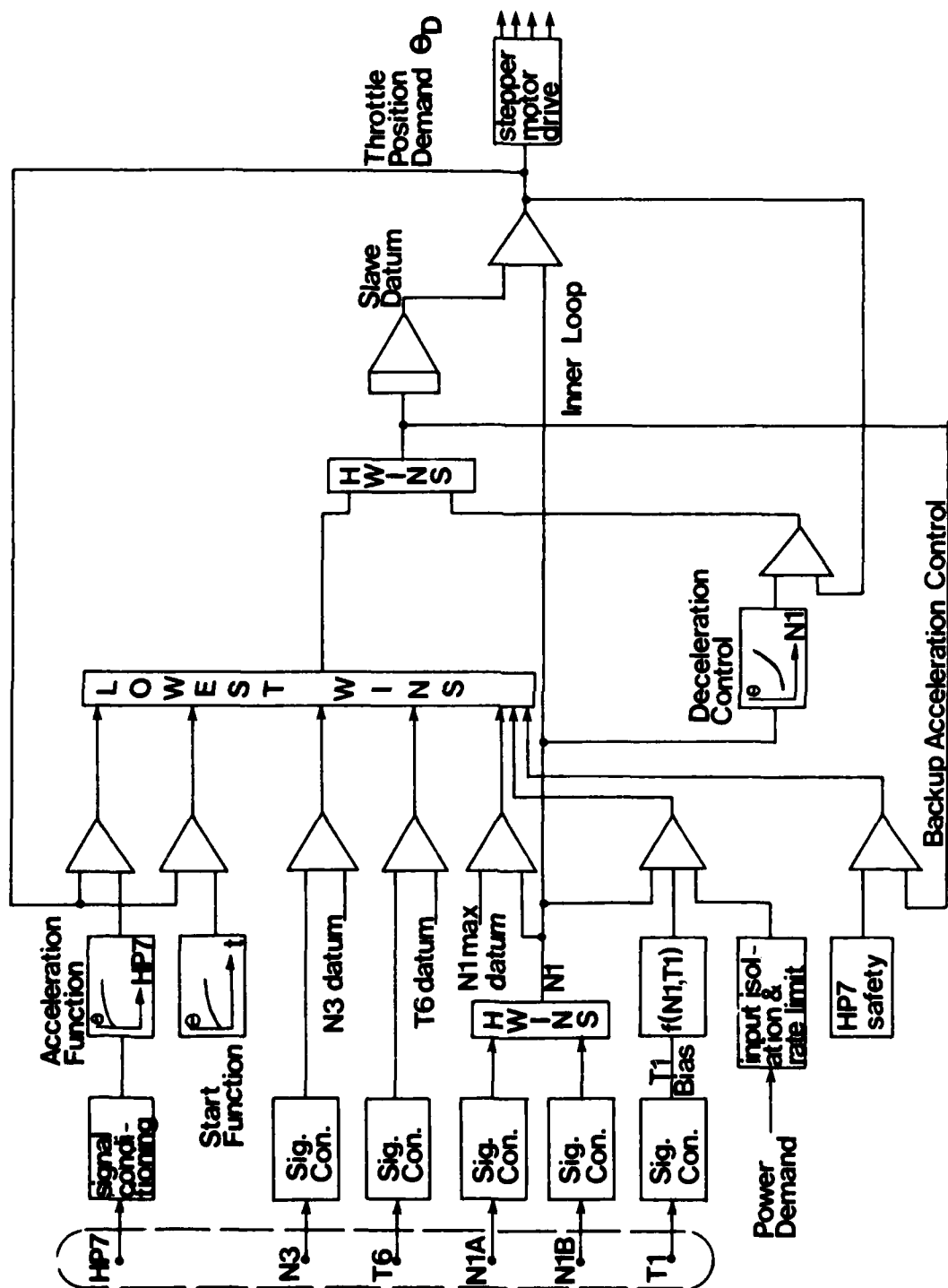
The normal drive to the face valve shaft is taken from the worm wheel via a tooth face coupling and bellows arrangement. When manual reversion is required a plunger is depressed to disengage the coupling and engage the manually operated bevel gear.

The throttle is then completely independent of the stepper motor and electronic control, and the engine can still be run manually if either of these fail. This leads on to other subjects of importance, namely safety, reliability and maintainability. The design features incorporated to achieve the high standard in these areas required by the engine manufacturer and operators will now be discussed.

#### SAFETY

The important areas from the point of view of maintaining engine and control integrity are as follows:-

- a) Gas generator and power turbine overspeed.
- b) Engine stall or flame-out.
- c) Engine overtemperature.
- d) Unscheduled shutdown.
- e) Unscheduled power changes.
- f) Manoeuvring controllability.



**Electronic Control Functional Block Diagram**

**Fig. 1**



The control functional block diagram is shown in fig.1. A reset mode governing arrangement incorporating the Slave Datum control principle (2), (3) is used, comprising an inner proportional control loop whose datum is reset by an outer integral loop, which gives isochronous governing. This is a highly desirable feature giving consistent control of the engine over its power range from idle up to sprint rating.

System response depends critically on the timing of the inner proportional loop. The choice of parameter for this loop is however not critical. Engine pressure and  $N_1$  were both considered carefully for the present application, and  $N_1$  was chosen principally because it is the more easily and reliably measured.

The control parameters  $N_1$  and  $N_3$  are measured by conventional inductive pickoffs. HP7 is sensed by a strain-gauge transducer and  $T_6$  by chromel-alumel thermocouples. After conditioning these signals are compared with datum values as shown to form the required error signals. Control passes to the lowest of these error signals, except during deceleration, the winning error being integrated to give the required inner loop datum. Comparison of the datum with  $N_1$  then produces the throttle position command which is directly related to fuel flow.

Noteworthy points are that engine power is controlled by means of a range  $N_1$  control. This parameter was chosen because it was familiar to operators and met most of the requirements such as transducer reliability, accuracy, ease of measurement, and low variation of power with engine deterioration (4). Two transducers are used to meet the stringent integrity targets, and particularly to avoid unscheduled engine rundown. The acceleration control sets fuel flow as a function of engine HP7 pressure, thus giving automatic protection against engine stall, and additionally preventing the control from giving excessive overfuelling in the event of flameout. A backup acceleration control is incorporated giving a fixed slow acceleration. The deceleration control is set as a function of  $N_1$  to give safe deceleration without risk of flameout.

The fuel control throttle position is set by means of a servo control using a hybrid stepper motor.

#### Hydromechanical Fuel Control

The fuel control comprises a pump, throttle, pressure drop unit and flow distributor. The function of the control is to set engine fuel flow as a function of throttle position. It is required that the system should be highly reliable, accurate and repeatable, particularly because the acceleration and deceleration controls depend on the relationship between throttle position and fuel flow being accurately defined. The system has been designed to fail frozen in the event of electronic control failure, and is provided with direct manual throttle control as backup.

As mentioned previously, where existing technology has adequately proved itself in terms of life, reliability and performance, a decision to change to a new technology is not taken lightly (5). For this reason the well established marine standard piston pump currently on the Olympus TM3B has been retained for the Marine Spey.

The piston pump has the capability of high pressure operation which is advantageous from the point of view of combustion efficiency. Another outstanding feature is the high volumetric efficiency, which is maintained at low speeds so that light-up and starting at adequate fuel pressure presents no problem, even after many thousands of hours service.

## ENGINE MANUFACTURES REQUIREMENTS

The requirements for a Marine Gas Turbine Engine Control System may be stated broadly in two classes. Firstly, there are the control functions to be achieved and other specific requirements to be met and these can be quantified fairly readily. In case of the Marine Spey these include various governing functions, engine integrity requirements which need limiter and trip channels and safety circuits to be incorporated, reliability, life and environmental requirements.

Secondly there are requirements that, although important, are more difficult to quantify. This category included adaptability to different applications with minimum change, and ease of adjustment, maintenance and trouble shooting, which implies good accessibility and understandability of the equipment by crew members. There is also the implied requirement that any change from existing design or technology must bring with it significant and proven new benefits.

It is believed that the system described goes a long way to properly meeting both the above classes of requirement.

The electronics and hydromechanical parts of the system are described and the reasons for the choice of design at each stage given.

## DESCRIPTION OF THE SM1A CONTROL SYSTEM

### Electronic Control Unit

The electronic control unit is required to provide the following primary functions:-

- (a) Starting and Acceleration to Idle.
- (b) Power control from idle to normal maximum and sprint rating.
- (c) Engine acceleration and deceleration control.
- (d) Limiting of the following engine parameters:-

Low Pressure Shaft Speed,	$N_1$
Power Turbine shaft speed,	$N_3$
Power Turbine inlet temperature,	$T_6$
Maximum Fuel flow,	$F_6$
- (e) Emergency trips on  $N_3$  and  $T_6$ .
- (f) Comprehensive self monitoring capability.
- (g) Fail frozen and manual reversion capability.

This first major decision to be made was whether a digital or analogue system should be used. At the time this decision was made, digital control techniques in this context had not progressed to the point where they competed with analogue systems. Reliability had not been proven and development costs were expected to be much higher. However, the system concept chosen has the advantage that digital computing elements can be introduced in place of some of the analogue circuits at an appropriate time in the future, due to the modular design and construction technique adopted.

## CURRENT AND FUTURE DEVELOPMENTS IN MARINE GAS TURBINE CONTROL SYSTEMS

by Michael J Joby  
and Richard J Eves  
Lucas Aerospace Limited

A radical re-examination of engine control system requirements has arisen out of the development of the new generation of marine gas turbines such as the Rolls Royce SM1A. This paper describes a new analogue electronic control system designed and developed for the SM1A. Particular attention is given to discussing how the design has evolved to meet the engine manufacturer's specification, and the advantages in terms of performance, safety, reliability and maintainability which make the adoption of a new technology control worthwhile.

One of the most important components of the fuel control system is the stepper motor driven throttle valve developed for this application. The valve incorporates features which give it a fail frozen capability. Particular attention has been paid to overcoming the problems of contamination and corrosion so as to ensure a long trouble-free operating life in the marine environment.

Consideration is given to future developments. Fighting ships are likely to make increasing use of sophisticated data handling and control techniques. It is anticipated that these future requirements can best be met in the case of the engine controls, by introducing digital techniques. An example is given showing how the existing SM1A analogue control system could be modified to give a full-authority digital engine control, without taking the high-risk path of completely redesigning the control system. The advantages of adopting a digital approach in this context are analysed.

### INTRODUCTION

The current range of Rolls Royce Marine Gas Turbine Engines use well proven and reliable hydromechanical fuel control systems developed over a period of nearly 20 years. It has, however, been recognised that future generations of Marine Gas Turbines would follow the same path as their aircraft and industrial counterparts, namely towards the use of electronics controls for the regulation of engine power and other engine parameters.

The specification requirements and evaluation of possible system configurations for these new electronic controls and their associated simplified hydromechanical fuel systems have been the subject of study for some time (1) (2) but activity crystallised with the decision to proceed with the Rolls Royce Marine Spey (SM1A) programme. The first part of this paper describes the electronic and hydromechanical fuel control system that has been designed and developed for this application. Proving of the system in prototype form by means of engine test bed running is scheduled for this year and pre-production is planned for next year. Largely analogue techniques have been used in the electronic control, but consideration is also given here to likely future developments involving the use of digital techniques.

## CONCLUSIONS

The advantages inherent in adopting a control system comprising isolated sub-systems corresponding to the functional zones of the propulsion machinery have been put forward. It has been shown how the functional-to-hardware design approach offers the following benefits;

- Increased system integrity : The overall system is more likely to survive partial system or plant failure.
- Increased flexibility : changes to one functional zone do not effect other control zones. This allows for the inevitable changes in the operational requirements of the ship during its lifetime.
- Easier operation and maintenance : the system is simpler to understand, and fault finding is less time-consuming, due to the manner in which the system is arranged.

The concept of a geographically distributed control system, using on-plant controllers, has been outlined. When an analogue implementation was considered, it was suggested that the advantages were outweighed by the practical problems.

However, the introduction of microprocessor-based sub-systems linked by serial data links was shown to make a distributed system viable. A distributed system using microprocessor and serial data links has the following advantages:-

- Reduced vulnerability to battle damage : The use of geographically separate plant control units and duplicated serial data links greatly increasing survivability.
- Reduced costs : Less cabling bringing about a saving in both cost and weight, the use of common elements of both hardware and software reducing the cost of development and spares.
- Increased flexibility : The plant controllers are functionally isolated, allowing changes to be made to one without affecting the system as a whole.
- Reduced mean time to repair : The spare processing power available can be used for auto-testing and to aid fault diagnosis.

The use of a data network using some form of adaptive routing technique was discussed. Practical problems were shown to indicate that a better immediate solution involved the introduction of a System Control Unit to control the distribution of commands and data throughout the system.

## Acknowledgements

The author wishes to thank Hawker Siddeley Dynamics Engineering Limited for permission to publish this paper. He also gratefully acknowledges the help given by his colleagues, past and present, in its preparation.

reversionary modes of operation. The PCU's will contain a local panel displaying information essential to the safe operation of that item of plant. From this position the operator can exercise the plant via the microprocessor in the PCU. Thus, safe operation may be ensured for the plant itself; however, communication with either the SCC or the other PCU's will be necessary to ensure that the design limitations of the propulsion machinery as a whole are not exceeded. In the event of the PCU itself failing, local manual operation is possible, bypassing the microprocessor system.

An alternative fallback mode involves remote manual operation of the plant, often termed servo-manual. The servo-manual system operates directly upon the plant actuators. Controls for servo-manual are usually located in the SCC and allow remote operation of the plant independent of the microprocessor system.

#### Relative Advantages

Adaptive routing packet switching is a technique widely used for inter-computer communication: there exists a wealth of theory and of practice. However, ARPS is a new technique in propulsion control system. Such a system would require considerable development, in terms of hardware in the HAU and more especially in terms of the message handling software. Once developed, however, an ARPS system would be sufficiently flexible to be ship independent.

As an interim measure, a system utilising the concept of a SCU offers a more straight forward solution at the expense of slightly greater vulnerability to failure or battle damage. A microprocessor system similar to that described previously has yet to be implemented in a Royal Naval Warship, thus the use of a SCU removes some of the unknown quantities inherent in the development of a completely new type of propulsion control system.

The technology required to build a microprocessor-based system exists: HSDE Limited have experience in designing equipment similar to the various component parts of the system, but operation of the system as a whole has yet to be tried. The mining equipment division of HSDE Limited use a multiplexed data ring system for conveyor belt control and surveillance system. In addition HSDE Limited have undertaken digital studies for the Royal Navy and for a major foreign navy. The technology exists, however, a full understanding of the implications inherent in the adoption of such a system is vital if full advantage is to be taken of the power of the microprocessor. HSDE have developed and run a digital fuel control system on such diverse gas turbines as the Gnome Helicopter, Pegasus vectored thrust and Marine Olympus engines. The Olympus Application included a HSDE made, microprocessor based, user-programmable industrial controller for start/stop sequencing.

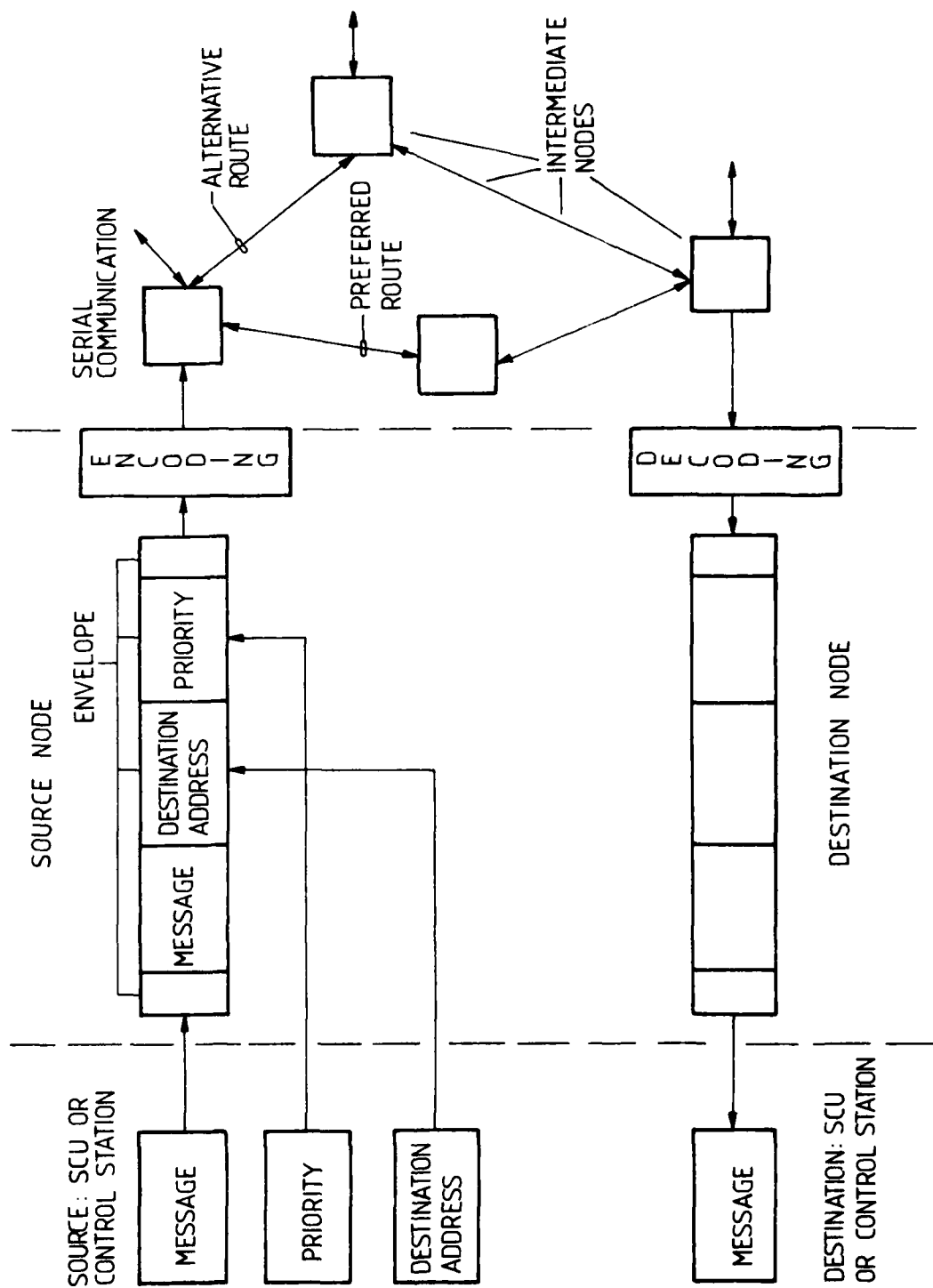


Figure 13: Operation of Adaptive Routing Packet Switching

Each board has its fault indication lamp, driven by the Safety circuits to indicate if a fault is present. Thus it is possible to diagnose a fault and replace a board with a spare one extremely rapidly.

There are also monitoring points on the front panel of each board, and some boards have potentiometers for screwdriver adjustment of datums and schedules.

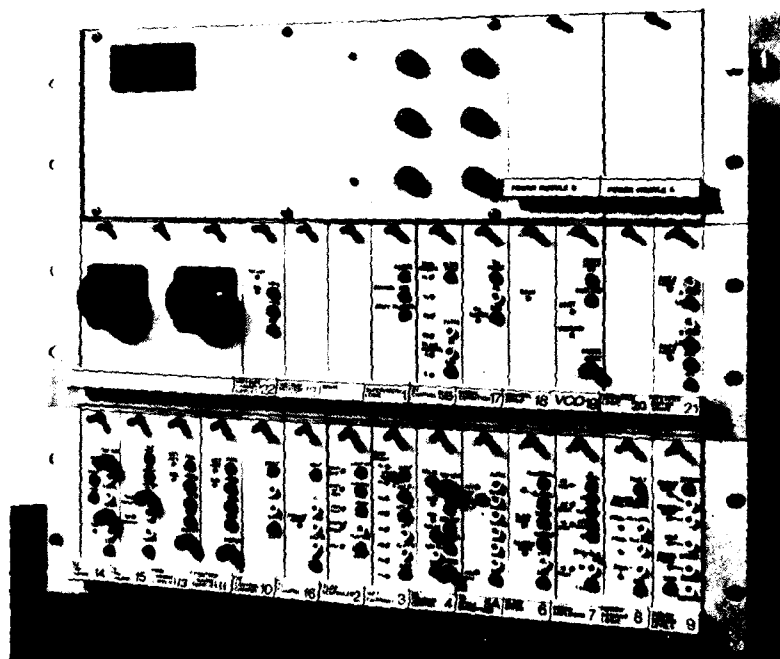


FIGURE 5

The boards containing the trip channels have test buttons which inject dummy transducer signals into the trip circuits, i.e. an a.c. signal for the speed trip circuits and a simulated thermocouple signal for the temperature trip circuit. Reset buttons are also provided to reset the trip channels ready for operation.

Purpose built test equipment is also provided for connection via the two test sockets. The test equipment provides simulated transducer signals to all inputs, which may be varied for test purposes. The equipment also provides an engine simulation for closed loop testing of the governors without running the engine.

## FUTURE DEVELOPMENTS

The analogue controller described above has been designed to meet the specification of requirements put up by the engine manufacturer and agreed by the final customer. The development programme has involved the closest possible liaison to ensure that the system accurately reflects the customer's requirements without significant over-engineering. The electronic controller has been designed particularly to have very high integrity and maintainability. This has been achieved at the expense of some complexity in the safety circuits. A digital control system puts most of its safety functions into the computer program and a minimum amount into actual hardware. This is one good reason for examining whether there is a case for a digital variant of the present control in the future

### Digital System

A digital computer is ideally suited to applications where there is a requirement to make use of its main capabilities namely:-

- Data acquisition and storage
- Data processing
- Arithmetic and logical operations

Consider the incorporation of a digital computer in the present system. The minimum change digital system is shown in Fig.6. All the input signal conditioning channels are retained, and these are fed to a multiplexer along with the datum signals. The computer can then select the required channel which is input to the computer via an analogue to digital converter. The starting, acceleration, deceleration and demand function generators are deleted, as are the error amplifiers and slave datum control. The safety circuits and supervisory logic would also no longer be required. The motor position control loop would be replaced by a simplified circuit producing the required stepping sequence at a rate set by the computer. Other new elements would be processor and store, multiplexer and analogue to digital converter, computer monitor and computer power supply. A fault display drive circuit would be required to take over the indicating functions of the supervisory logic. Based upon in-house experience with digital engine controls dating back to 1970 it would seem that the most suitable computer for a marine engine control would use one of the modern 16-bit microprocessors currently available to a military temperature range. A hardware multiply and divide facility is regarded as being essential. A 16-bit machine is preferred to the more widely used 8-bit processor because the higher computing power allows the control system and engine manufacturers far greater scope in product development programmes, since the basic control, safety and display functions do not use the machine's full computing power. For the basic control and self-check routines around 2K x 16-bits PROM store would be required together with 256 x 16-bit words of RAM. If it were required to extend the system functions then the fixed PROM store would increase in size.

System input signals would be processed using the existing signal conditioning. The computer would then select these signals as required by means of a multiplexer. A 10-bit analogue to digital converter would convert the selected signal to the required digital form. The datum signals would be similarly input to the computer from potentiometers, allowing straight forward limited authority adjustment.

Operations from this point on come under software control. The input signals are sampled as indicated above at regular intervals of time, typically every 10-20ms for control variables. A software safety check is carried out in which each input is checked to see that it is within defined limits and has not changed by an unreasonable amount since the previous sample period. A fault integrator routine is used to ensure that minor transient input disturbances do not cause a fault



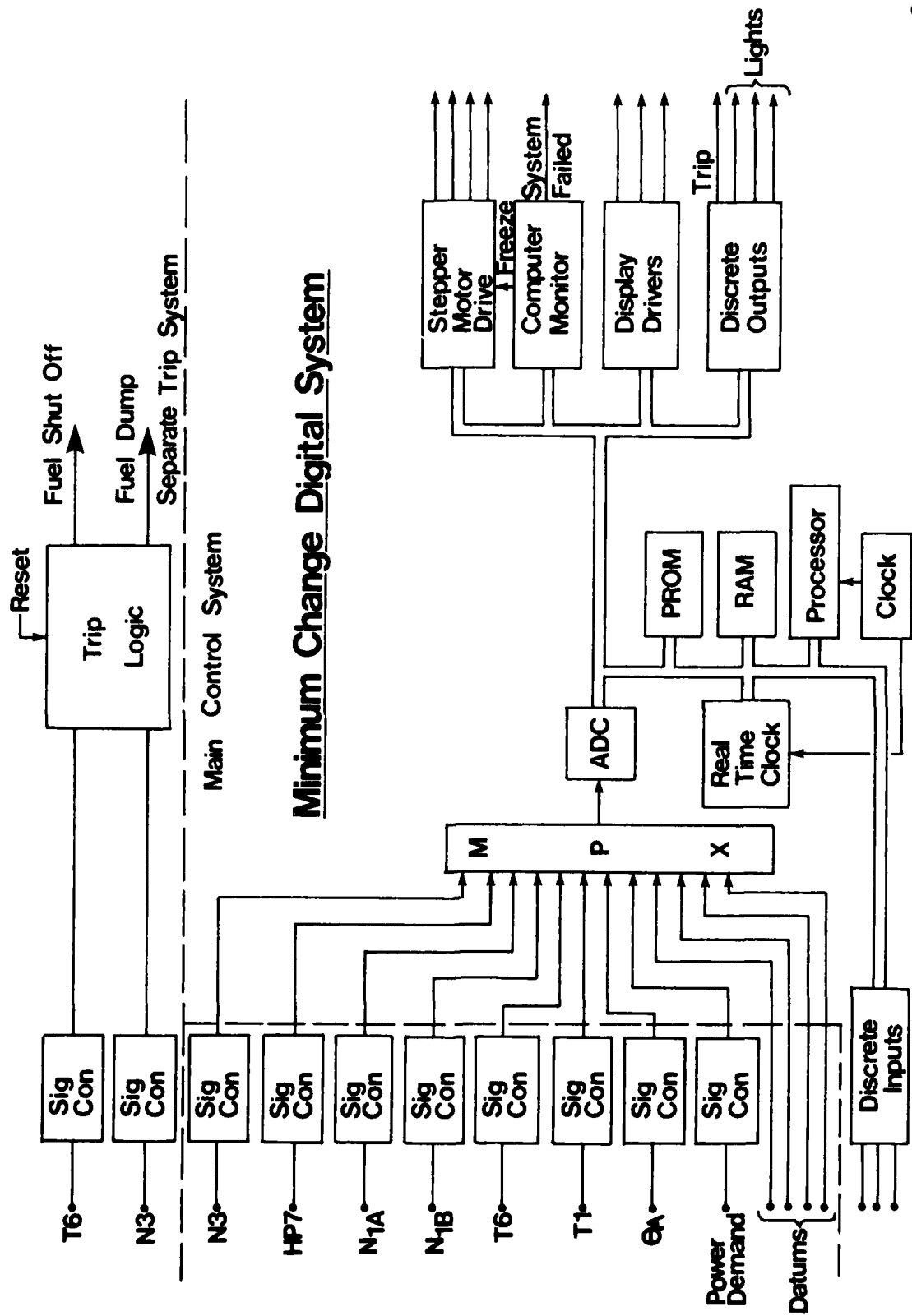


Fig. 6

to be declared. The computer program then processes the validated signals generating the required error signals and functions, applying compensation to the signals and executing the rest of the control calculations. The resulting output is a stepping rate command to the throttle actuator.

#### Safety and Reliability

The order in which particular calculations are executed can be important. A typical sequence is listed below:-

Service computer monitor

Output to actuator drive

Read in control parameters

Validate inputs

Execute control calculations

Safety routines

The computer monitor consists of a timer, comparator and fault counter. Operation is as follows. At the beginning of each control sample period the computer must output a number calculated by the safety program within a preset interval. If this number is incorrect the actuator drive is frozen, and the fault counter incremented. If the correct answer is obtained next time round then normal operation is resumed. Similarly if the computer does not service the monitor at the correct time a temporary freeze occurs. If this is repeated over a sufficient number of cycles, then the fault counter permanently disables the system and indicates a critical fault.

The safety routines allow the designer considerable flexibility in deciding when to freeze the control or when to by-pass a non-critical failure by means of suitable backup control program which allows a measure of 'graceful degradation' in the system.

The reliability of the minimum change control has been estimated using the same data source as the analogue control and the table below compares relevant figures. The analysis shows the digital system to have a marginally better failure rate than the analogue control without safety circuits. When these are also taken into account the difference is significant.

	Analogue	Digital
Failure Rate (%)	100	82
Dormant Fault Rate (%)	22	5

Table 1. Comparison of analogue and digital control failure rates.

## Maintainability

The lower failure rate of the digital controller and its high probability of detecting any system fault combine to give better system availability and lower maintenance costs. It can be argued that the difference in system availability will be trivial in practice, since a repair by replacement policy in modular systems allows single failures to be readily rectified, whether or not the safety circuits have indicated the location of the fault. In the present example tracing a dormant fault in the analogue system would require trying out more boards than for the digital system. However, changing a module is an operation which does not normally affect engine running and takes only a few minutes. It is therefore expected that the analogue system will achieve better than 99.9% availability in-service.

Maintenance costs may be divided into three categories in order to obtain a simple comparison between systems.

- (1) Maintenance staff, spares, tooling etc.
- (2) Special test costs.
- (3) Maintenance actions, spares utilisation.

The first area is related to the complexity of the control and is affected by the number of distinctly different subsystems and technologies applied. The second relates to those parts of each system which cannot be checked out automatically by the electronic control system and require additional inspection, engine and rig running to determine fault locations. The third area has been related directly to complexity taking into account all the system components including duplication.

Defect rate is taken as a measure of complexity allowing similar systems to be compared. In order that hydromechanical and electronic components may be included in the comparison, the hydromechanical defect rates are multiplied by a suitable weighting factor. This factor is generally not critical and experience suggests that a factor of 3 is suitable. Thus the maintenance staff, spares and tooling cost is given by summing individual defect rates as shown:-

Cost = (Throttle valve + PDU + Pump) 3 + electronic control + trips

The special test cost recognises those parts of the system which cannot be checked out simply by switching on the control, and in the case of the trips by pressing test buttons. Thus the special test cost is calculated

Cost = (PDU + Pump) 3 + electronics control (dormant faults)

The maintenance action and spares utilisation cost in the particular example is the same as the first cost item above. Differences arise in these terms when there are significant amounts of redundancy built into the design. The maintenance costs of the complete engine controls are summarised below:-

Maintenance Cost (%)	
Analogue	100
Digital	87

Thus in terms of improved reliability and lower maintenance costs a digital controller looks an attractive proposal. This of course is only a small part of the story, and in any decision to adopt a new control the development costs of the hardware and software must be traded against potential in-service economies. Not only would the hardware development represent a significant part of the development cost, but so also would the computer software.

#### Additional Functions

The case for adopting a digital control is strengthened if additional system functions are considered. It is likely that the next generation of fighting ships will follow the trends already in evidence on both civil and military aircraft, which are making increasing use of standardised serial digital highways for data transmission. Typical uses could include outputting information to a central data logging system or for display purposes.

The optimum arrangement for in-service engine health monitoring still appears to be to use those parameters already required for instrumentation and control with relatively few additions, but in conjunction with established manual techniques (7). The additional gains associated with more extensive systems are not, in most cases justified. Typical pieces of information which are readily available include low cycle fatigue counting, creep life calculation and even the simple but effective bearing check afforded by measuring the time taken by the engine shafts to come to rest after shutdown.

The use of a serial digital highway can enhance the conventional display functions already provided by analogue and digital meters adjacent to the unit. Meters in the machinery control room could be driven via a digital data link, thus simplifying wiring, and a visual display could be provided giving both graphical and alphanumeric information simultaneously. Further refinements are possible with the inclusion of colour which can give easy to assimilate fault or condition information.

#### CONCLUSION

The paper has shown how an analogue electronic control system and simple hydromechanical fuel system has been applied to the Rolls Royce Marine Spey engine. The benefits of this approach have been discussed, particularly those such as safety, reliability and maintainability. It has also been shown that further benefits could be obtained in the future by introducing digital techniques in place of some of the analogue circuitry.

#### ACKNOWLEDGEMENTS

The authors wish to thank the directors of Lucas Industries Limited for permission to publish the information in this paper, and also to acknowledge the help provided by colleagues at Lucas Aerospace Limited in discussing and preparing this paper.

#### NOMENCLATURE

- F - Fuel flow rate
- HP7 - 7th Stage High Pressure Compressor Delivery Pressure
- $N_1$  - Low Pressure Shaft Speed
- $N_2$  - High Pressure Shaft Speed
- $N_3$  - Power Turbine Shaft Speed
- $T_1$  - Ambient Air Temperature
- $T_6$  - Power Turbine Inlet Temperature
- $\theta$  - Required Throttle Valve Position
- $\theta_A$  - Actual Throttle Valve position
- $\theta_D$  - Throttle Position Demand (Datum for Position Control Loop).

#### REFERENCES

- (1) Joby, M.J and Perring, S.G. 'Electronic Based Power Control Systems for Gas Turbine propelled ships'. Fourth ship control systems symposium, The Hague, The Netherlands.
- (2) Binns, J.M. and Joby, M.J. 'A simplified Electronic Based Engine Control for Industrial Gas Turbines A.S.M.E. Paper 74-GT-128, 1974.
- (3) British Patent No. 946111
- (4) Saville, H. and Wheeler, D.J. "The Selection of fuel control systems for use with Marine Gas Turbines'. Third ship control systems symposium, Bath, England, 1972.
- (5) Saville, H. and Wheeler, D.J. "The use and Experience of Hydraulic Fuel Systems in the control of Marine Propulsion Gas Turbines. Fourth ship control systems symposium, The Hague, The Netherlands.
- (6) Reliability Predictions for Military Avionics. Reliability Prediction Method No. 250 Issue 1 March 1977. Division OL3, RSRE Malvern, UK.
- (7) Tipton, J 'A Digital Approach to Industrial Gas Turbine Control. A.S.M.E. Paper 78-GT-39, 1978.

# A HIGH POWER SUPERCONDUCTING SHIP PROPULSION SYSTEM - ITS CONTROL FUNCTIONS AND POSSIBLE CONTROL SCHEMES

by I.C. Bartram, IRD Ltd.,  
and R.T.S. Looock, Ministry of Defence (UK)

## ABSTRACT

This paper describes the control system for a prototype superconducting propulsion system. The equipment included a superconducting generator providing power to a low speed superconducting motor. The paper covers the requirements of the control system and its realisation. The paper then examines some case studies employing superconducting machinery and describes a range of control systems designed to meet the differing requirements of various ship types.

## INTRODUCTION

Superconductivity is that property of certain materials which, when cooled below a certain critical temperature, exhibit no resistance to the flow of electricity. The property is, however, restricted by other physical conditions, namely the current density in the superconductor and the magnetic flux density in which it is required to operate. Fig. 1 shows the operating boundary of temperature, current density and flux density for niobium-titanium alloy. It may be seen that the critical temperature is about 10 K, therefore any winding employing superconductors must be cooled to below this value. In fact, the temperature of liquid helium at atmospheric pressure is 4.2 K and this coolant is used when exploiting the property of superconductivity.

IRD has been engaged for several years in the development of superconducting devices, particularly machines, and under sponsorship, particularly from the Royal Navy, has built several d.c. superconducting machines. The advantage of superconductivity in relation to large d.c. machines is that sufficient ampere turns may be employed to provide magnetic fields in air which are higher than the saturation level of the iron cores used in conventional machines. This leads to higher power to weight ratios and by using the homopolar (or Faraday disc) principle the design limit for d.c. machines is increased by at least a factor of 10.

Fig. 2 shows a prototype propulsion system under test at IRD. This system was built for the Royal Navy and a paper presented at the Third Ship Control Systems Symposium shows computer predictions of its performance.

## MOTOR CONTROL PHILOSOPHY

Large d.c. superconducting motors may be employed for direct drive to propellers, 50 000 hp at 50 rev/min being well within the design boundary. Such high torque motors necessarily have a high total flux produced by the superconducting windings, giving rise to a large magnetic stored energy. To charge such a field rapidly would require a large input and output power controller, itself running to several megawatts. It was therefore decided at an early stage that control of these machines would be by varying the applied voltage to the armature, the field level remaining constant. This gives rise to a range of basic control systems related to the Ward-Leonard drive. Having rejected motor field control as a primary (i.e. rapid) control function it should be noted that changes taking several minutes are

© International Research & Development Co. Ltd., 1978

practical and such changes are available to the system designer as a secondary function for, say, matching the propeller characteristics to engine characteristics in multi-engine configurations. Such a feature may considerably improve the running economy by acting as, effectively, a variable ratio gearbox.

The refrigeration and other plant may be regarded from a control viewpoint as a service similar to lubeoil and cooling water systems which when operational put the propulsion motor plant into the 'GO' state. No complex interaction therefore exists between this plant and the propulsion control system

#### CONTROL SYSTEM FOR THE 1 MW PROTOTYPE PROPULSION SYSTEM

The development system shown in Fig. 2 consisted of a 'Deltic' diesel engine driving a superconducting d.c. generator electrically coupled to a propulsion motor. The diesel engine was to run at nominally constant speed. The propulsion control system was required to perform the following principal functions:

- (1) To provide a variable voltage, reversible, d.c. power supply capable of charging and discharging the field of the superconducting generator and maintaining the excitation at a selected level.
- (2) To sequence the selection of the thyristor bridges, the positions of the changeover-isolator, and the field circuit breaker from the existing condition to the demanded condition.
- (3) To sequence the operation of armature circuit breakers to insert energy absorbing resistors during reversal manoeuvres.
- (4) To provide various levels of manual control.

An arrangement satisfying item (1) gives a variable voltage output from the generator whilst operating at constant speed. This function was realised by a pair of thyristor bridges supplied from an exciter driven from the 'Deltic' engine. One bridge was supplied directly from the exciter and provided a variable 'forcing' voltage to charge and discharge the field winding. The second bridge was supplied from the same source via a 40:1 step down transformer, and provided a small range of voltages for maintaining the current at the desired level after the use of the 'forcing' bridge. The second thyristor controller fulfilled two systemic requirements: firstly, it reduced the 'ripple' voltage applied to the superconducting coil under steady conditions, and secondly it reduced the reactive volt-amperes from the exciter under the same conditions. The two thyristor bridges were connected in parallel and supplied a changeover mechanised isolator to provide reversibility of polarity on the d.c. side. Fig. 3 shows a schematic of this plant.

The propulsion control system included additional feedback loops to prevent engine overload and to prevent excessive load build-up and rejection.

Fig. 4 shows the propulsion control console which was designed to be compatible with a system of earlier design. The development was planned initially for eventual sea trials to drive one shaft in a twin screw vessel. The left-hand panel includes a 'mimic' diagram for the electrical plant showing important parameters. The handwheel in the foreground is the input to the automatic controller. The panel to the right is a surveillance aid showing the state of the plant. The upper block shows the state of the various auxiliary pumps and power supplies. The lower block gives warning of the excursion of chosen parameters beyond set limits (an audible alarm was also provided). The centre block repeats the parameters at the upper end of the lower block at a greater level of excursion and items in this block may be selected in advance to shut down the offending plant. Judgement on the selection for this procedure would of course

depend on whether this system was being used to propel a ship or as a shore test facility.

Fig. 5 shows the system performance. Some design margin (about 10%) was built into the hardware and in fact this was used to give performance better than the specified minimum.

The performance of the control system demonstrated that the underlying theory was realisable in practice.

#### DEVELOPMENT OF SUPERCONDUCTING PROPULSION SYSTEMS

Concurrently with the development of the superconducting machines and the realisation of their limitations in certain circumstances, there has been a development in control and system concepts, giving a range of schemes to meet the varying requirements of different ship types. Fig. 6 illustrates four of the options available for control systems and these are described briefly below:

Type 1 has a constant speed engine driving a variable field superconducting generator connected to a fixed field superconducting motor. This arrangement was used on the 1 MW system described above and it is suitable for an engine speed of about 1500 rev/min or below, and, to avoid undue complication in the generator, with moderate transient performance in high power systems. This scheme was proposed for large tanker and similar drives employing medium speed diesels (400 to 600 rev/min). A major advantage is that auxiliary power generation can be taken from a.c. generators driven by the constant speed engine.

Type 2 has a variable speed engine driving a fixed field superconducting generator connected to a fixed field superconducting motor. This concept requires armature reversal gear but allows rapid manoeuvring by engine speed control.

Type 3 has a constant speed engine driving a variable field conventional a.c. generator connected by rectifiers to a fixed field superconducting motor. This concept is similar to type 1 but requires armature reversal equipment. The scheme is particularly applicable to high speed engines such as gas turbines and allows rapid manoeuvring by generator field control whilst providing a constant speed drive for auxiliary generation.

Type 4 has a variable speed engine driving a variable field conventional a.c. generator connected by rectifiers to a fixed field superconducting motor. This scheme is particularly attractive to systems with more gas turbines than propeller shafts, especially in warship drives where the total installed propulsive power is only occasionally utilised.

#### STUDY ON A 260 000 TONNE D.W. CRUDE OIL CARRIER

This study was done on behalf of the UK Department of Industry by IRO in conjunction with a major UK shipbuilder and other consultants.

A major consideration was the requirements for crude carriers to have segregated ballast tanks. This meant that such vessels were volume rather than weight limited and it had been identified that superconducting electrical propulsion would reduce engine room volume in a large number of ship types. The schematic diagram for the system is shown in Fig. 7. In this case the vessel is propelled by a single shaft system employing 32 000 hp. Studies were performed for 86 and 110 rev/min propeller speeds, the power being provided by 3 medium speed diesel engines operating at constant speed and each driving a superconducting generator and an alternator. The superconducting generators provide propulsive and cargo pumping power, remaining load being taken from the alternators. The use of three diesels is related to the duty cycle of the vessel. Two engines only are required



for a ballast voyage and for cargo pumping one only is required. The out of service engine may be maintained during the ballast voyage as separate environmental enclosures are proposed. With one engine under maintenance during cargo pumping the third is available for emergency propulsion.

The layout of the main machinery (Figs. 8 and 9) results in a 20% reduction of the machinery space in this type of vessel over a conventional system. This is achieved by locating the main engines above the propulsion motor.

The system is configured as Type 1 (Fig. 6) and conventional d.c. motors are used to drive the cargo pumps. The propeller reversal time of 60 seconds requires small excitation plant for the generators and the rate of change of field current is low.

#### CASE STUDY FOR WARSHIP PROPULSION

This case study was completed as part of a programme sponsored by the Royal Navy. The scheme presented here is for a three engine, two shaft fit. The engine chosen is the SM1A gas turbine and the arrangement is of Type 4 (Fig. 6). Although the study covered different numbers of engines for a two shaft ship, the three engine system was chosen since odd numbers of prime movers are impractical with alternative transmission systems, particularly if the flexibility provided by the electrical system is to be maintained.

Fig. 10 shows a control functions block diagram. The power interconnection scheme is shown in Fig. 11. The switchgear shown consists entirely of off-load isolators except for CB1 and CB2 which are load making/breaking switches.

For ahead operation, only one engine is required for speeds up to about 66% of maximum, two engines are needed to reach about 87%, and three engines thereafter. Clearly, any generator may be used for propulsion in the one engine mode and any two in the two engine mode. The motors (or generators) need to be paralleled in the one and three engine modes in order to share power. In the two engine mode this is neither essential nor desirable since this mode gives independent speed control when motors are segregated. The transmission lines shown should be capable of carrying the total output current, so giving a high degree of security of supply in the event of failure or damage. It is anticipated that the single engine mode will be used in open water conditions for normal cruising, with two engines in use for manoeuvring and fast cruising. The three engine mode is, of course, for full power performance with rapid reversion to a segregated two engine system for high speed manoeuvring, the third engine idling ready for instant connection to meet power demands during such activities.

Reversal of the propeller rotation is, of course, a requirement of the system, the most arduous condition being the full ahead to full astern, crash stop, manoeuvre. The scheme proposed below is suitable for any number of prime movers in excess of two. The sequence of events is as follows:

- (1) Suppress generator field and set GS1-3 to OFF when supply currents have fallen to zero.
- (2) Open circuit breakers CB1 and CB2.
- (3) Open G1, G2, G3 and close G4.
- (4) Close CB1 and CB2.

(If the vessel is running with condition (3) already set up, items (2) to (4) may be omitted).

- (5) Allow ship and propeller to decelerate to about half speed under normal drag.
- (6) Open CB1 and CB2.
- (7) Set CS1 and CS2 to 'ASTERN' and CS1-3 so that the appropriate generators are connected (two out of three generators only required), i.e. at least one generator to each busbar BB1 and BB2.
- (8) Close CB1 and CB2.
- (9) Perform constant current (i.e. torque) braking by generator field control (i.e. maintain voltage across braking resistors constant at about 50% system voltage).
- (10) The motors (and propellers) are decelerated to standstill and accelerate astern without further switching, the system settling out about 18% full current and 26% of ahead full speed in reverse.

Braking resistors must now be removed.

- (11) Increase loading on one transmission line whilst reducing current in the second.
- (12) At current zero in second line, short out resistor.
- (13) Load up second line and unload first line.
- (14) At current zero in first line, short out resistor.
- (15) Equally load transmission lines and run segregated, if desired, by opening S4.

The items which determine the time for this manoeuvre are numbers (5) and (10); other items are logic functions, which in total will take less than 5% of the time for items (5) and (10). The system can be designed to operate so that the 'half speed' in item (5) may be anywhere between 0 and 100%, however the larger the value then the larger the total energy dissipated in the braking resistors.

The control system is a speed demanded function rather than a power demanded function. This is a particularly useful feature since the power system voltage, an easily measured parameter, is almost directly proportional to shaft speed. The system is also able to deal inherently with fluctuations in load, due to, say, the propeller leaving the water, since shedding full load on the motor results in an increase in motor speed of only 2% for an unchanged applied voltage. Load shedding by the gas turbines has to be dealt with by the governor and is a problem common to all transmission systems employing these engines, but should be achievable without causing engine speed to reach the 'shut down' level.

It is difficult to compare a three engine electric transmission system with a conventional (i.e. gearbox) equivalent from a fuel consumption viewpoint for reasons given earlier. However, a four engine system can be compared, and the same conclusions would apply for three engines if the gearbox equivalent were practical. The fuel flow against ship speed for the equivalent mechanical and electrical systems is shown in Fig. 12; these curves assume that the systems have equal efficiency. It can be seen that the flexibility of the electrical system allows fuel savings over certain speed bands. When this chart is modified by the duty cycle (an 'S' curve) the total fuel flow against cumulative time underway is as in Fig. 13; the difference in area under these curves represents the difference in overall fuel

- \* Fig. 13 should be interpreted as follows: for any fuel flow the corresponding time underway represents the proportion of the total mission time during which that fuel flow is not exceeded.

consumption. In this case the electrical system uses some 91% of the fuel of the mechanical system. This figure is, of course, reduced due to the losses in the electrical systems. The electrical system employs a fixed pitch propeller and does not claim the efficiency benefit of the fixed pitch over the controlled pitch propeller. This comparison indicates that the overall efficiency of the electrical system is higher than that of the mechanical system. Also, compared with the energy consumption, including refrigeration and other auxiliaries, the energy profile shows that the superconducting electrical system will indeed require 10% LESS fuel than a mechanical system.

This fuel advantage, plus the ability to operate engines running their own cycle for maximum life and the flexibility of layout and operation which the superconducting system provides, all make this system an important contender for future warship propulsion systems.

#### CONCLUSION

The method of control of superconducting d.c. electric propulsion systems is dependent upon the type and power of prime movers and upon the electrical hardware realisation, that is, whether a d.c. superconducting or an a.c. conventional generator is used. The required rate of response of the system influences, in its turn, the choice of generator.

The use of such machinery in the future is not dependent upon control strategy as it has been shown in this paper that a system may be selected to cover requirements for ship propulsion, including the provision of auxiliary electric power from the main engines. Superconducting d.c. machines are at a stage of development in which the basic concepts and characteristics are well established. The need remains, however, to demonstrate the long term reliability of the refrigeration and other machine systems to potential users, particularly in the marine field.

#### ACKNOWLEDGEMENTS

The authors wish to thank the United Kingdom Ministry of Defence (Procurement Executive), the United Kingdom Department of Industry (Ship and Marine Technology Requirements Board) and the Directors of International Research & Development Co. Ltd., for their permission to publish this paper.

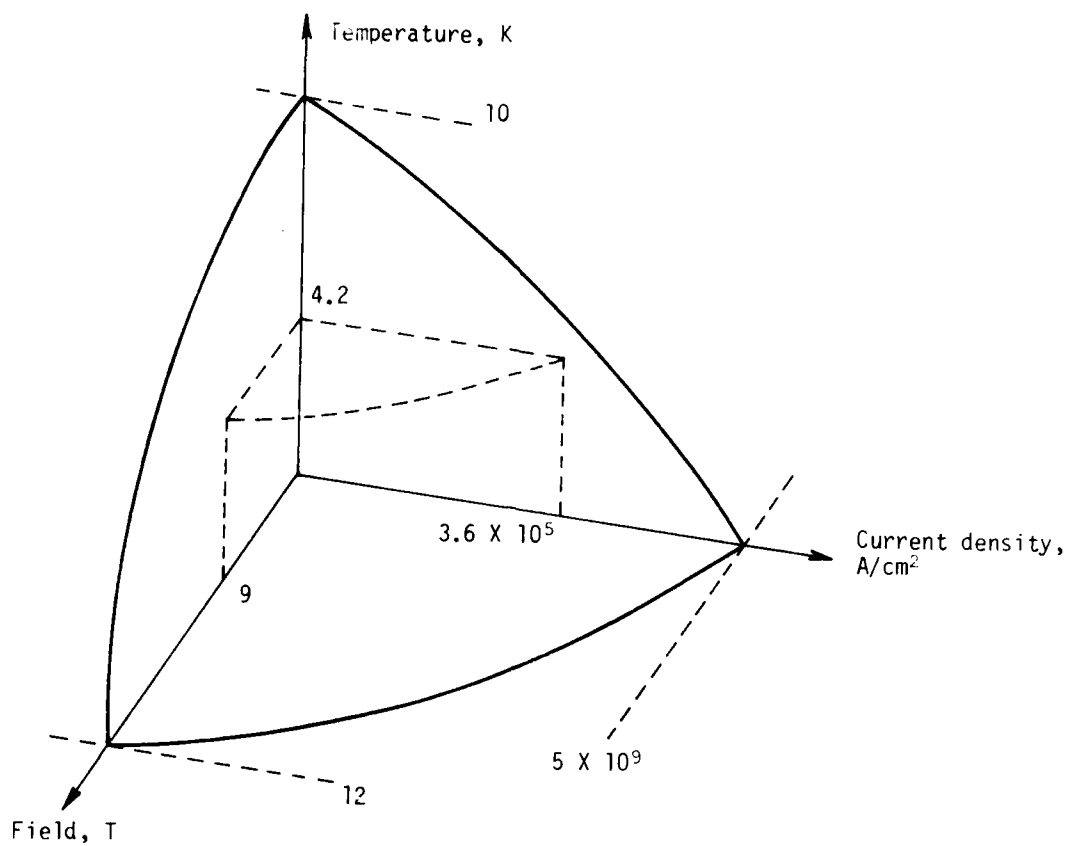


Fig. 1 Superconductor Limitations - Temperature, Current, Field

	Volume	Session	Page
French, C. Ministry of Defence (UK)	2	G	1-1
Friedman, I. Ingalls Shipbuilding	1	B	3--
Frivold, H. Det Norske Veritas (Norway)	4	N	1-1
George, D. H. Panama Canal Co. (Canal Zone)	3	K1	3-1
Gibson, F. W. Royal Military College of Canada (Canada)	4	M	2-1
Goff, C. N. Naval Training Equip. Center	4	N	4-1
Goransson, S. Statens Skeppsprovsningsanstalt (Sweden)	3	K1	3-1
Gorrell, E. L. Def & Civil Inst of Envir Medicine (Canada)	4	O1	2-1
Griswold, L. W. David W. Taylor Naval Ship R&D Center	4	O2	3-1
Haaland, E. Norcontrol (Norway)	4	N	3-1
Hall, D. D. Naval Ocean Systems Center	3	J1	1-1
Hara, M. Tokyo Univ of Mercantile Marine (Japan)	1	C	2-1
Harper, T. R. Propulsion Dynamics, Inc.	2	E2	1-1
Healey, E. J., CAPT Chairman, Session E2 Natl Defence Hdqtrs (Canada)			

	Volume	Session	Page
DeMattia, H. J. Naval Sea Systems Command	3	J1	1-1
Donnelly, J. W. Naval Ship Engineering Center Philadelphia Division	5	Q2	3-1
Dorrian, A. M. Y-ARD (UK)	2	G	1-1
Drager, K. H. Det Norske Veritas (Norway)	3	J1	2-1
Dresser, A. E. Bath Iron Works	5	Q2	1-1
Duberley, A. National Gas Turbine Establish- ment (UK)	4	N	2-1
Eda, H. Stevens Inst of Technology	3	J2	3-1
Ellsworth, W. Chairman, Session F2 David W. Taylor Naval Ship R&D Center			
Engebretsen, E. Ship Res Inst of Norway (Norway)	2	F1	1-1
Eves, R. J. Lucas Aerospace, Ltd (UK)	2	G	3-1
Fein, J. A. David W. Taylor Naval Ship R&D Center	4	O2	1-1
Feranchak, R. A. Westinghouse	3	K2	2-1
Fields, A. S. David W. Taylor Naval Ship R&D Center	1 & 5	C & R	4-1 & 2-1
Fitzpatrick, E., CDR, USN Naval Ship Engineering Center	1	A	1-1
Foltz, F. L. Hamilton Test Systems	2	F1	4-1

	Volume	Session	Page
Brink, A. W. Inst for Mech Const-TNO (Neth)	2 & 4	E1 & P	3-1 & 4-1
Broome, D. R. Univ College London (UK)	3	J2	1-1
Bruce, C. National Gas Turbine Establish- ment (UK)	3	H	1-1
Bystrom, L. Swedish State Shipbuilding Exp Tank (Sweden)	3	J2	2-1
Carruthers, J. F., CDR Canadian Forces-Navy (Canada)	1	A	3-1
Cassel, C. W. General Electric	5	Q2	1-1
Chan, Y. T. Royal Military College of Canada (Canada)	4	M	2-1
Clement, W. F. Systems Technology, Inc.	2	F2	2-1
Connelly, E. M. Perf Meas Assoc, Inc.	5	Q1	4-1
Cooling, J. E. Marconi Radar Systems, Ltd (UK)	5	R	4-1
Cooper, R. Eclectech Associates, Inc.	3	L	2-1
Cummins, W., Dr. Chairman, Session O2 David W. Taylor Naval Ship R&D Center			
Cummings, R. R. Ministry of Defence (UK)	2	F1	2-1
Davis, S. Naval Sea Systems Command	2	F2	4-1
Dejka, W. Chairman, Session H Naval Ocean Systems Center			

LIST OF SYMPOSIUM AUTHORS, SESSION CHAIRMEN,  
AND GUEST SPEAKERS

	Volume	Session	Page
Aas, T. Norcontrol (Norway)	4	N	3-1
Albee, T. L., CAPT, USN Chairman, Session G Naval Ship Engineering Center			
Allen, R. C., Dr. Chairman, Session Q2 David W. Taylor Naval Ship R&D Center			
Allen, R. W. Systems Technology, Inc.	2	F2	2-1
Anderson, A. Timm, CAPT, USN Chairman, Session B Naval Ship Engineering Center			
Baas, G. Inst for Mech Const-TNO (Neth)	4	P	4-1
Banham, J. W. Chairman, Session M Naval Ship Engineering Center Philadelphia Division			
Bartram, T. C. IRD, Ltd (UK)	2	G	4-1
Baxter, A. National Gas Turbine Establish- ment (UK)	3	H	1-1
Birbanescu-Biran, A. Israel Shipyards, Ltd (Israel)	3	K2	3-1
Blanke, M. Servolaboratoriet (Denmark)	6	C	3-1
Bowen, T. L. David W. Taylor Naval Ship R&D Center	2	E2	3-1
Bozzi, P. Operations Research, Inc.	1	C	4-1



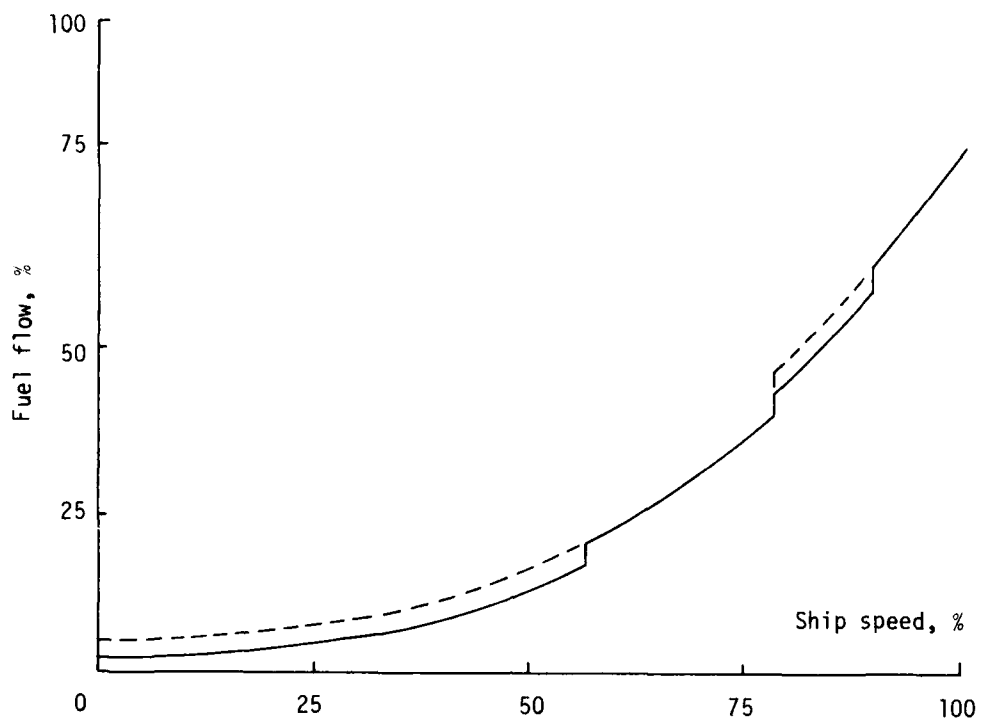


Fig. 12 Fuel Flow versus Ship Speed

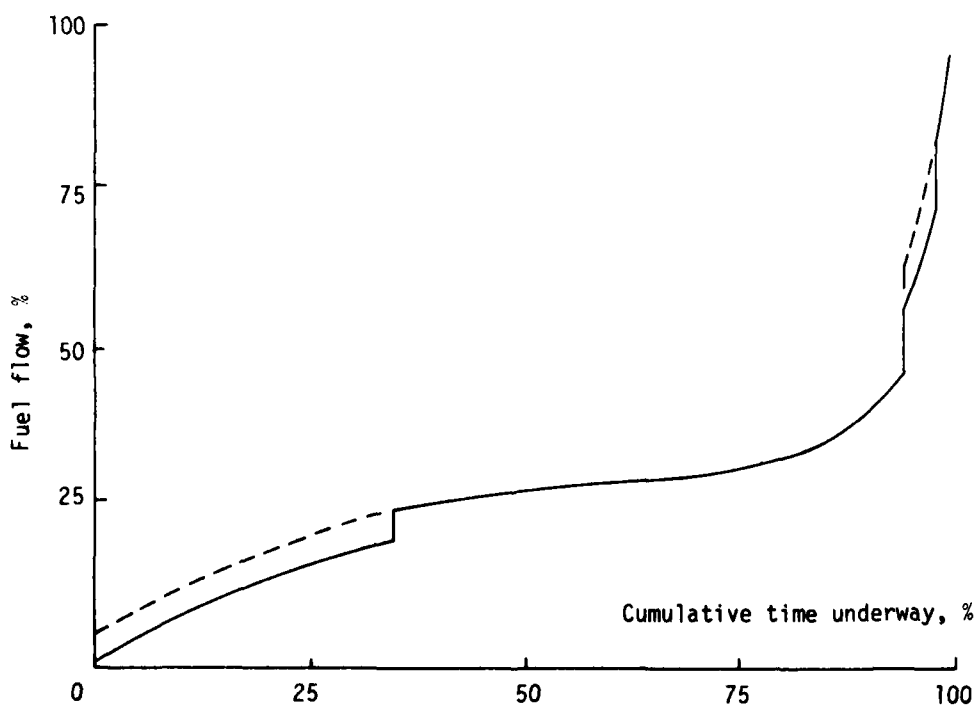
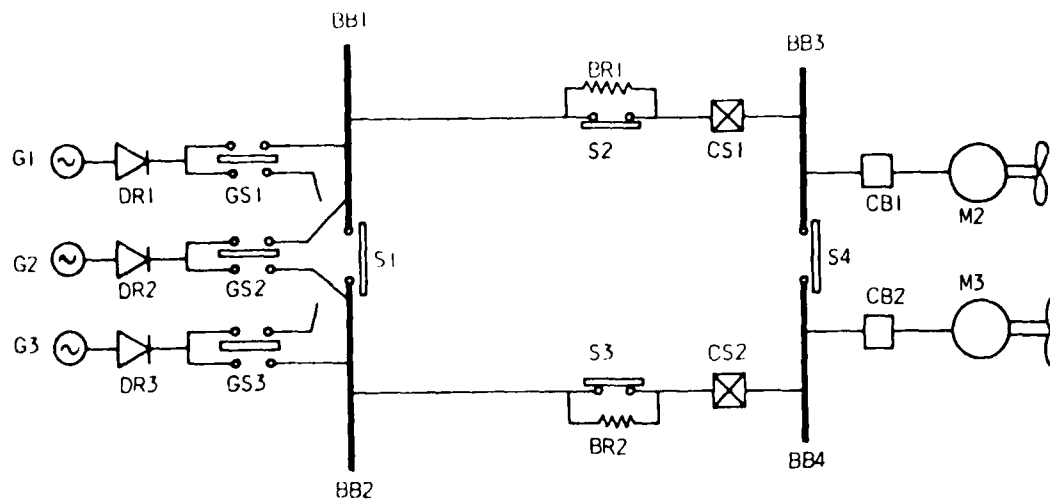


Fig. 13 Fuel Flow versus Time Underway

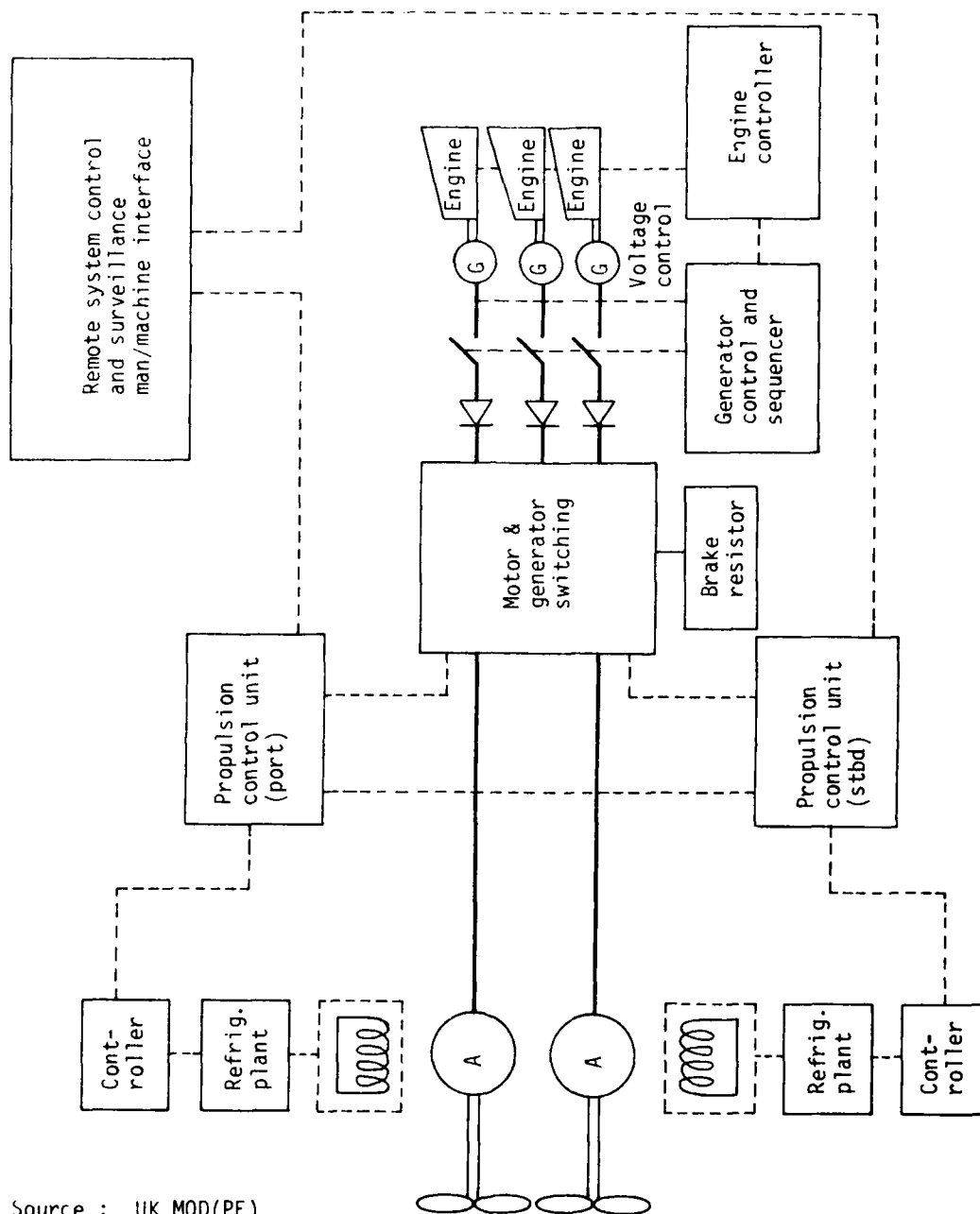


Switch positions											Loaded generators
GS1	GS2	GS3	S1	S2	S3	S4	SC1	SC2	CB1	CB2	
P	1	0	C	C	C	0	AH	AH	C	C	G1
S	0	0	C	C	C	0	AH	AH	C	C	G1
0	P	0	C	C	C	0	AH	AH	C	C	G2
0	S	0	C	C	C	0	AH	AH	C	C	G2
0	0	P	C	C	C	0	AH	AH	C	C	G3
0	0	S	C	C	C	0	AH	AH	C	C	G3
P	P	0	C	C	C	0	AH	AH	C	C	G1 G2
P	S	0	0/C	C	C	0	AH	AH	C	C	G1 G2
S	S	0	C	C	C	0	AH	AH	C	C	G1 G2
P	0	P	C	C	C	0	AH	AH	C	C	G1 G3
P	0	S	0/C	C	C	0	AH	AH	C	C	G1 G3
S	0	S	C	C	C	0	AH	AH	C	C	G1 G3
0	P	P	C	C	C	0	AH	AH	C	C	G2 G3
0	P	S	0/C	C	C	0	AH	AH	C	C	G2 G3
0	S	S	C	C	C	0	AH	AH	C	C	G2 G3
P	P	S	C	C	C	0	AH	AH	C	C	G1 G2 G3
P	S	P	C	C	C	0	AH	AH	C	C	G1 G2 G3
P	S	S	C	C	C	0	AH	AH	C	C	G1 G2 G3
S	S	P	C	C	C	0	AH	AH	C	C	G1 G2 G3
S	P	S	C	C	C	0	AH	AH	C	C	G1 G2 G3
S	P	P	C	C	C	0	AH	AH	C	C	G1 G2 G3

P = Port  
 0 = Open (Off)  
 AH = Ahead

S = Starboard  
 C = Closed  
 (AS = Astern)

Fig. 11 Basic Power Interconnection Scheme and Switch Positions for Ahead Travel - Two Motor/Three Generator System



Source : UK MOD(PE)

Fig. 10 Block Diagram of Control System

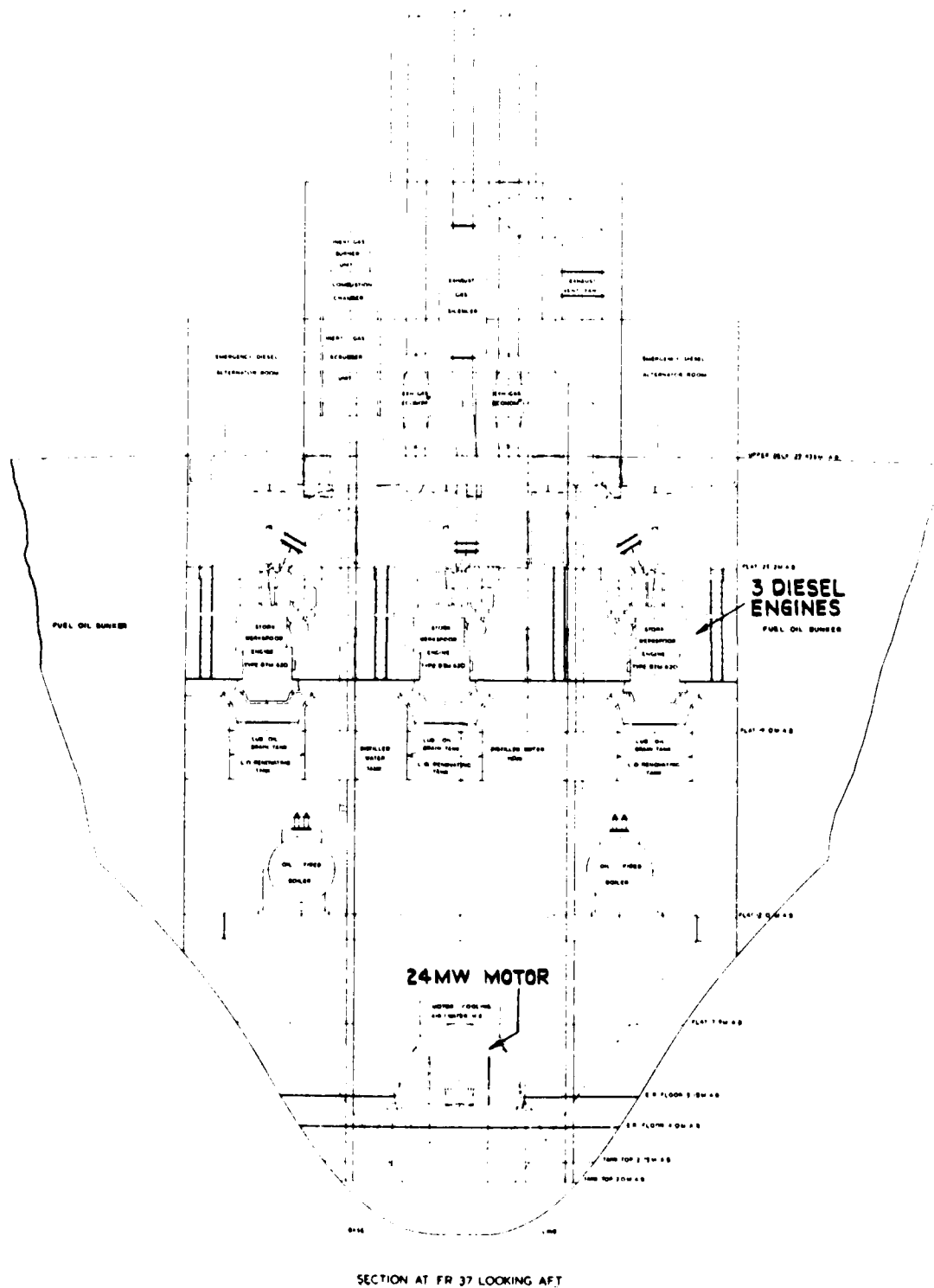


Fig. 9 Superconducting Propulsion Installation - Cross-section

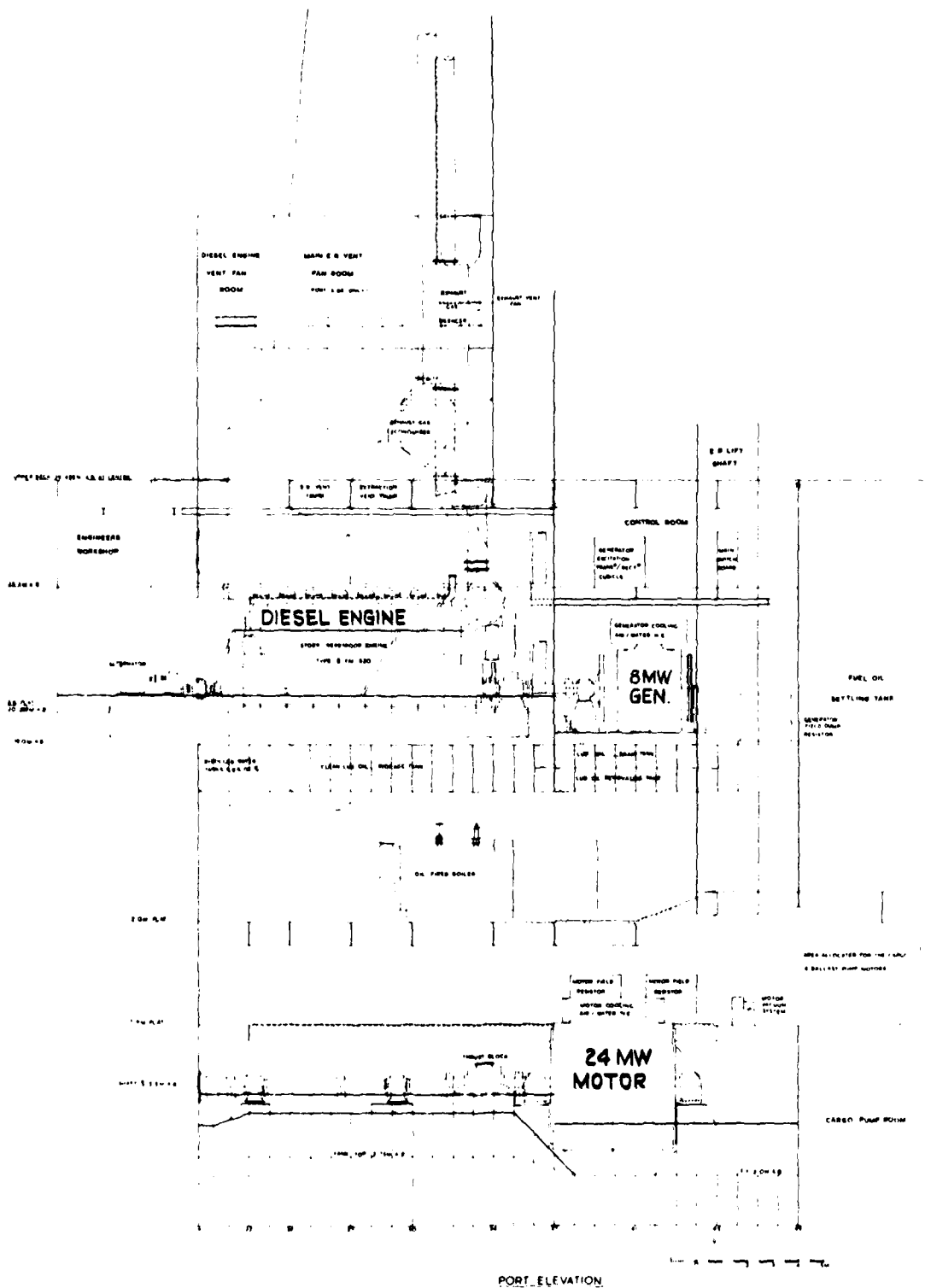


Fig. 8 Superconducting Propulsion Installation - Port Elevation

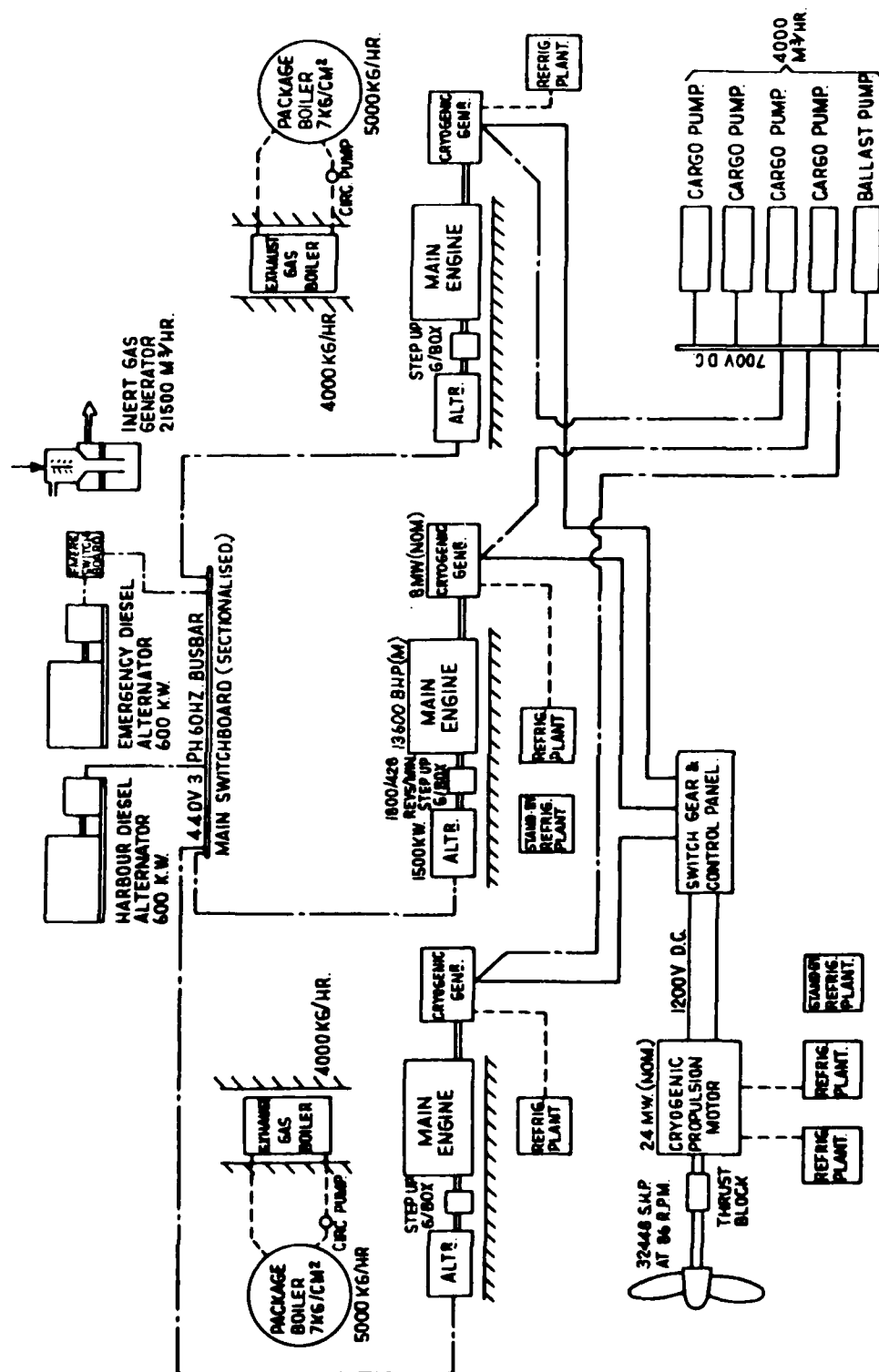


Fig. 7 Principal Machinery - Electrical Installation

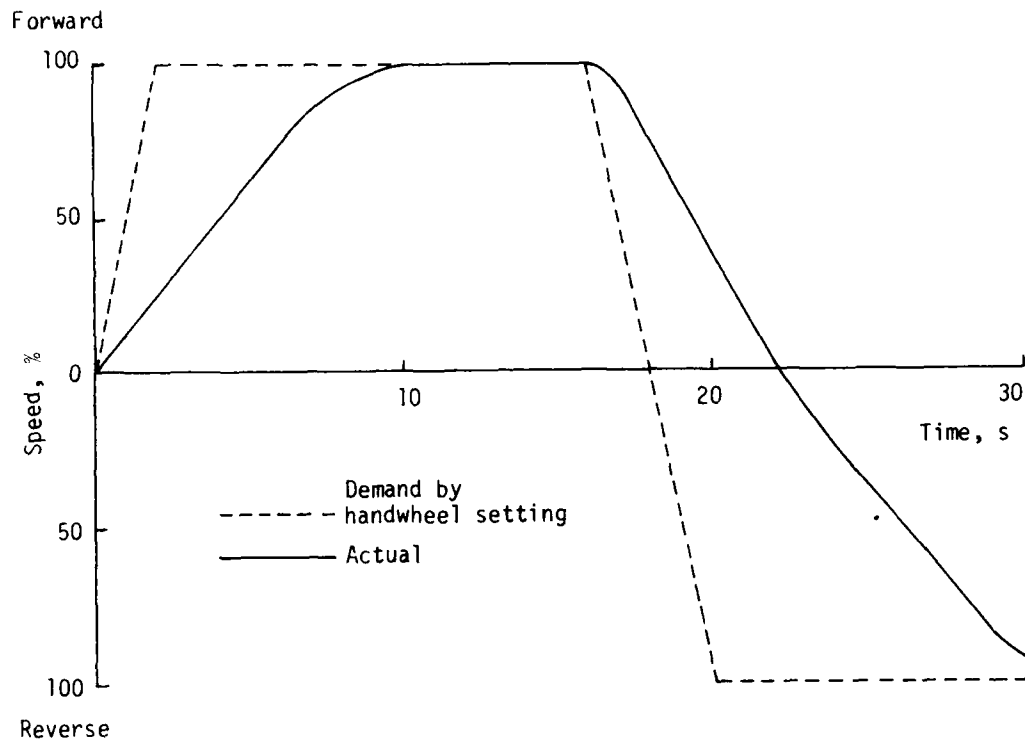


Fig. 5 System Performance Diagram - Speed and Demanded Speed against Time

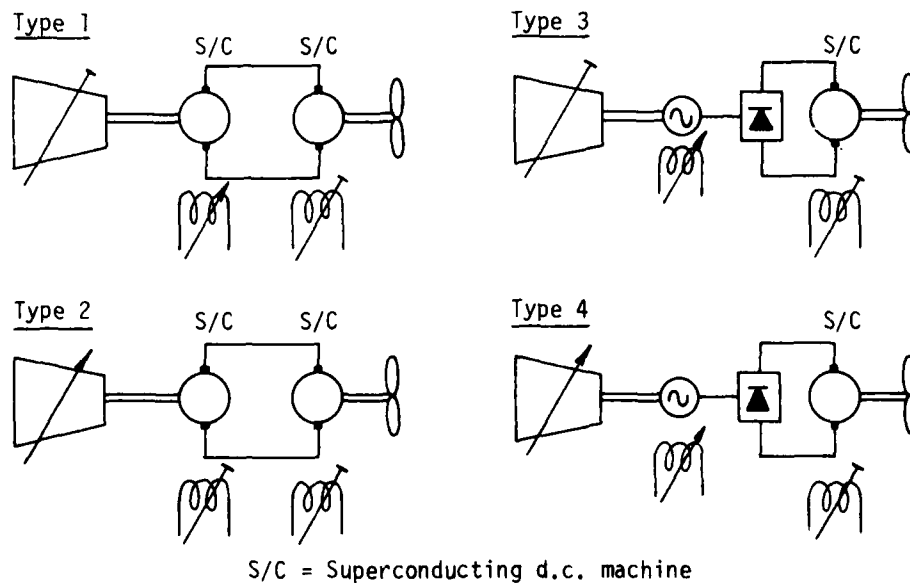


Fig. 6 Four Control Schemes

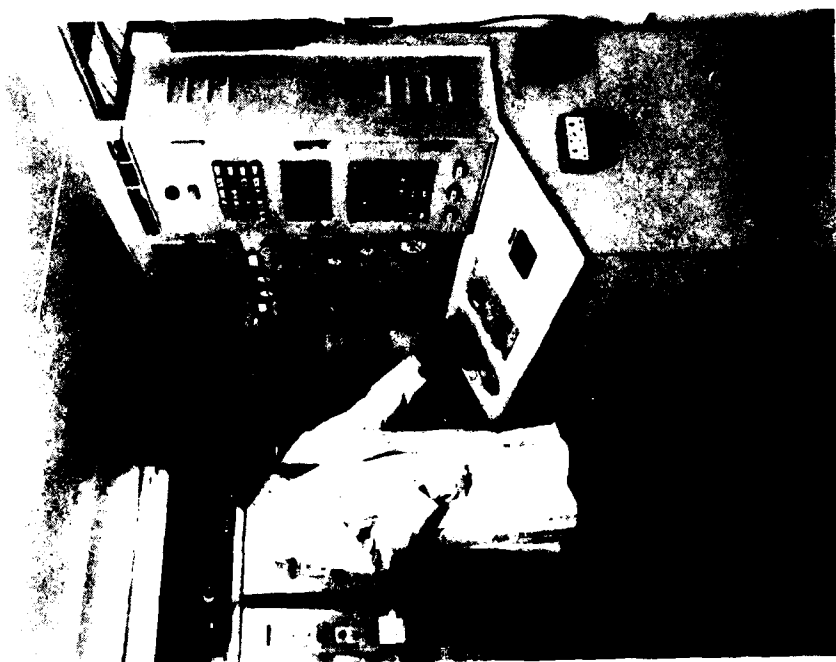
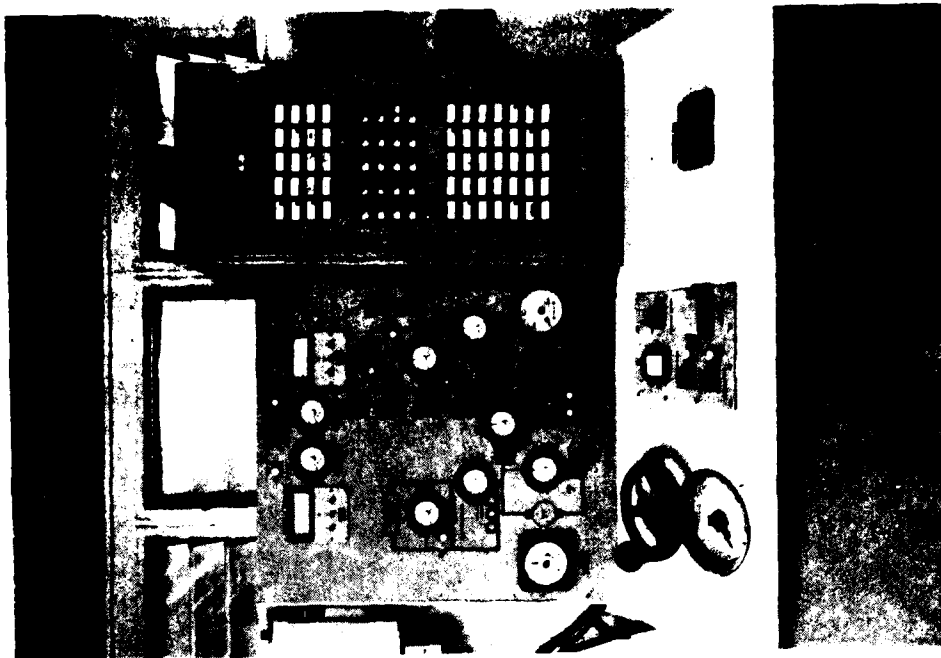


Fig. 4 Representative Control Console



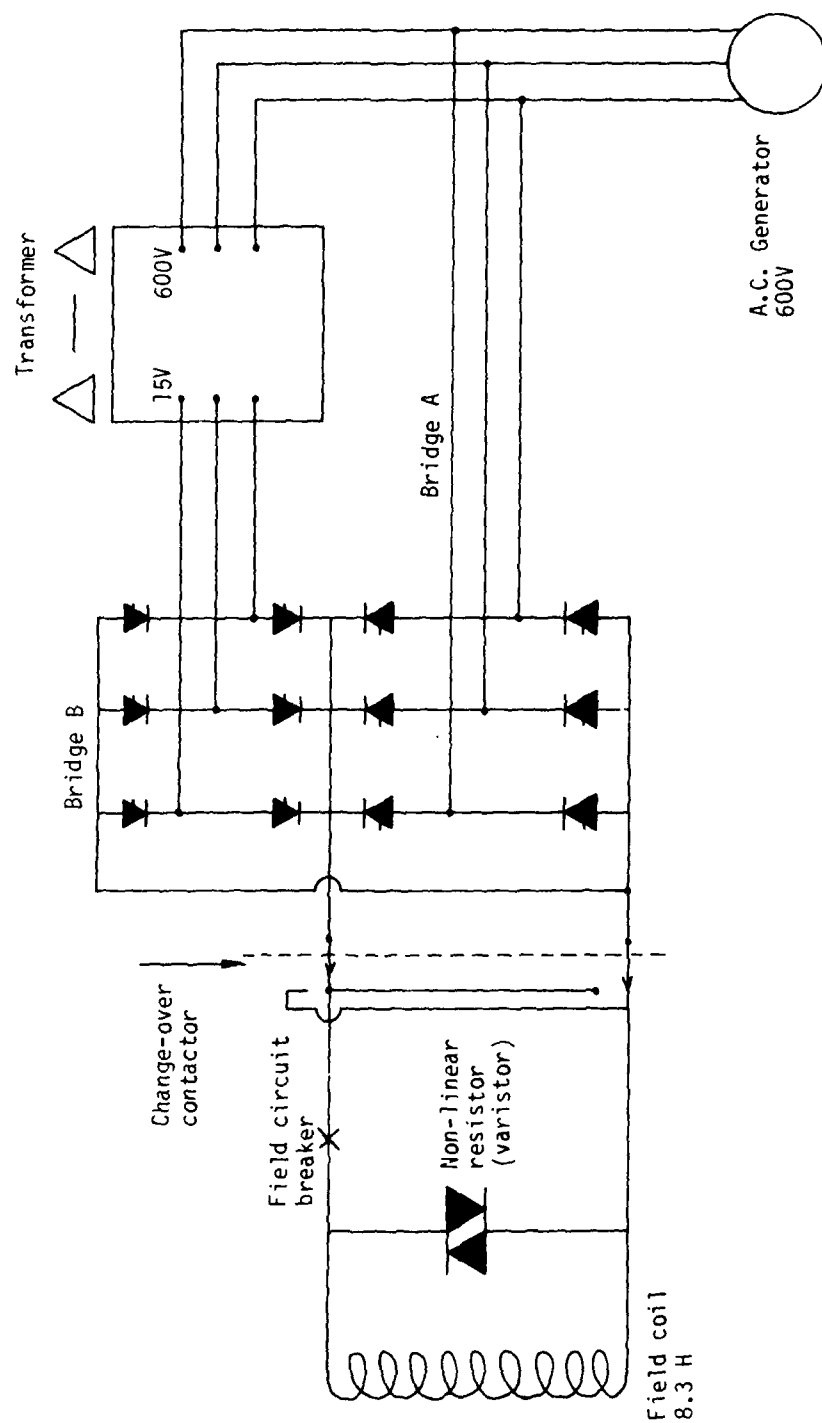


Fig. 3 Field Circuit for 1 MW Generator

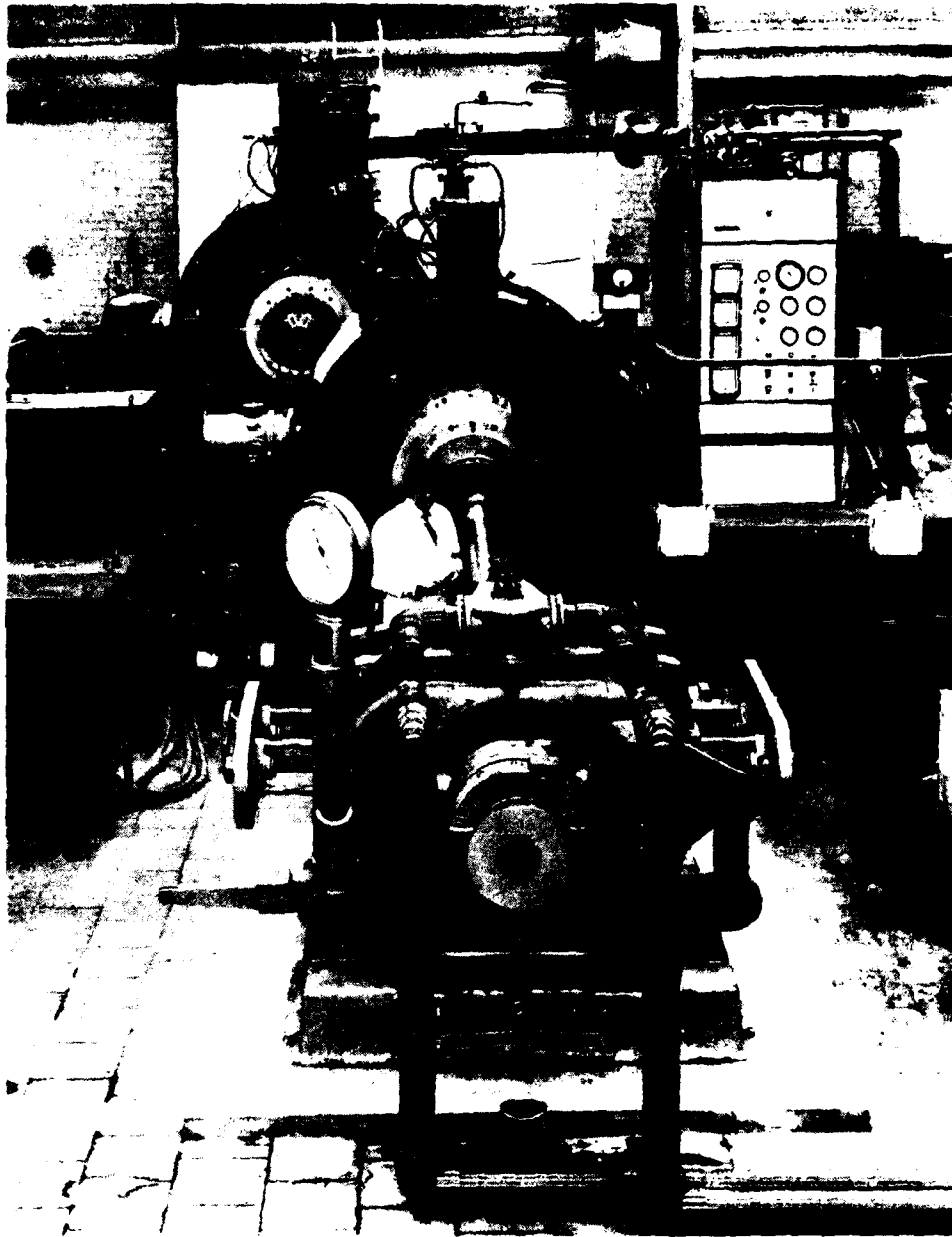


Figure 1. Gas turbine engine of the gas turbine system

	Volume	Session	Page
Hindmarsh, G. J. Vosper Thornycroft, Ltd (UK)	5	R	3-1
Hoffman, D. Hoffman Maritime Consultants, Inc.	4	P	3-1
Holland, G. E. Naval Ship Engineering Center	1	A	1-1
Horigome, M. Tokyo Univ of Mercantile Marine (Japan)	1	C	2-1
Houlihan, T. M. Naval Postgraduate School	3	K2	1-1
Joby, M. J. Lucas Aerospace, Ltd (UK)	2	G	3-1
Johnson, R. David W. Taylor Naval Ship R&D Center	3	J1	3-1
Kallstrom, C. Lund Inst of Tech (Sweden)	3	J2	2-1
Kammerer, J. G. Naval Ocean Systems Center	3	J1	1-1
Kaplan, P. Oceanics, Inc.	2	F2	4-1
Karasuno, K. Kobe Univ of Mercantile Marine (Japan)	2	D	3-1
Keating, G. Decca Radar, Ltd (UK)	2	F1	3-1
Kern, D. Chairman, Session L Specialized Systems, Inc.			
Keyes, P. R. MARA-TIME Marine Services Corp.	3	K1	1-1
King, Randolph W., RADM (Ret) Speaker, Symposium Dinner Maritime Transportation Res Bd Natl Res Council			

	Volume	Session	Page
Mann, David E., Dr. Speaker, Keynote Address Assistant Secretary of the Navy (Research, Engineering and Systems)			
Mara, T. MARA-TIME Marine Services Corp.	3	K1	1-1
Martin, D. Chairman, Session J1 Naval Material Command			
Martin, P. LMT Simulators (France)	2	D	1-1
Matsuki, S. Kobe Univ of Mercantile Marine (Japan)	2	D	3-1
McHale, J. B. Y-ARD (UK)	3	H	2-1
McLane, J. T. Chairman, Session O1 David W. Taylor Naval Ship R&D Center			
McWhirter, W. David W. Taylor Naval Ship R&D Center	3	J1	3-1
Messalle, R. F. David W. Taylor Naval Ship R&D Center	4	O2	1-1
Moon, J. R. Ferranti (UK)	2	E1	2-1
Moran, D. D., Dr. David W. Taylor Naval Ship R&D Center	4	O2	1-1
Moran, T. L. David W. Taylor Naval Ship R&D Center	6	P	2-1
Moss, D. G. General Electric	1	B	1-1

	Volume	Session	Page
Norrbin, N., Dr. Chairman, Session C Swedish State Shipbuilding Exp Tank	3	K1	3-1
Ohtsu, K. Tokyo Univ of Mercantile Marine (Japan)	1	C	2-1
Okumura, M. Kobe Univ of Mercantile Marine (Japan)	2	D	3-1
Olson, B. M. Gibbs & Cox, Inc.	5	Q2	1-1
Orton, J. EASAMS, Ltd (UK)	4	O1	1-1
Parkin, L., LCDR, USCG U.S. Coast Guard	3	L	3-1
Parsons, M., Dr. Chairman, Session J2 Univ of Michigan			
Pesch, A. J. Eclectech Associates, Inc.	3	L	2-1
Phelps, M. A., LCDR, RN HMS SULTAN (UK)	2	D	2-1
Pijcke, A. C. Chairman, Session F1 The Netherlands Maritime Inst (Neth)			
Pirie, I. W. Ministry of Defence (UK)	3	H	2-1
Plant, J. B. Royal Military College of Canada (Canada)	4	M	2-1
Probert, N. D. Hawker Siddeley Dynamics Engr, Ltd (UK)	2	G	2-1
Puglisi, J. Maritime Administration	3	K1	1-1

	Volume	Session	Page
Putman, T. H. Westinghouse	3	K2	2-1
Rains, D. A. Ingalls Shipbuilding	1	B	3-1
Reeves, P., CAPT, RN Ministry of Defence (UK)	1	A	2-1
Reid, R. E. Univ of Virginia	1	C	1-1
Rinehart, V. Maritime Administration	3	L	2-1
Risberg, R. J. Panama Canal Co. (Canal Zone)	3	K1	3-1
Robey, H. N. David W. Taylor Naval Ship R&D Center	4	O2	2-1
Rohkamm, E. Blohm + Voss AG (W. Ger)	2	E2	2-1
Ronning, O., CAPT Royal Norwegian Navy (Norway)	2	F1	1-1
Ropstad, O. Kongsberg, Vapenfabrikk (Norway)	2	E1	1-1
Rubis, C. J. Propulsion Dynamics, Inc.	2	E2	1-1
Ruland, J. K., LCDR, USN Office of Chief of Naval Operations	1	A	4-1
Schubert, E. Forschungsinstitute fur Anthro- potechnik (W. Ger)	5	Q1	2-1
Schubert, F., CAPT, USCG Chairman, Session K1 U.S. Coast Guard Hdqtrs			
Schuffel, H. Inst for Perception-TNO (Neth)	3	K1	2-1

	Volume	Session	Page
Shipley, P. Birkbeck College (UK)	5	Q1	3-1
Simanowith, R. C. David W. Taylor Naval Ship R&D Center	5	R	2-1
Smalley, J. P. E. EASAMS, Ltd (UK)	4	01	1-1
Smith, W. E. David W. Taylor Naval Ship R&D Center	6	P	2-1
Spencer, J. B. Chairman, Session K2 Ministry of Defence (UK)	1	A	2-1
Stankey, R. Chairman, Session E1 Naval Ship Engineering Center			
Steinhausen, J., LCDR, RN Ministry of Defence (UK)	4	01	1-1
Stuurman, A., LT Royal Navy (Neth)	2	E1	3-1
Sugimoto, A. Mitsubishi Heavy Industries, Ltd (Japan)	4	P	1-1
Thomas, J. R. E. Ferranti (UK)	2	E1	2-1
Thompson, R. V. Univ of Newcastle Upon Tyne (UK)	5	Q2	2-1
Tiano, A. Laboratorie per l'Automazione Navale (Italy)	4	P	4-1
Toney, J., LT, USN Naval Postgraduate School	3	K2	1-1
Turner, R. J. College of Nautical Studies (UK)	4	01	3-1
Turner, T. Vosper Thorneycroft, Ltd (UK)	2	F1	2-1

	Volume	Session	Page
van Amerongen, J. Delft Univ of Technology (Neth)	3	J2	4-1
van Dam, J. Royal Netherlands Naval College (Neth)	3	J1	4-1
van de Linde, J. G. C., RADM Chairman, Session Q1 Royal Netherlands Navy (Neth)			
van Nauta Lemke, H. Chairman, Session P Delft Univ (Neth)	3	J2	4-1
Verhage, W., LCDR Chairman, Session D The Royal Netherlands Naval College (Neth)			
Verlo, G. Det Norske Veritas (Norway)	3	J1	2-1
Volta, E. Laboratoria per l'Automazione Navale (Italy)	4	P	4-1
Ware, J. Operations Research, Inc.	1	C	4-1
Whalen, J. Operations Research, Inc.	4	O2	2-1
Whalley, R., LCDR, RN Ministry of Defence (UK)	3	H	3-1
Wheatley, S. Chairman, Session N Natl Maritime Res Center			
Wheeler, D. J. Rolls Royce (UK)	1	B	2-1
Whitesel, H. K. David W. Taylor Naval Ship R&D Center	4	O2	3-1



	Volume	Session	Page
Whyte, P. H. D.R.E.A. (Canada)	2	F2	3-1
Williams, K. E. MARA-TIME Marine Serv Corp.	5	Q1	1-1
Williams, V. E. National Maritime Research Center	1	C	1-1
Wolford, J. C. Naval Weapons Support Center	5	R	1-1
Zuidweg, J. Royal Netherlands Naval College (Neth)	3	J1	4-1

DATE  
FILMED  
-8